Application of Dynamic Partial Least Squares to Complex Processes

A Thesis submitted by

Bothinah A. Altaf

For the degree of Doctor of Philosophy

School of Chemical Engineering and Advanced Materials

Newcastle University

September 2013

Abstract

Multivariate statistical modelling and monitoring is an active area of research and development in both academia and industry. This is due to the economic and safety benefits that can be attained from the implementation of process modelling and monitoring schemes. Most industrial processes in the chemistry-using sector exhibit complex characteristics including process dynamics, non-linearity and changes in operational behaviour which are compounded by the occurrence of non-conforming data points. To date, modelling and monitoring methodologies have focussed on processes exhibiting one of the aforementioned characteristics. This Thesis considers the development and application of multivariate statistical methods for the modelling and monitoring of the whole process as well as individual unit operations with a particular focus on the complex dynamic nonlinear behaviour of continuous processes.

Following a review of Partial Least Squares (PLS), which is applicable for the analysis of problems that exhibit high dimensionality and correlated/collinear variables, it was observed that it is inappropriate for the analysis of data from complex dynamic processes. To address this issue, a multivariate statistical method Robust Adaptive PLS (RAPLS) was proposed, which has the ability to distinguish between non-conforming data, i.e. statistical outliers and a process fault. Through the analysis of data from a mathematical simulation of a time varying and non-stationary process, it is observed that RAPLS shows superior monitoring performance compared to conventional PLS. The model has the ability to adapt to changes in process operating conditions without losing its ability to detect process faults and statistical outliers.

A dynamic extension, RADPLS, using an autoregressive with exogenous inputs (ARX) representation was developed to model and monitor the complex dynamic and nonlinear behaviour of an Ammonia Synthesis Fixed-bed Reactor. The resultant model, which is resistant to outliers, shows significant improvement over other dynamic PLS based representations. The proposed method shows some limitations in terms of the detection of the fault for its full duration but it significantly reduces the false alarm rate.

The RAPLS algorithm is further extended to a dynamic multi-block algorithm, RAMBDPLS, through the conjunction of a finite impulse response (FIR) representation and multiblock PLS. It was applied to the benchmark Tennessee Eastman Process to illustrate its applicability for the monitoring of the whole process and individual unit operations and to demonstrate the concept of fault propagation in a dynamic and nonlinear continuous system. The resulting model detects the faults and reduces the false alarm rate compared to conventional PLS.

Acknowledgments

I take this opportunity to sincerely thank my supervisors, Prof. Elaine Martin and Prof. Gary Montague, for firstly offering me the opportunity to undertake research under their supervision and secondly their guidance, encouragement and support throughout the period of my PhD. In particular, I would like to thank Prof. Elaine for her effort for going through my thesis draft many times.

Special thanks to Dr.Aruna Manipura for his constant support and encouragement to finish the thesis.

Special thanks to my friends Nouf, Maryam and Aisha for being patience and for all the support. I also would like to thank my office mate, Chris, Remi, Richrad and Grace for the support and encouragement.

Financial support provided from Ministry of Higher Education and King Abdulaziz University, Saudi Arabia is also acknowledged.

This thesis belongs together with all my love and gratitude to my sisters and brothers Sarah, Ohood, Saeed, Sahal, Reem, my sister in low Lujain and my lovely nephew Abdulla.

Above all, I am forever grateful to my parents Abdullah Altaf and Samira Asali for their loving support, endless inspiration, kindness, understanding and encouragement. Without them, I would not be writing this thesis.

Table of Contents

CHAPTER 3

CHAPTER 4

List of Figures

List of Tables

List of Symbols

a	Number of latent variables
a , b	Parameters of $ARMA$ model (§3.9) Parameters of $ARIMA$ model (§3.10)
$\mathbf{A}_i$	Coefficient matrix for the lagged output variables - Dynamic PLS
$\mathbf{B}_i$	Coefficient matrix for the lagged input variables - Dynamic PLS
$\mathbf{B}$	Matrix of PLS inner relation coefficients
$\mathbf{B}_{PLS}$	PLS regression coefficients
BL	Block size for recursive PLS
B	Number of block – Multiblock PLS
b_i	Coefficient of PLS inner regression relationship
B	Parameter of $ARMA$ model (§3.9) Parameter of $ARIMA$ model (§3.10)
B	Block number
$\mathbf{C}$	Matrix of coefficients - Dynamic PLS
$\mathbf{G_i}$	Linear dynamic model
$\mathbf{E}$	Residual matrix for PLS inputs (Chapter 3) Residual matrix for PCA (Chapter 2) Noise matrix (§ 3.7.1)
$\mathbf{F}$	Residual matrix for PLS outputs
K	Number of quality variables
	Time delay - Dynamic PLS (§ 3.7.1)
k	Increment for ramp signal (§ 3.9.2)
LV	Number of latent variables (Chapter 5)
m	Number of variables for PCA (Chapter 2) Number of input variables for PLS (Chapter 3)
m_b	Number of input variables in block b
N	Number of samples for PLS and PCA
n_u	Time lags for input variables - Dynamic PLS
n_y	Time lags for output variables - Dynamic PLS
$\mathbf{P}, \mathbf{p}$	PLS input loading matrix/vector (Chapter 3) PCA loading matrix/vector (Chapter 2)
$\boldsymbol{P}_b, \boldsymbol{p}_b$	MBPLS - Block loadings matrix/vector
R	Adjusted Wold's criteria
R	Ramp signal

$\mathbf{T}, \mathbf{t}$	PLS input score matrix/vector (Chapter 3)
	PCA score matrix/vector (Chapter 2)
$\boldsymbol{T_b}, \boldsymbol{t_b}$	MBPLS - Block scores matrix/vector
$\boldsymbol{T_T}, \boldsymbol{t_T}$	MBPLS - Super scores matrix/vector
$\mathbf{Tol}$	Convergence
T_b^2	Hotelling's T² statistic for block b
T_α^2	Confidence limit for Hotelling's T² statistic
T_n^2	Hotelling's T² for the nth sample
$\mathbf{U}, \mathbf{u}$	PLS output score matrix/vector
$\mathrm{u_h}$	Signal generated from $ARMA$ model (§ 3.9)
	Signal generated from $ARIMA$ model (§ 3.10)
$\mathbf{Q}, \mathbf{q}$	Output loading matrix/vector
$\mathbf{q}_a$	MBPLS output weight
S	Number of subsets in cross validation
SPE_b	Squared prediction error for an individual block
$\mathrm{SPE}_\mathrm{X}^{(\mathrm{i})}$	Square prediction error of the input space for the ith sample
$\mathrm{SPE}_\mathrm{Y}^{(\mathrm{i})}$	Square prediction error of the output space for the ith sample
$\mathbf{W}, \mathbf{w}$	PLS weight matrix/vector
$\boldsymbol{W_b}, \boldsymbol{w_b}$	MBPLS block weight matrix/vector
$\boldsymbol{W_T}$, $\boldsymbol{w_T}$	MBPLS super weight matrix/vector
$\mathbf{X}, \mathbf{x}$	PLS input matrix/vector
$\widehat{\mathbf{X}}, \hat{\mathbf{x}}$	PLS predicted input matrix/vector
$\mathbf{X_{new}}$	Input matrix for recursive PLS
$\boldsymbol{X_b}$	Block input matrix
$\mathbf{Y}, \mathbf{y}$	PLS output matrix/vector
$\widehat{\mathbf{Y}}, \hat{\mathbf{y}}$	PLS predicted output matrix/vector
$\mathbf{Y_{new}}$	Output matrix for recursive PLS
$\boldsymbol{\Lambda_a}$	Matrix of a retained latent variables
α	Significance level
$\boldsymbol{\Lambda_b^{-1}}$	Inverse of the covariance matrix
χ_α^2	Chi-squared distribution with degrees of freedom a, i.e. number of latent variables and alpha (α) is the significance level.
ε_{ii}	Random signal from normal distribution
z^{-1}	Back shift operator

Acronyms

ADPLS	Adaptive Dynamic PLS
AIC	Akaike’s Information Criterion
AMBDPLS	Adaptive MultiBlock Dynamic PLS
APLS	Adaptive PLS
ARL	Average Run Length
ARX	Auto-Regressive with Exogenous input
DPLS	Dynamic PLS
FAR	False Alarm Rate
FDR	Fault Detection Rate
FIR	Finite Impulse Response
MBDPLS	MultiBlock Dynamic PLS
MBPLS	MultiBlock PLS
PLS	Partial Least Squares
RADPLS	Robust Adaptive Dynamic PLS
RAMBDPLS	Robust Adaptive Multiblock Dynamic PLS
RAPLS	Robust Adaptive PLS
RMSE	Root Mean Squared Error
RPLS	Recursive PLS

Chapter 1

Thesis Introduction and Overview

The focus of this thesis is on the application of multivariate statistical projection based techniques for the monitoring of complex and dynamic behaviour of industrial continuous process. Two aspects were considered, the monitoring of the whole process and individual unit operations using multivariate performance monitoring techniques based on partial least squares and the extension of these to incorporate dynamic behaviour and ensure the monitoring scheme is robust to outliers. The aim of this chapter is to provide an overview of the research problem and the challenges addressed as well as provide an overview of the thesis structure and the main contributions of the research.

1.1 Introduction

The chemicals sector is of strategic importance in the European Union and as shown in Figure 1.1 it was the most important trading region compared to the rest of the world (Cefic: the European Chemical Industry Council, 2012). The chemicals sector faces several challenges including improving production efficiency, coping with varying production requirements (product demand), competing with emerging producers such as China and India and the need for improved health and safety in the production environment. One tool to assist in the delivering of these goals is that of process performance monitoring.

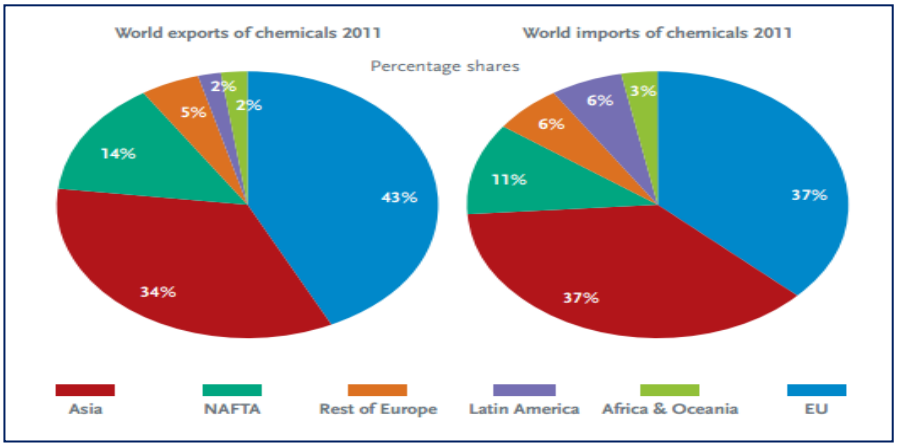

Figure 1.1 - World exports and imports of chemicals by regional share (source: Cefic, the European Chemical Industry Council (2012))

1.1.1 Process Performance Monitoring

Process performance monitoring is an important topic in the highly competitive chemicals sector (Gosselin and Ruel, 2007; Kruger and Xie, 2012). It is a means for assessing the performance and identifying the potential sources of variation inherent within the process of interest. Process monitoring is implemented to maintain high quality consistent production and for improving the performance of the process. In addition, process monitoring provides the operator with critical information about the progress of the process and hence early warning of the onset of an operational change thereby enabling correction action to be taken in a timely manner thereby ensuring process efficiency is preserved and there is no loss of product and energy, health and safety are not compromised.

A number of monitoring methods have been proposed and these are briefly summarised in the following section. The very first process performance monitoring scheme was known as statistical process control (SPC) and was proposed by Walter A. Shewart in 1920s. It was based on an individual control chart that monitors the performance of the quality products. It has been used for maintaining and improving the performance of industrial processes (Raich and Çinar, 1996; Montgomery, 2005; Summers and Donna, 2010)

1.1.2 Process Monitoring Methods

Process monitoring can be based on one of three strategies: model based, knowledge based and data driven approach. A detailed description of the three methods can be found in Ge et al. (2013) with a three part review by Venkatasubramanian et al. (2003a; 2003b; 2003c)

Model based methods are based on a first principles model of the physical and/or chemical relationships between the inputs and outputs of a process. Hence a mathematical model representing the process underpins the process performance monitoring scheme, i.e. the actual process behaviour is compared to the mathematical model and any deviation between them is expressed as a residual and this is used for process monitoring and fault detection. Even though model based methods provide a representative model, the development of theoretical models requires significant time, effort and financial resources and is challenging for complex processes (Seborg et al., 1989).

Knowledge based methods depend on a detailed understanding of the system and is expressed in terms of facts, rules and the known nominal behaviour. This information is organized into a scheme that is utilised for process monitoring. The idea is to compare the actual behaviour of the system with the information contained within the monitoring scheme and any inconsistency indicates a system abnormality (Frank, 1990; Ramesh et al., 1992). Unlike model based methods, it does not involve mathematical models or detailed physical and chemical relationships. However, it is time consuming since it requires detailed knowledge and experience of the system to develop the monitoring scheme.

Data driven methods are primarily constructed from process measurements and contain information about the process. They do not require any knowledge of the physical and chemical relationships hence they have been termed black-box methods. In contrast to model based and knowledge based methods, they can be implemented on processes which exhibit complex characteristics and high dimensions in a shorter time-frame (Chiang et al., 2001). One of the main data based monitoring methods is that of multivariate statistical process control.

1.1.3 Statistical Process Performance Monitoring Methods

Statistical process control (SPC) was initially introduced by the pioneering work of Walter A. Shewhart in 1920, who worked for Bell Telephone laboratories. He proposed the philosophy of process monitoring, i.e. to monitor the performance of a process and identify source of process variability through the development of monitoring charts (Montgomery, 2005; Kruger and Xie, 2012). Process variability can be subdivided into background noise that is present in the process due to the nature of the process, i.e. common cause variation, and uncontrolled variation that is caused by assignable causes and is not part of the process and hence, that should be isolated and eliminated (Kaskavelis, 2000). A process is considered to be in a state of statistical control if the variation is from common causes (Oakland, 2008). The traditional SPC tools are well established and their primary role is to indicate whether product quality is satisfactory. They compare current performance against process behaviour when the process represented normal operating condition which is defined in terms of in statistical control limits. Examples of univariate SPC charts are Shewhart chart ($\overline{X}$-bar and range chart), cumulative sum (CUSUM), and exponentially weighted moving average (EWMA) charts. Significant paybacks have been realised through the implementation of

univariate SPC (Montgomery, 2005; Summers and Donna, 2010). However, it has been criticized for the following reasons:

- Inability to handle high dimensional data as it is based on the individual charting of a limited number of process variables, most often product quality resulting in an inaccurate analysis of process performance (MacGregor and Kourti, 1995; Nomikos and MacGregor, 1995; Kruger and Xie, 2012). By monitoring only the quality variable, the information on the process variables is ignored. Additionally by only considering the process variables the relationships between these variables (i.e. the interactions) are ignored (Reynolds and Lu, 1997).
- If implemented, a large number of control charts would be required for large scale processes and it can be difficult to be monitor and interpret these simultaneously (Martin et al., 1996; Bersimis et al., 2007). In summary, ignoring interactions can be misleading in terms of identifying process malfunction and an excessive number of false alarms may materialise. This results in acceptable quality product being destroyed or reworked and time wasted in seeking out process issues which were not present.

The aforementioned aspects have lead to the introduction of Multivariate SPC which aims to tackle the limitations of the univariate version of SPC. In the last two decades, the statistical multivariate projection techniques of Principal Component Analysis (PCA) and Partial Least Squares (PLS) have been widely applied for the monitoring of industrial processes (Jackson, 1991; MacGregor et al., 2005; Cinar et al., 2007; Mujica et al., 2008; Kourti et al., 2009; Tavares et al., 2011; Kruger and Xie, 2012; Qin, 2012; Yin et al., 2012). The philosophy underpinning their use was:

- They are able to transform high dimensional, correlated and noisy variables, which are typical characteristics of modern industrial data, into a limited number of new latent variables that are uncorrelated.
- The resulting latent variables are linear combinations of the original variables and are used to capture the information relating to the process variation and hence, a simplified yet representative process model is developed (Kourti et al., 1996; Simoglou et al., 2000).
- The most significant feature is that a limited number of control charts are required to monitor the process based on the statistical monitoring indices of Hotelling's T^2 and the squared prediction error (SPE) (Kourti and MacGregor,

1995; Gallagher and Wise, 1996; Martin et al., 1996; Raich and Çinar, 1996; Qin, 2003)

Principal Component Analysis (PCA) aims to transform the original variables (input data matrix) into a new set of principal components, PCs, by exploiting the correlation structure between the process variables to reduce the dimensionality of the data set without loss of information (Jolliffe, 2002). The PCs, which capture the sources of variation in the data are orthogonal and are ordered in terms of decreasing levels of variability. An overview of PCA is given in Chapter 2. Although PCA has been successfully applied to many processes, it only considers the input data matrix and thus where the interest is in monitoring the output, it is not applicable. As the aim of the thesis is to monitor the outputs of the whole process as well as individual unit operations, PCA is not considered in detail and the focus is on partial least squares (PLS).

Partial Least Squares (PLS) is the most commonly applied multivariate statistical modelling technique, with the goal of predicting a set of quality variables from a high dimensional input space (Wold et al., 2001; Vinzi et al., 2007; Abdi, 2010). In contrast to PCA, the PLS latent variables are constructed using both the input and output data matrices and the aim is to maximize the covariance between the two matrices and hence predict the quality variables. PLS has been widely applied for the modelling and monitoring of multivariate industrial data (Kaskavelis, 2000; Wold et al., 2001; Yacoub and MacGregor, 2003; Wold et al., 2004). A detailed description of PLS is given in Chapter 3.

By utilising projection based statistical techniques, an empirical model of the process is developed from experimental data and from this monitoring metrics are calculated including Hotelling's T^2 and Squared Prediction Error (SPE). It has been stated that statistical monitoring approaches based on empirical models are effective tools due to their reliability, speed of development and implementation, degree of knowledge required and cost of implementation (Kano et al., 2002; Qin, 2003; Cinar et al., 2007; Alghazzawi and Lennox, 2008; Kourti et al., 2009; Kruger and Xie, 2012).

1.1.4 Industrial Processes and Multivariate Projection Methods

Multivariate statistical projection approaches, PCA and PLS, are designed to handle data from steady state processes. MacGregor (1997) summarised some of the challenges associated with handling industrial data including data set size, quality of the data and

variable correlations. Monitoring schemes for steady state process can be developed based on PCA and PLS and although these approaches show superior performance compared to traditional SPC methods in terms of extracting information from large data sets in the presence of correlated variables, other challenges materialises. Most modern industrial processes exhibit complex behaviour including dynamic, non-stationary, nonlinear and time varying (Gallagher et al., 1997; Choi et al., 2006). Hence the steady state approaches need to be extended or modified to produce reliable monitoring schemes for more complex systems, which exhibit dynamic, non-linear and changing operational behaviour. These extensions have been developed based on understanding the nature of the data collected from the system under study. Therefore understanding process characteristics is an important factor in the construction of statistical monitoring systems.

Another important aspect is the type of operation namely batch or continuous (Ge et al., 2013). Sharratt (1997) defined a batch process as a series of operations that are carried out over a finite period of time on a separate and identifiable portion of materials. Batch processes are favoured when producing high value products. It is also favoured because of the flexibility in production process and low cost of equipment. However, Rippin (1983) stated that several issues are associated with batch processes including lack of reproducibility, fluctuations in product quality and high specific power consumption. Examples of batch processes include fine chemical production and process within the bio-chemical industry. On the other hand, a continuous process is a process where all the operations are executed continuously based on un-identifiable portions of material. These processes are operated at the optimal conditions after start up and produce consistent output. Although the cost of equipment used for continuous processes is high, the production rate and quality are high (Plumb, 2005). They can be operated automatically to produce large quantities of products and reduce the work force required. Examples of continuous processes include chemical processes such as petroleum refining, cement, commodity chemical such as ammonia and fertilizer Industry. Although both types are widely implemented, continuous systems are the focus of this thesis and application of the techniques to batch processes would be a further area of research.

The research to date has primarily focussed on the monitoring of individual unit operations as opposed to multiple units comprising the whole process. A product from a continuous process is typically manufactured from a series of operational units. The

product will be processed in a number of unit operations which are connected through transfer streams and control loops for example. Consequently the functionality of an individual unit operation will be affected by other operations. As a result, if an abnormal event has occurred in a specific unit, it will propagate through to the other unit operations hence it is essential to understand the whole process as well as the individual unit operations. The interactions between individual units, the time delay between different units, the recycling strategies, the control system and the nature of the task itself are all factors that increase the complexity of the monitoring task of continuous systems.

1.2 Thesis Motivation

Multivariate statistical process monitoring methods have been shown to be efficient for the early detection of abnormal behaviour. One family of approaches to handle steady state process that exhibits linear relationships between the process measurements are these based on Partial Least Squares (PLS). A number of extensions to PLS have been proposed to address specific characteristics including dynamic PLS. Negiz and Çlinar (1997a) reported that in some cases, these dynamic extensions were unable to capture small changes in the process dynamics. Furthermore, limited attention has been given to the application of recursive projection based approaches with adaptive confidence limits to model and monitor dynamic and nonlinear processes in real time and is a focus of this thesis. An issue in recursive monitoring is the presence of statistical outliers in the data as it is important to detect and handle these appropriately with respect to the model updating.

As mentioned continuous processes comprise a number of unit operations and hence the monitoring of such process is challenging when the totality of the process is considered. Research in this area has focused on the application of multiblock approaches (Wangen and Kowalski, 1989; MacGregor et al., 1994; Qin et al., 2001; Westerhuis and Smilde, 2001; Smilde et al., 2003). However, there are still issues that need to be investigated including how to incorporate process dynamics into the multiblock algorithm and how a fault propagates through a dynamic large scale processes. These aspects are also considered in this thesis.

Figure 1.2 summarises a number of challenges relating to the implementation of PLS for industrial process performance monitoring and those that were addressed in this thesis. Figure 1.2 also provides some of the currently available PLS based algorithms

which address individual aspects including the use of multiblock PLS methods for the modelling and monitoring of large scale processes and the use of recursive PLS with adaptive confidence limits for the modelling and monitoring of process that exhibits changing behaviour such as time varying or non-stationary. The next level (coloured level) presents the solutions proposed in this thesis to address a combination of the issues. For example, robust adaptive PLS (RAPLS) is proposed to develop a recursive model that is resistant to outliers and thus is able to model processes that exhibit changing behaviour. Multi block Dynamic PLS (MBDPLS) based on a finite impulse response time series is developed to model a large scale dynamic process. Robust adaptive multiblock dynamic PLS (RAMBDPLS) is proposed to model and monitor all unit operations simultaneously as well as individual unit operation of a large scale dynamic process in a recursive manner where the model is robust to statistical outliers.

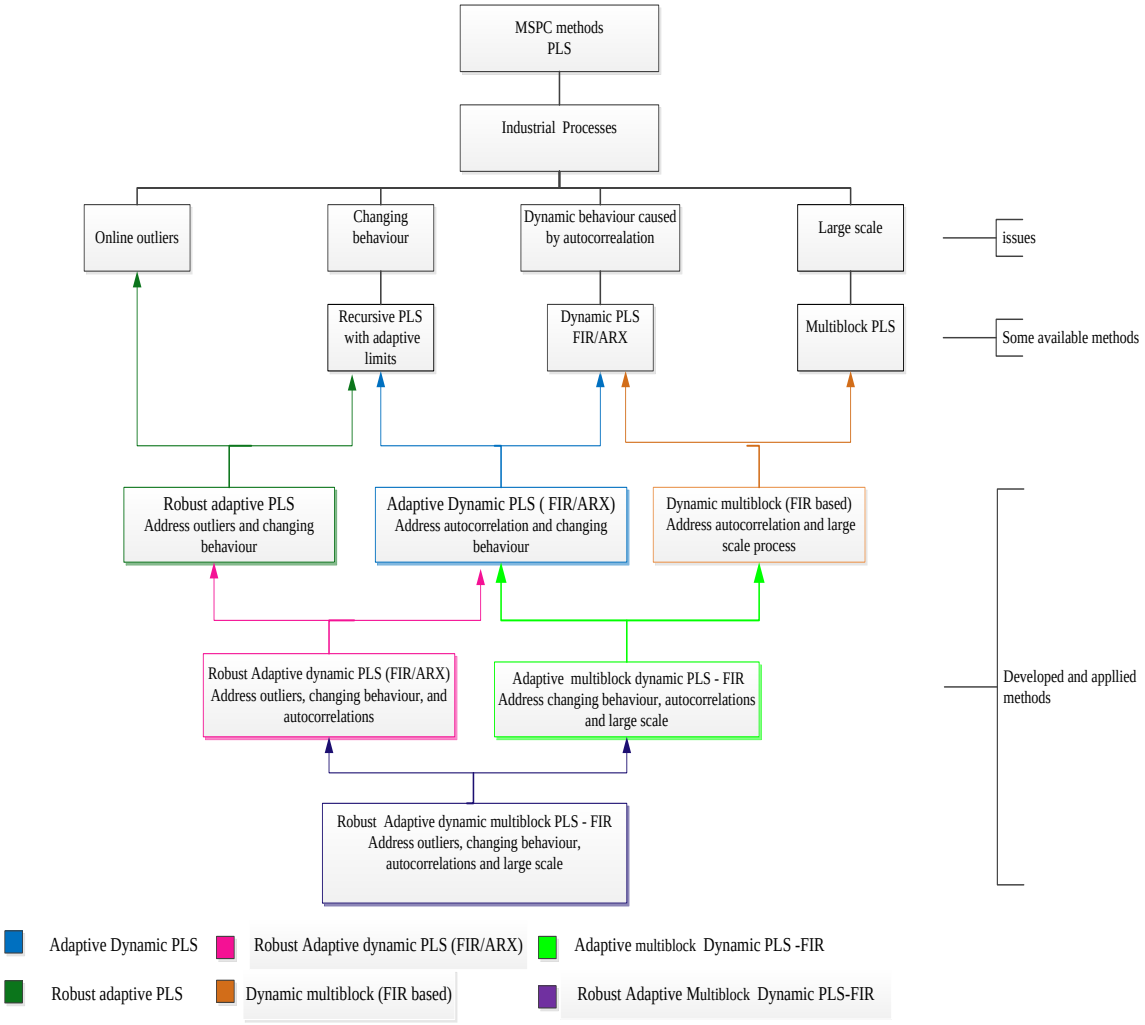

Figure 1.2 - Challenges that are addressed in this thesis

1.3 Aims and Objectives of the Thesis

The ultimate goal of this thesis is to address the applicability of multivariate statistical projection based approaches as well as a number of extensions for the monitoring of complex dynamic behaviour of both the whole process and individual unit operations for a continuous process. More specifically the objectives of this research include:

- To review the current multivariate projection based approaches that have been applied for the monitoring of continuous systems which are based on Partial Least Squares (PLS), more specifically Dynamic PLS (DPLS), Multiblock PLS (MBPLS) and Recursive PLS (RPLS)
- To model and monitor complex dynamic behaviour using different variants of multivariate projection based techniques to demonstrate how different process characteristics impact on the developed monitoring schemes.
- To model and monitor the complex characteristics of multivariate processes that exhibit time varying and non-stationary behaviour in a recursive manner and in the presence of outliers. This materialised in the development of a robust adaptive partial least squares (RAPLS) algorithm.
- To model and monitor the complex characteristics of multivariate processes including the dynamic behaviour of large scale processes. A multiblock dynamic partial least squares based on Finite impulse response (MBDPLS) was developed.
- To describe how the current approach of RAPLS, can be modified and extended to address current limitations such as accounting for process dynamics. Robust adaptive dynamic Partial Least Squares (RADPLS) was proposed.
- To statistically evaluate the quality and capabilities of the models and monitoring charts developed based on different projection approaches using the statistical indices of Root Mean Squared Error (RMSE), Average Run Length (ARL), False Alarm Rate (FAR) and Fault Detection Rate (FDR).
- To develop a methodology, Robust Adaptive Multiblock Dynamic PLS (RAMBDPLS), based on current extensions to PLS, including dynamic PLS, recursive PLS and multiblock PLS that has the ability to handle unusual samples (i.e. outliers) when monitoring a unit operation and the whole system.
- Demonstrate the application of PLS and the existing and proposed extensions, Dynamic PLS (DPLS), Adaptive Dynamic PLS (ADPLS) and Robust Adaptive dynamic PLS (RADPLS), to monitor the complex behaviour of an ammonia

synthesis reactor. This is an example of the monitoring of a unit operation that exhibit complex process dynamics.

- Monitoring of both the whole process and the individual unit operations of the Tennessee Eastman process using Dynamic PLS based on a finite impulse response (FIR) model, Adaptive Multiblock Dynamic PLS (AMBDPLS) and Robust Adaptive Multiblock Dynamic PLS (RAMBDPLS) and the investigation of fault propagations in a continuous system.

1.4 Contributions of the Thesis

The contributions of this thesis are based on the application of the multivariate statistical projection based technique of Partial Least Squares (PLS) and its extension for the real time monitoring of complex behaviour of multivariate dynamic systems. More specifically the contributions are:

- A number of multiblock PLS algorithms have been proposed in the literature for monitoring large scale process. They aim to divide the process into meaningful blocks to simplify the interpretation and monitoring of the process. In particular, the multiblock PLS algorithm proposed by Westerhuis and Coenegracht (1997) is analysed and extended to multiblock dynamic PLS through the incorporation of a finite impulse response time series representation. The rational for selecting this algorithm, (Westerhuis and Coenegracht, 1997), is that it is well known that its parameters can be calculated from the application of conventional PLS hence it can be extended to monitor large scale dynamic process through the application of dynamic PLS based on a time lagged approach.
- Several recursive PLS algorithms have been proposed in the literature to update the PLS reference model to account for changes in process operations. In particular, the recursive PLS algorithm with adaptive confidence limits (APLS) by Wang et al.(2003) is analysed. The reason for selecting this algorithm is that it is well known for its ability to reduce the number of false alarms compared to conventional PLS and sample wise recursive PLS proposed by Qin (1993). In addition, because this algorithm can be extended to monitor the whole process as well as individual unit operations by incorporating it with multiblock PLS. The adaptive PLS (APLS) algorithm has been extended to account for auto-correlated measurements hence an adaptive dynamic PLS (ADPLS) algorithm was developed.

- As the recursive approaches aim to update a PLS model whenever new data become available, it is important to identify whether to implement the recursive update step due to the presence of statistical outliers. A novel robust adaptive PLS (RAPLS) algorithm for the modelling and monitoring of a continuous process was developed. The approach has the ability to distinguish between normal, non-conforming observations (fault) and outliers. The approach was extended to robust adaptive multiblock dynamic (RAMBDPLS) for modelling and monitoring of dynamic systems and the monitoring of individual unit operations as well as whole process
- A comparative assessment of different extensions to PLS (conventional, adaptive and robust adaptive PLS) in terms of model prediction, fault detection and false alarm rate using data from a mathematical simulation of time varying and non-stationary processes was performed.
- The algorithm, APLS, proposed by Wang et al.(2003) was incorporated with an Autoregressive with exogenous input model to account for process dynamic behaviour caused by autocorrelation and it was extended to a robust variant for the modelling and monitoring of the complex dynamic behaviour of an ammonia synthesis reactor. To the knowledge of the author, no existing studies have been conducted to model the complex behaviour and detect faults of ammonia synthesis fixed-bed reactor using dynamic partial least squares and the extensions.
- In the same study, several scaling techniques and time series structures were considered along with PLS to investigate the most appropriate model for the ammonia synthesis fixed-bed reactor. The developed models and monitoring schemes were evaluated using the statistical indices of root mean squared error, average run length and false alarm and fault detection rates.
- The algorithm, APLS, proposed by Wang et al.(2003) was incorporated with a Finite impulse response model to account for process dynamics. It was extended to a robust variant to be enabled to distinguish between normal operating condition samples, outliers and abnormal samples. It was also extended using multiblock PLS to monitor the whole process and individual unit operations and was applied to the Tennessee Eastman Process (TEP).
- In most applications of recursive PLS, the aim is to account for process changes. In this thesis, the recursive PLS along with its variants to account for process

non-linearity in the two case studies, ammonia synthesis fixed-bed reactor and the TEP.

1.5 Thesis Layout

Chapter 1 provided a brief introduction to the research problem and introduces the aims, objectives, challenges and contributions.

A general procedure for process performance monitoring and a brief introduction to multivariate statistical projection based technique, Principal Component Analysis (PCA) with associated limitations are discussed in Chapter 2. In addition, the complex characteristics of industrial processes are described as these provided the need for the extensions to steady state multivariate projection based approaches.

Chapter 3 is a review of partial least squares (PLS) with the historical background and theoretical aspect of PLS being presented as well as the limitations of conventional PLS. Conventional PLS is then used to model data from both a mathematical simulation of a time varying process and a non-stationary process. This chapter also presents a number of extensions to PLS including dynamic PLS and multiblock PLS

In Chapter 4, the recursive partial least squares (RPLS) algorithm is reviewed along with its variants and the limitations of RPLS when applied to real time monitoring. The main theoretical contributions of the thesis are also presented in this chapter with the conjunction of recursive PLS and adaptive confidence limits resulting in robust adaptive PLS (RAPLS). The developed approach is applied to distinguish between normal and non-conforming operational behaviour and outliers when monitoring the complex dynamics of a continuous chemical processes. This is a novel approach which has not previously been reported in the published literature.

The modelling and monitoring of the complex dynamic behaviour of an Ammonia Synthesis fixed-bed Reactor using partial least squares and its extensions is investigated in Chapter 5. In this chapter, the proposed approach, RAPLS, is extended through the incorporation of AutoRegressive with eXogenous (ARX) time series to account for the process dynamics and hence, RAPLS is extended to robust adaptive dynamic PLS (RADPLS).

In Chapter 6, the proposed approach (RAPLS) is incorporated with a Finite Impulse Response (FIR) time series representation to model the dynamic behaviour of the

Tennessee Eastman Process (TEP). In addition, the approach is extended to handle multiple unit operations as well as the whole process. The concept is applied to the Tennessee Eastman Process (TEP).

The Fault detection capability of the approaches described in Chapter 6 is investigated through considering a series of fault types introduced to the Tennessee Eastman Process is presented in Chapter 7. The fault detection ability is evaluated by using statistical metrics of fault detection and false alarm rate. Additionally, the fault detection delay within the whole process and individual unit operations is investigated.

Chapter 8 is reports on the conclusions, recommendations and future research.

The overall thesis layout is presented in Figure1.3.

1.6 Chapter Summary and Conclusions

In this chapter, the research problem and the challenges to be addressed in the subsequent chapters of the thesis are briefly presented. More specifically, the chapter has presented the main limitations of univariate statistical process control and how it has been extended resulting in multivariate statistical process control. In addition, an overview of statistical projection based techniques to monitor individual industrial unit operations as well as whole process is discussed. Furthermore, a brief outline of each chapter and the contributions were summarised. Chapter 2 describes the general monitoring procedure and a briefly introduces principal component analysis. In addition, it also describes the main industrial characteristics a process and more recent multivariate monitoring methods.

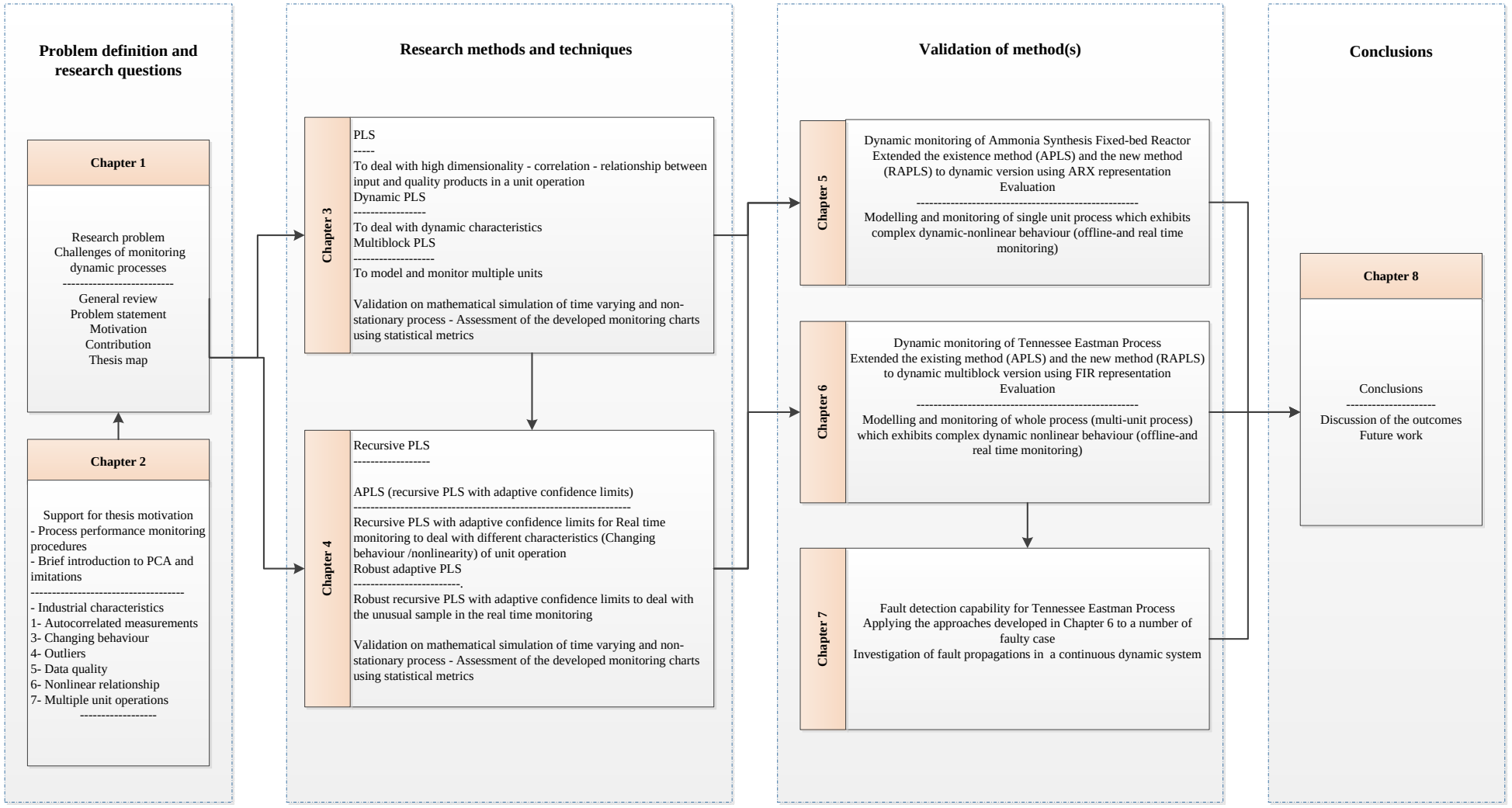

Figure 1.3 – Thesis layout and linkage

Chapter 2

Review of Data-Based Process Performance Monitoring

2.1 Introduction

Statistical process performance monitoring has become an important element in terms of attaining an enhanced understanding of the process and hence for its monitoring. These two elements ensure that the process and production are satisfactory in terms of safety, quality, environmental and economic requirements. In this chapter a general procedure for process performance monitoring is described. In addition, a brief introduction to the multivariate statistical projection based technique, Principal Component Analysis (PCA) is described and its associated limitations. The challenges resulting from the complex characteristics of industrial processes are used as a basis to introduce more recent research in the field of performance monitoring.

2.2 Process Monitoring Procedure

The general framework for the development of a monitoring procedure is summarised in Figure 2.1. Attaining data is the initial and crucial step in the development of any data based monitoring representation. In the data generation step, three aspects should be considered: analysis and understanding of the process characteristics, generation or collection of training and validation data sets and ensuring that the data quality is satisfactory and the data is representative of the process. Data quality in terms of addressing issues including missing data, measurement magnitudes and sampling interval is fundamental and hence, it is crucial to have an understanding of the nature of process thereby ensuring the data is informative and interpretable. In addition, data should be collected at an appropriate sampling interval thereby ensuring it captures information that is representative and relevant to the process (Martens et al., 1989; Miletic et al., 2004). This issue is investigated in Chapters 5 and 6 where the data is collected from two simulations, an Ammonia Synthesis Fixed-bed Reactor and the Tennessee Eastman Process. The use of data set that are not representative results in a monitoring model that does not represent the industrial process and can materialise in unacceptable false alarms or the missed detection of abnormal events (Martens et al., 1989; Ge et al., 2013).

The literature indicates that there is no established criterion for selecting an appropriate monitoring technique (Chen, 2010; Ge et al., 2013). It is therefore important to consider the characteristics of the process to provide an insight into the level of complexity of the required process monitoring model. The next step is to determine among available techniques which one is more appropriate. At this stage the monitoring method is applied to a training data set which is generated or collected based on normal process operating conditions (Martens et al., 1989; Qin, 2012; Ge et al., 2013).

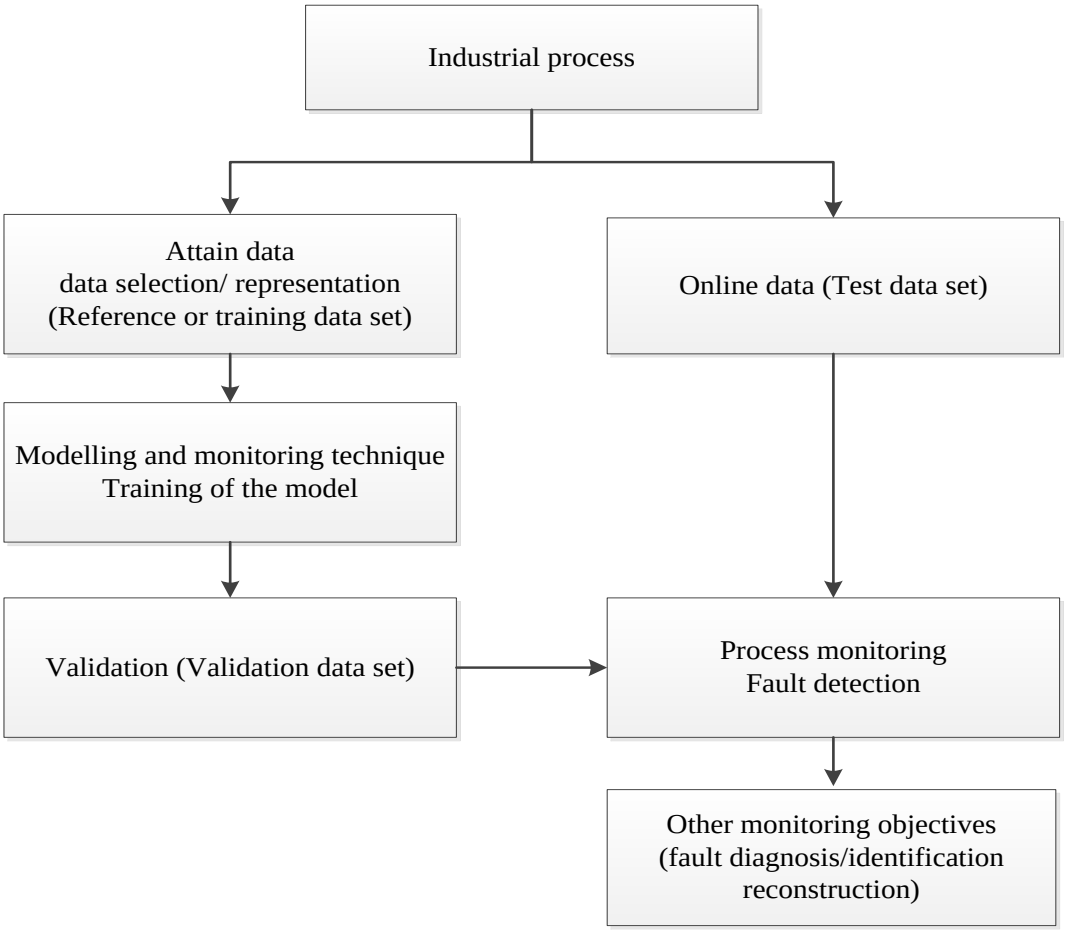

Figure 2.1 – Process monitoring procedure

Validation of the model is an important step prior to its use for online monitoring to ensure the model developed based on the training data performs in a similar manner to new unseen data (Martens et al., 1989; Qin, 2012; Ge and Song, 2013; Ge et al., 2013). Two procedures can be implemented for the validation step. First the model can be applied to a new data set, the validation data set, generated under the same operating conditions. Alternatively, cross validation can be used where the training data set is divided into a number of subsets, all subsets are used for the model development with an excluded subset being used for validation. This is repeated for all subset

combinations (Diana and Tommasi, 2002; Li et al., 2002). A description of cross-validation technique is given in Chapter 3 (§3.3.4).

After constructing a process monitoring model, monitoring indices are developed based on the model and are used for monitoring the process. The monitoring of any process consists of four tasks: fault detection, fault diagnosis, fault reconstruction and fault identification (Chiang et al., 2001; Qin, 2003; Kruger and Xie, 2012; Ge et al., 2013). Fault detection is the initial and essential step of process monitoring and is where a decision is taken with regards to the state of the process as to whether an abnormal event has occurred (Himmelblau, 1978; Qin, 2003). Monitoring indices and their confidence limits play an important role in fault detection as violating the limits indicates the potential presence of an abnormal event. Fault diagnosis is the next step where the aim is to identify the relevant component or the root cause of the abnormal event (Weighell et al., 1997; Chiang et al., 2001). This task is challenging as the variables are correlated and hence the fault may impact on more than one variable. Qin (2003) and Ge et al. (2013) defined fault reconstruction as the step where the direction and the magnitude of the fault can be explored to examine detailed information pertaining to the fault which will help isolate the fault and recover the process. In addition, it might prevent the occurrence of further related faults. Finally, fault identification involves the assigning of the fault to its corresponding class. This step is of greatest importance as it helps the process operator to implement appropriate corrective action. In this work the focus is on the initial step of process monitoring (i.e. fault detection) in complex industrial processes.

2.3 Multivariate Statistical Projection Techniques

Central to the development of multivariate statistical process control (MSPC) were the statistical projection techniques of Principal Component Analysis (PCA) and Partial Least Squares (PLS). These approaches have been successfully applied for the monitoring of industrial processes. The underlying philosophy is to transform high dimensional data into a limited number of latent variables, which can be used as the basis for the development of the monitoring statistics of Hotelling's T^2 and the Squared Prediction Error (SPE). The following section introduces the principal component analysis (PCA) whilst a detailed description of partial least squares is presented in Chapter 3.

2.3.1 Principal Component Analysis

Industrial processes are typically well instrumented and hence the resulting data will be of high dimension and correlated variables. The multivariate statistical technique of Principal Component Analysis (PCA) has been shown to be an efficient method for monitoring the behaviour of industrial processes (Martin et al., 1996; Wold and Sjöström, 1998; Brauner and Shacham, 2000; Kano et al., 2001; Kruger and Xie, 2012). It was originally introduced by Pearson in 1901, and further developed by Harold Hotelling in 1933. It is also termed Singular Value Decomposition (SVD) in numerical analysis, characteristic vector analysis in physical science and Hotelling transformation in image analysis (Wold et al., 1987). A number of books and papers provide a detailed description of the methodology including Wold et al. (1987), Jackson (1991), Jolliffe (2002), and Kruger and Xie (2012).

The basic concept underpinning principal component analysis is the application of a linear transformation of the original variables resulting in a new set of factors called principal components (Jackson, 1991; Jolliffe, 2002). These principal components capture the main source of variability in the data and are used for calculating the monitoring statistics of Hotelling's $T^2$and square prediction error.

The original data matrix $\mathbf{X}$ comprises n rows and m columns, where each variable is represented by a column and each sample is represented by a row. Mathematically, PCA can be calculated by number of algorithms including Singular Value Decomposition (SVD), §2.3.1.1, and the Non-Linear Iterative Partial Least Squares (NIPLAS) algorithm (§2.3.1.2) (Wold et al., 1987). In both cases, the data matrix $\mathbf{X}$ is decomposed into the sum of a product of a pairs of scores and loadings vectors ($\mathbf{t}_i$ and $\mathbf{p}_i$) plus a residual matrix $\mathbf{E}$:

$$\mathbf{X} = \sum_{i=1}^{a} \mathbf{t}_i * \mathbf{p}_i' + \mathbf{E} = \mathbf{T}\mathbf{P}' + \mathbf{E} \qquad (2.1)$$

where the columns of the matrix $\mathbf{T}$ are the scores vectors, which are the coordinates of the original samples in principal component (PCs) space. The columns of the matrix $\mathbf{P}$ are the loadings vectors, which are the weights of the original variables in the PCs and can be used to identify both the relationships between variables and the importance of each variable in individual PCs (Wold et al., 1987). a is the number of retained PCs and $a \leq \min(n, m)$ and $\mathbf{E}$ is the residual matrix which contains the noise (Jackson, 1991;

Jolliffe, 2002). One of the major benefits of modelling a multivariate process using PCA is the ease of visualization of multivariate data though the interpretation of the loading and scores plots.

2.3.1.1 Singular Value Decomposition

Singular value decomposition is one method for the calculation of the scores and loadings of the data matrix **X**:

$$\text{SVD}(\mathbf{X})=\mathbf{USV}' \qquad (2.1)$$

where **V** is a matrix containing the eigenvectors (i.e. loadings) and **S** is a diagonal matrix which contains the square root of the ordered eigenvalues (i.e. singular values) of the covariance matrix of **X**. The scores are the column of the matrix **US** (Wold et al., 1987)

2.3.1.2 Non-Linear Iterative Partial Least Squares (NIPALS) for PCA

The NIPALS algorithm is an alternative method for calculating the scores and loadings of the data matrix **X**. The NIPALS algorithm for PCA (Wold et al., 1987), is as follows:

Step 1. Set i $= 1$, (i=1,2,..*a*) and $\mathbf{E}_0 = \mathbf{X}$, "Tol" is the convergence threshold

Step 2. Select $\mathbf{t}_\text{i}$ to be a column of $\mathbf{E}_{\text{i}-1}$

Step 3. Calculate the loading vector $\mathbf{p}_\text{i}$ by projecting $\mathbf{E}_{\text{i}-1}$ onto $\mathbf{t}_\text{i}$:

$$\mathbf{p}_\text{i}' = \mathbf{t}_\text{i}'\mathbf{E}_{\text{i}-1}/\mathbf{t}_\text{i}'\,\mathbf{t}_\text{i}$$

Step 4. Normalize $\mathbf{p}_\text{i}$ to unity:

$$\mathbf{p}_\text{i} = \mathbf{p}_\text{i}/\|\mathbf{p}_\text{i}\|$$

Step 5. Calculate the new scores vector $\mathbf{t}_\text{i}$ by projecting $\mathbf{E}_{\text{i}-1}$ onto $\mathbf{p}_\text{i}$:

$$\mathbf{t}_\text{i} = \mathbf{E}_{\text{i}-1}\mathbf{p}_\text{i}/\mathbf{p}_\text{i}'\mathbf{p}_\text{i}$$

Step 6. Check for convergence, if the difference between the eigenvalue $\tau_{new} = (\mathbf{t}'_\text{i}\mathbf{t}_\text{i})$ and τ_{old}(from last iteration) is larger than "Tol", return to step 3, otherwise proceed to step 7

Step 7. Calculate the residual:

$$\mathbf{E}_\text{i} = \mathbf{E}_{\text{i}-1} - \mathbf{t}_\text{i}\mathbf{p}_\text{i}'$$

Step 8. If additional principal component are required to be calculated set $i = i + 1$ and return to step 2.

Dimensionality reduction is achieved by retaining these principal components that explain main source of process variability. A number of approaches have been proposed including the SCREE plot, parallel analysis, broken stick rule, cross validation as well as an empirical rule for selecting the number of PCs (Jackson, 1991; Kaskavelis, 2000; Diana and Tommasi, 2002; Kruger and Xie, 2012). The cross validation approach is described in Chapter 3 as it is used to determine the number of latent variables to be retained in Partial Least Squares (PLS).

2.3.1.3 Limitations of Principal Component Analysis

PCA has been successfully applied to many processes for monitoring purposes. For example, Kruger and Xie (2012) applied PCA to data generated from a process that produced solvent chemicals, and showed that PCA efficiently detects and diagnoses process faults. Chiang et al. (2001) used PCA for the detection and diagnoses of faults using the Tennessee Eastman Process. However, PCA is not directly applicable to these processes as the underlying processes exhibiting complex behaviour (§2.4) since the underlying assumption of PCA is steady state behaviour. If applied to processes that do not satisfy this assumption, it may result in missed detection of process operational changes or an increase in the number of false alarms.

Secondly PCA only considers the **X** data matrix and thus where interest is in monitoring the output, partial least squares (PLS) should be considered as it considers both the data matrix **X** and the output matrix **Y**. Therefore, for the monitoring of the whole process, PLS is appropriate and form the basis of the work in this thesis and a detailed description is given in Chapter 3.

2.4 Industrial Process Characteristics

The monitoring of industrial processes is challenging due to the complex nature of the data (Kourti and MacGregor, 1995; MacGregor and Kourti, 1995; Kaskavelis, 2000; Alghazzawi and Lennox, 2008). A brief analysis of some of the characteristics of the measurements from industrial processes is presented in the following subsections and these are used as a basis to introduce more advanced monitoring methods in the subsequent chapters. A more detailed description of the characteristics of industrial data

and more recently proposed methods for process monitoring is given in Kruger and Xie (2012), Qin (2012), Ge and Song (2013) and Ge et al. (2013).

The MSPC techniques based on PCA and PLS have limitations in terms of their basic configurations as they are designed to model steady state processes. For example, for the monitoring of industrial processes that has dynamic relationships between the measurements, a dynamic model is required (Ku et al., 1995; Lakshminarayanan et al., 1997a). Therefore, the characteristics of the data collected from an industrial process is an important factor in terms of determining the basis of the monitoring system and hence extensions to PCA and PLS have been proposed including non-linear algorithms, recursive algorithm, multi-block approaches and dynamic variants. Other data-based methods that have been combined with MSPC techniques are proposed in the literature for the monitoring processes that exhibit complex characteristics. For example, Support Vector Data Description (SVDD) is a classification based method which is used to construct a monitoring scheme for non-Gaussian processes. However, the main focus of this thesis is the direct extensions of the traditional MSPC techniques.

2.4.1 Data Autocorrelation

Autocorrelation between samples is a typical feature of data from most industrial chemical processes, i.e. samples are related to previous samples due to the use of feedback control systems and disturbances (Ku et al., 1995; Kourti et al., 1996; Runger, 1996; Qin, 2012; Ge et al., 2013). The level of the time dependency is dependent on the nature of the process.

Applying statistical methods, which assume that the samples are independent in time, is inappropriate and can materialise in an increase in the number of false alarms and incorrect information on the status of the process (Montgomery and Mastrangelo, 1991; Christina and Douglas, 1995; Negiz and Çlinar, 1997a; Qin, 2012). For example, Ku et al. (1995) applied steady state PCA to data from two case studies; a mathematical simulation and the Tennessee Eastman process. They showed that by applying conventional PCA to data from a process containing dynamic information, the underlying relationships between the process variables will not be revealed and hence an excessive number of false alarms were generated.

Process dynamics can be addressed by collecting the data at a higher sampling interval. However, this can result in the loss of significant information relating to the process and

unreliable monitoring performance (Seborg et al., 1989). Therefore, the monitoring of dynamic processes requires process monitoring methods that consider the time dependency. Several approaches have been proposed including dynamic PCA and dynamic PLS, time series analysis and state-space modelling methods. One dynamic MSPC approach is to incorporate into the data matrix historical lags of the original variables and apply the original algorithm to the modified matrices (Kaspar and Ray, 1993; Ku et al., 1995) However, determining the appropriate time history is challenging and is discussed in Chapters 5 and 6 where level of time dependency is determined for two dynamic processes; an ammonia synthesis fixed-bed reactor and the Tennessee Eastman Process. On the other hand, other methods such as state-space models and time series analyses have been proven to be effective for the monitoring of dynamic processes (Alwan and Roberts, 1988; Negiz and Çlinar, 1997b; Negiz and Çlinar, 1997a). These methods are not considered in this thesis.

2.4.2 Changing Behaviour

Gallagher et al. (1997) stated that the behaviour of most industrial processes changes over time. The rationale for this can be the switching from one operating condition to another due to seasonal effects, changes in operating conditions or raw materials for example. Switching from one operating condition to another has been termed multimode operation whilst changes in process behaviour over time is referred to as time varying behaviour (Ge and Song, 2013; Ge et al., 2013). Both scenarios require advanced methods to construct reliable monitoring representations.

Several methods have been proposed to account for the time varying behaviour of a process. For example, several forms of recursive and adaptive PCA and PLS have been proposed (Helland et al., 1992; Qin, 1993; Dayal and MacGregor, 1997b; Qin, 1998b; Wang et al., 2003). The recursive methods can be seen as a linearization method as they aim to update the model and hence reflect current operating conditions. Although these methods are cost effective in terms of updating the model instead of identifying new models whenever new data becomes available, these methods are implemented without consideration of sample type and hence outliers or process faults may be included in the model updating process. Therefore, it is important to develop criterion to ensure that only representative data are used for model updating.

Multi-mode techniques have also been proposed to model processes exhibiting changes in the operation mode. The aim is to develop a different model for each operational

mode, store them in a library and switch between these models based on the current operational mode. A description of data based monitoring methods for multimode processes is given by Qin (2012), Ge and Song (2013) and Ge et al. (2013)

2.4.3 Outliers

A further feature of industrial processes is the existence of outliers. Outliers are samples that exhibit behaviour that is different compared to that of other samples. Many definitions have been proposed in the literature. For example, Barnett and Lewis (1994) defined outliers as "an observation which appears to be inconsistent with the remainder of the dataset". Another definition of an outlier is "An observation that deviates so much from other observations as arouse suspicions that is was generated by a different mechanism" (Cateni et al., 2008). The existence of such samples could significantly change the results of the statistical monitoring approach. A considerable amount of literature has been published on the impact of data type when developing monitoring schemes (Geladi and Kowalski, 1986; Wold et al., 2001; Haenlein and Kaplan, 2004; Hodge and Austin, 2004; Kruger and Xie, 2012; Vinzi and Russolillo, 2012).

Therefore, most statistical techniques required a pre-processing step to initially identify and treat outliers. Several methods have been proposed to detect and treat outliers offline including filtering, detection based on monitoring statistics, application of the Mahalanobis distance and the use of robust estimators (Cummins and Andrew, 1995; Kaskavelis, 2000; Pell, 2000; Hubert and Branden, 2003; Kruger et al., 2008a).

In the case where a model is continuously updated whenever new data becomes available such as recursive modelling, real time outliers may occur and hence, they will contribute to the model updating process. Therefore, it is important to distinguish between different types of samples and hence, only representative data is used for updating the process monitoring model. Therefore, there is a need for an online methodology that helps to detect outliers in real time to ensure reliable monitoring results. This feature is investigated in detail in Chapter 4.

2.4.4 Data Quality

Another common characteristic is the quality of the data in terms of missing data and variables of different magnitude. Missing data is a characteristic in industrial data and can occur periodically due to device failure or maintenance for example. Two types of missing values can be found in industrial data, missing at random and not missing at

random. In the first case no further analysis is required in terms of identifying the cause. For the non-random missing values, an enhanced analysis to determine the reason why they are missing requires to be undertaken (Kaskavelis, 2000). Several methods have been proposed to account for missing data and their treatment prior to developing a monitoring system (Nelson et al., 1996; Lakshminarayan et al., 1999; Schafer and Graham, 2002; Scheffer, 2002). This is discussed in §3.3.6.

Other important characteristics when building the monitoring model is whether the variables are comparable. Many measurements can be collected including temperature, pressure, compositions, flow rates and level indicators, which have different magnitudes and units. The impact of this can be that measurements with the greatest ranges dominate the process model and potentially dilute the importance of those variables with a smaller range. Therefore, scaling of the data is important and is application dependent (Wold et al., 1987). For example, when process variables have the same magnitude, the scaling of variables is not required, however this is not the norm and hence different scaling methods have been proposed including mean centring and normalization. The effect of scaling on process modelling is investigated further in Chapter 5. Figure 2.2 shows the impact of normalization on the process variables that have different magnitudes. Figure 2.2 (a) shows variables from different ranges whilst Figure 2.2 (b) shows the scaled variables and that these variables (Figure 2.2 (a)) cannot be compared in terms of process behaviour.

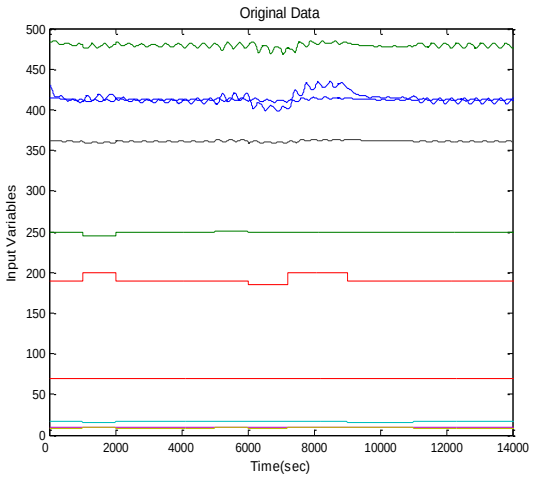

Figure 2.2 (a) -Time series of non scaled data

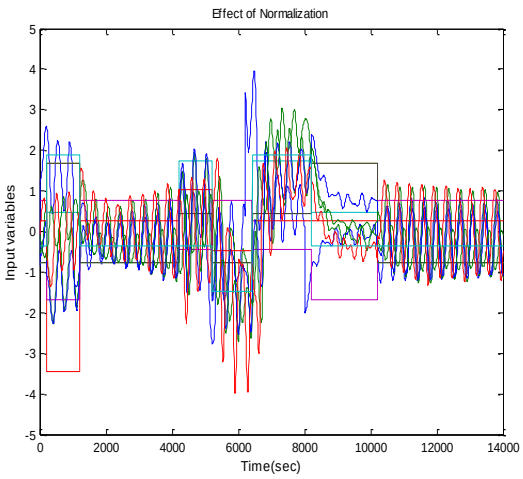

Figure 2.2 (b) -Time series of scaled data

2.4.5 Nonlinear Relationships

Nonlinear relationships between process's measurements (process variable and quality product) are common in industrial processes. Such relationships are difficult to model and monitor compared to linear relationships. The change in the operating conditions of a process exhibiting non-linear behaviour increases the complexity of the monitoring task. Several methods have been proposed to model and monitor nonlinear processes including neural networks, kernel based approaches and linear approximation methods (Ricker, 1995; Baffi et al., 2000; Cho et al., 2005; Geng and Zhu, 2005; Iketubosin, 2011; Qin, 2012).

While all these methods are applied to construct monitoring systems for nonlinear process, the linear MSPC methods of PCA and PLS, which are the central focus of this work, may be applicable. The rationale for this is that stable production is key to the manufacture of consistent high quality product and typically it is produced under steady state operating conditions. It is argued that a process can be linearized even if the relationship between the process measurements are nonlinear (Qin, 2012; Ge and Song, 2013; Ge et al., 2013). Therefore, although fundamentally most industrial processes are nonlinear, linear MSPC has been extensively applied to monitor those processes. For example, Yin et al. (2012) and Chiang et al. (2001) applied a number of linear monitoring approaches to monitor the Tennessee Eastman process which exhibits non-linear behaviour. In this work RPLS approaches are used to account for process nonlinearity by breaking down the modelling period to small enough intervals thereby ensuring process operated under steady state hence accounting for process nonlinearity.

2.4.6 Multiple Unit Operations

Most industrial processes comprise multiple operational units. These operational units typically interact and hence, these interactions increase the complexity of the monitoring task. By developing a monitoring system for the whole process, it can be determine as to how a fault affects the overall performance. Process faults typically occur in a specific part of the process, but fault propagation will materialise due to the inter-relationship between the unit operations. As a result, the detection of the source of the fault is a challenging task. Therefore, understanding the whole process requires the understanding of the individual unit operations and this will help detect failures more rapidly and identify the primary source of the operational issue thereby improving the overall performance of the process. Several approaches have been proposed to construct

monitoring systems for the whole process utilising the individual process units based on MSPC including hierarchal and multiblock monitoring methods (Wangen and Kowalski, 1989; MacGregor et al., 1994; Wold et al., 1996; Westerhuis et al., 1998; Qin et al., 2001; Wang et al., 2001; Westerhuis and Smilde, 2001; Lee and Vanrolleghem, 2002; Ge and Song, 2013). One of the unexplored areas is the analysis of fault propagation in industrial processes with multiple unit operation that exhibit dynamic behaviour. Chapter 6 discusses an example of fault propagation through the application of dynamic and recursive variants of PLS on a process that comprises multiple operational units.

2.5 Recent Data Based Monitoring Methods

As mentioned in the previous subsections, the main issue with the traditional approach to MSPC is that it does not consider the complex characteristics of modern industrial processes. Ge et al. (2013) presented a review of different data based monitoring methods for batch and continuous processes which is summarised in Figure 2.3. It shows some of the most common characteristics of industrial processes including dynamic, time varying and multimodal, nonlinear and non-Gaussian processes. The review comprises a discussion of different data based methods including direct extensions of the traditional MSPC techniques and other methods that unrelated to projection based approaches. Examples of direct extension of MSPC include dynamic PCA and PLS and recursive PCA and PLS with support vector data description being an example of a non multivariate approach to monitor non- Gaussian processes.

Kruger and Xie (2012) also reviewed the basic monitoring methods of PCA and PLS and its variants for the monitoring of time varying process. Yin et al. (2012) reviewed the basic MSPC methods and their variants including dynamic PCA and PLS and other data based techniques including Fisher Discriminant analysis, which is dimensionality reduction technique that has been well studied in the field of pattern classification. The aim was to evaluate the performance of the reviewed techniques based on their application to the Tennessee Eastman Process. Qin (2012) also reviewed recent advances in MSPC techniques that are used to address more complex process characteristics including nonlinearity, changing operational behaviour and data autocorrelation.

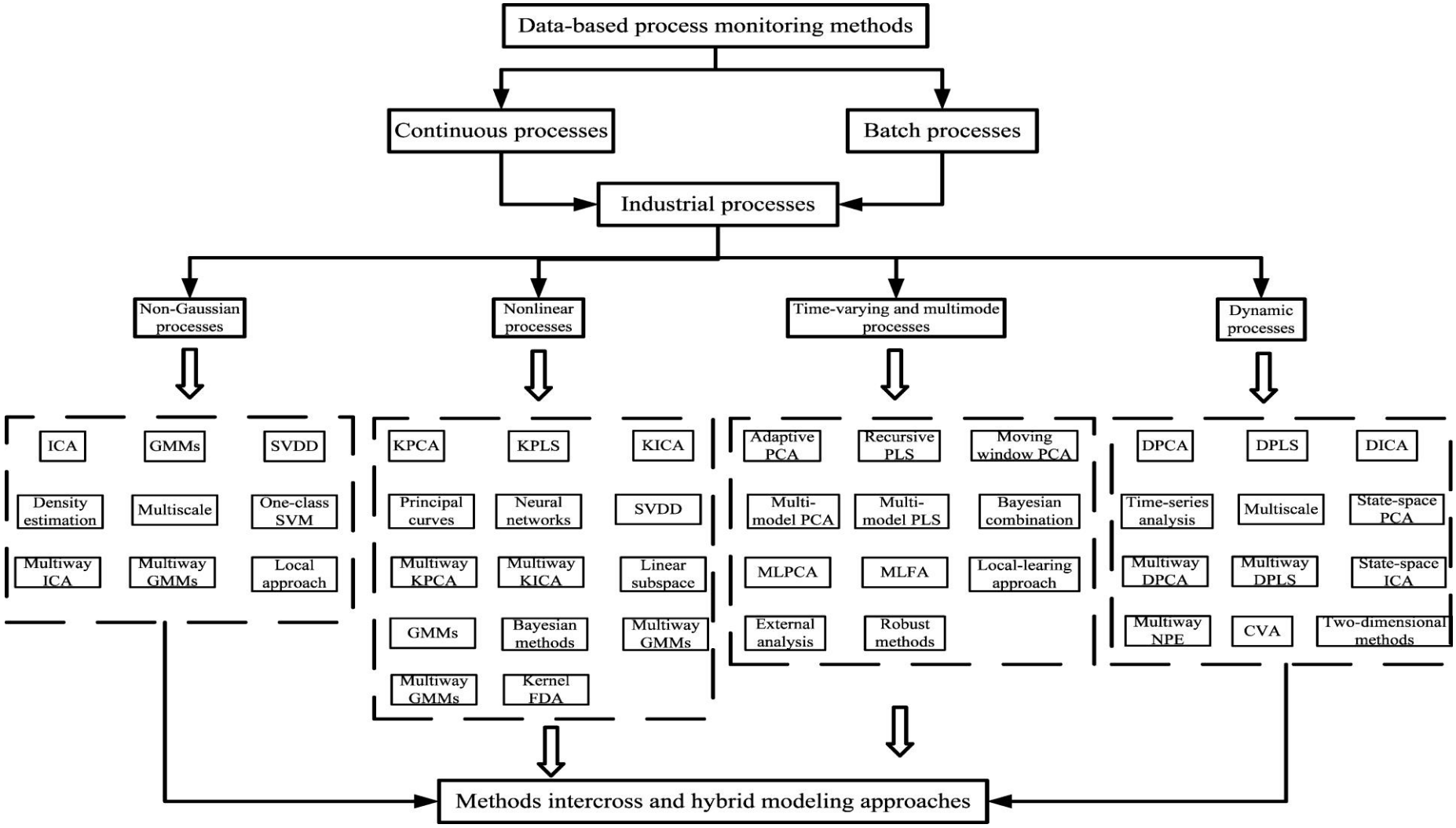

Figure 2.3 - Systematic view of different data-based process monitoring methods (Ge et al., 2013)

2.6 Chapter Summary and Conclusions

This chapter has described a general procedure for the implementation of statistical monitoring. It also has provided an overview of Principal Component Analysis (PCA) and highlighted that PCA only considers the variations related to input data matrix and for process monitoring the output variables should be taken into account as they contain information on the process. Therefore, PCA is inappropriate in this case and Partial Least Squares (PLS) is more applicable. This chapter also presented an evaluation of various data characteristics including data autocorrelation, changing operational behaviour, the presence of outliers, data quality and process nonlinearity. The multivariate statistical techniques with appropriate extensions can be considered as a practical method for monitoring complex modern industrial process. One of the key areas to be investigated in this thesis is the monitoring of the dynamic behaviour, caused by measurements autocorrelation, industrial processes which increases the complexity of the monitoring task.

Chapter 3 presents a detailed description of Partial Least Squares and two of its variants dynamic PLS and multiblock PLS. These approaches can be employed for both the monitoring of the whole process as well individual unit operations. These approaches can be combined to offer enhanced monitoring of complex industrial applications. Chapter 3 also presents the application of conventional PLS to a time varying and non-stationary processes and evaluates the monitoring charts using the statistical metrics of false alarm and fault detection rates.

Chapter 3

Review of Partial Least Squares and Extensions with Application for Process Complex Behaviour

3.1 Introduction

In this chapter, partial least squares (PLS) and two extensions, dynamic PLS (DPLS) and multiblock PLS (MBPLS) are reviewed. Partial least squares is one of the most widely applied statistical projection technique for the modelling and monitoring of multivariate data (Kaskavelis, 2000; Wold et al., 2001). Once the data has been collected, a model is developed based on latent variables (a linear combination of the original variables). These latent variables are extracted to capture most of the information contained in the process variables that is useful for the prediction of the response variables. A number of approaches have been proposed to calculate the PLS latent variables. The most popular being Non-linear Iterative Partial Least Squares (NIPLAS).

Reviews of the application of PLS for industrial process analysis, process control and fault detection have been given in Abdi (2010), Helland (2001), Wold et al. (2001), Höskuldsson (1988) and Geladi and Kowalski (1986). The fundamental PLS algorithm is designed to model a process that is operating at steady-state which is not the case for most process applications and hence a number of variants have been proposed for the modelling of time varying, non-stationary, non-linear and dynamic processes including dynamic PLS and recursive PLS. In addition, when the process comprises multiple unit operations multiblock PLS is applicable.

3.2 Objectives

The goal of this chapter is to review conventional PLS as it forms the basis for the subsequent chapters. The first stage is to introduce the PLS algorithm prior to describing the application of Partial Least Squares (PLS) for the monitoring of processes that exhibit complex behaviour including dynamic, time varying and non-stationary behaviour. The next step is to introduce monitoring schemes that monitor both the whole process and individual unit operation. Finally, the monitoring charts introduced are evaluated in terms of their performance. The key areas addressed include:

- Is the multivariate statistical technique of PLS an effective process monitoring tool for the modelling and monitoring of complex process behaviour, i.e. time varying and non-stationary?
- How do the PLS approaches perform in terms of prediction and monitoring for time varying and non-stationary processes? The results are assessed using the statistical metrics of root mean squared error (RMSE), the average run length (ARL), fault detection rate (FDR) and false alarm rate (FAR).

3.3 Partial Least Squares

3.3.1 Historical Background to Partial Least Squares

Figure 3.1 summarises the historical development of Partial Least Squares (PLS). PLS was originally proposed by Herman Wold in the 1960's. The original algorithm Non-linear Estimation by Iterative Least Squares (NILES) was an iterative algorithm that extracted latent variables for two situations: principal component analysis and two blocks (quality and process data for example). In 1973, the algorithm was renamed NIPALS (Non-linear Iterative Partial Least Squares) and was modified by Wold and Martens in the early 1980s (Wold et al., 2001). PLS was originally applied in the social and economical sciences but application extended to the field of chemistry and chemometrics (Höskuldsson, 1988). PLS is applicable for chemical studies due to its ability to extract information from ill-conditioned data unlike ordinal least squares. This was demonstrated in the application of PLS to multi-collinear data by Svante Wold and Harald Marten (Wold et al., 2001). In the late 1980's and 1990's, some of the challenges associated with PLS including the interpretation of the PLS model and the use of a PLS model for control system design were addressed (Höskuldsson, 1988; Kaspar and Ray, 1992).

PLS was initially designed to model steady state processes, but this is not the case for many industrial application. Therefore in the 1990's modifications and extensions to PLS were proposed including non-linear PLS, neural network PLS and dynamic PLS (Kresta, 1992; Wold, 1992; Kaspar and Ray, 1993; Lakshminarayanan et al., 1997b) and recursive PLS (Helland et al., 1992; Qin, 1993; Qin, 1998b). Applications of PLS to both industrial batch and continuous processes have been widely reported (Kaspar and Ray, 1992; Simoglou et al., 2000; Yacoub and MacGregor, 2003; Marjanovic et al., 2006; Mu et al., 2006; Tang et al., 2011) with a detailed description of PLS given in

Vinzi, E. V. and Russolillo, G. (2012), MacGregor et al.(2005), Garthwaite(1994), Höskuldsson (1988) and Geladi and Kowalski (1986).

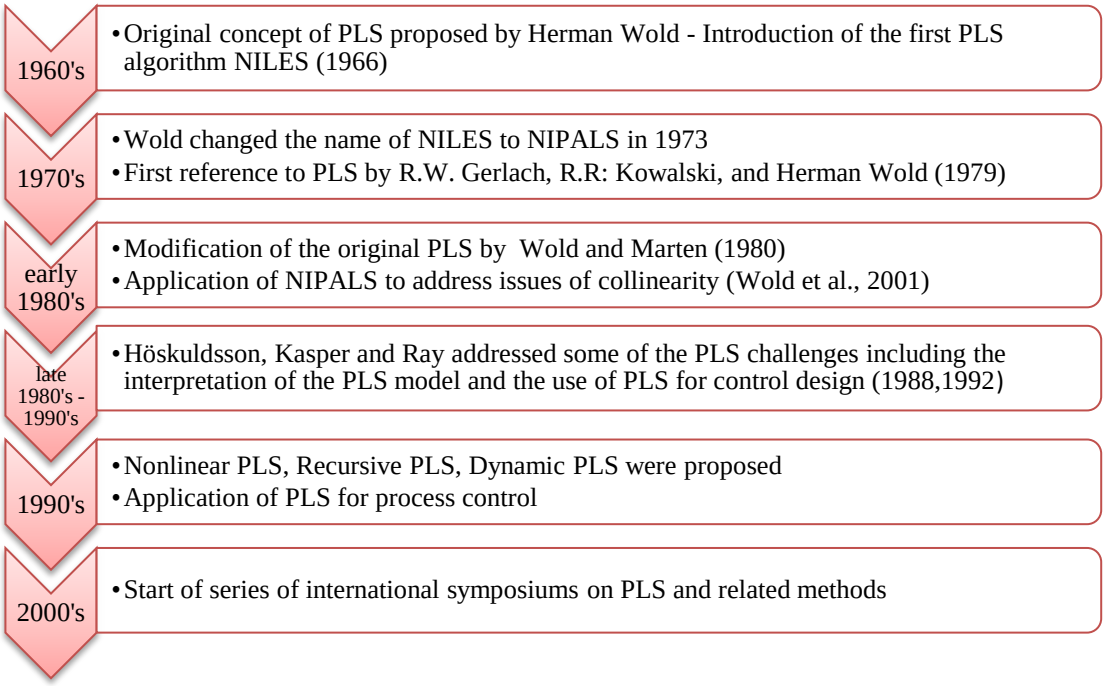

Figure 3.1- Historical development of PLS

3.3.2 PLS Methodology

The basic philosophy of PLS is to project high dimensional data down onto a low dimensional subspace defined in terms of latent variables. In contrast to principal components, the latent variables are constructed using the predictor variables **X** together with the response variables **Y**. The latent variables are calculated to maximize the covariance between the process variables and response variables with the goal of predicting the response by retaining a limited number of latent variables (a). For illustration, consider a process variable matrix **X**, with n rows and m columns and a product quality (output) matrix **Y**, with n rows and k columns. A PLS model consists of two types of relationships, an outer relationship, which deals with **X** and **Y** individually, and an inner relationship, which relates the **X** block and the **Y** block. PLS defines a set of latent variables $\mathbf{t}_i$ and $\mathbf{u}_i$ $(i = 1,2, \ldots . a)$ as follows:

$$\begin{aligned} \mathbf{t}_i &= \mathbf{X}_i \mathbf{w}_i \qquad (i = 1,2, \ldots . a) \\ \mathbf{u}_i &= \mathbf{Y}_i \mathbf{q}_i \end{aligned} \tag{3.1}$$

where $\mathbf{w}_i$ and $\mathbf{q}_i$ represent the weight and loading vectors of **X** and **Y** respectively. Both $\mathbf{w}_i$ and $\mathbf{q}_i$ have unit length and are determined by maximizing the covariance between $\mathbf{t}_i$ and $\mathbf{u}_i$, i.e. maximize $(\mathbf{u}_i'\mathbf{t}_i)$ for $\|\mathbf{w}_i\| = \|\mathbf{q}_i\| = 1\,, (i = 1,2, \ldots . a)$. Equation 3.1 is referred to as the outer relationship for the **X** and **Y** blocks respectively. An inner linear relationship is defined as:

$$\mathbf{u}_i = b_i\mathbf{t}_i \qquad (i = 1,2, \ldots . a) \tag{3.2}$$

where b_i is the coefficient of the ith inner regression estimated by $\hat{b}_i = (\mathbf{t}_i'\mathbf{t}_i)^{-1}\mathbf{t}_i'\mathbf{u}_i$. The next step is to deflate **X** and **Y** as follows:

$$\begin{aligned} \mathbf{X}_{i+1} &= \mathbf{X}_i - \mathbf{t}_i\mathbf{p}_i'\,, & \mathbf{X}_1 &= \mathbf{X} \\ \mathbf{Y}_{i+1} &= \mathbf{Y}_i - \hat{b}_i\mathbf{t}_i\mathbf{q}_i'\,, & \mathbf{Y}_1 &= \mathbf{Y} \end{aligned} \tag{3.3}$$

Letting $\hat{\mathbf{u}}_i = \hat{b}_i\mathbf{t}_i$ be the prediction of $\mathbf{u}_i$, the matrices **X** and **Y** can be decomposed as:

$$\begin{aligned} \mathbf{X} &= \mathbf{T}_a\mathbf{P}_a' + \mathbf{E} \\ \mathbf{Y} &= \hat{\mathbf{U}}_a\mathbf{Q}_a' + \mathbf{F} \end{aligned} \tag{3.4}$$

where $\mathbf{P}_{m\times a}$ and $\mathbf{Q}_{k\times a}$ are the loadings, $\mathbf{T}_{n\times a}$ and $\hat{\mathbf{U}}_{n\times a}$ are the scores and estimated scores for the input and output spaces respectively and $\mathbf{E}_{n\times m}$ and $\mathbf{F}_{n\times k}$ are the residuals matrices of **X** and **Y** respectively. A graphical representation of the PLS decomposition, Equation 3.4, is shown in Figure 3.2.

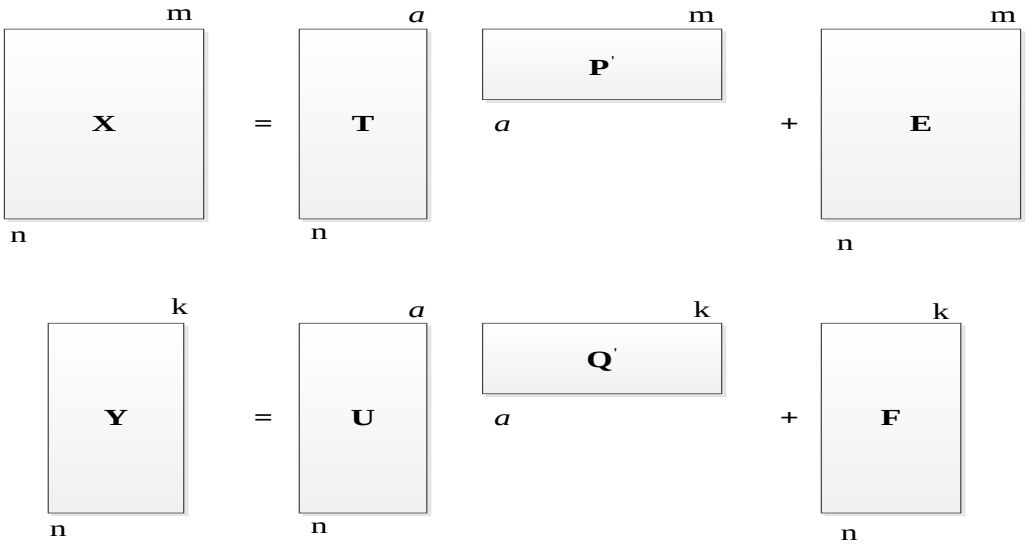

Figure 3.2 - Graphical representation of PLS decomposition (Geladi and Kowalski, 1986)

PLS is termed PLS1 where there is only one output, i.e. k = 1 and PLS2 when k > 1. When k > 1, a separate PLS1 model can be developed for each quality variables or alternatively all quality variables can be included, i.e. PLS2 develops a model incorporating all the outputs.

3.3.3 PLS Algorithms

A number of different algorithms have been proposed for the calculation of the PLS latent variables. The most popular is the NIPALS (Non-linear Iterative Partial Least Squares) algorithm, and it forms the basis of this work (Figure 3.3). It is also known as the standard partial least square algorithm and it is summarised as follows:

Step 1. Set $\mathbf{E}_{i+1} = \mathbf{E}_i$ and $\mathbf{F}_{i+1} = \mathbf{F}_i$ and i =1 (i=1,2,3,…,*a*) with $\mathbf{E}_1 = \mathbf{X}$

And $\mathbf{F}_1 = \mathbf{Y}$, Set $\mathbf{u}_i$ equal to any column of $\mathbf{F}_0$

Step 2. Regress the columns of $\mathbf{E}_i$ on $\mathbf{u}_i$ to calculate the weight coefficients $\mathbf{w}_i$:

$$\mathbf{w}_i' = \mathbf{u}_i'\mathbf{E}_i/\mathbf{u}_i'\mathbf{u}_i$$

Step 3. Normalise $\mathbf{w}_i$ to unit length:

$$\mathbf{w}_i = \mathbf{w}_i/\|\mathbf{w}_i\|$$

Step 4. Calculate the input scores, the latent variables of $\mathbf{E}_i$:

$$\mathbf{t}_i = \mathbf{E}_i\mathbf{w}_i/\mathbf{w}_i'\mathbf{w}_i$$

Step 5. Regress $\mathbf{F}_i$ on $\mathbf{t}_i$ to calculate the output loading coefficients:

$$\mathbf{q}_i' = \mathbf{t}_i'\mathbf{F}_i/\mathbf{t}_i'\mathbf{t}_i$$

Step 6. Normalise $\mathbf{q}_i$ to unit length:

$$\mathbf{q}_i = \mathbf{q}_i/\|\mathbf{q}_i\|$$

Step 7. Calculate the new output scores $\mathbf{u}_{new}$:

$$\mathbf{u}_{new} = \mathbf{F}_i\mathbf{q}_i/\mathbf{q}_i'\mathbf{q}_i$$

Step 8. Check convergence of $\mathbf{u}$, if yes continue to step 9, else go to step 2 and replace $\mathbf{u}_i$ by $\mathbf{u}_{new}$

Step 9. Regress the rows of $\mathbf{E}_{i-1}$ on $\mathbf{t}_i$ to calculate the input loadings $\mathbf{p}_i$:

$$\mathbf{p}_i' = \mathbf{t}_i'\mathbf{E}_{i-1}/\mathbf{t}_i'\mathbf{t}_i$$

Step 10. Regress the column of **U** on **T** to find the inner regression coefficients b_i for the latent variable:

$$b_i = \mathbf{t}_i'\mathbf{u}_i / \mathbf{t}_i'\mathbf{t}_i$$

Step 11. Deflate the matrices by calculating the input and output residuals:

$$\mathbf{E}_{i+1} = \mathbf{E}_i - \mathbf{t}_i\mathbf{p}_i' \ , \ \mathbf{F}_{i+1} = \mathbf{F}_i - \mathbf{t}_i b_i \mathbf{q}_i'$$

Step 12. To calculate additional latent variable by repeating steps 1 to 11. This step is important as in PLS, each latent variable contains independent information about the inputs and outputs of the process. Therefore, the contribution of the first latent variable must be subtracted from the matrices **X** and **Y** before proceeding to the calculation of the next latent variables.

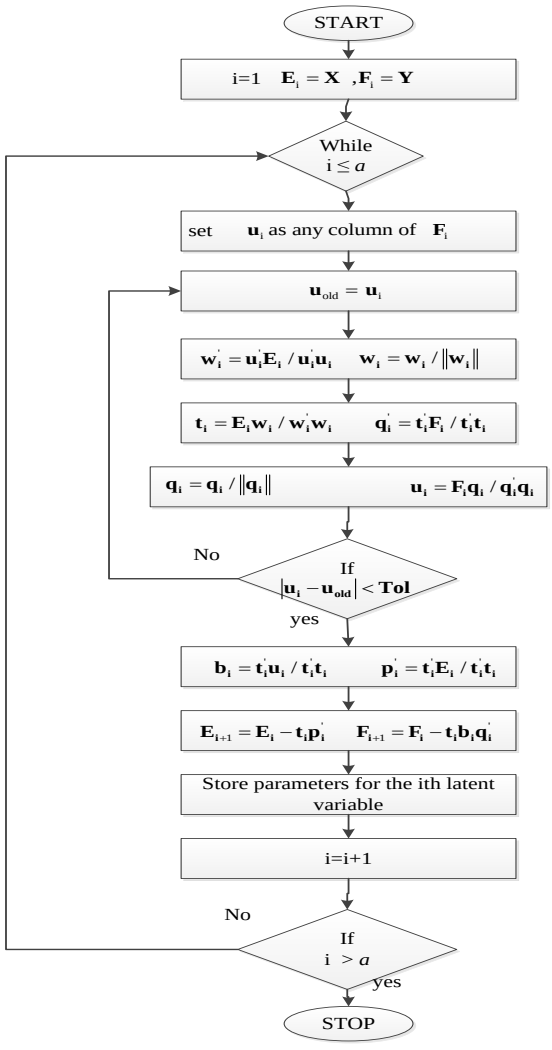

Figure 3.3 – NIPALS algorithm

For PLS1, the convergence in step 8 is no longer necessary as $\mathbf{u} = \mathbf{y}$. The predictors in the $\mathbf{X}$ block are related to the response variables in $\mathbf{Y}$ through the estimate of the PLS regression coefficients given by:

$$\widehat{\mathbf{B}}_{\mathrm{PLS}} = \mathbf{W}_a(\mathbf{P}_a'\mathbf{W}_a)^{-\mathbf{1}}\mathbf{Q}_a' \tag{3.5}$$

$$\widehat{\mathbf{Y}} = \mathbf{X}\widehat{\mathbf{B}}_{\mathrm{PLS}} \tag{3.6}$$

A number of publications have investigated the performance of PLS1 and PLS2. They concluded that PLS1 showed superior performance for the applications considered (Garthwaite, 1994; Breiman and Friedman, 1997). Therefore, building an individual model in the case of two or more quality variables may result in a better process model in term of prediction accuracy. In this thesis PLS1 forms the basis for all the algorithmic extensions and application studies whilst PLS2 is used in the mathematical simulations. For convenience the following notation is used to represent the application of PLS:

$$\{\mathbf{X}, \mathbf{Y}\} \overset{\mathrm{PLS}}{\longrightarrow} \{\mathbf{T}, \mathbf{P}, \mathbf{Q}, \mathbf{U}, \mathbf{W}, \mathbf{B}\} \tag{3.7}$$

There are a number of alternative PLS algorithms, Table 3.1, including the statistically inspired modification of PLS, SIMPLS (De Jong, 1993) the algorithm is given in Appendix A. The main differences compared to NIPALS, is there is no need to deflate the data matrices $\mathbf{X}$ and $\mathbf{Y}$ individually since the deflation is carried through the covariance matrix $\mathbf{S} = \mathbf{X}'\mathbf{Y}$. Additionally, De Jong (1993) calculated the score vectors using the original data matrix $\mathbf{X}$ whilst in NIPALS they are calculated in terms of residuals. The advantage of SIMPLS over NIPALS is that the calculation of the scores and loadings is conducted directly from the original variables and thus the algorithm is not iterative resulting in faster computation of the latent variables. However, through the use of computers, the limitations in terms of algorithm speed can be overcome.

Another approach is kernel PLS (Lindgren et al., 1993) which calculates the PLS parameters based on the kernel function ($\mathbf{X}'\mathbf{Y}\mathbf{Y}'\mathbf{X}$) and the deflation is conducted on the covariance matrices ($\mathbf{X}'\mathbf{Y}$) and ($\mathbf{X}'\mathbf{X}$). The kernel PLS algorithm was modified by De Jong and Ter Braak (1994) and Dayal and MacGregor (1997a) through the simplification of the deflation step thereby reducing computational effort. The first modification, kernel PLS 1, by De Jong and Ter Braak (1994) simplifies the deflation procedure for both ($\mathbf{X}'\mathbf{Y}$) and ($\mathbf{X}'\mathbf{X}$) whilst the second modification, kernel PLS 2, by Dayal and MacGregor (1997a) showed that the necessary deflation can be carried for

either ($\mathbf{X}'\mathbf{Y}$) or ($\mathbf{X}'\mathbf{X}$). The advantage of the kernel PLS algorithms over NIPALS is computational effort where NIPALS is calculated in an iterative manner whilst kernel PLS is calculated directly from the covariance matrices. However, by the use of computer this limitation can be overcome. The kernel PLS algorithm and its modified variant are given in Appendix A. Table 3.1 presents a summary of the main PLS algorithms.

Table 3.1 – Summary of the conventional PLS algorithms.

Method	Author	Comments
NILES	Wold (1966)	- Original PLS algorithm
Modified NIPALS	Wold (1982)	- PLS algorithm - based on an iterative procedure
SIMPLS	De Jong (1993)	- Deflation is performed on the matrix $\mathbf{S} = \mathbf{X}'\mathbf{Y}$ - PLS loadings and scores are calculated directly from the original variables.
Kernel PLS	Lindgren et al.(1993)	- PLS parameters are calculated based on the kernel function - Deflation based the covariance matrices
Modified kernel PLS 1	De Jong and Ter Braak (1994)	- Modification of the original kernel PLS algorithm proposed by Lindgren et al.(1993) - The equations used for deflation of the covariance matrices are modified to reduce the computational effort.
Modified kernel PLS 2	Dayal and MacGregor (1997a)	- Modification the kernel PLS 1 algorithm proposed by Dayal and MacGregor (1997a) - For the kernel PLS algorithm, either ($\mathbf{X}'\mathbf{Y}$) and ($\mathbf{X}'\mathbf{X}$) is deflated to reduce the computational effort.

3.3.4 Selection of the Number of Latent Variables

In general, one latent variable is not sufficient to capture the variation contained within the process for the prediction of the quality variables $\mathbf{Y}$. Therefore, it is necessary to

determine the desirable number of latent variables to retain to describe the major sources of variation in the data and hence predict the quality variables.

Retaining a large number of latent variables can cause over fitting due to the inclusion of latent variables that explain process noise thereby impacting on the quality of the model prediction when the resulting model is applied to new unseen data. In contrast, retaining too few latent variables will result in a model under fitting hence process behaviour is not captured and the resulting prediction will be poor.

A number of approaches have been proposed for selecting the appropriate number of latent variables. For example, Akaike's Information Criteria, which is calculated based on the residual sum of squares and Wold's R criteria and adjusted Wold's R criteria, which are based on cross validation. A comprehensive comparison between these approaches was conducted (Li et al., 2002) and it was concluded that the adjusted Wold's R criteria resulted in more representative models compared to the other two approaches based on two case studies. The philosophy of the adjusted Wold's R criterion is to include a latent variable in a PLS model if and only if it results in significantly improved model prediction. The methodology is based on cross validation (Wold, 1978) and is as follows:

- Divide the data into a number of subsets s ($(s-1)$ subsets as used for training and the excluded set is used for testing).
- A one latent variable model is built from the training subsets and applied to the test data set. An individual PRedicted Error Sum of Squares (PRESS) is calculated. By repeating this procedure until that each set is excluded once, a series of individual PRESS values is calculated and the total PRESS is calculated.
- The procedure is repeated for 2, 3,…. $\min(n, m)$ latent variables and a corresponding total PRESS is calculated.

The adjusted Wold's R metric is given by

$$R = \frac{\text{PRESS}(a+1)}{\text{PRESS}\,(a)} \geq \alpha \qquad (3.8)$$

where a is the number of latent variable and the threshold α is 0.95. Several cross validation algorithms have been proposed which differ based on way the subsets are

formed for model building and testing (Wold, 1978). Although cross validation is time consuming especially for large data sets, it has been used extensively in the literature for selecting the number of PC's and latent variables for PCA and PLS respectively. Figure 3.4 shows an example of the predicted error sum of squares versus latent variable where the PRESS decreases rapidly for the first four latent variables and after that the rate of decrease in PRESS becomes quite small. Table 3.2 shows the value of the adjusted Wold's criteria, Equation 3.8, for $\alpha = 0.95$. Based on the adjusted Wold's criteria 4 latent variables would be selected.

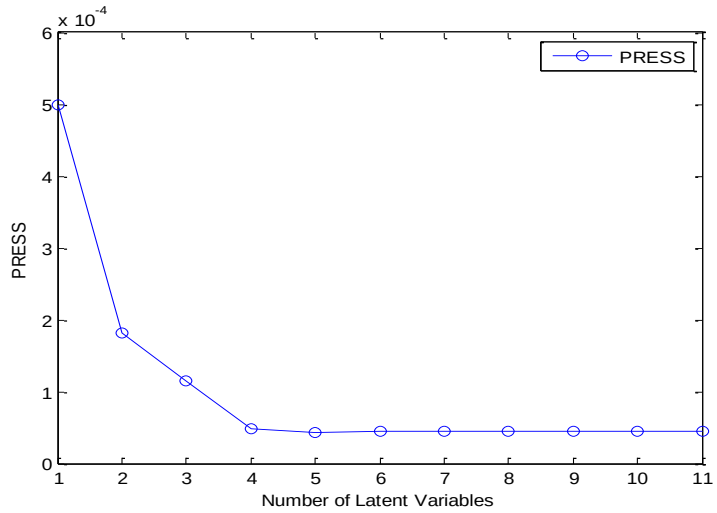

Figure 3.4 – Example of the predicted error sum of squares for each latent variable

Table 3.2 – Results for adjusted Wold criteria for $\alpha = 0.95$

Latent variable	1	2	3	4	5	6	7	8	9	10
R	0.39	0.63	0.42	0.96	1.005	1.00	1.00	1.00	1.00	1.00

Another approach for selecting the number of latent variables is by considering the variance captured by the model relating to **Y**. This approach was adopted by Kresta et al. (1991). The data used for calculating the number of latent variables using adjusted Wold's criteria is again used and Figure 3.5 shows the variance captured by the model relating to the **Y** block, again 4 latent variables were selected. It can be observed that the fifth latent variable does not add any significant information since the variance captured by the fifth latent variable is less than 1%. Hence 4 latent variables is appropriate for the

PLS model. In this thesis, the variance captured and the adjusted Wold's criteria based on cross validation are used to determine the number of latent variables to retain in the model.

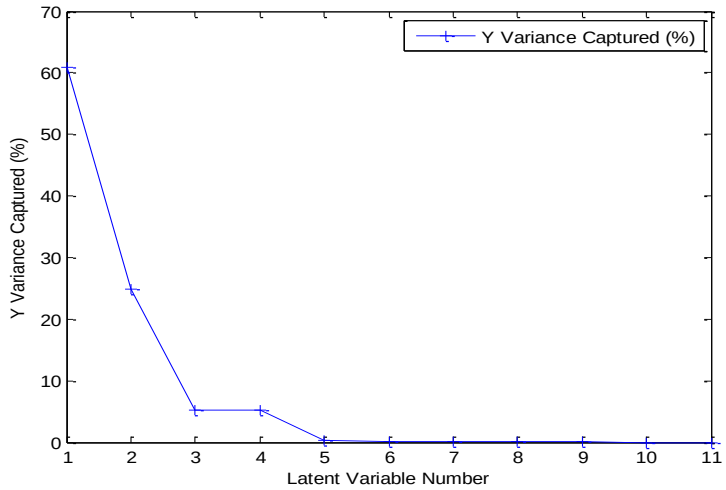

Figure 3.5 - Example of latent variable selection approach

3.3.5 Advantages of PLS

PLS can handle the typical characteristics of multivariate industrial processes, for example, measurement noise and high dimensionality. The handling of measurement noise is achieved by projecting the high dimensional data onto a lower dimensional subspace and the variation related to noise is captured in the last few latent variables and through their exclusion, measurement noise is addressed. Therefore, it is important to retain the appropriate number of latent variables (a) (section 3.3.4).

A further advantage of PLS is that it can handle correlated variables which are typical in industrial process (Wold et al., 1984; Fyfe, 2005). This is a consequence of the latent variables being linearly independent (orthogonal). Additionally, PLS has the ability to handle collinearity which occurs when some variables are linearly dependent, i.e. when at least one variable can be written as an approximate or exact linear combination of other variables (Martens et al., 1989). Collinearity is a serious issue for ordinary least squares since it causes the estimation of the regression coefficients $\mathbf{b} = (\mathbf{X}'\mathbf{X})^{-1}\mathbf{X}'\mathbf{Y}$ to be ill-conditioned due to the singularity of the matrix $(\mathbf{X}'\mathbf{X})^{-1}$ and hence the estimation of $\mathbf{b}$ becomes unstable and a small change in the analysed data can caused a large change in $\mathbf{b}$ (Wold et al., 1984; Martens et al., 1989). To address the issue of collinearity, two solutions are available. The first is to remove highly correlated

variables consequently the redundant information is removed. Secondly, through implementation of PLS, the highly correlated and collinear variables are incorporated in uncorrelated components (Wold et al., 1984).

A further advantage of PLS is that it can be applied in the case where the number of samples is less than the number process variables. This is a major issue in multiple linear regression and in such case a unique solution cannot be calculated. Geladi and Kowalski (1986) described PLS as a remedy for the weak points of regression methods due to its robustness and ability to handle ill conditioned data.

Unlike many statistical analysis techniques, there are no underlying constraints in terms of the distribution of the data for PLS modelling (Fornell and Bookstein, 1982; Haenlein and Kaplan, 2004). However, the calculation of confidence limits for monitoring charts requires the data to be normally distributed, Nomikos and MacGregor (1995) stated that the confidence limits can be calculated even if the original data are non-normal since the latent variables are linear combinations of the original variables and by the central limit theorem they are approximately normally distributed, thereby addressing the issue of non-normality.

3.3.6 Pre-processing of Process Data

Prior to the application of the PLS algorithm, the data may be required to be pre-processed. This is an additional step where a preliminary analysis is conducted to attain a general overview of the data however, it is important for two reasons. First because the performance of the PLS model depends on the quality of the data and secondly it helps eliminate some data problems such as outliers and missing data. Pre-processing procedures include the treatment of missing data, outlier detection, centring and scaling. The first step in pre-processing is the visual inspection of the original data signals to investigate whether the data contains problems such as missing data.

The presence of missing data is most likely to be due to instrumentation problems and one possible treatment for the missing data is the use of the in-filling techniques. A number of methods have been proposed for in-filling of missing values, for example mean imputation, zero-order linear interpolation and prediction of missing data methods (Nelson et al., 1996; Kaskavelis, 2000; Schafer and Graham, 2002).

- Mean imputation: missing value is replaced by the average value of the available data.

- Zero-order linear interpolation: missing value is replaced by the last point available before the missing value.
- Prediction method: missing value is replaced by the predicted value through auto-regressive time series models, for example.

A detailed description of other methods can be found in Schafer and Graham (2002), Kaskavelis (2000) and Nelson et al. (1996).

As defined in Chapter 2, an outlier is a sample differs significantly from the rest of the data due to a recording error. Several methods have been proposed for detecting outliers including Mahalanobis distance, which is a measure of how far the sample is from the centre of multivariate space, as well as through the use of basic plots, time series or scatter plot. The scores plot from principal component analysis can also be used to identify outliers. A detailed description of outlier detection methods is given by Hodge and Austin (2004). Once an outlier is detected, it should be either ignored or corrected prior to model development (Barnett and Lewis, 1994). A considerable amount of literature has been published on the treatment of outliers in PLS modelling and methods to address them have included filtering and the use of robust estimators (Kruger et al., 2008a; Kruger et al., 2008b; Wang and Srinivasan, 2009).

Centring and scaling is another important pre-processing step that is used when the collected data represent different measurements and units. Centring and scaling techniques should be implemented with care as it is important to preserve the information contained within the process. Also, inappropriate pre-processing may introduce additional variation into the process and result in the loss of important features in the original signals (Bro and Smilde, 2003). The impact of different scaling methods is investigated in Chapter 5.

3.4 Performance Evaluation of PLS Model

A core step in PLS modelling is to assess the performance of the resulting model. Model assessment should be conducted in three stages, i.e. training, validation and testing. The training stage is the first stage and is where the model is built based on a data set that is representative of the process, i.e. a historical data set, and the number of latent variables to be retained is determined (§3.3.4). The model fit for the training is assessed through the root mean squared error of the training data (RMSE):

$$\mathrm{RMSE} = \sqrt{\frac{\sum_{i=1}^{n}(y_i - \hat{y}_i)^2}{n}} \qquad (3.9)$$

where y_i , $\hat{y}_i$ are the measured and predicted values of the i^{th} sample respectively and n is the total number of samples used in the training data set. The training model is validated by applying the model to unseen data (validation data set) that is generated under normal operating conditions. Then the model is assessed using RMSE to check the consistency of the model and the ability to explain the characteristics of the validation data. The test stage involves the application of the model to a totally independent test set of samples, which may have different characteristics compared to the training data set and it is used to test the ability of the model to detect abnormal events.

3.5 Process Monitoring Based on a PLS Representation

One application of PLS is for process monitoring, the two key monitoring statistics are Hotelling's T^2 and the squared prediction error (SPE) (Qin, 2003; Qin, 2012). Based on historical data from nominal process operation, a PLS model is constructed (§3.3) and the confidence limits for Hotelling's T^2 (§3.5.1) and SPE (§3.5.2) are attained. Future behaviour is then compared to these statistics (Gallagher and Wise, 1996; Qin, 2003; Qin, 2012). PLS monitoring has been reported for a number of industrial applications. For example, Kruger and Xie (2012) constructed monitoring charts based on PLS for a distillation process whilst Yin et al. (2012) applied several methods including PLS to compare their performance based on data generated from the Tennessee Eastman process. Tavares et al. (2011) applied PLS to a municipal solid waste (MSW) for process control and monitoring. Kresta (1992) applied PLS to data collected from a fluidized bed reactor and Methanol-Acetone water distillation column. They concluded that PLS performed well in terms of detecting process abnormal events.

Three metrics form the basis of PLS monitoring; Hotelling's T^2 which is based on the input scores ; SPE_X which is calculated from the residuals of the input variation and SPE_Y which is based on the residuals of the output variation (Qin, 2003; Kruger and Xie, 2012). Hotelling's T^2 and the squared prediction error SPE_X complement each other. Hotelling's T^2 detects a disturbance within the identified model whilst SPE_X detects a disturbance outside the identified model, i.e. residuals.

3.5.1 Hotelling's T² Chart

Hotelling's T² is constructed from the scores of the PLS model:

$$T_i^2 = \mathbf{t}_i' \boldsymbol{\Lambda}_a^{-1} \mathbf{t}_i \quad (3.10)$$

where $\mathbf{t}_i$ represents the vector of t-scores for the ith data point (i=1,2,3….n) and $\boldsymbol{\Lambda}_a$ is the covariance matrix of the a retained latent variables. The associated confidence limit is given by:

$$T_\alpha^2 = \chi_\alpha^2(a) \quad (3.11)$$

where χ^2 is chi-squared distribution with degree of freedom a, equal to the number of latent variables retained and alpha (α) is the significance level (Nomikos and MacGregor, 1995; Qin, 2003). Details are provided in Appendix A. Hotelling's T² describes the overall process variation within the monitoring model. Consequently, values of Hotelling's T² lying outside the confidence limits represent a change in the variation of the variables and hence is an indicative of a change in the process (Gallagher and Wise, 1996; Qin, 2003; Kruger and Xie, 2012).

3.5.2 Squared Prediction Error Charts

The squared prediction error is the squared difference between the measured and predicted values:

$$SPE_X^{(i)} = \|\mathbf{x}_i - \hat{\mathbf{x}}_i\|_2^2 \quad (3.12)$$

$$SPE_Y^{(i)} = \|\mathbf{y}_i - \hat{\mathbf{y}}_i\|_2^2 \quad (3.13)$$

where $\mathbf{x}_i$, $\mathbf{y}_i$ and $\hat{\mathbf{x}}_i$, $\hat{\mathbf{y}}_i$ represent the vectors of the measured and predicted values of the predictor and response variables of the i th data point, (i=1,2,3….n) respectively. $\| \quad \|_2^2$ represents the squared norm of a vector. For a significance level α, the confidence limit is given by:

$$SPE_\alpha = g\chi_\alpha^2(h) \quad (3.14)$$

where χ^2 is the chi-squared distribution with degree of freedom h, $g = \frac{\theta_2}{\theta_1}$, $h = \frac{\theta_1^2}{\theta_2}$ and $\theta_i = \sum_{j=a+1}^{m} \lambda_j^i$, and λ_j is the eigenvalue of the covariance matrix (Box, 1954; Jackson and Mudholkar, 1979; Nomikos and MacGregor, 1995; Qin, 2003). Values of the SPE_X , for individual samples, that lie outside of the confidence limits indicates a change

in the relationship between the predictor variables whilst values of SPE_Y that breach the confidence limit is an indication of a mismatch between past process operation when the PLS was determined and current process operation (Nomikos and MacGregor, 1995; Qin, 2003). Alternative confidence limit is provided in Appendix A.

3.6 Evaluation of PLS Monitoring Charts

3.6.1 Average Run Length

The Average Run Length (ARL) is a performance measure which is defined as the expected number of samples that occur before an out of control is detected. It has been used as a means of comparison to assess the performance of monitoring schemes. The average run length can be calculated in a number of ways including the use of Markov chain (Brook and Evans, 1972). In this work the average run length is calculated using a Monte Carlo approach (Javaheri and Houshmand, 2001). The aim of the Monte Carlo approach is to generate a large number of control charts under the same conditions and then to calculate the run length (RL) for each chart, i.e. the number of samples that remain within the statistical limits from the start of monitoring period until an out of control is detected. The average run length is then calculated as the average of the values of the run length (RL) that are obtained from different control charts.

For each control chart there are two types of ARL: the in-control ARL (ARL0) and the out-of-control ARL (ARL1). ARL0 is the average number of samples from the start of the monitoring period until an out of control signal is detected given that there is no change affecting the process. On the other hand, ARL1 is the average number of samples from the occurrence of the change in the process until an out of control signal is detected. An effective control chart should have a high ARL0 when a process is operating under normal operating conditions and a low ARL1 when a change has been introduced into a process, i.e. the change in the process is detected rapidly.

3.6.2 False Alarm and Fault Detection Rates

False alarm rate (FAR) and fault detection rate (FDR) are statistical indices also used to evaluate the efficiency of monitoring charts (Chiang et al., 2001; Lee et al., 2006b; Yin et al., 2012). A false alarm is generated when the control chart identifies an out of

control signal while in practice the process is operating normally. FAR and FDR are given by:

$$\mathrm{FDR} = \frac{\text{No. of samples } (\mathrm{i} > \mathrm{ith} \,|\mathrm{f} \neq 0)}{\text{total samples } (\mathrm{f} \neq 0)} \times 100 \tag{3.15}$$

$$\mathrm{FAR} = \frac{\text{No. of samples } (\mathrm{i} > \mathrm{ith} \,|\mathrm{f} = 0)}{\text{total samples } (\mathrm{f} = 0)} \times 100 \tag{3.16}$$

where i represents the value of the statistic used to construct the monitoring chart (i=1,2,3….n), "ith" is the corresponding confidence limit and f indicates the occurrence of the fault. Since the fault may be detected in either Hotelling's T^2 or Squared prediction error (SPE_X), it useful to calculate a joint FDR, which take into account both univariate statistics. Additionally a joint FAR is also useful as the false alarm may be occurred in both monitoring chart.

3.7 Dynamic PLS

PLS was proposed to model steady state processes but for many industrial process the relationship between the measurements is dynamic, i.e. the current state of the process not only depends on the current values of the variables, it is also dependent on the previous values. A dynamic model thus captures the relationships between variables at time t and also at previous time points($t-1,\ t-2,\ldots$). A number of algorithms have been proposed for dynamic PLS (DPLS) including the modification of the PLS inner relationship, the augmentation of time lagged measurements and a filter approach (Ricker, 1988; Kaspar and Ray, 1993; Lakshminarayanan et al., 1997a).

One approach is to include lagged measurements in the input block, through the incorporation of a time series representation (Ricker, 1988; Qin, 1993; Qin and McAvoy, 1993). If the input matrix includes only lagged values of the input variables, it is termed a PLS finite impulse response (FIR) model while an auto-regressive with exogenous input (ARX) model is built if both lagged input and output values are included in the input matrix (Ricker, 1988; Qin, 1993; Qin and McAvoy, 1993; Ljung, 1999). Although the use of lagged variables approach is widely adopted, the size of the input matrix can be large and hence the computational load increases. In addition, including a large number of lagged values can materialise in the generation of additional noise that may be difficult to characterize (Chiang et al., 2001). This can be observed from the increase of variance captured by the model whilst model prediction was not

significantly improved as shown in Chapter 6. In this thesis, dynamic PLS is examined through both an auto-regressive with exogenous inputs (ARX) approach and a finite impulse response (FIR) representations for the modelling of an ammonia synthesis reactor (Chapter 5) and the Tennessee Eastman Process (Chapter 6) respectively. In addition, the two dynamic PLS approaches are extended to adaptive and multiblock algorithms and applied for modelling and monitoring. The general framework of dynamic PLS based on lagged variables is introduced in this subsection and a detailed description of the approaches is presented in Chapter 5 and Chapter 6.

Another dynamic PLS method proposed by Kaspar and Ray (1993) aims to model dynamic processes by the finding a dynamic transformation of the input data and relate the transformed input to the output hence an algebraic relationship is attained. The dynamic filter, i.e. dynamic transformation, can be designed either through prior knowledge of the system or by minimizing the sum of squares of the output residual. The next step is to apply the conventional PLS to the matrix of the dynamic transformation. Kaspar and Ray (1993) demonstrated their approach through the application of the method for control purposes to a distillation column at the University of Wisconsin and to a heated rod process. Kaspar and Ray (1993) stated that the limitation of this approach is that the filter order must be specified, otherwise no dimensional reduction is conducted in the dynamic part of the model, i.e. the dynamic transformation may result in increase in the dimensions of the matrix used for PLS in the next step.

Another dynamic PLS modelling approach was proposed by Lakshminarayanan et al. (1997b) which is based on the modification of the inner relationship of the conventional PLS algorithm (Equation 3.2), i.e. instead of relating $\mathbf{u}_i$ and $\mathbf{t}_i$ using a linear model, they proposed the use of a dynamic model such as autoregressive with exogenous input. Consequently, the dynamic representation of the decomposition of the response $\mathbf{Y}$ (Equation 3.4), is given by:

$$\mathbf{Y} = \sum_{i=1}^{a} \mathbf{G}_i(\mathbf{t}_i)\mathbf{q}_i' + \mathbf{F} \tag{3.17}$$

where $\mathbf{G_i}$ denotes the linear dynamic model (e.g. ARX). The approach was primarily designed for controller synthesis employing univariate controller design and tuning techniques. This method was applied to the Wood and Berry distillation column (Wood

and Berry, 1973), an acid-base neutralization process and a multivariable distillation column. Table 3.3 provides an overview of the dynamic PLS approaches.

Table 3.3 - Overview of the dynamic PLS algorithms.

Methods	Author	Comments
DPLS lagged variables	Ricker (1988) Qin (1993) Qin and McAvoy (1993)	- The advantage of this approach is that the steady state PLS method can be used to develop the dynamic model. - A limitation is that the computational effort is increased if a large number of lagged variables is included
DPLS Modification of inner relationship	(Lakshminarayanan et al., 1997b)	- The inner relationship of the PLS algorithm is modified. - Primarily applied in control application
DPLS Filter approach	(Kaspar and Ray, 1993)	- Based on the dynamic filtering of the input data - Prior knowledge of the process is required to design the filter. - Primarily applied in control application

3.7.1 Lagged Variables Method

A finite impulse response (FIR) representation is denoted by:

$$\mathbf{y}(t) = \sum_{j=1}^{n_u} \mathbf{B}_j \mathbf{u}(t-j) + \mathbf{e}(t) \tag{3.18}$$

whilst an auto-regressive with exogenous input (ARX) representation is denoted by:

$$\mathbf{y}(t) = \sum_{i=1}^{n_y} \mathbf{A}_i \mathbf{y}(t-i) + \sum_{j=1}^{n_u} \mathbf{B}_j \mathbf{u}(t-j-k+1) + \mathbf{e}(t) \tag{3.19}$$

where $\mathbf{y}(t)$, $\mathbf{u}(t)$ and $\mathbf{e}(t)$ are the process output, input and noise vectors respectively. $\mathbf{A}_i$ and $\mathbf{B}_i$ are the matrices of the coefficients that are identified using PLS regression hence steady state PLS is applied to model the dynamic process. n_y and n_u are the number of time lags for the output and input data vectors respectively; k is the time

delay between the input and output variables in the system and is typically 1 if there is no dead-time in the system. In practical applications, the delay should be taken into account. This is investigated in Chapter 5 where a dynamic PLS method based on an ARX representation is used to model the dynamic behaviour of an ammonia synthesis fixed-bed reactor.

For a FIR model, the regressor row vector $\mathbf{x}(t)$ comprises lagged input data values and is defined as:

$$\mathbf{x}(t) = [\mathbf{u}(t-1), \mathbf{u}(t-2), \dots\dots, \mathbf{u}(t-n_u)] \tag{3.20}$$

and for an ARX model, the regressor row vector $\mathbf{x}(t)$ comprises lagged output and input data values and is defined as:

$$\mathbf{x}(t) = [\mathbf{y}(t-1), \dots, \mathbf{y}(t-n_y), \mathbf{u}(t-k), \dots\dots, \mathbf{u}(t-n_u-k+1)] \tag{3.21}$$

Both representations can be written as:

$$\mathbf{y}(t) = \mathbf{C}.\mathbf{x}(t) + \mathbf{e}(t) \tag{3.22}$$

where $\mathbf{C}$ for the FIR representation is given by:

$$\mathbf{C} = [\mathbf{B}_1, \mathbf{B}_2, \dots\dots, \mathbf{B}_{n_u}] \tag{3.23}$$

and for the ARX representation is given by:

$$\mathbf{C} = [\mathbf{A}_1, \mathbf{A}_2, \dots\dots, \mathbf{A}_{n_y}, \mathbf{B}_1, \mathbf{B}_2, \dots\dots, \mathbf{B}_{n_u}] \tag{3.24}$$

The input and output matrices for the PLS model can be arranged in the following matrix format:

$$\mathbf{X} = \begin{bmatrix} \mathbf{x}(1) \\ : \\ \mathbf{x}(t) \end{bmatrix}, \mathbf{Y} = \begin{bmatrix} \mathbf{y}(1) \\ : \\ \mathbf{y}(t) \end{bmatrix}, \mathbf{E} = \begin{bmatrix} \mathbf{e}(1) \\ : \\ \mathbf{e}(t) \end{bmatrix} \tag{3.25}$$

and are related through:

$$\mathbf{Y} = \mathbf{XC} + \mathbf{E} \tag{3.26}$$

A number of applications and extensions of DPLS, through the incorporation of a time series representation have been reported in the literatures. For example, Baffi et al. (2000) extended the DPLS algorithm described above to the non-linear case to model

non-linear dynamic processes. They applied the new approach to a simulation of a pH neutralization process and concluded that the prediction capabilities of the DPLS algorithm improved when a non-linear regression model is used. Chen and Liu (2002) employed the idea of lagged variables to improve the performance of multiway PLS for batch process, hence a batch dynamic PLS was developed. They applied the proposed method to a DuPont industrial batch polymerization process, more specifically a semi-batch emulsion polymerization and an exothermic batch chemical reactor. The proposed approach accounted for serial correlation within each batch and cross-correlation between batches. In this thesis, dynamic PLS is extended by combining it with recursive PLS to model the complex behaviour of two dynamic and nonlinear processes in Chapters 5 and 6.

3.8 Multiblock PLS

Industrial process typically comprise a large number of variables that are associated with different operational units, and for the modelling and monitoring of these process a variant of PLS, Multiblock PLS (MBPLS), was proposed. The first multiblock PLS method was termed PLS path modelling, Gerlach et al. (1979). The basic concept of MBPLS is to divide the input data matrix into informative blocks that may relate to different unit operations. It is primarily used to simplify the interpretation of a PLS model when a process is complex and can be used for any number of blocks with any kind of relationships existing between the blocks (Westerhuis and Coenegracht, 1997). However, there are no specific rules for dividing a process into different blocks consequently engineering knowledge is required to determine the block structure. The main advantage of MBPLS in term of process monitoring is it enables the identification of the block where the fault has occurred.

The general idea of the MBPLS method is summarised in Figure 3.6. The basic algorithm is similar to that of conventional PLS, however, the matrix of input variables is divided into a number of blocks $\boldsymbol{X}_b$ and b =1,2,3….B as shown in Figure 3.6. The latent variable for the bth block is denoted by $\boldsymbol{t}_b$ and for the response block, $\boldsymbol{u}$. A number of MBPLS algorithms have been proposed and are based on different criteria, deflation, construction of super scores and weight and score normalization (Frank and Kowalski, 1985; Wangen and Kowalski, 1989; MacGregor et al., 1994; Westerhuis and Coenegracht, 1997; Westerhuis et al., 1998). The basic algorithm (Figure 3.6) is

presented prior to the description of the different variants of MBPLS and is summarized as follows:

Step 1. Set $\boldsymbol{u}$ equal to any column of $\boldsymbol{Y}$

Step 2. Regress the $\boldsymbol{u}$ on each block $\boldsymbol{X}_b$ (b =1,2,3….B) to attain block weights $\boldsymbol{w}_b$:

$\boldsymbol{w}_b = \boldsymbol{X}_b'\boldsymbol{u}$ (b =1,2,3….B)

Step 3. Normalize the block weights $\boldsymbol{w_b}$ to length one and calculate the block latent variable, $\boldsymbol{t}_b$:

$\boldsymbol{w}_b = \boldsymbol{w}_b/\|\boldsymbol{w}_b\|$

$\boldsymbol{t}_b = \boldsymbol{X}_b\boldsymbol{w}_b$

Step 4. Combine the latent variables to form a super block $\boldsymbol{T}$:

$\boldsymbol{T} = [\boldsymbol{t}_1, \boldsymbol{t}_2, \dots, \boldsymbol{t}_b, \dots \boldsymbol{t}_B]$

Step 5. Calculate the super weights and normalize them:

$\boldsymbol{w}_T' = \boldsymbol{T}'\boldsymbol{u}$

$\boldsymbol{w}_T = \boldsymbol{w}_T/\|\boldsymbol{w}_T\|$

Step 6. Calculate the super scores:

$\boldsymbol{t}_T = \boldsymbol{T}\,\boldsymbol{w}_T$

Step 7. Regress matrix $\boldsymbol{Y}$ on $\boldsymbol{t}_T$ to calculate the output loading coefficients:

$\boldsymbol{q} = \boldsymbol{Y}'\boldsymbol{t}_T/\boldsymbol{t}_T'\boldsymbol{t}_T$

Step 8. Calculate the new output scores as:

$\boldsymbol{u} = \boldsymbol{Y}\boldsymbol{q}/\boldsymbol{q}'\boldsymbol{q}$

Step 9. Go to step 2 until convergence of $\boldsymbol{u}$

Step 10. After convergence of $\boldsymbol{u}$, calculate the block loading $\boldsymbol{p}_b$.

Step 11. Deflate the data matrices, the response and blocks matrices, and calculate the next factor if required.

The deflation formula differs based on the discussion given below.

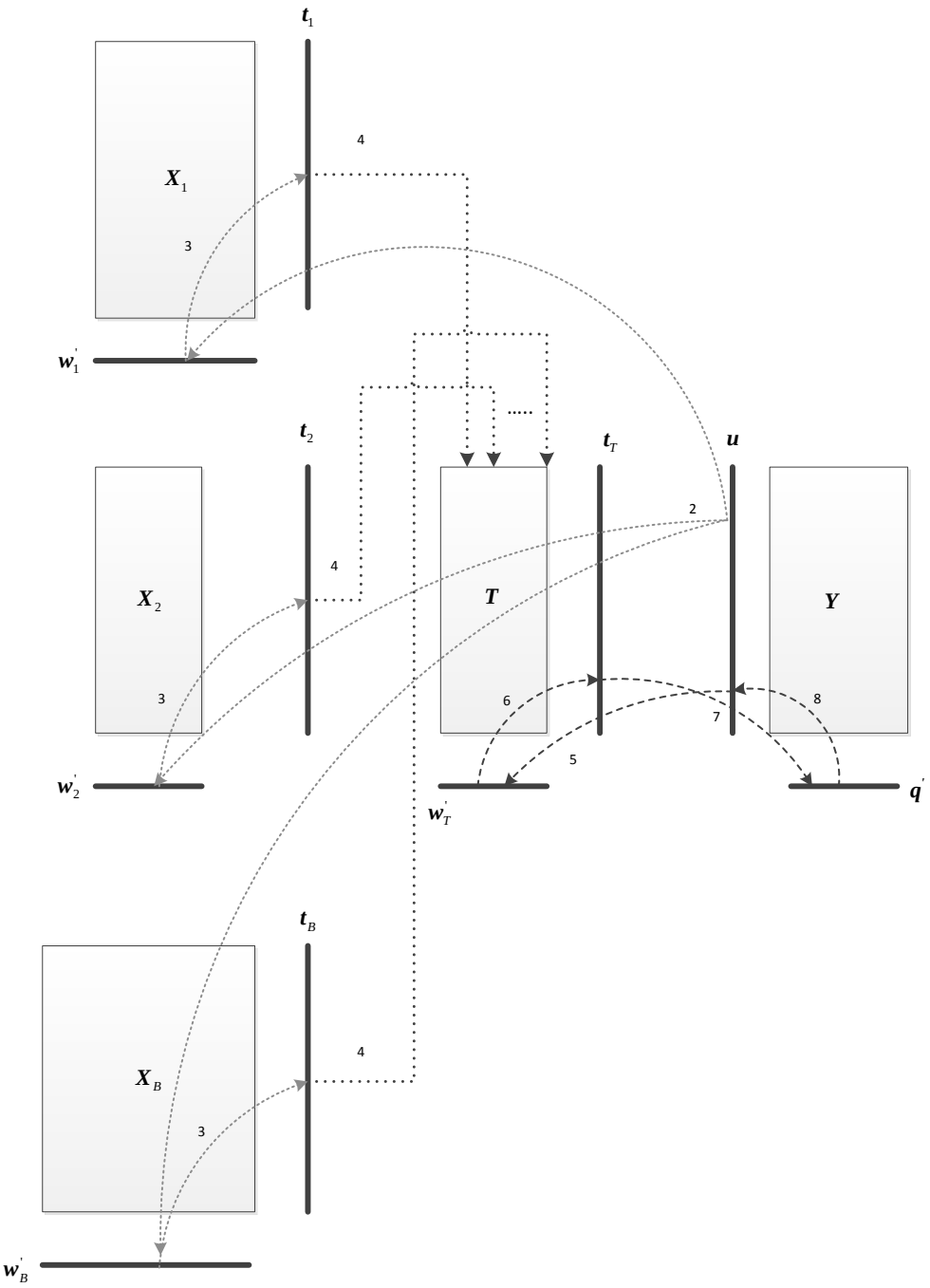

Figure 3.6 – Multiblock PLS method (Vinzi et al., 2007)

MacGregor et al. (1994) and Wangen and Kowalski (1989) proposed a MBPLS algorithm, referred to as block score updating MBPLS$_b$, that uses the block scores, $\boldsymbol{t}_b$, for the calculation of the of loadings and residuals:

$$\boldsymbol{p}_b = \boldsymbol{X}_b \boldsymbol{t}_b / \boldsymbol{t}_b' \boldsymbol{t}_b$$

$$\boldsymbol{X}_b = \boldsymbol{X}_b - \boldsymbol{t}_b \, \boldsymbol{p}_b'$$

Wold et al. (1996) proposed a hierarchical multiblock PLS algorithm, HMBPLS, the aim of which is to block the variables and then employ the hierarchical PLS algorithm. The algorithm consists of two levels, super level and sub-level. The sublevel contains the input and output blocks and each bock is modelled in terms of its block scores and loadings. At the super level, the input and output matrices are replaced by the block scores from the sub-level. Finally the super level matrices are used in conventional PLS and the output scores are normalized. Details of HMBPLS can be found in Wold et al. (1996).

Frank and Kowalski (1985) proposed a MBPLS algorithm, super scores updating algorithm $MBPLS_T$, that calculates the block loadings and the residuals based on the super scores $\boldsymbol{t}_T$:

$$\boldsymbol{p}_{bT} = \boldsymbol{X}_b \boldsymbol{t}_T / \boldsymbol{t}_T' \boldsymbol{t}_T$$

$$\boldsymbol{X}_b = \boldsymbol{X}_b - \boldsymbol{t}_T \, \boldsymbol{p}_{bT}'$$

Westerhuis and Coenegracht (1997) showed that this method results in exactly the same result as conventional PLS when all the variables are combined in one large block. Consequently, conventional PLS can be used directly to calculate the parameters of $MBPLS_T$. Qin et al. (2001) introduced a further analysis on $MBPLS_b$ and $MBPLS_T$ and demonstrated how the algorithms can be used for statistical monitoring. The $MBPLS_T$ method proposed by Westerhuis and Coenegracht (1997) is used as the basis of the subsequent chapters. Hence, the algorithm is first introduced and then the relationship between conventional PLS and $MBPLS_T$ is given.

Applications of variants of MBPLS have been widely reported in the literature. For example, Westerhuis and Coenegracht (1997) applied MBPLS to model a pharmaceutical process comprising wet granulation and tableting. Wold et al. (1996) applied a hierarchical MBPLS to data collected from a residue catalytic cracker (RCCU) unit at the Statoil Mongstad refinery in Norway. They concluded that the application of MBPLS provided enhanced interpretation compared to conventional PLS as it enabled them to investigate which part of the process caused a certain event.

3.8.1 Multiblock PLS - MBPLS$_T$

For a given output variable matrix $\mathbf{Y}_{n\times k}$ and process variable matrix $\mathbf{X}_{n\times m}$ where $\mathbf{X}_{n\times m}$ can be sub-divided into multiple blocks B according to:

$$\mathbf{X} = [\boldsymbol{X}_1, \boldsymbol{X}_2, \ldots \boldsymbol{X}_b \ldots\ldots \boldsymbol{X}_B] \tag{3.27}$$

The number of variables in each block is m_b where $m = \sum_{b=1}^{B} m_b$. The MBPLS$_T$ approach calculates the loadings, scores, and weights for each block and also the super weights and supper scores (Equation 3.28), and uses these to deflate the input and output matrices. The parameters of MBPLS$_T$ are:

$$\{\boldsymbol{X}_1, \boldsymbol{X}_2, \ldots\ldots\ldots \boldsymbol{X}_b, \boldsymbol{Y}\} \xrightarrow{\text{MBPLS}_T} \{\boldsymbol{W}_b, \boldsymbol{W}_T, \boldsymbol{T}_b, \boldsymbol{T}_T, \boldsymbol{Q}, \boldsymbol{U}, \boldsymbol{P}_b\}, \quad b = 1,2 \ldots B \tag{3.28}$$

where $\boldsymbol{P}_b$ is a matrix of block loadings, $\boldsymbol{W}_b$ and $\boldsymbol{W}_T$ are the matrices of the block weights and super weights respectively, $\boldsymbol{T}_b$ and $\boldsymbol{T}_T$ are the matrices of the block scores and super scores respectively and $\boldsymbol{Q}$ and $\boldsymbol{U}$ are the output weights, scores matrices respectively. The MBPLS$_T$ algorithm is implemented as follows:

Step 1. Set $\boldsymbol{X}_{b,\mathbf{1}} = \boldsymbol{X}_b$, $\boldsymbol{Y}_1 = \boldsymbol{Y}$ and $a = 1$

Step 2. Choose a starting $\boldsymbol{u}_a$ and iterate through the following steps until convergence:

$$\boldsymbol{w}_{b,a} = \boldsymbol{X}'_{b,a}\boldsymbol{u}_a / \left\|\boldsymbol{X}'_{b,a}\boldsymbol{u}_a\right\|$$

$$\boldsymbol{t}_{b,a} = \boldsymbol{X}_{b,a}\boldsymbol{w}_{b,a}$$

$$\boldsymbol{T}_a = [\boldsymbol{t}_{1,a}, \boldsymbol{t}_{2,a}, \ldots\ldots \boldsymbol{t}_{B,a}]$$

$$\boldsymbol{w}_{T,a} = \boldsymbol{T}'_a\boldsymbol{u}_a / \|\boldsymbol{T}'_a\boldsymbol{u}_a\|$$

$$\boldsymbol{t}_{T,a} = \boldsymbol{T}_a\boldsymbol{w}_{T,a}$$

$$\boldsymbol{q}_a = \boldsymbol{Y}'_a\boldsymbol{t}_{T,a} / \boldsymbol{t}'_{T,a}\,\boldsymbol{t}_{T,a}$$

$$\boldsymbol{u}_a = \boldsymbol{Y}_a\boldsymbol{q}_a / \boldsymbol{q}'_a\boldsymbol{q}_a \quad \text{and} \quad b_a = \boldsymbol{t}_{T,a}\boldsymbol{u}_a / \boldsymbol{t}'_{T,a}\,\boldsymbol{t}_{T,a}$$

Step 3. Deflate residuals

$$\boldsymbol{p}_{b,a} = \boldsymbol{X}'_{b,a}\boldsymbol{t}_{T,a} / \boldsymbol{t}'_{T,a}\,\boldsymbol{t}_{T,a}$$

$$\boldsymbol{X}_{b,a+1} = \boldsymbol{X}_{b,a} - \boldsymbol{t}_{T,a}\boldsymbol{p}'_{b,a} \quad \text{and} \quad \boldsymbol{Y}_{a+1} = \boldsymbol{Y}_a - \boldsymbol{t}_{T,a}\,b_a\boldsymbol{q}'_a$$

Step 4. Set $a = a + 1$ and return to step 2.

The MBPLS_T algorithm is related to conventional PLS algorithm and the parameters of the individual blocks can be calculated directly from the PLS algorithm as shown by Westerhuis and Coenegracht (1997) and Qin et al. (2001). The theoretical proofs is given by Qin et al. (2001), Appendix A, and the relationships are summarised as follows:

Step 1. The first step was to combine all variables into one block **X** and PLS is then applied:

$$\{\mathbf{X}, \mathbf{Y}\} \overset{\text{PLS}}{\longrightarrow} \{\mathbf{T}, \mathbf{P}, \mathbf{Q}, \mathbf{U}, \mathbf{W}, \mathbf{B}\}$$

where **T** and **P** are the input scores and loadings matrices, **U** and **Q** are the output scores and loadings matrices, **W** is matrix of weights and **B** is the diagonal matrix of the PLS inner regression coefficients following the application of conventional PLS. Then the PLS parameters, loadings and scores, were divided into the corresponding blocks hence the parameters of the individual blocks are attained following the steps:

Step 2. The MBPLS_T super scores $\boldsymbol{T}_T$ was identical to the score of the conventional PLS **T**:

$$\mathbf{T} = \boldsymbol{T}_T \tag{3.29}$$

Step 3. The conventional PLS weights $\mathbf{w}_a$ for the ath latent variable were sub-divided:

$$\mathbf{w}_a = \begin{bmatrix} \mathbf{w}_{1,a} \\ \mathbf{w}_{2,a} \\ \vdots \\ \mathbf{w}_{b,a} \\ \vdots \\ \mathbf{w}_{B,a} \end{bmatrix} \tag{3.30}$$

Step 4. The MBPLS_T block weights for the ath latent variable are then given by:

$$\boldsymbol{w}_{b,a} = \mathbf{w}_{b,a} / \left\| \mathbf{w}_{b,a} \right\| \tag{3.31}$$

Step 5. The MBPLS_T super weights $\boldsymbol{w}_{\text{T},a}$ for the ath latent variable are given by:

$$\boldsymbol{w}_{T,a} = \begin{bmatrix} \|\boldsymbol{w}_{1.a}\| \\ \|\boldsymbol{w}_{2.a}\| \\ \vdots \\ \|\boldsymbol{w}_{b.a}\| \\ \vdots \\ \|\boldsymbol{w}_{B.a}\| \end{bmatrix} \tag{3.32}$$

Step 6. The MBPLS$_T$ block loadings $\boldsymbol{p}_{b,a}$ for the ath latent variable is given by:

$$\boldsymbol{p}_{b,a} = \mathbf{p}_{b,a} \tag{3.33}$$

Step 7. The MBPLS$_T$ block scores $\boldsymbol{t}_{b,a}$ for the ath latent variable:

$$\boldsymbol{t}_{b,a} = \boldsymbol{X}_{b,a} * \boldsymbol{w}_{b.a} \tag{3.34}$$

Step 8. The MBPLS$_T$ output weights for the ath latent variable:

$$\boldsymbol{q}_a = \mathbf{q}_a \tag{3.35}$$

By using conventional PLS parameters for the calculations of the monitoring statistics, the overall process performance can be described whilst monitoring charts for the individual blocks can be constructed based on individual block parameters derived based on Equations 3.29 to 3.35. Hence, monitoring charts for both the whole process as well as the individual units are attained. This approach is used in this thesis and has been extended to multiblock dynamic PLS (MBDPLS) based on FIR representation, adaptive multiblock dynamic PLS (AMBDPLS) and robust adaptive multiblock dynamic PLS (RAMBDPLS) (Chapter 6).

Like PLS, the monitoring statistics for MBPLS$_T$ utilise the univariate statistics of Hotelling's T² and square prediction error (SPE). Qin et al.(2001) concluded that as a consequence of the equivalence between MBPLS$_T$ and conventional PLS, monitoring indices for the overall process and the individual blocks are calculated as:

- The squared prediction error for the individual blocks can be calculated as

  $$\mathrm{SPE_b} = \left\| \boldsymbol{X}_b - \widehat{\boldsymbol{X}}_b \right\|^2 \tag{3.36}$$

  where $\widehat{\boldsymbol{X}}_b$ is the prediction of the process measurements in block *b*.

- The Hotelling's T² for the individual block is calculated based on the scores from MBPLS$_T$:

  $$\mathrm{T}_b^2 = \boldsymbol{T}_b' \boldsymbol{\Lambda}_b^{-1} \boldsymbol{T}_b \tag{3.37}$$

  where $\boldsymbol{T}_b$ is the block scores and $\boldsymbol{\Lambda}_b^{-1}$ is the inverse of the covariance matrix of the score matrix $\boldsymbol{T}_b$. If the covariance matrix is singular, a pseudo-inverse should be used.

- The squared prediction error of the overall process can be calculated either from MBPLS$_T$ or conventional PLS since the residuals from MBPLS$_T$ and

conventional PLS are identical (Qin et al., 2001). Therefore Equation 3.12 is used and the confidence limit is calculated according to Equation 3.14.

- Since the super scores of $MBPLS_T$ are used to calculate the overall Hotelling's T^2 metric and are identical to the scores from conventional PLS (Equation 3.28), the overall Hotelling's T^2 can be calculated according to Equation 3.10 and the confidence limit is calculated according to Equation 3.11.

3.9 Application of PLS to a Time Varying Process

3.9.1 Time Varying Behaviour

When the process operating conditions change as a consequence of changes in the raw materials, disturbances such as a drift in the set point or the ageing of the main components for example, the process behaviour is characterized as being time varying. It has been noted that most industrial process are time variant (Gallagher et al., 1997; Choi et al., 2006). In this section, it is demonstrated that a steady state PLS approach is not appropriate for the modelling and monitoring of a process that exhibits time varying behaviour through a simulation study.

3.9.2 Simulation of Time Varying Process

A data set from a simulation of a time varying process comprising two predictor variables and two response variables x_{1h}, x_{2h}, y_{1h} and y_{2h} respectively is considered. The first step is the generation of the initial predictor signals u_h. These are generated from an Autoregressive Moving Average (ARMA) model:

$$u_h(z^{-1}) = \frac{1 + az^{-1}}{1 + bz^{-1}}\, \varepsilon(z^{-1}) \tag{3.38}$$

where a and b are 0.5 , $\varepsilon(z^{-1})$ is obtained from a standard normal distribution and z^{-1} is a back shift operator. The predictor and response variables are then defined as:

$$\begin{pmatrix} y_{1h} \\ y_{2h} \end{pmatrix}_t = \begin{bmatrix} c_{11} & c_{12} \\ c_{21} & c_{22} \end{bmatrix} \begin{pmatrix} x_{1h} \\ x_{2h} \end{pmatrix}_t \tag{3.39}$$

$$\begin{pmatrix} x_{1h} \\ x_{2h} \end{pmatrix}_t = \begin{pmatrix} u_h \\ u_h \end{pmatrix} + \begin{pmatrix} \varepsilon_{1h} \\ \varepsilon_{2h} \end{pmatrix} \tag{3.40}$$

where c_{11}, c_{12}, c_{21} and c_{22} are constant parameters and are -0.2, 0.3, 0.1 and -0.05 respectively. $\varepsilon_{1h}$and ε_{2h} are uncorrelated random signals from a $N(0,0.2)$ distribution

and u_h is an ARMA signal of the h^{th} time instance defined according to Equation 3.38. The subscript t refers to the actual process values. A random signal from a $N(0,0.1)$ distribution was augmented to the actual signal for both the predictor and response variables to mimic measurement noise:

$$\begin{pmatrix} y_{1h} \\ y_{2h} \end{pmatrix}_m = \begin{pmatrix} y_{1h} \\ y_{1h} \end{pmatrix}_t + \begin{pmatrix} \varepsilon_{3h} \\ \varepsilon_{4h} \end{pmatrix} \quad (3.41)$$

$$\begin{pmatrix} x_{1h} \\ x_{2h} \end{pmatrix}_m = \begin{pmatrix} x_{1h} \\ x_{1h} \end{pmatrix}_t + \begin{pmatrix} \varepsilon_{5h} \\ \varepsilon_{6h} \end{pmatrix} \quad (3.42)$$

where m denotes the measured values and ε_{3h}, ε_{4h}, ε_{5h} and ε_{6h} are random signals. Time varying behaviour was attained through the introduction of a ramp signal with an increment $k = 0.005$ added to the c_{22} coefficent at t = 300.

$$r(t) = \begin{cases} c_{22}t < 300 \\ k^t c_{22}t \geq 300 \end{cases} \quad (3.43)$$

This simulation is taken from Wang et al. (2003). In this study, 200 samples were used for model development and 800 samples for validation. A further data set was generated which included a step change in the second input variable at time instance t=500. This additional data set was generated to test the ability of the PLS monitoring charts to differentiate between time varying behaviour and a step change that is not considered as normal operation. Model development and the monitoring charts are presented in the subsequent sections.

3.9.3 Model Development

The data are generated from the same signal hence there are no issues pertaining to different measurement units hence scaling was not considered. The results from the application of PLS to the calibration data set are summarized in Table 3.4, Figures 3.7 and 3.8. Each raw provides the amount of variation captured by the latent variables and the total variation, Cumulative variation, captured by the retained latent variables. The number of latent variables to retain was identified as one from cross validation. From Table 3.4, the PLS model with one latent variable captures 95.36% of the total variation in the X-block and explains 88.33% of the variation in the Y-block. The second latent variable does not add any improvement to the model as it only captures 4.64% of the variation in the X-block and explains 0.01% of the variation in the Y-block as shown in Table 3.4.

Table 3.4 - Percentage variance captured from PLS model for time varying process

LV	X-block		Y-block	
	LV	Cumulative	LV	Cumulative
1	95.36	95.36	88.33	88.33
2	4.64	100.00	0.01	88.34

Figures 3.7 and 3.8 show the time series plots for the two quality variables for the calibration data set with each plot has a zoomed in plot (residuals plots are given in Appendix A). An offset is observed in both plots indicating that the underlying behaviour is not fully captured by the model. When the model is applied to the validation data set (Figures 3.9 and 3.10), it fails to predict the time varying behaviour as seen from the second quality variable (Figure 3.10). When the model is applied to a test data set which contains both time varying behaviour and a step change, the model again fails to predict the process behaviour (Figure 3.11 and 3.12).

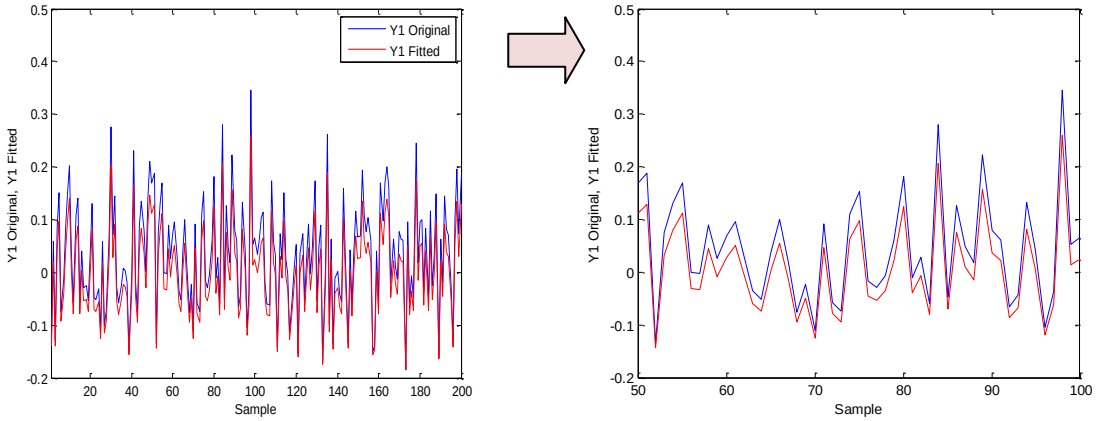

Figure 3.7 – Time series plot of original and fitted values for the first quality variable for the calibration data set

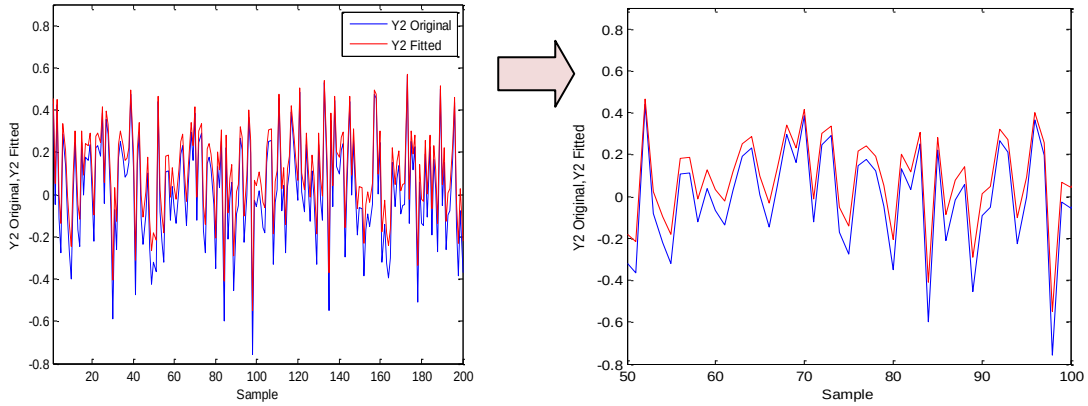

Figure 3.8 – Time series plot of original and fitted values for the second quality variable for the calibration data set

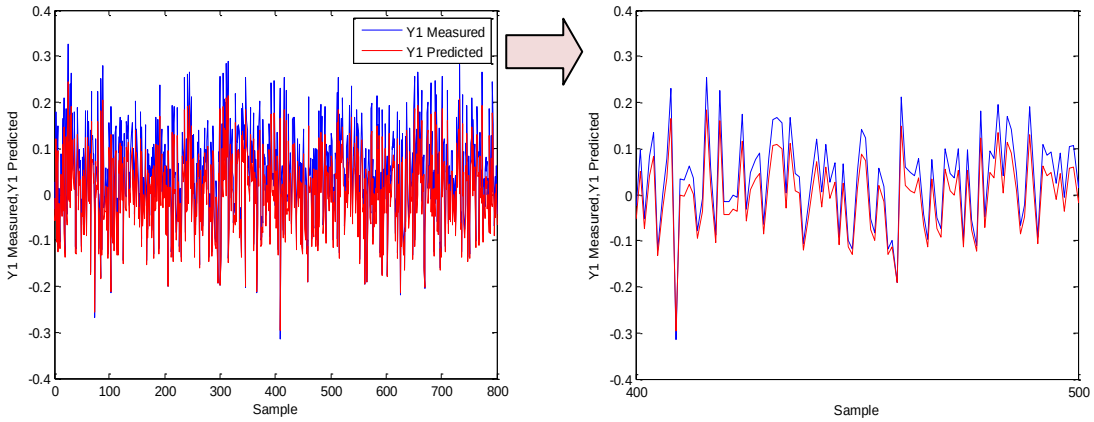

Figure 3.9 - Time series plot of measured and predicted values for the first quality variable for the validation data set

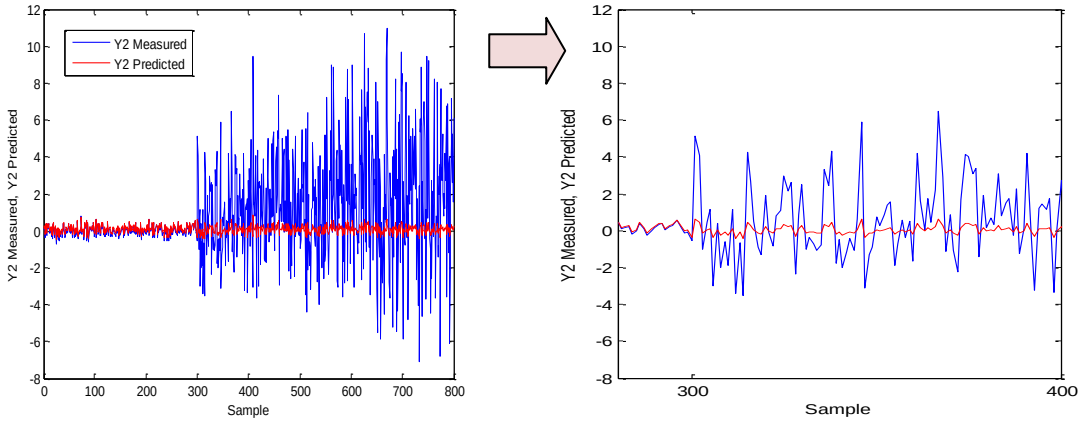

Figure 3.10 - Time series plot of measured and predicted values of the second quality variable for the validation data set

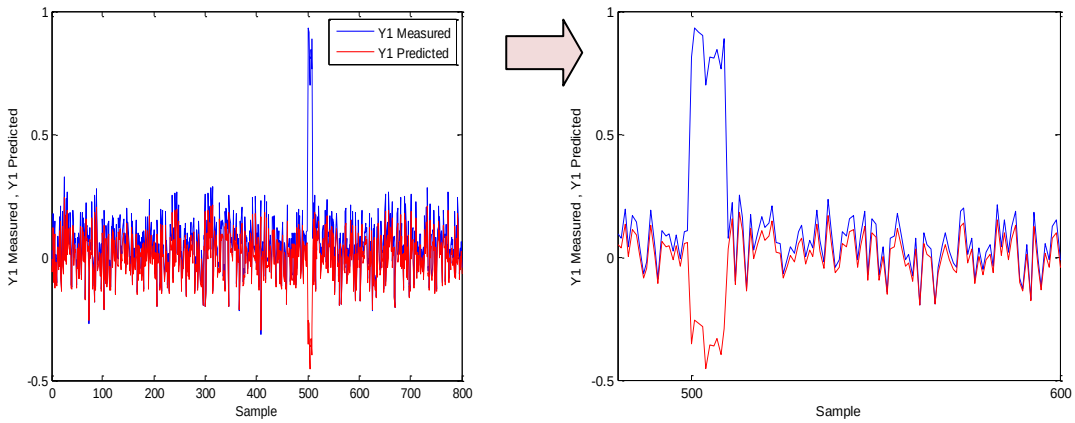

Figure 3.11– Time series plot of measured and predicted values for the first quality variable for the test data set

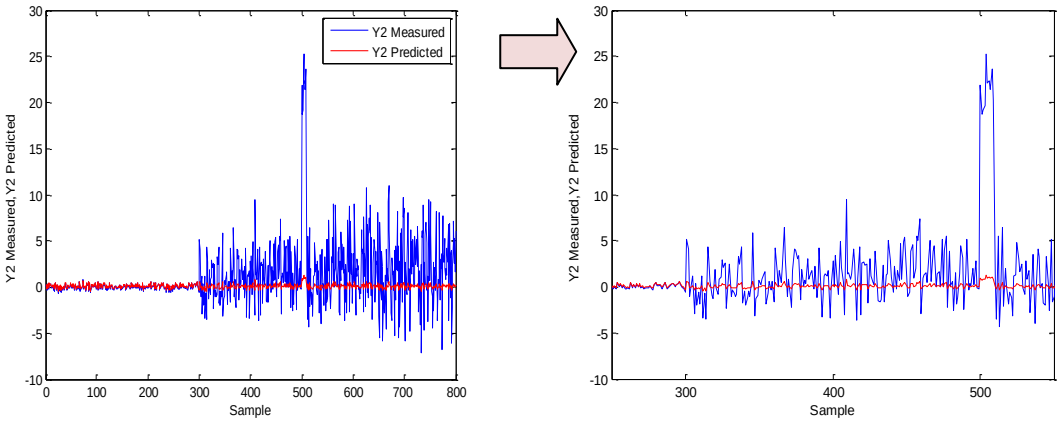

Figure 3.12– Time series plot of measured and predicted values for the second quality variable for the test data set

Figures 3.11 and 3.12 show that both quality variables are affected by the step change at sample number 500 and lasts for 10 samples. However, the PLS model fails to predict the process behaviour during this period. The residuals plots for both quality variables for the validation and test data sets show that conventional PLS model fails to predict the time varying behaviour (Appendix A).

Table 3.5 summarises the root mean squared error for the calibration, validation and test data sets. It can be seen that the root mean squared error of the first quality variable is not affected by the time varying behaviour and is well predicted and presents an acceptable value for the RMSE. However, the RMSE for the test data set is significantly large since the model fails to predict the behaviour of the quality variable under the introduced step change. The RMSE of the second quality variable has significantly increased since the model fails to predict both the time varying behaviour and the step change. It can be conclude that conventional PLS is inappropriate for modelling time varying process. The RMSE of the second quality variable is higher than the first quality variable due to the difference in the variability of the two variables, the first quality variable variability was ±0.3 whilst for the second quality variable, it was ±12.

Table 3.5 - RMSE of the calibration, validation and test data sets for the time varying process

Quality variables	Calibration data set	Validation data set	Test data set
	RMSE	RMSE	RMSE
Y1	0.03	0.05	0.137
Y2	0.09	2.62	3.49

3.9.4 Monitoring Charts

The monitoring results for the simulation exhibiting time varying process using conventional PLS are illustrated in Figures 3.13 and 3.14 for the calibration and validation data sets respectively. Figure 3.13 shows the time series plot for Hotelling's T^2 and the squared prediction error of the input and output spaces SPE_X and SPE_Y respectively. The three metrics indicate 1% and 5% of the signals lie out of statistical control for the 99% and 95% confidence limits respectively and this is statistically acceptable. More specifically the false alarm rate for Hotelling's T^2 and the squared prediction error of the input and output spaces SPE_X and SPE_Y are 5%, 5% and 5% respectively for the 95% confidence limits and 1% for the 99% confidence limit as shown in Table 3.6.

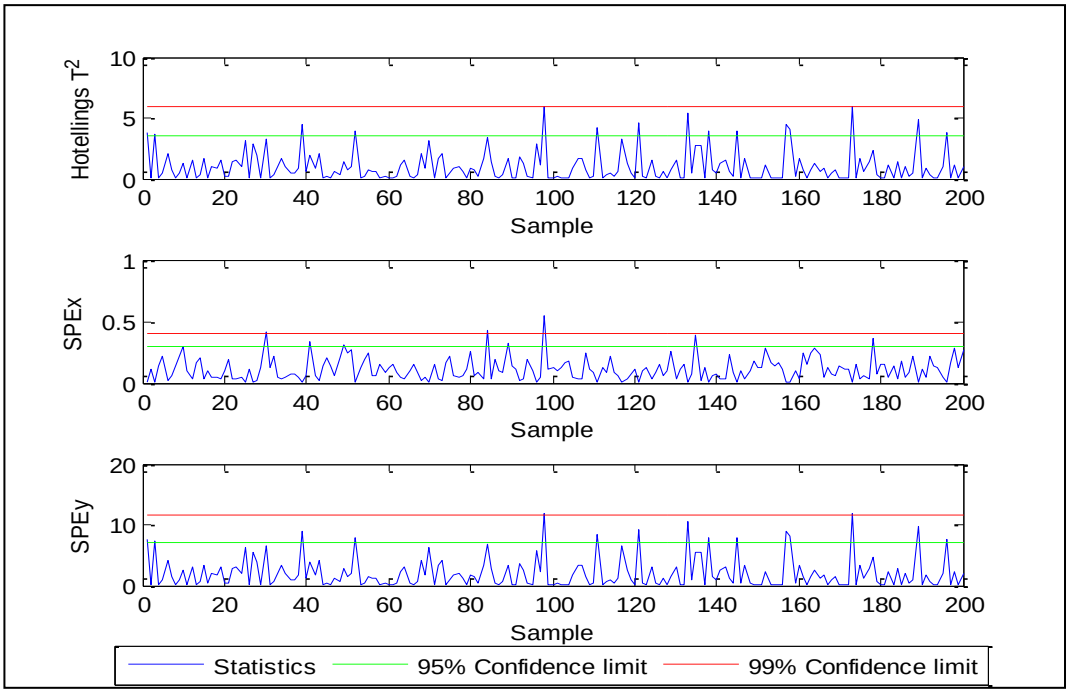

Figure 3.13 – Monitoring statistics for the calibration data set for time varying process

Table 3.6 - FDR and FAR based on conventional PLS

Data set	Calibration data set		Validation data set		Test data set	
Chart	FAR -95%	FAR -99%	FAR -95%	FAR -99%	FDR -95%	FDR -99%
Hotelling's T^2	5%	1%	4.75%	1%	90%	90%
SPE_X	5%	1%	4.87%	0.2%	90%	90%
SPE_Y	5%	1%	33.75%	31.8%	100%	100%

Figure 3.14 shows the monitoring charts for the validation data set where the time varying behaviour is observed in the SPE_Y metric as the behaviour differs to that of the calibration data set. The 95% and 99% confidence limits were these attained from the calibration data set. For Hotelling's T^2 and SPE_X indices, the number of out of statistical control signals was within the statistically acceptable limits of 5% and 1% of the total number of samples. The false alarm rate is 4.75% and 4.87% for Hotelling's T^2 and SPE_X monitoring chart respectively for the 95% confidence limit and 1% for the 99% confidence limit as shown in Table 3.6. On the other hand, for the SPE_Y which is affected by the time varying behaviour the number of false alarms is 33% and 31.8% which is not statistically acceptable as it exceeds 5% and 1% for the 95% and 99% confidence limits respectively as shown in Table 3.6.

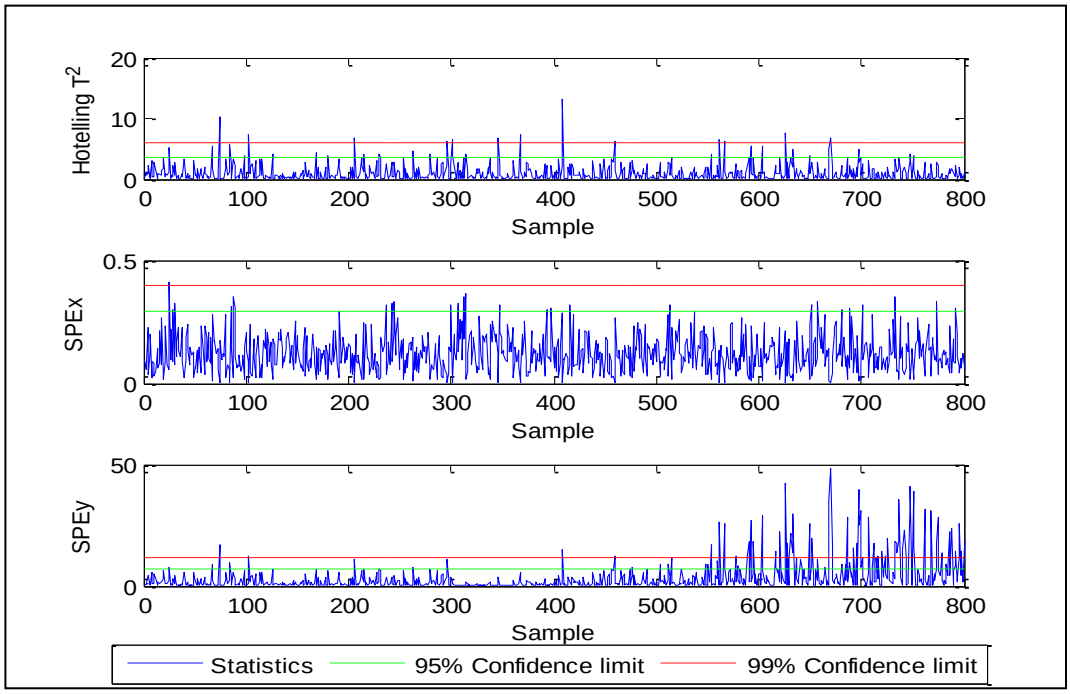

Figure 3.14 – Monitoring statistics for the validation data set for time varying process

For the validation data set, ARL0 is calculated based on a Monte Carlo approach where the simulation was repeated 50 times and for each run the run length (RL) was recorded and the ARL0 was calculated (Table 3.7). It can be seen that the ARL0 for the Hotelling's T^2 and SPE_X monitoring charts are satisfactory as the metrics remain within statistical control for a satisfactory number of samples prior to an out of statistical control being detected compared to the ideal ARL0 of 100 samples for the confidence level of 0.01. In contrast, the ARL0 for the SPE_Y chart is unsatisfactory as the time varying behaviour was detected and considered as an out of statistical control. This

indicates that the monitoring charts based on conventional PLS are not appropriate for the monitoring of time varying processes.

Table 3.7 - Average run length of the time varying process using PLS.

Chart	ARL0	ARL1
Hotelling's T^2	60	5
SPE_X	66	5
SPE_Y	7	6

Figures 3.15, 3.16 and 3.17 show Hotelling's T^2, SPE_X and SPE_Y for the test data set respectively. The confidence limits are those from the calibration data set. It can be seen that all three statistics are affected by the step change in the second predictor variable whilst only the SPE_Y is affected by the time varying behaviour, i.e. the behaviour of SPE_Y differs compared to that of the calibration data set due to the introduction of the ramp signal. The SPE_Y continuously violates the confidence limits, starting at t = 400, after the introduction of the ramp signal. During this period a step change was introduced at t = 500 and it can be seen that the signal violates the limit prior to, during and after the step change. The fault detection rate for the SPE_Y is 100% since the monitoring index continuously violate the limit post t=500. This concludes that the SPE_Y does not differentiate between the step change and time varying behaviour.

Similar to the conclusions of Wang et al.(2003), it can be concluded that conventional PLS is not appropriate for monitoring processes that exhibit time varying behaviour. Hotelling's T^2 and SPE_X monitoring charts are not affected by the time varying behaviour as the data is comparable to that used to the calibration data set. In addition both indices detect the step change successfully. The fault detection rate for both monitoring charts is 90 % (Table 3.6).

For the test data set, ARL1 is calculated based on a Monte Carlo approach (Table 3.7). For the current case it can be seen from the charts that the step change (process fault) is detected 1 sample after the introduction of the step change for Hotelling's T^2 and SPE_X. When the Monte Carlo method is applied, Table 3.7 shows the results for ARL1 which indicates that on average there is a delay in the fault detection. For example, Hotelling's T^2 and SPE_X detect the fault after 5 samples and SPE_Y detects the fault after 6 samples. These results are based on the 50 data sets generated under the same conditions.

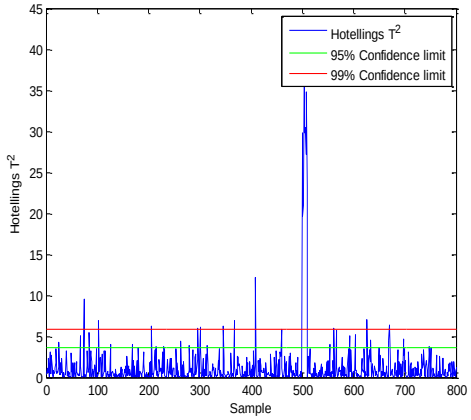

Figure 3.15 - Hotelling's T^2 for the test data set for time varying process

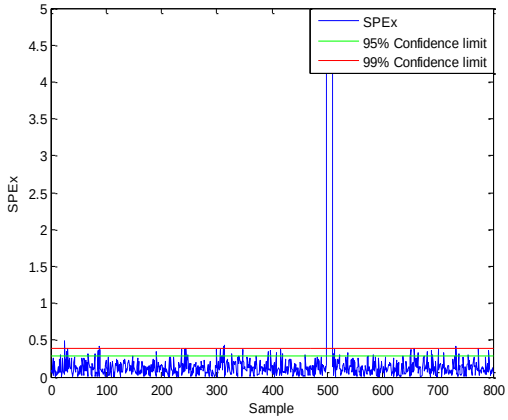

Figure 3.16 - SPE_X for the test data set for time varying process

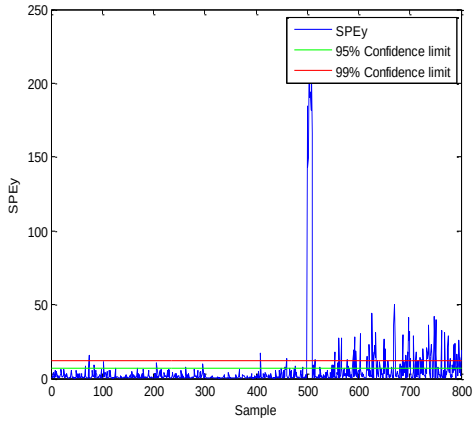

Figure 3.17- SPE_Y for the test data set for time varying process

The main conclusions following the application of conventional PLS to a time varying process are as follows:

- The conventional PLS algorithm fails to adapt to time varying behaviour.
- The prediction of the quality variables for the validation data set is poor compared to the calibration data set due to the failure of PLS to predict the time varying behaviour.
- The false alarm rate increases compared to the calibration data set
- Although the fault detection rate was high, the model failed to differentiate between the effect of the time varying behaviour and the process fault.

3.10 Application of PLS to a Non-stationary Process

3.10.1 Non-stationary Process Behaviour

Non-stationary behaviour is another area that challenges standard modelling and monitoring techniques (Box and Tiao, 1965; Box et al., 2008). The statistical properties of a non-stationary process include a time varying mean or a time varying variance or both hence underlying behaviour is unpredictable. Non-stationary behaviour can be a random walk, a deterministic trend, cyclical or a combination. A random walk non-stationary process is where there is a slow steady change in process behaviour and it can be with or without drift. A random walk with drift implies a change in the process mean and variance whilst a random walk without drift implies a change in the process variance. A deterministic trend is a non-stationary process where the process mean changes around a constant and is independent of a time trend. A cyclical non-stationary process implies that the process behaviour fluctuates around the mean. The non-stationary behaviour can be a consequence of a number of reasons for example seasonal changes or a filling and emptying cycle. In this section, it is demonstrated that conventional PLS is not appropriate for the monitoring of a non-stationary process through a simulation study.

3.10.2 Simulation of Non-stationary Process

A data set from a simulation of a non-stationary processes comprising two predictor variables and two response variables x_{1h}, x_{2h}, y_{1h} and y_{2h} respectively is constructed. The first step is to generate the initial predictor signal u_h from an Autoregressive Integrated Moving Average (ARIMA) model:

$$u_h(z^{-1}) = \frac{1 + az^{-1}}{(1 + bz^{-1})(1 - z^{-1})}\, \varepsilon(z^{-1}) \tag{3.44}$$

where a and b are 0.5, $\varepsilon(z^{-1})$ is obtained from a standard normal distribution $N(0,1)$ and z^{-1} is a back shift operator. The predictor and response variables are then defined as:

$$\begin{pmatrix} y_{1h} \\ y_{2h} \end{pmatrix}_t = \begin{bmatrix} c_{11} & c_{12} \\ c_{21} & c_{22} \end{bmatrix} \begin{pmatrix} x_{1h} \\ x_{2h} \end{pmatrix}_t \tag{3.45}$$

$$\begin{pmatrix} x_{1h} \\ x_{2h} \end{pmatrix}_t = \begin{pmatrix} u_h \\ u_h \end{pmatrix} + \begin{pmatrix} \varepsilon_{1h} \\ \varepsilon_{2h} \end{pmatrix} \tag{3.46}$$

where c_{11}, c_{12}, c_{21} and c_{22} are constant and are -0.2, 0.3, 0.1 and -0.05 respectively. ε_{1h} and ε_{2h} are uncorrelated random signals generated from a $N(0,0.2)$ distribution and u_h is the ARIMA signal for the h^{th} time instant and the subscript t refers to the actual process values. A random signal from a $N(0,0.1)$ distribution was augmented to the actual signal of the both predictor and response variables to mimic measurement noise:

$$\begin{pmatrix} y_{1h} \\ y_{2h} \end{pmatrix}_m = \begin{pmatrix} y_{1h} \\ y_{1h} \end{pmatrix}_t + \begin{pmatrix} \varepsilon_{3h} \\ \varepsilon_{4h} \end{pmatrix} \quad (3.47)$$

$$\begin{pmatrix} x_{1h} \\ x_{2h} \end{pmatrix}_m = \begin{pmatrix} x_{1h} \\ x_{1h} \end{pmatrix}_t + \begin{pmatrix} \varepsilon_{5h} \\ \varepsilon_{6h} \end{pmatrix} \quad (3.48)$$

where m denotes the measured values and ε_{3h}, ε_{4h}, ε_{5h} and ε_{6h} are random signals. This simulation is taken from Wang et al. (2003). In this study, 200 samples were used for model development and 800 samples for validation. A further data set was generated in this study which included a step change in the first input variable at sample t=500. This additional data set was generated to test the ability of the PLS monitoring charts to differentiate between non-stationary behaviour and a step change that is not considered as normal operation. Model development and the monitoring charts are presented in the following subsequent sections.

3.10.3 Model Development

The data is generated from the same signal, hence scaling was not considered as there is no issue resulting from different unit measurements. The results from the application of PLS to the calibration data are summarized in Table 3.8, Figures 3.18 and 3.19. The number of latent variables to retain was identified as one latent variable from cross-validation. From Table 3.8, the PLS model with one latent variable captures 99.2% of the total variation in the X-block and explains 83.5% of the variation in the Y-block. It can be seen that the second latent variables dose not capture any additional variation hence, one latent variable is sufficient to describe the process.

Table 3.8 - Percentage variance captured from PLS model for non-stationary process

LV	X-block		Y-block	
	LV	Cum	LV	Cum
1	99.2	99.2	83.5	83.5
2	0.8	100	0.1	83.6

Figure 3.18 and Figure 3.19 show the time series plots for the quality variables respectively for the calibration data set. An offset can be seen between the original and fitted values which is expected as the model does not explain all the variation within the process. The residual plots are given in Appendix A showing the difference between measured and fitted values.

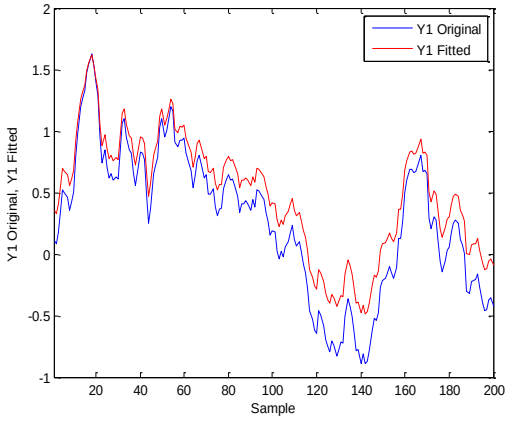

Figure 3.18 - Time series plot of original and fitted values for the first quality variable for the calibration data set

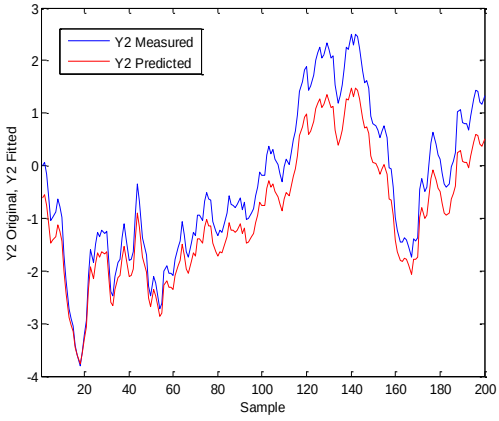

Figure 3.19 - Time series plot of original and fitted values for the second quality variable for the calibration data set

When the PLS model is applied to the validation and test data sets, Figures 3.20, 3.21, 3.22 and 3.23, it is evidence that there is an offset between the measured and predicted values. In addition, Figures 3.22 and 3.23 show that the model fails to predict the abnormal behaviour, step change at t=500. The residuals plots for the validation and test data sets, Appendix A, approved these observations.

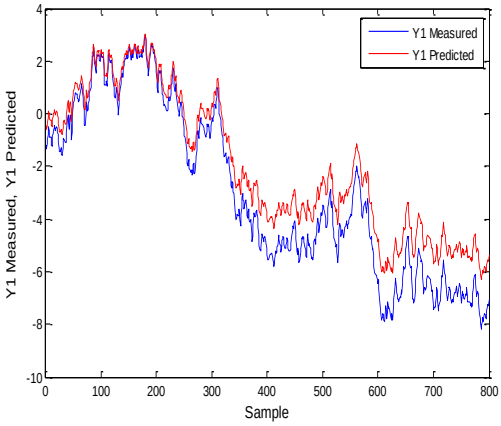

Figure 3.20 - Time series plot of measured and predicted values for the first quality variable for the validation data set

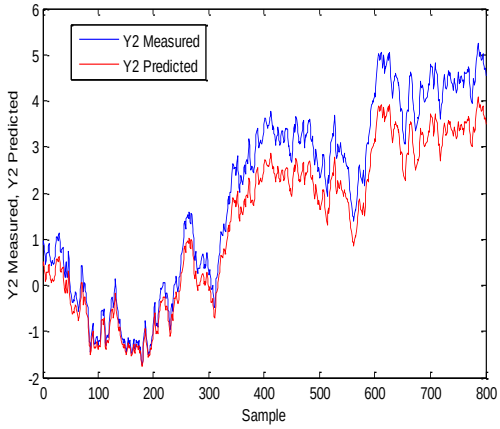

Figure 3.21 - Time series plot of measured and predicted values for the second quality variable for the validation data set

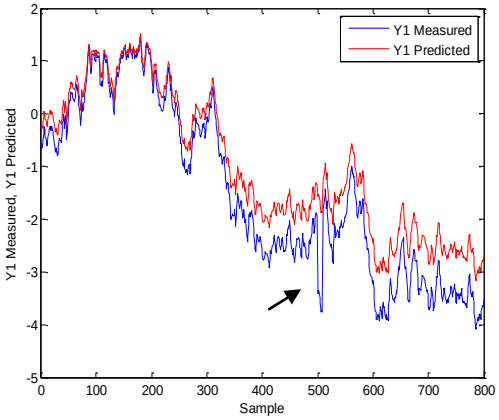

Figure 3.22 - Time series plot of measured and predicted values for the first quality variable for the test data set

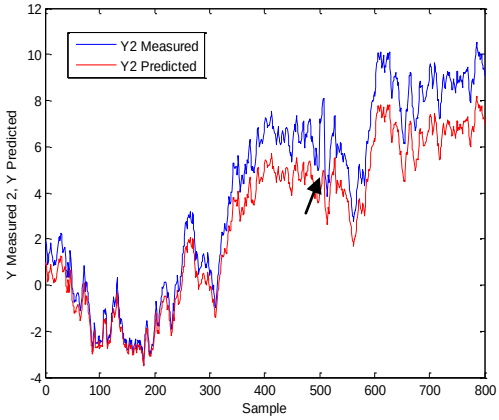

Figure 3.23 - Time series plot of measured and predicted values for the second quality variable for the test data set

Table 3.9 summarises the root mean squared error (RMSE) for the calibration, validation and test data sets. It can be seen that the RMSE for the validation and test data sets are larger in magnitude compared to the RMSE for the calibration data set for both quality variables. Although the prediction follows the trend for both quality variables, the number of false alarm is high when constructing the monitoring charts indicating that the model developed based on the calibration data set is inappropriate for the modelling of non-stationary processes. The results of the monitoring charts are presented in the following sections.

Table 3.9 - RMSE for the calibration, validation and test data sets

Quality variables	Calibration data set	Validation data set	Test data set
	RMSE	RMSE	RMSE
Y1	0.23	0.56	0.60
Y2	0.58	1.42	1.46

3.10.4 Monitoring Charts

The monitoring results for the non-stationary behaviour using conventional PLS are given in Figures 3.24 and 3.25. Figure 3.24 shows the monitoring metrics of Hotelling's T^2, SPE_X and SPE_Y for the calibration data set. It can be clearly seen that the charts show an acceptable number of out of statistical control samples as they are within the 5% of for the 95% confidence limit. The false alarm rate is 5%, 5% and 4.5% for the Hotelling's T^2, SPE_X and SPE_Y respectively as shown in Table 3.10.

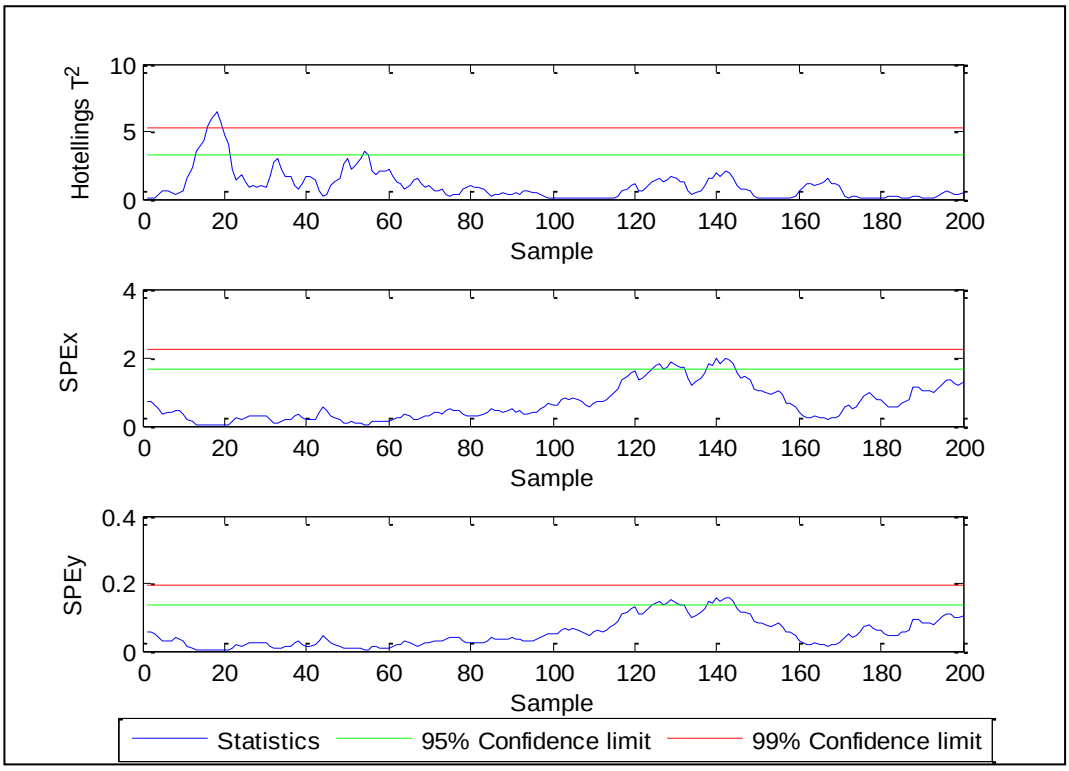

Figure 3.24- Monitoring statistics for the calibration data set

The monitoring result for the validation data set shows unsatisfactory performance as the number out of statistical control samples is more than 55% and for all the monitoring charts when the process represents nominal behaviour as shown in Figure 3.25. The false alarm rate confirms this as it is 58.1%, 59.9% and 60% for Hotelling's T^2, SPE_X and SPE_Y respectively for the 95% confidence limit and 55.7%, 58.1% and 58.7% for Hotelling's T^2, SPE_X and SPE_Y respectively for the 99% confidence limit which is statistically unacceptable (Table 3.10). These issues are caused by the non-stationary nature of the process and hence demonstrating that conventional PLS is inappropriate for the modelling of a non-stationary process.

Table 3.10- FDR and FAR based on conventional PLS

Data set	Calibration data set		Validation data set		Test data set	
Chart	FAR – 95%	FAR – 99%	FAR – 95%	FAR – 99%	FDR – 95%	FDR – 99%
Hotelling's T^2	5%	2.5%	58.1%	55.7%	-	-
SPE_X	5%	0%	59.9%	58.1%	100%	100%
SPE_Y	4.5%	0%	60%	58.7%	100%	100%

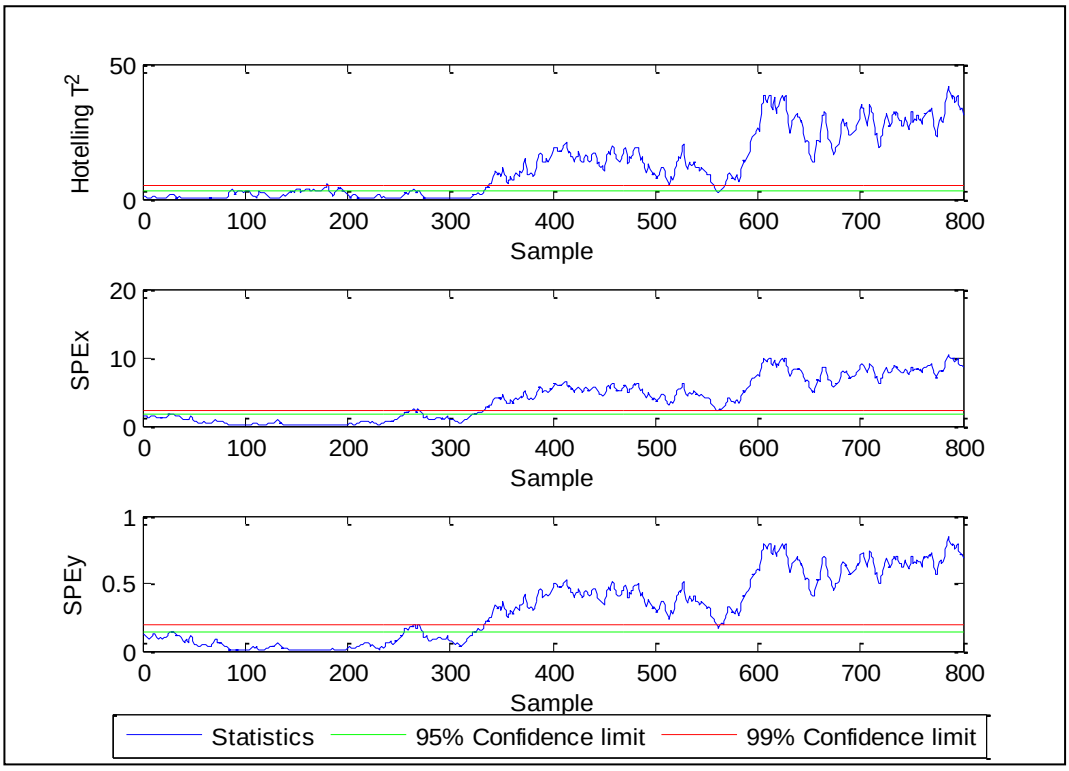

Figure 3.25- Monitoring results by PLS for validation data set

The ARL0 is calculated for the validation data set based on a Monte Carlo approach where the simulation was repeated 50 times (Table 3.11). For the data set illustrated, it can be seen that the monitoring metrics violate the limits after a few samples during the monitoring period (Figure 3.25). More specifically, the Hotelling's T^2, SPE_X and SPE_Y metrics violate the confidence limits at t = 80, t = 13 and t=15 respectively. Following the implementation of the Monte Carlo method, the ARL0 is 47, 37 and 33 for Hotelling's T^2, SPE_X and SPE_Y respectively (Table 3.11).This indicates that the monitoring charts based on conventional PLS tend to produce early false alarms compared to the ideal ARL0 of order of 100 samples, i.e. the monitoring metrics violates the confidence limits more rapidly while the process represents nominal operations.

Table 3.11 - The average run length for the non-stationary process.

Chart	ARL0	ARL1
Hotelling's T^2	47	5
SPE_X	37	3
SPE_Y	33	4

The monitoring charts following the application of the model to the test data set where a step change was introduced at t = 500 are given in Figures 3.26, 3.27 and 3.28. Figures 3.27 and 3.28 show that the SPE_X and SPE_Y charts detected the step change however, it can be seen that the samples prior to and after the step change are already out of statistical control due to a failure of PLS to model the non-stationary behaviour. Consequently, the PLS model fails to discriminate between a process fault, a step change, and the non-stationary nature of the process. The Hotelling's T^2 monitoring chart (Figure 3.26) was not affected by the step change as there is no evidence of the presence of a step change at t = 500. Therefore, the fault detection rate is not calculated. Although the fault detection rate, Table 3.10, is 100% for the SPE_X and SPE_Y monitoring charts, it is unreliable as all the metrics violate the confidence limits from t = 320 due to the non-stationary nature of the process.

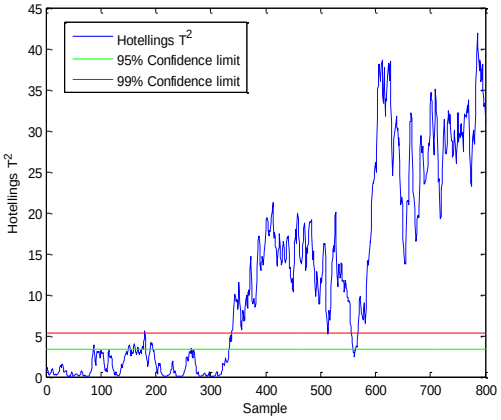

Figure 3.26 – Hotelling's T^2 for the test data set

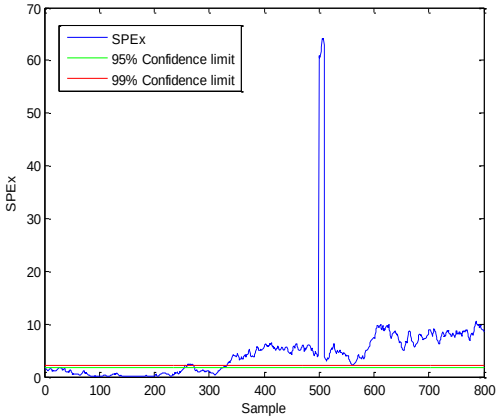

Figure 3.27 – SPE_X for the test data set

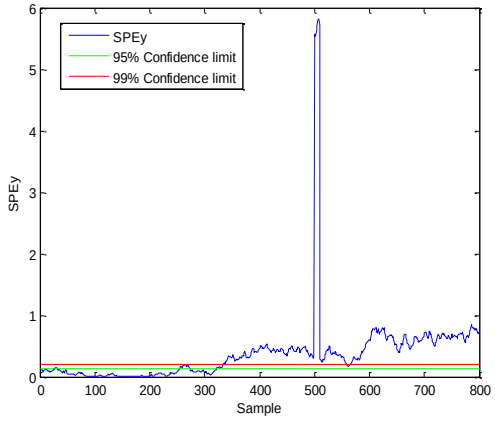

Figure 3.28 – SPE_Y for the test data set

The ARL1 is calculated for the test data set for all the monitoring charts based on the Monte Carlo method. For the illustrated test data set used for constructing the monitoring chart (Figures 3.26 to 3.28), it can be seen that the ARL1 is 0 for the SPE_X and SPE_Y monitoring charts. However, this occurred as the monitoring metrics in the period prior to the step change are already in violation of the confidence limits. This indicates that the fault is detected immediately. Following the implementation of the Monte Carlo method, it can be seen that the step change is detected after 5, 3 and 4 samples for Hotelling's T^2, SPE_X and SPE_Y charts respectively indicating that on average there is a time delay in the fault detection.

The main conclusions following the application of conventional PLS to a non-stationary process are as follows:

- The conventional PLS algorithm fails to model the non-stationary behaviour.
- The prediction of the quality variables for the validation and test data sets is poor compared to the calibration data set due to the failure of PLS to predict the non-stationary behaviour.
- There is a significant increase in the number of false alarms.
- The fault detection rate is high due to the nature of the process as most of the samples violate the confidence limits. Consequently, the model fails to distinguish between the fault and the nature of the process hence the fault detection rate is unreliable.

3.11 Chapter Summary and Conclusions

In this chapter, a general overview has been presented of the multivariate projection approach of partial least squares (PLS). A major part of the chapter focused on describing PLS and two of its extensions, dynamic PLS (DPLS) and multiblock PLS (MBPLS). These are the core methodologies that are combined and extended in the subsequent chapters. The motivation for reviewing these methodologies was based on the fact that most industrial processes exhibit dynamic characteristics and consist of multiple units operations and hence it is important to consider both characteristics simultaneously. These extensions help to achieve the ultimate goal of the thesis, the monitoring of the whole process as well as that of individual unit operations. In addition, two or three of the approaches can be combined to develop monitoring schemes for specific applications. For example the combination of multiblock PLS and

dynamic PLS is used for constructing a monitoring scheme for the Tennessee Eastman process in Chapter 6.

It has been shown that conventional PLS is inappropriate to model time varying and non-stationary processes. This is a consequence of the model being developed from nominal data under specific operating conditions and being then applied to unseen data which were collected under different operating conditions due to the time varying or non-stationary behaviour of the process. Consequently monitoring performance deteriorates over time. This conclusion was previously reported by Wang et al. (2003). In this thesis, the statistical concepts of average run length (ARL), fault detection rate (FDR) and false alarm rate (FAR) are used to evaluate the efficiency of the monitoring charts. The conclusions drawn from the metrics ARL, FDR and FAR indicate that the monitoring charts based on conventional PLS are inefficient for processes that exhibit time varying and non-stationary behaviour.

An issue that is of increasing importance is that of the differentiation between changes in operating conditions and process faults as conventional PLS failed to do so. This was observed from the failure of the PLS to discriminate between a step change effect and time varying and non-stationary behaviour. This issue is often ignored in the published literature and it is important to investigate further extensions of PLS to meet this requirement. The next chapter presents recursive PLS approaches providing a critical review of the methodology and its adaptive limits and introduces a robust recursive PLS algorithm with adaptive limits.

Chapter 4

Real Time Monitoring using Recursive PLS and its Extensions

4.1 Introduction

Most industrial processes exhibit changing behaviour over time materialising in time varying and non-stationary process behaviour. In some cases the process dynamics change as a result of a change in the relationship between process variables and hence the model that was built based on historical data is unable to describe the current state of the process. In the previous chapter, it was shown that conventional Partial Least Squares (PLS) was inappropriate for the monitoring of non-stationary and time varying processes. Furthermore, it has been shown in the literature that conventional PLS is unable to capture process dynamics caused by autocorrelation (Kaspar and Ray, 1993; Lakshminarayanan et al., 1997b) and model the nonlinear relationships between measurements (Wold, 1992; Dong and McAvoy, 1996). Despite the ability of conventional PLS to reduce the dimensionality of a problem and deal with ill-conditioned data, the statistical indices of false alarm rate (FAR) and average run length (ARL) indicated that the false alarm was increased and it was unable to identify the onset of the fault when applied to industrial processes that did not exhibit steady state behaviour.

One solution to the aforementioned issues, changing behaviour, is recursive PLS (RPLS) (Helland et al., 1992; Qin, 1998b). RPLS is an on-line modelling and monitoring approach that was proposed to capture dynamic changes in a system and its application has been extended to model time varying processes (Helland et al., 1992; Qin, 1993; Qin, 1998b). Different RPLS approaches have been proposed in the literature and these are reviewed in this chapter. One issue that can arise in online modelling is the presence of outlying samples and these are used to update the PLS model, then the resulting model will not be representative of process behaviour.

In this chapter an improved methodology, robust adaptive PLS (RAPLS), is proposed that recursively updates the PLS model, if and only if the incoming sample represents nominal process behaviour. The proposed approach also enables the detection of outliers which is an enhancement over the approach proposed by Wang et al. (2003). This approach can be extended to, robust adaptive dynamic PLS (RADPLS), to account for autocorrelated data, i.e. where the process samples are not time independent. The concept has also been extended to deal with processes that comprise multiple

operational units (Chapter 6). The proposed approach is tested on a simulation of a time varying process and a non-stationary process and in Chapters 5 and 6 the concepts are applied to simulated industrial processes.

4.2 Objectives

Within this chapter

- The existing RPLS methods for the real time modelling and monitoring of complex process behaviour are reviewed prior to extending the concept to incorporate adaptive confidence limits (APLS) (Wang et al., 2003)
- The RPLS with adaptive confidence limits (APLS) approach is further extended adaptive dynamic PLS (ADPLS) to handle autocorrelated samples in a recursive manner and apply confidence limits that are updated based on the monitoring statistics of the processes,
- A robust adaptive PLS (RAPLS) algorithm is developed to handle statistical outliers.
- The Robust Adaptive PLS (RAPLS) concept is extended to handle autocorrelated samples, robust adaptive dynamic PLS (RADPLS).
- The statistical indices of average run length (ARL), false alarm rate (FAR) and fault detection rate (FDR) are used to quantify the efficiency of the monitoring charts for APLS, RAPLS, ADPLS and RADPLS.

4.3 Recursive PLS (RPLS) Methods

Recursive PLS (RPLS) aims to update the calibration model (Equation 4.1) when new data $\{\mathbf{X}_i, \mathbf{Y}_i\}$ becomes available:

$$\{\mathbf{X}, \mathbf{Y}\} \xrightarrow{\text{PLS}} \{\mathbf{T}, \mathbf{P}, \mathbf{Q}, \mathbf{U}, \mathbf{W}, \mathbf{B}\} \tag{4.1}$$

where $\mathbf{X}$ and $\mathbf{Y}$ are the initial input and output matrices, $\mathbf{T}$ and $\mathbf{U}$ are the scores matrices; $\mathbf{P}$ and $\mathbf{Q}$ are the loadings of the input and output matrices respectively; $\mathbf{W}$ is the matrix of PLS weights and $\mathbf{B}$ is a diagonal matrix of the inner model coefficients. The following section presents the historical development and a review of the existing RPLS approaches.

The first step involves developing a reference model based on one of the existing PLS models previously reviewed in Chapter 3 (Table 3.1). Two families of recursive

algorithms are described in the literature to update a linear PLS model. The first one is based on the NIPLAS algorithm, where the PLS parameters are calculated in an iterative manner (Helland et al., 1992; Wold, 1994; Qin, 1998a; Wang et al., 2003). The second family utilises the kernel PLS algorithm (Lindgren et al., 1993; Dayal and MacGregor, 1997b). In this thesis, the methods from the first family of algorithms are reviewed. Figure 4.1 summarises the different recursive PLS approaches and their specific features.

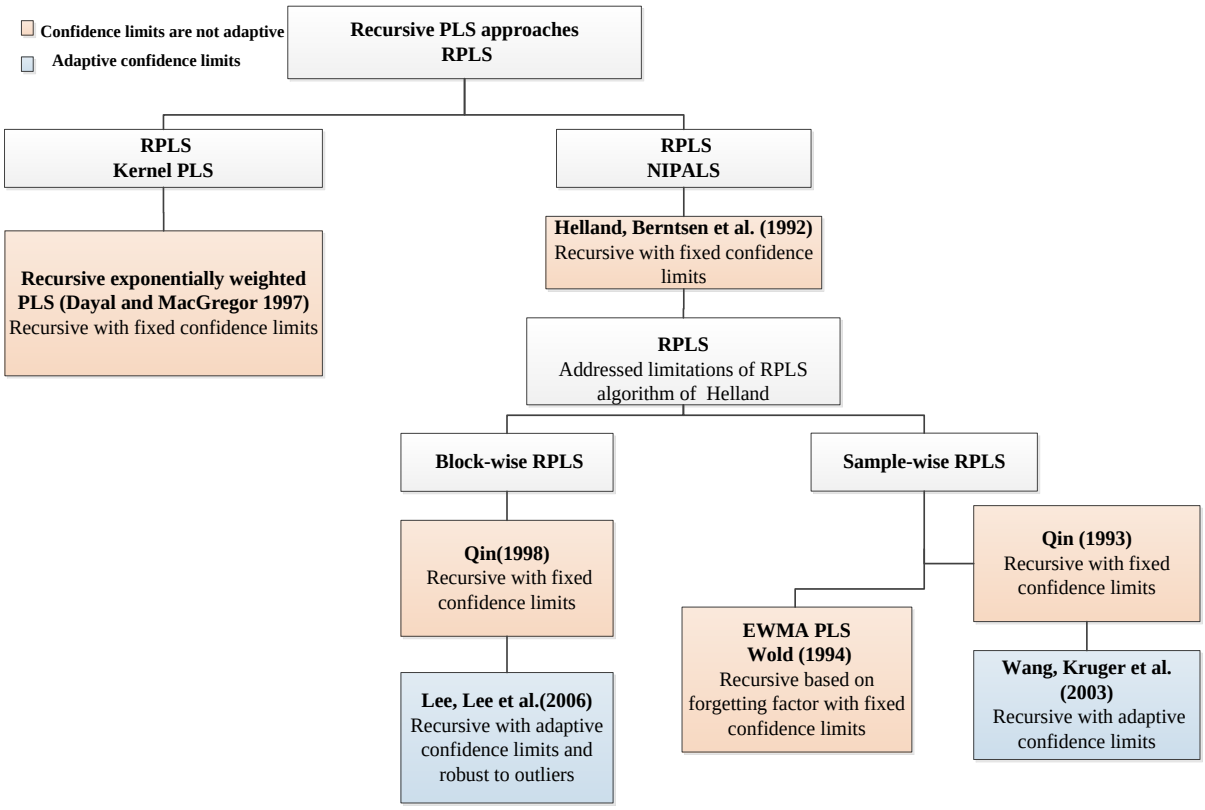

Figure 4.1- Recursive PLS approaches

The first recursive PLS (RPLS) algorithm was proposed by Helland et al. (1992). Their approach mainly comprised two steps. First, the original data sets ($\mathbf{X}_{\text{old}}$) and ($\mathbf{Y}_{\text{old}}$) were represented by their PLS loading matrices and diagonal matrix of inner model coefficients (i.e. **P**, **Q** and **B** matrices) and the new data $\mathbf{X}_{\text{i}}$ and $\mathbf{Y}_{\text{i}}$ was appended to these loading matrices (Equation 4.2). PLS was then applied to the updated data matrices. Consequently, the previous PLS model is updated in a recursive manner.

$$\mathbf{X}_{\text{new}} = \begin{bmatrix} \mathbf{P}' \\ \mathbf{X}_{\text{i}} \end{bmatrix};\ \mathbf{Y}_{\text{new}} = \begin{bmatrix} \mathbf{BQ}' \\ \mathbf{Y}_{\text{i}} \end{bmatrix} \tag{4.2}$$

Helland et al. (1992) stated that for their RPLS algorithm only a few latent variables should be retained. However, Qin (1993) pointed out that by retaining only a few latent variables during model updating, a loss of information may materialise. Consequently, he proposed retaining the number of latent variables equal to the rank of **X**. A limitation of the approach of Helland et al. (1992) was discussed by Dayal and MacGregor (1997b) who stated that the RPLS algorithm was slow compared to kernel based recursive PLS.

Wold (1994) proposed an exponentially weighted moving average (EWMA) approach for both principal component analysis (EWMA-PCA) and partial least squares (EWMA-PLS). The EWMA-PLS approach consists of two main parts. The first is one step ahead forecasting of the scores and predicting of the response. Moreover, the initial model is conserved through memory matrices to control the updating process. The second part involves updating the existing PLS model and the memory matrices. The details of the EWMA-PLS algorithm are provided by Wold (1994) and in general the EWMA-PLS algorithm comprises the following steps:

Step 1. Select the forgetting factor (λ) based on the historical data or experience

Step 2. Select the initial data matrices $\mathbf{X}_0$ and $\mathbf{Y}_0$, and calculate centring and scaling parameters, i.e. mean and standard deviation

Step 3. Derive the initial PLS model from the normalized data with *a* latent variables

Step 4. Initiate the EWM-PLS memory matrix by including initial data vectors that correspond to the maximum and minimum score values of each model dimension

Step 5. Initiate the weight memory matrices $\mathbf{W}_{\mathrm{mem},a}$ for each latent variable by including $\mathbf{w}_a'$ as first raw.

Step 6. Initiate the long memory matrices $\mathbf{Q}_{\mathrm{ref},a}$ identical to $\mathbf{W}_{\mathrm{mem},a}$

Step 7. Calculate a one-ahead forecast of the scores $\hat{\mathbf{t}}_{a,\mathrm{t+1}}$ using the forgetting factor as follows:

$$\hat{\mathbf{t}}_{\mathrm{t+1}} = \lambda \mathbf{t}_t + (1-\lambda)\hat{\mathbf{t}}_{\mathrm{t}}$$

Step 8. Calculate one-ahead predicted response $\hat{\mathbf{y}}_{\mathrm{t+1}}$ using Step 7

Step 9. Get the observed sample at t+1 and check against spikes, unwarranted rotations by comparing with memory matrices in order to force the new updated model to not

differ compared to the initial model. The new observation is then normalized using scaling parameter from the previous step. The actual scores and residuals are then calculated.

Step 10. Update the scaling parameters by means of residuals

Step 11. Update PLS model by iterating until convergence

Step 12.Update memory matrices as described in steps 4 to 6. Go for step 7 for the next time point.

Wang et al. (2003) pointed out that the value of the weighting parameter, λ, used to update the PLS model may control the outcome, since it determines the balance between the old and the new data in the updating procedure. This balance may not be appropriate all the time especially when implemented on an industrial process that exhibits complex behaviour. In addition, the use of initial model to control the updating process is not appropriate since the initial model does not reflect the current behaviour. Furthermore, Wold (1994) described the second part of the algorithm as complicated. Consequently, it is impractical to implement such an approach when a huge amount of data is available over a short time period due to the use of data acquisition systems.

Qin proposed two recursive algorithms for the updating of a PLS model; sample-wise RPLS (1993) and block-wise RPLS (1998b). The aim of the block-wise RPLS algorithm is to develop a PLS sub-model using the NIPALS algorithm based on a block of new data. The block-wise RPLS procedure (Figure 4.2) comprises 3 steps, first a block size is selected, BL, that is used for the model updating process. Secondly, a PLS model is developed based on the reference data set $\{\mathbf{X}_1, \mathbf{Y}_1\}$ and the model is represented though its loadings and inner regression coefficients matrices, i.e. $\mathbf{P}_1$ $\mathbf{Q}_1$ and $\mathbf{B}_1$. When a new block of data, $\{\mathbf{X}_2, \mathbf{Y}_2\}$, the size being equal to that of the block size, a sub-model is developed and represented by its loadings and inner regression coefficients matrices, i.e. $\mathbf{P}_2$ $\mathbf{Q}_2$ and $\mathbf{B}_2$. The next step is to combine the parameters of the first and second PLS models to form the recursive data matrices:

$$\mathbf{X}_{\text{new}} = \begin{bmatrix} \mathbf{P}_1' \\ \mathbf{P}_2' \end{bmatrix}, \mathbf{Y}_{\text{new}} = \begin{bmatrix} \mathbf{B}_1\mathbf{Q}_1' \\ \mathbf{B}_2\mathbf{Q}_2' \end{bmatrix}$$

The final step is to apply PLS to the new data matrices and represent the model by the loadings and inner regression coefficients matrices, i.e. $\mathbf{P}_{2c}, \mathbf{Q}_{2c}$ and $\mathbf{B}_{2c}$, consequently the previous model is updated and these steps are repeated whenever a new block of

data becomes available. Qin (1998b) extended this approach to block-wise RPLS based on a forgetting factor λ, that is used to weight the parameters of the initial model and to discount the old information in favour of the information contained in the new block, and applied block-wise RPLS to an industrial application, a catalytic reformer to predict octane number.

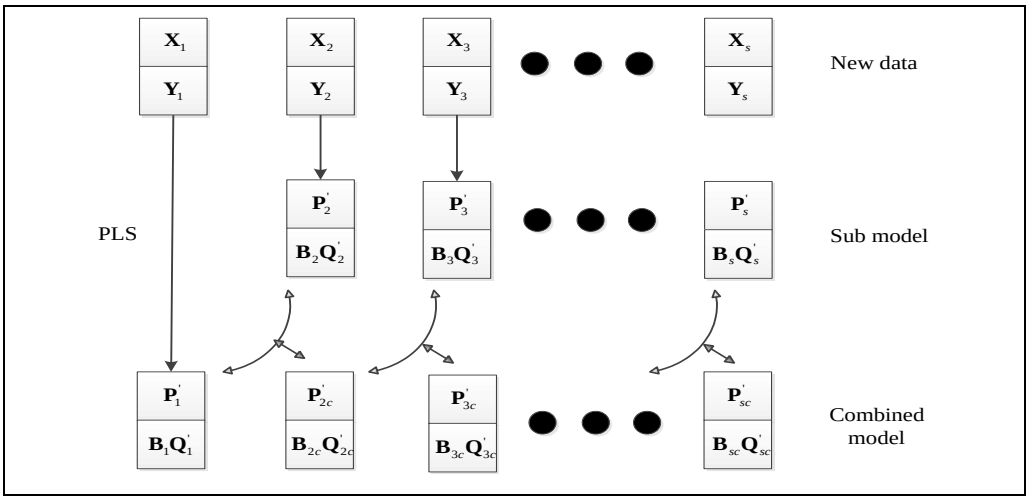

Figure 4.2 – A recursive process for Block-wise RPLS (Qin, 1998b)

This procedure requires significant computational effort in terms of developing the sub-models and then reapplying PLS to update the old model. This algorithm is considered to be a form of "blind" updating as the new data may contain non-conforming samples thereby influencing the model. Furthermore, the confidence limits of the reference model are used for the block-wise RPLS monitoring charts consequently they are not reflective of the updated model. Wang et al. (2003) discussed some limitations of block-wise RPLS:

- The number of the samples included in the sub-PLS model may affect the results. When the block size is small the PLS model is updated quickly whereas for large block sizes, model update is delayed. Consequently, different block sizes result in different PLS models.
- The normal operating data used for modelling is discounted in favour of the new block that may not represent the process since the data can be generated during an abnormal event.
- The forgetting factor may discount the old model based on specified weight which may not accurate all the time.

The sample-wise RPLS algorithm proposed by Qin (1993) updates the PLS model whenever a new data sample is available. In addition, he proposed its extension to

system identification, consequently the RPLS model can account for process dynamics caused by autocorrelation. This approach updates the PLS model recursively to account for changes in the process and is used as a basis for developing the proposed methods in this thesis (§4.3.1). Issues that may arise include:

- The confidence limits used are based on the historical or reference data which may not represent the current state of the process.
- The new sample is allowed to contribute to model updating without considering that the sample may represent an outlying sample. Consequently, this form of RPLS may be viewed as "blind" model updating. This issue is discussed in detail in §4.3.3.1.

Wang et al. (2003) extended the sample-wise recursive PLS algorithm to include adaptive confidence limits, Adaptive PLS (§4.3.2). The main idea besides model updating is to update the confidence limits of the monitoring statistics using a window of length (L) of the previous monitoring statistics, i.e. Hotelling's T^2, SPE_X and SPE_Y. These statistics will typically reflect the performance of the current sample and therefore, are more meaningful when calculating the confidence limits as they tend to exhibit same behaviour. However, both sample wise RPLS and APLS update the model without considering whether the sample is reflective of normal operation, i.e. the new coming samples may be an outlier or generated from abnormal event. These approaches are used as the basis for developing a new improved APLS algorithm in this work (§4.4).

Lee et al. (2006a) extended the block-wise RPLS algorithm to robust adaptive block-wise RPLS. The idea is to screen the incoming data based on the combined index, mainly combines the univariate monitoring statistics of Hotelling's T^2 and squared prediction error (SPE_X), prior to the development of a PLS sub-model. If the data represents nominal process operation, i.e. the combined index remains within a state of statistical control, the data will be used for the model updating process (Figure 4.3). They proposed two strategies to deal with outlying data. First when the combined index breaches the confidence limit, a hard threshold is proposed, i.e. all the outlying data are excluded from the model update, alternatively a soft threshold can be applied where the entire data is weighted prior to model updating process. The robust adaptive block-wise RPLS algorithm starts with the development of a reference model based on historical data. When a new block of data becomes available, the monitoring statistics including

Hotelling's T^2, squared prediction error (SPE_X) and the combined index are calculated. For the hard threshold, the outlying samples are discarded from the model updating process with the remaining new data used for model updating. For the soft threshold approach, a weight is calculated based on the combined index that results in the outlying samples behaving as they were generated from nominal process. The weight calculation is discussed in §4.3.3.1.

Two issues associated with this approach materialise. First, all the data that violate the combined index threshold are considered to be outlying data and there is no distinguishing between whether they are generated as statistical outliers or due to process fault. This thus allows for a process fault to contribute to the RPLS model. Secondly, different block size will result in different models.

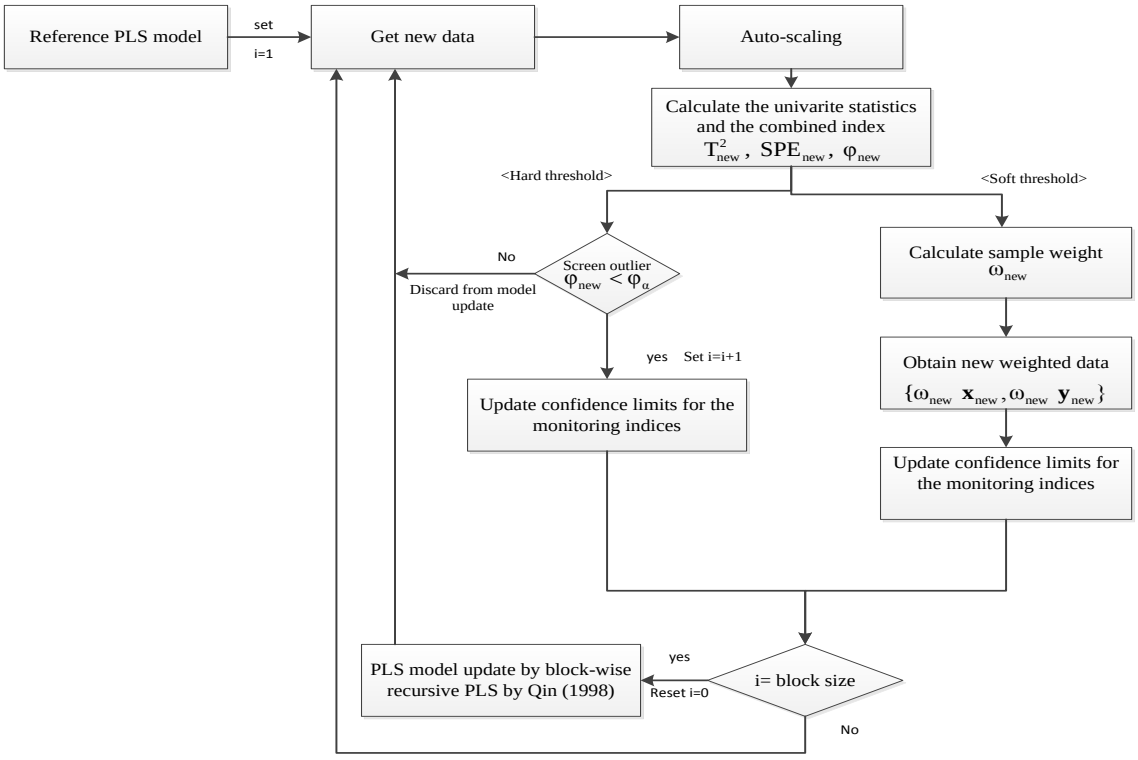

Figure 4.3 - Robust block-wise RPLS (Lee et al., 2006a)

The other class of methods are based on the kernel PLS algorithm. The first recursive algorithm was exponentially weighted PLS (Dayal and MacGregor, 1997b). In this approach the model is updated in a recursive manner based on a forgetting factor, which helps determine how much previous information should be discounted in favour of new data. The forgetting factor can be either fixed or variable. In the case of a constant forgetting factor, the old data is discounted continuously without any investigation as to

whether the new data contains representative information hence, information may therefore be lost. On the other hand, for a variable forgetting factor the old data is only discounted when the new data contains information. The full algorithm is presented in Appendix B.

Although this approach considers the relevance of the new data, it does not identify if the information in the new data results from a change in the process conditions or from outlying samples. The confidence limits of the monitoring statistics are assumed to be calculated based on the historical data as no information on this aspect was provided in the paper (Dayal and MacGregor, 1997b).

4.3.1 Sample-wise Recursive PLS

In sample-wise RPLS proposed by Qin (1993), a reference model (Equation 4.1) is developed based on normal operating data using the PLS algorithm (NIPALS). Once a new sample $\{\mathbf{x}_i, \mathbf{y}_i\}$ becomes available, the PLS model is updated through the application of PLS to the new matrices:

$$\mathbf{X}_{\text{new}} = \begin{bmatrix} \mathbf{P}' \\ \mathbf{x}_i \end{bmatrix};\ \mathbf{Y}_{\text{new}} = \begin{bmatrix} \mathbf{BQ}' \\ \mathbf{y}_i \end{bmatrix} \tag{4.3}$$

where **P** and **Q** are the loadings of the input and the output matrices **X** and **Y** respectively. **B** is a diagonal matrix of the inner regression coefficients. Qin (1993) pointed out that applying PLS to the data matrix in Equation 4.3 results in the same PLS model as would be attained when applying PLS to the following data matrices:

$$\mathbf{X}_{\text{new}} = \begin{bmatrix} \mathbf{X} \\ \mathbf{x}_i \end{bmatrix};\ \mathbf{Y}_{\text{new}} = \begin{bmatrix} \mathbf{Y} \\ \mathbf{y}_i \end{bmatrix} \tag{4.4}$$

The approach proposed by Qin (1993) significantly reduces the computational effort and time required to identify the RPLS model compared to the approach based on Equation 4.4. This is because the dimension of the data matrices is reduced when using PLS parameters and hence the model can be identified faster than when using the whole data set each time to identify the RPLS model. In addition, it requires less memory as only the previous PLS parameters, which represent the old data, are retained for model updating. Qin (1993) stated that in practical applications, the number of latent variables (a) to be retained may vary and hence cross validation or variance explained

should be used. In this thesis, the effect of varying the number of latent variables is assessed in Chapter 5.

Similar to conventional PLS, the monitoring statistics of RPLS are based on the univariate statistics of Hotelling's T^2 and Squared Prediction Error (SPE_X and SPE_Y) of the input and output spaces respectively. For a new observation $\{\mathbf{x}_i, \mathbf{y}_i\}$ the monitoring statistics can be calculated based on §3.5.

Qin (1993) did not provide an updating procedure for calculating the confidence limits. Consequently, the confidence limits calculated from the reference model are used for the monitoring statistics of the new observation which may result in an increase or in some case a decrease in the number of false alarms. The calculation of the confidence limits was previously presented in Chapter 3 (Equation 3.9 and Equation 3.12). In addition, the algorithm updated 'blindly' as no investigation has been carried on the sample type.

4.3.2 Adaptive PLS (APLS)

Wang et al. (2003) further extended the sample-wise RPLS approach by introducing adaptive confidence limits, adaptive PLS (APLS), and extending it to recursive multiblock PLS. The APLS algorithm is presented in Figure 4.4. As for sample-wise PLS, the first step in APLS is to develop a reference PLS model from historical data. When a new sample becomes available, Hotelling's T^2 and Squared Prediction Error (SPE_X and SPE_Y) of the input and output spaces respectively are calculated according to §3.5.

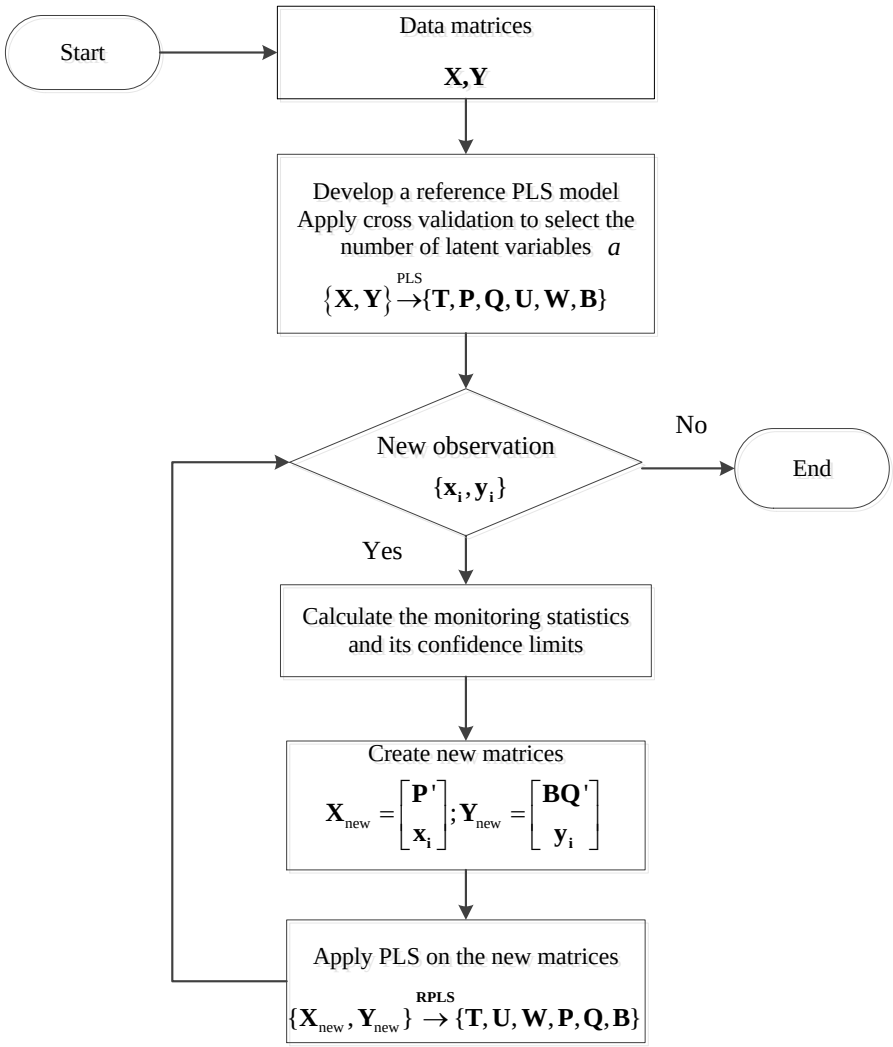

Figure 4.4 - Recursive PLS with adaptive confidence limits (APLS)

The adaptive confidence limits by Wang et al. (2003) were developed on the following basis:

- MacGregor and Kourti (1995) noted that any univariate statistics (ξ) that are calculated based normally distributed process variables, follow a Chi-squared distribution. Based on that, the univariate monitoring statistics following the application of PLS follow the Chi-squared distribution. This is because they are calculated based on the latent variables, which are linear combination of the original variables and by the central limit theorem they are approximately normally distributed.
- As each univariate statistic (ξ), i.e. Hotelling's T^2,SPE_X and SPE_Y, represents a sum of squared values, Box (1954) and Jackson and Mudholkar (1979) stated

that the confidence limits of a univariate statistic ($\xi > 0$), which has a mean of $\bar{\xi}$ and a variance of σ_ξ, can be obtained as:

$$\xi^{(1-\alpha)} = g\chi^2(\alpha, h) \quad (4.5)$$

where $\xi^{(1-\alpha)}$ represent the confidence limit, g and h are given by:

$$g = \sigma_\xi/(2\,\bar{\xi}) \quad (4.6)$$

$$h = (2\bar{\xi}^2)/\sigma_\xi \quad (4.7)$$

Consequently, the confidence limits for Hotelling's T² and Squared Prediction Error (SPE_X and SPE_Y) for the current sample i can be calculated as follows:

1. Consider a window of length (L) of the previous statistics given by
   $$S_i = \{\xi_{i-L}, \ldots\ldots\ldots \xi_{i-1}\} \quad (4.8)$$
2. Calculate the mean ($\bar{\xi}$) and variance (σ_ξ) of S_i
3. The limits are then calculated according to Equations 4.5, 4.6 and 4.7.

Through the implementation of this approach, adaptive confidence limits are obtained for the monitoring statistics. However, as noted by Wang et al. (2003) determination of the length of the window, used for the calculation of the adaptive confidence limits, is a challenge and is application dependent. Selecting a short window length may provide very sensitive confidence limits giving rise to false alarms, since it enables the confidence limits to adapt to strong variations. In contrast a wide window may make the confidence limits insensitive (Wang et al., 2003). To the researcher knowledge this area is required more investigation as there is no rule that can be generalized for all the applications and for different types of variation.

Wang et al. (2003) applied the proposed approach to a mathematical simulation of a time varying and a non-stationary process. They noted that through the application of the APLS approach the number of false alarms decreased significantly compared to conventional PLS (§3.9 and §3.10). The application of APLS to the mathematical simulations is revisited and further analysed in this chapter (§4.6 and §4.7). Additionally Wang et al. (2003) applied APLS to two industrial simulations; a fluid catalytic cracking unit (FCCU) and a distillation unit for purifying butane. They concluded that APLS can accommodate the process variation and that abnormal behaviour introduced into the process was detected. Wang et al. (2003) further extended

this approach to monitor the individual blocks of a process through utilising the relationship between the conventional PLS algorithm and multiblock PLS based on the super scores (§3.8). They stated that the application of the APLS algorithm to a process with auto-correlated data required further investigation and this is addressed in (§4.3.2.1).

4.3.2.1 Adaptive Dynamic PLS

Most industrial processes exhibit dynamic behaviour as a result of measurements autocorrelation and hence it is useful to extend the recursive PLS with adaptive confidence limits (APLS) algorithm to adaptive dynamic PLS (ADPLS) as follows:

- The reference model can be modified through the incorporation of a time series representation to account for the autocorrelation in the data hence a dynamic PLS model is developed. A detailed description of the development of a dynamic PLS model using time series was described in Chapter 3.
- When a new sample becomes available, it has to be incorporated into a dynamic representation and the monitoring statistics and confidence limits are calculated as for the APLS algorithm.
- The model is then updated by combining the new sample with the previous PLS model, Equation 4.3, and PLS is applied to the updated matrices.

In this thesis, the ADPLS approach is based on two time series representations, Finite Impulse Response (FIR) and Auto-Regressive with eXogenous input (ARX) and this aspect is investigated in terms of model prediction and monitoring performance through their application to two industrial simulations (Chapter 5 and Chapter 6). The approach is also extended to adaptive multi-block dynamic PLS, Chapter 6.

4.3.3 Limitations of Recursive PLS with Adaptive Confidence Limits

The approach proposed by Wang et al. (2003) significantly decreases the number of false alarms compared to conventional PLS when the process is operated under normal operating conditions. However, if the APLS approach of Wang et al. (2003) is implemented for real time monitoring, the model is updated regardless of the type of new observation. This is an issue when the new data is not representative of nominal process behaviour.

4.3.3.1 Sample Types in Real Time Monitoring

In real time monitoring, one of two types of samples can be generated, a sample from normal operating conditions or a sample which deviates from the nominal behaviour. With respect to model updating, the normal operating observations can be used. The issue is how to handle non-conforming samples and outliers. These two types of samples behave in a similar manner as both deviate from the rest of the samples and are defined as:

- A statistical outlier is unlikely to be generated consecutively. Barnett and Lewis (1994) define an outlying sample as one that appears to deviate significantly from other members of a sample. This type of outlying sample can be recorded within normal operating conditions as a result of noise or an erroneous reading. One of the main issues with the existence of outliers is their impact on identifying the model and associated confidence limits. In some cases, it may contain useful information about the process and hence it is important to use such information (Barnett and Lewis, 1994; Pell, 2000; Kruger et al., 2008a; Kruger et al., 2008b).
- Non-conforming samples that are generated consecutively will typically materialise due to a disturbance or process fault and thus represent abnormal behaviour Choi et al.(2006). This type of sample contains irrelevant information which is not useful for model development.

In off-line PLS modelling, i.e. the development of a reference model, there is only a risk of including the first type of outlying samples since the data represents normal operating conditions. A number of papers have been published on the impact of data type when developing a PLS reference model (Geladi and Kowalski, 1986; Martens et al., 1989; Wold et al., 2001; Haenlein and Kaplan, 2004; Kruger and Xie, 2012; Vinzi and Russolillo, 2012). They all pointed out that a PLS model should be developed on data that is outlier free and that is representative of nominal process behaviour.

A number of approaches have been proposed for the detection and treatment of outliers off-line including filtering, visual detection and application of robust estimator (Cummins and Andrew, 1995; Pell, 2000; Hubert and Branden, 2003; Kruger et al., 2008a). Filtering can materialise in a change in a data structure to reduce the effect of outliers and hence it is not implemented in this work. Visual detection can be achieved

through monitoring charts such as Hotelling's T^2 and the squared prediction error SPE_X or through scores plots following the application of principal component analysis. A number of approaches have been proposed to calculate a representative value of a statistical outlier, robust estimator, thereby ensuring it behaves as generated from nominal process so that the statistical outliers can be included in the PLS modelling (Barnett and Lewis, 1994; Cummins and Andrew, 1995; Pell, 2000; Kruger et al., 2008a; Kruger et al., 2008b).

When recursive PLS is used to update a PLS model in real time, there is a risk of including both types of samples. If a PLS model is continually updated using outlying samples the following issues may materialise:

- There is a risk of missed detection of future outlying samples as the inclusion of outliers in the model updating procedure may act as a mask and prevent the detection of future outliers and non-confirming data (Barnett and Lewis, 1994).
- If a sequence of outlying samples is included, the model may be considered to be non-representative of the nominal operating conditions of the process and hence issues materialise with its ability to predict future observations and also detect process changes.

In the APLS algorithm of Wang et al. (2003), there was no investigation into the type of samples used in the updating procedure. Consequently, it may be updated using statistical outliers or samples representing abnormal behaviour, furthermore the adaptive confidence limits will adapt to the abnormal behaviour. This issue is illustrated in Figure 4.5 which shows the results of the implementation of the APLS on the FCCU when the process was affected by one of the programmed faults (i.e. degradation in the flow of the regenerated catalyst). It can be clearly seen that the three monitoring statistics indicate the presence of the fault and since the fault lasted for approximately 150 consecutive samples, the following issues are observed:

- In terms of the fault, which affects the process at sample numbers 950 to 1100, during this period all the samples are included in the model updating procedure. Hence the model is not representative of nominal process behaviour during this period.
- The monitoring statistics indicate the presence of the fault but violate the confidence limits for only few samples and then the confidence limits adapt to

this event, consequently no alarm is produced. This issue is described in §4.3.3.2.

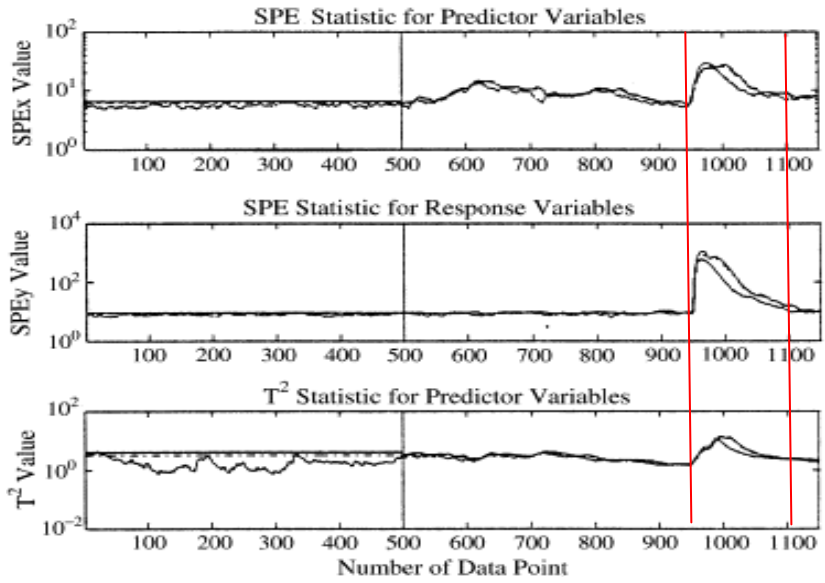

Figure 4.5 – APLS monitoring charts representing the degradation in the flow of regenerated catalyst (Wang et al., 2003)

Two strategies can be used to deal with statistical outliers in adaptive modeling. One approach is to delete the sample and hold the model updating until the next new sample is considered. This approach may result in a loss of process information for PLS modeling as pointed out by Barnett and Lewis (1994), Lee et al. (2006a), Choi et al. (2006) and Kruger et al. (2008a). The second approach is to replace the outlier by a representative value to reduce its effect on the updated model as previously described for off-line PLS which form the basis of treating outliers in this work.

There is only a limited amount of published literature on how to detect and treat outliers for real time multivariate statistical projection based monitoring. For example:

- Liu et al. (2004) proposed an online filtering approach, the revised MT filter-cleaner, to detect and address the presence of statistical outliers online to provide clean data for online PLS and PCA monitoring. The approach involves two steps, first the process model is estimated online using an autoregressive model and the second is to apply a Modified Kalman filter, which is an algorithm used to calculate a statistically optimal estimate of the process thereby removing outliers from the data. After cleaning outliers from the data, PLS or PCA can be applied. Liu et al. (2004) stated that this approach had been applied to different

types of data including auto-correlated data, non-stationary and time varying data. The main issue with this approach is that filters can change the structure of the raw data hence they are not considered in this work.

- Galicia et al. (2012) proposed a multivariate approach based on principal component analysis (PCA) and a Bayesian supervisory approach to detect and then differentiate between types of outliers. They applied the proposed approach to the adaptive modelling and monitoring of data from a simulation of a Kamyr digester. Extending this approach to PLS when constructing a process model is a research area for future.
- One way to check the presence of statistical outliers in real time is to check the monitoring charts of Hotelling's T^2 and SPE_X (Choi et al., 2006). Lee et al.(2006a) proposed the use of a combined index, which is a combination of the univariate monitoring statistics of Hotelling's T^2 and squared prediction error, SPE_X, to detect outlying samples for block-wise RPLS. The aim is to use the combined index for detecting outlying sample and then for calculating a weight function that is used to reduce the impact of the outlying data on the block-wise RPLS model. More specifically, the combined index is used to calculate an estimated value to be included in the model updating process instead of the outlying sample.

  The idea of using a weight function was first proposed by Cummins and Andrew (1995). They selected the Cauchy and Fair weight functions to suppress the impact of an outlier on the static PLS model, (Table 4.1), i.e. they calculated a robust estimator based on the weight. However, their idea was to use the residual resultant from the application of cross validation technique to calculate the parameter μ in the weight function. Pell (2000) adopted the same weight function for static PLS but instead of using the cross validated residual they used the fitted residual. Instead of residuals, Lee et al. (2006a) used the combined index and its limit as the combined index combines both the principal and residual variation of the process, which is contained in Hotelling's T^2 and SPE_X respectively (§4.4.1). They showed that the weight function based on the combined index results in improvement in the root mean squared error of block-wise RPLS compared to conventional PLS and RPLS for a waste water treatment process.

Table 4.1 – Different weight function used for PLS and recursive PLS methods.

Function	Residual weight function	Combined index weight function
Cauchy	$\omega_i = 1/[1 + (\mu/c)^2]$	$\omega_i = 1/[1 + (\varphi_i/c\,\varphi_\alpha)^2]$
Fair	$\omega_i = 1/[1 + (\mu/c)]^2$	$\omega_i = 1/[1 + (\varphi_i/c\,\varphi_\alpha)]^2$

* μ is the residual divided by the median absolute deviation from the median - φ_i is the value of the combined index, $\varphi_\alpha$is the correspondence confidence limits and c is tuning parameter.

The value of the weight ranges from 0 to 1 in both cases, where a weight that is close to zero forces the outlying sample to behave as if generated from normal operating conditions. The weight initially is set to one and when the combined index violates the confidence limit, hence the value of the combined index and its confidence limits are used to calculate the weight (Table 4.1). In this case the entire samples are weighted prior to model updating. Each weight function has a tuning parameter c which is determined empirically based on the application under study to achieve the best performance in term of prediction (Cummins and Andrew, 1995; Pell, 2000; Lee *et al.*, 2006a).

In this work, the combined index threshold is used along with sample wise recursive PLS to develop a new and improved APLS approach that recursively updates the PLS model and is robust to statistical outliers (§4.4). Additionally, the Robust Adaptive PLS (RAPLS) algorithm uses the adaptive confidence limits only when the samples are confirmed to be representative of nominal operating conditions.

4.3.3.2 Adaptive Confidence Limits

Chiang et al. (2001) pointed out that one of most important feature of monitoring charts is the need to detect the fault as soon as possible after occurrence to allow investigation of the source of the fault to be carried out. Otherwise, if the monitoring chart showed that the process is within a state of statistical control during the faulty period, it may be assumed that the fault is auto-corrected, i.e. the control system implements a corrective action and the process return to a state of statistical control. Consequently, the process continues to be operated under the fault effect without investigation.

The use of adaptive confidence limits when the process is affected by a fault (non-conforming samples) is an issue. Figure 4.5 shows that the monitoring statistics indicates the presence of the fault, however, it only violates the limits for the first few samples and then the adaptive confidence limits adapt to this abnormal event. This occurred because the adaptive confidence limits are calculated based on a window of the previous statistics under the fault conditions; consequently it accommodates the change in the monitoring statistics and indicates that the process is within a statistical control state whilst it is not.

From the previous discussion, it can be concluded that adaptive confidence limits are useful only when the sample represent nominal process behaviour. Otherwise, the monitoring charts indicate that the process is within statistical control when it is affected by the fault. In the next section Robust Adaptive PLS algorithm is developed to overcome the limitations discussed in §4.3.3.1 and §4.3.3.2.

4.4 Robust Adaptive PLS (RAPLS)

This approach is proposed to overcome the limitations of the APLS algorithm i.e. to prevent the adaption of the model to outlying samples. Furthermore, it is extended to model and monitor processes that comprise autocorrelated observations. The algorithm comprises two steps, first the screening of new samples (§4.4.1) and the second is to update the PLS model based on the threshold outcome. The algorithm is described in (§4.4.2).

4.4.1 RAPLS Thresholds

In adaptive modelling, a reliable PLS model have been developed in the previous step thus it is necessary to decide whether the new sample is an outlier. The combined index (Qin and Yue, 2001) threshold is used and is extended to distinguish between a statistical outlier and non-conforming sample. The basis of the combined index is a combination of the univariate statistics of Hotelling's T^2 and the squared prediction error, SPE_X:

$$\varphi = \frac{T^2}{T_\alpha^2} + \frac{SPE_X}{SPE_\alpha} = \mathbf{x}'\mathbf{\Phi}\mathbf{x} \tag{4.9}$$

where T^2 and SPE_X are the values of the univariate statistics Hotelling's T^2 and the squared prediction error and T_α^2 and SPE_α are the value of the corresponding confidence

limits for a significance level of α for a new sample. The vector **x** is the input values of the new sample and the matrix **Φ** is given by:

$$\mathbf{\Phi} = \frac{\mathbf{P\Lambda^{-1}P'}}{T_\alpha^2} + \frac{\mathbf{I - PP'}}{SPE_\alpha} \tag{4.10}$$

where **P** is the loading matrix and **Λ** is given by $\mathbf{\Lambda} = \mathbf{T'T}/(n-1)$ and **T** is the matrix of scores of the reference PLS model and n the number of sample in the reference data set. In the case of adaptive PLS, these matrices are obtained from the model at the previous time point.

The confidence limits of the combined index are given in Qin and Yue (2001) are calculated based on $\varphi \sim g\chi^2(h) = \varphi_\alpha$ where g and h are given by:

$$g = \frac{tr(\mathbf{S\Phi})^2}{tr(\mathbf{S\Phi})} \tag{4.11}$$

$$h = \frac{[tr(\mathbf{S\Phi})]^2}{tr(\mathbf{S\Phi})^2} \tag{4.12}$$

where **S** is $cov(\mathbf{x})$ and **x** is the vector of the input values of the new sample.

As mentioned in Chapter 3 that the Hotelling's T² and SPE_X complements each other as the Hotelling T² represents the variation within the model, i.e. developed based on the retained scores, and the SPE_X represents the variation out of the model, i.e. developed based on the residuals. Therefore, in terms of monitoring charts there might be some samples violate the confidence limits of Hotelling's T² but not the SPE_X limits and the opposite is materialised. Therefore, implementing a single index is preferred for monitoring (Qin and Yue, 2001) as it can detect all the point out of the joint range of the confidence limits for Hotelling's T² and SPE_X.

As described in §4.3.3.1, statistical outliers are unlikely to be recorded consecutively in contrast to samples from abnormal events. Therefore, by utilising the Western Electric rule, where consecutive violations are considered to be an indication of a process abnormality, therefore, discrimination between a fault and statistical outliers can be achieved. If the new sample is confirmed to be a statistical outlier, it requires further treatment prior to model updating, i.e. the combined index is utilised for the calculation of the weight to be used in the treatment of the outliers (Table 4.1). The RAPLS threshold can thus be summarised as shown in Figure 4.6.

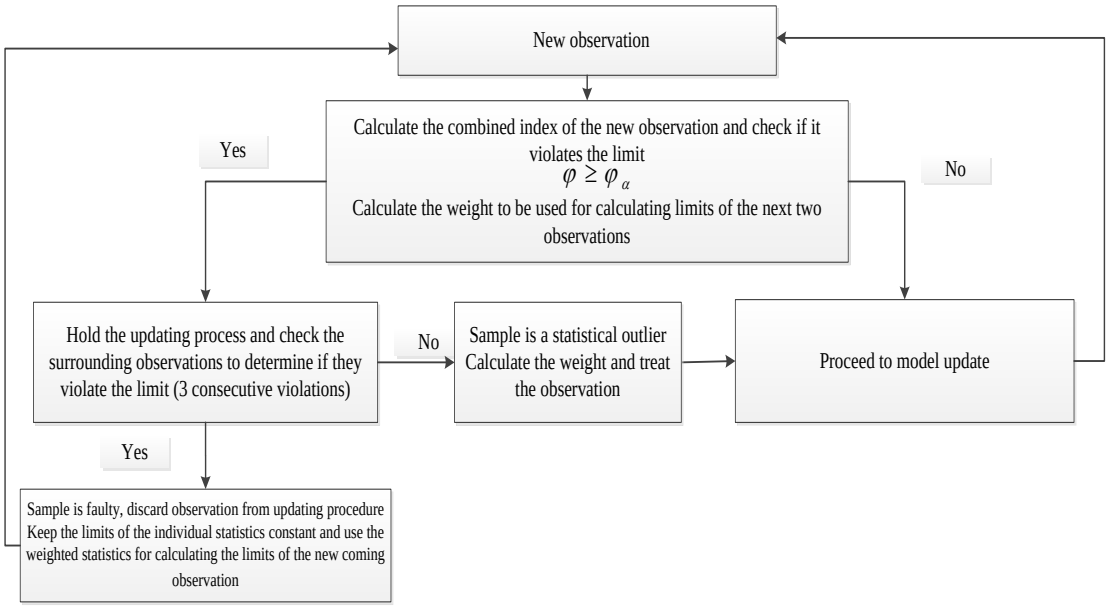

Figure 4.6 – RAPLS threshold

Table 4.2 summarizes the different cases for RAPLS thresholds. In each case, the first threshold tests the statistical status of the current sample whereas the second threshold checks the statistical status of the previous and next samples.

Table 4.2 - Different cases for RAPLS algorithm.

Case	First threshold	Second threshold				Final decision
	sample t	sample t-2	Sample t-1	sample t+1	sample t+2	
1	Nominal process behaviour	No need to check				Update model
2	Violates 1st threshold	Nominal process behaviour	Nominal process behaviour	Nominal process behaviour	Nominal process behaviour	sample is outlier
3	Violates 1st threshold	Violates the limit	Violates the limit	No need to check		sample is fault
4	Violates 1st threshold	Nominal process behaviour	Violates the limit	Violates the limit	No need to check	sample is fault
5	Violates 1st threshold	Nominal process behaviour	Nominal process behaviour	Violates the limit	Violates the limit	sample is fault

4.4.2 RAPLS Algorithm

The RAPLS algorithm is summarized in Figure 4.7. The first step of the algorithm is to develop a reference model from historical data, using conventional PLS (NIPALS). Once a new sample becomes available, the threshold (§4.4.1) is examined and a decision, whether to update the PLS model and the confidence limits depends on the outcome of the threshold analysis (Table 4.2). The observation is discarded from the model updating process if the sample represents abnormal behaviour, i.e. the combined index violates its limits for 3 consecutive samples. If the sample represents a statistical outlier, i.e. the combined index is only violated by the current sample, the sample is weighted prior to updating the model (§4.4.1).

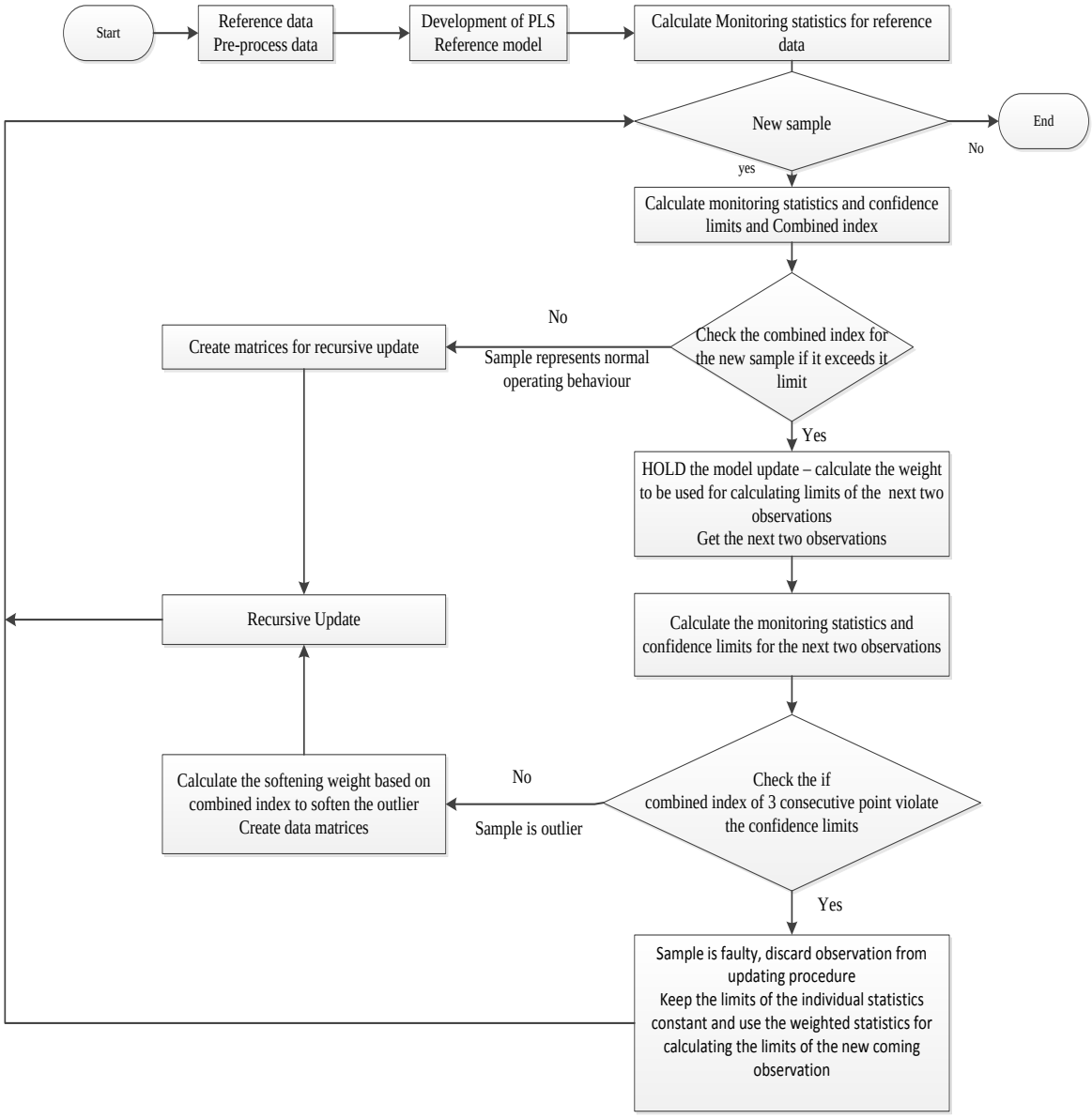

Figure 4.7 – Robust adaptive PLS algorithm

In this thesis, the RAPLS approach is extended to a dynamic variant where two time series representations are considered, Finite Impulse Response (FIR) and Auto-Regressive with eXogenous input (ARX), and the performance of the algorithms are investigated in terms of model prediction and monitoring performance through their application to two industrial simulations (Chapters 5 and 6). The approach is also extended to robust adaptive multiblock dynamic PLS, Chapter 6.

4.5 Evaluation of Recursive PLS Methods

The purpose of a monitoring scheme based on RAPLS is to provide a model that represents process behaviour and to identify abnormal behaviour when it occurs. Therefore, the model needs to be evaluated as well as the monitoring charts. As for conventional PLS, the root mean squared error of calibration, validation and prediction is used for model evaluation whilst the monitoring charts are evaluated in terms of number of false alarms; fault detection ability and the time taken to indicate a fault. Therefore, the statistical indices of false alarm rate (FAR), fault detection rate (FDR) and Average Run Length (ARL) are calculated.

4.6 Application of Recursive PLS Approaches to a Time Variant Process

In Chapter 3, it was shown that conventional PLS models and monitoring charts were inappropriate for processes that exhibit changing behaviour and the number of false alarm was significantly increased over that expected theoretically. This was determined through the application of conventional PLS to a simulation of a time variant process. In this section, the applicability of APLS and RAPLS for real time process monitoring of a time varying process is investigated.

4.6.1 Application of APLS to a Time Variant Process

The mathematical simulation representing time varying behaviour described in Chapter 3 (§3.9.2) forms the basis of this study. The first step in developing an APLS model is to attain a reference model. The PLS model comprising one latent variable developed in §3.9.3 is used as the basis of the analysis. For each new sample, the monitoring statistics, Hotelling's T^2 and Squared Prediction Error (SPE_X and SPE_Y) and the adaptive confidence limits were calculated prior to model updating according to Equations 4.5, 4.6, 4.7 and 4.8.

The APLS algorithm was applied to two data sets, the validation and the test data sets (Chapter 3). The objective of using two data sets was to investigate the ability of APLS to discriminate between time varying behaviour and a step change in the process.

Figures 4.8 and 4.9 show the time series plots of the measured and predicted values of the two quality variables where each plot has been zoomed in to show the differences. It can be seen that the APLS model has the ability to adapt to time varying behaviour compared to conventional PLS (Chapter 3). From Figure 4.8 an offset can be observed between the measured and predicted values for the first quality variable whilst the second quality variable shows small differences in the peaks as shown in Figure 4.9. In the case where a step change is introduced into the process at sample number t=500 and lasts for 10 consecutive samples, Figures 4.10 and 4.11 show the results in terms of time series plots of the measured and predicted quality variables. It can be seen that both variables were affected by the fault and they were well predicted through the implementation of APLS approach compared to conventional PLS. An offset can be seen between the measured and predicted values for both quality variables as shown in the Figures 4.10 and 4.11.

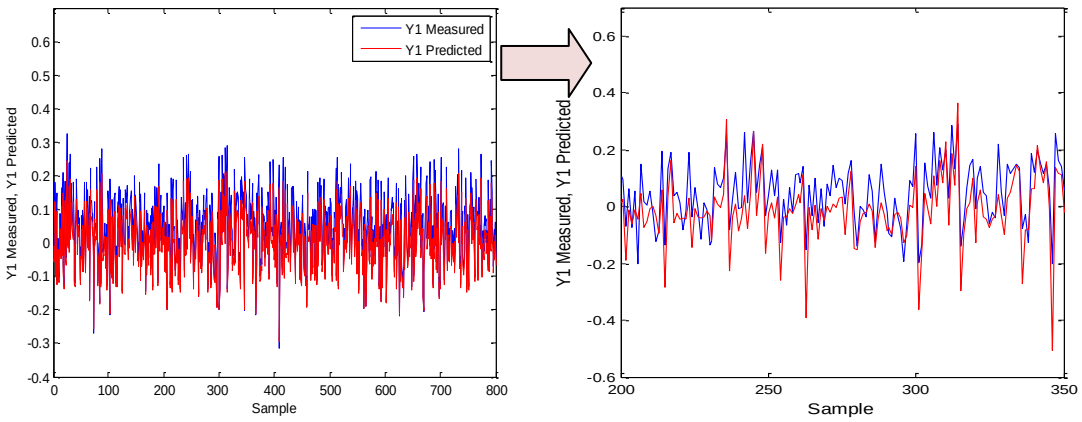

Figure 4.8 – Time series plot of measured and predicted values for the first quality variable - APLS (Validation data set)

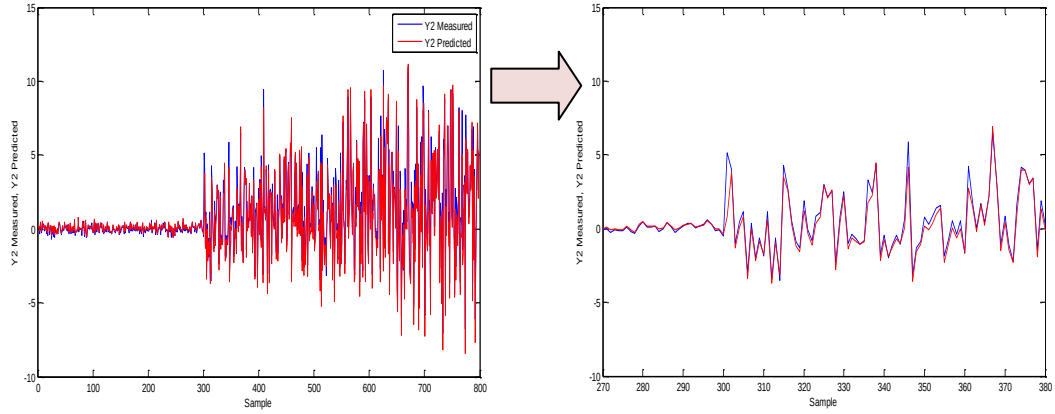

Figure 4.9 - Time series plot of measured and predicted values for the second quality variable - APLS (Validation data set)

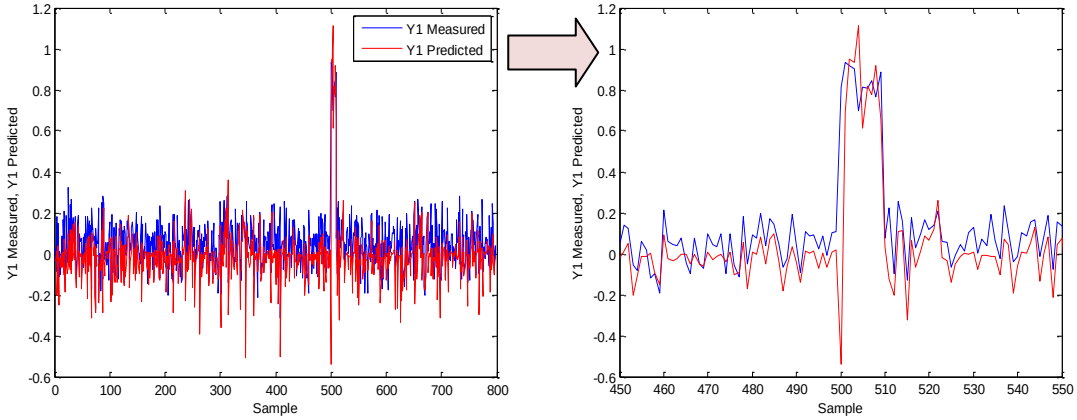

Figure 4.10 - Time series plot of measured and predicted values for the first quality variable - APLS (Test data set)

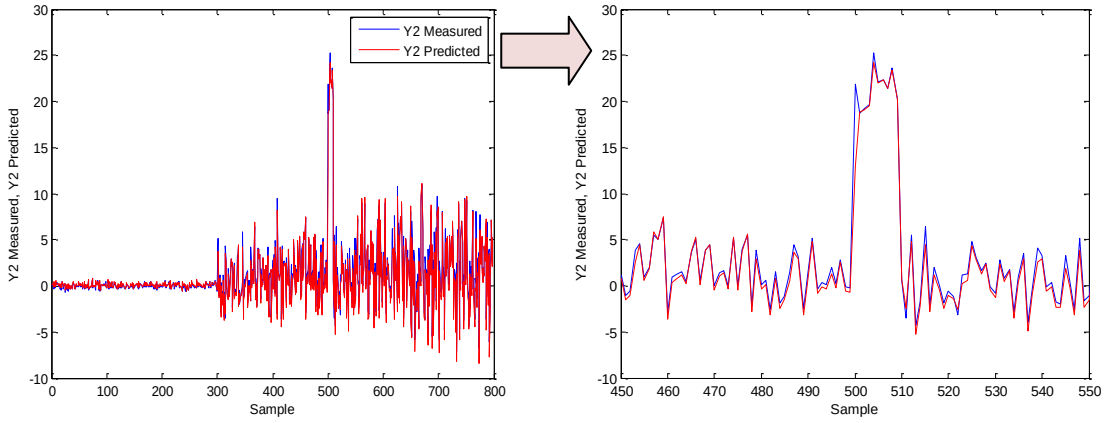

Figure 4.11 - Time series plot of measured and predicted values for the second quality variable - APLS (Test data set)

These improvements in the predictions are reflected in the RMSE of prediction for both the validation and test data sets (Table 4.3). For the validation data set, the RMSE of quality variables following the application of APLS, 0.04 and 0.57, were an

improvement over those from conventional PLS, 0.05 and 2.62 respectively. The improvements in the prediction is also reflected in the RMSE for the test data set as for APLS, 0.11 and 0.64, were lower than those result from conventional PLS, 0.137 and 3.49 for both quality variables. The RMSE of the second quality variable is higher than the first quality variable due to the difference in the variability of the two variables, the first quality variable variability was ±0.5 whilst for the second quality variable, it was ±12 for the validation data set and was ±3 for the first quality variable whilst for the second quality variable, it was ±25 for the test data set.

Table 4.3 - RMSE of the validation and test data sets by APLS

Quality variable	Validation data set	Test data set
	RMSE	RMSE
Y1	0.04	0.11
Y2	0.57	0.64

The monitoring results of the time varying process using the APLS model for the validation data set are illustrated in Figures 4.12, 4.13 and 4.14. It can be seen that the SPE_Y statistic is strongly affected by the time varying behaviour and in general the confidence limits adapt well to the change in process behaviour. This results in a reduction in the number of false alarms compared to conventional PLS results with the order of 5% and 1% out of statistical control samples corresponding to the 95% and 99% confidence limits as respectively (Table 4.4). The quantitative results for the FAR from the implementation of APLS shows a significant reduction compared to conventional PLS with the most noticeable difference being a drop of 32.25% for the SPE_Y monitoring chart.

For the test case, where a step change was introduced at t = 500 and which lasts for a duration of 10 samples, it can be seen that the three monitoring statistics were affected by the step change (Figures 4.15, 4.16 and 4.17). The monitoring charts indicate the presence of the step change for two samples and then the confidence limits start to adapt during the next few samples during which the process is still affected by the step change. Additionally, since the model and confidence limits were updated using samples and statistics generated during step change condition respectively, the model and the confidence limits were insensitive to the detection of further abnormal samples, i.e. after updating the model and the confidence limits with the first two samples of the step change, the monitoring charts failed to detect the full period of the step change.

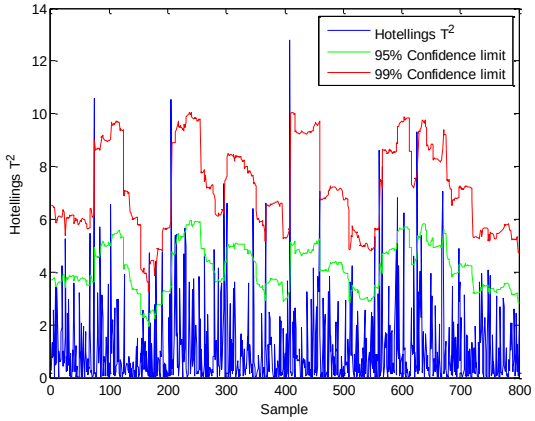

Figure 4.12 – Hotelling's T^2 for the validation data set – APLS

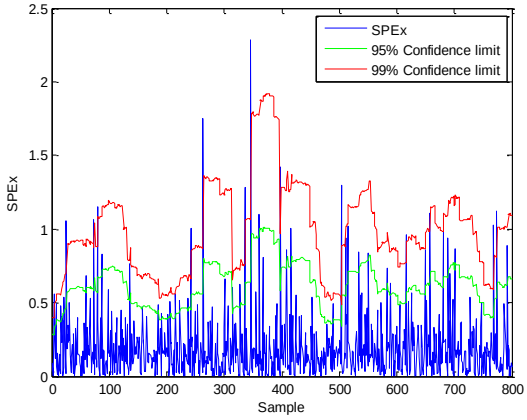

Figure 4.13 - SPE_X for the validation data set – APLS

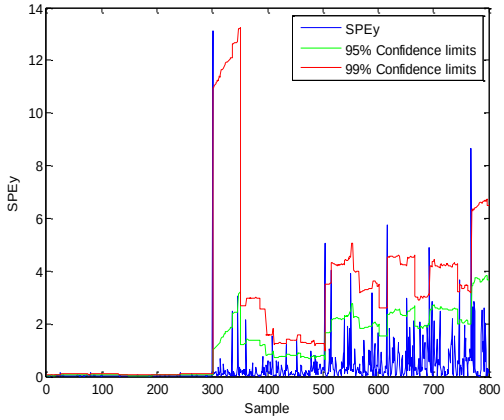

Figure 4.14 - SPE_Y for the validation data set – APLS

The fault detection rate (Table 4.4) reflect the previous observations since only 20%, 10% and 10% of the faulty samples were detected for the Hotelling's T^2, SPE_X and SPE_Y respectively for the 99% confidence limits. This is because the confidence limits adapt the faulty samples and hence the process returns to a state of statistical control. In reality where the fault or disturbance lasts for a significant period, the process model and confidence limits will be updated using these samples and may thus be considered to be non-representative of nominal process behaviour.

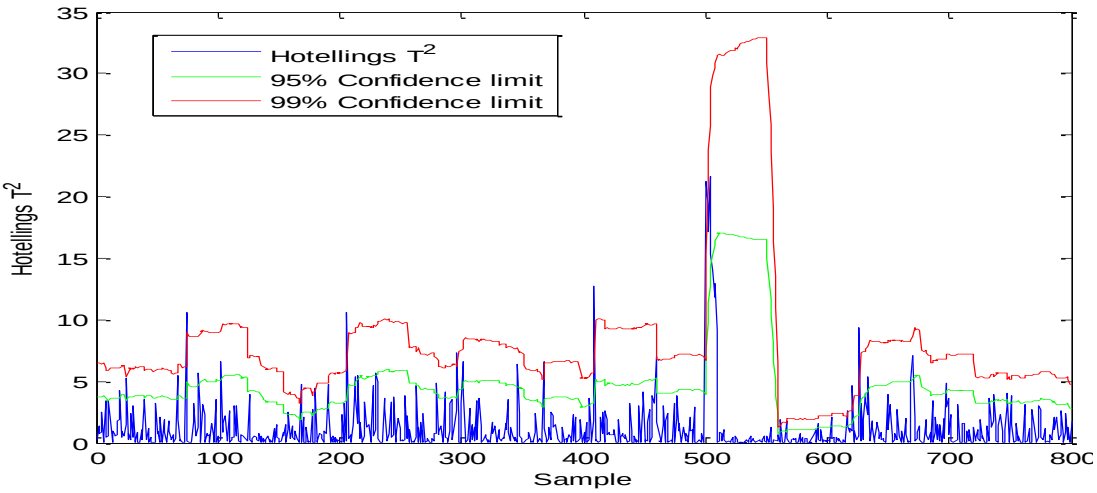

Figure 4.15 – Hotelling's T² for the test data set – APLS

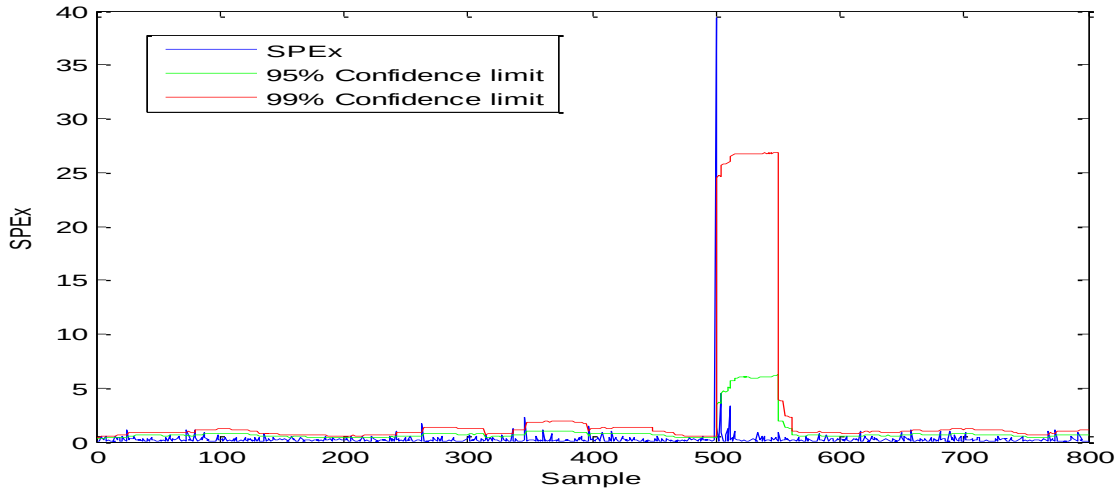

Figure 4.16 - SPE_X for the test data set – APLS

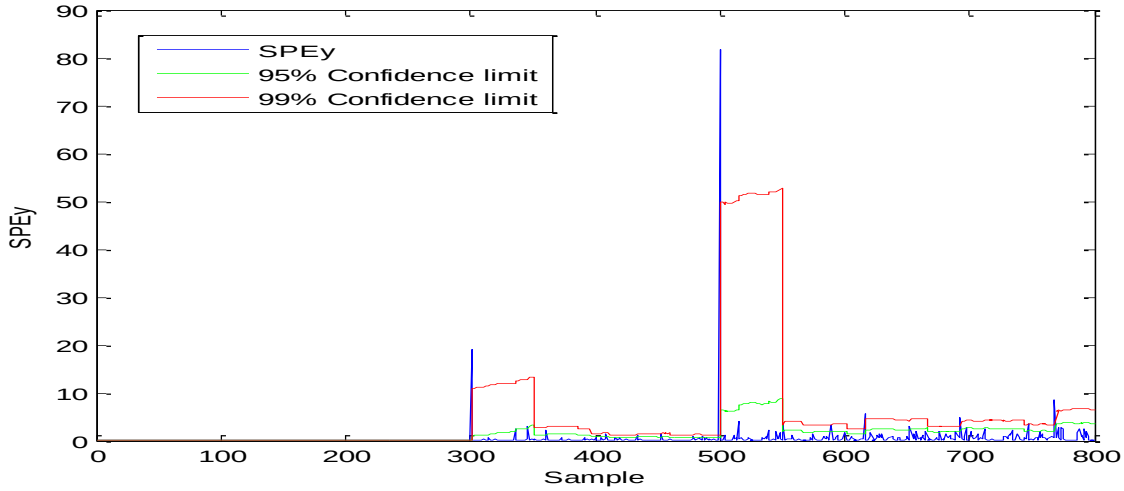

Figure 4.17 - SPE_Y for the test data set –APLS

Table 4.4 - FDR and FAR based on APLS

Chart	FDR – 95%	FDR – 99%	FAR – 95%	FAR – 99%
Hotelling's T^2	40%	20%	4.00 %	1.00%
SPE_X	30%	10%	4.12%	1.37%
SPE_Y	30%	10%	5.25%	1.50%

As mentioned in Chapter 3, the results for ARL0 and ARL1 were calculated based on a Monte Carlo simulation where the experiment was repeated 50 times and in each run, the run length (RL) was recorded and the ARL calculated. The ARL0 was calculated from the monitoring charts constructed based on the validation data set since the time varying behaviour is considered normal process behaviour whilst ARL1 was attained from the test data set following the introduction of a step change at t=500. The results from the Monte Carlo simulation are summarised in Table 4.5. It can be seen that the implementation of APLS produced monitoring charts that detect the fault rapidly compared to conventional PLS where the fault was indicted after 5 to 6 samples. Consequently, the ARL1 is better compared to conventional PLS (Chapter 3).The results also indicate that the monitoring charts remain within a state of statistical control for a satisfactory number of samples when the process represents normal operating conditions, the ideal ARL0 for the 99% confidence limit is 100 samples.

Table 4.5 - Average run length for the monitoring charts by APLS.

Chart	ARL0	ARL1
Hotelling's T^2	80	1
SPE_X	79	1
SPE_Y	74	1

Although the results from the application of APLS to the data representing time varying behaviour indicate that the number of false alarm was decreased, the fault detection rate was unsatisfactory as the monitoring charts detect 20% of the faulty samples hence the RAPLS is implemented.

4.6.2 Application of RAPLS to a Time Variant Process

The procedure presented in §4.4.2 described the construction of monitoring charts for the simulation of a time varying process. As for APLS, the first step was to develop a reference model using conventional PLS (§3.9.3). Once a new sample becomes available, the univariate monitoring statistics and the combined index are calculated and the first threshold is implemented to prevent the model adapting to outlying samples. Similarly, the confidence limits are not updated when the sample is generated from abnormal process behaviour. Details of the used weight are provided in Appendix B.

The results from the application of RAPLS for the validation data set are presented in Figures 4.18 and 4.19 where the first quality variable was unaffected by the time varying behaviour as the behaviour of the signal does not change compared to that prior to the introduction of the ramp signal (i.e. time varying behaviour) whilst the second variable was strongly affected by the time varying behaviour. It can clearly be seen that both quality variables are well predicted. The RMSE for the validation data set (Table 4.6) shows that the results are slightly improved compared to these of APLS (Table 4.3).

By checking the time series plot of the combined index, Figure 4.20, it can be seen that there is a few violations, appointed by arrows, indicating the presence of statistical outliers. The number of the violations was quantified from the monitoring chart of the combined index to be 18 samples corresponding to 2.25% of the violations for the 99% confidence limit and 59 samples corresponding to 7.37% of the violations for the 95% confidence limit. These rates are higher than the statistically acceptable rate of order of 5% and 1% for the 95% and 99% confidence limits respectively indicating that there is some samples is not caused by chance, i.e. outliers. Therefore, these outliers were weighted prior to model updating to reduce the impact on the RAPLS model. The time series plot and the calculations of the weight used for outlying samples are given in Appendix B. This approach results in the outliers behaving similar to the samples generated during normal operating conditions. Additionally, the treatment of the statistical outliers result in a slight improvement in the model predictions and this is reflected in the RMSE, 0.03 and 0.56 compared to APLS (0.04 and 0.57) for the first and second quality variables respectively. However, this improvement is still comparable to the result from APLS as the number of the outliers is small (18 samples) compared to the number of samples (800 samples).

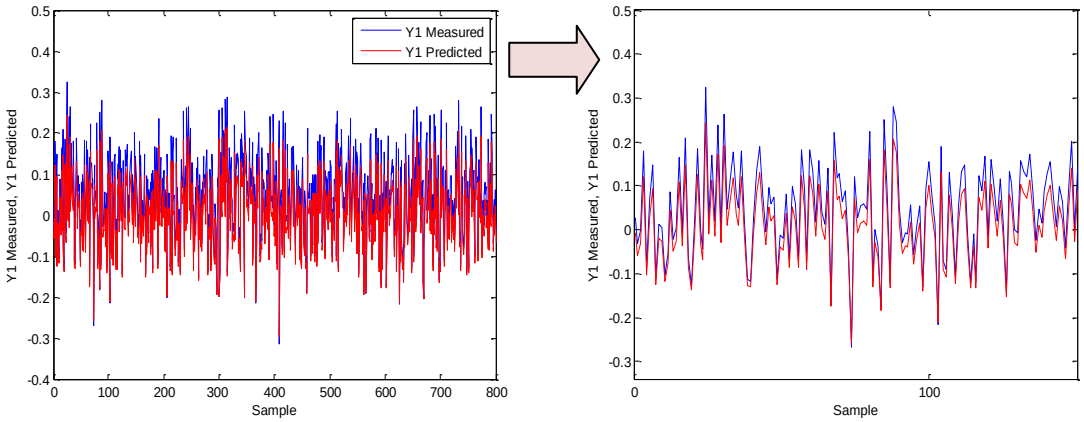

Figure 4.18– Time series plot of measured and predicted values for the first quality variable - RAPLS (Validation data set)

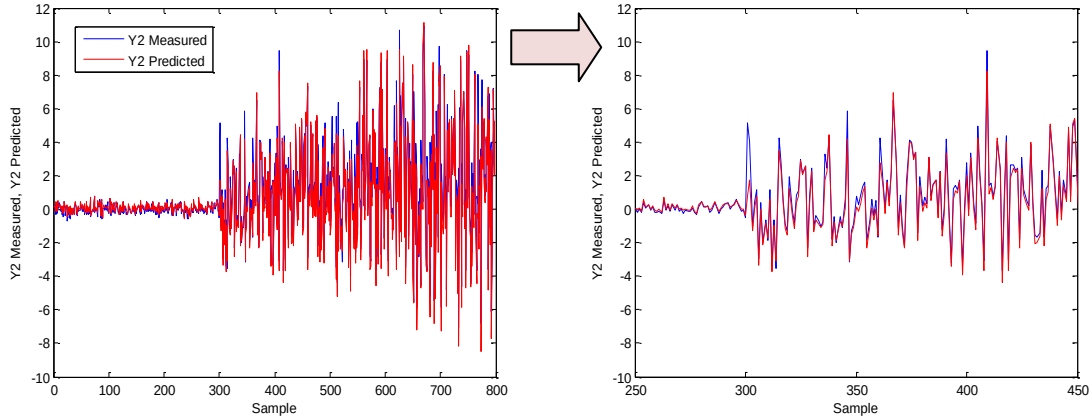

Figure 4.19 – Time series plot of measured and predicted values for the second quality variable – RAPLS (Validation data set)

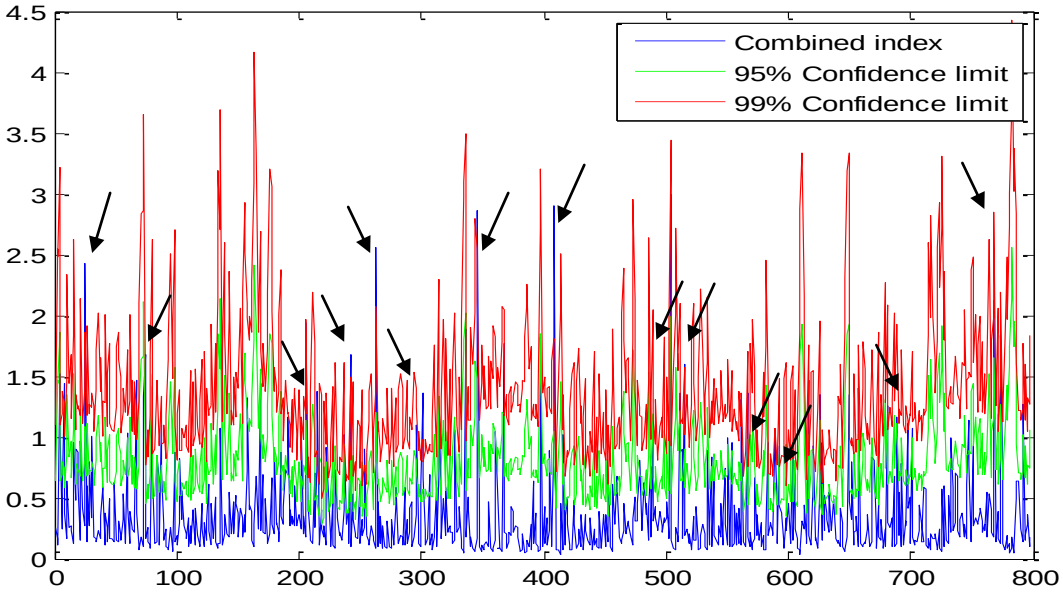

Figure 4.20 - Time series plot for the combined index - RAPLS (Validation data)

The results from the application of RAPLS to the test data set are presented in Figures 4.21 and 4.22. It can be observed that both quality variables are well predicted. However, during the step change period the model predicts the behaviour but with less accurately compared to APLS. This is because the samples during this period did not contribute to the model hence the accuracy of the prediction was less than that for APLS. From Table 4.6, the values of the RMSE, 0.12 and 1.16, were an improvement over those for conventional PLS (0.137 and 3.49) for the first and second quality variables respectively. However, the predictions for the test data set were slightly lower compared to the APLS results, RMSE= 0.11 and 0.64, for both quality variables. This was expected because the RAPLS approach prevents the abnormal samples (step change samples) from contributing to model updating and therefore the predictions during this period were calculated using the previous model. However, when the process returned to normal operating conditions, the prediction improved as shown in the time series plots (Figures 4.21 and 4.22). This shows that the model can discriminate between the step change (abnormal behaviour) and time varying behaviour (normal operating behaviour).

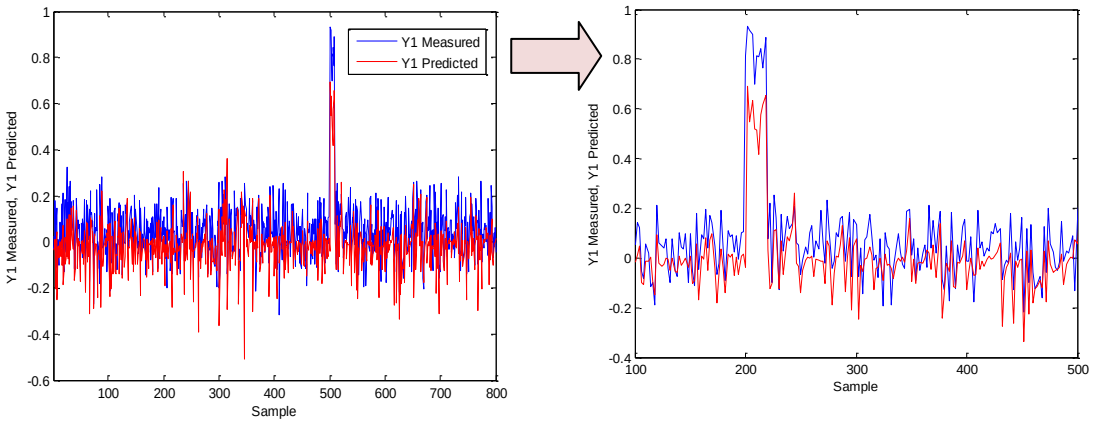

Figure 4.21 – Time series plot of measured and predicted values for the first quality variable - RAPLS (Test data set)

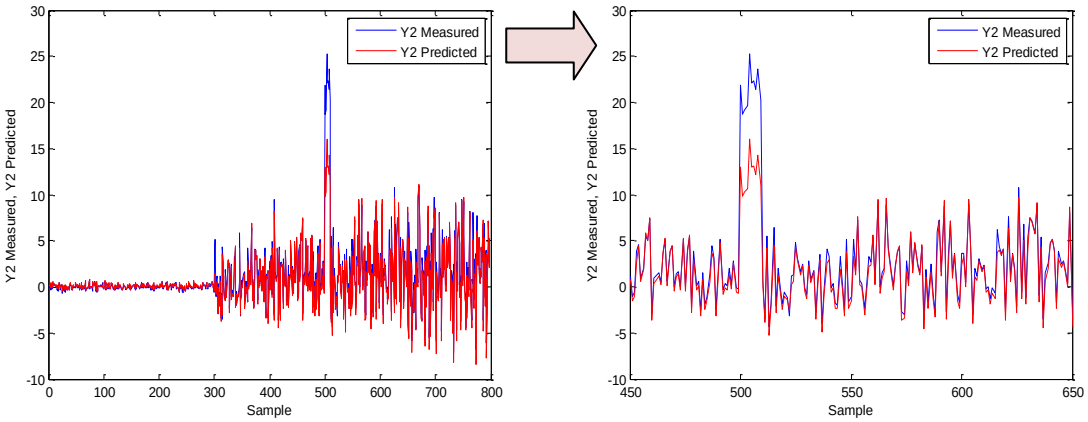

Figure 4.22 – Time series plot of measured and predicted values for the second quality variable - RAPLS (Test data set)

Table 4.6- RMSE of the validation and test data set - RAPLS

Quality variable	Validation data set	Test data set
	RMSE	RMSE
Y1	0.03	0.12
Y2	0.56	1.16

Figure 4.23 shows the combined index for the test data set and this will be used to determine whether to update the PLS model. The effect of the step change is evidence as the combined index violates the confidence limits during the step change period, hence the PLS model is not updated during this period.

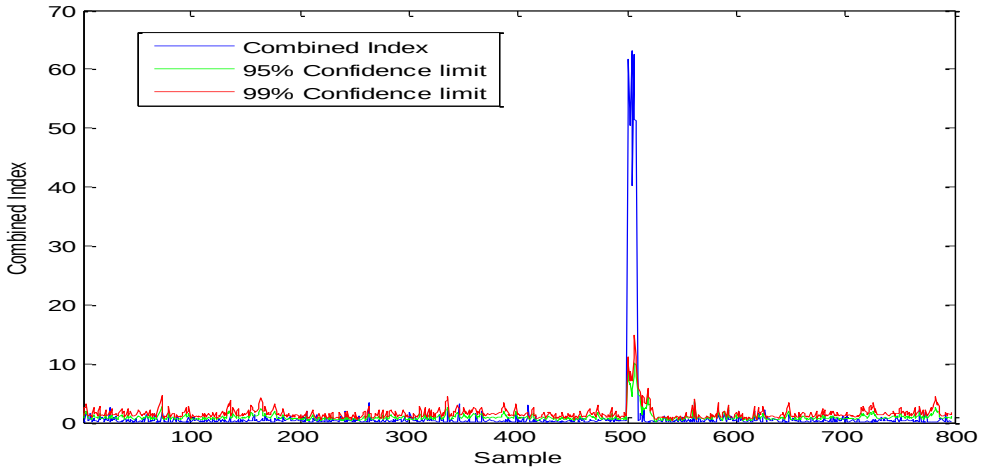

Figure 4.23 - Time series plot of the combined index - RAPLS (Test data set)

The monitoring results using the RAPLS model for the validation data set are illustrated in Figures 4.24, 4.25 and 4.26. It can be seen that they are similar to these for APLS. A few out of statistical control signals were detected. The number of the violations is acceptable as they did not exceed the 5% and 1% for 95% and 99% confidence limits respectively. This is reflected in the false alarm rate (Table 4.7) where the FAR form RAPLS, 1%, 1.25 and 1.25% for Hotelling's T^2, SPE_X and SPE_Y are approximately similar to these for APLS for the 99% confidence limit. The same observation can be concluded for the 95% confidence limit, the FAR form RAPLS, 4%, 4.25% and 5.12% for Hotelling's T^2, SPE_X and SPE_Y, is comparable to those from APLS.

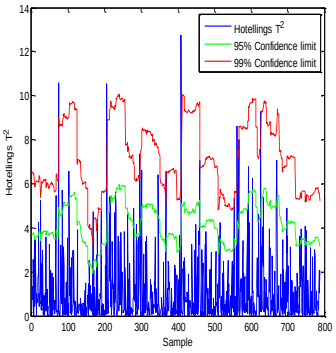

Figure 4.24 - Hotelling's T^2 for the validation data set

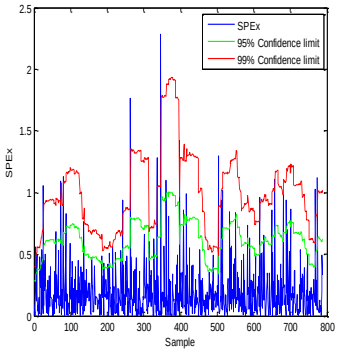

Figure 4.25 - SPE_X for the validation data set

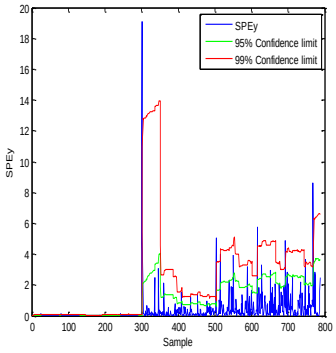

Figure 4.26 - SPE_Y for the validation data set

Figures 4.27, 4.28 and 4.29 show the monitoring results following the application of RAPLS to the test data set. The monitoring charts indicate the step change and the adaption to the time varying behaviour. The abnormal samples, i.e. samples during the step change, are detected through the monitoring charts of Hotelling's T^2, SPE_X and SPE_Y and they were not included in the model updating process since they are also indicated by the combined index chart (Figure 4.23). The quantitative results of the FDR, Table 4.7, indicates that the abnormal event is fully detected, FDR is 100%, by the three monitoring charts compared to the APLS monitoring charts where only 20%, 10% and 10% of the fault were detected by Hotelling's T^2, SPE_X and SPE_Y respectively.

Table 4.7 - FDR and FAR based on RAPLS

Chart	FDR – 95%	FDR – 99%	FAR – 95%	FAR – 99%
Hotelling's T^2	100%	100%	4%	1%
SPE_X	100%	100%	4.25%	1.25%
SPE_Y	100%	100%	5.12%	1.25%

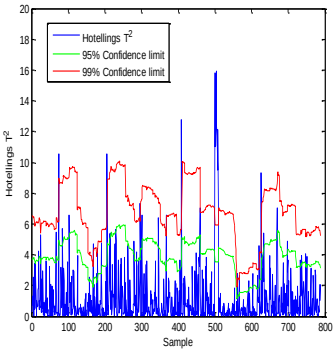

Figure 4.27- Hotelling's T^2 for the test data set

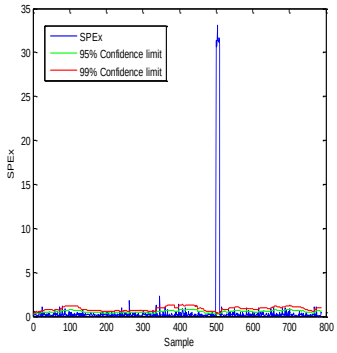

Figure 4.28 - SPE_X for the test data set

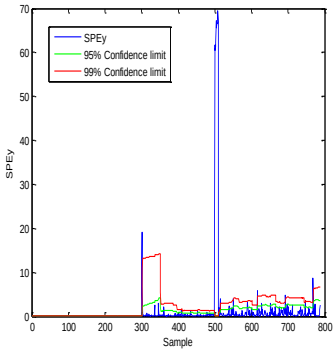

Figure 4.29 - SPE_Y for the test data set

Table 4.8 summarises the results of the statistical indices for the average run length; ARL0 and ARL1 based on a Monte Carlo simulation comprising 50 experiments. It can be seen that both indices provide good results with the ARL0 not indicating any false alarms for a sufficient period of 83, 81 and 79 for the three monitoring statistics compared to the ideal ARL0 of 100 samples whilst the ARL1 immediately indicates the abnormal event compared to conventional PLS as shown in Table 4.8

Table 4.8 - The average run length for the monitoring charts – RAPLS.

Chart	ARL0	ARL1
Hotelling's T^2	83	1
SPE_X	81	0
SPE_Y	79	1

The following observations can be made when comparing the performance of conventional PLS, APLS (Wang et al., 2003) and RAPLS algorithms.

- Both adaptive algorithms, APLS and RAPLS, have the ability to adapt to the time variant behaviour compared to conventional PLS.
- The quality variables are well predicted and the predictions from APLS and RAPLS are improvement over conventional PLS. The improvement identified by the adaptive algorithms is reflected in the lower values of the root mean squared error (RMSE). For the test data set, the prediction error of the RAPLS

model was slightly higher than the APLS as the samples from the abnormal event were discarded from model update.

- The RAPLS model identified a few outlying samples which results in a slight improvement in the model predictions compared to APLS and conventional PLS for the validation data set.
- The number of false alarms for all the monitoring charts decreased through the implementation of the adaptive approaches, APLS and RAPLS, compared to conventional PLS.
- RAPLS and conventional PLS perform better than APLS in terms of fault detection as the APLS algorithm allows the confidence limits to adapt to changes without consideration the sample type.

4.7 Application of Recursive PLS Approaches to a Non-stationary Process

In this section, the efficiency of APLS and RAPLS for real time monitoring for a non-stationary process is investigated. In Chapter 3, it was shown that conventional PLS is inappropriate for the modelling of processes exhibiting non-stationary behaviour with a large number of false alarms. One approach to account for non-stationary behaviour is the implementation of recursive PLS with adaptive confidence limits.

4.7.1 Application of APLS to a Non-Stationary Process

The mathematical simulation representing non-stationary process behaviour introduced in Chapter 3 (§3.10.2) forms the bases of this study. The APLS algorithm was applied to the validation data and the test data set previously discussed in Chapter 3. The objective of using two data sets is to investigate the ability of APLS to discriminate between non-stationary behaviour and a process fault, i.e. step change.

Figures 4.30 and 4.31 shows the time series plots for the measured and predicted values for the two quality variables and it can be clearly seen that APLS has the ability to adapt to non-stationary behaviour. For the case when the process is affected by the step change at sample number t=500, Figures 4.32 and 4.33 show the resulting time series plots of the measured and predicted quality variables and again the behaviour is well predicted. This is expected as the prediction was calculated using the updated PLS model utilising the previous time points. The results for the RMSE for the validation and test data sets (Table 4.9) reflect this observation. From Table 4.9, the RMSE

following the application of APLS to the validation data set (0.01 and 0.06) decreases compared to conventional PLS (0.56 and 1.42) for both quality variables. The same observation can be made for the test data set, the RMSE following the application of APLS (0.05 and 0.08) decreases compared to the RMSE for conventional PLS (0.60 and 1.46) for both quality variables respectively.

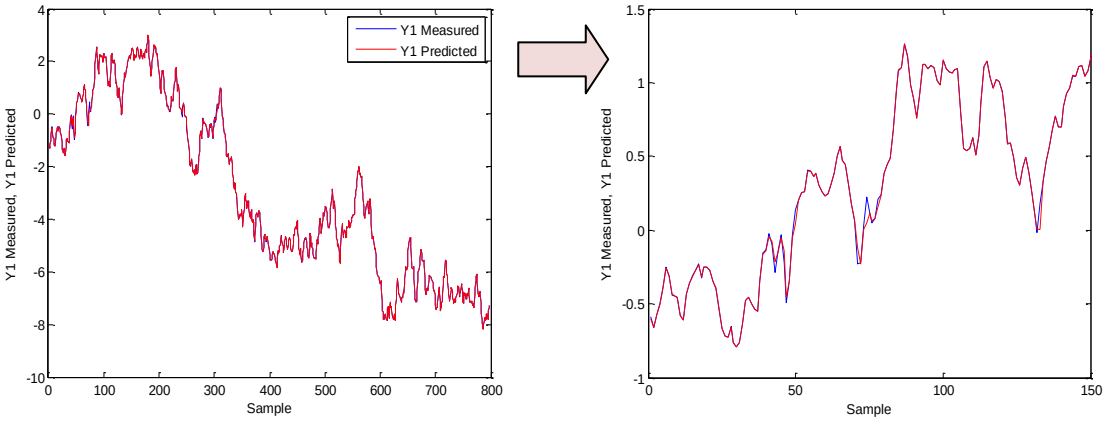

Figure 4.30 -Time series plot of measured and predicted values for the first quality variable - APLS (Validation data set)

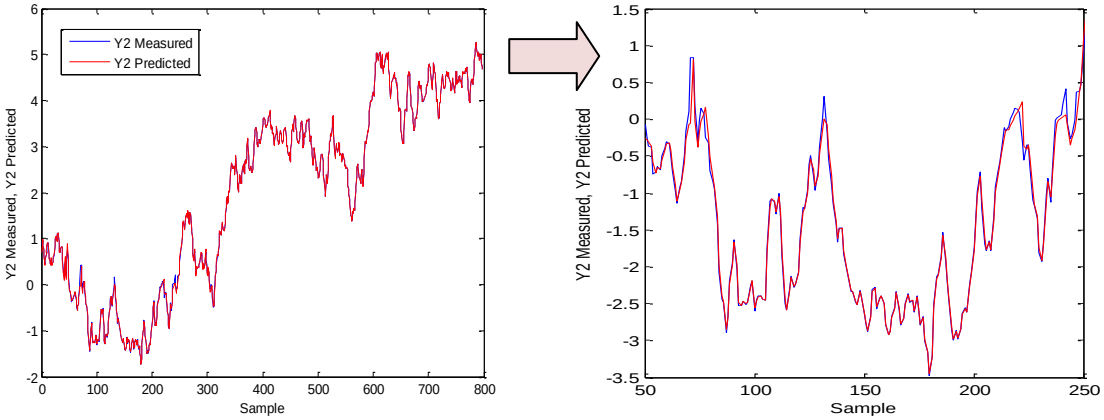

Figure 4.31 - Time series plot of measured and predicted values for the second quality variable- APLS (Validation data set)

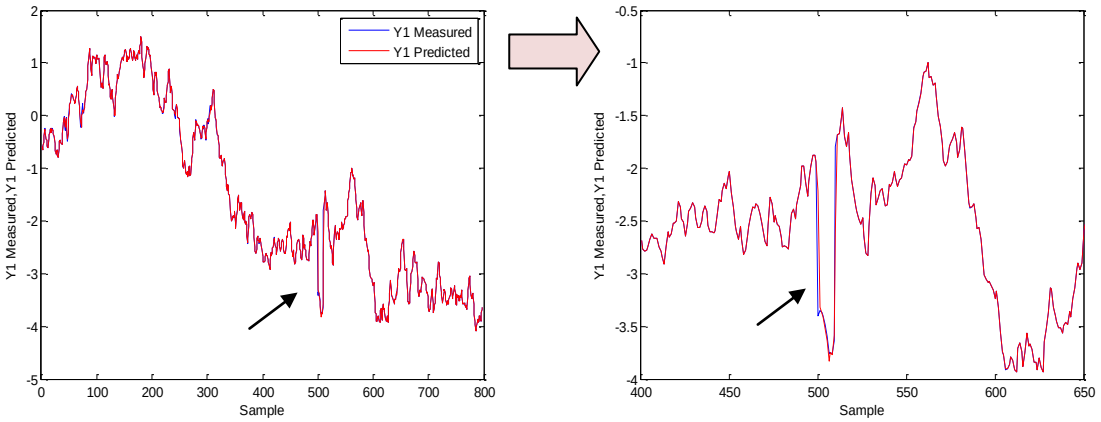

Figure 4.32-Time series plot of measured and predicted values for the first quality variable - APLS (Test data set)

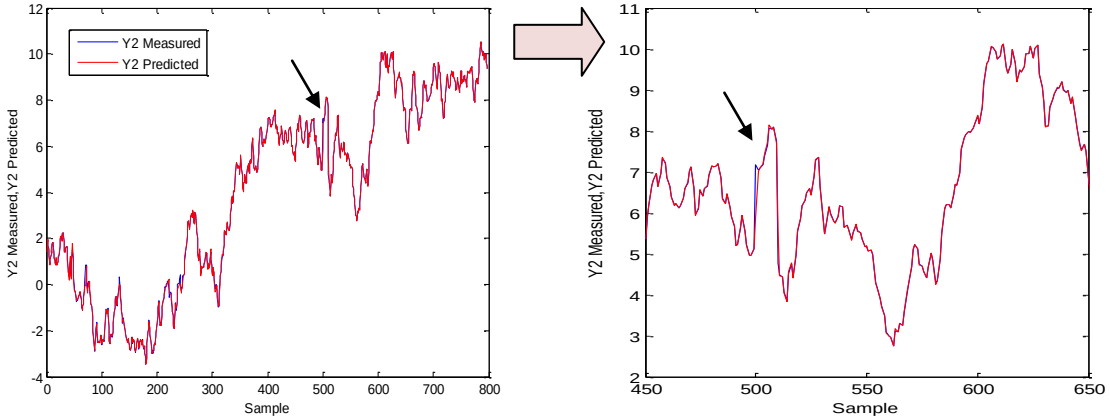

Figure 4.33-Time series plot of measured and predicted values of the second quality variable - APLS (Test data set)

Table 4.9- RMSE of the validation and test data set - APLS

Quality Variables	Validation data set	Test data set
	RMSE	RMSE
Y1	0.01	0.05
Y2	0.06	0.08

The results from the monitoring of the non-stationary behaviour using the APLS model for the validation data set are illustrated in Figures 4.34, 4.35 and 4.36. In general the confidence limits adapt to the non-stationary behaviour. This result in a significant reduction in the number of false alarms compared to conventional PLS. A few samples fell outside of the 95% and 99% confidence limits and this was expected to be of the order of 5% and 1% respectively. This is reflected in Table 4.10, where the rate of false alarms, 5.87%, 4.37% and 4.62% for the 95% confidence limit and the FAR, 1.25%,

1.12% and 1.75% for the 99% confidence limit for Hotelling's T^2, SPE_X and SPE_Y respectively. Therefore, the number of the false alarms is greatly reduced compared to those from conventional PLS, 58.12%, 59.87% and 60% (Chapter 3).

For the test data set where a step change was introduced, Hotelling's T^2 does not indicate the presence of the step change whilst the SPE_X and SPE_Y monitoring statistics indicated the presence of the step change at t = 500 (Figures 4.37, 4.38 and 4.39). However, they identified the first two samples and then the confidence limits started to adapt to the change. Consequently, the model and confidence limits were updated using samples that were affected by the step change hence the monitoring charts indicated that the process was back in statistical control whilst still affected by the abnormal event (step change). The quantitative fault detection rates (Table 4.10) reflect this as the monitoring chart of SPE_X and SPE_Y detect 20% of the fault whilst Hotelling's T^2 does not detect a fault as shown in Figure 4.37.

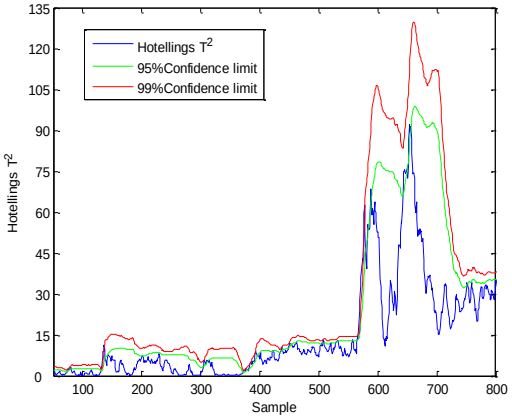

Figure 4.34 - Hotelling's T^2 for the validation data set

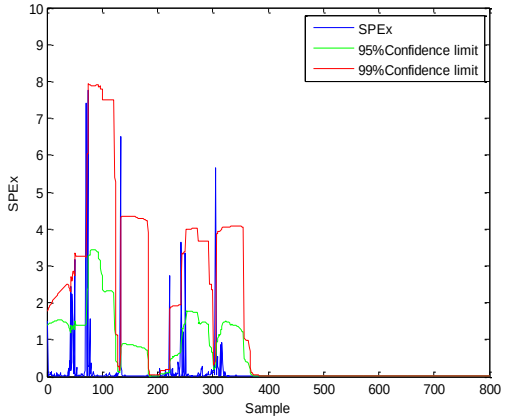

Figure 4.35 - SPE_X for the validation data set

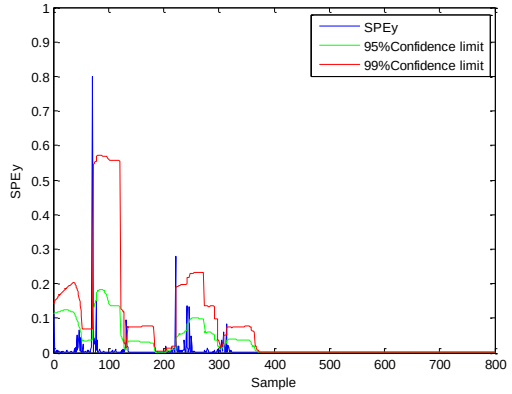

Figure 4.36 - SPE_Y for the validation data set

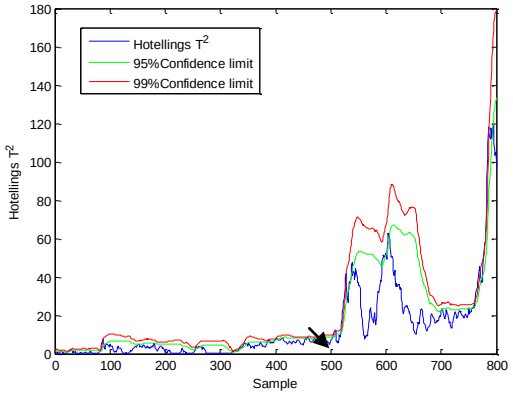

Figure 4.37 - Hotelling's T^2 for the test data set

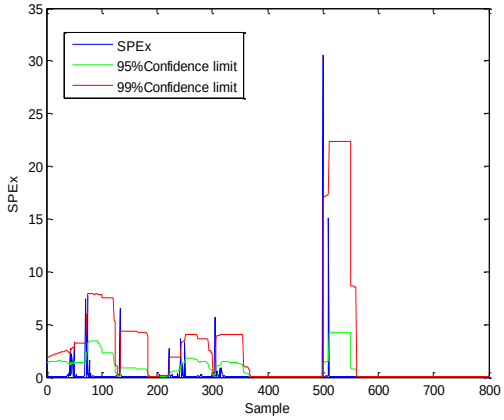

Figure 4.38 - SPE_X for the test data set

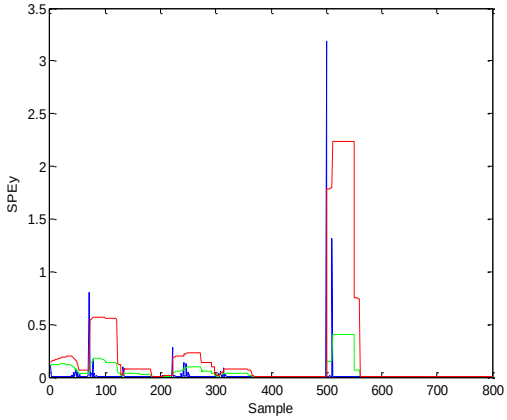

Figure 4.39 - SPE_Y for the test data set

Table 4.10 - FDR and FAR based on APLS

Chart	FDR – 95%	FDR – 99%	FAR – 95%	FAR – 99%
Hotelling's T^2	-	-	5.87 %	1.25 %
SPE_X	20%	20%	4.37 %	1.12 %
SPE_Y	20%	20%	4.62 %	1.75 %

Table 4.11 summarises the results from using a Monte Carlo simulation based on 50 experiments to calculate the average run length (ARL). The result shows that for the validation data set, the ARL0 indicated that the monitoring charts of the APLS model did not produce false alarms for an acceptable period of time, 59, 62 and 70 samples for the Hotelling's T^2, SPE_X and SPE_Y compared to these following the application of conventional PLS (Chapter 3), which were 47, 37 and 33 samples respectively. The ideal ARL0 is approximately 100 samples which indicate that the APLS improved the monitoring charts compared to conventional PLS. On the other hand, the results of the ARL1 indicated that the abnormal event is indicated rapidly compared to the monitoring charts based on conventional PLS. On average SPE_Y based on the APLS model indicates the abnormal event after a delay of one sample compared to a delay of 4 samples following the application of conventional PLS. In addition, SPE_X constructed based on APLS indicates the abnormal event immediately compared to the same monitoring chart from conventional PLS which required 3 samples to indicate its presence. Hotelling's T^2 was not affected by the abnormal event hence ARL1 is not calculated.

Table 4.11 - The average run length of the monitoring charts by APLS.

Chart	ARL0	ARL1
Hotelling's T^2	59	-
SPE_X	62	0
SPE_Y	70	1

4.7.2 Application of RAPLS to a Non-stationary Process

The RAPLS algorithm described in §4.4.2 is used to develop monitoring schemes for a process exhibiting a non-stationary behaviour. The reference model developed based on conventional PLS (§3.10.3) is utilized. The univariate monitoring statistics and the combined index for every new sample are calculated and the RAPLS thresholds are implemented prior to model update to prevent a non representative sample from contributing to the model updating process. Details of the used weight is provided in Appendix B.

Figures 4.40 and 4.41 show the measured and predicted values for both quality variables for the validation data set. It can be seen that the results are comparable to the results following the application of APLS. A few samples, 5 samples corresponding to 0.6% for the 99% confidence limit, can be detected based on the combined index (Figure 4.42). However, since only 5 samples are identified as outliers (when combined index violates its limit), there is no difference in the prediction results compared to the APLS algorithm. The RMSE of prediction (Table 4.12), i.e. 0.01 and 0.06 for both quality variables reflect this observation as it is similar to the RMSE following the application of APLS for the validation data set (Table 4.9)

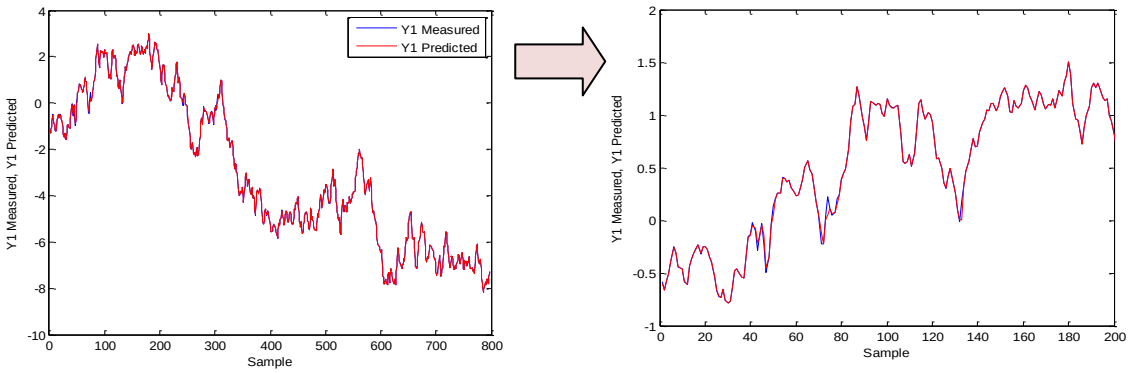

Figure 4.40 - Time series plot of measured and predicted values for the first quality variable - RAPLS (validation data set)

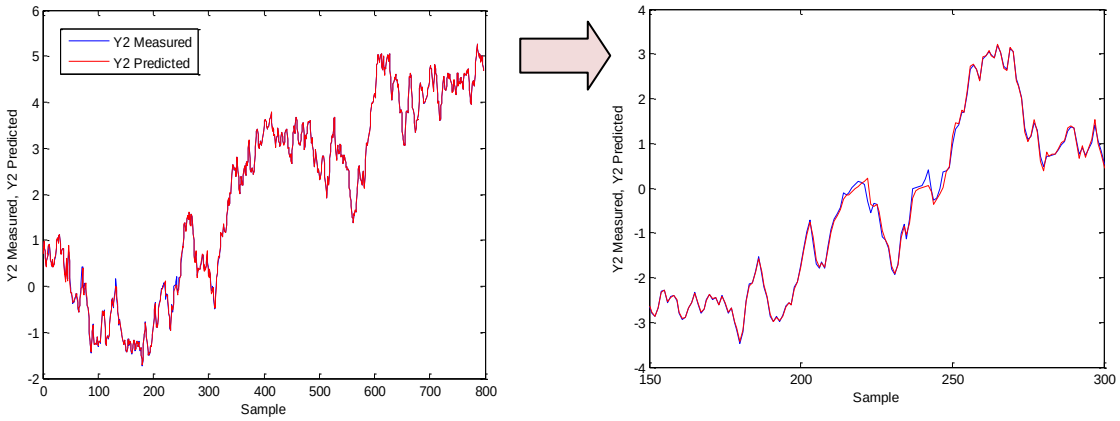

Figure 4.41 - Time series plot of measured and predicted values for the second quality variable - RAPLS (validation data set)

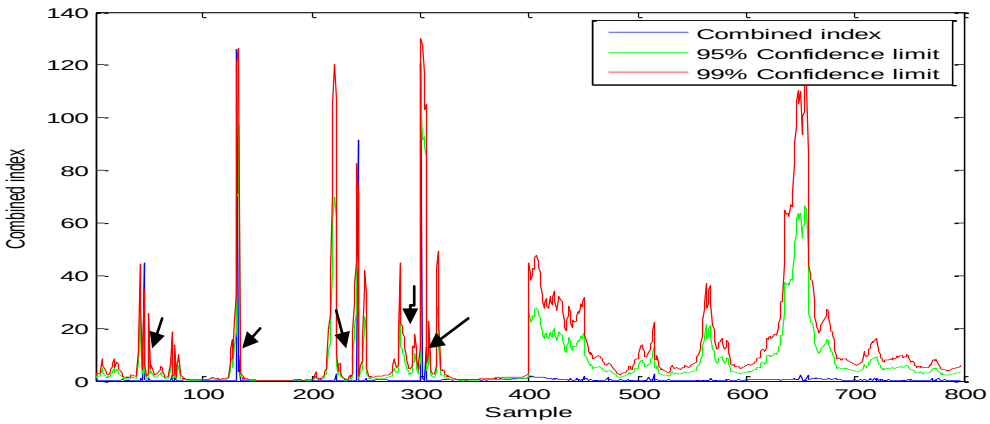

Figure 4.42- Time series plot of the combined index - RAPLS (validation data set)

The results from the application of RAPLS to the test data set are presented in Figures 4.43 and 4.45. It can be clearly seen that both quality variables were well predicted. However, during the step change period the prediction accuracy is less compared to that for APLS. This was expected as these samples were discarded from the model updating process and the model prior to the step change was used to predict the behaviour of the process during this period, consequently, the RMSE decreased as shown in Table 4.12. However, it can be clearly seen that the value of the RMSE, 0.13 and 0.16 for both quality variables following the application of RAPLS improved compared to that for conventional PLS, RMSE = 0.6 and 1.46, (Chapter 3).

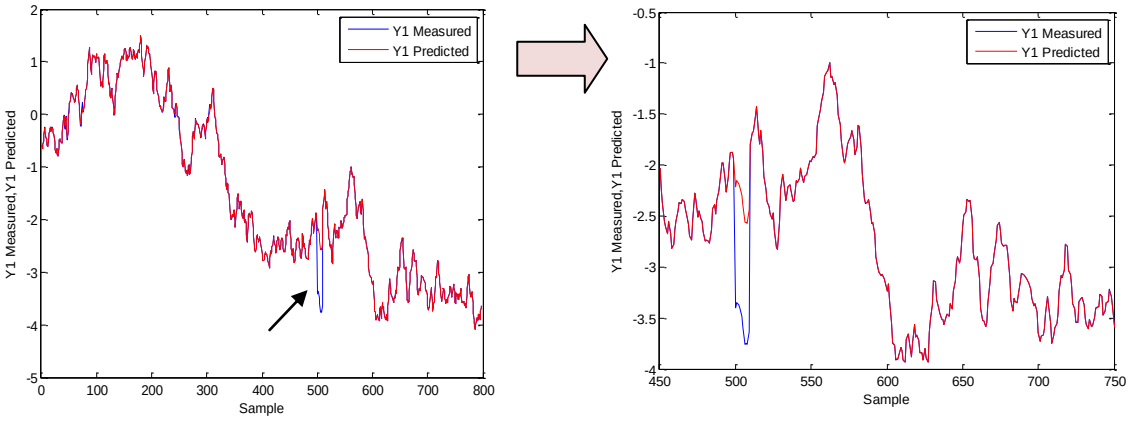

Figure 4.43 - Time series plot of measured and predicted values for the first quality variable - RAPLS (test data set)

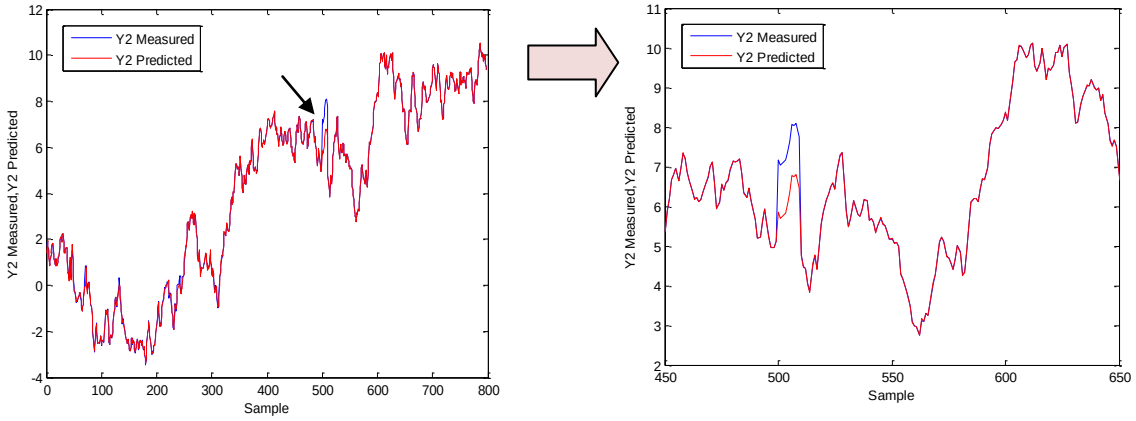

Figure 4.44 -Time series plot of measured and predicted values for the second quality variable - RAPLS (test data set)

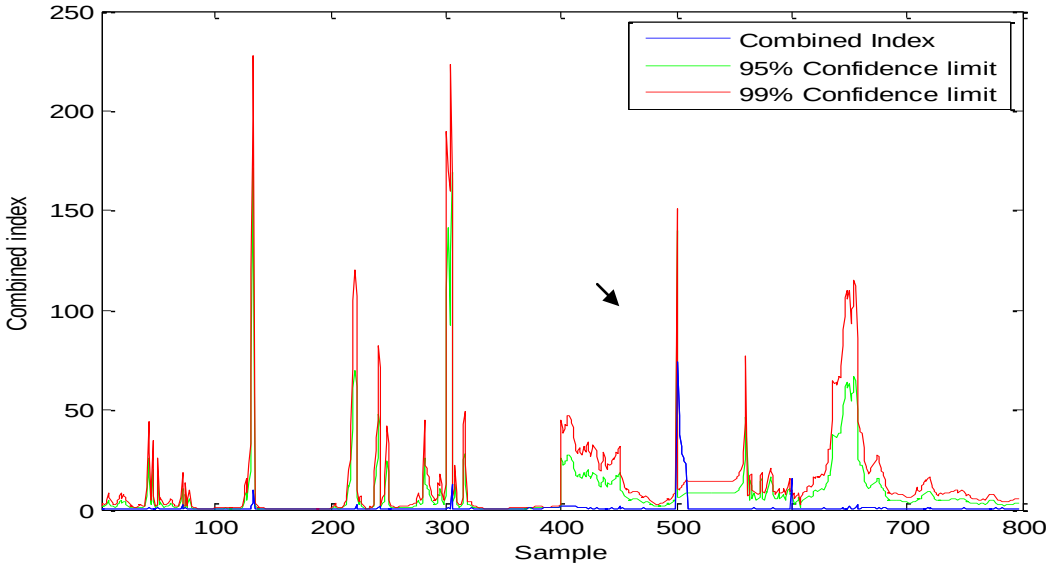

Figure 4.45 - Time series plot for the combined index - RAPLS (test data set)

Table 4.12- RMSE of the validation and test data sets by RAPLS

Quality variables	Validation data set	Test data set
	RMSE	RMSE
Y1	0.01	0.13
Y2	0.06	0.16

Figures 4.46, 4.47 and 4.48 show the monitoring charts following the application of RAPLS for the validation data set. The results for the validation data set are comparable to those for APLS. A few samples lie outside of the 95% and 99% confidence limits. Table 4.13 summarizes the quantitative results of the number of false alarms and it can be concluded that the rate of violations is acceptable for 95% and 99% confidence limits respectively. The FAR is 5.87%, 4.37% and 4.62% for the 95% confidence limit and 1.25%, 1.12% and 1.75% for the Hotelling's T^2, SPE_X and SPE_Y respectively for the 99% confidence limit. In addition these rates reveal that the number of violations is greatly reduced compared to conventional PLS (Chapter 3).

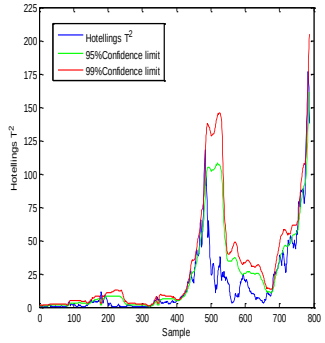

Figure 4.46- Hotelling's T^2 for the validation data set

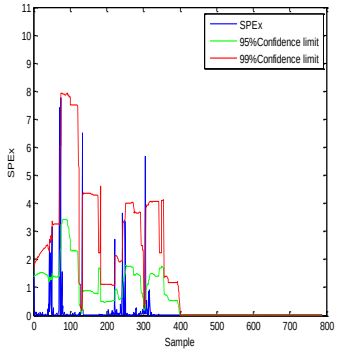

Figure 4.47 - SPE_X for the validation data set

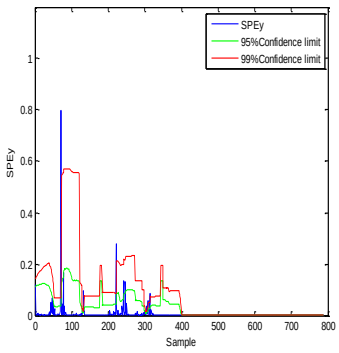

Figure 4.48 - SPE_Y for the validation data set

The monitoring results following the implementation of RAPLS to the test data set are illustrated in Figures 4.49, 4.50 and 4.51. It can be clearly seen that the monitoring charts SPE_X and SPE_Y are affected by the abnormal event and indicate the presence of the step change. Consequently, the confidence limits stop adapting process until the process is back to normal operating conditions. This is reflected in Table 4.13 where 100% of the abnormal event was detected compared to 20% following the implementation of APLS. Hotelling's T^2 is not affected by the step change and hence it does not violate the confidence limits and therefore the fault detection rate is not

calculated. This is because Hoteling's T^2 reflects a different change in the process compared to those reflected by SPE_X and SPE_Y monitoring charts.

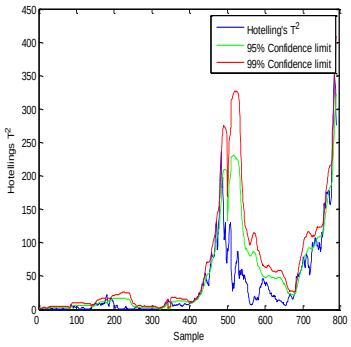

Figure 4.49- Hotelling's T^2 for the test data set

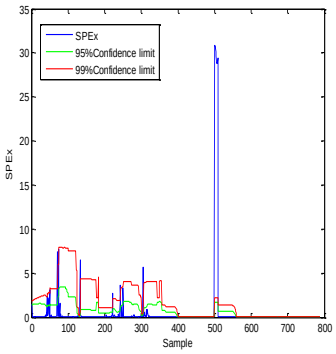

Figure 4.50 - SPE_X for the test data set

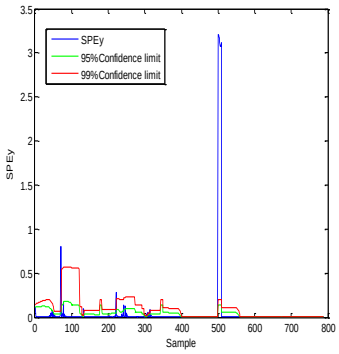

Figure 4.51 - SPE_Y for the test data set

Table 4.13- FDR and FAR based on RAPLS

Chart	FDR – 95%	FDR – 99%	FAR – 95%	FAR – 99%
Hotelling's T^2	-	-	5.87 %	1.25 %
SPE_X	100%	100%	4.37 %	1.12 %
SPE_Y	100%	100%	4.62 %	1.75 %

The concept of average run length is used again based on Monte Carlo simulation for 50 experiments, to evaluate the monitoring charts. Table 4.14 summarizes the results for ARL0 and ARL1. It can be seen that the monitoring charts based on RAPLS remain within state of statistical control for a sufficient number of samples, compared to the ideal ARL0 of 100 samples, as reflected by the ARL0 ,62, 65 and 73, for Hotelling's T^2, SPE_X and SPE_Y respectively and the results are slightly different to those following the application of APLS, 59, 62 and 70.

As only SPE_X and SPE_Y indicated the presence of the step change, the ARL1 is calculated for these two metrics. On average, the SPE_X chart based on RAPLS detects the abnormal event immediately and after 1 sample for SPE_Y. This result concludes that the monitoring chart is an improvement compared to that for conventional PLS.

Table 4.14 - The average run length of the monitoring charts by RAPLS.

Chart	ARL0	ARL1
Hotelling's T^2	62	-
SPE_X	65	0
SPE_Y	73	1

The following conclusions can be drawn from comparing the performance of the adaptive approaches and conventional PLS for a non-stationary process:

- The predictions following the application of the adaptive approaches are improved compared to those for conventional PLS. The root mean squared error (RMSE) of prediction reflects this observation as it lower than the corresponding values for conventional PLS.
- In term of the monitoring charts, the adaptive PLS (APLS) (Wang et al., 2003) monitoring charts indicate the presence of the abnormal events. However, the adaptive confidence limits are allowed to adapt to the new samples, consequently, the fault detection rate decreases.
- An alternative adaptive method RAPLS algorithm which performs better than APLS (Wang et al., 2003) in terms of fault detection shows that the FDR is high compared to APLS. In addition, it has the ability to identify outliers and determine whether a new sample is generated during normal operations or is an abnormal event.
- Both adaptive approaches, APLS and RAPLS, decrease the number of false alarms compared to conventional PLS.

4.8 Chapter Summary and Conclusions

A critical review of a number of recursive PLS methods presented in the literature was undertaken. From this analysis, the sample wise recursive PLS algorithm along with adaptive confidence limits proposed by Wang et al. (2003) was selected as the bases of the subsequent analysis for the following reasons:

- The efficiency of the model updating procedure which resulted in more accurate predictions.
- The ability of the model to account for changes in process behaviour.

- The ability of the model to be extended to construct monitoring charts for the whole process and individual unit operations as shown in Chapter 6.

However, two issues arose, first, the presence of outlying samples when performing real time modelling and monitoring and their impact on the adaptive confidence limits. To account for these issues, robust adaptive PLS with adaptive confidence limits (RAPLS) was developed. The proposed approach is resistant to statistical outliers and the updating procedure is not implemented in the presence of non-conforming samples. The results from the case studies showed that this approach is an improvement over the APLS algorithm in terms of process monitoring and fault detection rate.

Secondly, as most industrial processes have autocorrelated measurements and since conventional PLS does not deal with autocorrelated measurements, a dynamic extension to APLS and RAPLS was proposed. The recursive partial least squares models with adaptive confidence limits (APLS) proposed by (Wang et al., 2003) and RAPLS were extended to model and monitor dynamic processes with adaptive confidence limits.

The adaptive PLS (APLS) algorithm was applied to a time varying process and a non-stationary process and it was shown that the adaptive PLS approach reduced the false alarm rate compared to conventional PLS. However, the fault detection rate was reduced since the model as well as confidence limits were updated using non-conforming samples and hence out of control behaviour failed to be detected. Therefore, a RAPLS algorithm was proposed to overcome the aforementioned limitations. The adaptive PLS approach was used as the basis. But through the implementation of the combined index as a threshold, the model and the limits were only updated with samples representative of nominal operation.

From the application of the APLS and RAPLS algorithms to the simulations of time varying and non-stationary process, it can be concluded that the adaptive approaches reduced the number of false alarms compared to conventional PLS as discussed previously. The most significance difference between conventional PLS and the adaptive algorithms is observed in the SPE_Y chart for time variants processes. In addition, the RAPLS algorithm further decreased the number of false alarms compared to APLS for Hotelling's T^2, SPE_X and SPE_Y. This is due to the ability of the RAPLS algorithm to identify the outlying samples and hence it can accurately investigate the new samples. In terms of fault detectability, it can be concluded that the monitoring

charts following the application of RAPLS provide reliable results as the fault detection rate was higher than these for APLS.

In Chapters 5, the dynamic variants of PLS, adaptive PLS (APLS) and robust adaptive PLS (RAPLS) based on an Auto-Regressive with eXogenous input (ARX) are applied to model the complex dynamic behaviour of an ammonia synthesis fixed bed reactor.

Chapter 5

Statistical Monitoring of Complex Behavior of the Ammonia Synthesis Reactor

5.1 Introduction

This chapter presents the statistical monitoring of a unit operation that forms part of a continuous process. The application study involves data generated from a simulation of an ammonia synthesis reactor published by Morud and Skogestad (1998). The simulation is based on first principle models that are complex and time consuming to develop and from the literature it has been shown that the ammonia synthesis reactor is a dynamic system (Brian et al., 1965; Morud and Skogestad, 1998). In addition, it is demonstrated that the presence of recycling in the ammonia synthesis process increases the level of complexity (Denn and Lavie, 1982; Morud and Skogestad, 1998). Although the first principle models offers a detailed understanding of the physical behaviour of the process, empirical modelling provides a faster result and is forward in some application. Partial Least Squares (PLS) is the most common statistical approach that has been used for the development of empirical models and form the basis of modelling and monitoring schemes discussed in this chapter.

5.2 Objectives

Two objectives form the bases of this study. The first was to demonstrate the application of the statistical modelling technique of partial least squares to an industrial process that exhibits dynamic and nonlinear behaviour. The second goal was to apply the extensions of PLS, dynamic PLS (DPLS), adaptive dynamic PLS (ADPLS) and robust adaptive dynamic PLS (RADPLS) to develop real time monitoring charts. The purpose of the monitoring charts is to provide better insight and immediate information on the state of the process by detecting special cause variation. The key questions addressed are:

- Is the multivariate statistical technique of PLS or its variants DPLS, ADPLS and RADPLS appropriate for the understanding and prediction of reactor performance?
- Which pre-processing techniques have a significant impact on the dynamic PLS algorithm in terms of predicting the concentration of ammonia?
- Are the monitoring charts built, based on dynamic PLS and its variants, appropriate for detecting abnormal behaviour?

- Which PLS approach (conventional PLS, dynamic PLS, adaptive PLS or robust adaptive PLS) is more appropriate for monitoring performance and why?

The following section provides a description of the process characteristics and the simulation study.

5.3 Ammonia Synthesis Reactor

In the chemical industry, ammonia is considered to be an important chemical compound with 15% of the ammonia produced worldwide being used by industry (Appl, 1999) with fertilizer industry using 80% of the total amount of produced ammonia in the USA (Riegel and Kent, 2007). Furthermore, it is used for the production of a range of industrial products including fibres, plastics, organics and explosive components. The production of ammonia has expanded outside the USA with China, Russia and India being the main producing countries and more recently the Middle East. According to the US Geological Survey (U.S. Geological Survey, 2008), the main producer countries produce 55% of the total world production of ammonia.

5.3.1 Overview of the Ammonia Synthesis Reactor

Figure 5.1 shows a schematic diagram of the ammonia synthesis reactor. Ammonia synthesis is performed in a fixed-bed reactor, which consists of two core elements; the first is that 3 consecutive fixed-beds with each bed comprising 10 segments in which the reaction is carried out. The second element is the heat exchanger where heat is exchanged between the inlet stream and the outlet stream. As a result, the heat is recycled to the process. The produced ammonia leaves the reactor at the bottom of the third bed with product quality being defined in terms of concentration of the produced ammonia.

More specifically, the gases (H_2, N_2) pass through the first bed and the reaction initially takes place slowly and the ammonia (NH_3) concentration is low. The reaction rate increases as the temperature increases along the bed reaching equilibrium when all the influences are balanced or stable (Figure 5.1). Hot gases (H_2, N_2 and NH_3) are then passed out and the gas-mixture is cooled down by mixing with fresh feed (H_2, N_2) at quench point Q_2. In the second bed, the temperature increases again as the reaction takes place and once again reaches equilibrium and hot gas (H_2, N_2 and NH_3) is passed out. This operation is repeated when the stream is transferred from the second to the third bed with the gas exiting from the third bed and entering the heat exchanger. Heat

is exchanged between the hot gases (H_2, N_2 and NH_3) and the fresh feed (H_2, N_2) with the heated gases being transferred back to the first bed. This is mixed again with the fresh feed at quench point, Q_1 (Figure 5.1), and passed to the first bed and process is repeated.

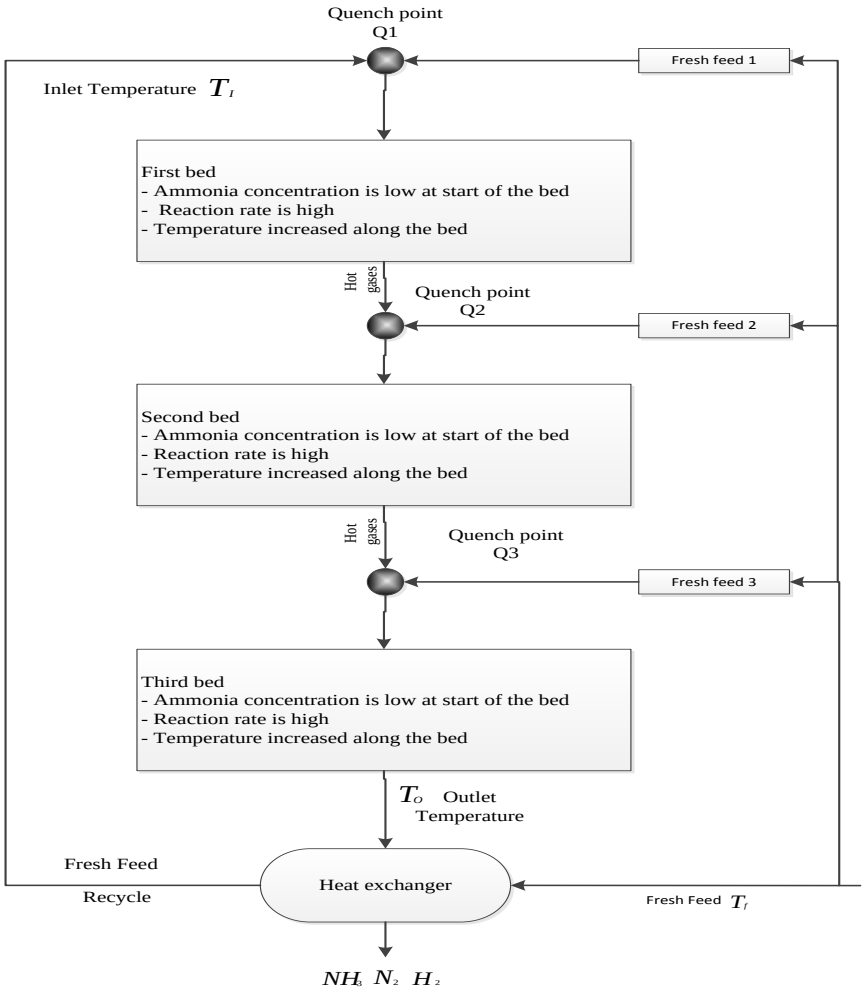

Figure 5.1- Schematic diagram of ammonia synthesis fixed-bed reactor

It is essential for the ammonia synthesis process to maintain the product concentration (ammonia) at the required level by maintaining the level of pressure of the reactor and the temperature of the total feed flow. In general to set up a controller for any process, it is necessary to understand the behaviour of the process under open loop control as a first step. Therefore, the statistical analysis of the ammonia synthesis undertaken is performed in the absence of a controller to enable process understanding. The findings and discussions in this chapter are based on the data generated from a simulation study published by Morud and Skogestad (1998). The purpose of using this simulation is to obtain data that is representative of dynamic behaviour of an industrial process.

5.4 Process Characteristics

5.4.1 Dynamic System with Recycle

The ammonia synthesis reactor considered in this case study is a dynamic system which exhibits complex dynamics due to recycling and quenching (Morud and Skogestad, 1998). Energy recycling in the ammonia process occurs when the hot stream of ammonia enters the heat exchanger and heats up the fresh feed before entering the first bed. The presence of recycling results in the process operating under a feedback mechanism i.e. recycling is equivalent to feedback control. In general, recycling in any dynamic process increases its sensitivity to disturbances, response time and hence can result in instability (Denn and Lavie, 1982; Morud and Skogestad, 1994). It is shown that the ammonia reactor becomes unstable and its temperature oscillates rapidly in two situations (Morud and Skogestad, 1998). The first occurs when the overall pressure drops below 170 bar and the total fresh feed temperature is kept at steady state. The second occurs when the total fresh feed temperature drops below 235°C and the overall pressure is maintained at steady state. Table 5.1 summarizes the operating conditions resulting in the ammonia reactor becoming unstable. Morud and Skogestad (1998) pointed out that these large and rapid oscillations of the temperature damage the catalyst in the reactor. This behaviour is called limit cycle behaviour and it is shown in Figure 5.2 where the instability is caused by a drop in the overall pressure.

Table 5.1- Situations where the ammonia reactor becomes unstable

Instability caused by	Total fresh feed temperature	Pressure
Case 1	Constant at 250°C	Drops below 170 bar
Case 2	Drops below 235°C	Constant at 200 bar

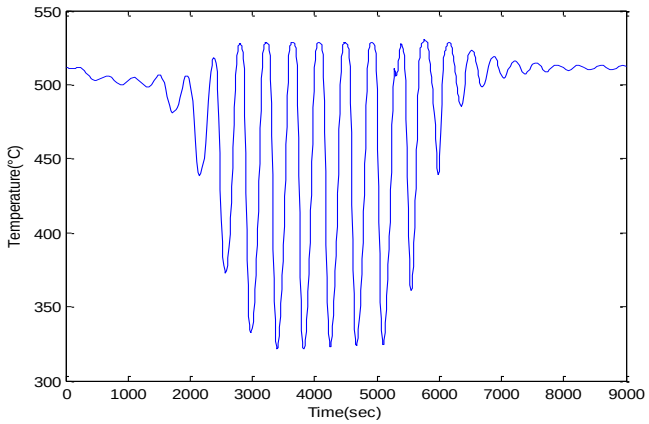

Figure 5.2 - Limit cycle behaviour of the ammonia synthesis reactor

In Figure 5.2, the reactor initially operates at 200 bar and then at t=0 sec the pressure is reduced from 200 to 170 bar and the temperature remains stable. The limit cycle behaviour starts when the overall pressure is reduced from 170 to 150 bar at 2000 sec. The temperature stabilises once the pressure is restored to 200 bar.

The analysis of the unstable behaviour of the ammonia fixed-bed reactor is extensive in the field of control engineering. Table 5.2 summarizes three key papers where the dynamic behaviour of the ammonia synthesis fixed-bed reactor has been analysed using theoretical models, i.e. first principle models, and control strategies. First principle models are built based on the fundamentals of chemistry and physics of the process but such models are difficult to develop, especially for complex processes such as ammonia synthesis (Seborg et al., 1989; Morud and Skogestad, 1994; Morud and Skogestad, 1998).

Table 5.2 - Key literature on the analysis and control of the ammonia synthesis reactor.

Type of analysis	Purpose of the analysis	References
Steady state analysis Nonlinear dynamic analysis Root locus analysis Frequency analysis	Explanation of dynamic behaviour of the reactor Development of first principle model	Morud and Skogestad (1998)
Simulation and control of the reactor using feedback control	To prove the claim that the reactor could be controlled using feedback control	Realfsen (2000)
Simulation and application of different control strategies	Different control designs were applied to stabilize the reactor.	Holter (2010)

Morud and Skogested (1998) performed an analysis on the instability of the behaviour of the ammonia reactor and they showed that steady state analysis is inappropriate. Nonlinear dynamic analysis was then used to study the cause of the instability of the ammonia reactor. Through the approaches of root locus analysis and frequency domain analysis, physical insight was attained into the cause of the instability. Finally they showed that the reactor can be stabilised through the implementation of a feedback controller (Morud and Skogestad, 1998). Realfsen (2000) also showed that a feedback controller can be used to stabilise the reactor. More recently Holter (2010) analysed the theoretical model developed by Morud and Skogested (1998) and applied different

control design including feed-forward and feedback control to stabilize the process. It was found that feed-forward design is inappropriate for stabilising the ammonia reactor.

5.5 Complexity of Process Behaviour and PLS Modelling

From the previous sections, it is clear that the complex dynamic behaviour of the ammonia fixed-bed reactor is a consequence of recycling. Moreover the theoretical modelling of such complex behaviour, which is based on a combination of differential and algebraic equations, requires significant effort, engineering experience and knowledge of the principles of chemistry and physics of the process to model process behaviour. Partial Least Squares (PLS) which is a black-box modelling approach provides an alternative approach for modelling such process behaviour. Moreover, it can be used to detect the onset of abnormal behaviour.

Despite the widespread application of PLS to model industrial processes under steady state and dynamic behaviour, limited attention has been paid to the use of recursive dynamic PLS with adaptive confidence limits to model dynamic nonlinear processes in the presence of recycling. For example, Wang et al. (2003) applied Recursive PLS with adaptive confidence limits for the modelling of a fluid catalytic cracking unit and a distillation column for purifying butane. Both processes presented time varying behaviour. However, the level of process dynamics was limited and consequently they were able to model the processes using linear steady state and recursive linear approaches. Hence, Wang et al. (2003) suggested that further investigation on autocorrelated processes (i.e. dynamic behaviour) was required. Another example is the process of wastewater treatment which exhibits time varying behaviour. It was modelled using robust block-wise recursive PLS (Lee et al., 2006a). However, block-wise recursive PLS results in different process models depending on block size. These approaches have been discussed in detail in Chapter 4. The ammonia synthesis reactor differs to the simulation studies in Chapter 4 showing strong dynamics due to the nature of the dynamic chemical equilibrium resulting from the continuous quenching of the fresh feed at the quench points. In this study, fixed parameter DPLS (conventional DPLS) and adaptive dynamic sample wise PLS were applied. The following sections provide a detailed description of the data collected from the ammonia synthesis fixedbed reactor and the development of fixed and adaptive dynamic PLS models.

5.6 Data Structure and Acquisition

The data in this study was generated from the simulation study published by Mourd and Skogested (Morud and Skogestad, 1998). The simulation was written in MATLAB©. In the simulation, the reactor was operated without a controller to allow for the understanding of process behaviour. It is known that the process operations of the ammonia synthesis are affected by changes in the overall pressure or the total fresh feed temperature as summarised in Table 5.1. An undesired oscillation (limit cycle behaviour) occurs if the settings in Table 5.1 occur. The initial operating conditions and start up values can be found in the original published work (Morud and Skogestad, 1998). For the development of an empirical model of the ammonia synthesis process using partial least squares regression, the data should be sampled on the basis of an appropriate sampling period, Δt. This should be selected to preserve the dynamic information contained in the process measurements and to avoid the problem of aliasing. The phenomenon of aliasing, i.e. where significant information relating to the process measurements is lost, materialises as a result of a long sampling period (Seborg et al., 1989). Figure 5.3 shows a schematic of the aliasing phenomenon where the purple signal represents the actual signal generated from a process and the blue signal is the signal collected based on long sampling interval indicating that the dynamic information in the actual signal is lost. If the sampling is too frequent, it can impact on the computer's ability to handle the data. In this study, the sampling period is determined based on the information from the time constant and is discussed in §5.6.1.

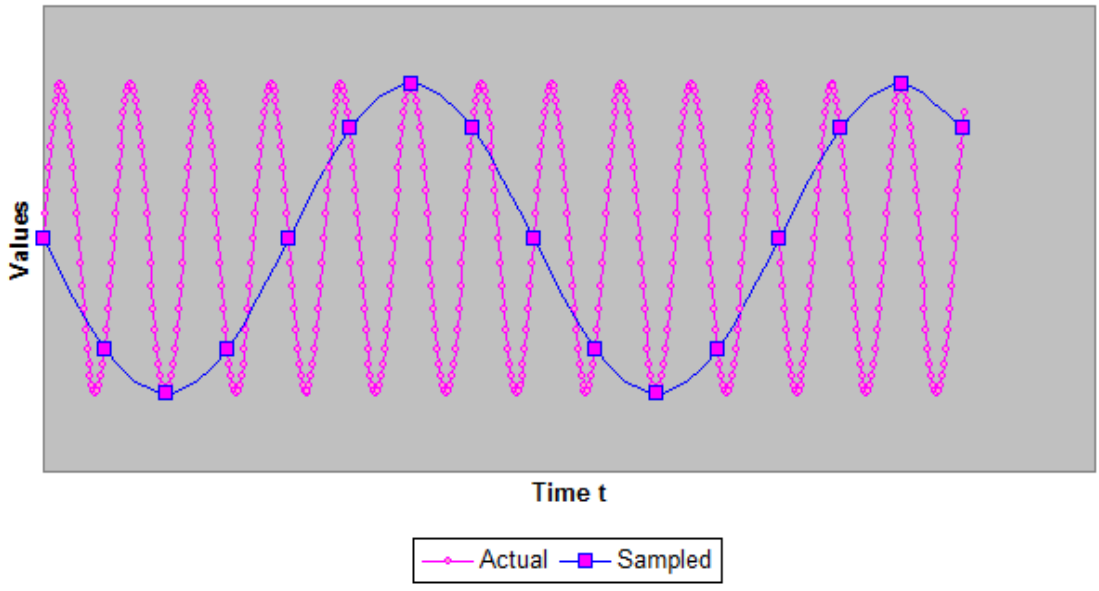

Figure 5.3 - Schematic diagram of aliasing phenomena (Seborg et al., 1989)

Table 5.3 - Predictor and responses variables of the ammonia synthesis reactor.

name	Tag		Description	Unit
C_3	y	1	Concentration of the ammonia (Response variable)	kg NH_3 /kg gas
T_i	x_1	2	Inlet temperature (Input variable)	^oC
T_f	x_2	3	Temperature of total fresh feed flow (Manipulated variable)	^oC
F_e	x_3	4	Total fresh feed (Input variable)	ton/h
Q_1	x_4	5	First quench flow rate (Input variable)	ton/h
Q_2	x_5	6	Second quench flow rate (Input variable)	ton/h
Q_3	x_6	7	Third quench flow rate (Input variable)	ton/h
T_{Q1}	x_7	8	Temperature of the first quench (Input variable)	^oC
T_{Q2}	x_8	9	Temperature of the second quench (Input variable)	^oC
T_{Q3}	x_9	10	Temperature of the third quench (Input variable)	^oC
P	x_{10}	11	Operating pressure (Manipulated variable)	bar

Table 5.3 summarises the predictor and response variables. The response variable is the ammonia concentration, y. The manipulated variables are the operating pressure and temperature of total fresh feed flow. For the ammonia synthesis reactor, different measured variables have their own dynamic characteristics. Consequently, they may respond differently to the same step in one of the manipulated variables. Figures 5.4 and 5.5 show the response of the inlet temperature and the concentration respectively for a step change in pressure. It appears that the response of the variables to reach a new steady state differ significantly.

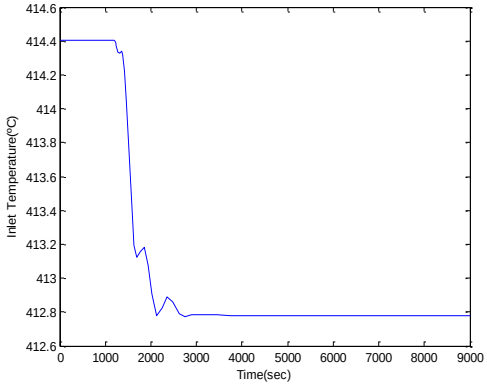

Figure 5.4 - The response of the inlet temperature for a step change in pressure

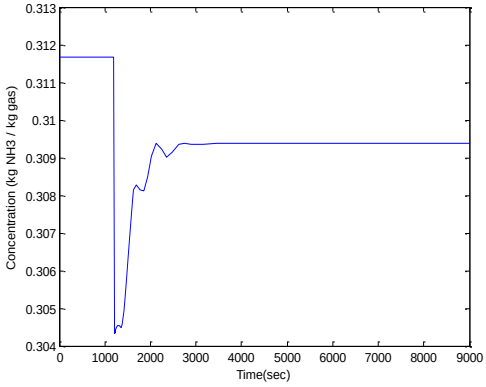

Figure 5.5 - The response of ammonia concentration for a step change in pressure

5.6.1 Time Constant

The time constant, τ, is important for determining the appropriate sampling frequency (i.e. sampling period). It is the time required by a system to reach 63.2% of a new steady state following a step change (Seborg et al., 1989). The time constant identifies how the process variables respond to a step change in the manipulated variables i.e. operating pressure or total fresh feed temperature in this study. The pressure and total fresh feed temperature are selected as they are the most common causes of disturbances in this system. Figure 5.6 shows a graphical determination of the time constant based on an open loop step response of the inlet temperature. From the graph, the following can be concluded:

Step change introduced:	t =1200 sec
Initial steady state value:	511.55 ^oC
Final steady state value:	502.5 ^oC
Differences between the two steady states:	9.05 ^oC
63.2% of the differences:	5.72 ^oC
63.2% of process (τ):	508.2 at t=1500 sec, 300 sec after the step

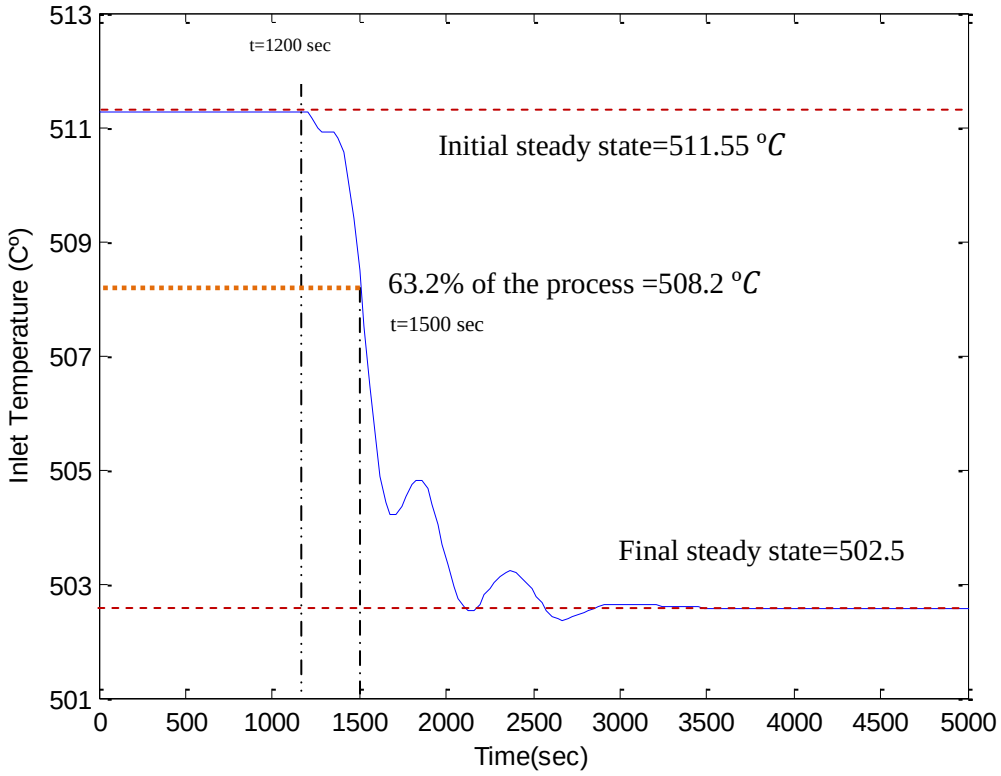

Figure 5.6 - Open loop step response and graphical determination of time constant

In Figure 5.6, the inlet temperature is used for calculating the time constant. Some of the other process variables such as second quench temperature give the same results for time constant. This can be observed from Figure 5.7 which shows an open loop response from the second quench temperature following a step change in the overall pressure. The time constant resulting from using the second quench temperature is exactly the same as for the inlet temperature, i.e. time constant, τ =300.

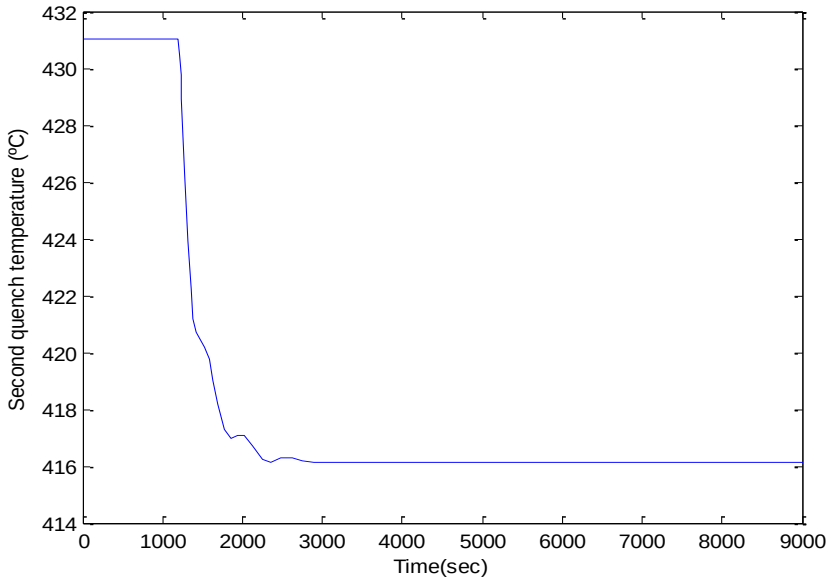

Figure 5.7- Response of the second quench temperature for a step change in pressure

5.6.2 Sampling Period

The calculation of the sampling period Δt is application based and in this work two criterion were used to help select the most appropriate sampling period (Seborg et al., 1989). The first helps identify the upper bound whereas the second one determines the lower bound. For an open loop system, the sampling period is calculated such that

$$\Delta t < (0.1)\,\tau \qquad (5.1)$$

where τ =300 and From Equation 5.1, any sampling period less than 30 sec would be theoretically appropriate for modelling the ammonia synthesis fixed-bed reactor.

The sampling period should be small enough to capture the significant information in the process, however, it should not be so small that the computational aspect of the analysis becomes an issue. It is therefore important to find an appropriate value for the

lower bound of the sampling period and for that Ziegler – Nichols control tuning rule (Seborg et al., 1989) is utilised:

$$0.01 < \frac{\Delta t}{\tau} < 0.05 \qquad (5.2)$$

Table 5.4 gives the results for the Ziegler – Nichols tuning rule utilising different sampling periods for the ammonia synthesis reactor. From both criterion, it can be seen that any sampling period less than 15 sec and greater than 2 sec is appropriate for capturing the process dynamics. A sampling rate of 10 sec was selected and this was determined based on constructing different models across this range. The models RMSE for the calibration and validation data sets and the variance captured together indicated that the model based on 10 sec was appropriate as has the lowest RMSE. It is important to mention that models based on different sampling periods in the range of 5 sec to 25 sec are performed well in terms of variance captured. The results from the different models are presented in Appendix C**.**

Table 5.4 – Different sampling periods for the ammonia reactor based on Ziegler – Nichols tuning rule (Seborg et al., 1989)

Δt	$\frac{\Delta t}{\tau}$	$0.01 < \frac{\Delta t}{\tau} < 0.05$
25	0.083	0.083 > 0.05
20	0.067	0.067 > 0.05
15	0.05	Equal to 0.05
10	0.033	0.01 < 0.03 < 0.05
5	0.016	0.01 < 0.016 < 0.05
2	0.006	0.006<0.01

Finally based on the previous discussion, the simulation was run over a period of 14000 sec with the samples taken every 10 sec. The first 4000 sec were used to build the reference model while the rest of the data was used for validation. In the test data sets, two types of disturbance were introduced to investigate the ability of the calibration model to predict and identify abnormal events. The following table summarise the features of the data used in the analysis and Figures 5.8 to 5.10 shows validation data set and two cases of test data set.

Table 5.5 - Summary of the data used in the analysis under different operating conditions

<table>
<tr><td colspan="4">Whole time of running the simulation 14000sec</td></tr>
<tr><td>t = 1 to t < 4000</td><td colspan="3">4000< t <= 14000</td></tr>
<tr><td>Calibration data set</td><td colspan="3">Validation data set t=1 to t=10000</td></tr>
<tr><td rowspan="4">Process pressure, fresh feed temperature are kept at steady state</td><td colspan="3">Process pressure, fresh feed temperature are kept within steady state range</td></tr>
<tr><td colspan="3">Test data set t=1 to t=10000</td></tr>
<tr><td colspan="2">t >= 1 to t<=3200</td><td>3200< t< 10000</td></tr>
<tr><td>Case 1</td><td>Pressure is dropped to 150 bar
Fresh feed temperature is kept at steady state</td><td>Process pressure is restored to steady state
Fresh feed temperature is kept at steady state</td></tr>
<tr><td></td><td>Case 2</td><td>Process pressure is kept at steady state
Fresh feed temperature is dropped to 235º C</td><td>Process pressure is kept at steady state
Fresh feed flow rate is restored to 250º C</td></tr>
</table>

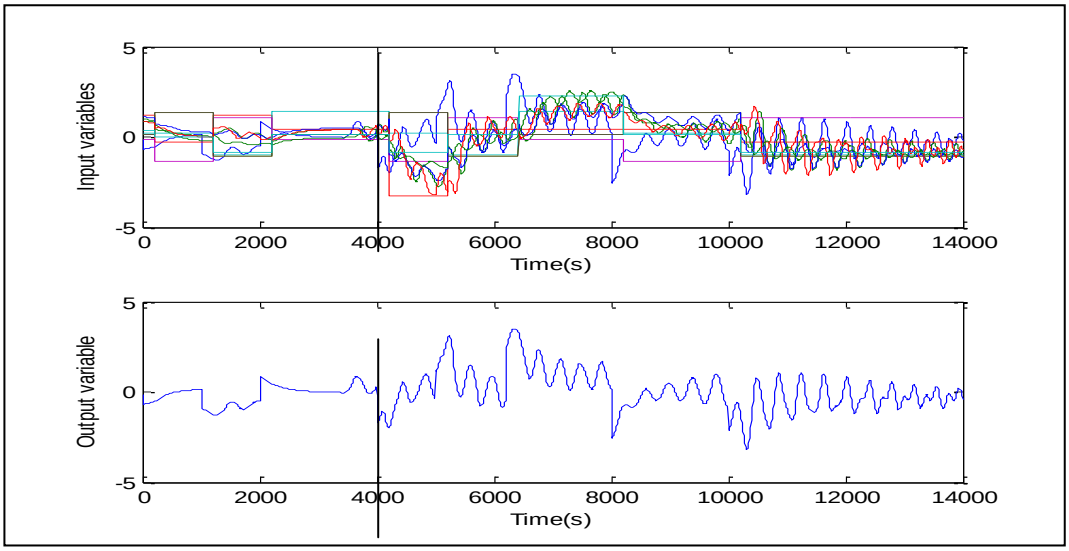

Figure 5.8 – Calibration and validation data sets

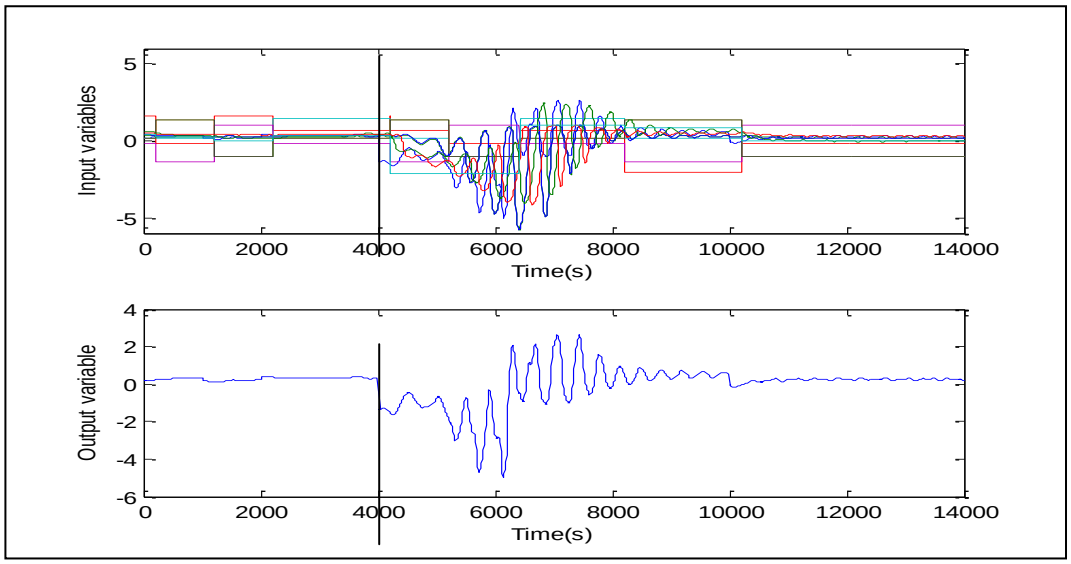

Figure 5.9 – Calibration and test data sets – Case 1

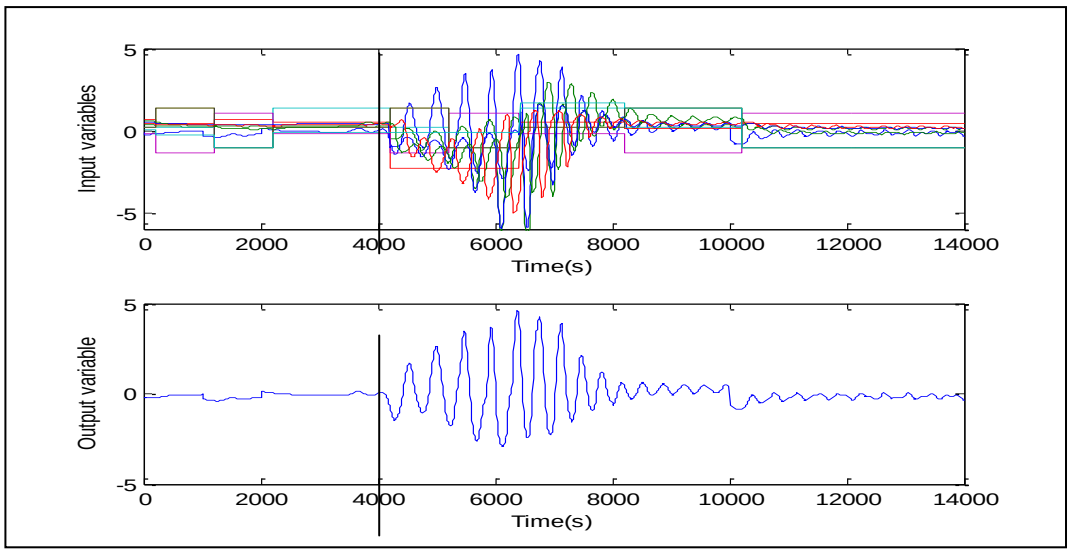

Figure 5.10 - Calibration and test data sets – Case 2

5.7 Modelling of Ammonia Concentration

Modelling the behaviour of the ammonia fixed-bed reactor is challenging because of the complex process dynamics and the presence of heat recycling along with the potential for the reactor to become unstable. The modelling was undertaken using the three PLS approaches described in Chapter 3 and Chapter 4 respectively (i.e. Conventional PLS, adaptive PLS and robust adaptive PLS). These approaches were modified to account for process dynamics caused by autocorrelation. The goal of the modelling task was:

- To model the complex behaviour of the ammonia synthesis fixed-bed reactor and analyse its performance.
- To predict ammonia concentration.

- To investigate the ability of the model to detect abnormal behaviour using dynamic PLS, adaptive dynamic PLS and robust adaptive dynamic PLS.

Prior to the development of the PLS model, identification of the dynamic representation and pre-processing of the data was undertaken. The following section introduces these stages and the rationale for the different approaches.

5.7.1 Identification of Reference Model using Dynamic PLS

5.7.1.1 Data Pre-Processing

Pre-processing of data is an important and recommended step prior to the modelling and monitoring stage (Bro and Smilde, 2003). However, it is important not to over treat the raw data otherwise information contained in terms of the original process is lost. In this study, the effect of pre-processing techniques on a dynamic PLS model is investigated with the goal of finding the most appropriate model for ammonia concentration. Pre-processing in this case study was limited to various forms of data scaling. Three different pre-processing techniques were considered in addition to the case where no pre-processing was undertaken. Model building data were generated by running the simulation of the first principle model without the addition of noise to reduce model complexity in this case study. Consequently, there was no requirement to filter the data. The following sections introduce the pre-processing techniques used in this case study.

5.7.1.1.1 Normalization

The first scaling technique considered was that of normalization, also known as standardization. By adopting this approach, all variables have the same weighting in the dynamic PLS model. The original data from the ammonia synthesis fixed-bed reactor contained variables with different standard deviations and measurement units. Such differences in units and variability can lead to biased predictions and inaccurate models. More specifically, the dynamic PLS model represents the original variables in a few latent variables that capture most of the process variation. Consequently variable with larger standard deviations can influence the model as it is over represented. Therefore, the variables can be normalized prior to implementing of dynamic PLS modelling.

$$x_{norm}(t) = \frac{x_p(t) - \bar{x}_p}{s_{x_p}} \tag{5.3}$$

$$y_{norm}(t) = \frac{y(t) - \bar{y}}{s_y} \tag{5.4}$$

where $x_p(t)$ and $y(t)$ are the input and output variables at time instance t respectively, $\bar{x}_p, \bar{y}$, s_{x_i} and s_y are the mean and standard deviation of the input and output variables respectively. The original and normalized variables from the ammonia synthesis fixed-bed reactor are shown in Figure 5.11 and Figure 5.12 respectively.

5.7.1.1.2 Mean Centring

Centring of variables involves the removal of the mean from each variable resulting in all variables taking a mean of zero. The centred variables are calculated by subtracting their average from the original values:

$$x_{pcentred}(t) = x_p(t) - \bar{x}_p \quad (5.5)$$

$$y_{centred}(t) = y(t) - \bar{y} \quad (5.6)$$

where $x_p(t)$ and $y(t)$ are the input and output variables at time instance t respectively, $\bar{x}_p$ and $\bar{y}$ are the mean of the input and output variables respectively. The cantered variables from the ammonia synthesis fixed-bed reactor are shown in Figure 5.13.

5.7.1.1.3 Mean Centring of Input Variables

For this case the input variables are mean centred as described in the previous section (Equation 5.5) but no pre-processing was applied to the output variable. The centred variables from the ammonia synthesis fixed-bed reactor are shown in Figure 5.14.

The difference between the original variables can be clearly seen in Figure 5.11 whereas in Figure 5.12 the variables are comparable following the application of the normalization approach. From Figures 5.13 and 5.14, it can be seen that there are differences in the ranges between the input variables and the output variables following the application of the mean cantering of the input and output variables and the application of mean cantering of the input variables respectively. The selection of the appropriate pre-processing approach was made based on the performance of the dynamic PLS model in terms of the Root Mean Squared Error (RMSE) and coefficient of determination, R^2, for the validation data set (§5.7.2).

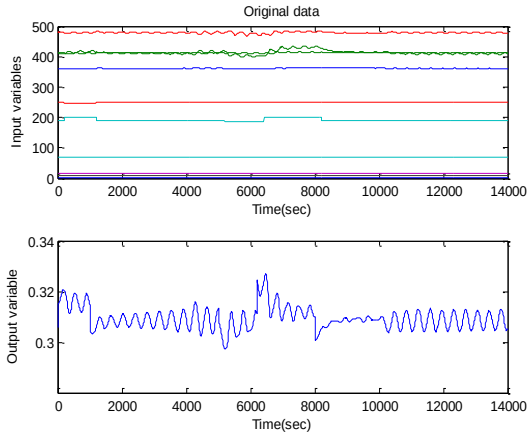

Figure 5.11 - Time series of the original (input/output) variables

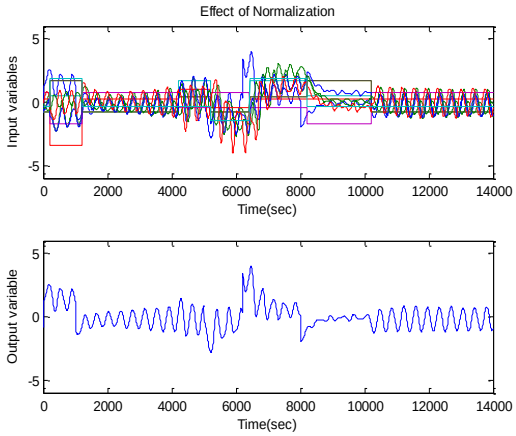

Figure 5.12- Time series of the normalized (input/output) variables

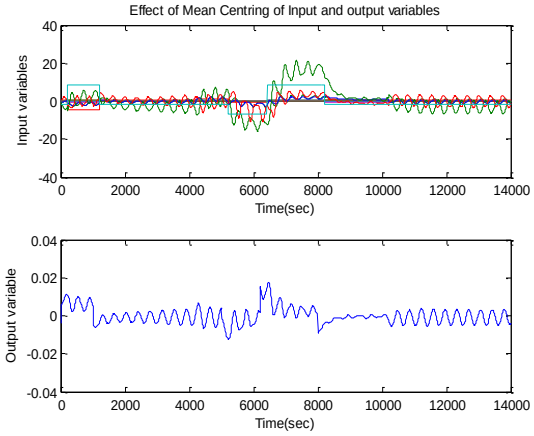

Figure 5.13- Time series of the mean centred (input/output) variables

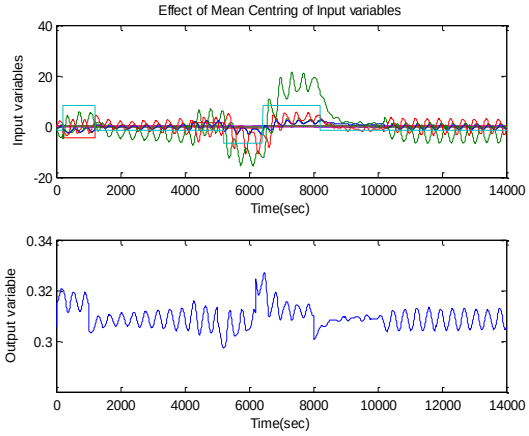

Figure 5.14-Time series of the mean centred input variables

5.7.1.2 Identification of Data Structure

In this process, the concentration of the ammonia was measured at the end of the third bed, therefore a time delay is expected between the process of measuring the input and output variables. The presence of the time delay has an impact on system stability (Kolmanovskii et al., 1999). From Table 5.6 it can be seen that there is approximately no correlation between the input and output variables at time instance t and hence a time delay between input and output variables exist as it is known that the variables are correlated and should be determined prior to PLS modelling. The presence of heat recycling and the time delay in the process increases the complexity of the dynamic behaviour as discussed in §5.4. Also as explained in Chapter 3, PLS assumes that the relationship between the variables is linear and static. However, the dynamic behaviour caused by autocorrelation of the process variables violates this assumption.

Therefore, it is necessary to include process dynamics and time delay in the structure of the data used for modelling and monitoring based on PLS through the application of a dynamic time series representation.

Table 5.6 – The correlation coefficients between input and output variables at time instance t

$\mathbf{x}_i(t)$	$\mathbf{x}_1(t)$	$\mathbf{x}_2(t)$	$\mathbf{x}_3(t)$	$\mathbf{x}_4(t)$	$\mathbf{x}_5(t)$	$\mathbf{x}_6(t)$	$\mathbf{x}_7(t)$	$\mathbf{x}_8(t)$	$\mathbf{x}_9(t)$	$\mathbf{x}_{10}(t)$
$\mathbf{y}(t)$	0.026	-0.042	0.0297	-0.016	0.016	0.016	0.0784	0.151	0.182	0.097

It is mentioned in Chapter 3 that the PLS model can account for process dynamics through the incorporation of a time series representation (e.g. AutoRegressive with eXogenous inputs (ARX) or Finite Impulse Response (FIR). In this study, an ARX model is used to build the dynamic representation. The advantage of an ARX model compared to FIR is the reduction in the number of parameters to be determined as the FIR model requires a large number of parameters to account for the process dynamics. The next section provides a brief description of the ARX representation and how it was implemented in terms of the data generated from the ammonia synthesis fixed-bed reactor simulation.

5.7.1.2.1 AutoRegressive with eXogenous Inputs Representation

An AutoRegressive with eXogenous input (ARX) representation is a linear relationship between the output of the process $\mathbf{y}(t)$ and past finite time series of the process output and process input $\mathbf{u}(t)$. The ARX representation is defined as:

$$\mathbf{y}(t) = \sum_{i=1}^{n_y} \mathbf{A}_i \mathbf{y}(t-i) + \sum_{j=1}^{n_u} \mathbf{B}_j \mathbf{u}(t-j-k+1) + \mathbf{e}(t) \qquad (5.7)$$

where $\mathbf{y}(t)$, $\mathbf{u}(t)$ and $\mathbf{e}(t)$ are the process output, input and noise vectors respectively. $\mathbf{A}_i$ and $\mathbf{B}_j$ are the matrices of the coefficients to be identified using PLS regression hence steady state PLS is used to model the dynamic process. n_y and n_u are the number of time lags for the output and input data vectors respectively; k is the time delay in the system. The ARX model can be expressed in a simpler matrix format such that the regressor row vector which consist of lagged output and input data values time instance t is:

$$\mathbf{x}(t) = [\mathbf{y}(t-1), \ldots, \mathbf{y}(t-n_y), \mathbf{u}(t-k), \ldots, \mathbf{u}(t-n_u-k+1)] \quad (5.8)$$

and the ARX representation can be written as:

$$\mathbf{y}(t) = \mathbf{C}.\mathbf{x}(t) + \mathbf{e}(t) \quad (5.9)$$

where $\mathbf{C}$ is the matrix of model coefficients given by:

$$\mathbf{C} = [\mathbf{A_1}, \ldots, \mathbf{A}_{n_y,}\mathbf{B_1}, \ldots, \mathbf{B}_{n_u}] \quad (5.10)$$

The ammonia synthesis fixed-bed reactor process is a multi-input system therefore the entry $\mathbf{u}(t-k)$ in Equation 5.8 is a row vector which consists of the process input variables listed in Table 5.3.

$$\mathbf{u}(t-k) = [\mathbf{x}_1(t-k), \mathbf{x}_2(t-k), \ldots \mathbf{x}_{10}(t-k)] \quad (5.11)$$

whereas the entry $\mathbf{y}(t-1)$ in Equation 5.8 is

$$\mathbf{y}(t-1) = [\mathbf{y}(t-1)] \quad (5.12)$$

It can be seen that the structure of the ARX representation depends on 3 values; the time lagged values (i.e. n_y and n_u) and the delay, k. Therefore an ARX model with n_y lagged values of output variables and n_u lagged values of the input variables and delay k is presented as $\mathrm{ARX}(n_y, n_u, k)$. The order n_y, n_u and k of the ARX representation is determined using Akaike's Information Criterion AIC (Akaike, 1974).

5.7.1.2.2 Akaike's Information Criterion (AIC)

AIC is an information measure used to help identify the most appropriate model among a class of competing models specified from recorded data (Akaike, 1974). Initially a set of candidate models need to be identified based on knowledge of the system under study and then AIC for each model can be calculated using the residual sums of squares of the model:

$$\mathrm{AIC} = n * \ln\left(\frac{\mathrm{RSS}}{n}\right) + 2 * A \quad (5.13)$$

Where n is the number of samples used for calibration; RSS is the residual sum of squares and A is the number of parameter in the ARX model. The model with the lowest AIC is then selected as the most appropriate model.

For identifying the most appropriate ARX representation for the data from the ammonia synthesis fixed-bed reactor, 11 sets of ARX representations were identified according to §5.7.1.2.1.

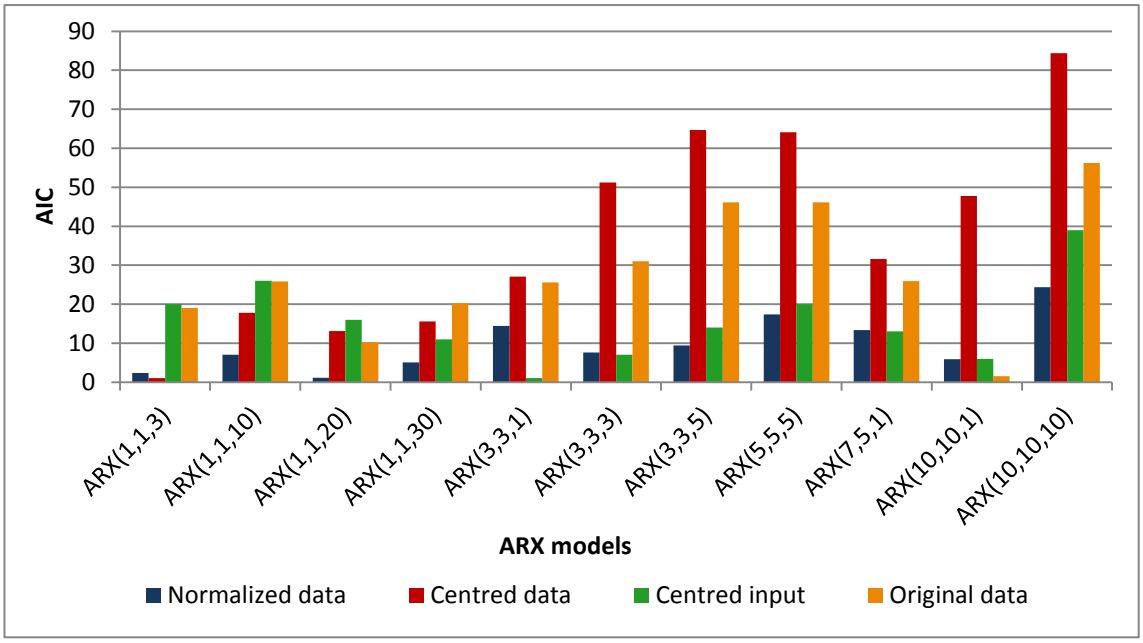

Figure 5.15 - The AIC for different ARX structures and pre-processing methods

Figure 5.15 shows a plot of AIC for the different ARX structures where the data is being processed according to the three aforementioned pre-processing approaches. The goal is to identify the structure associated with the lowest AIC value. It is important to mention that the value of AIC varies according to two factors; the structure of the ARX representation and the pre-processing approach. From the chart, the normalization approach tends to produce smaller AIC values for most of the cases compared to other pre-processing approaches. The centred data (input, output) and the original data produce high AIC values in most cases which indicate that the model built based on them will not fit the process data. The values of AIC based on the centred input data are variable. Therefore, at this stage the structure selected based on the lowest AIC value for each pre-processing method is listed in Table 5.7. The selected structure for each pre-processing approach is then used for PLS modelling in the following section.

Table 5.7 – ARX structure for the pre-processing methods with smallest AIC

Pre-processing method	Normalized data	Centred data	Centred input	Original data
ARX structure	ARX(1,1,20)	ARX(1,1,3)	ARX(3,3,1)	ARX(10,10,1)

The lowest AIC value based on the normalization approach is associated with an ARX(1,1,20) structure which shows a large time delay between the input and the output variables. This value is close to the AIC value associated with the ARX(1,1,3) structure which show only three samples delay. The structure ARX(1,1,20) is used in this thesis as the modelling results of the ammonia synthesis fixed-bed reactor based on the ARX(1,1,3) structure presented in Appendix C show that the structure based on an ARX(1,1,20) produced more accurate modelling results in term of predictions of the ammonia concentration. Therefore ARX(1,1,20) is used for the normalization data

To ensure that the time delay identified in the ARX structure is appropriate, a step is introduced into the process manipulated variables and the corresponding time delay is investigated (Appendix C). It is found that the time taken for the variables to respond to a step change differ significantly as some variable respond within 10 sec to 30 sec (i.e. 1 to 3 samples) and some of them respond within 180 sec to 200 sec (i.e. 18 to 20 samples). Hence for models that have a small time delay (e.g.ARX(3,3,1)), the dominant variables are these with a quicker response. However, for models that have a large time delay (e.g.ARX(1,1,20)), the dominant variables are these which responded after 180 to 200 sec.

5.7.2 Dynamic PLS Model

The reference model is constructed from the data representing normal operating conditions (i.e. the calibration data set in Table 5.5). The calibration data was pre-processed according to § 5.7.1.1. The data structure was selected based on the results provided in Table 5.7 (§5.7.1.2.2). The number of latent variables was determined based on cross validation. The model was then applied on unseen data representing normal operating conditions (i.e. the validation data set in Table 5.5) to test its ability to predict process behaviour. The selection of the appropriate model was based on the value of the Root Mean Squared Error (RMSE) and the coefficient of determination (R^2). The results from applying dynamic PLS on the calibration and validation data sets are summarised in Table 5.8.

Table 5.8 – RMSE and R^2 of PLS model based on different pre-processing approaches for calibration and validation data sets.

Pre-processing	RMSEC	RMSEV	R^2Cal	R^2Val
Normalization	0.0003	0.0009	0.9632	0.9346
Centring input and output	0.0006	0.0023	0.8787	0.7727
Centring input	0.0006	0.0032	0.8706	0.5143
No pre-processing	0.0004	0.0019	0.9297	0.8493

The main conclusion drawn from Table 5.8 is that the dynamic PLS model for the normalized data performed better than the other models for the validation data. This indicates that the model build based normalized data is more appropriate to model the data from the ammonia synthesis fixed-bed reactor. The details of the dynamic PLS model based on the normalized data is discussed in the next section. The model is then tested on the test data sets (i.e. the test data set in Table 5.5) which contain a disturbance to investigate the ability of the monitoring charts to identify process faults.

5.7.2.1 Dynamic PLS Model of Normalized Data

Dynamic PLS (DPLS) was applied to the normalized data and the dynamic structure identified in §5.7.1 was used. The first step was to determine the number of latent variable (LVs) through the application of cross validation. Figure 5.16 shows the RMSE of the calibration and RMSE of cross validation. Both indices indicate that four latent variables are appropriate. Table 5.9 shows that four latent variables correspond to 94.6% of the total amount of variance explained in the X-block and 96.3% of the variance explained in the output.

Figure 5.17 shows the time series of the original and fitted response, Figure 5.18 shows the original vs. fitted response and Figure 5.19 is the time series plot of the residuals. From Figure 5.18 it can be seen that the model fits the data. However, three samples are far from the regression line and by looking at the time series of the residuals, (Figure 5.19), it can be seen that the values of the residuals are close to zero which indicates that the model fits the data well with three peeks related to the points in Figure 5.18. This indicates that the model cannot cope with the change in the process at these points.

Table 5.9 - Percentage variance captured from DPLS model

LV	X-block		Y-block	
	%Variance	% Cumulative	%Variance	% Cumulative
1	35.15	35.15	60.90	60.90
2	29.48	64.64	24.97	85.87
3	22.40	87.04	5.26	91.13
→ 4	7.59	94.63	5.19	96.32
5	1.68	96.31	0.39	96.71
6	3.05	99.36	0.00	96.71
7	0.64	100.00	0.01	96.72
8	0.00	100.00	0.00	96.72
9	0.00	100.00	0.00	96.72
10	0.00	100.00	0.00	96.72
11	0.00	100.00	0.00	96.72

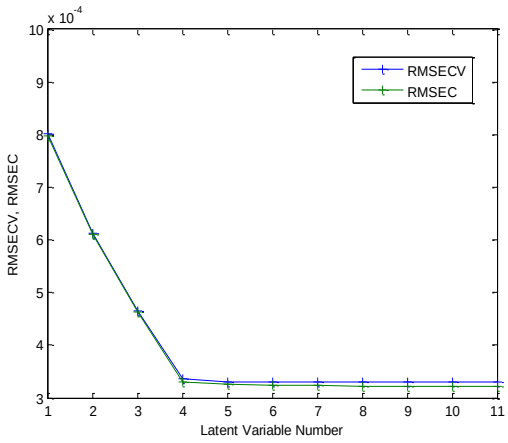

Figure 5.16 - Cross-validation results for determining the number of LV (DPLS)

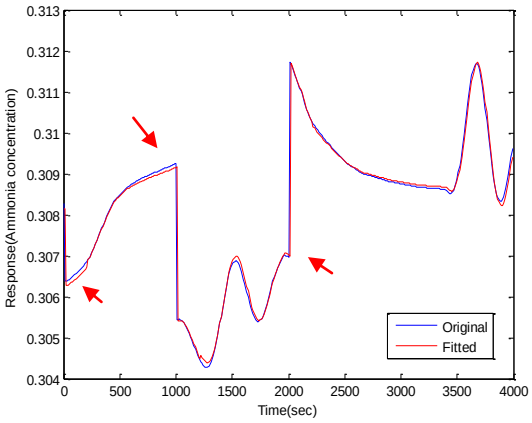

Figure 5.17 - Time series plot of the original and fitted response (DPLS)

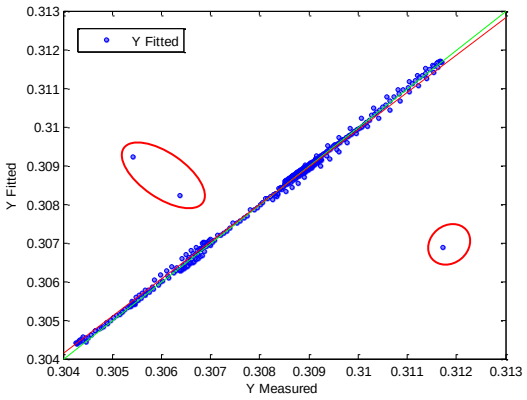

Figure 5.18 – Original vs. fitted response (DPLS)

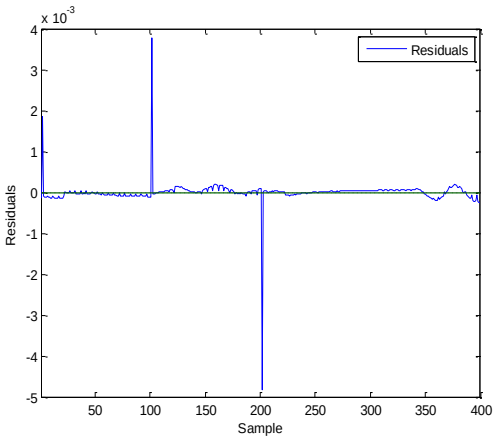

Figure 5.19 –Time series plot of the residuals for reference model (DPLS)

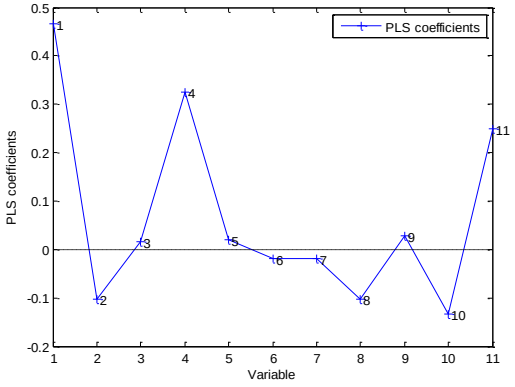

Figure 5.20 – DPLS coefficients

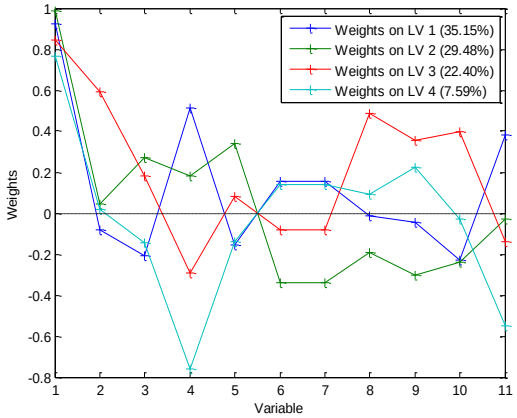

Figure 5.21 – DPLS weights

Figure 5.20 shows the DPLS coefficients, one past output variables and one past input contains 10 variables. It can be seen that the first variable coefficient is larger than the other variables. By analysing the process characteristics, other variables also seem to be important such as quench variables. However, from the DPLS coefficients they seem to less important compared to first variable. This is because of the strong correlation between some of the predictor variables which sometime cause the significant variable to appear as insignificant variable in the regression coefficients. One possible solution is to remove one of the correlated variables. But for the statistical analysis of the ammonia synthesis process, all the predictor variables are required as they are responsible for the process dynamics. For example, one of the correlated pair is the first and second quench variables (x_5, x_6). They are highly correlated and provide the same information. However they are important for the process, as they are a source of the dynamics in the process (§5.4.1). One advantage of a PLS model is its ability to deal with correlated data, hence there is no need to remove any variable in the predictor matrix. From Figure 5.20, it can also be seen that the fourth and eleventh variables (i.e. total fresh feed and the overall pressure) are significantly affecting the ammonia concentration. The importance of the variables for the analysis can be investigated by looking to DPLS weights

Figure 5.21 shows the DPLS weight for the first four latent variables. It is known the PLS weights give an indication of the correlation structure between the predictor and latent variables. From the figure, it is clear that for each retained latent variable, different sets of variables are of high importance. This concludes that all the variables included in the predictor matrix are important for the analysis and have an effect in the behaviour of the process.

The results from applying the DPLS model to the validation data is presented in Figures 5.22 to 5.24. It can be seen that the model fits the data well. However, a few samples lie far from the regression line and by looking at the time series of the residuals (Figure 5.24) it can be seen that the values of the residuals are close to zero which indicates that the model does fit the data well with a few peaks relating to the points in Figure 5.23. This is explained by looking at the time series plot of the original and fitted values (Figure 5.22) where the fitted value does not match the original for a few samples. The RMSE and R^2 in Table 5.8 of the validation data set indicate that the model fits the data well. The next steps are to apply the model to the test data set and to construct a monitoring scheme based on the developed model.

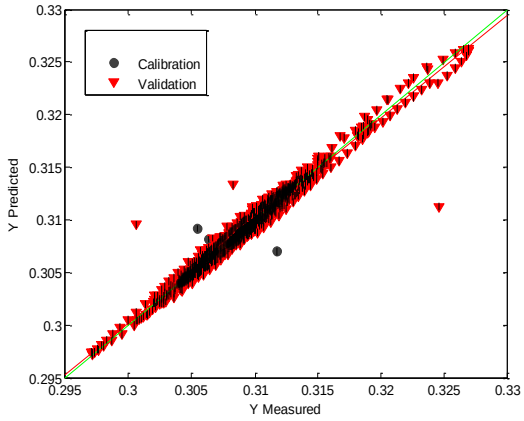

Figure 5.22 - Measured vs. predicted response for the validation data set (DPLS)

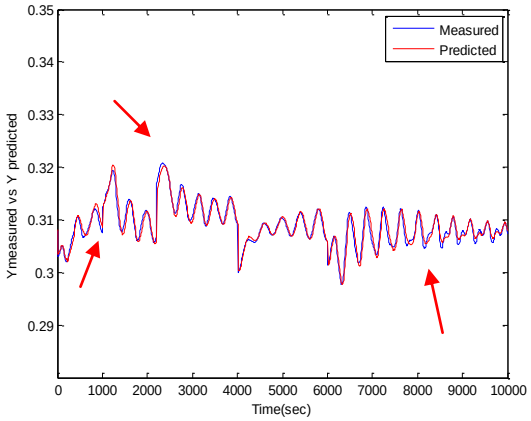

Figure 5.23 – Time series of measured and predicted response for the validation data set (DPLS)

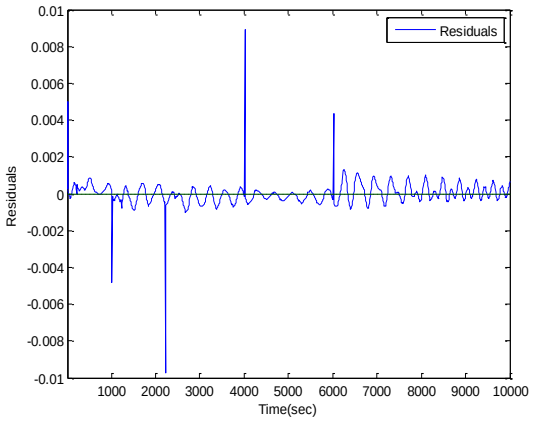

Figure 5.24 - Time series plot of the residuals for the validation data set (DPLS)

The results from applying the DPLS model to the two test data sets corresponding to case 1 and case 2 (Table 5.5) are presented in Table 5.10 and Figures 5.25 to 5.30. The major conclusions drawn are as follows:

- The DPLS model performs well in terms of predicting the data in both cases where different operating conditions were impacting on the process. However, an offset can be seen in the time series plots of the measured and predicted response and this is confirmed by looking at the time series plot of the residuals.
- The root mean squared error of prediction is increased compared to the RMSE for the calibration and validation data. However, the value is still considered to be small but it can potentially be improved by using an adaptive dynamic PLS approach (section 5.8).

Table 5.10 - RMSE and R^2 of the test data sets by DPLS

Case	RMSE	R^2
Case 1	0.0120	0.93
Case 2	0.0235	0.91

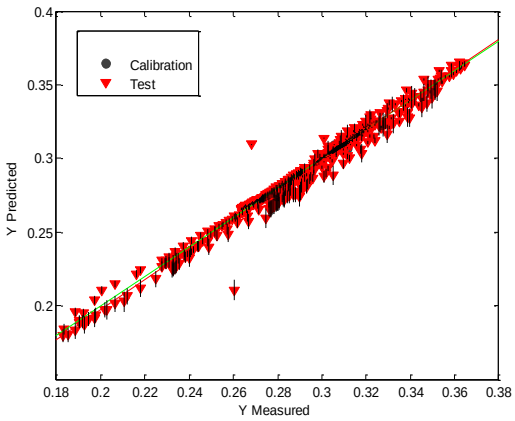

Figure 5.25- The measured vs. predicted response (case 1- DPLS)

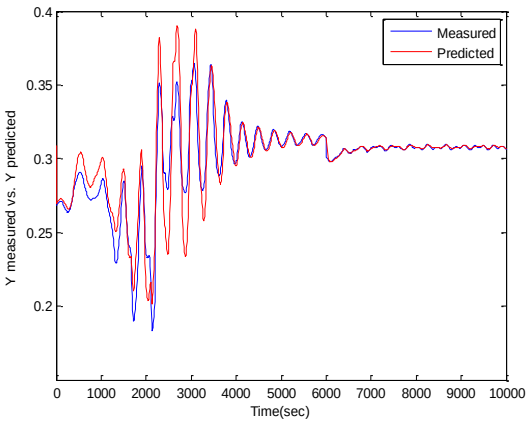

Figure 5.26 - Time series plot of the measured and predicted response (case 1 - DPLS)

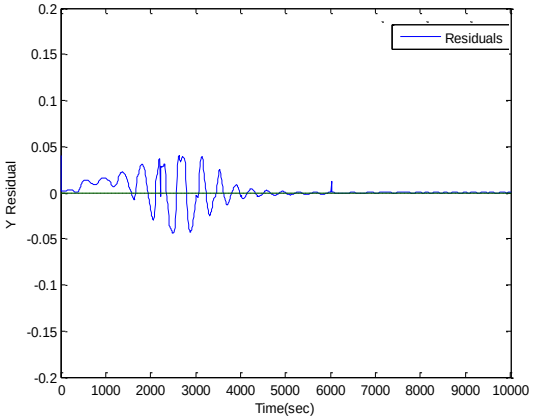

Figure 5.27 - Time series plot of the residuals (case 1 - DPLS)

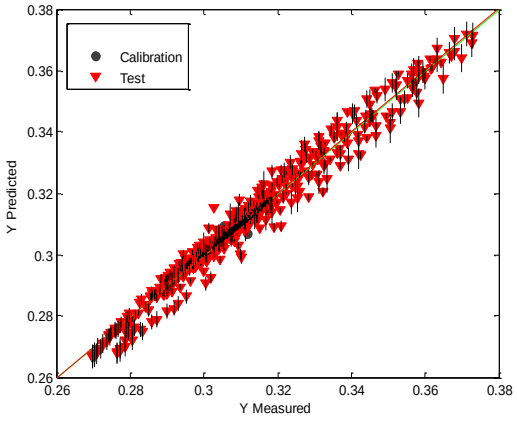

Figure 5.28 - The measured vs. predicted response (case 2 - DPLS)

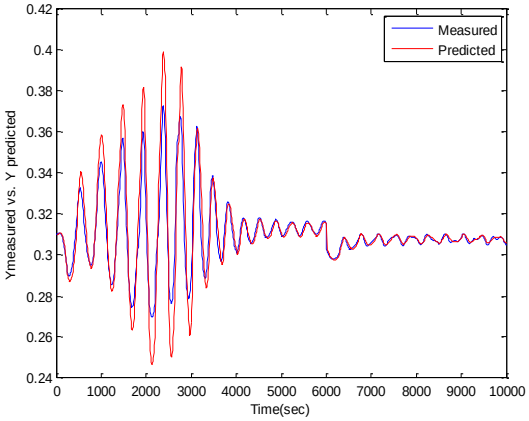

Figure 5.29 - Time series plot of the measured and predicted response (case 2 - DPLS)

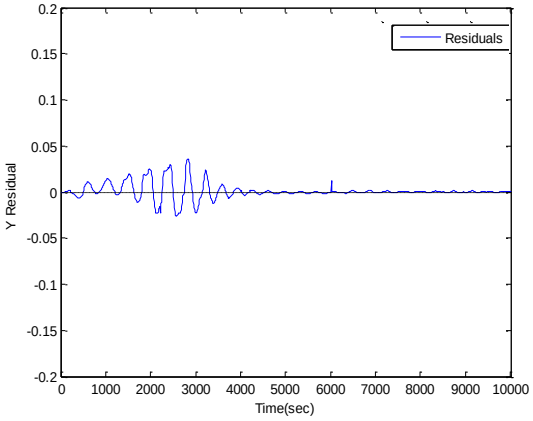

Figure 5.30 - Time series plot of the residuals (case2 - DPLS)

5.7.2.2 Monitoring Statistics Based on Dynamic PLS

5.7.2.2.1 Monitoring Statistics for Calibration and Validation Data sets

The results from the monitoring of the ammonia synthesis fixed-bed reactor using the dynamic PLS (DPLS) model developed in the previous section are illustrated in Figures 5.31 to 5.33. Each figure shows the time series plot of Hotelling's T^2 and the Squared Prediction Error of the input and output space SPE_X and SPE_Y respectively. The 99% and 95% confidence limits were calculated based on the reference data set. It can be seen that the three indices include a number of out of statistical control signal. However, they did not exceed 1% and 5% of the total number of samples for the 99% and 95% confidence limits respectively which is statistically acceptable based on the calculated false alarm rate (Table 5.11). The false alarm rate for Hotelling's T^2, SPE_X and SPE_Y are 5%, 5% and 2.25% for the 95% confidence limit and 1%, 0.75% and 1.75% for the 99% confidence limit respectively. The monitoring charts for the calibration data set presented in Figures 5.31 to 5.33 are used as the baseline monitoring charts for adaptive dynamic PLS and robust adaptive dynamic PLS.

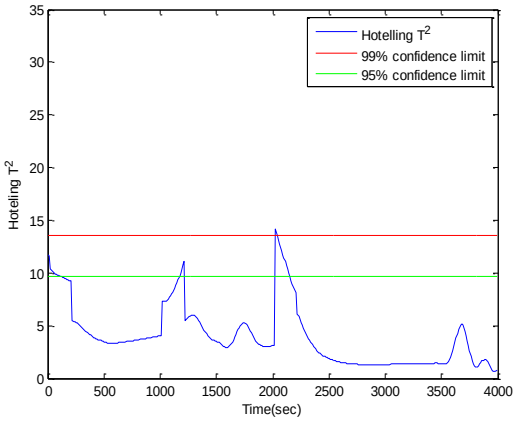

Figure 5.31 - Hotelling's T^2 for the reference data set (DPLS)

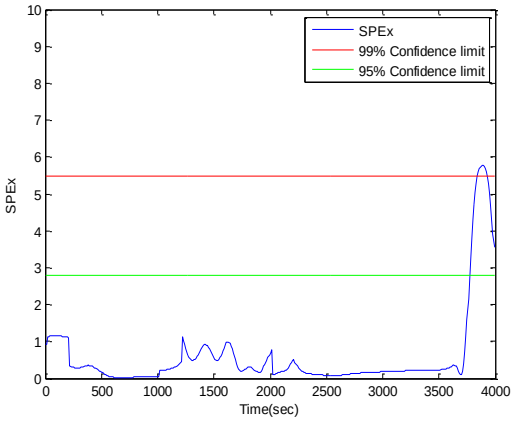

Figure 5.32 - SPE_X for the reference data set (DPLS)

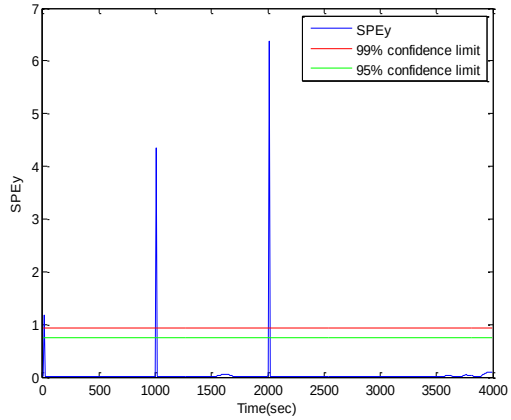

Figure 5.33 - SPE_Y for the reference data set (DPLS)

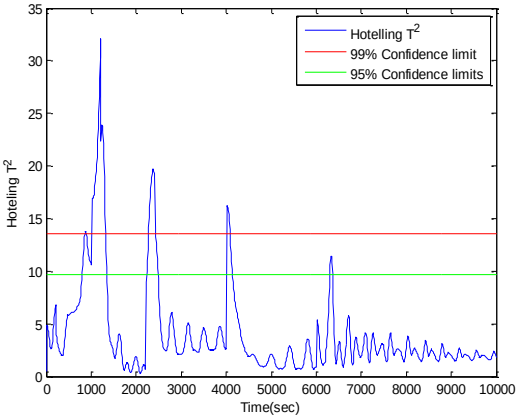

Figure 5.34 - Hotelling's T^2 for the validation data set (DPLS)

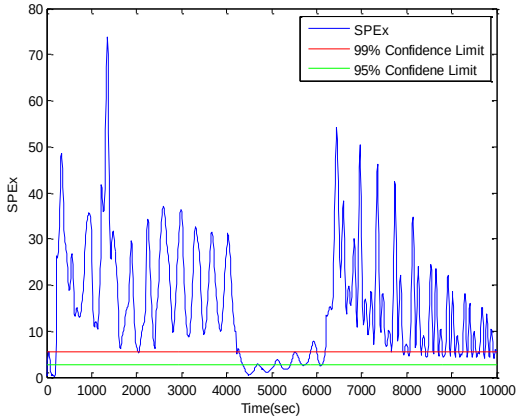

Figure 5.35 - SPE_X for the validation data set (DPLS)

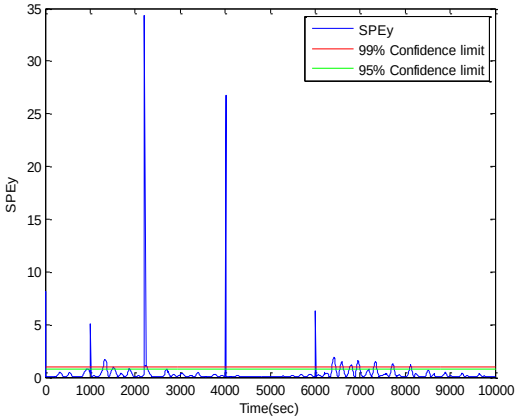

Figure 5.36- SPE_Y for the validation data set (DPLS)

Figures 5.34 to 5.36 present Hotelling's $T^2$and the Squared Prediction Error for the inputs and output space SPE_X and SPE_Y for the validation data set (Table 5.5). It can be seen that SPE_X and SPE_Y continuously violate the confidence limits even though the process represents nominal operating. The false alarm rates of the monitoring charts for the validation data set, 12 %, 92 % and 24.5 % for Hotelling's T^2, SPE_X and SPE_Y are much higher than the acceptable level of 5% for the 95% confidence limits (Table 5.11). This is because the confidence limits for the validation were those from the calibration data which may not appropriate for reflecting the dynamics contained in the validation data. This concludes that the process requires advance dynamic modelling to produce reliable monitoring charts.

Table 5.11 - False alarm rate of monitoring charts for the calibration and validation data sets using dynamic PLS

Chart	False alarm rate 95% confidence limits	False alarm rate 99% confidence limits
	Calibration data set	
Hotelling's T^2	5%	1%
SPE_X	5%	0.75%
SPE_Y	2.25%	1.75%
	Validation data set	
Hotelling's T^2	12 %	8 %
SPE_X	92 %	75.1%
SPE_Y	24.5 %	9.5 %

5.7.2.2.2 Monitoring Statistics for the Test Data Sets

The model was applied to the test data sets (Table 5.5). Figure 5.37 presents Hotelling's T^2 and the Squared Prediction Error for the input and output space, SPE_X and SPE_Y respectively. The first part of the plot represents the monitoring statistics for the reference data set (i.e. the monitoring indices presented in Figures 5.31 to 5.33). The drop in the pressure and total feed temperature which resulted in rapid oscillations in the process variables, as discussed in section 5.4, was detected 1800 sec (180 samples) after the actual time of the occurrence of the event for Hotelling's T^2 and it continue to violate the 95% and 99% confidence limits until normal operating conditions are restored at t = 7200 sec. The SPE_X and SPE_Y statistics detect the disturbance after 500 sec (50 samples) and they continue to violate the confidence limits even after normal operating conditions were restored. The continuous violation of the squared prediction error metrics indicate that there is a significant event that was not captured in the reference model which is true for the period from t=4001 sec to t=7200 sec; however, after t=7200 sec the normal operating conditions were restored and the monitoring statistics should not violate the confidence limits. Figures 5.38 to 5.40 present the monitoring statistics for the test data set when normal operating conditions were restored according to Table 5.5 (i.e. the Hotelling's T^2 and the Squared Prediction Error SPE_X and SPE_Y after t = 7200 sec). It is clearly seen that the SPE_X and SPE_Y continue to violate the 95% and 99% confidence limits when the process operating

conditions are restored to the normal ranges. Therefore, it can be concluded that the dynamic PLS model has some limitations for modelling such dynamic process resulting in unreliable monitoring charts.

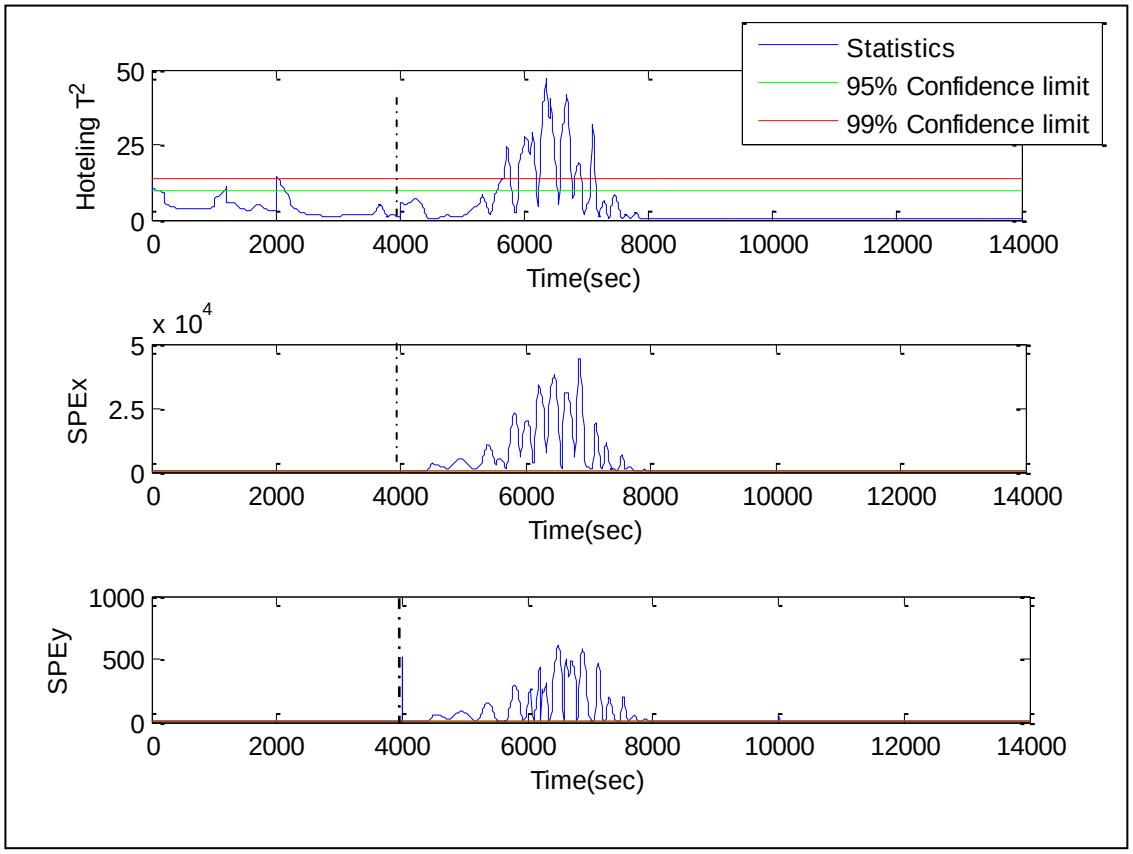

Figure 5.37 – Monitoring statistics of ammonia synthesis rector for the test data set (DPLS)

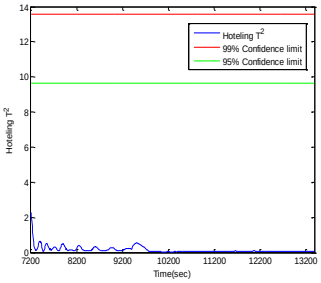

Figure 5.38 – Hotelling's T^2 for the test data set after t =7200 sec (DPLS)

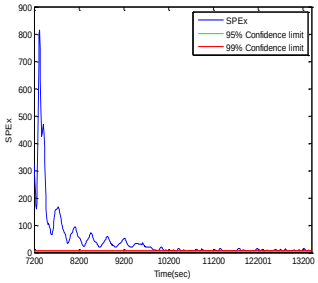

Figure 5.39 - SPE_x for the test data set after t =7200 sec (DPLS)

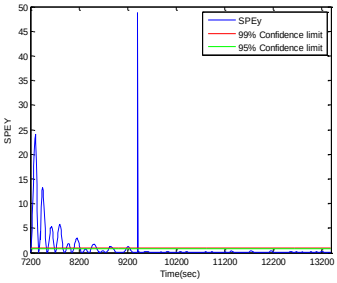

Figure 5.40 - SPE_Y for the test data set after t = 7200 sec (DPLS)

In this study, the average run length ARL0 and ARL1, are calculated based on a Monte Carlo simulation, 50 experiments, where the data sets were generated under the same operating conditions (i.e. different step changes in the same range of the normal operating conditions). The results for ARL0 and ARL1 for the dynamic PLS monitoring

charts are presented in Table 5.12. The overall conclusion is that the performance of the monitoring charts is unacceptable. This is because there is a delay in indicating the onset of the fault. For example, for Hotelling's T^2 the fault is indicated on average after 110 samples from its onset. On the other hand, when the process is operating under normal operating conditions, the monitoring charts produce false alarm after a short period of time. It can be concluded that the monitoring charts based on dynamic PLS for the monitoring of the ammonia synthesis fixed-bed reactor are unreliable.

Table 5.12 - ARL0 and ARL1 for Hotelling's T^2, SPE_X and SPE_Y

Chart	ARL	DPLS
Hotelling's T^2	ARL0	45
	ARL1	110
SPE_X	ARL0	20
	ARL1	50
SPE_Y	ARL0	30
	ARL1	50

In the next sections, the application of adaptive sample-wise dynamic PLS and robust adaptive dynamic PLS approaches are presented.

5.8 Adaptive Dynamic PLS (ADPLS)

5.8.1 Modelling Using ADPLS

The adaptive PLS (APLS) approach was summarised in Chapter 4. The main idea of APLS is to update the PLS model once a new observation becomes available and hence the monitoring charts are constructed based on the updated PLS model. Two modifications were introduced to the APLS algorithm as discussed in Chapter 4. Firstly, the reference model for APLS is developed based on a dynamic representation to account for process dynamics (i.e. the DPLS model developed based on calibration data §5.7.2.1 is used as a reference model). Secondly, once an observation becomes available, it has to be incorporated into the dynamic representation given in §5.7.1.2 prior to model updating and hence the model is updated recursively in a sample-wise manner, i.e. it has to be presented in the form of ARX(1,1,20). In addition, the number of latent variables was updated using cross validation every time the model was updated to prevent over or under fitting when calculating the prediction. This is very important

at that step since the process behaviour changes significantly especially when the disturbance affects the process behaviour. The ADPLS algorithm for the ammonia synthesis fixed-bed reactor is presented in Figure 5.41. The reference model developed in § 5.7.2.1 with 4 latent variables is used as a reference model for ADPLS. The ADPLS was then implemented on unseen data, i.e. validation data set, which represents normal operating conditions. Two versions are implemented, the ADPLS with a fixed number of latent variables and the ADPLS with a variable number of latent variables.

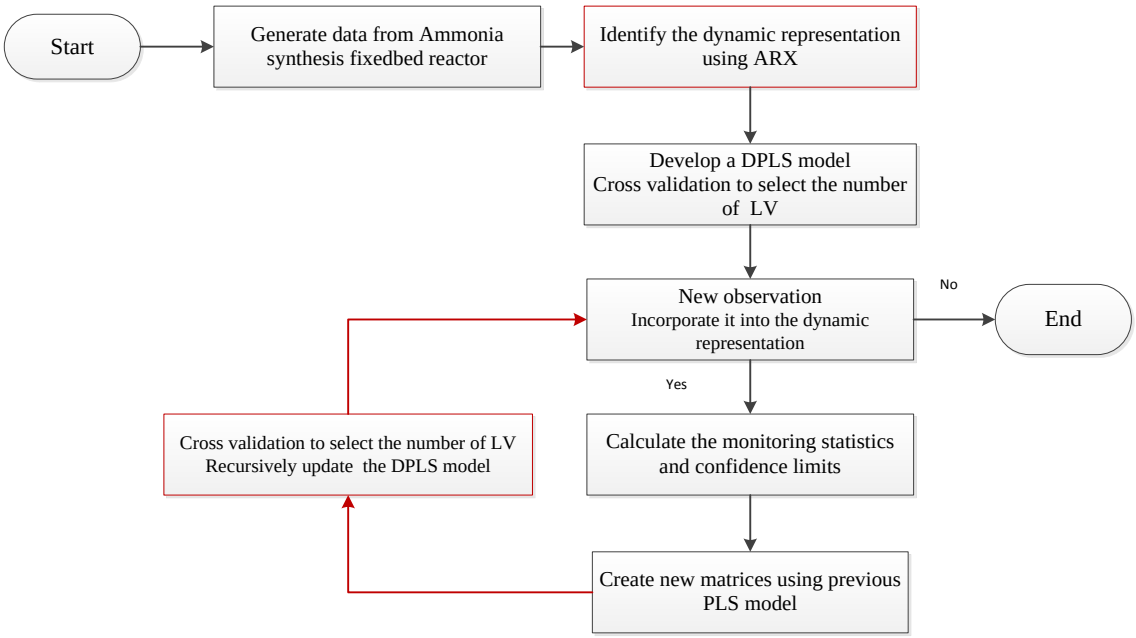

Figure 5.41 – ADPLS approach for modelling ammonia synthesis reactor

The results from the application of the modified ADPLS algorithm using a fixed and variable number of latent variables on the validation data set are summarised in Table 5.13. Compared to the DPLS model, the model fit and quality have improved. This can be concluded by comparing the RMSE and R^2 of the DPLS and the ADPLS models. Figures 5.42 and 5.43 show the time series plot of the measured and predicted response for the ADPLS model for a fixed and variable number of latent variable respectively. From the figures, no differences can be observed between the time series of the ADPLS fixed and varied latent variable model. Although there is no significance difference between the models, however, it is critical to have an approach that can capture real changes in the process which can be achieved through the variation of number of latent variables. The residuals plots for both cases are given in Appendix C.

Table 5.13- RMSE and R^2 of the validation data sets by ADPLS

Fixed number of LVs		Variable number of LVs	
RMSE	R^2	RMSE	R^2
0.00062	0.97	0.0006	0.98

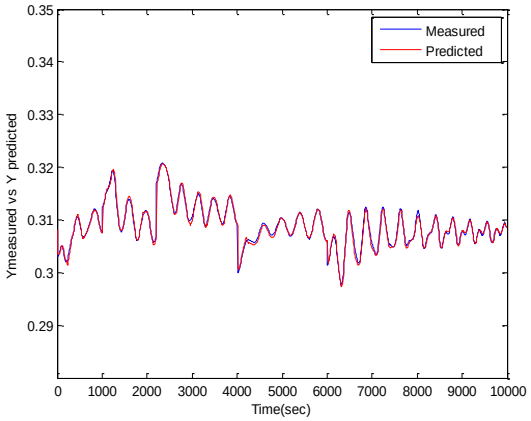

Figure 5.42 - Time series plot of measured and predicted response for the validation data set (fixed LVs-ADPLS)

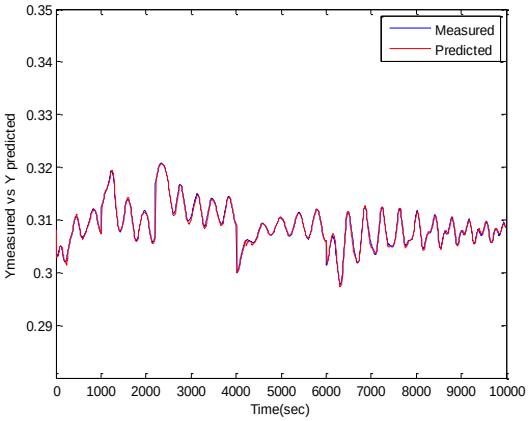

Figure 5.43 - Time series plot of measured and predicted response for the validation data set (variable LVs -ADPLS)

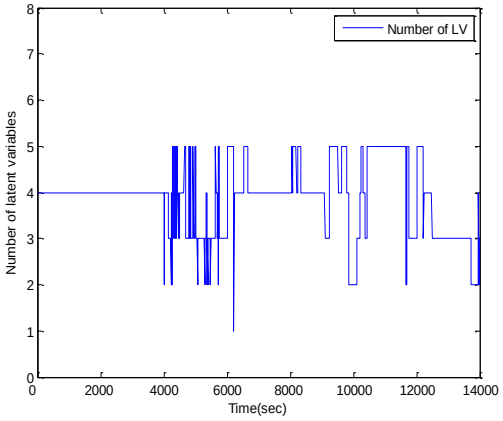

Figure 5.44 - Number of LVs used by ADPLS - validation data set

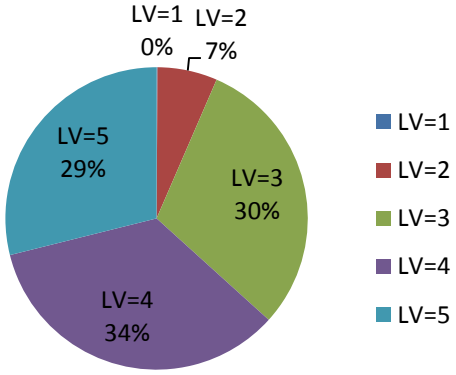

Figure 5.45 - Percentages of number of LVs used by ADPLS - validation data set

Figure 5.44 shows the time series plot of the number of latent variables determined by cross validation and Figure 5.45 shows the percentage of latent variables used through the analysis. It can be seen that the number of latent variable lies between 3, 4 and 5. This variation results in no real improvement to the model prediction. Figures 5.46, 5.47, 5.48 and 5.49 show the time series plot of the measured and predicted response for case 1 and case 2 respectively. From Figures 5.46 to 5.49, no

difference can be observed between the time series of the ADPLS model for the fixed and variable number of latent variables. The RMSE and R^2 of the prediction indicates that model quality is marginally better based on a variable number of latent variables (residuals are given in Appendix C)

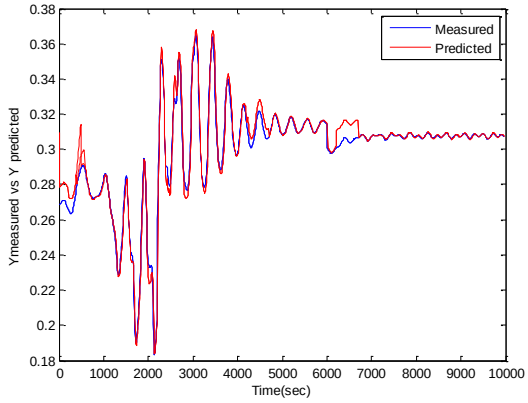

Figure 5.46- Time series plot of measured and predicted response (fixed LVs - ADPLS)- case1

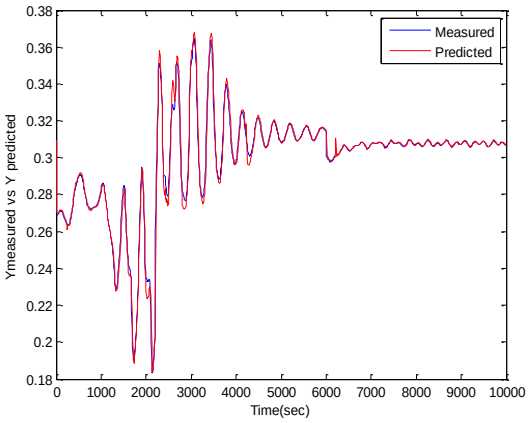

Figure 5.47- Time series plot of measured and predicted response (variable LVs - ADPLS) - case1

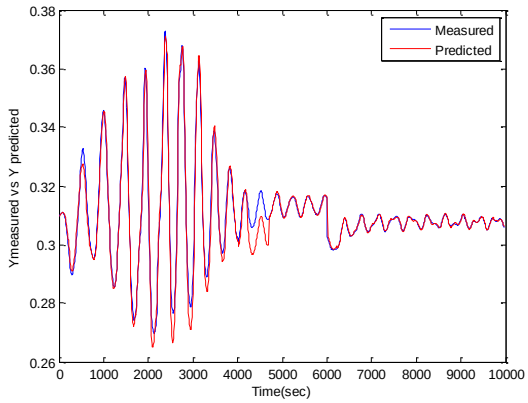

Figure 5.48- Time series plot of Measured and predicted response (fixed LVs - ADPLS) – case 2

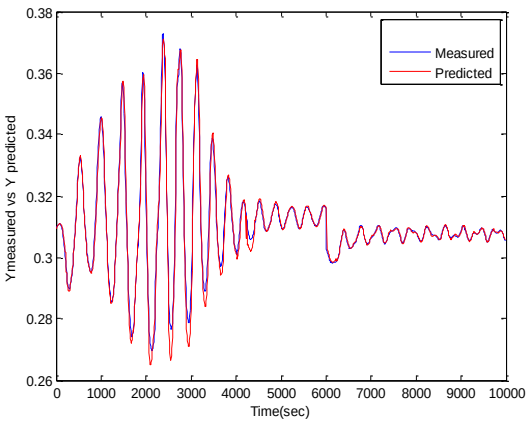

Figure 5.49- Time series plot of Measured and predicted response (variable LVs - ADPLS) – case 2

Table 5.14 - RMSE and R^2 of the prediction for the test data set by ADPLS

Cases	Fixed number of LVs		Variable number of LVs	
	RMSE	R^2	RMSE	R^2
Case 1	0.008	0.94	0.007	0.95
Case 2	0.007	0.95	0.005	0.96

Figures 5.50 and 5.51 show the time series plot of the number of latent variables for the two cases determined by cross validation. Figures 5.52 and 5.53 show the percentage of the number of latent variables for case 1 and 2. It can be seen that the number of latent variable in both cases lies between 3 and 5 latent variables. This variation results in a slight improvement, marginal improvement, in the model prediction as observed from Table 5.14.

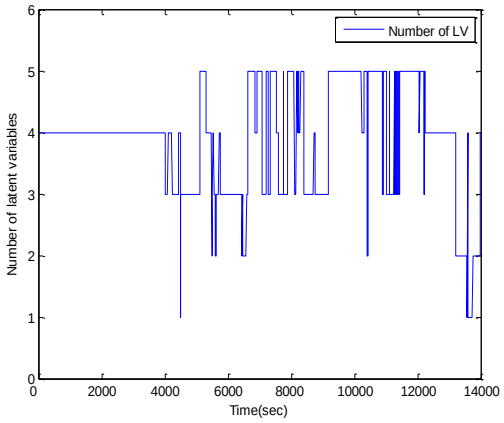

Figure 5.50- Time series plot of number of LVs (case 1-ADPLS)

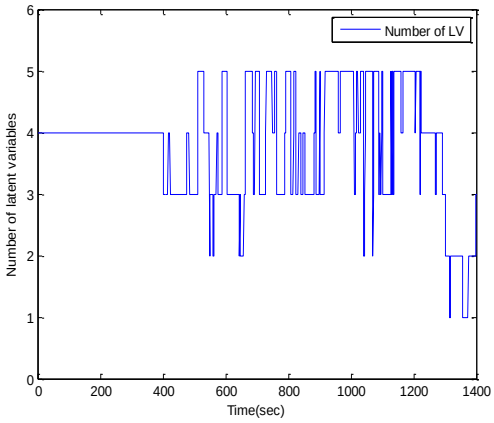

Figure 5.51- Time series plot of number of LVs (case 2-ADPLS)

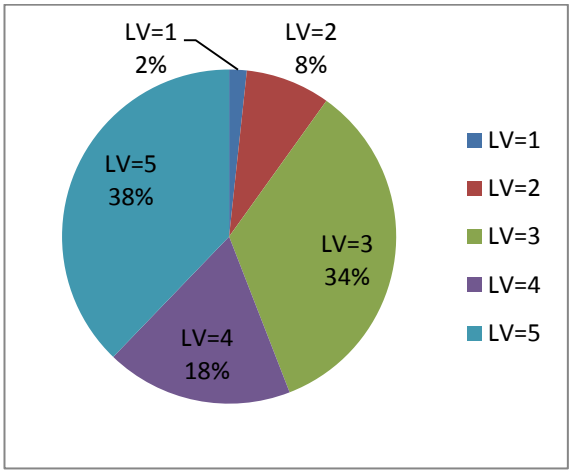

Figure 5.52- Percentage of number of LVs used by ADPLS – case 1

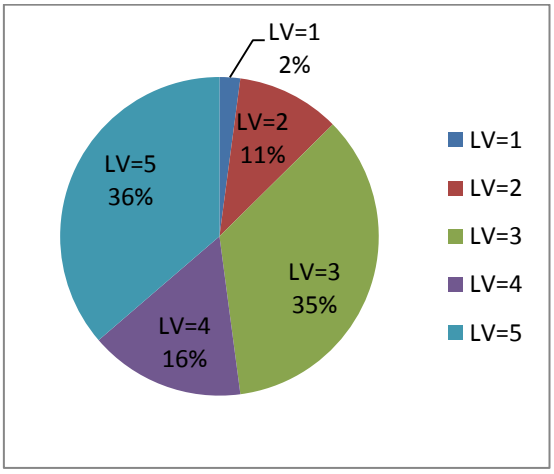

Figure 5.53- Percentages of number of LVs used by ADPLS – case 2

The difference in the number of latent variables included for the validation and test cases gives an indication that the number of latent variables selected is dependent on process behaviour. Since the results show that the ADPLS with a variable number of latent variables marginally improves the model quality, the monitoring results will be constructed based on the ADPLS with a variable number of latent variables.

5.8.2 Monitoring Statistics Based on ADPLS Model

5.8.2.1 Monitoring Statistics for Validation Data set

The results of monitoring the ammonia synthesis fixed-bed reactor with a scheme developed from the ADPLS algorithm for the validation data set are presented in Figures 5.54, 5.55 and 5.56. It can be seen that the monitoring charts adapt to the change in the process dynamics. The number of samples outside of the statistical control limits materialise but as it is the order 1% and a 5% corresponding to the 99% and 95% confidence limits. More specifically the false alarm rates, 4.95%, 4.91% and 4.1% for Hotelling's T^2, SPE_X and SPE_Y respectively indicate that the number of violations are within the acceptable rate (5%) for the 95% confidence limits and 1.3%, 1% and 1% for Hotelling's T^2, SPE_X and SPE_Y respectively for the 99% confidence limits (Table 5.15).

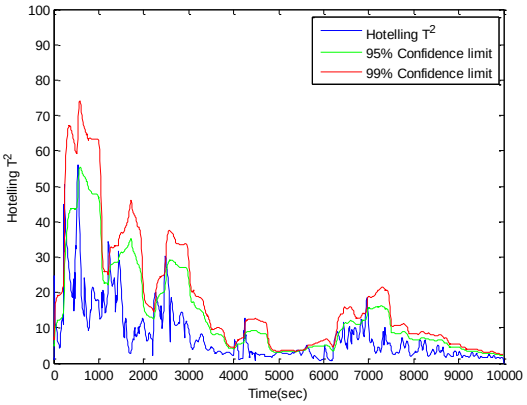

Figure 5.54 – Hotelling's T^2 based on ADPLS for the validation data set

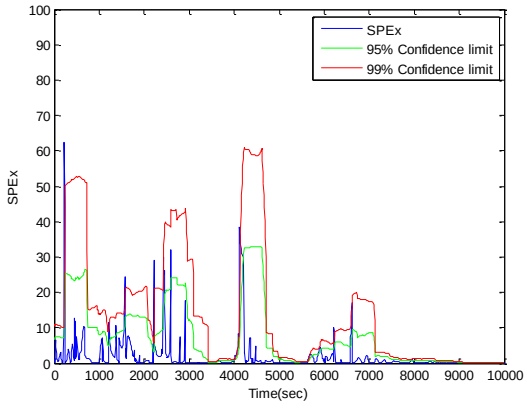

Figure 5.55 – SPE_X for based on ADPLS for the validation data set

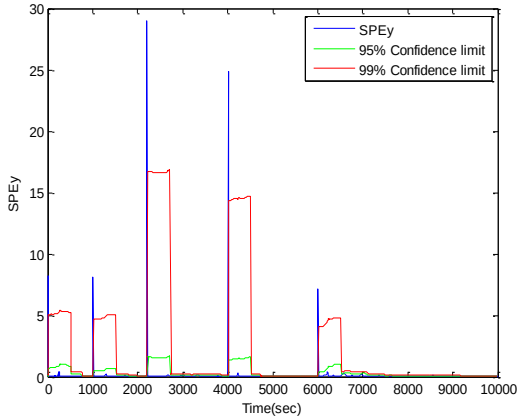

Figure 5.56 – SPE_Y based ADPLS for the validation data set

Table 5.15- False alarm rate of monitoring charts for the validation data set using ADPLS

Chart	False alarm rate 95% confidence limits	False alarm rate 99% confidence limits
	Validation data set	
Hotelling's T^2	4.95%	1.30%
SPE_X	4.91%	1.00%
SPE_Y	4.10%	1.00%

5.8.2.2 Monitoring Statistics for the Test Data Sets

The results for the test data sets are presented in Figures 5.57 to 5.62 for a variable number of latent variables included in the monitoring based on ADPLS model. The main observations drawn from the monitoring charts are:

- The statistical metrics (Hotelling's T^2, SPE_X and SPE_Y) are affected by the fault (i.e. the drop in the pressure and the drop in the fresh feed temperature, case 1 and 2 respectively) and successfully indicate the presence of fault.
- The confidence limits adapt to the fault in the monitoring charts and indicate that the process remains within statistical control state.

The purpose of confidence limits is to indicate whether a process is out of statistical control but in the case of monitoring of the ammonia synthesis reactor based on ADPLS, it can be seen that they adapt to the effect of the fault and do not indicate that the process is out of statistical control. Even though the prediction is improved using ADPLS, there is a need to include a threshold to prevent adaption to abnormal events. The fault detection rates of the monitoring charts for case 1 and case 2 are presented in Table 5.16 which shows that the monitoring charts detect less than 20% of the faulty samples. More specifically the fault detection rates for case 1, 7.4%, 10.9% and 14.4% for Hotelling's T^2, SPE_X and SPE_Y for the 95% confidence limits respectively and 4.2%, 6.3% and 4.7% for Hotelling's T^2, SPE_X and SPE_Y for the 99% confidence limits respectively (Table 5.16). For case 2, the monitoring charts of Hotelling's T^2, SPE_X and SPE_Y detect 3.8%, 12.5% and 9.1% for the 95% confidence limit respectively and 1.5%, 2.2% and 3.1% for the 99% confidence limit respective. These indicate that the fault

was not detected by the monitoring charts. Therefore, Robust Adaptive Dynamic PLS (RADPLS) is applied to address this limitation.

Table 5.16 – Fault detection rate for test data sets by ADPLS

Chart	Fault detection rate 95% confidence limits	Fault detection rate 99% confidence limits
	Test data set - Case 1	
Hotelling's T^2	7.4%	4.2%
SPE_X	10.9%	6.3%
SPE_Y	14.4%	4.7%
	Test data set - Case 2	
Hotelling's T^2	3.8%	1.5%
SPE_X	12.5%	2.2%
SPE_Y	9.1%	3.1%

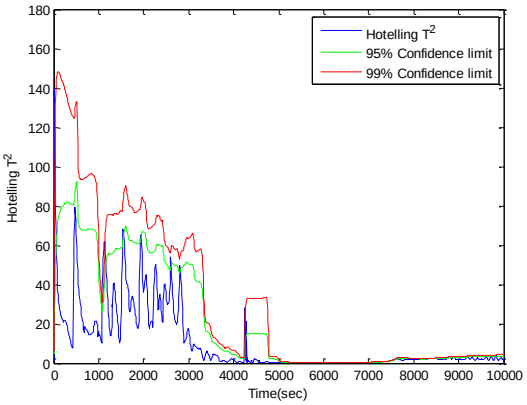

Figure 5.57 - Hotelling T^2 based on ADPLS for the test data set – case 1

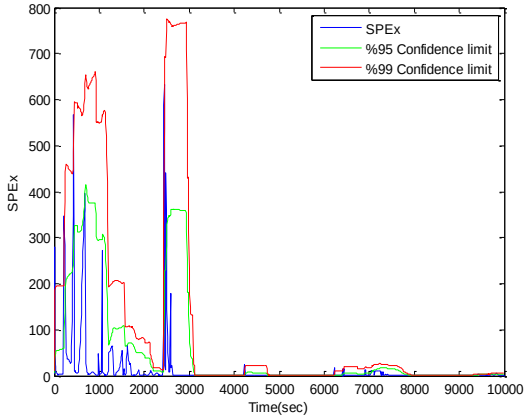

Figure 5.58 –SPE_X based on ADPLS for the test data set- case 1

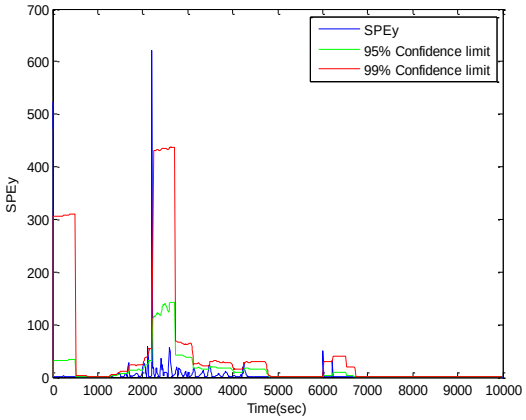

Figure 5.59 – SPE_Y based ADPLS for the test data set – case 1

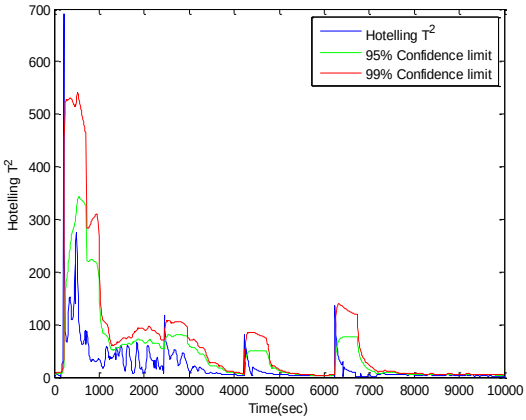

Figure 5.60 - Hotelling T^2 based on ADPLS for the test data set – case 2

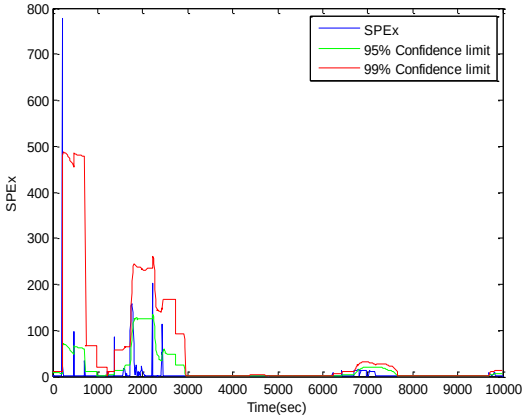

Figure 5.61 –SPE_X based on ADPLS for the test data set – case 2

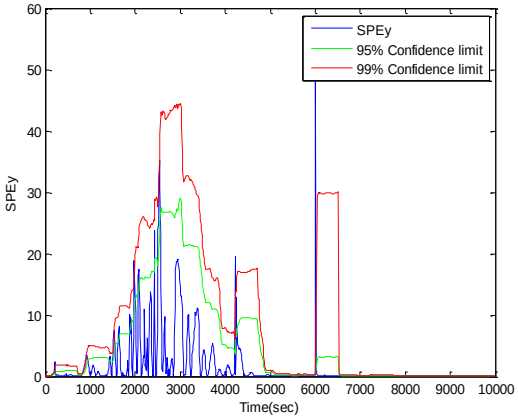

Figure 5.62 –SPE_Y based on ADPLS for the test data set – case 2

The results for ARL0 and ARL1 based on Monte Carlo simulation, 50 experiments, for the ADPLS monitoring charts are presented in Table 5.17. What is interesting in this table are the results for ARL1 for all the three monitoring metrics. From the monitoring charts of the test data sets, it can be clearly seen that the indices are affected by the disturbances. However, the confidence limits of the monitoring charts adapt to the change in the monitoring metrics and this results in a longer ARL1 as the monitoring metrics remain in a statistical control as shown in Table 5.17. In contrast, the ARL0, which is calculated for the validation data set shows satisfactory results for the monitoring charts as no false alarm was detected for sufficient period of time compared to the ideal ARL0 of 100 samples (Table 5.17).

Table 5.17 – ARL0 and ARL1 for Hotelling'sT^2, SPE_X and SPE_Y using ADPLS

Chart	ARL	ADPLS
Hotelling's T^2	ARL0	80
	ARL1	30
SPE_X	ARL0	75
	ARL1	20
SPE_Y	ARL0	82
	ARL1	35

5.9 Robust Adaptive Dynamic PLS (RADPLS)

5.9.1 Modelling Using RADPLS

The Robust Adaptive PLS (RAPLS) algorithm was summarised in Chapter 4. In this study, two modifications were introduced to the original RAPLS proposed in Chapter 4. First, the reference model was developed from a dynamic representation to account for the process dynamics hence a dynamic PLS (DPLS) model is developed. Secondly, once a sample becomes available, it has to be incorporated into a dynamic representation prior to model update. Once it is confirmed that the process is operating under normal operating conditions, the dynamic model is updated recursively in a sample-wise manner. The modified algorithm for the modelling of the ammonia synthesis fixed-bed reactor is summarised in Figure 5.63.

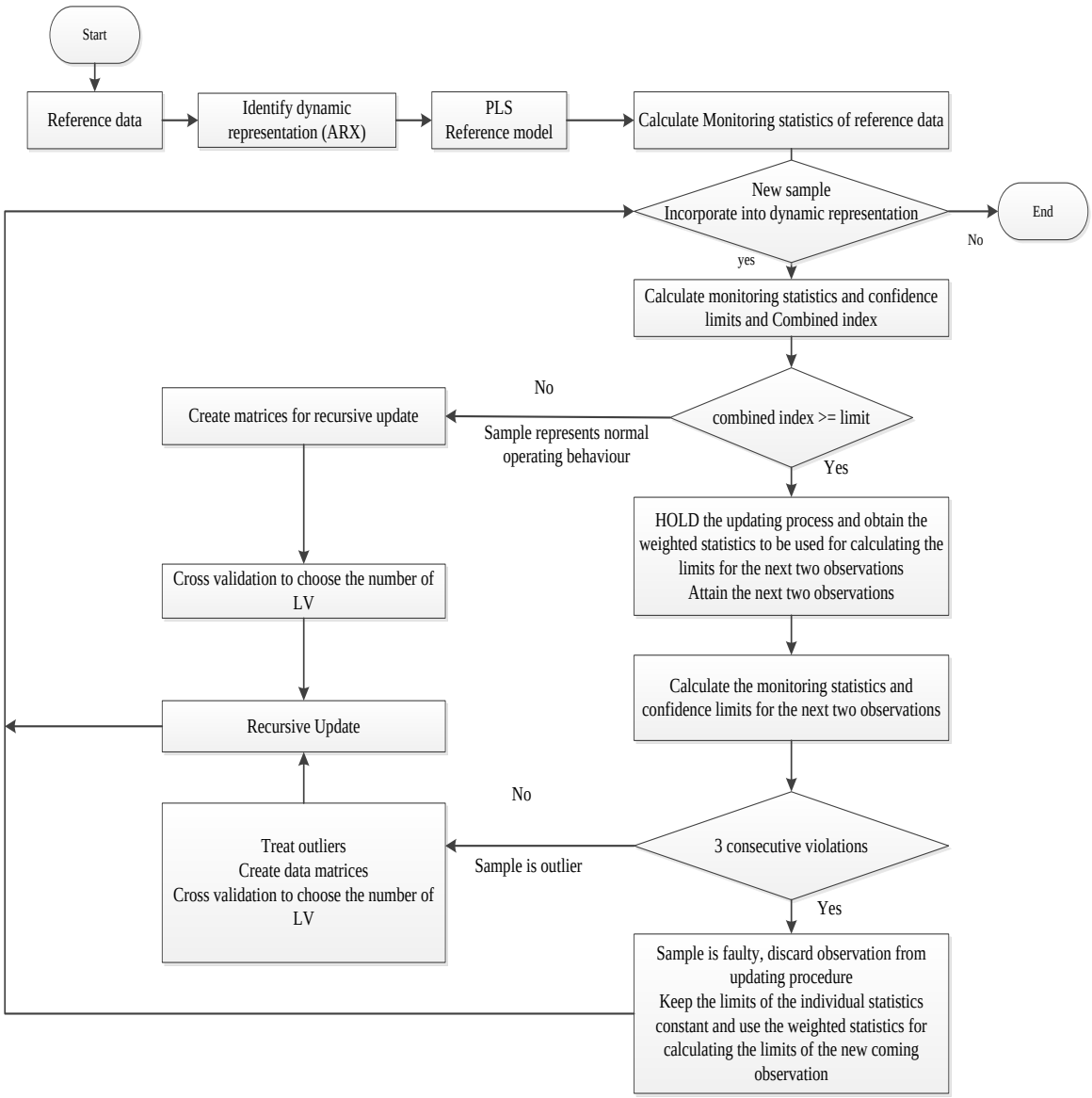

Figure 5.63 - RADPLS approach for ammonia synthesis process

The reference model developed in §5.7.2.1 is used as a reference model for the RADPLS algorithm. It was built based on the calibration data set in Table 5.5. The next step was to update the model once a new sample became available. For this step, the validation and test data sets in Table 5.5 are used and the ability of the algorithm to distinguish between data from normal operating conditions and a disturbance is examined. The results from the application of RADPLS with a fixed and a variable number of latent variables for the validation data set are presented in Figures 5.64 and 5.65. They show the time series plots of the measured and predicted response. It can be seen that the response is well predicted for both fixed and variable latent variables cases.

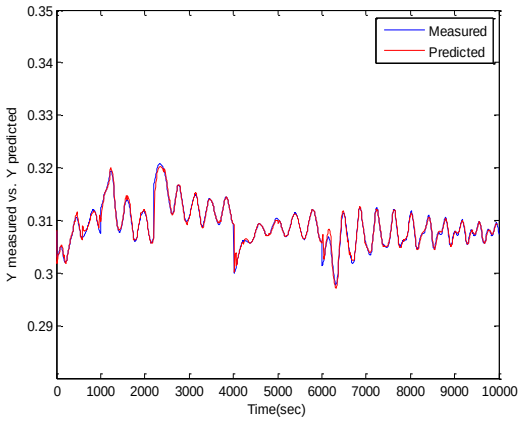

Figure 5.64 - Measured and predicted response - validation data set (fixed number of LVs - RADPLS)

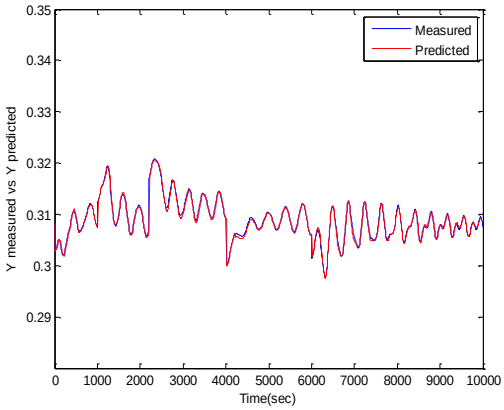

Figure 5.65 - Measured and predicted response - validation data set (variable number of LVs - RADPLS)

The prediction of the RADPLS model is not enhanced when the number of latent variables was allowed to vary within the adaption procedure. This is confirmed by investigating the values of the RMSE and coefficient of determination, R^2, for the validation data set where the difference is very small (Table 5.18) (residuals are given in Appendix C).

Table 5.18 - RMSE and R^2 of the validation data set by RADPLS

Fixed Number of LV		Variable number of LV	
RMSE	R^2	RMSE	R^2
0.00059	0.98	0.00057	0.98

Figure 5.66 shows the time series plot of the number of the latent variables determined by cross validation and Figure 5.67 shows the percentage of latent variables. It can be seen that the number of latent variable lies between 3 and 5. This variation does not result in an improvement in the model prediction (Table 5.18). The rational for no real difference is that a very little variability was explained by the few latest latent variables. Hence adding one or more latent variable would not improve the model prediction. However, it is important to have a flexible approach that can capture real changes in the future. Therefore, the algorithm with variable number of latent variables was considered.

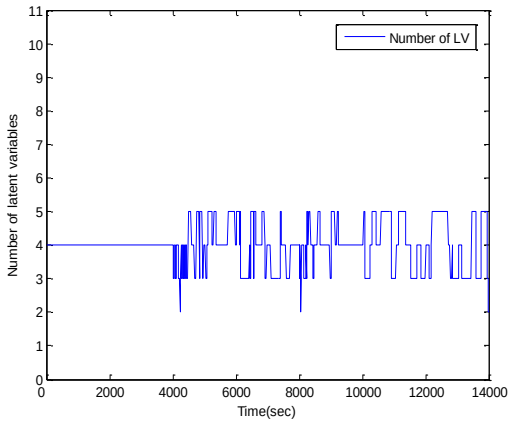

Figure 5.66 - Number of LVs used by RADPLS - validation data set

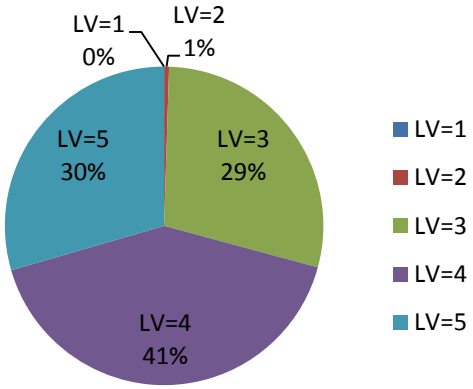

Figure 5.67- Percentages of number of LVs used by RADPLS- validation data set

The results from the application of the modified RADPLS using a fixed and variable number of latent variables to the test data sets are summarised in Figures 5.68, 5.69, 5.70 and 5.71. They show the time series plots of the measured and predicted response. It can be seen for both data sets, the fixed and variable number of latent variables cases, the response was well predicted. The prediction is not really improved when the number of latent is varied as shown in Table 5.19.

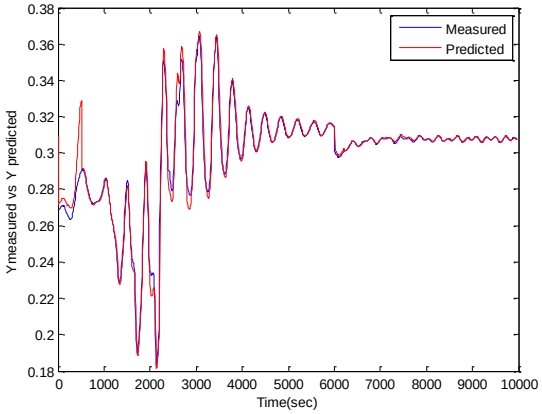

Figure 5.68 -Measured and predicted response (fixed LVs) - case1 RADPLS

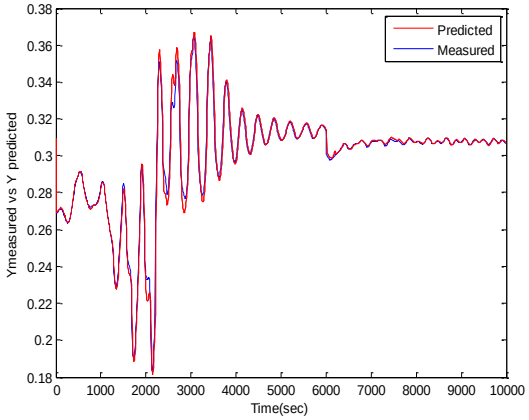

Figure 5.69 - Measured and predicted response (variable LVs)-case1 RADPLS

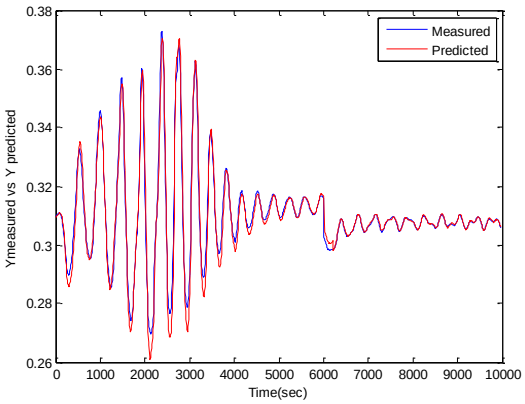

Figure 5.70 - Measured and predicted response (fixed LVs) - case 2 RADPLS

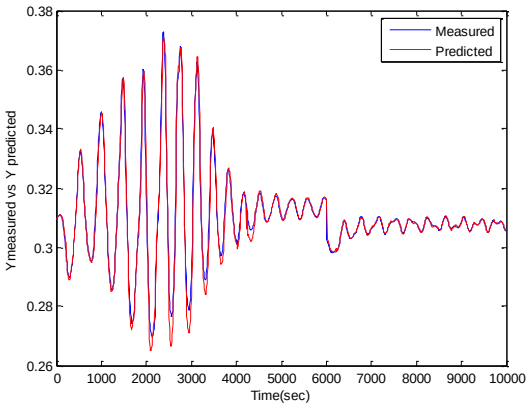

Figure 5.71 - Measured and predicted response (variable LVs) - case 2 RADPLS

Table 5.19- RMSE and R^2 for the test data sets using RADPLS

Cases	Fixed LVs		Variable LVs	
	RMSEP	R^2	RMSEP	R^2
Case 1	0.005	0.96	0.004	0.97
Case 2	0.004	0.96	0.003	0.96

The time series plots of the number of latent variables based on RADPLS for the test data sets are presented in Figures 5.72 and 5.73. The percentage of latent variables is presented in Figures 5.74 and 5.75. It can be seen that the number of latent variable lies between 3 and 5 with 3 latent variable being dominated. The variation in the number of latent variables results in no real improvements in model quality and model predictions as shown in Table 5.19. All monitoring results will be generated based on RADPLS using variable number of latent variables as it is important to capture any real change in the process operation that may results in a change in the underlying model.

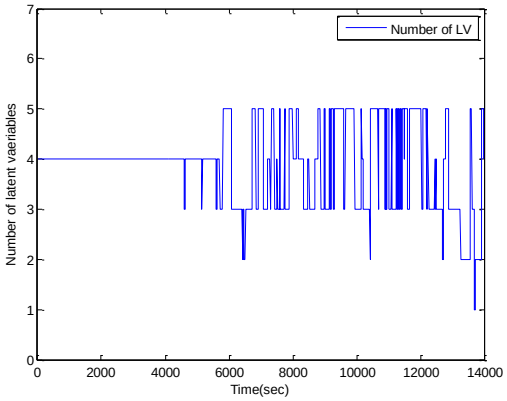

Figure 5.72 - Number of LVs used by RADPLS – case 1

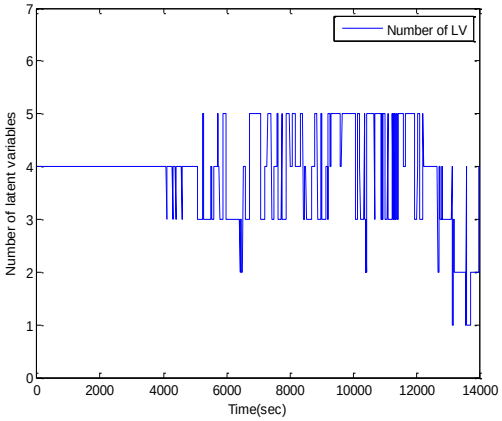

Figure 5.73 - Number of LVs used by RADPLS – case 2

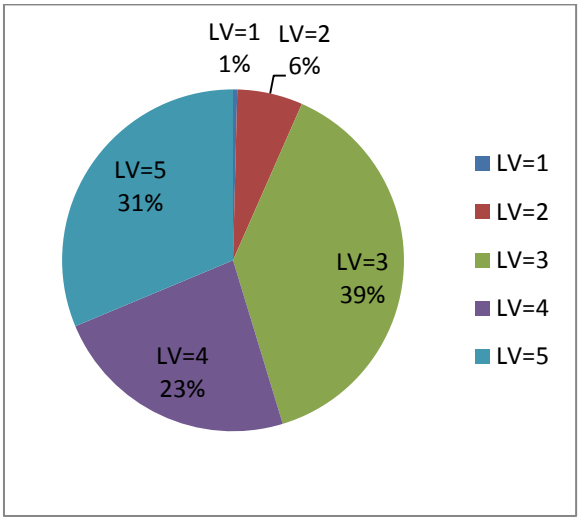

Figure 5.74 - Percentage of number of LVs by RADPLS – case 1

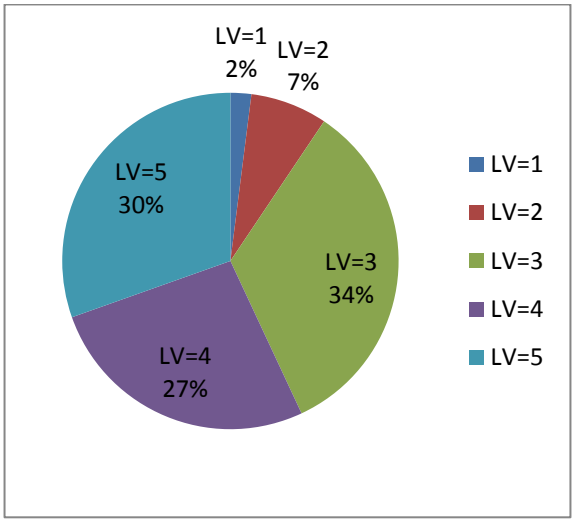

Figure 5.75 - Percentages of number of LVs by RADPLS – case 2

5.9.2 Monitoring Statistics Based on RADPLS Model

5.9.2.1 Monitoring Statistics for Validation Data Set

The monitoring results from the application of RADPLS to the validation data set are presented in Figures 5.76, 5.77 and 5.78. It can be concluded that the process is in a state of statistical control since the statistical metrics (Hotelling's T^2, SPE_X and SPE_Y) lie within the statistical confidence limits. A few samples violate the 99% and 95% confidence limits. The false alarm rates are shown in Table 5.20 which indicate that the rate of violation is within the statistically acceptable rate of 1% and 5% respectively.

Table 5.20.False alarm rate of monitoring charts for the validation data set by RADPLS

Chart	False alarm rate 95% confidence limits	False alarm rate 99% confidence limits
	Validation data set	
Hotelling's T^2	4.85%	1.11%
SPE_X	4.51%	0.90%
SPE_Y	3.10%	0.80%

The control chart of the combined index (Figure 5.79) which shows that the combined index remains within statistical control and the few violations identify the statistical outliers for the RADPLS algorithm. The False alarm rate for the combined index chart, 6% and 1.7% for the 95% and 99% confidence limits respectively, indicate that there are some points which can be considered as outliers. This is because the FAR is higher than the statistically acceptable rate of order of 5% and 1% for the 95% and 99% confidence limits respectively. These samples are treated by implementing combined index weight prior to model updating, hence the impact of the outliers on model update is reduced.

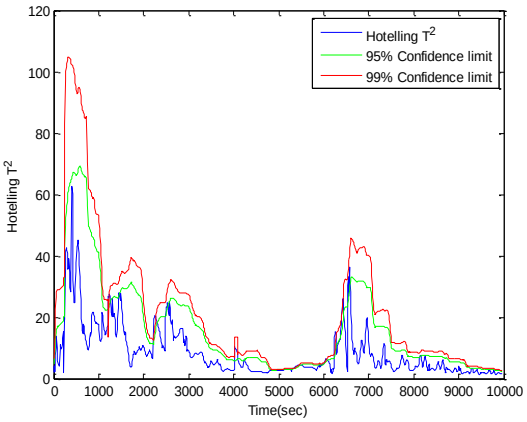

Figure 5.76- Hotelling's T^2 based on RADPLS for the validation data set

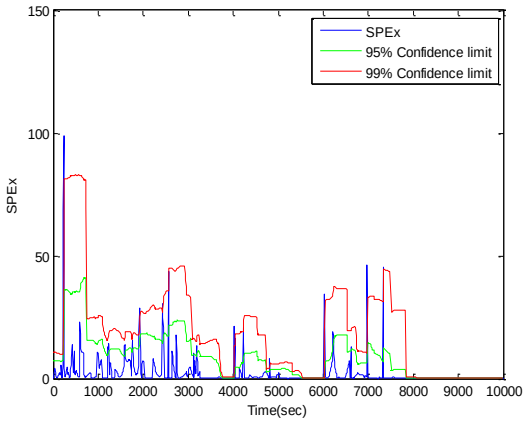

Figure 5.77 - SPE_X based on RADPLS for the validation data set

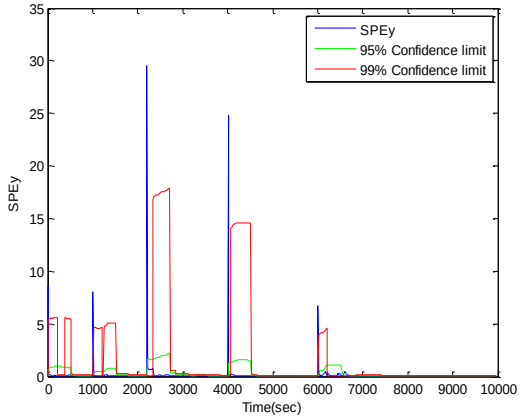

Figure 5.78 - SPE_Y based on RADPLS for the validation data set

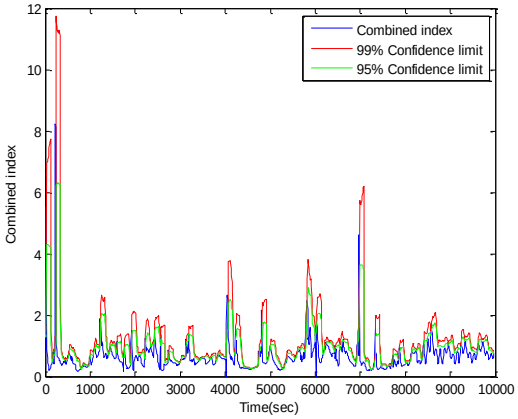

Figure 5.79 - Combined index based on RADPLS for the validation data set

5.9.2.2 Monitoring Statistics for the Test Data Sets

From Table 5.5, the process disturbance was introduce at t =1 sec after running the simulation for 4000 sec under normal operating conditions. The disturbances affect the process for 3200 sec and hence the number of samples affected by the fault is identified as 320 consecutive samples. The monitoring results based on the RADPLS are presented in Figures 5.80 to 5.87 for the test data sets (Table 5.5). In both cases the statistical indices are affected by the fault. For the first case, it can be seen that the monitoring indices clearly indicate that the process has deviated from statistical control. Hotelling's T^2 indicates the disturbance at t = 20 sec (i.e. second sample after introducing the disturbance), the SPE_X indicates it at t = 50 sec (i.e. fifth sample after the introduction of the disturbance) and SPE_Y indicate it at t = 60 sec (i.e. sixth sample after introduction of the disturbance). For the second case, it can be seen that the monitoring indices clearly indicate that the process deviates from statistical control. Hotelling's T^2 indentifies the disturbance at t = 40 sec (i.e. forth sample after the onset of the disturbance), SPE_X at t=30 sec (i.e. third sample after the onset of the disturbance) and SPE_Y t= 60 sec (i.e. sixth sample after introduction of the disturbance). The monitoring charts show the process is out of statistical control approximately until t=1800 sec and t= 1200 sec for the first and second cases respectively. However, in this period a few points are in statistical control when it was known that the disturbance lasts until t=3200 sec (i.e. all the samples from t=1 until 3200 are affected by the disturbance Table 5.5). This may have occurred for the following reasons:

- The model parameters have been updated incorrectly when the fault occurs for a few samples. During process oscillations, when the signal passes through the region of normal operation, it causes the model to update. However, at this time the dynamic characteristics of the process are not representative of normal operation. This situation becomes more severe the longer the fault persists as the magnitude and frequency of the oscillation both increase (Figure 5.69 and 5.71).
- Rapid oscillations resulting from the fault (the fast dynamic behaviour of the signal) has an impact on the statistical indices as Hotelling's T^2 and SPE_X are calculated as a function of the measured value of the current sample and the parameters of the previous PLS model.
- Additionally, the combined index was calculated as a function of the two statistics (Hotelling's T^2 and SPE_X), their adaptive limits and the previous PLS model. Once an observation is identified as a statistical outlier, the observation itself is weighted prior to model updating. However, the adaptive limits are allowed to adapt to the statistical outlier. Hence the limits of the statistical outlier are used to calculate the combined index and its limit. This could have an impact on the functionality of the combined index as seen in Figure 5.83 and Figure 5.87 where an outlier was identified at time t=450 and t=1000 for case1 and case 2 respectively.

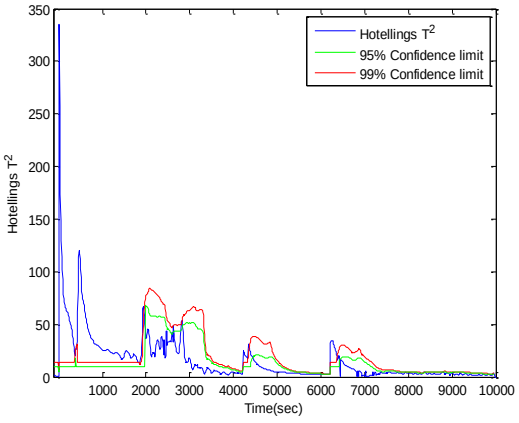

Figure 5.80 – Hotelling's T^2 based on RADPLS for the test data set – case 1

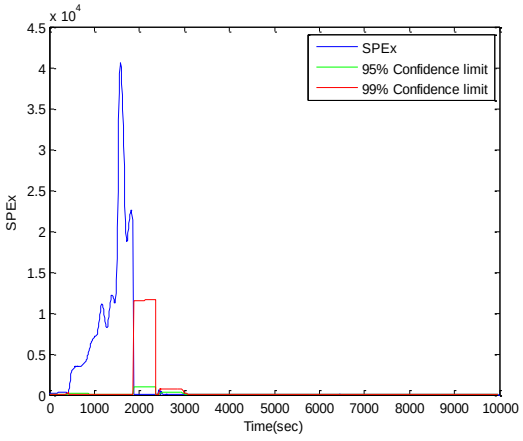

Figure 5.81- SPE_X based on RADPLS for the test data set – case 1

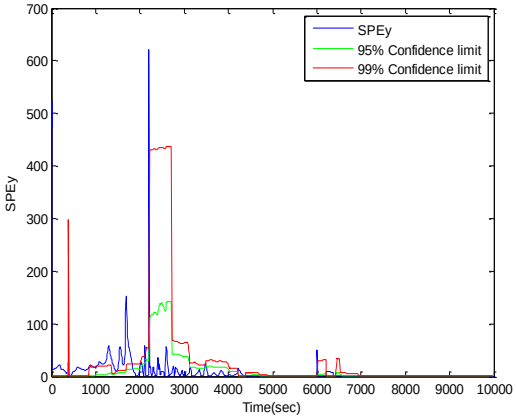

Figure 5.82- SPE_Y based on RAPLS for the test data set – case 1

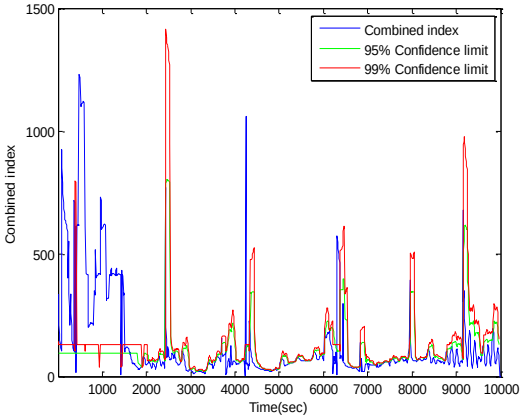

Figure 5.83- Combined index based on RAPLS for the test data set – case 1

The same observations can be seen for the second testing data set where the fresh feed temperature affects the behaviour of the ammonia reactor.

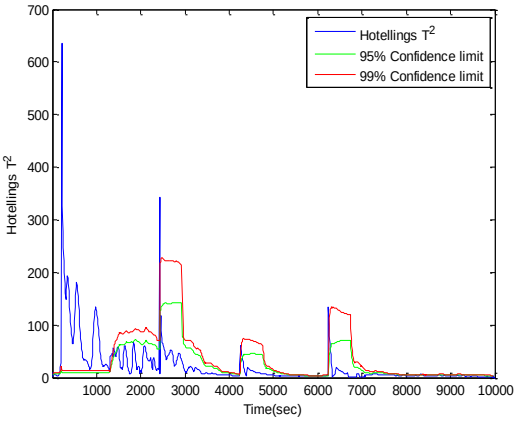

Figure 5.84- Hotelling's T^2 based on RAPLS for the test data set – case 2

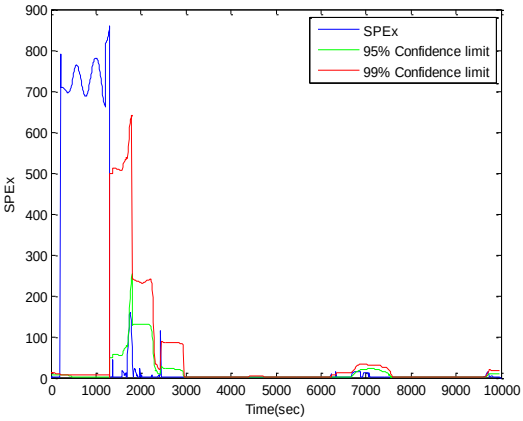

Figure 5.85- SPE_X based on RAPLS for the test data set – case 2

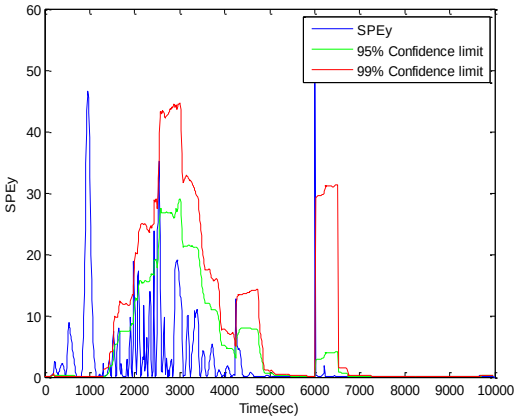

Figure 5.86- SPE_Y based on RADPLS for the test data set – case 2

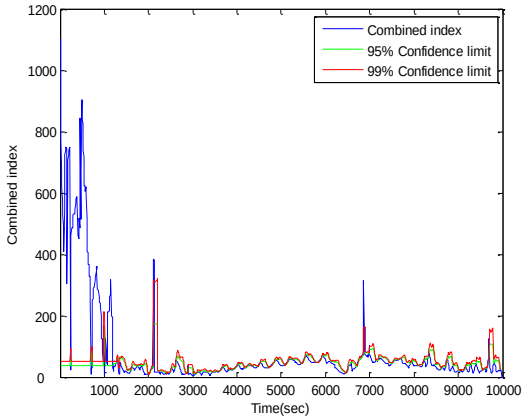

Figure 5.87- Combined index based on RADPLS for the test data set – case 2

A different fault duration was investigated (i.e. the pressure falls to 150 bar for 100 recorded samples). From Figures 5.88 to 5.91 it can be observed that the fault was clearly identified.

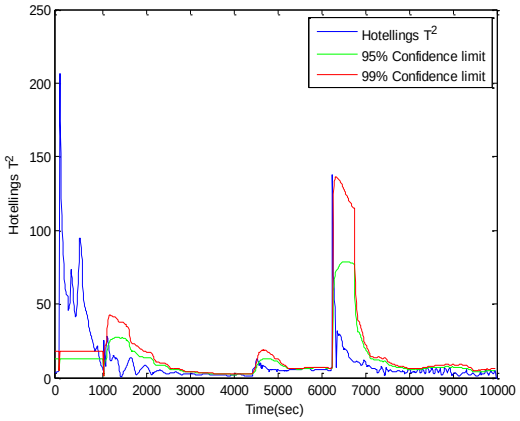

Figure 5.88. Hotelling's T^2 based on RADPLS for test data set (100 samples)

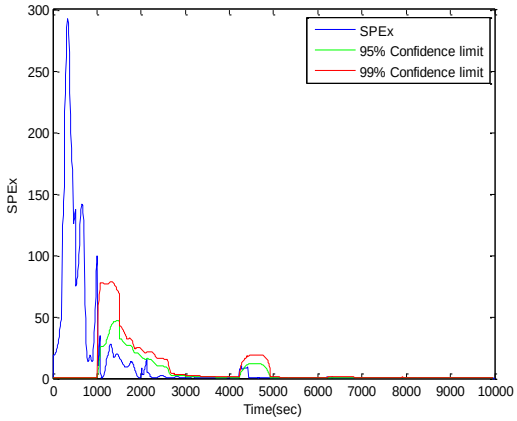

Figure 5.89. SPE_X based on RADPLS for test data set (100 samples)

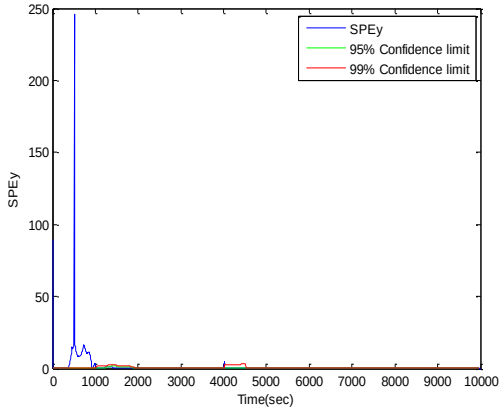

Figure 5.90- SPE_Y based on RADPLS for test data set (100 samples)

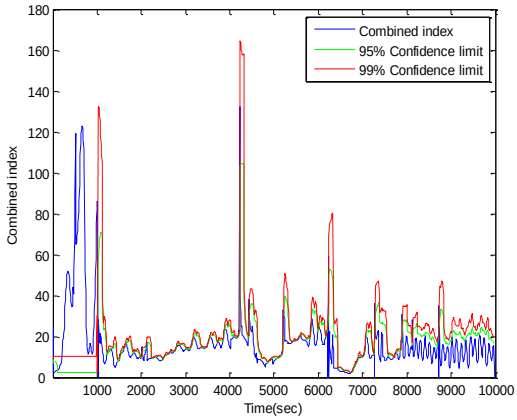

Figure 5.91-Combined index based on RADPLS for test data set (100 samples)

From Table 5.21, there is strong evidence that an improvement has materialised when comparing these results against the results based on ADPLS, where the fault detection rate were low (Table 5.16), and DPLS, where the false alarm rate were high (Table5.11). The fault detection rate is significantly increased when the fault occurs for a short duration as shown in Table 5.21. For case 1, the monitoring charts on average detect 60% and 57% of the process faults for the 95% and 99% confidence limits respectively whilst for case 2, the monitoring charts on average detect 38.5% and 36.5% of the process faults for the 95% and 99% confidence limits respectively. The fault detection rate has significantly increased when the faults occurs for a short

duration as the monitoring charts detect 93.5% and 90% of the process faults for the 95% and 99% confidence limits respectively.

Table 5.21 – Fault detection rate for monitoring charts based on RADPLS.

Chart	Fault detection rate 95% confidence limits	Fault detection rate 99% confidence limits
	Test data set - Case 1	
Hotelling's T^2	59.68%	56.25%
SPE_X	58.12%	54.68%
SPE_Y	62.18%	59.37%
	Test data set - Case 2	
Hotelling's T^2	39.06%	35.93%
SPE_X	34.37%	33.75%
SPE_Y	42.18%	39.68%
	Test data set (100 samples)	
Hotelling's T^2	97%	95%
SPE_X	99%	95%
SPE_Y	85%	80%

Again the concept of average run length ARL0 and ARL1 is used to evaluate the monitoring charts based on RADPLS. There is a strong evidence of an improvement as can be seen in Table 5.22 where the value of ARL1 indicates the disturbance after few samples compared to ARL1 following the application of DPLS and ADPLS. On the other hand when the process was operating under normal operating conditions, the ARL0 was high compared to those following the application of the DPLS and ADPLS algorithms. The values of ARL0 and ARL1 were calculated on the basis of Monte Carlo approach (50 experiments).

Table 5.22 – ARL0 and ARL1 for Hotelling's T^2, SPE_X and SPE_Y using RADPLS

chart	ARL	RADPLS
Hotelling's T^2	ARL0	90
	ARL1	5
SPE_X	ARL0	88
	ARL1	10
SPE_Y	ARL0	90
	ARL1	12

5.10 Discussion

In this Chapter, five statistical indices are used to assess model quality and the performance of monitoring charts. the root mean squared error (RMSE) and coefficient of determination (R^2) are used for assessing the models whereas average run length (ARL), false alarm rate (FAR) and fault detection rate (FDR) are used for assessing the monitoring charts. In the following sections the statistical metrics are assessed comparing DPLS, ADPLS and RADPLS to obtain a better understanding of the ability of each approach in terms of prediction and monitoring.

5.10.1 Root Mean Squared Error (RMSE)

The following sections provide a comparison of the RMSE following the application of the modelling approaches for the validation and test data sets (Table 5.5).

5.10.1.1 RMSE of Validation Data Set

Figure 5.92- (a) shows a comparison between the RMSE of the modelling approaches and Figure 5.92- (b) shows a comparison between adaptive modelling approaches. Of all the approaches it can be seen that adaptive approaches give a bower RMSE indicating that the adaptive approaches result in better model predictions (Figure 5.92- (a)). Of the adaptive approaches, it can be concluded that the RADPLS approach with a variable number of latent variables results in slightly improved predictions as shown in Figure 5.92- (b). Although the improvements in the adaptive approaches are marginal, the monitoring results show that the RADPLS results in more reliable monitoring charts.

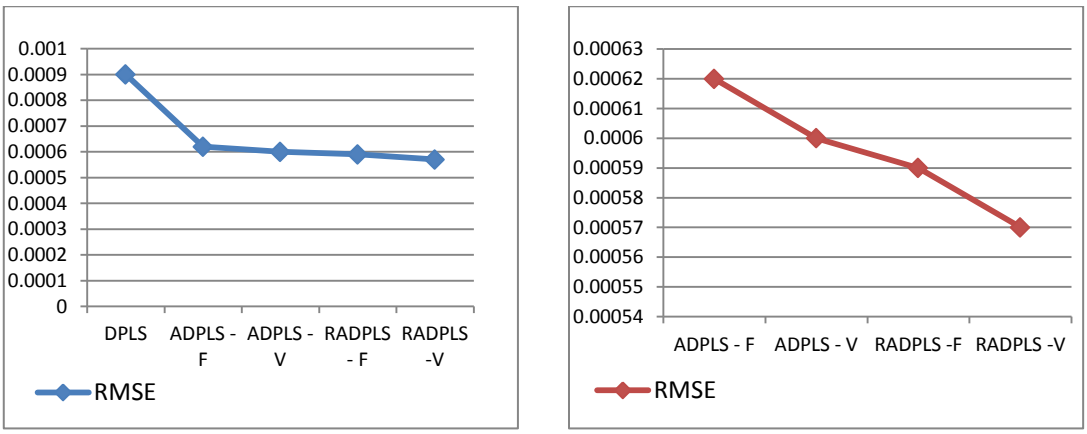

(a) (b)

Figure 5.92 – RMSE of PLS approaches for the validation data set

5.10.1.2 RMSE of the Test Data Sets

Figures 5.93 and 5.94 show the root mean square error of all PLS approaches for the test data sets (Table 5.5). Again the comparison was conducted on two bases. The first one was a comparison of all modelling approaches (Figures 5.93- (a) and 5.94 - (a)) and the second one was a comparison between the adaptive modelling approaches (Figures 5.93 - (b) and 5.94 - (b)). For both cases, it can be seen that RADPLS with a variable number of latent variables provides slight better predictions. Although the improvement is small compared to ADPLS however, the monitoring charts based on the RADPLS have the ability to detect the fault compared to ADPLS (Tables 5.16 and 5.21). A significant difference between the RMSE of DPLS and the adaptive approaches is observed. This concludes that the adaptive approaches provide better results than the fixed parameter dynamic PLS (DPLS).

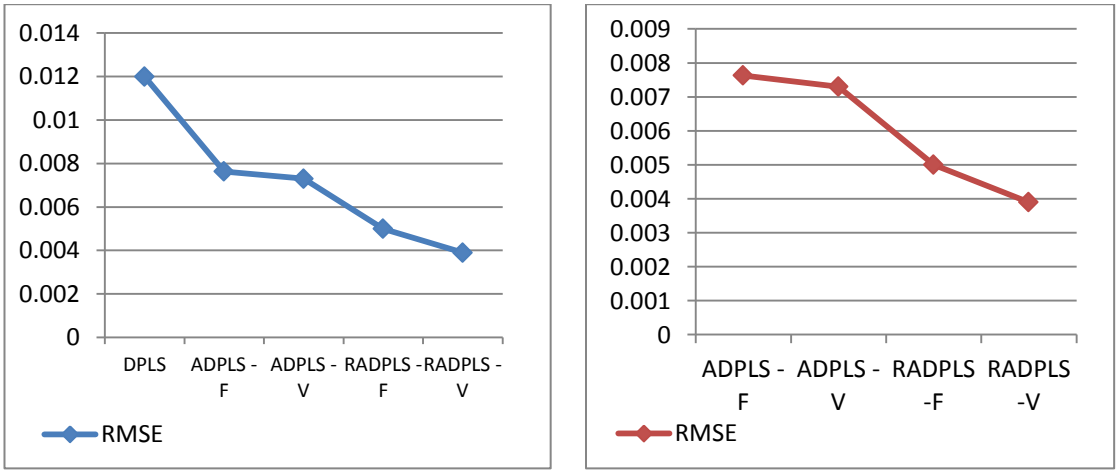

(a) (b)

Figure 5.93 – RMSE of PLS approaches for the test data set – case 1

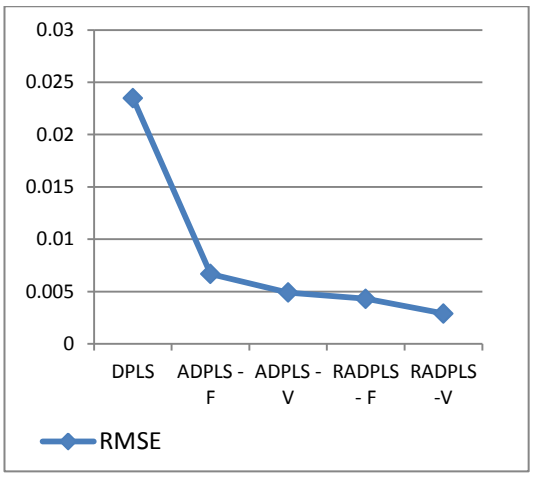

(a)

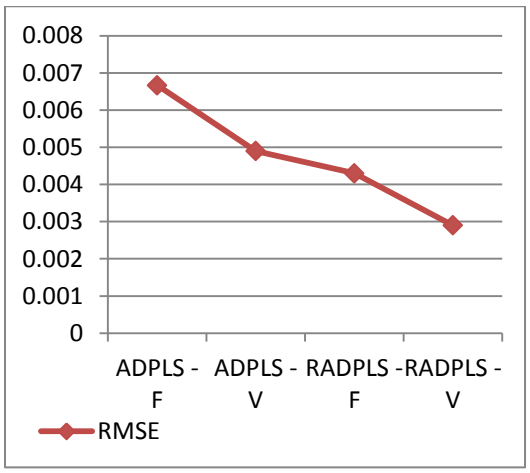

(b)

Figure 5.94 – RMSE of PLS approaches for the test data set – case 2

5.10.2 Coefficient of Determination

The following sections provide a comparison of the Coefficient of Determination following the application of the modelling approaches for the validation and test data sets (Table 5.5).

5.10.2.1 R^2 for the Validation Data Set

The value of the coefficient of determination following the application of the modelling approaches to the validation data set is presented in Figure 5.95. It can be seen that the model quality of the adaptive approaches is better than the quality of the dynamic PLS model (Figure 5.95 – (a)). Of the adaptive approaches, the quality of the RADPLS models is marginally better than the ADPLS approaches as shown in Figure 5.95 – (b) .

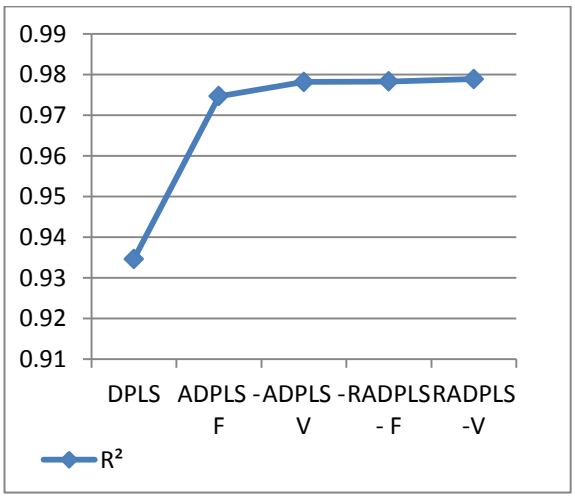

(a)

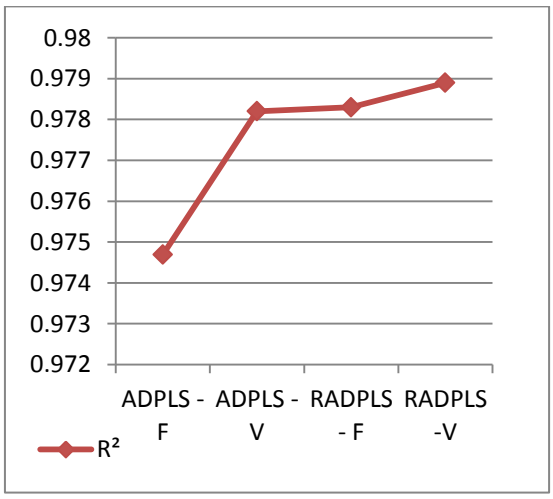

(b)

Figure 5.95 – R^2 for the validation data set for all approaches

5.10.2.2 R^2 for the Test Data Sets

Figures 5.96 and 5.97 show the coefficient of determination following the application of the DPLS variants to the test data sets. It can be concluded that the adaptive approaches are significantly better than DPLS as shown in Figures 5.96-(a) and 5.97-(a). Of the adaptive approaches (Figures 5.96-(b) and 5.97-(b)), the RADPLS models exhibit a slight enhanced performance compared to all approaches.

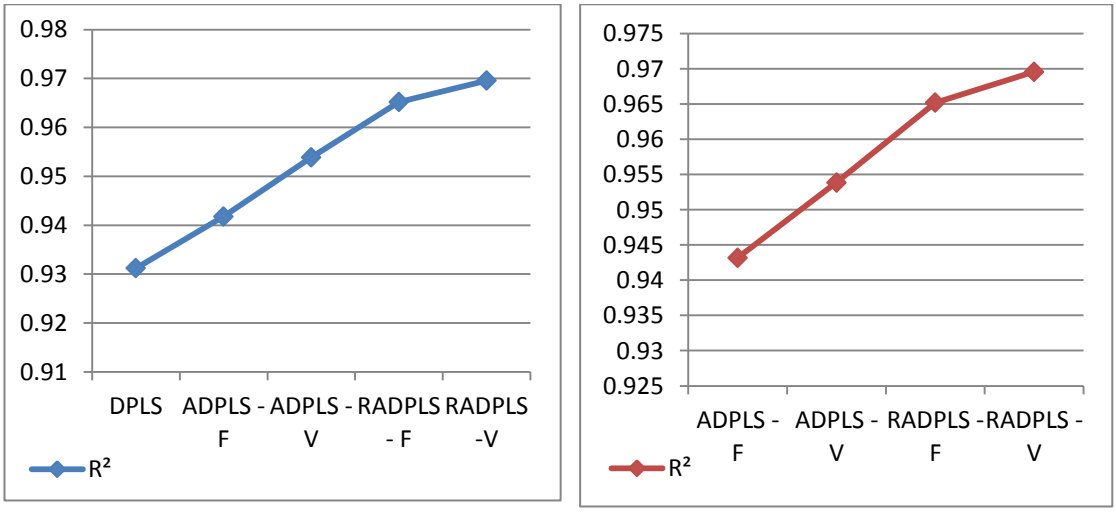

(a) (b)

Figure 5.96 – R^2 for the test data set case 1 for all approaches

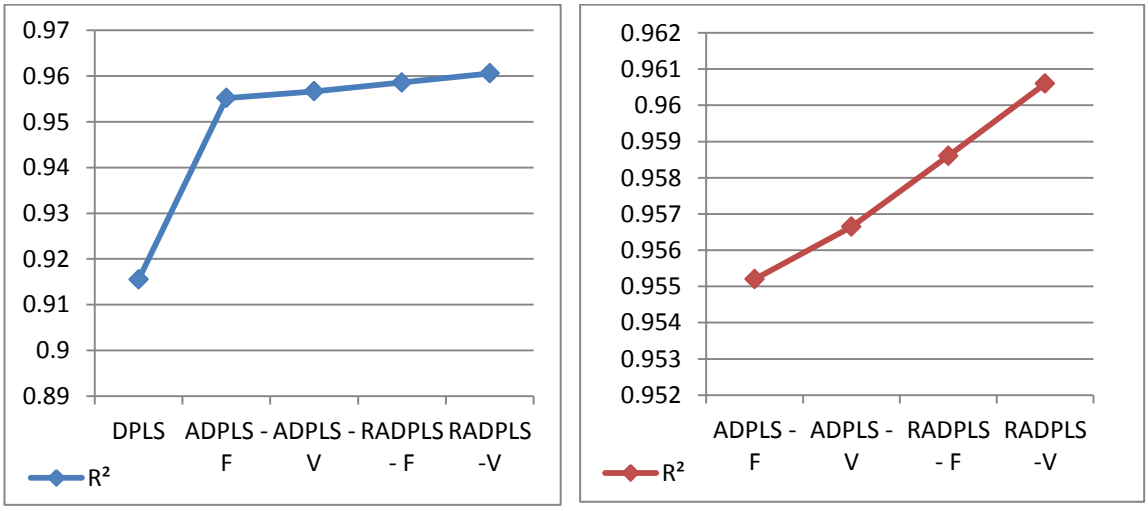

(a) (b)

Figure 5.97 – R^2 for the test data set case 2 for all approaches

Although the improvements in the adaptive approaches are marginal, the monitoring results show that the RADPLS results in more reliable monitoring charts.

5.10.3 Average Run Length

The results of ARL0 and ARL1 for Hotelling's T^2, SPE_X and SPE_Y are presented in Figures 5.98 to 5.100. Under normal operating conditions, Hotelling's T^2 (Figure 5.98) based on the adaptive approaches (ADPLS and RADPLS) perform better than DPLS. The same observation can be concluded for SPE_X and SPE_Y (Figures 5.99 and 5.100). On the other hand, when the process was affected by the fault, Hotelling's T^2 based on RADPLS performed significantly better than ADPLS and DPLS. This can be also seen in the SPE_X and SPE_Y monitoring charts.

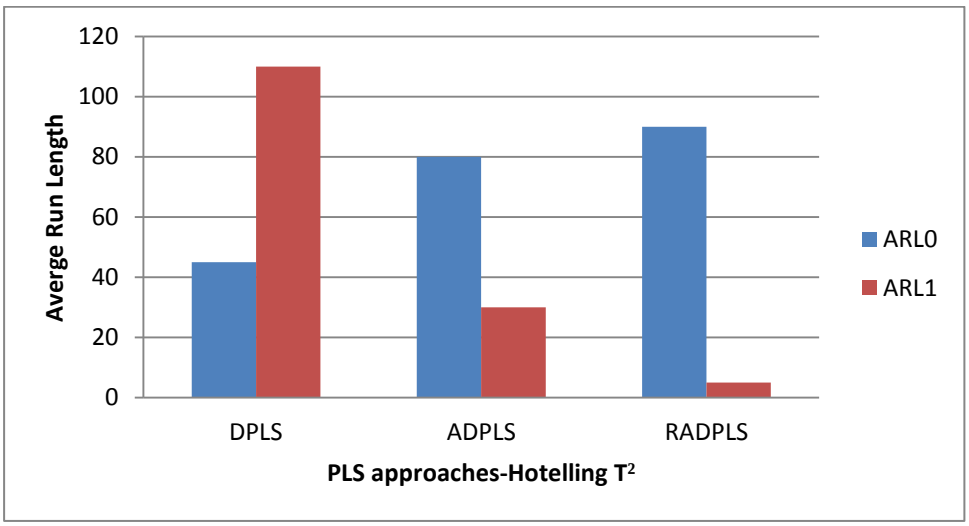

Figure 5.98 – Average run length for Hotelling's T^2

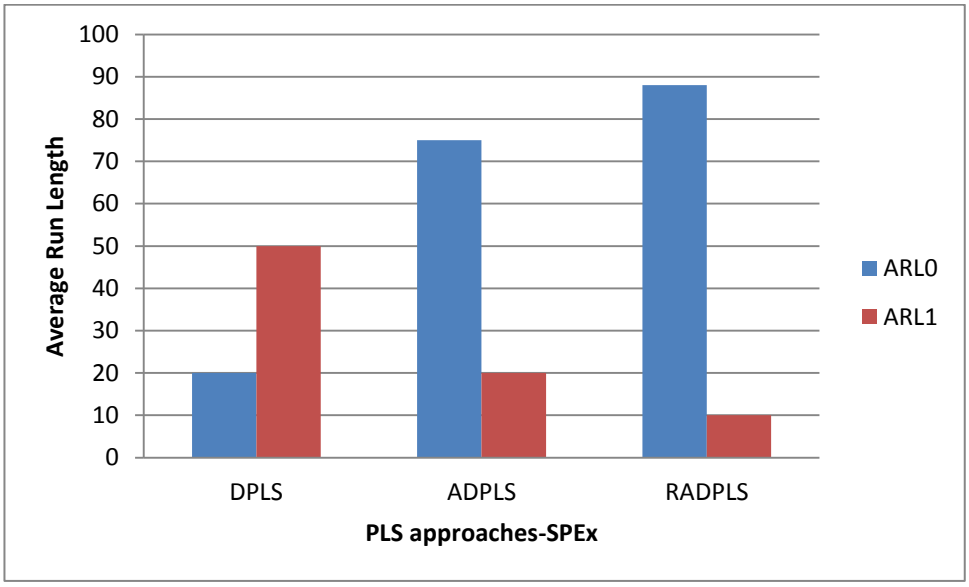

Figure 5.99 – Average run length for SPE_X

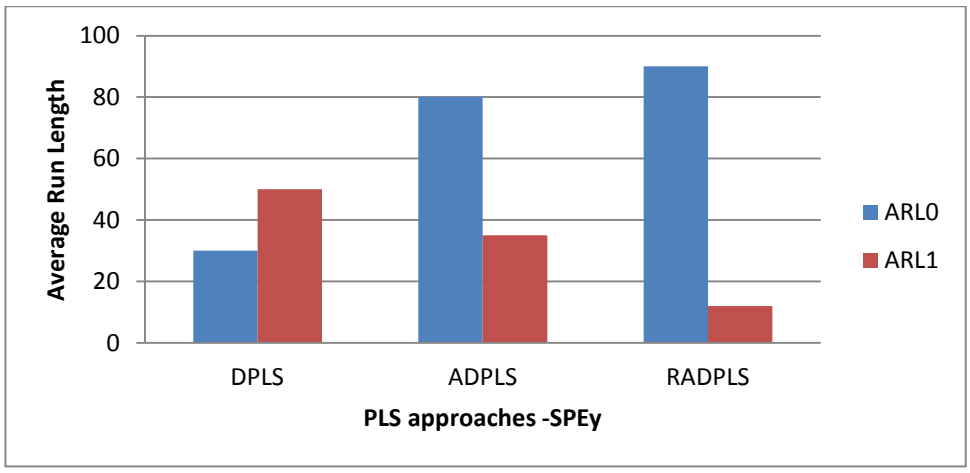

Figure 5.100 – Average run length for SPE_Y

5.10.4 Fault Detection Rate and Fault Alarm Rate

Figures 5.101 and 5.102 show the FAR for the three approaches for the validation data set for the 95% and 99% confidence limits respectively. It can be seen that DPLS increased the FAR compared to the adaptive approaches. A slight improvement can be seen between ADPLS and RADPLS as shown in Tables 5.16 and 5.21.

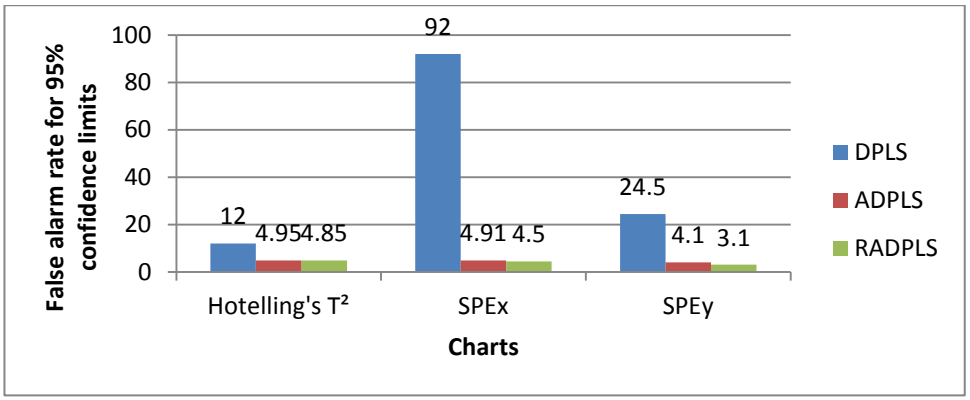

Figure 5.101 – False alarm rate for PLS approaches based on 95% confidence limits

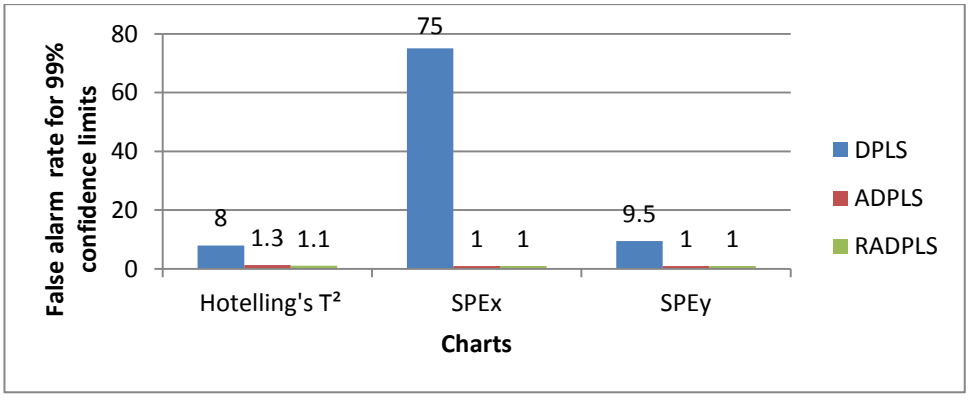

Figure 5.102 – False alarm rate for PLS approaches based on 99% confidence limits

Figures 5.103 and 5.104 show the FDR for the adaptive approaches for the test data sets for the 95% and 99% confidence limits respectively. It can be seen that there is a significant increase in the FDR based on RADPLS compared to the ADPLS approaches.

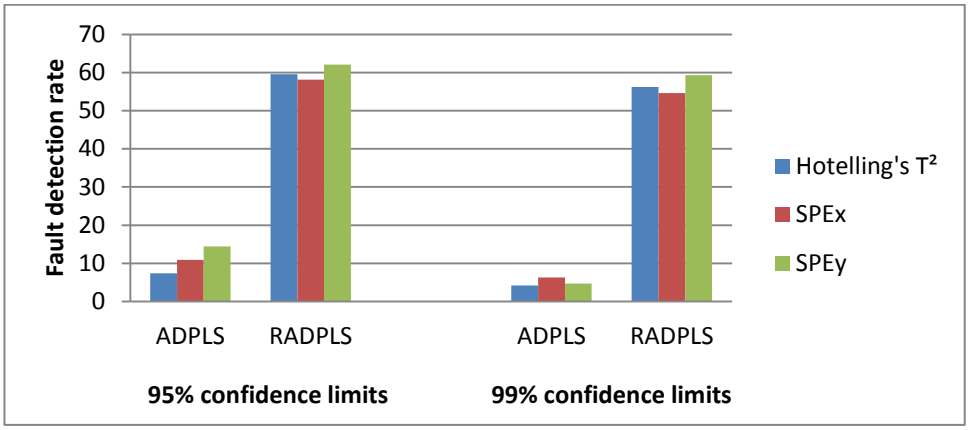

Figure 5.103 – FDR for PLS approaches for 95% confidence limits (case 1)

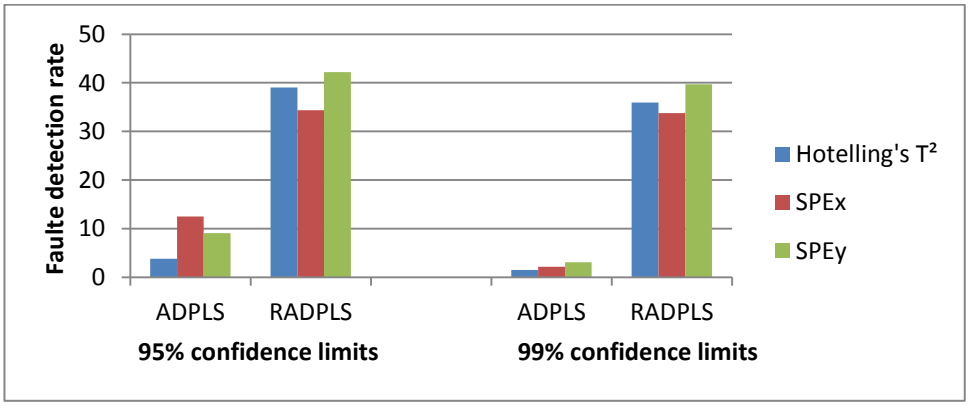

Figure 5.104 – FDR for PLS approaches for 99% confidence limits (case 2)

5.11 Chapter Summary and Conclusions

In this chapter, statistical modelling and monitoring of data generated from an ammonia synthesis fixed-bed reactor was preformed. Two main issues were addressed, the modelling of the complex dynamic behaviour of the ammonia synthesis fixed-bed reactor using statistical approaches and the building of monitoring schemes to monitor process behaviour.

For the first part, the empirical model was built using DPLS. By calculating the appropriate sampling interval and identifying the most appropriate dynamic representation, the dynamics in the process were taken into account. Different scaling approaches were considered and normalization was adopting. Based on this work, the complex behaviour of the ammonia synthesis fixed-bed reactor was modelled and the DPLS method showed good performance in terms of fitting and prediction as

quantifying by the RMSE and R^2. However, the false alarm rates following the application of DPLS indicate that the ammonia synthesis fixed bed reactor requires an advanced techniques to construct reliable monitoring charts.

The ADPLS and RADPLS approaches were used to regularly update the process model. ADPLS was used to update the reference model once a new sample became available. This showed an improvement in model fit and predictions. However, there was no threshold to prevent an abnormal event being included in the updating procedure. RADPLS was proposed to overcome this limitation. The results from ADPLS and RADPLS demonstration improved model fit and predictions compared to DPLS. RADPLS showed slightly improved performance compared to ADPLS. However, the performance of the monitoring charts following the application of RADPLS had the ability to decrease the number of false alarms compared to DPLS monitoring charts and increase the fault detection rate compared to the monitoring charts following the application of ADPLS.

The only limitation on the application of the proposed method (RADPLS) was the effect of the complex dynamic behaviour of the ammonia fixed-bed reactor signal on the functionality of RADPLS. This was due to the very strong dynamics contained in the data generated from ammonia simulation. The strong dynamic characteristics force the monitoring statistics to pass through the normal operating conditions area whilst the process was affected by the fault. Hence, the model and the confidence limits were updated incorrectly causing the next faulty samples to be identified as generated from normal operating conditions.

The performance of the RADPLS is tested on the benchmark of the Tennessee Eastman simulation process in Chapters 6 and 7. In addition, the extension of the RAPLS method to construct a scheme for monitoring the whole process as well as individual units is presented in Chapters 6 and 7.

Chapter 6

Statistical Monitoring of Tennessee Eastman Process

6.1 Introduction

As discussed in the previous chapters, the rapid development of process monitoring methods is a consequence of the increasing demand for more reliable processes and the need to manufacture products of consistent quality. By detecting the onset of abnormal events, the root causes of operational issues can be addressed and hence process efficiency and quality is enhanced. For the analysis of different data-driven monitoring approaches, it is normal practice to use data generated from simulation studies. In this chapter the statistical monitoring of the Tennessee Eastman Process (TEP) is considered. The TEP simulator is widely accepted as a test-bed for investigating process monitoring and fault diagnoses methodologies. It is a complex dynamic and nonlinear process, which was developed as a result of a collaboration between the Eastman Chemical Company and University of Tennessee (Downs and Vogel, 1993). In this chapter, a number of Partial Least Squares (PLS) based monitoring techniques are developed for the monitoring of the whole process as well as the individual unit operations. Monitoring charts are evaluated through a number of statistical indices that quantify false alarm and fault detection rates.

As discussed in previous chapters, monitoring based on PLS consists of two steps. First a process model that represents normal process behaviour is developed. Secondly, the developed model is used for constructing a monitoring scheme that has the ability to provide reliable detection of process abnormality. In Chapter 7, a number of operational changes are considered including a step change, random variation, change in reaction kinetics and an unknown change.

6.2 Objectives

The main objective of this chapter is to develop models and monitoring schemes based on the techniques discussed in Chapters 3 and 4 for the TEP in terms of both the whole process as well as the individual unit operations. More specifically the goals of the chapter are to:

- Apply and extend the PLS techniques introduced previously to develop process models that describe the performance of the TEP. Model fitting and prediction performance will be evaluated in terms of the root mean squared error (RMSE).
- Investigate the efficiency of the PLS techniques with respect to process monitoring.
- Develop monitoring schemes that allow for the monitoring of the whole process as well as the individual unit operations using multiblock PLS.

The monitoring charts will be assessed using the statistical index of false alarm rate (FAR) and fault detection rate (FDR). Table 6.1 summarises the modified PLS techniques applied in this chapter while Table 6.2 provides the criteria used to assess the performance of the modelling and monitoring approaches.

Table 6.1- Summary of the approaches applied and the underlying objectives.

Approach	Objective(s)
Partial Least Squares (PLS) Original PLS method	Modelling the process and monitoring the whole process using steady state fixed parameter PLS.
Dynamic PLS (DPLS) and multiblock variants (MBDPLS) Modified by incorporating FIR	Dynamic modelling of the process and monitoring of the whole process and individual unit operations using fixed parameter DPLS and MBDPLS
Recursive dynamic PLS with adaptive confidence limits (ADPLS) and multiblock variant (AMBDPLS) Modified by incorporating FIR	Recursive dynamic model with real-time monitoring of the whole process and individual unit operations with adaptive confidence limits
Robust recursive dynamic PLS with adaptive confidence limits (RADPLS) and multiblock variants (RAMBDPLS) Modified by incorporating FIR	Recursive dynamic model that is robust to outlying samples for the real-time monitoring of the whole process and individual unit operations with adaptive confidence limits

Table 6.2- Assessment criteria for models and the statistical monitoring of the process

Criteria	Tool
Goodness of fit	RMSE of calibration data set
Accuracy of prediction	RMSE of validation data set
Monitoring efficacy	Monitoring charts, FAR and FDR

6.3 Tennessee Eastman Process

6.3.1 Background

In 1993, Downs and Vogel summarized the potential applications of the TEP. These included the application of different control strategies, process optimization, predictive control, nonlinear control and process diagnostics. They also provided FORTRAN subroutines to be used for the aforementioned application areas and these subroutines are available in the public domain (Downs and Vogel, 1993). The TEP has been used in a wide variety of studies including the application of control strategies, process monitoring and fault diagnosis (Ricker, 1995; Kano et al., 2002; Lee et al., 2004; Molina et al., 2011; Yin et al., 2012).

6.3.2 Process Description

The TEP comprises five unit operations: reactor, condenser, compressor, separator and stripper. Figure 6.1 provides a detailed diagram of the process units and the positioning of the valves (Downs and Vogel, 1993). A description of the process as well as notation and symbols is given in Downs and Vogel (1993).

The process has two quality products represented by G and H that are produced from four reactants, A, C, D and E. In addition to the products G and H, an inert, B, and a by-product, F, are removed from the system. All the reactions are exothermic and irreversible and are given by:

$$\begin{aligned} A(g) + C(g) + D(g) &\rightarrow G(l) \\ A(g) + C(g) + E(g) &\rightarrow H(l) \\ A(g) + E(g) &\rightarrow F(l) \\ 3D(g) &\rightarrow 2F(l) \end{aligned} \qquad (6.1)$$

The reactant (gas phase) is fed to the exothermic reactor where the main reaction is carried out. The reactor product stream is then cooled by the condenser and the

condensed components are transferred to the vapour/liquid separator with some of the unused materials in the vapour being recycled back to the reactor through a compressor. A portion of the recycle stream is purged to prevent the inert and by-product accumulating in the system (Downs and Vogel, 1993). Liquid components from the separator are sent to the stripper, where the remaining reacted components are further reacted and stripped. The quality products are produced in the striper and the unused material is recycled back into the reactor.

For ease of understanding, a schematic of the TEP is presented in Figure 6.2. It shows the five unit operations with a simplified workflow and does not include the control structure. Additionally, it identifies the units that represent the process blocks used in the multiblock analysis. Figures 6.1 and 6.2 show the interactions between the process units (blocks). Since the process is continuous and some of the control loops are connected (dashed lines), it is expected that further interactions will materialise between process units. For example, when the condenser cooling water rate is increased, it has an effect on the amount of liquid exiting from the condenser outlet, thereby determining the liquid level in the separator. The separator has a set point for the liquid level and this is connected to the underflow of the separator via a valve. Whenever, the liquid level is increased in the separator, the excess liquid is purged by opening the valve to allow more liquid to flow into the stripper. This is an example of how a change in the state of one unit operation is transmitted to another unit (i.e. stripper).

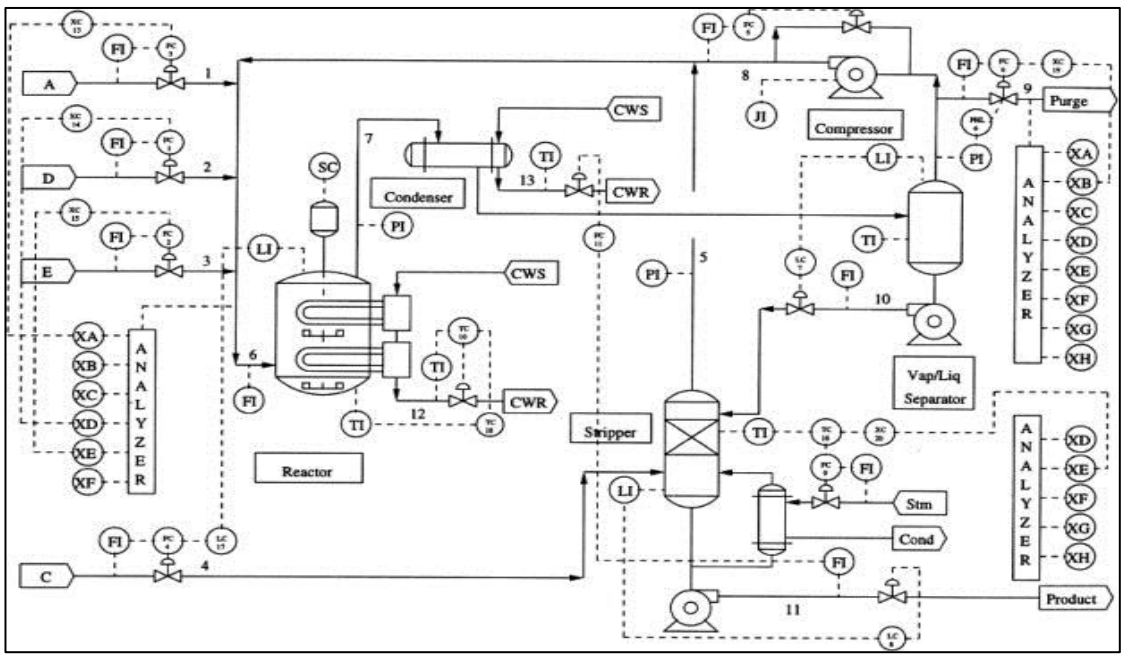

Figure 6.1 - Tennessee Eastman Process (Downs and Vogel, 1993)

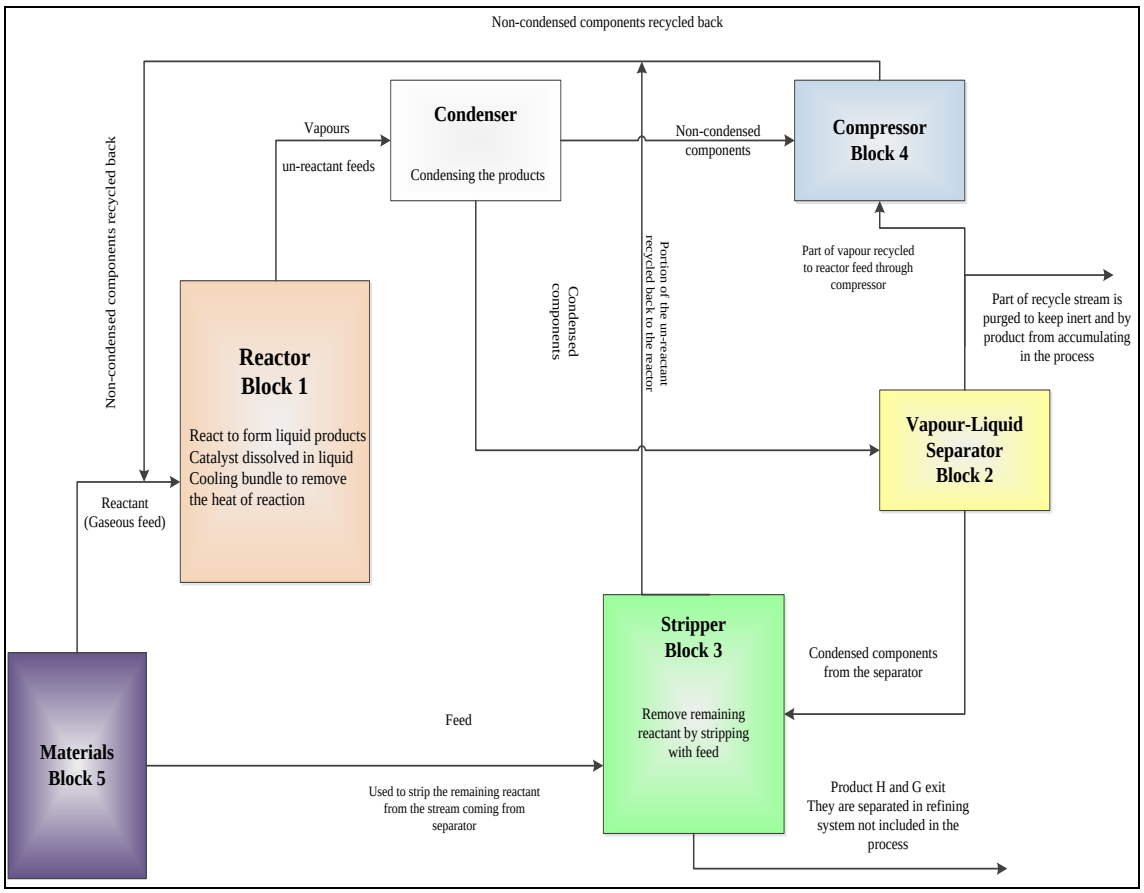

Figure 6.2 - Simplified Tennessee Eastman work flow

6.3.3 Data Acquisition

For this study, the data sets published by Chiang et al. (2001) that had been generated from the FORTRAN formed the bases of the analysis. These data sets have previously been used for process monitoring and fault diagnoses studies in Yin et al. (2012) and Chiang et al. (2001). The data set comprises 53 variables recorded every 3 min of which 22 are process measurements, XMEAS(1)…., XMEAS(22), 19 are composition measurements, XMEAS(23)….,XMEAS(41) and 12 are manipulated variables defined as XMV(1), XMV(2),…XMV(12). A description of the process variables and manipulated variables is presented in Tables 6.3 and 6.4.

The composition measurements are taken from streams 6, 9 and 11 (Figure 6.1) and the compositions form streams 6 and 9 are recorded every 6 min whilst the compositions from stream 11 are recorded every 15 min. Chiang et al. (2001) provided 22 training data sets encompassing both normal operating conditions and abnormal behaviour. They used the same sampling interval, 3 min for all variables to simplify the implementation of data the driven methods (Chiang et al., 2001). Chiang et al. (2001) stated that by

applying the same sampling interval for all the variables, the measurement taken from stream 6 and 9 are available for every two samples and for stream 11, they are available every five samples. Chiang et al. (2001) sorted the differences in the sampling interval between process variables and the measurement taken from stream 6,9 and 11 to have a sampling period of 3 min for all the measurement. By preserving the measurement taken from stream 6, 9 and 11 until a new measurement is recorded. In this work, the quality variable (composition G) is the only measurement taken from stream 9 with a 6 min time delay, i.e. a new measurement is available every two samples (3 min sampling).

The normal operating condition data set was collected for 25 operational hours. The data sets that incorporated abnormal behaviour were collected for 48 hr and the abnormal event was introduced after 8 hr of the operating period. The total number of data sets comprising identified faults is 21 (Downs and Vogel, 1993; Chiang et al., 2001). Table 6.5 summarises the abnormal data sets and the associated faults.

For the development of the monitoring scheme, 22 measurements XMEAS(1)…., XMEAS(22) and only 11 manipulated variables XMV(1),…….XMV(11) were used to define input matrix, $\mathbf{X} = [\mathbf{z}_1, \ldots \ldots \mathbf{z}_{33}]$. The manipulated variables were included as input variables because they are not independent of the process variables due to the process being operated under feedback control (Yin et al., 2012). In this study, the composition G (XMEAS(35)) is used to denote the product quality and is labelled, $\mathbf{v}_{13}$.

6.3.4 Process Characteristics

The Tennessee Eastman Process (TEP) exhibits nonlinear and dynamic characteristics. Although the process is nonlinear, it is known from the literature that a nonlinear system can be approximated by a linear model if it is operated within a certain operating region (Ge and Song, 2013; Ge et al., 2013). The TEP is operated under closed loop control and hence the process measurements are auto and cross correlated. Consequently, a process monitoring method that takes into account the correlation structure in the process data is necessary.

Table 6.3 - Process measurements and manipulated variables

Process Measurements		
Variables	Description	Label*
XMEAS(1)	A Feed (Stream 1)	z_1
XMEAS(2)	D Feed (Stream 2)	z_2
XMEAS(3)	E Feed (Stream 3)	z_3
XMEAS(4)	Total Feed (Stream 4)	z_4
XMEAS(5)	Recycle Flow	z_5
XMEAS(6)	Reactor Feed Rate	z_6
XMEAS(7)	Reactor Pressure	z_7
XMEAS(8)	Reactor Level	z_8
XMEAS(9)	Reactor Temperature	z_9
XMEAS(10)	Purge Rate (Stream 9)	z_{10}
XMEAS(11)	Product Separator Temperature	z_{11}
XMEAS(12)	Product Separator Level	z_{12}
XMEAS(13)	Product Separator Pressure	z_{13}
XMEAS(14)	Product Separator Underflow	z_{14}
XMEAS(15)	Stripper Level	z_{15}
XMEAS(16)	Stripper Pressure	z_{16}
XMEAS(17)	Stripper Level Underflow	z_{17}
XMEAS(18)	Stripper Temperature	z_{18}
XMEAS(19)	Stripper Steam Flow	z_{19}
XMEAS(20)	Compressor Work	z_{20}
XMEAS(21)	Reactor cooling Water outlet temperature	z_{21}
XMEAS(22)	Separator cooling Water outlet temperature	z_{22}
Manipulated Variables		
Variable	Description	Label*
XMV(1)	D Feed Flow (Stream 1)	z_{23}
XMV(2)	E Feed Flow (Stream 2)	z_{24}
XMV(3)	A Feed Flow (Stream 3)	z_{25}
XMV(4)	Total feed (Stream 4)	z_{26}
XMV(5)	Compressor Recycle Valve	z_{27}
XMV(6)	Purge Valve (Stream 9)	z_{28}
XMV(7)	Separator Pot Liquid Flow (Stream 10)	z_{29}
XMV(8)	Stripper Liquid Product Flow (Stream 11)	z_{30}
XMV(9)	Stripper Steam Valve	z_{31}
XMV(10)	Reactor Cooling Water Flow	z_{32}
XMV(11)	Condenser Cooling Water Flow	z_{33}
XMV(12)	Agitator speed	**

Label* denotes the variables used in the multivariate analysis. The manipulated variable XMV(12) is not used in the analysis

Table 6.4 - Composition measurements

Variable	Description	Label	Stream	Sampling interval (min)
XMEAS(23)	Component A	v_1	6	6
XMEAS(24)	Component B	v_2	6	6
XMEAS(25)	Component C	v_3	6	6
XMEAS(26)	Component D	v_4	6	6
XMEAS(27)	Component E	v_5	6	6
XMEAS(28)	Component F	v_6	6	6
XMEAS(29)	Component A	v_7	9	6
XMEAS(30)	Component B	v_8	9	6
XMEAS(31)	Component C	v_9	9	6
XMEAS(32)	Component D	v_{10}	9	6
XMEAS(33)	Component E	v_{11}	9	6
XMEAS(34)	Component F	v_{12}	9	6
XMEAS(35)	Component G	v_{13}	9	6
XMEAS(36)	Component H	v_{14}	9	6
XMEAS(37)	Component D	v_{15}	11	15
XMEAS(38)	Component E	v_{16}	11	15
XMEAS(39)	Component F	v_{17}	11	15
XMEAS(40)	Component G	v_{18}	11	15
XMEAS(41)	Component H	v_{19}	11	15

Table 6.5 - Process faults

Fault	Description	Type
Fault (1)	A/C feed ratio, B composition constant	Step
Fault (2)	B composition, A/C feed ratio constant	Step
Fault (3)	D feed Temperature	Step
Fault (4)	Reactor cooling water inlet temperature	Step
Fault (5)	Condenser cooling water inlet temperature	Step
Fault (6)	A feed loss	Step
Fault (7)	C header pressure loss-reduced availability	Step
Fault (8)	A, B, and C feed composition	Random variation
Fault (9)	D feed temperature	Random variation
Fault (10)	C feed temperature	Random variation
Fault (11)	Reactor cooling water inlet temperature	Random variation
Fault (12)	Condenser cooling water inlet temperature	Random variation
Fault (13)	Reaction kinetics	Slow drift
Fault (14)	Reactor cooling water valve	Sticking
Fault (15)	Condenser cooling water valve	Sticking
Fault (16)	Unknown	Unknown
Fault (17)	Unknown	Unknown
Fault (18)	Unknown	Unknown
Fault (19)	Unknown	Unknown
Fault (20)	Unknown	Unknown
Fault (21)	The valve fixed at steady state position	Constant position

6.4 Statistical Monitoring of TEP

A number of data driven methods have been applied to the TEP for monitoring purposes including partial least squares (PLS), principal component analysis (PCA) and independent component analysis (ICA). Recently Yin et al. (2012) undertook a comparative study on the application of a number of data driven methods to the TEP including PCA, PLS, ICA, Fisher Discriminant Analysis, total PLS (TPLS) and Subspace Aided Approach (SAP). They found that the SAP method provided better fault detection rate (FDR) than the other methods. In addition they concluded that the number of parameters, components and latent variables, associated with PLS, PCA and ICA influence the performance of the process monitoring methods. However, the PLS methods used in their study did not consider the autocorrelation inherent within the process variables. In addition they did not provide any information with regards to model quality.

Chiang et al. (2001) reviewed the application of multivariate statistical monitoring approaches to the TEP including PCA, Dynamic PCA (DPCA), and Canonical Variate Analysis (CVA). They found that CVA produced a high false alarm rate compared to PCA and DPCA. Additionally, DPCA is sensitive to the TEP faults compared to standard PCA, i.e. it detects the small changes in the TEP rapidly. In general, they found that the performance of the multivariate process monitoring methods varied for the different test data sets, more specifically when the fault affects a large number of process variables, detection performance is improved. Other multivariate statistical monitoring studies have also been undertaken on the TEP (Raich and Çinar, 1996; Kano et al., 2002; Li et al., 2010; Liu et al., 2012).

Within this study, the data driven methods presented in Table 6.1 are applied to the TEP for the purpose of monitoring. In contrast to previous studies, the approaches considered are based on the dynamics of the process and compared against the more traditional approaches of standard PLS. A further aspect of this study is to compare the results when monitoring the whole process as well as the individual unit operation. The multiblock PLS algorithm of Westerhuis et al. (1998) forms the bases of the monitoring of the individual unit operations and presented in Chapter 3. In the multiblock analysis, the first step was to divide the process variables and manipulated variables (Table 6.3) into five blocks namely reactor, separator, stripper, compressor and materials block respectively. The condenser unit data is combined with the reactor data since it contains

only one variable, condenser cooling water flow. Each block comprises a different number of variables ($m_b, \mathrm{b} = 1,2,..,5$) and given in Table 6.6, i.e. the number of the variables is 7, 6, 7, 5 and 8 for the reactor, separator, stripper, compressor and materials block respectively.

Prior to the implementation of statistical monitoring methods, pre-processing of the data was performed. In term of scaling, block scaling was applied, i.e. each variable in data block $\boldsymbol{X}_b$ is scaled to have zero mean and variance, $\frac{1}{m_b}$. After scaling, the variant PLS methods were applied.

Table 6.6 - Process variable assigned to corresponding blocks

Block name	Variables name	Variable	Labels
Block 1 Reactor	Reactor Feed Rate	XMEAS(6)	z_6
	Reactor Pressure	XMEAS(7)	z_7
	Reactor Level	XMEAS(8)	z_8
	Reactor Temperature	XMEAS(9)	z_9
	Reactor cooling Water outlet temperature	XMEAS(21)	z_{21}
	Reactor Cooling Water Flow	XMV(10)	z_{32}
	Condenser Cooling Water Flow	XMV(11)	z_{33}
Block 2 Separator	Product Separator Temperature	XMEAS(11)	z_{11}
	Product Separator Level	XMEAS(12)	z_{12}
	Product Separator Pressure	XMEAS(13)	z_{13}
	Product Separator Underflow	XMEAS(14)	z_{14}
	Separator cooling Water outlet temperature	XMEAS(22)	z_{22}
	Separator Pot Liquid Flow (Stream 10)	XMV(7)	z_{29}
Block 3 Stripper	Stripper Level	XMEAS(15)	z_{15}
	Stripper Pressure	XMEAS(16)	z_{16}
	Stripper Level Underflow	XMEAS(17)	z_{17}
	Stripper Temperature	XMEAS(18)	z_{18}
	Stripper Steam Flow	XMEAS(19)	z_{19}
	Stripper Liquid Product Flow (Stream 11)	XMV(8)	z_{30}
	Stripper Steam Valve	XMV(9)	z_{31}
Block4 Compressor	Recycle flow	XMEAS(5)	z_5
	Purge Rate (Stream 9)	XMEAS(10)	z_{10}
	Compressor Work	XMEAS(20)	z_{20}
	Compressor Recycle Valve	XMV(5)	z_{27}
	Purge Valve (Stream 9	XMV(6)	z_{28}
Block 5 Materials	A Feed (Stream 1)	XMEAS(1)	z_1
	D Feed (Stream 2)	XMEAS(2)	z_2
	E Feed (Stream 3)	XMEAS(3)	z_3
	Total feed (Stream 4)	XMEAS(4)	z_4
	D Feed Flow (Stream 1)	XMV(1)	z_{23}
	E Feed Flow (Stream 2)	XMV(2)	z_{24}
	A Feed Flow (Stream 3)	XMV(3)	z_{25}
	Total Feed (Stream 4)	XMV(4)	z_{26}

6.4.1 Static PLS Model

PLS was applied to the scaled TEP process data, where the data was collected on 3 min sampling period. The predictor matrix (500×33) containing the predictor variables was sub-divided as follows:

$$\mathbf{X} = [\boldsymbol{X}_1, \boldsymbol{X}_2, \boldsymbol{X}_3, \boldsymbol{X}_4, \boldsymbol{X}_5] \quad (6.2)$$

The matrices $\boldsymbol{X}_1, \boldsymbol{X}_2, \boldsymbol{X}_3, \boldsymbol{X}_4$ and $\boldsymbol{X}_5$ are the individual unit matrices (reactor, separator, stripper, compressor and materials respectively). The response vector, (500×1) is given by:

$$\mathbf{y} = [\mathbf{v}_{13}] \quad (6.3)$$

where $\mathbf{v}_{13}$ represent the quality variable (composition G).

The results from the application of static PLS are presented in Table 6.7. The first step was to determine the number of latent variables (LVs). Figure 6.3 shows the percentage of variance captured by the individual latent variables. From the scree plot, it appears that 3 latent variables is appropriate with 10.46% of the variation in the response variable **y** being explained by 44.12% of the variation in the predictor block **X** indicating that the PLS model fails to capture the dynamics in the process and does not represent the behaviour of the process. This can be clearly seen in Figures 6.4 and 6.6 which shows the time series plot of the measured and predicted for the calibration and validation data sets. Figures 6.5 and 6.7 show the time series plot of the residuals from static PLS for the calibration and validation data set respectively. From Table 6.7, it can be seen that by increasing the number of latent variables to 6, only an additional 2% of the variability in the Y-block is captured and thus it can be concluded that static PLS is not appropriate in this case. The root mean squared error of the calibration data set, 0.9422, indicates along with Figure 6.4 that the model prediction is not appropriate.

Table 6.7 - Percentage variance captured by the conventional PLS model

Latent Variables	X-block		Y-block	
	LV	Cum	LV	Cum
1	16.13	16.13	8.55	8.55
2	10.95	27.09	1.20	9.75
3	17.03	44.12	0.71	10.46
4	7.10	51.22	0.77	11.23
5	4.79	56.02	0.66	11.89
6	3.37	59.40	0.85	12.74

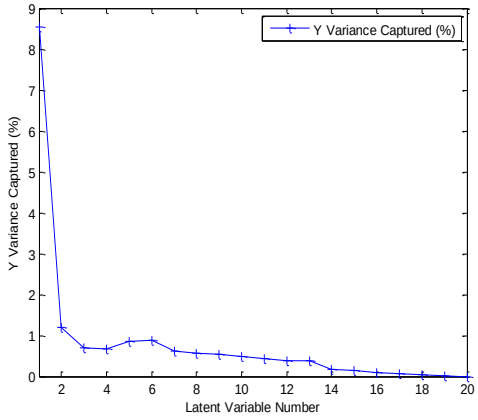

Figure 6.3 - Percent of variance captured by individual LV

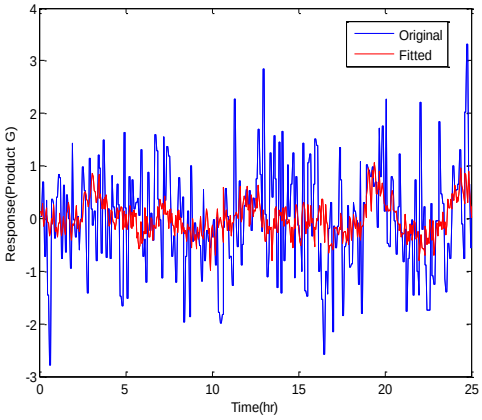

Figure 6.4 - Time series plot of the original and fitted data from static PLS (3 LV) - Calibration data set

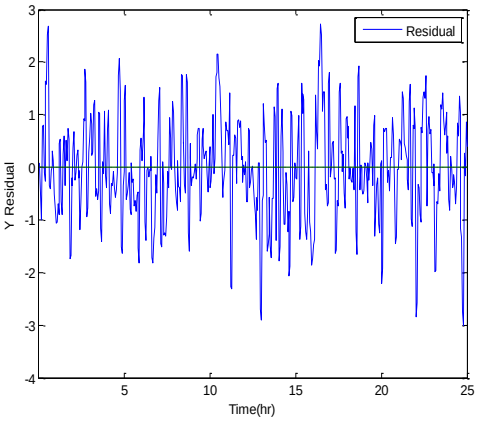

Figure 6.5 - Time series plot of the residuals for static PLS (3 LV) – Calibration data set

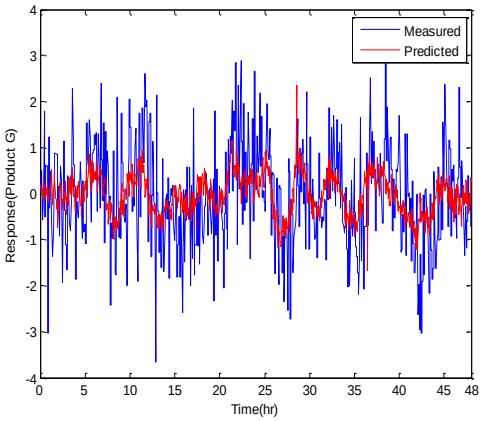

Figure 6.6 - Time series plot of the measured and predicted data from static PLS (3 LV) – Validation data set

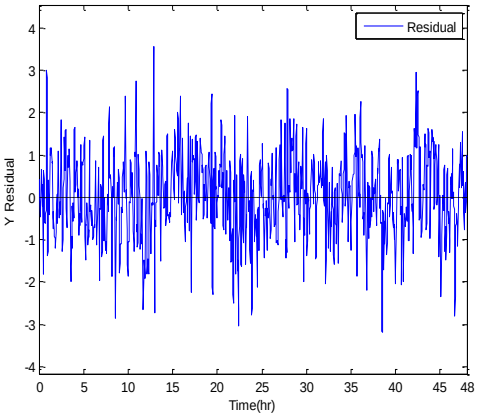

Figure 6.7 - Time series plot of the residuals from static PLS (3 LV) - Validation data set

Zhou et al. (2010) and Yin et al. (2012) mentioned that for the same data sets utilising standard auto-scaling, a PLS model with 6 latent variables was appropriate. Table 6.8 summarizes the model details generated on the basis of these suggestions. It can be seen that a PLS model based on 6 latent variables captures 12.53% of the variation in the Y-block and 42.10 % in the X-block**.** This is 0.21% lower than for a PLS model based on 6 latent variables and block scaling and 2.07 % greater than for a PLS model based on 3 latent variables and block scaling which indicates that the model that had been used was also inappropriate in terms of capturing the process dynamics and predicting the quality variable **y**. The RMSE of the calibration data set (RMSE=0.9425) indicates that the model prediction is not appropriate. Figures 6.8 and 6.9 show the time series plots of the measured and predicted response for the calibration and validation data sets based on a PLS model with 6 latent variables.

Table 6.8 - Percentage variance captured from conventional PLS model

Latent Variables	X-block		Y-block	
	LV	Cum	LV	Cum
1	16.11	16.11	8.72	8.72
2	4.43	20.54	2.27	10.98
3	5.92	26.46	0.48	11.46
4	4.92	31.38	0.35	11.81
5	5.71	37.09	0.30	12.11
6	5.01	42.10	0.42	12.53

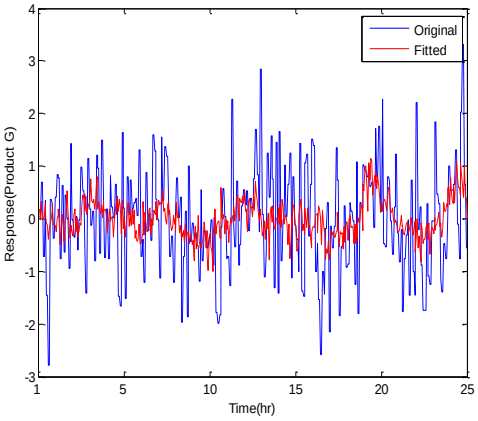

Figure 6.8 - Time series plot of the original and fitted data from static PLS (6 LV) - Calibration data set

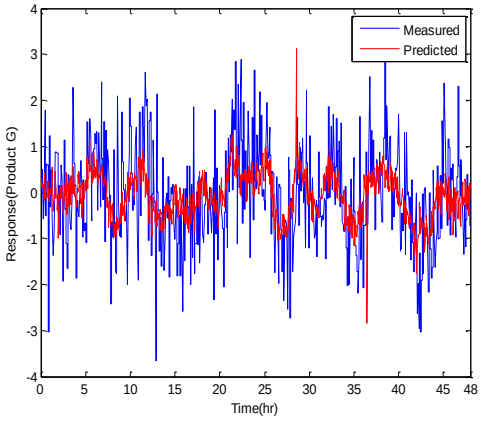

Figure 6.9 - Time series plot of the measured and predicted data from static PLS (6 LV) - Validation data set

The monitoring statistics for the static PLS model with 6 latent variables based on auto-scaled data and static PLS model with 6 latent variables based on block-scaled data set are presented in Appendix D. It was concluded that the monitoring charts following the application of static PLS produced a high false alarm rate which indicates that the static PLS model based on the different scaling methods was inappropriate to model the dynamics of the TEP. The false alarm rate (FAR) shows small differences between the two models (Figure 6.10). The false alarm rate of the individual monitoring charts for the calibration and validation data sets is given in Appendix D. The overall false alarm rate FAR is calculated based on the joint use of the monitoring statistics, Hotelling's T^2 and SPE_X. The overall FAR obtained from Yin et al. (2012) for the calibration data, 10, is very close to the FAR obtained from static PLS based on block-scaling, 9.5. The overall FAR for the validation data set following the application of PLS based on auto-scaling and block-scaling, 47 and 45.7 respectively, was higher than the FAR for calibration data set. This indicates that both models produced high false alarm rates and they are inappropriate to construct monitoring scheme for the TEP.

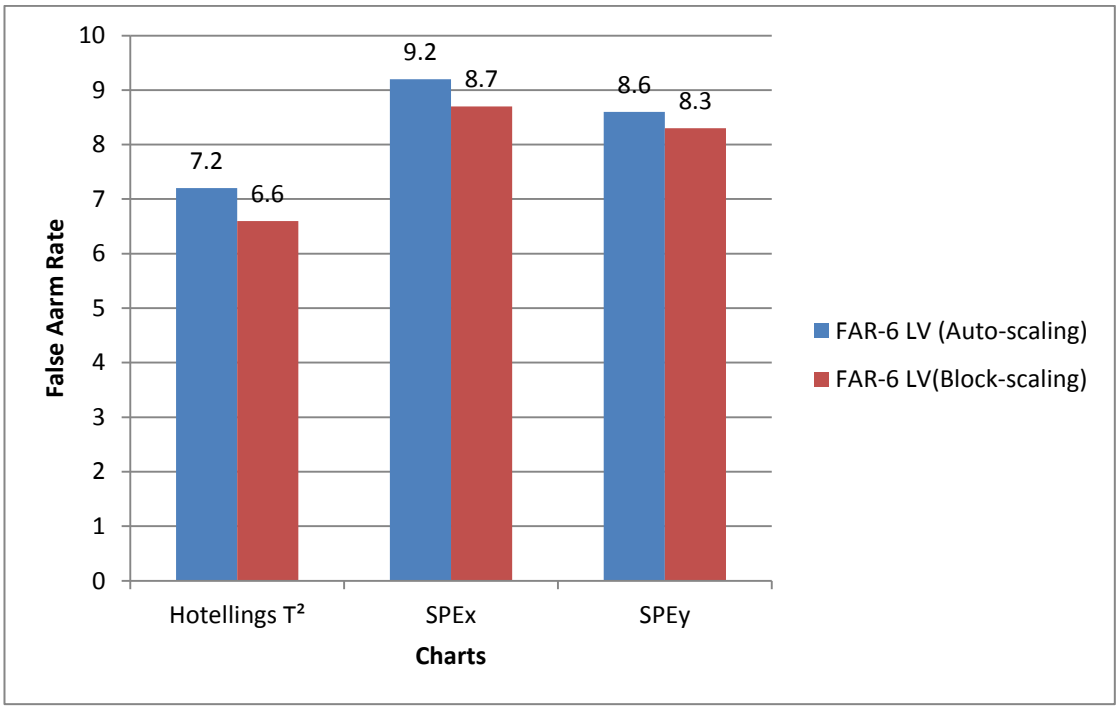

Figure 6.10 - False alarm rate from static PLS models (6 LV) based on auto-scaled and block-scaled data for the calibration data set

From the above discussion, it can be concluded that static parameters and steady state PLS is inappropriate to model the TEP (dynamic process). Consequently, dynamic PLS models are developed in the following section.

6.4.2 Dynamic PLS (DPLS)

The TEP is a dynamic process due to the feedback control system and hence, a dynamic model is required to take into account the process dynamics thereby enhancing the performance of the monitoring statistics (Ku et al., 1995; Kano et al., 2002).

A number of studies have reported the application of dynamic methods to the TEP. For example, Ku et al. (1995) developed a DPCA algorithm to deal with autocorrelation and their approach correctly identified a number of the faults introduced to the TEP. However, PCA does not consider the variation in the quality product variables. Juricek et al. (2001) used the TEP to compare multiple inputs, multiple outputs (MIMO) dynamic models identified using canonical variate analysis (CVA), autorgressive with exogenous input (ARX) and numerical algorithm for state space system identification (N4SID) methods. Their dynamic model included 7 inputs and 10 outputs. They found that the CVA and the state space algorithm give better results compared to the other methods. However, it is beyond the scope of this thesis to investigate dynamic models based on state space methods. Lee et al. (2004) combined system decomposition and dynamic PLS through an autoregressive moving average model for the diagnoses of multiple faults based on samples generated every 1 min. System decomposition is a fault diagnosis method where the process is decomposed based on the local qualitative relationship of each variable. Their diagnosis results for a single fault showed satisfactory accuracy in terms of fault diagnoses compared to the statistical methods used by Chiang et al. (2001) who applied PCA, DPCA and Independent component analysis (ICA) for fault detection and diagnosis. Lennox (2005) applied dynamic PLS, based on an ARX model and a 3 min sampling interval to integrate fault detection and isolation with model predictive control. He demonstrated that through the application of DPLS to the TEP, the diagnostic information relating to the control system can be extracted. Dynamic principal component analysis based on decorrelated residuals (DPCA-DR) has also been applied for fault detection on the TEP (Rato and Reis, 2013).

In this work, dynamic empirical modelling through a Finite Impulse Response (FIR) time series representation is considered. By using a FIR representation, a steady state PLS approach can be used for the modelling and monitoring of the TEP. The reason for

selecting FIR to model the TEP rather than ARX is that the application of multiblock approaches requires the division of the input matrix, into corresponding unit operation. By using ARX, the output variables require being included in the input matrix and it was not deemed to be informative in terms of the behaviour of the unit operations.

Figure 6.11 shows the systematic development of the PLS model using a dynamic representation for modelling and monitoring of TEP. The first step is to identify the model objectives and analyse the properties of the TEP. The goal is to develop a monitoring scheme for the whole process and the individual unit operation. The process exhibits dynamic nonlinear behaviour. Consequently, it is important to take this into account when developing a process model. Based on this, the data should be sampled such that it preserves the significant information in the process and captures the process dynamics. Three data sets are considered in the monitoring of the TEP, calibration data set which is used to develop the monitoring model, the validation data set which is used to ensure that the model captures the process behaviour and finally a test data set which is used for process monitoring and fault detection.

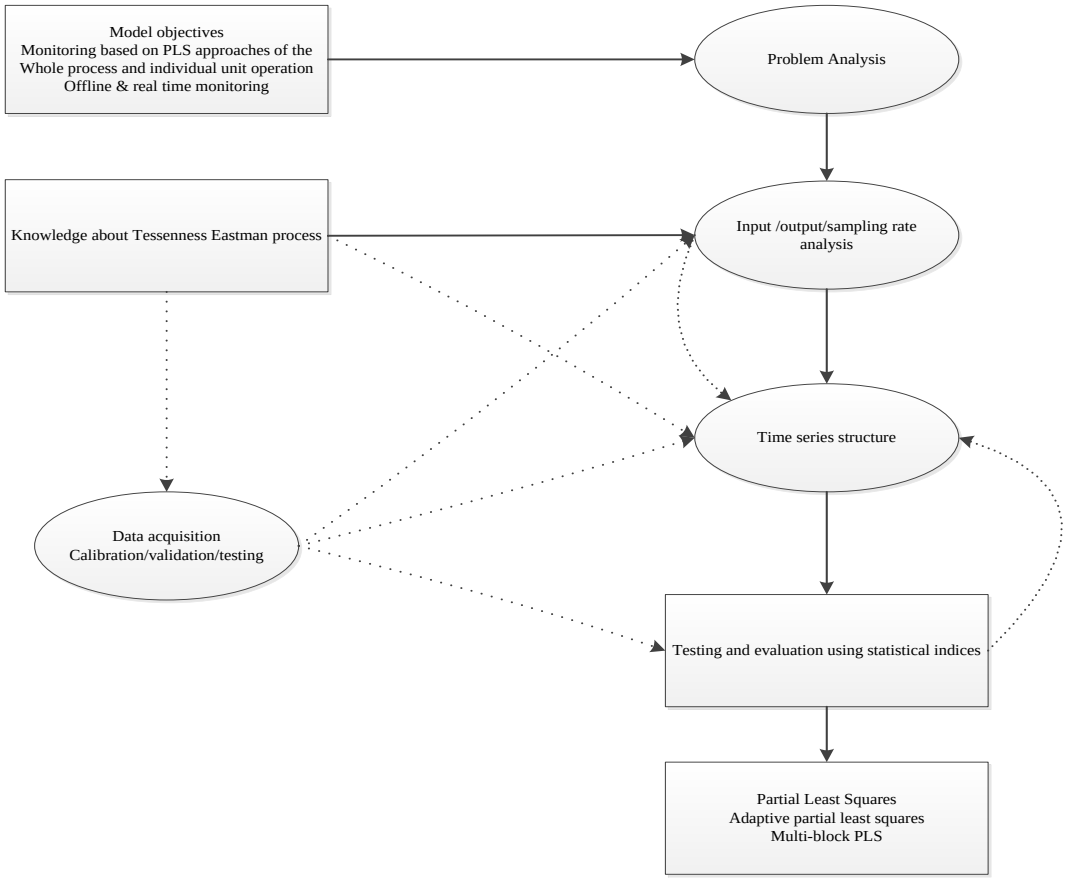

Figure 6.11 - Systematic development of a TEP monitoring scheme.

6.4.2.1 Finite Impulse Response (FIR) model

The use of a finite impulse response model for the modelling of process dynamics has been reviewed by a number of authors (Ricker, 1988; Kaspar and Ray, 1993; Dayal and MacGregor, 1996). A number of methods have been proposed to estimate the FIR coefficients. For example, ordinary least squares (OLS) but it can result in a biased estimation when the process input variables are correlated. This is because the inverse of the matrix $\mathbf{XX}'$ will be singular for correlated input. In 1984, Wold proposed the use of PLS to estimate the FIR model coefficients. Since then it has been applied by many authors to model dynamic systems (Ricker, 1988; Dayal and MacGregor, 1996; Nikolaou and Vuthandam, 1998; Baffi et al., 2000; Box et al., 2008). A FIR model accounts for process dynamics by including lagged input variables into the regressor matrix. The only limitation of the FIR approach is the need for a large number of parameters to be estimated. This can increase the computational complexity and the time required for identifying the model, especially when an adaptive dynamic PLS algorithm is implemented. Selecting the appropriate sampling interval can potentially reduce the number of parameters included in the FIR representation. The TEP data is generated based on a sampling interval of 3 min to allow for more rapid fault detection, identification and diagnosis (Chiang et al., 2001). On the other hand, from a system identification prospective (Ljung, 1999), one should sample according to:

$$\frac{1}{10}(\tau) \leq \Delta t < \frac{1}{5}(\tau) \tag{6.4}$$

where Δt is the sampling period and τ is the process time constant. In the TEP, the estimated time constant under closed loop control was approximately two hours (Chiang et al., 2001). According to this the sampling interval would be the order of:

$$12 \leq \Delta t < 24 \text{ min} \tag{6.5}$$

The FIR approach requires approximately $3(\tau)$ of history to capture the process dynamics. Therefore, the appropriate number of lags for the FIR model needs to be identified. A general overview of FIR modelling is presented below followed by a study to identify the appropriate number of lags based on different sampling intervals. The goal is to find the FIR representation that can take into account the dynamics in the

system with the smallest number of coefficients to simplify the implementation of the adaptive and multi-block PLS approaches.

The FIR representation is given by:

$$\mathbf{y}(t) = \sum_{j=1}^{n_u} \mathbf{B}_j \mathbf{u}(t-j) + \mathbf{e}(t) \tag{6.6}$$

where $\mathbf{u}(t)$ is the process input data vector, n_u is the number of time lags for the input data vectors; $\mathbf{e}(t)$ is the noise vector at the current time point t and the $\mathbf{B}_j$ is the coefficient matrix. Steady state PLS can be used to model the dynamic process. From Qin (1993), the regressor vector which consists of lagged input values can be expressed as follows:

$$\mathbf{x}(t) = [\mathbf{u}(t-1), \mathbf{u}(t-2), \dots\dots, \mathbf{u}(t-n_u)] \tag{6.7}$$

Equation 6.6 can be presented in a simplified form as:

$$\mathbf{y}(t) = \mathbf{C}.\mathbf{x}(t) + \mathbf{e}(t) \tag{6.8}$$

where $\mathbf{C}$ is defined as :

$$\mathbf{C} = [\mathbf{B}_1, \mathbf{B}_2, \dots, \mathbf{B}_{n_u}] \tag{6.9}$$

From Equations 6.7 and 6.8, the vectors $\mathbf{x}(t)$, $\mathbf{y}(t)$ and $\mathbf{e}(t)$ can be arranged in matrix form:

$$\mathbf{X} = \begin{bmatrix} \mathbf{x}(1) \\ \mathbf{x}(2) \\ : \\ : \\ \mathbf{x}(t) \end{bmatrix}, \mathbf{Y} = \begin{bmatrix} \mathbf{y}(1) \\ \mathbf{y}(2) \\ : \\ : \\ \mathbf{y}(t) \end{bmatrix}, \mathbf{E} = \begin{bmatrix} \mathbf{e}(1) \\ \mathbf{e}(2) \\ : \\ : \\ \mathbf{e}(t) \end{bmatrix} \tag{6.10}$$

Consequently, Equation 6.6 is re-written as following:

$$\mathbf{Y} = \mathbf{X} \,.\, \mathbf{C} + \mathbf{E} \tag{6.11}$$

The values of $\mathbf{C}$ are determined using PLS regression. For the TEP, the regressor matrix without lagged variables is given in Equation 6.2. The graphical representation of the steady state PLS matrices and the DPLS based on a FIR representation (3 lags is used as an example) is shown in Figure 6.12 and Figure 6.13, respectively.

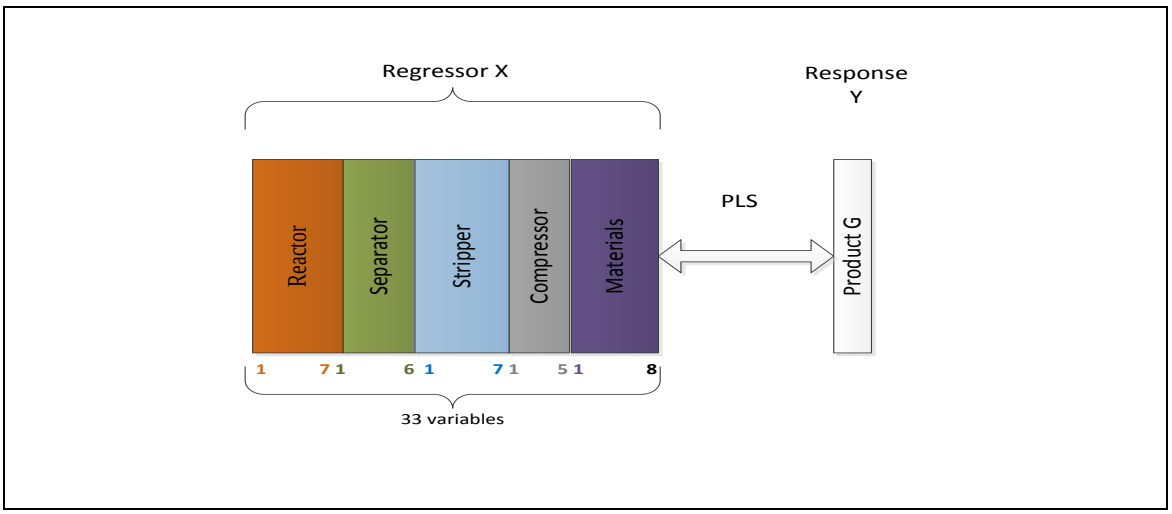

Figure 6.12 - Graphical representation of the input and output matrices for PLS

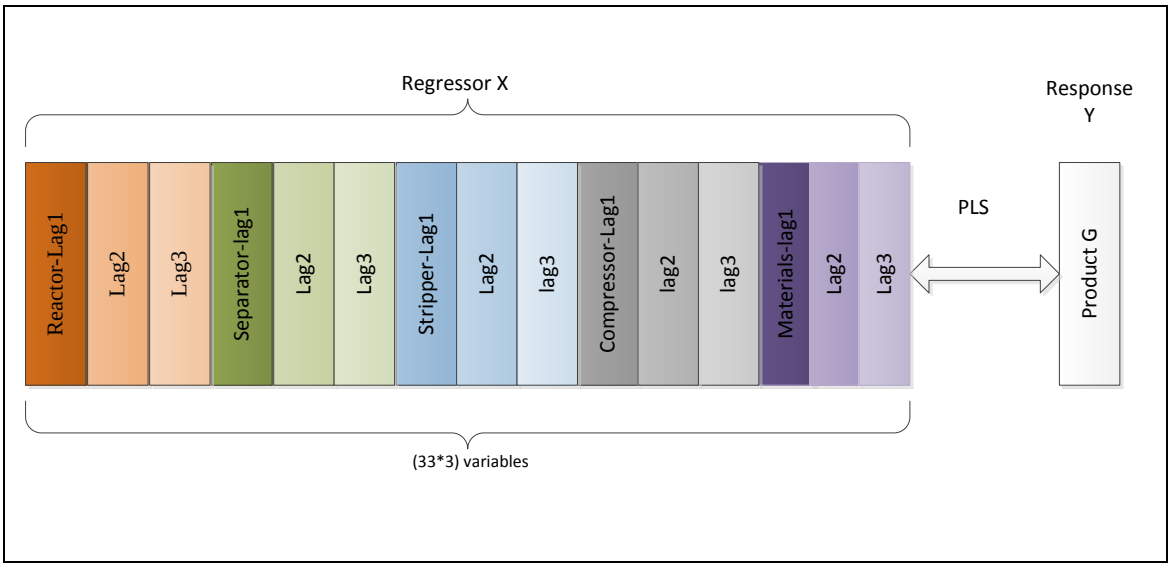

Figure 6.13 - Graphical representation of the input and output matrices for DPLS using FIR representation with 3 lags as an example

It is important to select the regressor matrix appropriately since by including additional lags in the regressor matrix the robustness of the model could be compromised. This occurs because the extra lags will increase the dimensionality of the matrix and noise may be being captured by the model (Chiang et al., 2001). On the other hand, it is known that FIR requires a large number of lags to capture the process dynamics, i.e. a history of 3(τ). According to this, the FIR representation requires approximately 6 hours of data to capture the dynamics in the TEP and hence the impact of including additional lags in the FIR model was also investigated.

Table 6.9 summarizes the maximum number of lags and number of FIR coefficients corresponding to different sampling intervals. For example if the sampling interval was

selected at 3 min, the maximum number of lags required to capture the dynamics in the TEP is of the order of 120 lags with 3960 coefficients (based on a 6 hour time history). This essentially increases the computational complexity of implementing the adaptive and multiblock approaches and is time consuming.

Table 6.9 - Number of FIR coefficient for different sampling intervals

Sampling interval	maximum number of lags (for 6 hour time history)	Corresponding number of coefficients in FIR
3	120	3960
12	30	990
18	20	660
24	15	495

In this study, the root mean squared error (RMSE) is used to evaluate the goodness of fit of the model. One approach to identifying the appropriate model is through an exhaustive search of all models. This requires significant computational time and effort. On the other hand, an experimental design approach could be applied to test the significance of increasing the number of lags and help to select the model structure. However, the use of data generated by Chiang et al. (2001), where only one data set is generated for calibration that represents normal operating conditions resultants in the application of an exhaustive search approach.

For the identification of an appropriate model, the sampling intervals considered were 3 min, 12 min, 18 min and 24 min based on Equations 6.4 and 6.5. The number of lags, n_u, considered were 1, 2 ,4 and 6 lags. The model was calculated based on the training data generated under normal operating conditions. The most important factor that needs to be considered is whether by sampling at a lower rate, the model can capture the important information contained in the process signals based on Equation 6.4. In addition, the number of FIR coefficients needs to be kept to a minimum to simplify the implementation of the adaptive and multiblock approaches.

Table 6.10 summarises the effect of sampling intervals and number of lags on the development of the PLS model. The selection of the most appropriate model was made based on two criteria, the RMSE of the calibration and the variance captured in the Y-block by the model. From the different combinations considered, the best model from

each sampling interval category was selected and then compared with other intervals. From Figures 6.14 to 6.17 and Table 6.10, it can be seen that the calibration model based on an 18 min and 24 min sampling interval gives the best level of variance captured as well as RMSE of calibration. The sampling interval of 18 min with 6 lags was selected for 3 reasons; (1) although the model built based on 24 min gives more accurate predictions and captures more variation in the Y-block, according to Equation 6.5, from a system identification prospective, the sampling interval should be less than 24 min. (2) The difference in RMSE of the models for both sampling intervals is minimal (3) It is known that the system measurements include Gaussian noise, hence incorporating more lags allows for the noise to contribute to the model (Chiang et al., 2001).

Table 6.10 – The impact of sampling interval and number of lags on DPLS model

Num	Sampling interval	Num of lags	RMSE -Calibration	Variance captured
1	3	0	0.9422	10.46
2	3	1	0.9250	11.90
3	3	2	0.8636	25.8021
4	3	4	0.8083	34.9972
5	3	6	0.5875	39.9065
6	12	0	0.8574	32.6302
7	12	1	0.8053	36.3717
8	12	2	0.7349	47.0142
9	12	4	0.6113	63.3365
10	12	6	0.5399	71.3499
11	18	0	0.7384	43.7319
12	18	1	0.6812	44.3853
13	18	2	0.6217	62.9014
14	18	4	0.4269	82.5087
15	18	6	0.2821	91.4618
16	24	0	0.6936	54.2931
17	24	1	0.6715	56.3781
18	24	2	0.4764	78.0396
19	24	4	0.3826	92.2723
20	24	6	0.2713	97.2255

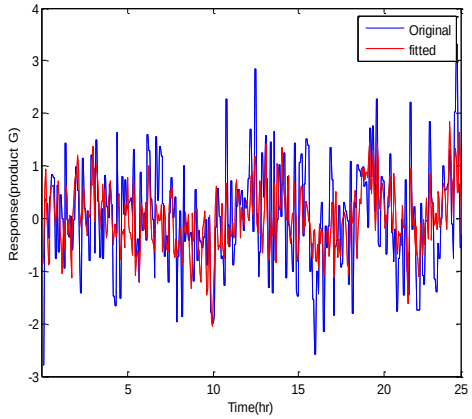

Figure 6.14 - Original and fitted response based on 3 min sampling interval - 6 lags

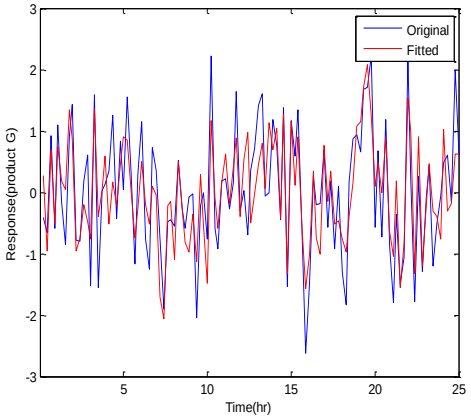

Figure 6.15 - Original and fitted response based on 12 min sampling interval - 6 lags

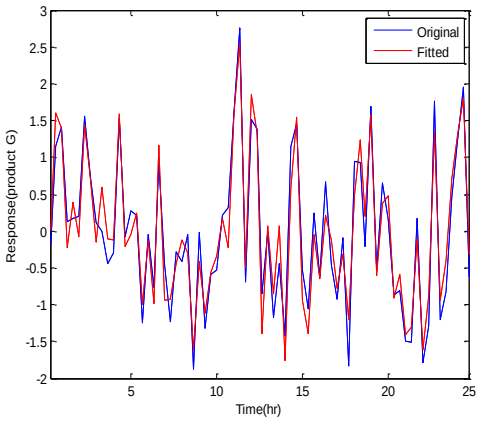

Figure 6.16 - Original and fitted response based on 18 min sampling interval - 6 lags

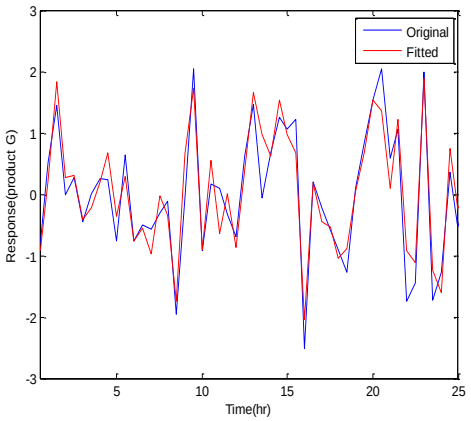

Figure 6.17 - Original and fitted response based on 24 min sampling interval - 6 lags

6.4.2.2 Dynamic PLS Model

From the previous section the PLS model based on an 18 min sampling interval and a 1.8 hr time history was selected. The total number of coefficients is 198. Figure 6.18 shows the variance captured by the individual latent variable and from this 5 latent variables were selected for the DPLS model giving a RMSE = 0.2821 for the calibration data set. Table 6.11 shows that five latent variables correspond to 28.7 % of the total variance explained in the **X**-block which is related to 91.43 % of the variance explained in the **Y**-block.

Table 6.11 - Percentage variance captured by the dynamic PLS model

Latent Variables	**X**-Block		**Y**-block	
	LV	Cum	LV	Cum
1	11.18	11.18	34.36	34.36
2	4.85	16.03	32.61	66.97
3	6.53	22.56	11.10	78.07
4	2.68	25.24	9.03	87.10
5	3.46	28.70	4.36	91.46

Figure 6.19 and Figure 6.20 are the time series plots of the original and fitted response and the residuals respectively. It can be seen that the model fits the data from the residual values, which are randomly scattered around zero. The results from applying the DPLS model to the validation data set are presented in Figures 6.21 and 6.22. It can be seen that the model approximately follows the trend of the validation data set. However, the magnitude of the residuals has increased from a range of ± 0.6 to ± 3 and these are more significant due to the dynamic and non-linear characteristics of the TEP. Hence, the information in the calibration data set was insufficient to describe the dynamic and non-linear information in the validation data set. The RMSE = 1.3015 for the validation data set and shows a significant increase compared to the RMSE of the calibration data set. This is potential due to the fact the process dynamics differ to these in the calibration data set hence a more advance approach for the modelling of the dynamic behaviour is required.

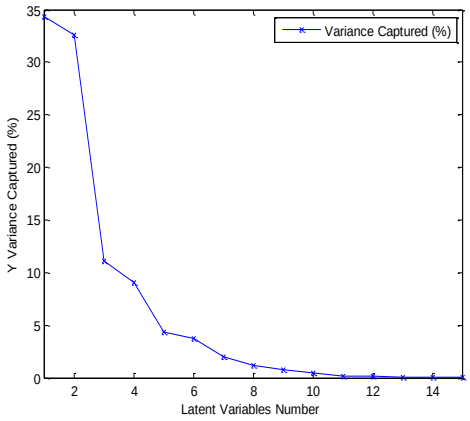

Figure 6.18 – Variance captured by latent variables

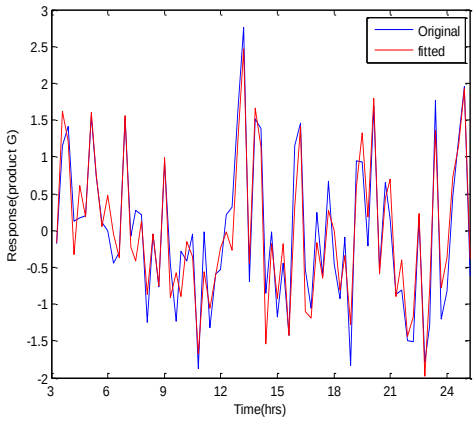

Figure 6.19 - Time series plot of the original and fitted data from DPLS - Calibration data set

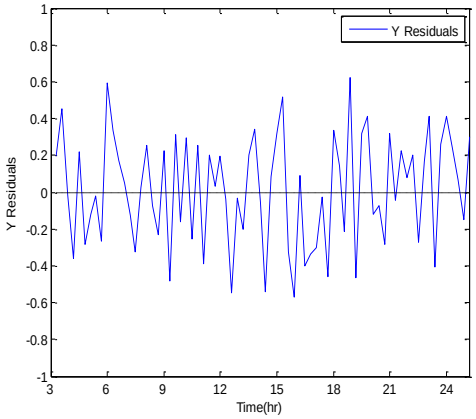

Figure 6.20 - Time series plot of the residuals from DPLS for the calibration data set

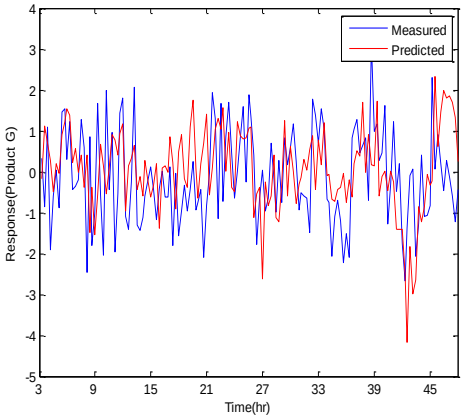

Figure 6.21- Time series plot of the original and fitted data from DPLS - Validation data set

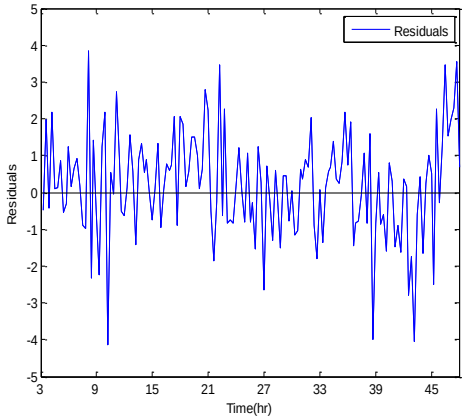

Figure 6.22 - Time series plot of the residuals from DPLS – Validation data set

6.4.2.3 Multiblock Dynamic PLS Model

In this study, multiblock PLS ($MBPLS_T$) was extended to multiblock dynamic PLS ($MBDPLS_T$) to allow for the monitoring of the individual unit operations of the process using a dynamic representation. An introduction to multiblock PLS ($MBPLS_T$) was presented in Chapter 3. As described in Chapter 3 conventional PLS can be used to calculate the parameters of $MBPLS_T$ and information about the individual unit operation of the process as well as the overall process can be attained (Westerhuis and Smilde, 2001). As no constrains are imposed on the number of input variables used in this relationship, any number of input variable can be used to form the multiblock analysis. For the TEP, a dynamic reference model was developed based on the FIR representation, DPLS model, in §6.4.2.2. This model can be extended to develop a

multiblock dynamic PLS model, MBDPLS$_T$ and for that the regressor matrix **X** which contains the lagged variables can be divided to multiple blocks *B* according to:

$$\mathbf{X} = [\boldsymbol{X}_1, \boldsymbol{X}_2, \dots \boldsymbol{X}_b \dots \dots \boldsymbol{X}_B] \quad (6.12)$$

where $\boldsymbol{X}_b, b = 1,2, \dots B$, contains the lagged variables for each block and each block comprises m_b variables. **y** is the response vector.

For the TEP, there are 5 blocks, B =5, and these were defined in Table 6.6. Each block contains 6 lags of the original variables as discussed in §6.4.2.1. The total number of variables is thus 198. The parameters of the multiblock dynamic PLS model, i.e. loadings, scores, weights, super scores and super weights, can be calculated in similar manner to the MBPLS$_T$ (§ 3.8.1). The monitoring statistics and the confidence limits for the whole process and the individual unit operations are calculated in a similar manner to those of PLS and MBPLS$_T$ with the only difference being that the lagged matrices are used to construct the individual block model.

An alternative to multiblock dynamic PLS (MBDPLS) proposed by Tessier et al. (2012) who used the idea of multiblock dynamic PLS for the monitoring of the performance of aluminium reduction cells based on a multiple input, multiple output system. However, in their approach they did not use a time series structure such as FIR or ARX instead they used their knowledge about the process to identify the number of lags to include into the regressor matrix, more specifically they ran the experiment until a process disturbance was observed, which usually occurs within 3 months for the aluminium reduction cells, and then included all the experimental results prior to fault occurrence into regressor matrix. In addition for some blocks, average values over a period of time were used instead of time lagged variables. Their approach to identifying the dynamic structure is only applicable to their experimental study.

6.4.2.4 Monitoring Based on DPLS and MBDPLS$_T$

Similar to conventional PLS, monitoring based DPLS approaches utilises the univariate statistics of Hotelling's T^2 and the squared prediction error of the input and output spaces, SPE$_X$ and SPE$_Y$ respectively. In addition, the monitoring statistics for multiblock dynamic PLS (MBDPLS$_T$) are calculated as for MBPLS$_T$. The calculation of these statistics and their corresponding confidence limits were discussed in Chapter 3

(§3.8.1). Through the use of the monitoring statistics from DPLS in conjunction with the monitoring statistics from $MBDPLS_T$, the performance of both the overall process and the individual units can be monitored.

The monitoring results from the application of DPLS and $MBDPLS_T$ for the TEP under normal operating conditions for the calibration data are presented in Figures 6.23 to 6.25. The Hotelling's T^2 and SPE_X statistics for the overall process (sub-plot 1) and the individual blocks (sub-plot 2 to 6) are presented in Figures 6.23 and 6.24 respectively and the SPE_Y for the response variable is given in Figure 6.25. The 95% and 99% confidence limits were calculated based on the calibration data set. It can be seen that a few out of statistical control signals were detected in all the sub-figures. However, they did not exceed 1% and 5% of the total number of samples for the 99% and 95% confidence limits respectively which is statistically accepted since they are expected to violate the limits by chance.

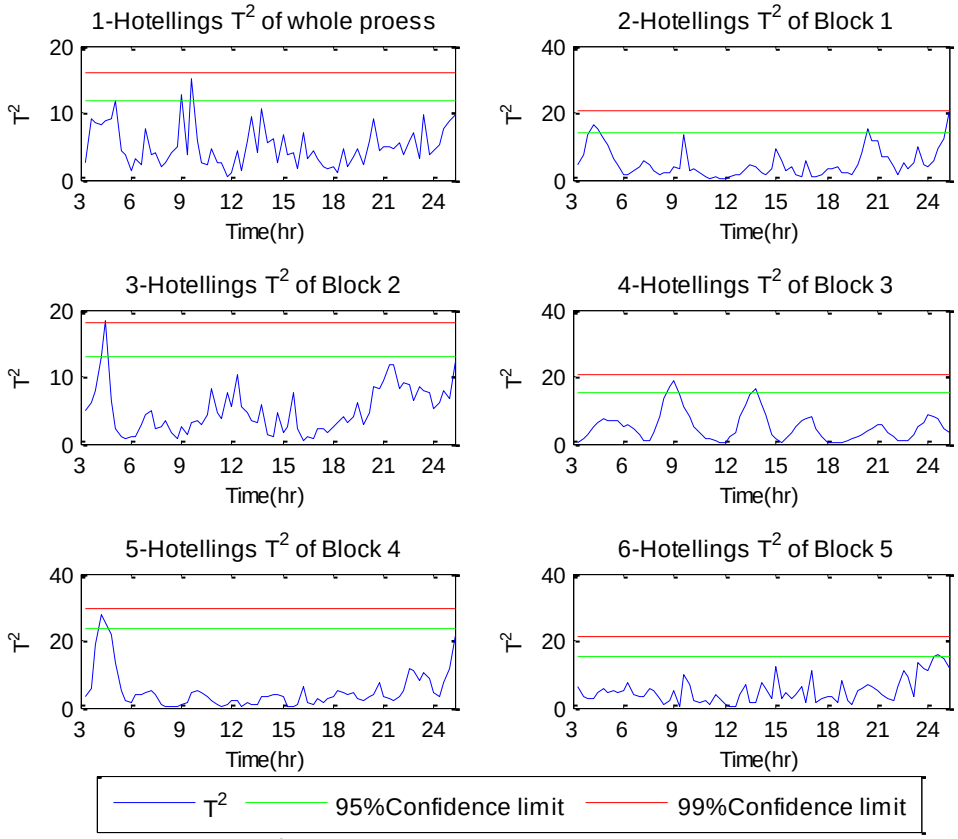

Figure 6.23 - Hotelling's T^2 for (1) overall process and (2-6) individual blocks based on DPLS and $MBDPLS_T$ approaches – Calibration data set

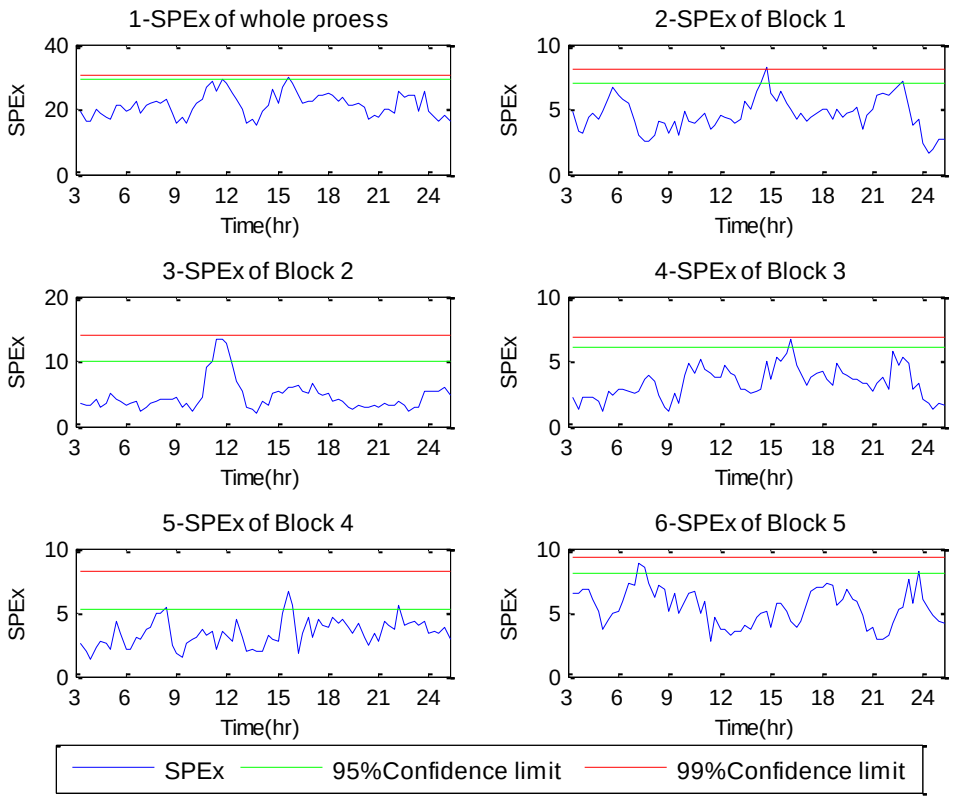

Figure 6.24 - SPE_X for (1) overall process and (2-6) individual blocks based on DPLS and $MBDPLS_T$ approached – Calibration data set

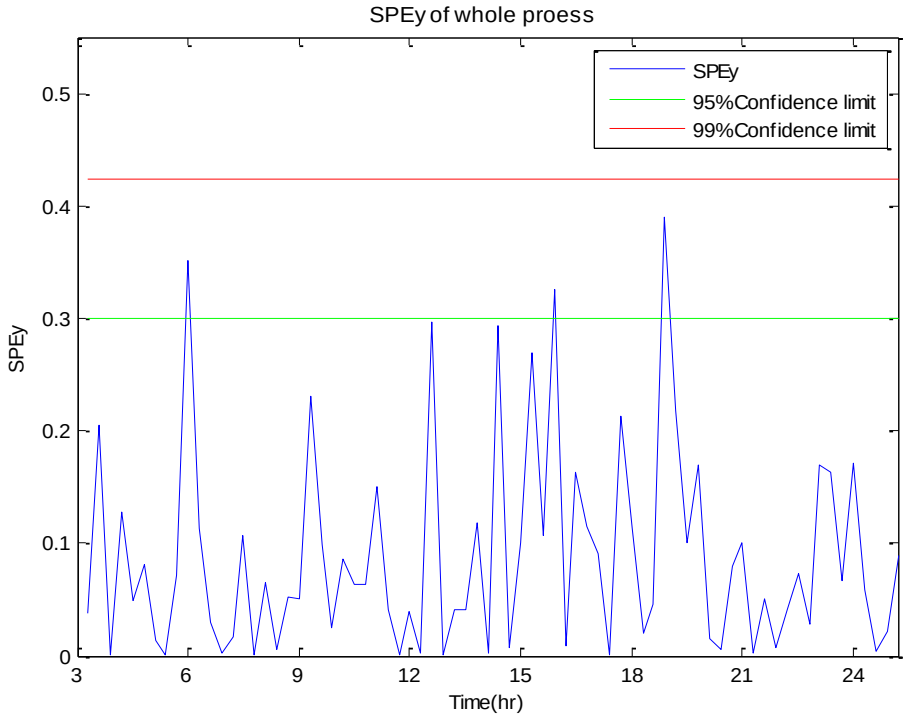

Figure 6.25 –SPE_Y based on DPLS approach - Calibration data set

The false alarm rate (FAR) defined in Chapter 3 (Equation 3.16) was calculated for the monitoring charts for the whole process and the individual chart based on DPLS and $MBDPLS_T$. Table 6.12 summarises the results from the monitoring charts of the calibration data set, where a number of samples are expected to violate the confidence limits by chance. It can be seen that these percentage are within the acceptable range, 5% and 1%, for the 95% and 99% confidence limits respectively. The overall FAR is calculated based on the joint use of the monitoring statistics of the whole process, Hotelling's T^2 and SPE_X. It was 8.10 which is better than the FAR = 9.5 provided by static PLS based on block-scaled data (§6.4.1). In addition the FAR for Hotelling's T^2, SPE_X and SPE_Y are 4.05%, 2.70% and 4.05% respectively is decreased compared to the same rate by static PLS model given in Appendix D.

Table 6.12 - False alarm rate for the monitoring charts for the calibration data set

Part	Chart	FAR 95%	FAR 99%
whole process	Hotelling's T^2	5.40%	0
	SPE_X	2.70%	1.35%
	SPE_Y	4.05%	0
Block 1 Reactor	Hotelling's T^2	5.40%	0
	SPE_X	4.05%	1.35%
Block 2 Separator	Hotelling's T^2	4.05%	0
	SPE_X	4.05%	0
Block 3 Stripper	Hotelling's T^2	4.05%	0
	SPE_X	2.70%	1.35%
Block 4 Compressor	Hotelling's T^2	4.05%	0
	SPE_X	5.40%	0
Block 5 Materials	Hotelling's T^2	4.05%	0
	SPE_X	4.05%	0

The dynamic PLS model developed in §6.4.2.2 was applied to a validation data set corresponding to 48 hr of nominal operation. Figures 6.26, 6.27 and 6.28 present the results of Hotelling's T^2 and the squared prediction error of the input and output spaces SPE_X and SPE_Y for the overall process (sub-figure 1) and the individual unit operation (sub-figures 2 to 6). It can be seen that the metrics violate the confidence limits for a large number of samples for the 95% and 99% confidence limits respectively. The

quantification of these violations is presented in Table 6.13 for the whole process and the individual unit operations respectively. It can be seen the FAR for the monitoring metrics is unsatisfactory since they exceeded the 1% and 5% for the 95% and 99% confidence limits respectively. Although the overall FAR = 24.66% based on the DPLS is an improvement compared to the FAR = 45.7% from static PLS (Appendix D), however, it is still high. The high FAR produced when the model is applied to the validation data set, which represents nominal behaviour, indicates that the dynamics of the calibration data set do not adequately explain the dynamics in the validation data set. In addition, the false alarm rate for the individual unit operations is also high as it is more than 30% for some units including materials and compressor blocks. Moreover, the FAR for the reactor, separator and stripper is more than 10% for the 95% confidence limit. This indicates that the monitoring charts based on $MBDPLS_T$ are unsatisfactory. Therefore, the TEP requires a more advanced method to account for the dynamics and non-linear characteristics.

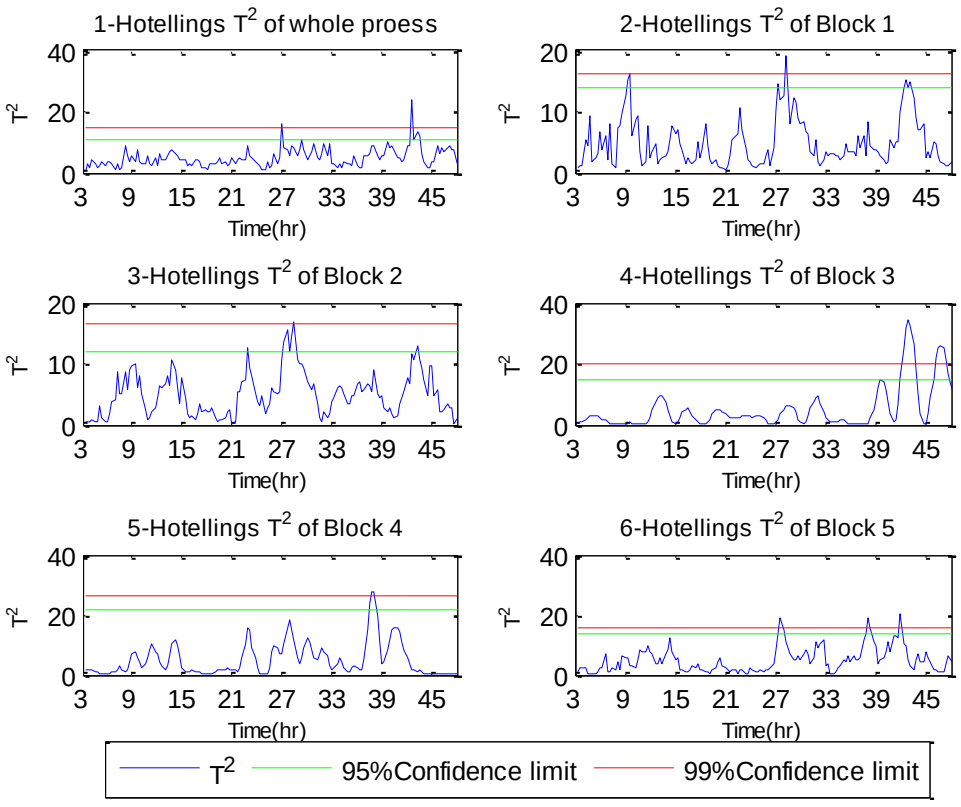

Figure 6.26 – Hotelling's T^2 for (1) overall process and (2-6) individual blocks based on DPLS and $MBDPLS_T$ approaches - Validation data set

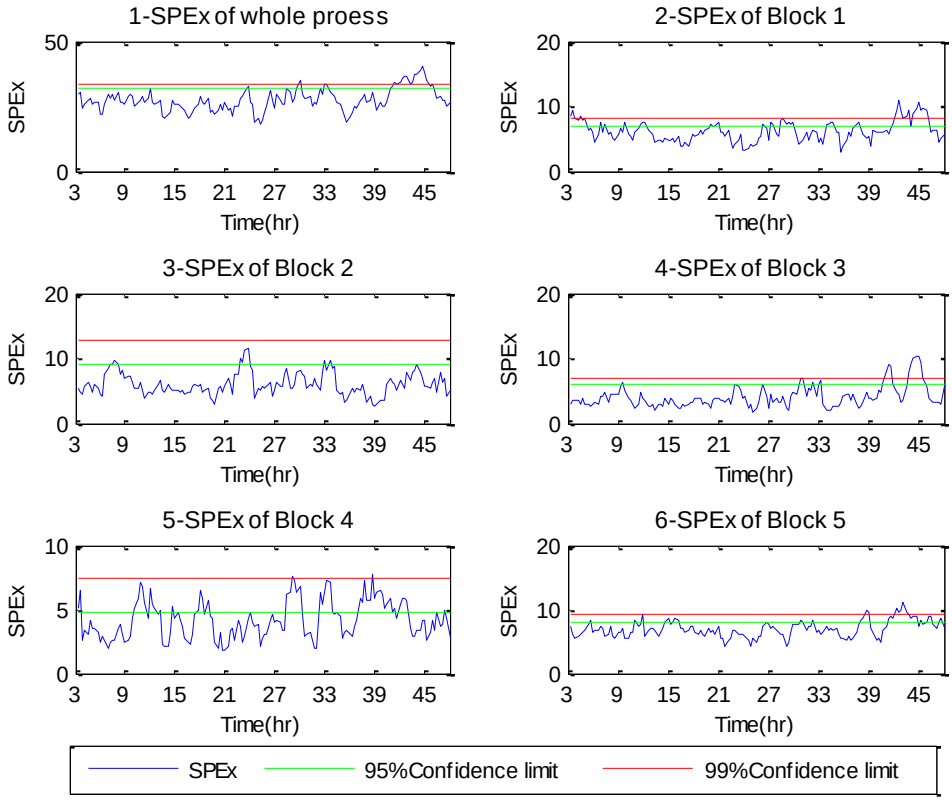

Figure 6.27 – SPE_X for (1) overall process and (2-6) individual blocks based on $MBDPLS_T$ approach - Validation data set

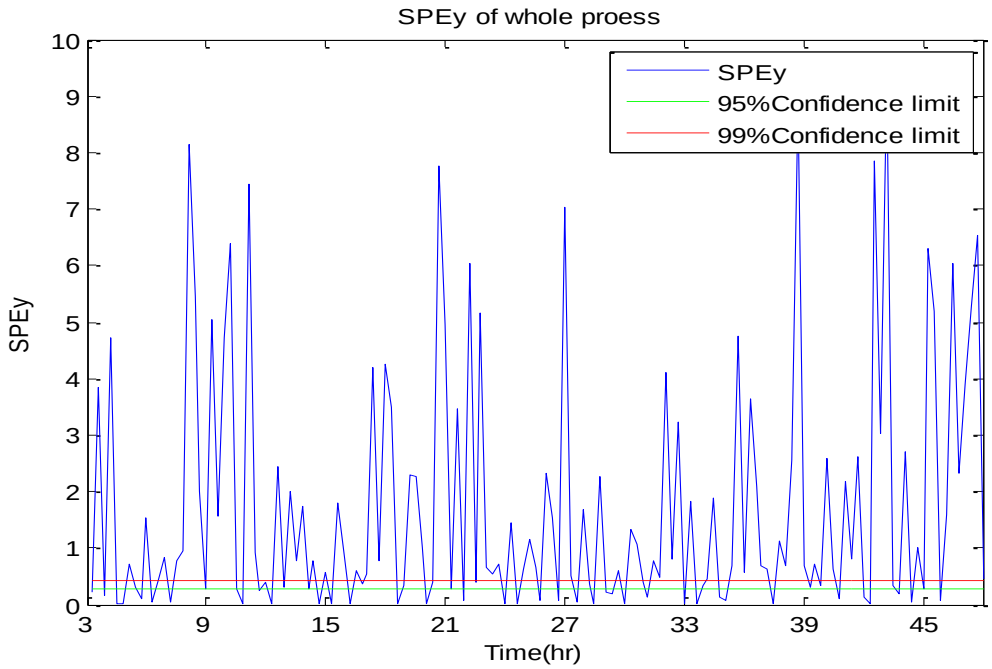

Figure 6.28 – SPE_Y based on DPLS and $MBDPLS_T$ approaches - Validation data set

Table 6.13 - False alarm rate for the monitoring charts for the Validation data set.

Part	Chart	FAR 95%	FAR 99%
whole process	Hotelling's T^2	5.34%	2.66%
	SPE_X	20.66%	8.66%
	SPE_Y	74%	62.66%
Block 1 Reactor	Hotelling's T^2	5.34%	2%
	SPE_X	30.66%	24%
Block 2 Separator	Hotelling's T^2	5.34%	0.66%
	SPE_X	11.48%	0.66%
Block 3 Stripper	Hotelling's T^2	10.6%	6.66%
	SPE_X	17.33 %	8%
Block 4 Compressor	Hotelling's T^2	4.66%	1.33%
	SPE_X	32%	1.33%
Block 5 Materials	Hotelling's T^2	6.66%	4%
	SPE_X	37.33%	20%

6.4.3 Adaptive Multiblock Dynamic PLS

Although dynamic PLS (DPLS) has the ability to predict the response variable (Product G), unsatisfactory performance is observed in terms of the monitoring metrics for both the whole process and the individual unit operations. The strong dynamics of the TEP requires a more advanced modelling method that accommodates the changes in the process dynamics and non-linear characteristics. The next step was to use the recursive PLS with adaptive confidence limits (APLS) as proposed in Chapter 4.

Two modifications were introduced to the APLS algorithm. Firstly, the reference model for APLS is developed based on a dynamic representation to account for the process dynamics, i.e. the reference DPLS model developed in §6.4.2 is used as the reference model. Secondly, once an observation becomes available, it has to be arranged according to the FIR dynamic structure identified in §6.4.2.1, i.e. the sample input vector should include 6 past values of the input variables. In addition the sample is scaled based on block scaling, that is each variable is scaled to have zero mean and variance $\frac{1}{m_b}$. The block scaling is used because the algorithm will be integrated in the next section into a multiblock version. In the case of other processes which only consist

of one unit operation, an appropriate scaling method should be selected and applied. Then, the monitoring statistics and the adaptive confidence limits are calculated prior to model updating according to §4.3.2. The model is then updated recursively in a sample wise manner and hence adaptive dynamic PLS (ADPLS) was developed within this thesis. The new ADPLS algorithm overcomes the DPLS model deficiency and accommodates the dynamic change in the TEP. It is presented in Figure 6.29.

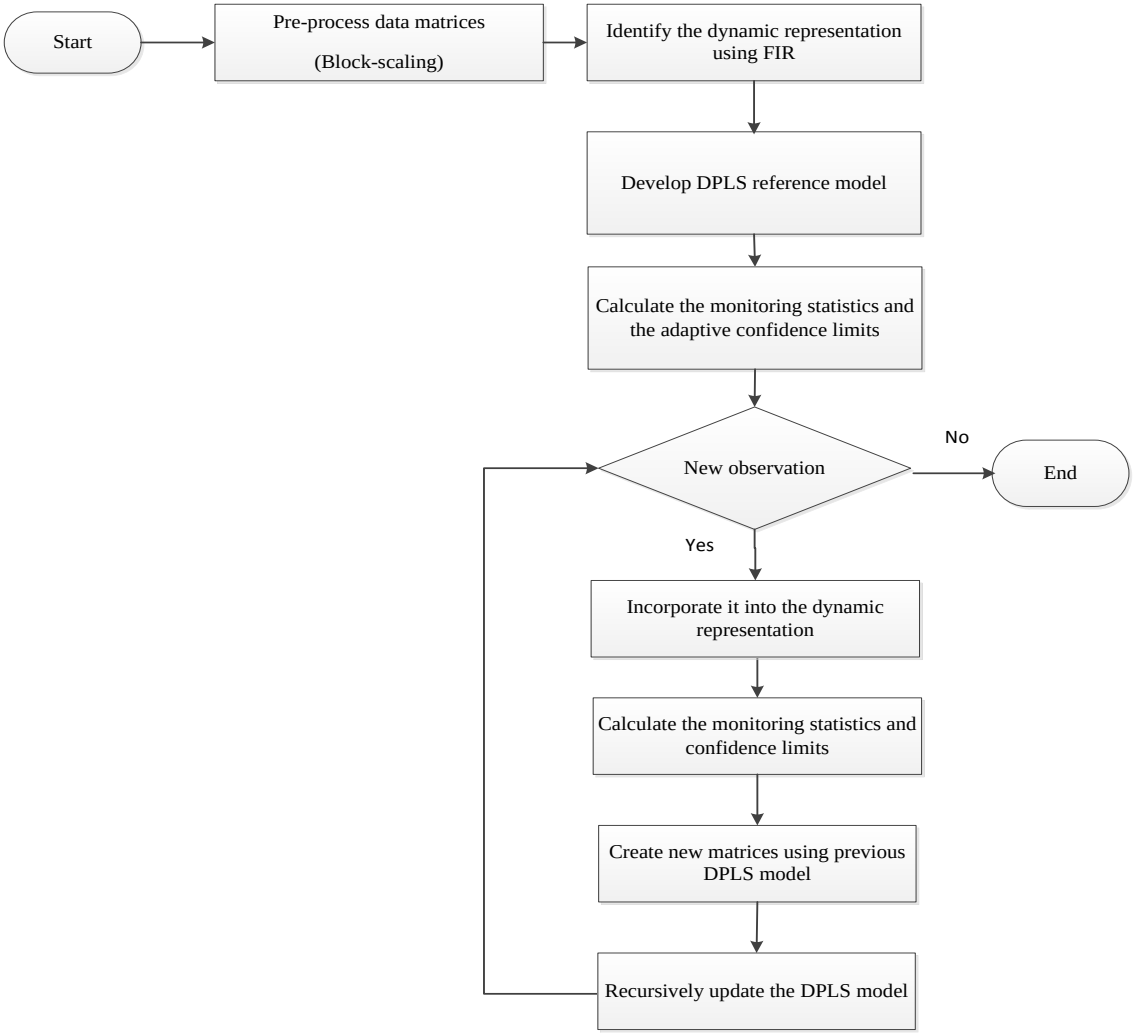

Figure 6.29 – The adaptive dynamic PLS algorithm (ADPLS)

From this, the relationship between DPLS and MBDPLS$_T$ was implemented in a recursive manner. A flow diagram of the algorithm is presented in Figure 6.30. The block parameters are calculated in a recursive manner as follows:

1. Calculate the reference model according to §6.4.2

$$\{\boldsymbol{X}_1, \boldsymbol{X}_2, \dots \boldsymbol{X}_b \dots \dots \boldsymbol{X}_B, \mathbf{y}\} \xrightarrow{\text{MBDPLS}_T} \{\boldsymbol{W}_b, \boldsymbol{W}_T, \boldsymbol{T}_b, \boldsymbol{T}_T, \boldsymbol{Q}, \boldsymbol{U}, \boldsymbol{P}_b\}$$

2. Calculate the block parameters using the relationship between DPLS and $MBDPLS_T$ (§6.4.2.3).
3. Once a new observation $\{\mathbf{x}_{new}, \mathbf{y}_{new}\}$ becomes available, it should be incorporated into the dynamic representation according to §6.4.2.1, i.e. 6 past values of the input variables should be included.
4. The monitoring statistics and the adaptive confidence limits are calculated according to §4.3.1 and §4.3.2 respectively.
5. Create the recursive matrices for model updating:

$$\mathbf{Xrec} = \begin{bmatrix} \mathbf{P}' \\ \mathbf{x}_{new} \end{bmatrix}, \mathbf{Yrec} = \begin{bmatrix} \mathbf{BQ}' \\ \mathbf{y}_{new} \end{bmatrix} \quad (6.21)$$

   where **B** is the inner regression coefficients **Q** and **P** are the weight and loadings from the previous DPLS model
6. Update the PLS model, the recursive matrices and return to step 2 for the calculation of the blocks parameters.

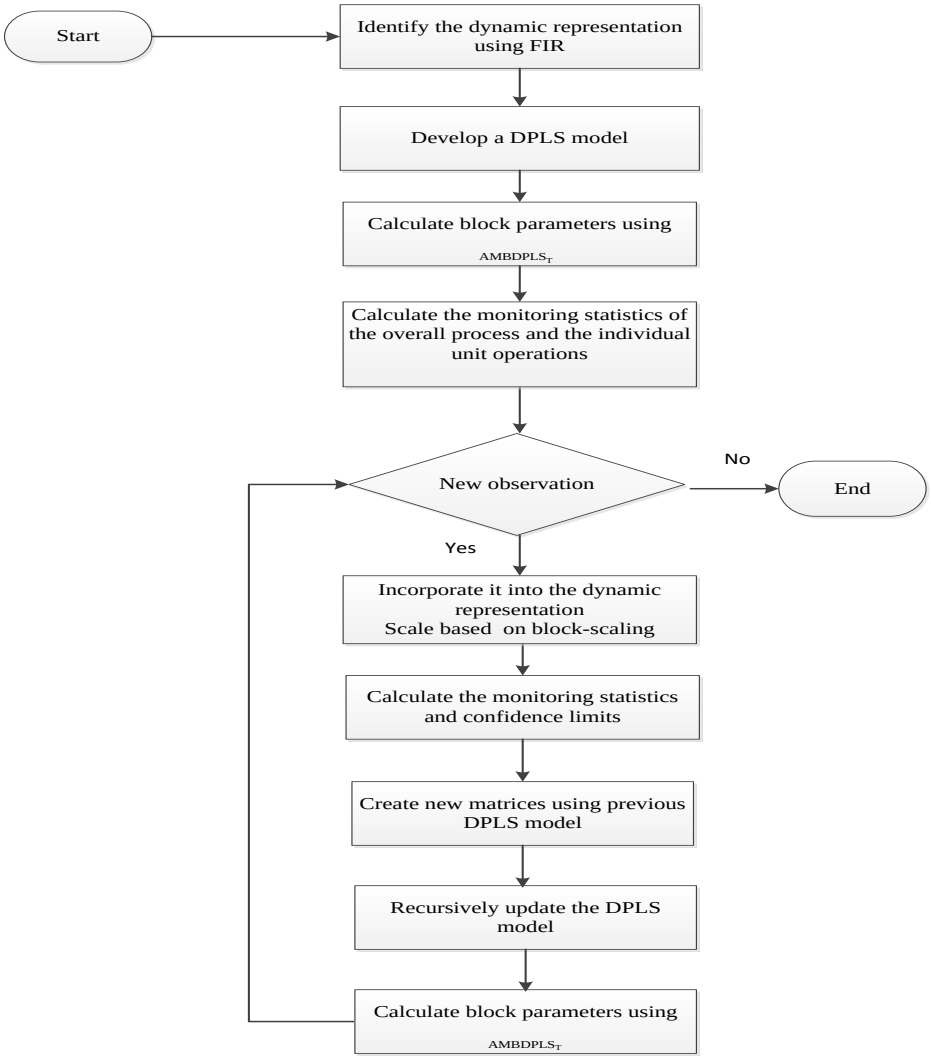

Figure 6.30 – The adaptive multiblock dynamic PLS algorithm

The results from the application of ADPLS to the validation data set show that the RMSE of the validation data set (RMSE = 1.2754) has improved compared to DPLS (RMSE = 1.3015). Hence the model fit and quality were improved. Figure 6.31- plot (1) shows the time series plot of the measured and predicted response for ADPLS. From Figure 6.31 and the RMSE of the validation data set, the application of ADPLS results in an improvement to the overall model. Figure 6.31- plot (2) shows the time series plot of the residuals where a few points can be considered as outliers. Although these points are not distinctive significantly from the samples in the validation data set, the results in Table 6.14 show that the false alarm rate exceeds the accepted level of violations (5% and 1% for the 95% and 99% confidence limits respectively). This increase in the false alarm rate could be a result of the identified outliers.

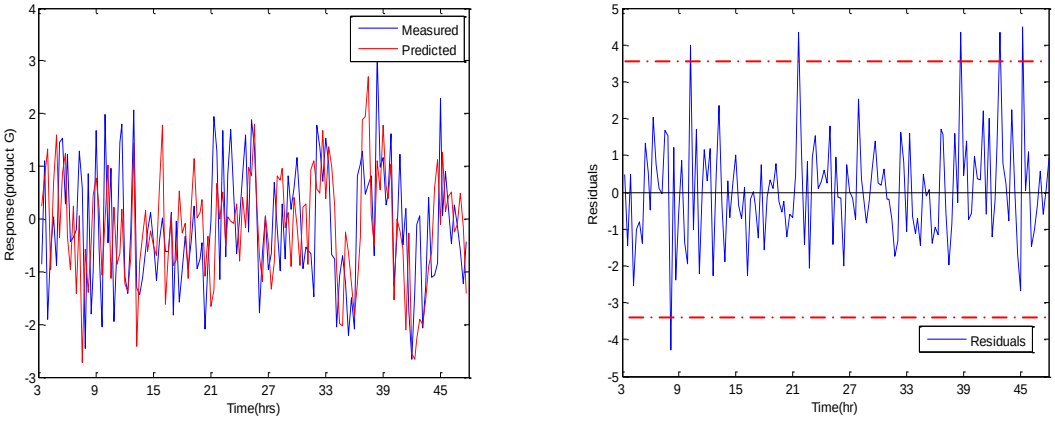

(1) (2)

Figure 6.31 – Results from ADPLS algorithm (1) Measured and predicted response from ADPLS algorithm (2) Time series plot of the residuals

The monitoring results of the overall process for the TEP attained with ADPLS model and the individual blocks resulting from the application of $AMBDPLS_T$ developed in §6.4.3 for the validation data set are presented in Figures 6.32 to 6.34.

Figures 6.32, 6.33 and 6.34 show the Hotelling's T^2, SPE_X and SPE_Y metrics for the overall process (sub-plot 1) and the individual blocks (sub-plot 2 to 6). The 95% and 99% confidence limits were calculated adaptively. It can be seen that a few out of statistical control signals were detected in all sub-figures. It is expected to have 5% and 1% violations for the 95 % and 99 % confidence limits by chance. The false alarm rate (FAR) was calculated and the results are presented in Table 6.14. The most significant improvement is seen in the monitoring chart of the SPE_Y (Figure 6.34), where the confidence limits adapt to the change and hence the FAR decreases compared to the

DPLS results, i.e. FAR = 8.66% based on ADPLS compared to 74% based on DPLS. The percentage of violations for the SPE_X plots, overall process and the individual unit operations, demonstrates a significant decrease compared to the fixed parameter DPLS (Table 6.13). The overall FAR, 9.33%, which is 15.33% less than the overall FAR from DPLS for the validation data set. These results along with the RMSE indicate that the process model has improved in terms of prediction and monitoring quality. In addition to the improvements in the monitoring charts of the overall process, the number of false alarm of the monitoring charts for the individual unit operations has decreased. This can be seen from the FAR of the monitoring charts in Table 6.14. The FAR for most of the charts is within the acceptable rate of 5% and 1% for the 95% and 99% confidence limits respectively.

Although the application of ADPLS and $AMBDPLS_T$ improved the monitoring charts, as mentioned in Chapter 4 the main limitation of the approach is the failure to take into consideration statistical outliers which is expected in this case study as the process measurements are incorporated with Gaussian noise. Consequently, robust adaptive dynamic PLS (RADPLS) and the multiblock variant ($RAMBDPLS_T$) were proposed and these algorithms are applied in the next section.

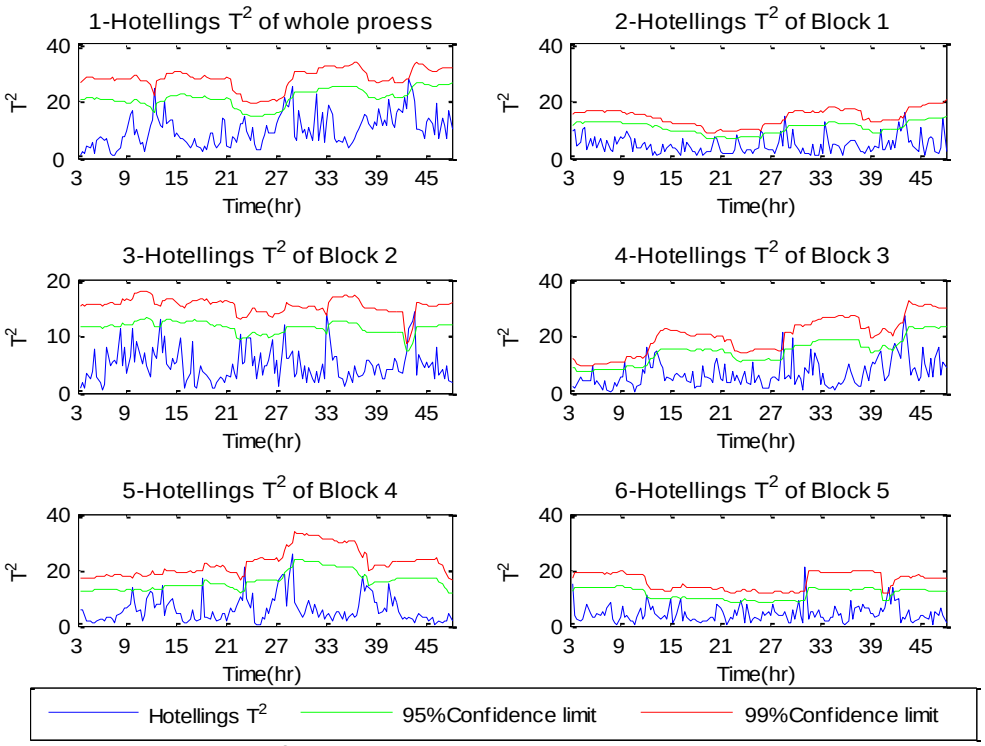

Figure 6.32 - Hotelling's T^2 for (1) overall process and (2-6) individual blocks based on ADPLS and $AMBDPLS_T$ approach –Validation data set

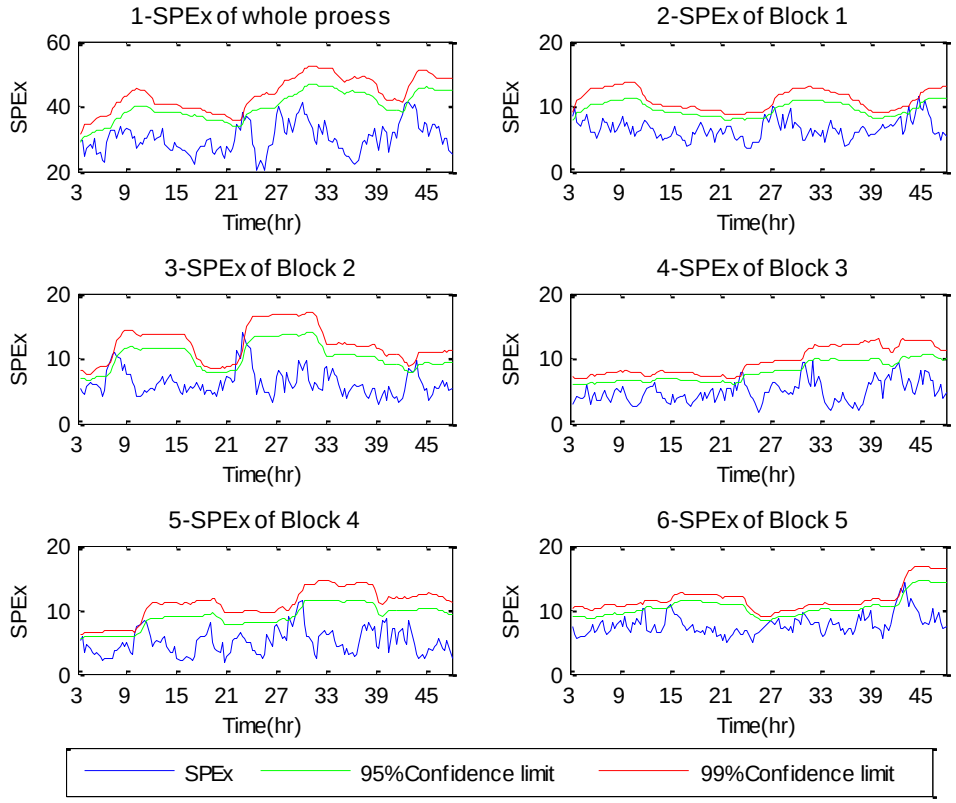

Figure 6.33 - SPE_X for (1) overall process and (2-6) individual blocks based on ADPLS and $AMBDPLS_T$ approach –Validation data set

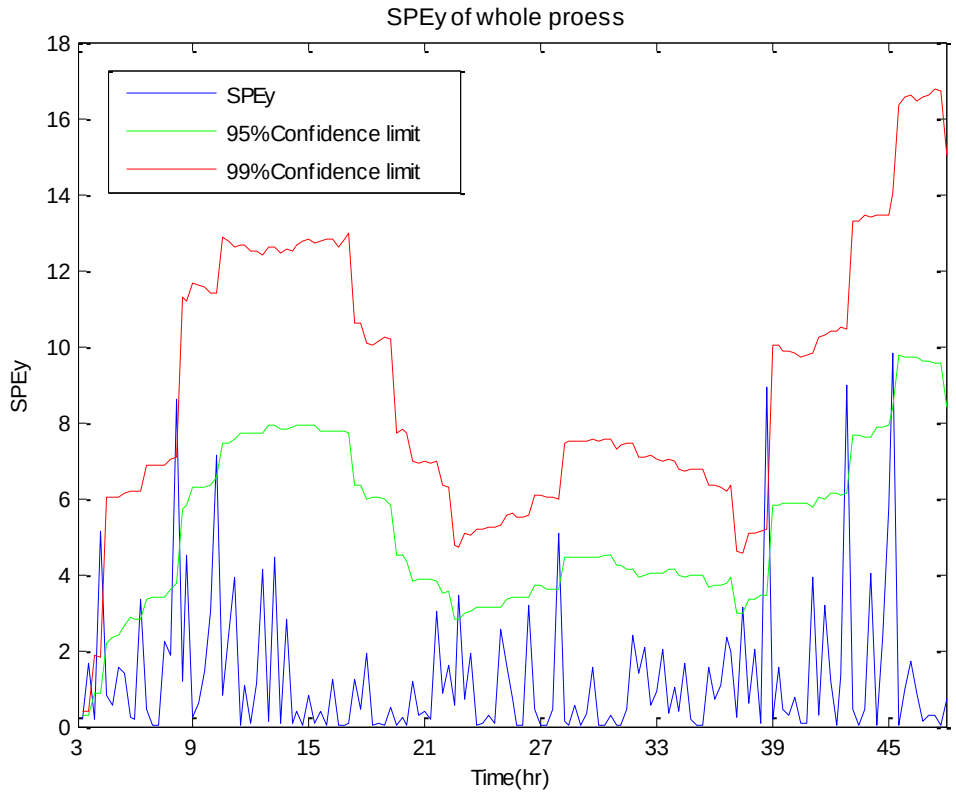

Figure 6.34 - SPE_Y for overall process based on ADPLS – Validation data set

Table 6.14 - False alarm rate for the monitoring charts of the validation data set

Part	Chart	FAR 95%	FAR 99%
whole process	Hotelling's T^2	5.33%	1.33%
	SPE_X	5.33%	1.33%
	SPE_Y	8.66%	4%
Block 1 Reactor	Hotelling's T^2	5.33%	1.33%
	SPE_X	4.6%	2 %
Block 2 Separator	Hotelling's T^2	5.33%	2%
	SPE_X	6.66%	3.33%
Block 3 Stripper	Hotelling's T^2	6.66%	2%
	SPE_X	5.33%	1.33%
Block 4 Compressor	Hotelling's T^2	4.66%	0.66%
	SPE_X	5.33%	1.33%
Block 5 Materials	Hotelling's T^2	5.33%	1.33%
	SPE_X	6%	1.33%

6.4.4 Robust Adaptive Multiblock Dynamic PLS (RAMBDPLS)

The Robust Adaptive Dynamic PLS (RADPLS) algorithm for the TEP is summarised in Figure 6.35. The main concept behind robust adaptive PLS method was previously presented in Chapter 4. In contrast to the approaches presented in Chapter 4, where steady state PLS was used for the development of the PLS reference model, dynamic PLS based on a time series representation is used here. This is to account for the dynamics associated with the TEP. The dynamic PLS model presented in §6.4.2 is used as the reference model. The main goal of the algorithm is to prevent the adaptive procedure including outlying samples and this was addressed through the combined index (Equation 4.12). The main difference between the RAPLS presented in Chapter 4 and the RADPLS is the inclusion of the dynamic information though dynamic PLS and its integration into a multiblock algorithm where the monitoring charts of the overall process and individual unit operation can be constructed.

The algorithm starts in a similar manner to ADPLS (§6.4.3). The differences are as follows:

- Once a new sample becomes available, the combined index (Equation 4.12) is calculated.
- A threshold is used to check whether the new sample represents the normal operating conditions. If the sample violates the threshold, another test is conducted to identify whether the sample represents a statistical outlier or process abnormality. A detailed explanation of the thresholds is given in §4.4.1 and calculation of observation weight is given in the Appendix.
- The DPLS model is updated based on the threshold outcome, i.e. the model is only updated if the sample represents normal operating conditions or when the sample represents a statistical outlier which has been weighted prior to model update. The calculation of the weight was previously described in Chapter 4 (Table 4.1).

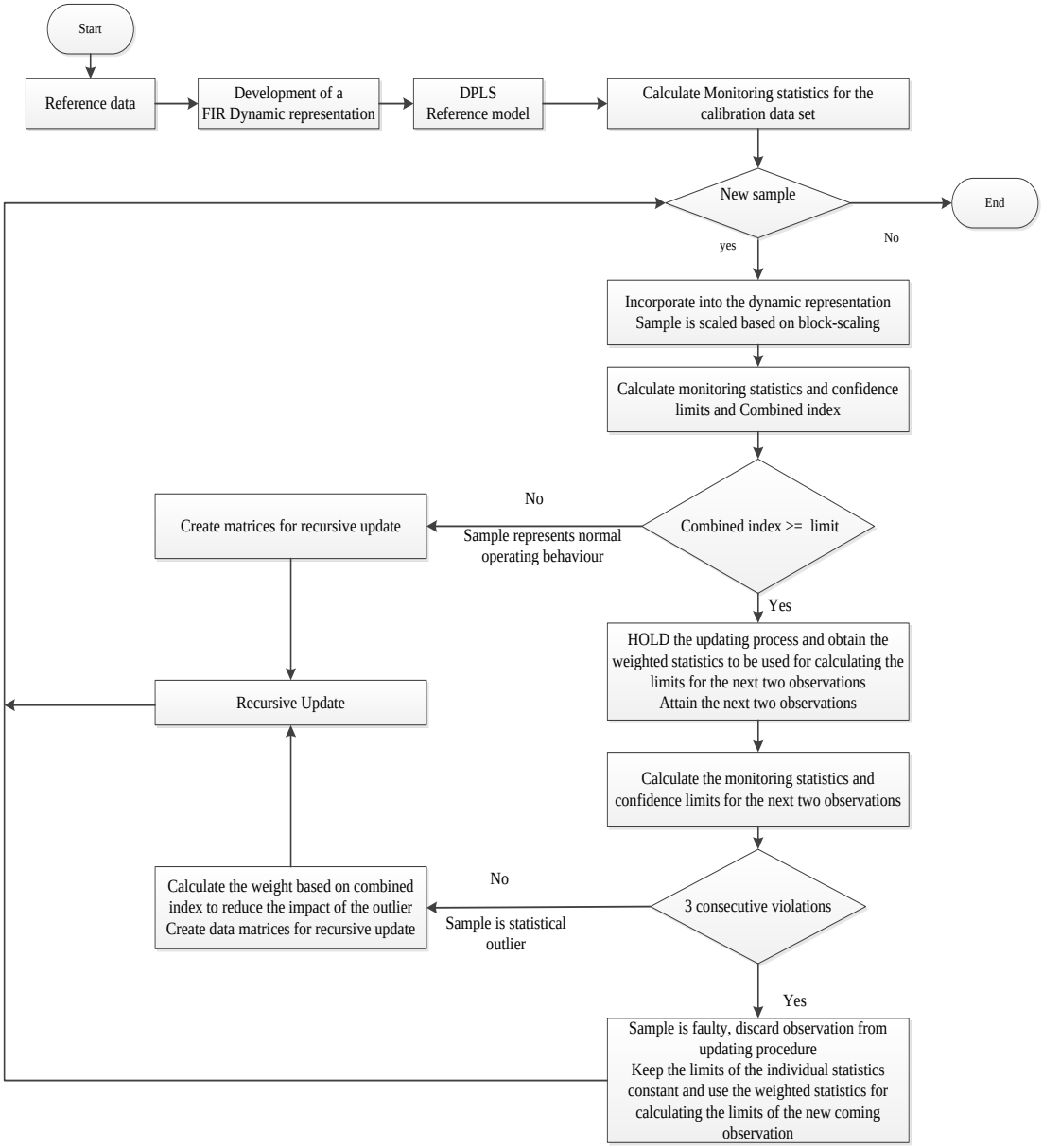

Figure 6.35 - The robust adaptive dynamic PLS (RADPLS) algorithm

The RADPLS algorithm is extended to Robust Adaptive Multiblock Dynamic PLS ($RAMBDPLS_T$) for monitoring the overall performance of the TEP process and the individual unit operations (Figure 6.36). Two steps were included in the RADPLS algorithm:

- The parameters of the individual unit operation were calculated for the first time after the development of the reference DPLS model and they were updated once the overall model has been updated.
- The monitoring statistics and the corresponding confidence limits for the individual blocks were calculated whenever a new sample became available according to §3.8.1 and §4.3.2 respectively.

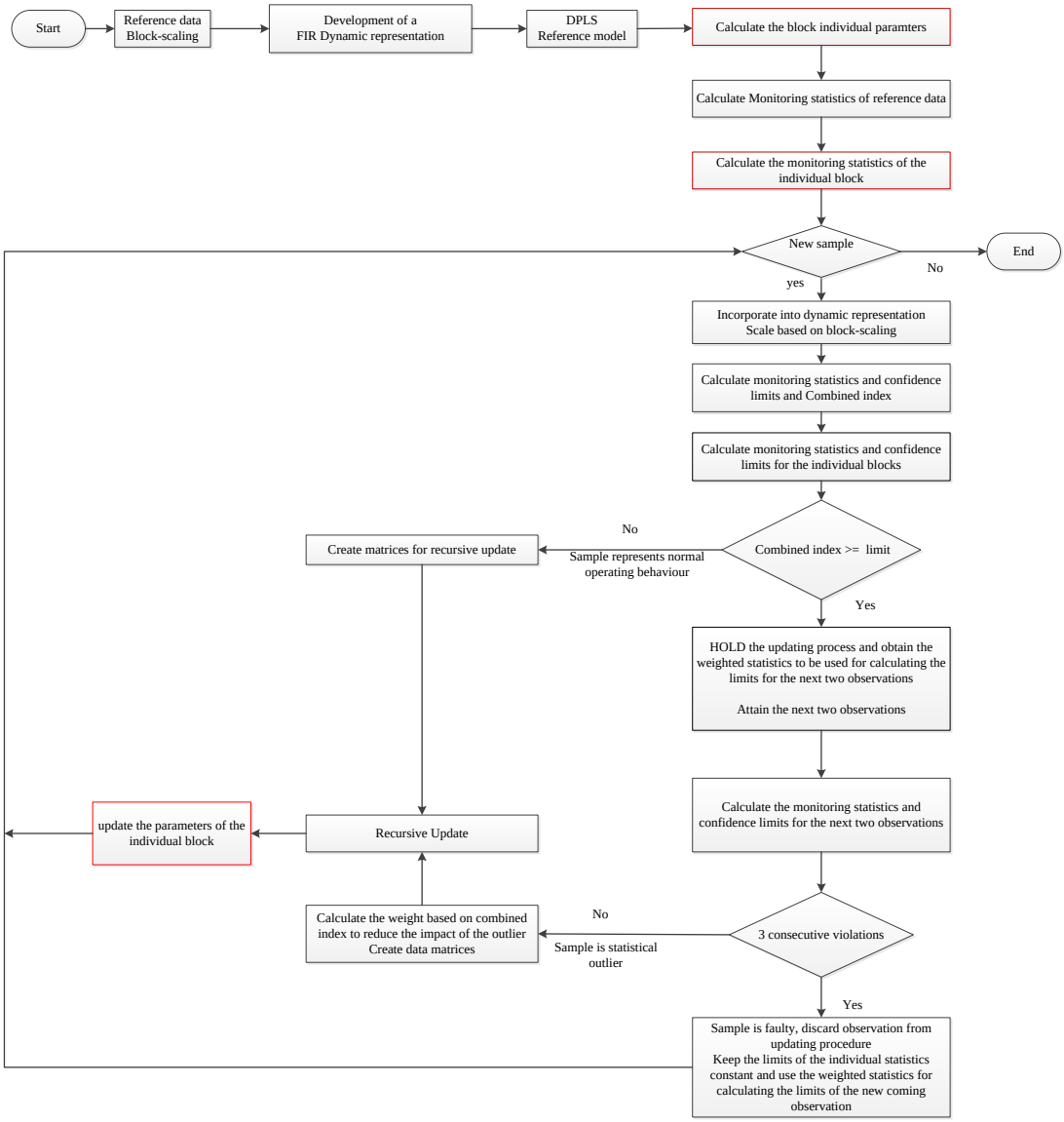

Figure 6.36 - The robust adaptive multiblock dynamic PLS ($RAMBDPLS_T$) algorithm

The results from the application of robust adaptive dynamic PLS (RADPLS) to the validation data set shows a slight improvement, RMSE = 1.2534, compared to DPLS and ADPLS in §6.4.2 and §6.4.3 respectively. Figure 6.37 – plot (1) shows the time series plot of the measured and predicted response, product G, from the application of RADPLS to the validation data set, which did not show a significant visual improvement. However, the RMSE showed a very slight improvement. This slight improvement in the RMSE was expected since the RADPLS identified a few statistical outliers as shown in Figure 6.37 – plot (2), time series plot of the residuals. These few points deviate slightly from the majority of samples were detected in the combined index plot (Figure 6.38)

According to the RADPLS algorithm, these statistical outliers were treated prior to model updating to reduce the impact on the DPLS model. As mentioned in Chapter 4, if the PLS model is updated using statistical outliers continuously, this would potentially deteriorate the prediction of the model. In this case, only 8 outliers were identified and treated over a period of 150 samples; this will not result in a great improvement in the results. These violations are corresponding to 5.33% for the 95% confidence limit. In the case of ADPLS where the model was updated without inspection, the RMSE of the validation data set was higher than the RMSE based on RADPLS.

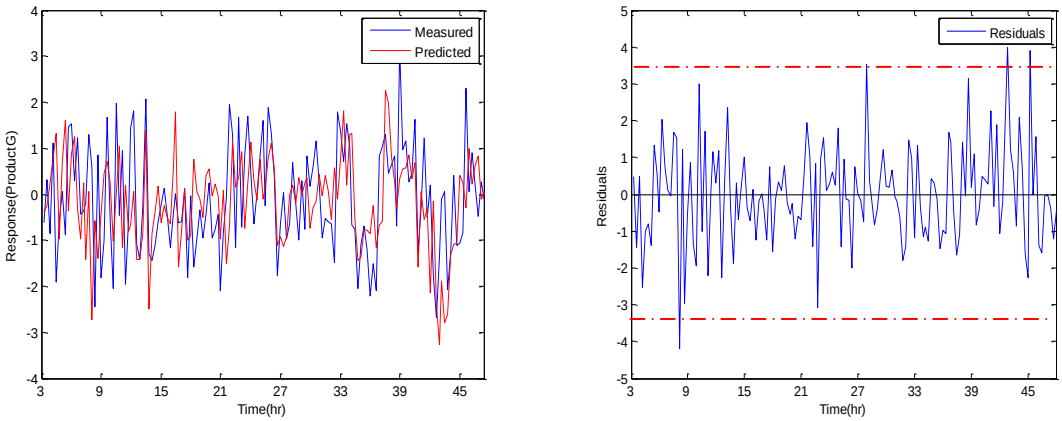

(1) (2)

Figure 6.37 - Results from application of RADPLS algorithm to validation data set (1) Measured and predicted response from RADPLS algorithm (2) Time series plot of the residuals

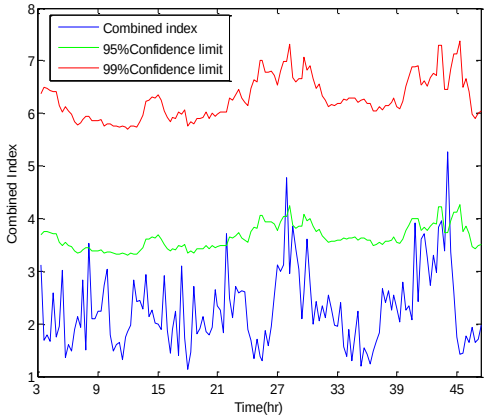

Figure 6.38 – Combined index based on RADLPS – Validation data set

Figures 6.39 and 6.40 show the results for Hotelling's T^2 and SPE_X for the whole process (sub-plot 1) and the individual unit operations (subplot 2-6). Figure 6.41 shows the SPE_Y of the process. It can be seen that there are few out of statistical control samples. However, the number of violation is acceptable as it is within the rate of 5% and 1% of the violations for 95% and 99% confidence limits respectively.

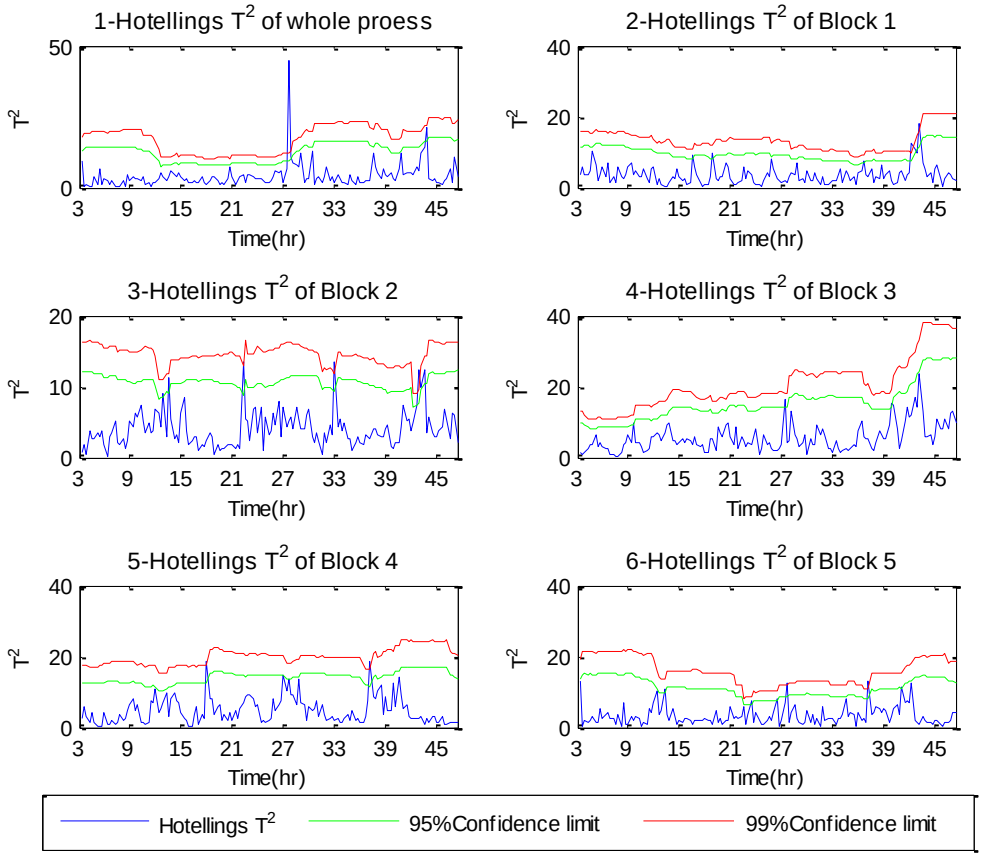

Figure 6.39 - Hotelling's T^2 for (1) overall process and (2-6) individual blocks based on RADPLS and $RAMBDPLS_T$ approach –Validation data set

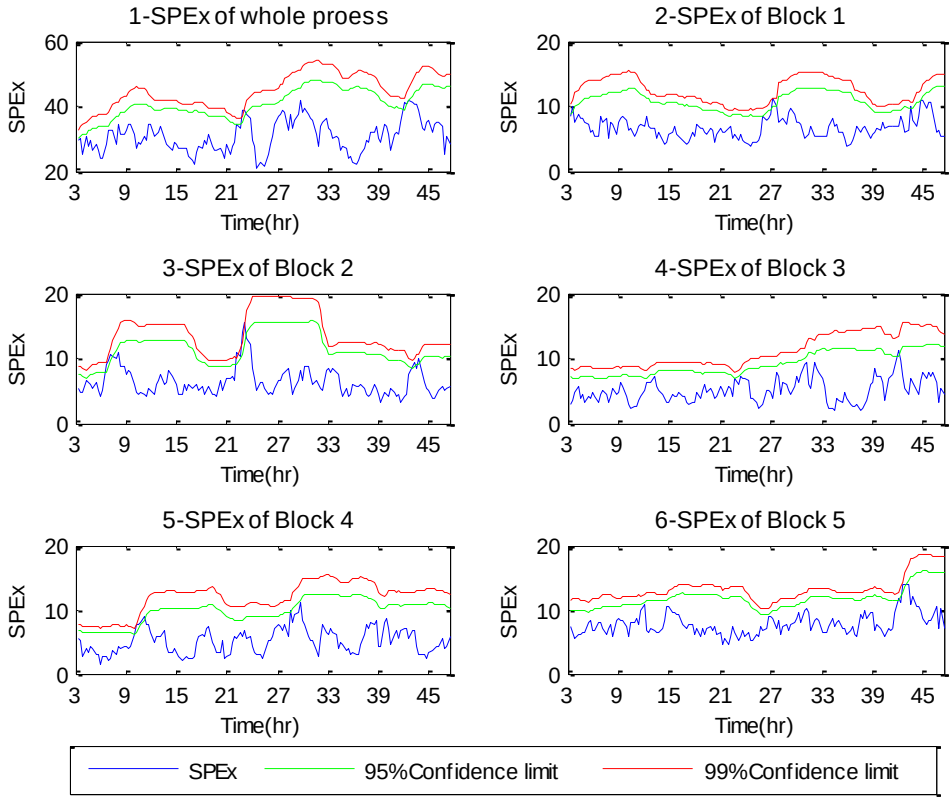

Figure 6.40 - SPE_X for (1) overall process and (2-6) individual blocks based on RADPLS and $RAMBDPLS_T$ approach –Validation data set

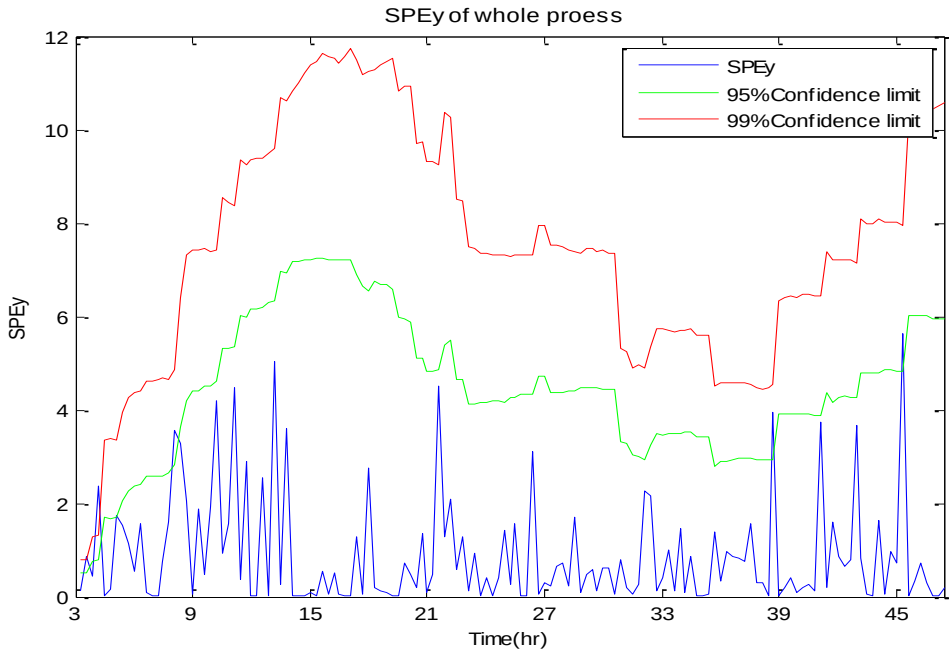

Figure 6.41 - SPE_Y for the TEP based on RADPLS and $RAMBDPLS_T$ approaches – Validation data set

The results of the false alarm rate show real improvement compared to fixed parameter DPLS. In addition, some of charts were slightly improved compared to ADPLS.

The monitoring charts for the overall process and the individual blocks were evaluated using FAR, which quantify the number of violations (Table 6.15). Figure 6.39 shows Hotelling's T^2 for the overall process (sub-figure 1) and individual blocks (sub-figure 2-6). It can be seen that the metrics violate the confidence limits in all the sub figures with an acceptable range of 5% and 1% for the 95% and 99% confidence limits respectively. These violations are slightly less compared to Hotelling's T^2 based on ADPLS. In particular the monitoring charts for block 3 where the FAR decreased from 6.66 % to 3.33%. The same observation can be drawn for SPE_X monitoring charts**.** The most significant improvement compared to DPLS and ADPLS was seen in the FAR for the SPE_Y metric, where the FAR decreased from 74% and 8.66% to 4.66%. Consequently the monitoring charts based on RADPLS bring the number of violations to the acceptable level. The overall FAR, which is calculated jointly based on Hotelling's T^2 and SPE_X, was 6.66% which is 2.67% less than the FAR based on ADPLS.

Table 6.15 - False alarm rate for the monitoring charts of the Validation data set (RADPLS).

Part	Chart	FAR 95%	FAR 99%
whole process	Hotelling's T^2	3.33%	1.33%
	SPE_X	3.33%	1.33%
	SPE_Y	4.66%	1.33%
Block 1 Reactor	Hotelling's T^2	3.33%	1.33%
	SPE_X	2%	0.66%
Block 2 Separator	Hotelling's T^2	6%	2%
	SPE_X	6%	2%
Block 3 Stripper	Hotelling's T^2	3.33%	0.66%
	SPE_X	5.33%	1.33%
Block 4 Compressor	Hotelling's T^2	3.33%	0.66%
	SPE_X	5.33%	1.33%
Block 5 Materials	Hotelling's T^2	4%	0.66%
	SPE_X	4%	1.33%

6.5 Discussion

In this Chapter, two statistical indices, Root Mean Square Error (RMSE) and False Alarm Rate (FAR) are used to assess the model quality and the monitoring charts respectively. In the following section the three approaches proposed in this chapter are assessed to attain enhanced understanding of their performance in terms of model prediction and the monitoring charts.

6.5.1 Root Mean Squared Error

Figure 6.42 shows the RMSE for the validation data set based on DPLS, ADPLS and RADPLS. The figure indicates that the prediction based on the adaptive approaches is better than that for fixed parameter DPLS. This improvement resulted from the continuous updating of the PLS parameters. As previously described in §6.4.3, the identification of a few statistical outliers using RADPLS also contributes to this improvement. This is because the identification and the weight of the statistical outliers maintained the robustness of the PLS model.

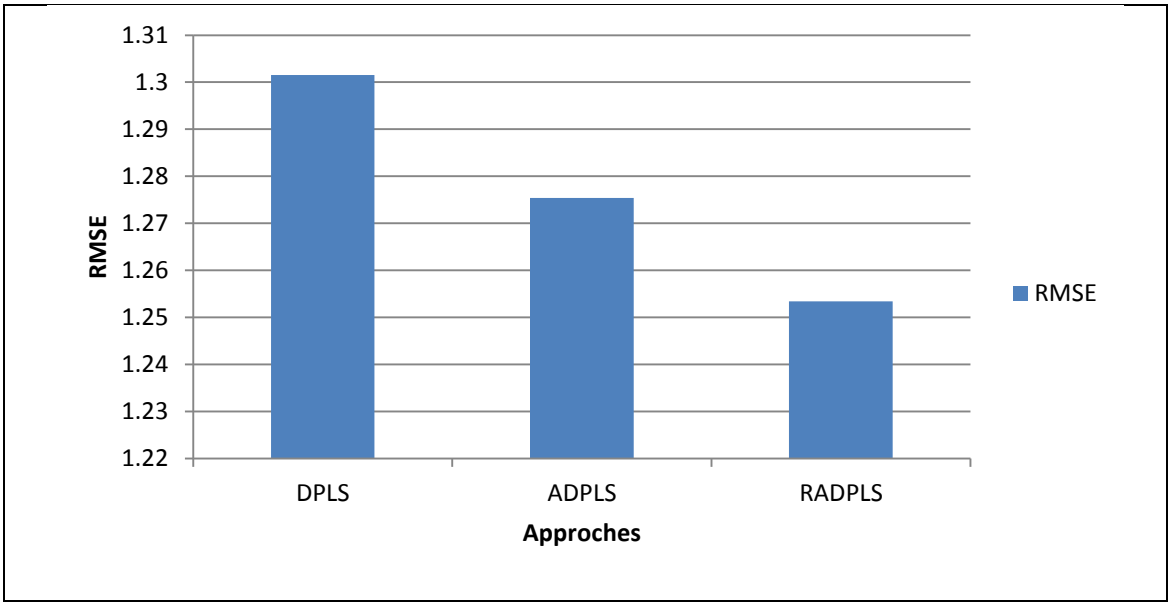

Figure 6.42 – RMSE based on DPLS, ADPLS and RADPLS

6.5.2 False alarm Rate

The concept of FAR, is used to assess the efficiency of the monitoring charts constructed based on the DPLS, ADPLS and RADPLS for the validation data set. Figure 6.43 shows comparative results for the FAR for SPE_X for the overall process and the individual blocks. It can be seen that the adaptive methods resulted in a low false

alarm rate compared to the fixed parameter DPLS. Consequently the monitoring charts based on the adaptive approaches are reliable in terms of describing the performance of the TEP process. In addition, the SPE_X monitoring charts of the overall process and blocks 1 and 2 based on RADPLS generated in a less false alarm rate compared to ADPLS.

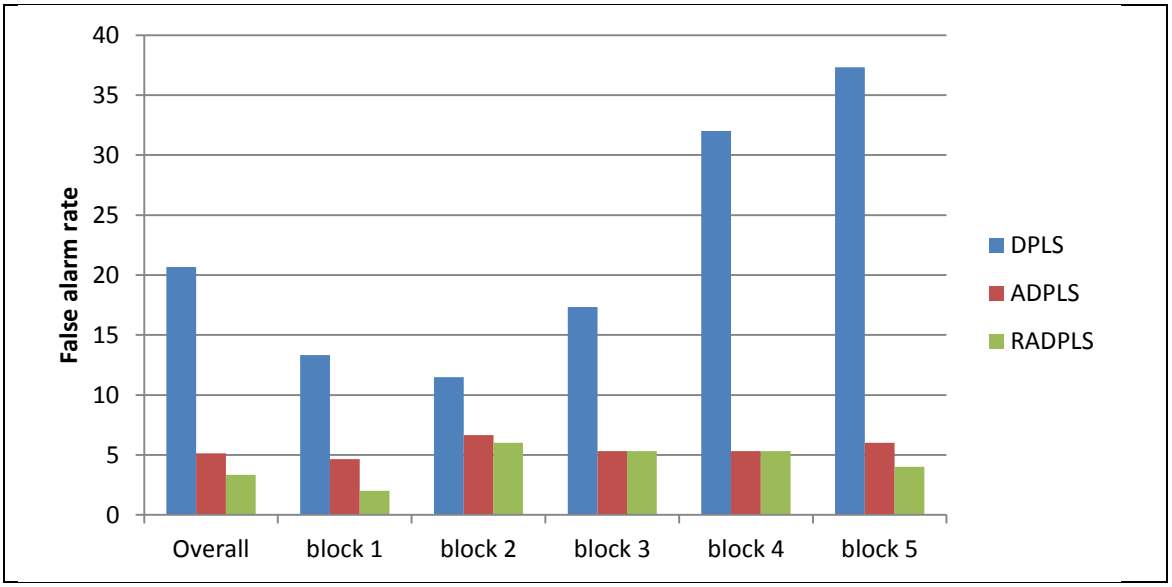

Figure 6.43 – False alarm rate for SPE_X charts based on DPLS, ADPLS and RADPLS for the overall process and the individual bocks

Figure 6.44 shows a FAR comparison between Hotelling's T^2 charts based on the three approaches. It can be seen that the robust adaptive approach reduced the FAR compared to the fixed parameter DPLS and ADPLS approaches. Additionally, the FAR for the individual Hotelling's T^2 charts based on RADPLS is lower than FAR following the application of DPLS and ADPLS. However, the FAR for block 2 following the application of RADPLS is higher than the DPLS and ADPLS but the percentage is within the acceptable rate.

A similar observation can be concluded from a comparative figure for the SPE_Y monitoring charts based on DPLS, ADPLS and RADPLS (Figure 6.45). The FAR from the robust adaptive approaches reduced the false alarm compared to fixed parameter DPLS. In addition, there is a slight difference between the ADPLS and RADPLS results with the results following the application of RADPLS showing fewer false alarms as a consequence of the identification of potential outliers.

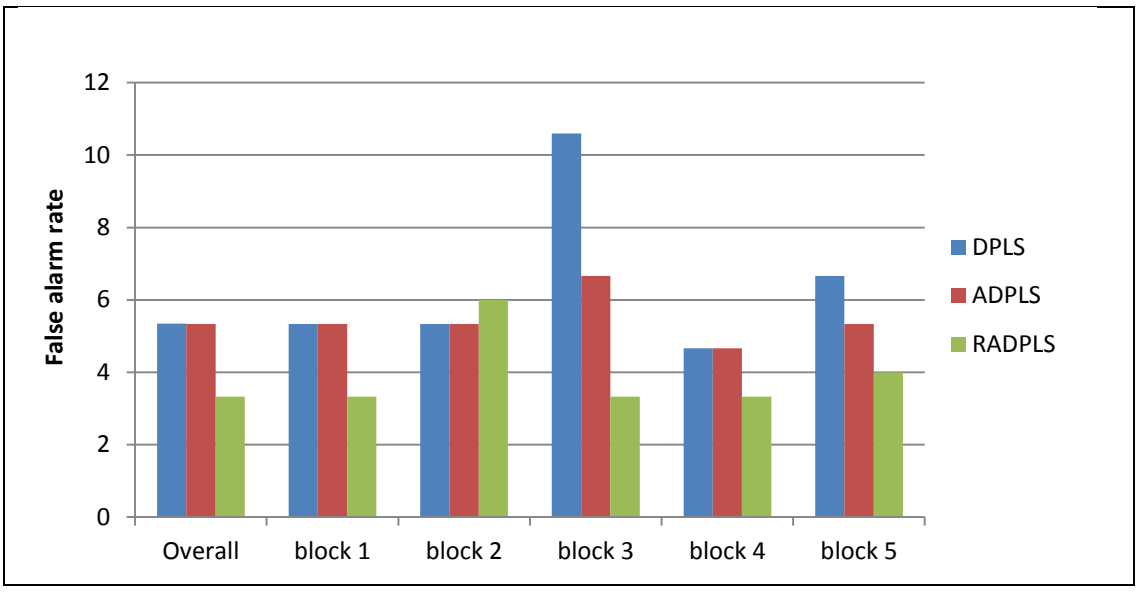

Figure 6.44 – False alarm rate for Hotelling's T^2 charts based on DPLS, ADPLS and RADPLS for the overall process and the individual bocks

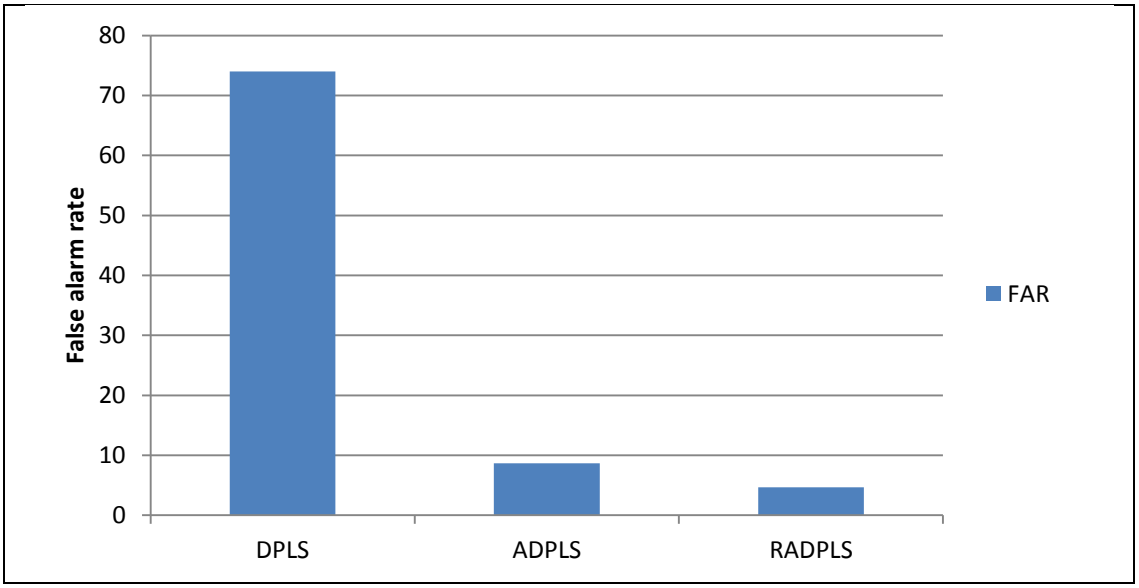

Figure 6.45 – False alarm rate for SPE_Y charts based on DPLS, ADPLS and RADPLS for the overall process and the individual bocks

6.6 Chapter Summary and Conclusions

In this Chapter, the PLS method was extended to multiblock dynamic PLS (MBDPLS) through the use of a finite impulse response time series representation. The aim was to construct monitoring systems that have the ability to monitor the whole process and the individual unit operations for the TEP while accounting for process dynamics. In addition, multiblock dynamic PLS was extended to a recursive version with adaptive confidence limits. This extension was used to linearize the process around the steady

state conditions and hence, exploit the linear methods ability to improve the monitoring of a nonlinear dynamic process. These extensions were applied to the Tennessee Eastman process to test their efficiency in terms of constructing a reliable monitoring system and to reduce the false alarm rate. The main contributions and conclusions were:

- The first part of the chapter involved the identification of an appropriate dynamic representation that take into account the process dynamics caused by autocorrelation. Several models based on different sampling intervals and different time history were developed in order to identify the most appropriate model to describe the dynamic behaviour of the TEP. The selected model was acceptable in terms of fitting and prediction with respect to the root mean squared error.
- Dynamic PLS, which was based on a FIR representation using an 18 min sampling period and 6 lags of time history, improved the model fit and prediction compared to static PLS and dynamic PLS using a 3 min sampling interval. However, the false alarm rate was high for the monitoring charts following the application of the model for the validation data due to changes in process dynamics and nonlinearity. This is not acceptable since the data set used at this stage was for validation of the model using normal operating condition data. Consequently, the process required a more advanced methods to construct a reliable monitoring scheme.

- The first extension was the recursive version of multiblock dynamic PLS with adaptive confidence limits, i.e. adaptive dynamic PLS (ADPLS) and adaptive multiblock dynamic PLS ($AMBDPLS_T$) which updates the model and the confidence limits whenever a new sample becomes available. This extension improved model prediction and overcame the limitations presented in DPLS and $MBDPLS_T$, however, it is criticised for the following reasons:
  - The model was updated blindly and hence there is a risk of including outlying observations that are generated either randomly or from a process disturbance. By including such a sample, the PLS model will be compromised.
  - The confidence limits were allowed to adapt all the changes in the process, consequently, the fault detection rate decreased as described in the next chapter.

- The second extension was robust adaptive dynamic PLS (RADPLS) and adaptive multiblock dynamic PLS (RAMBDPLS$_T$) which aims to update the model and confidence limits based on an inspection of the incoming sample. The model and confidence limits will not be updated when the samples are generated from a disturbance. On the other hand, where the outlying samples are generated randomly, the model and the confidence limits are updated based on the weighted outliers. The main advantage is that the limitations observed following the application of DPLS and ADPLS in terms of identifying statistical outliers was addressed and the false alarm rate is decreased.
- Two statistical indices were used to assess the efficiency of the model and the monitoring charts, the root mean squared error (RMSE) and the false alarm rate (FAR). Both metrics showed superior performance for the adaptive methods compared to fixed parameter DPLS

The aforementioned process monitoring methods are evaluated in term of fault detection for the TEP process in Chapter 7. The statistical index of fault detection rate is used to quantify the detection rate for the overall process and the individual unit operations following the application of the monitoring methods.

Chapter 7

Fault Detection Capability on Tennessee Eastman Process

7.1 Introduction

In this Chapter, the process monitoring methods proposed in Chapter 6, DPLS, MBDPLS$_T$, ADPLS, AMBDPLS$_T$, RADPLS and RAMBDPLS$_T$, are compared through their application to the Tennessee Eastman Process (TEP) for fault detection. The aim is to investigate fault detection ability of the algorithms with respect to the overall process and the individual unit operations. In addition, the issue of fault propagation in dynamic processes is investigated.

The process description, definition of the process data and disturbances were previously described in Chapter 6. Of the 21 process faults identified in Table 6.5, four different categories of process faults were selected for investigation in this chapter. The first case study, Fault (18), represents an unknown process fault, the second case study, Fault (1), represents a step change in the feed ratio to the reactor unit, the third case study, Fault (13), represents a slow drift in the reaction kinetics and finally the last case study, Fault (10), represents random variation in the one of the material temperatures. The fault detection and false alarm rates are calculated to investigate the efficiency of the monitoring approaches.

7.2 TEP Faults

As mentioned in Chapter 6 data sets are available comprises data that represents normal process operating conditions and the remaining sets incorporate abnormal behaviour. Additionally, the faulty data sets were collected for 48 hr and the abnormal event was introduced after 8 hr of normal operation (§6.3.3). As the time constant of the TEP was approximately 2 hours, a delay is expected between fault occurrence and the response of the system. For example, by sampling every 3 min according to Chiang et al. (2001), Fault (1) has an impact on the system after 7 samples, which correspond to 21 min of operation post fault introduction.

7.3 Evaluation of the Monitoring Charts

In this chapter, two statistical indices are used to investigate the reliability of the monitoring charts, false alarm rate and fault detection rate. The false alarm and fault

detection rates were calculated as a combination of Hotelling's T^2 and SPE_X for the period prior to and post fault occurrence respectively, i.e. the false alarm rate is calculated for the period of 8 hr prior to fault introduction whilst the fault detection rate is calculated post fault introduction. In addition, these metrics were calculated for the overall process and the individual unit operations (blocks).

7.4 Results and Discussion

7.4.1 Case Study on Fault (18)

This fault represents an unknown fault. In reality the chance for getting unknown faults is high as the environment and conditions may change based on the experiment. In the case for the TEP, there is no information regarding this fault or which variables are related to the fault hence the DPLS approach and extensions are applied to detect the fault and provide details regarding its behaviour.

7.4.1.1 Monitoring Charts by DPLS and $MBDPLS_T$ for Fault (18)

The DPLS algorithm described in §6.4.2.2 was applied to the data generated in the presence of Fault (18). The resulting DPLS monitoring charts are given in Figures 7.1, 7.2 and 7.3. The fault occurred after 8 hr of nominal operation hence the monitoring statistics are expected to remain within statistical control prior to this period. However, the monitoring indices, SPE_X and SPE_Y violate the confidence limits prior to the onset of the fault, i.e. within the first 8 hr of nominal operations. This is confirmed through the calculation of the false alarm rate in this period (Table 7.1). The false alarm rate (FAR) for the overall process is 33% and for SPE_Y is 73.3%. In addition, the FAR for all the individual unit operations exceeds 5% as shown in Table 7.1. Even though the fault effect is indicated in almost all the monitoring charts as shown in Table 7.1, where the overall process and the quality product monitoring chart detect 92% and 86.5% of the faulty samples respectively, the FAR indicates that the implementation of DPLS and $MBDPLS_T$ increases the number of false alarms hence they are inappropriate for the monitoring of the TEP. Therefore, the ADPLS and $AMBDPLS_T$ are implemented.

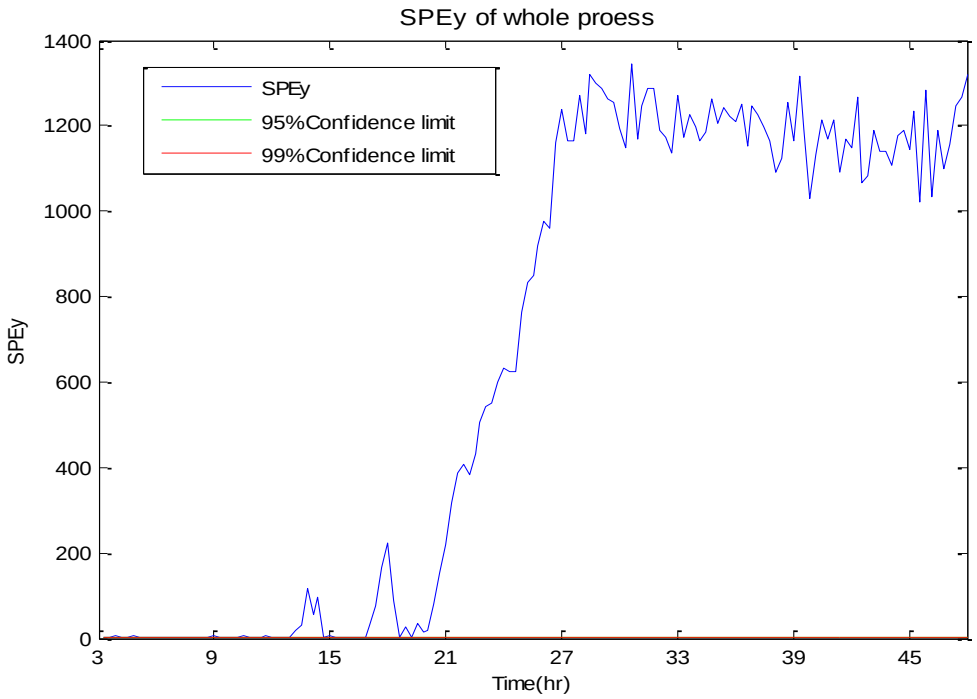

Figure 7.1 - SPE_Y for the TEP based on DPLS – Fault (18)

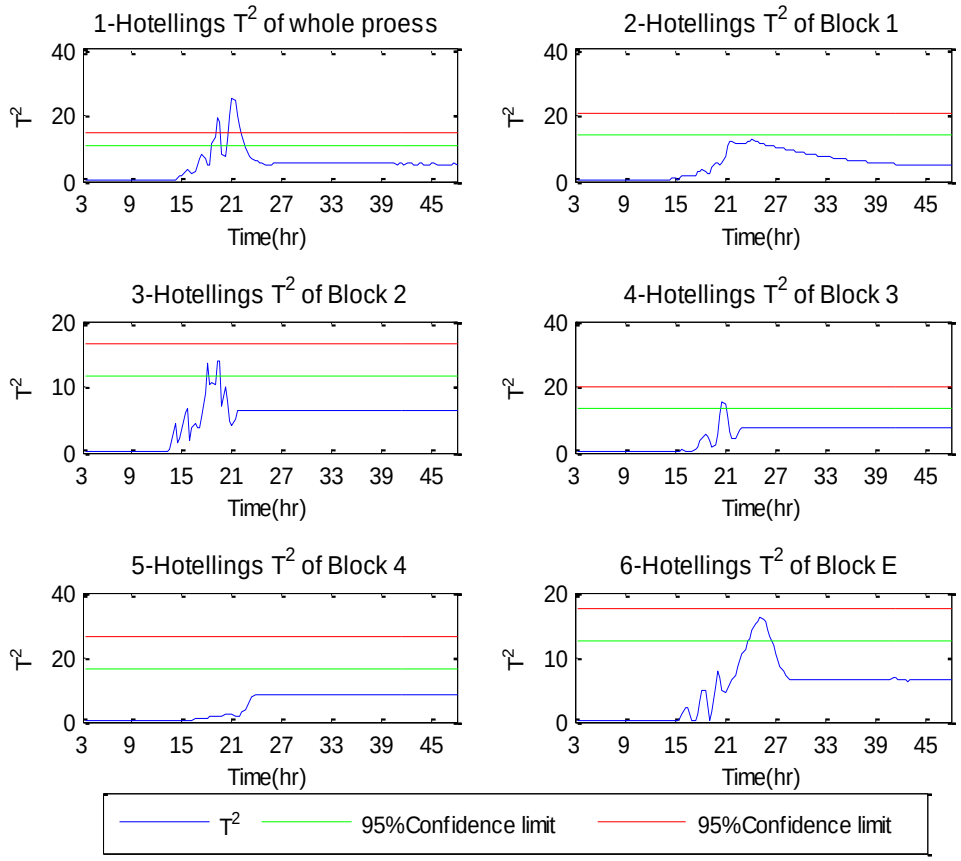

Figure 7.2 - Hotelling's T^2 for (1) overall process and (2-6) individual blocks based on DPLS and $MBDPLS_T$ approaches – Fault (18)

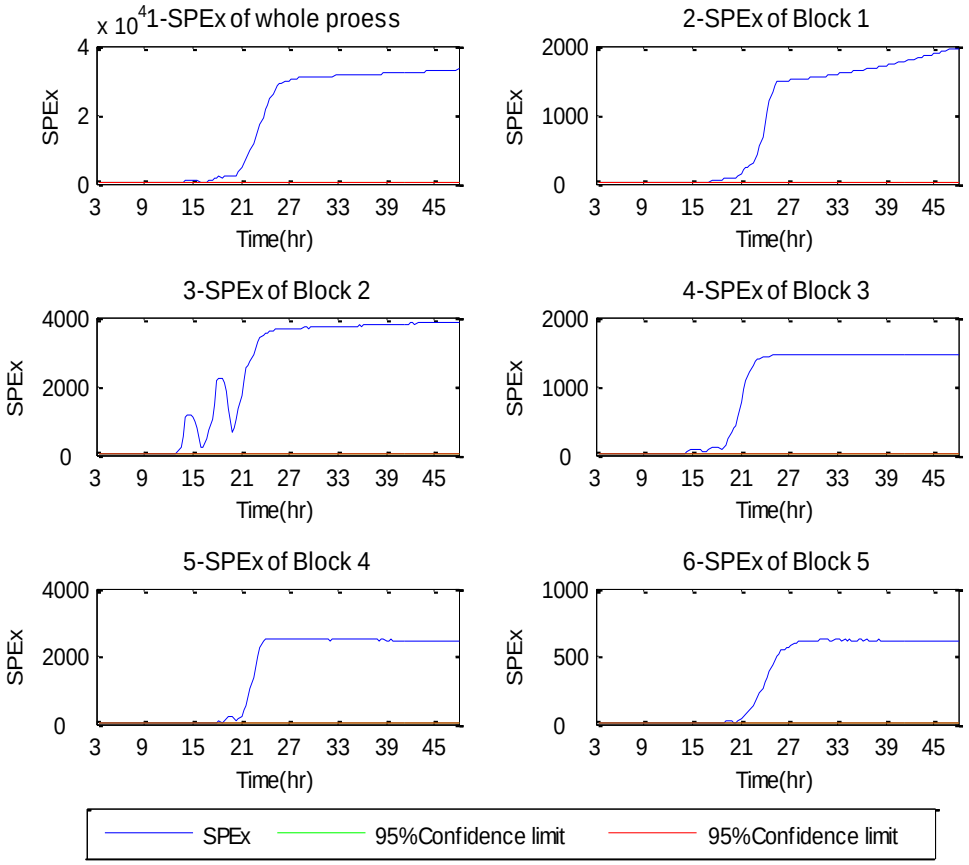

Figure 7.3 - SPE_X for (1) overall process and (2-6) individual blocks based on DPLS and $MBDPLS_T$ approach – Fault (18)

Table 7.1 – Fault detection and false alarm rates based on DPLS and $MBDPLS_T$ for Fault (18).

Part	Fault detection rate	False alarm rate
Overall process	92.4%	33.3%
Block 1 – Reactor	88.9%	13.3%
Block 2 - Separator	94.8%	13.3%
Block 3 – Stripper	88.1%	13.3%
Block 4 – compressor	91.1%	6.7%
Block 5 – Materials	81.2%	13.3%
SPE_Y	86.5%	73.3%

7.4.1.2 Monitoring Charts by ADPLS and AMBDPLS$_T$ for Fault (18)

The results from the implementation of the ADPLS and AMBDPLS$_T$ algorithms are given in Figures 7.4, 7.5 and 7.6. The quantitative results for all the monitoring charts are presented in Table 7.2. It can be seen that the ADPLS approach overcomes the limitation observed in DPLS and MBDPLS$_T$ algorithm, where the monitoring charts produced a high number of false alarms. The FAR following application of ADPLS and the AMBDPLS$_T$ algorithm for the overall process and the SPE$_Y$ were reduced by 26.6% and 46.6% respectively. However, it can be seen that the process remains within the statistical control after the onset of the fault (Figures 7.4, 7.5 and 7.6). This is due to the fact the confidence limits are allowed to adapt to the change in the process. In addition, the ADPLS algorithm allows the samples produced from the unknown fault to contribute to the model updating process, consequently, the efficiency of the ADPLS monitoring charts in term of fault detection decreases. Table 7.2 shows a significant decrease in the FDR for the monitoring charts for the overall process and individual block compared to the DPLS and AMBDPLS$_T$ algorithms. The monitoring charts of the overall process detect only 23.3% of the faulty samples with the individual blocks detecting 15 % to 28% of the faulty samples as summarised in Table 7.2. The monitoring chart for SPE$_Y$ detects only 26.7% of the faulty samples compared to the DPLS chart which detected 86.5% of the faulty samples. This is a clear indication of the deficiency of the monitoring charts following the application of ADPLS and hence RADPLS algorithm was implemented.

Table 7.2 – Fault detection and false alarm rates based on ADPLS and AMBDPLS$_T$ for Fault (18).

Part	Fault detection rate	False alarm rate
Overall process	23.3%	6.7%
Block 1 – Reactor	28.6%	6.7%
Block 2 - Separator	15.0%	13.3%
Block 3 – Stripper	18.8%	6.7%
Block 4 – compressor	24.8%	6.7%
Block 5 – Materials	24.1%	6.7%
SPE$_Y$	12.0%	26.7%

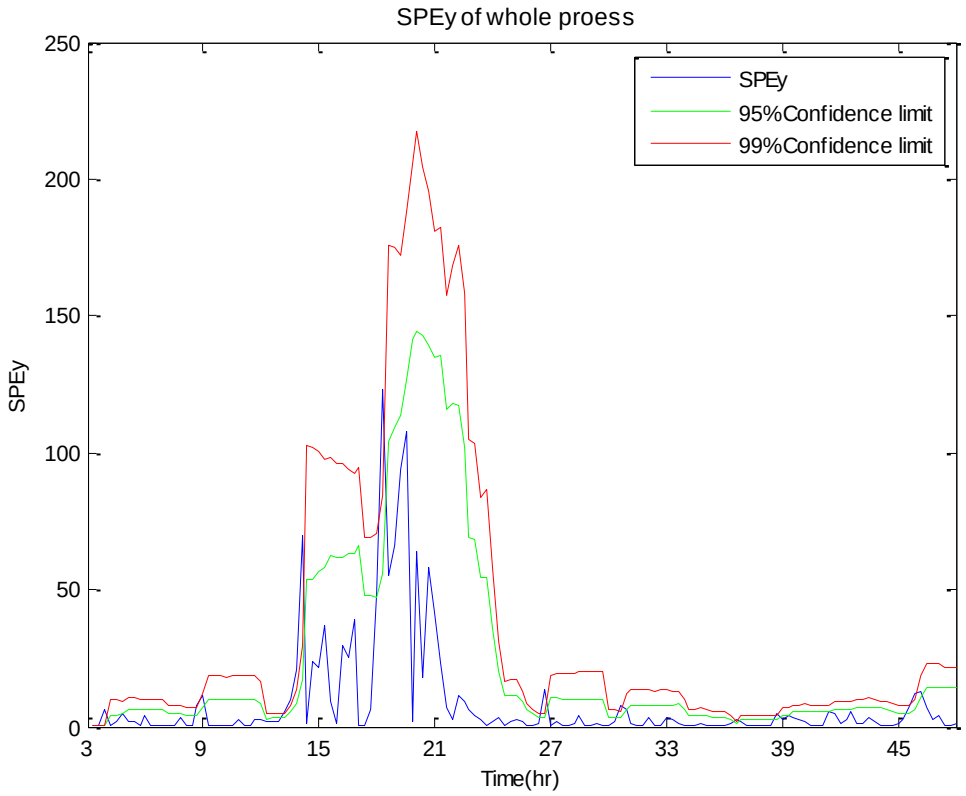

Figure 7.4 - SPE_Y for the TEP based on ADPLS – Fault (18)

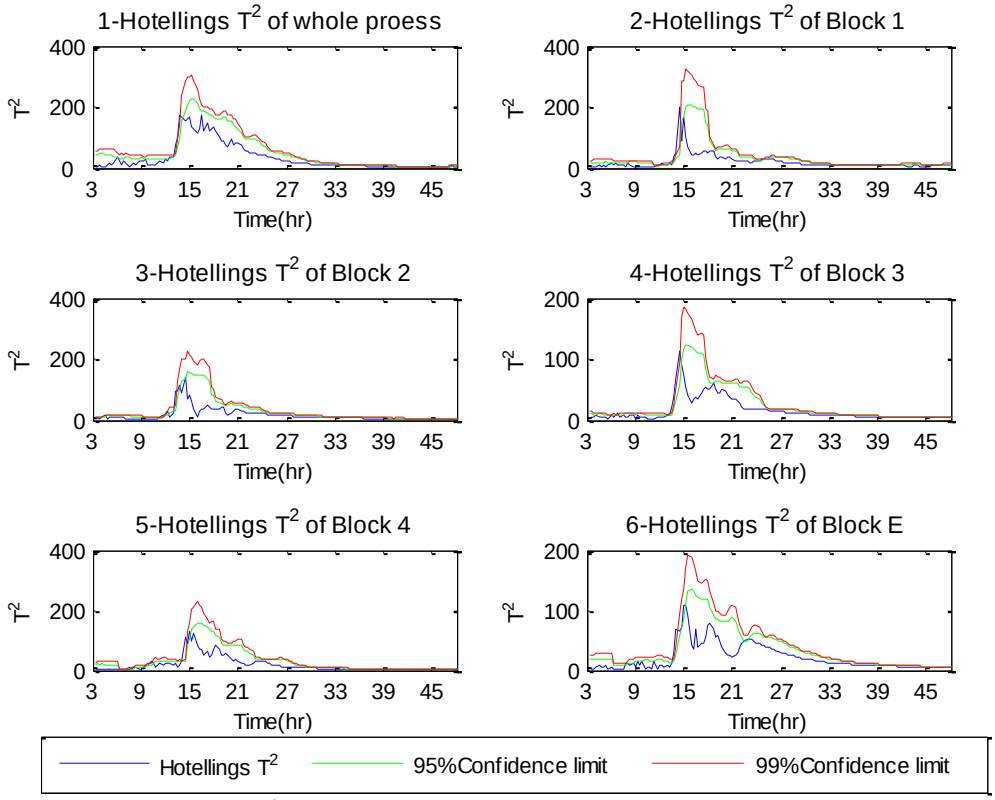

Figure 7.5 - Hotelling's T^2 for (1) overall process and (2-6) individual blocks based on ADPLS and $AMBDPLS_T$ approaches –Fault (18)

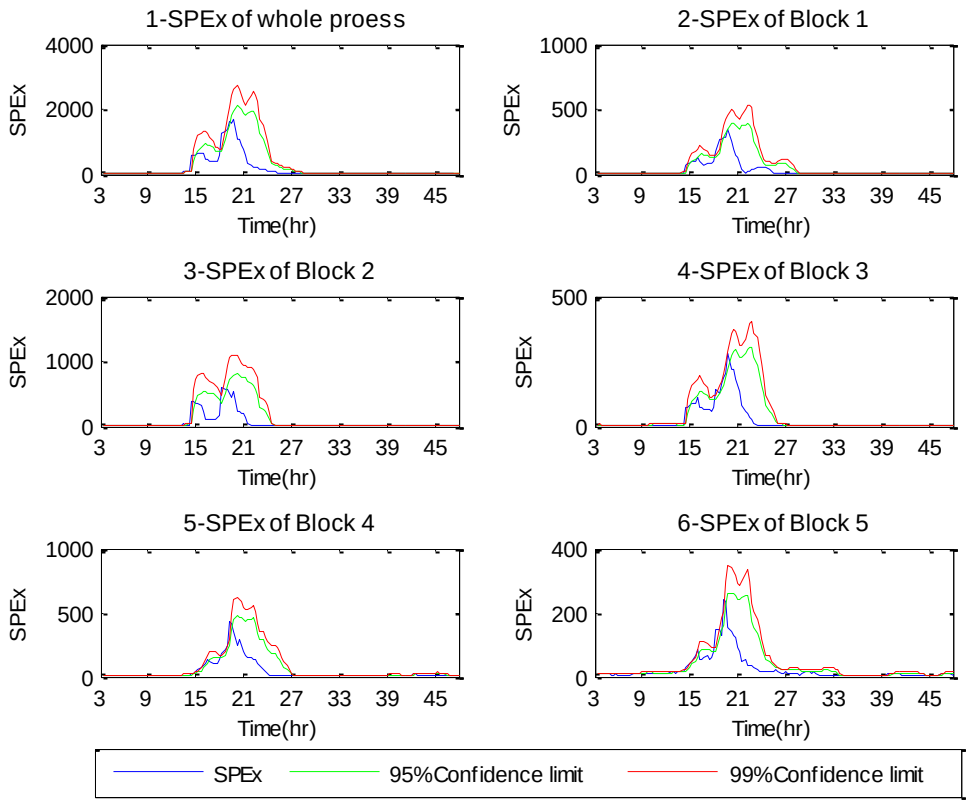

Figure 7.6 - SPE_X for (1) overall process and (2-6) individual blocks based on ADPLS and $AMBDPLS_T$ approaches –Fault (18)

7.4.1.3 Monitoring Charts by RADPLS and $RAMBDPLS_T$ for Fault (18)

The application of RADPLS and $RAMBDPLS_T$ provides an enhanced monitoring system as they calculate one additional monitoring statistic namely the combined index. This provides information regarding the total variation in the process. The combined index is presented in Figure 7.7 and it clearly indicates the process is out of statistical control. This indication by the combined index halts the updating procedure thereby ensuring the robustness of the model. From Table 7.3, it can be seen that the FDR for the combined index monitoring chart is 92.4% whilst the false alarm rate for the same chart is 0%.

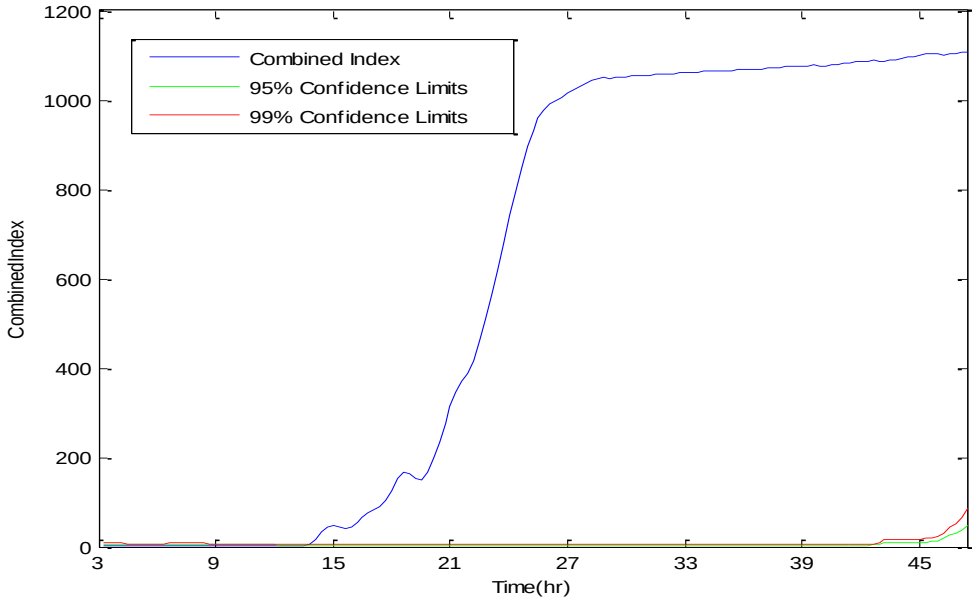

Figure 7.7 – Combined index for the TEP based on RADPLS and RAMBDPLS$_T$ approaches – Fault (18)

The monitoring charts for Hotelling's T², SPE$_X$ and SPE$_Y$, following the application of RADPLS and RAMBDPLS$_T$ are given in Figures 7.8, 7.9 and 7.10 respectively. It can be seen that the monitoring indices are affected by the fault (whole process and individual blocks). Additionally, the limitations observed following the application of DPLS and ADPLS, i.e. an increase in the false alarm rate when the process represents normal operation and a decrease in the fault detection rate when the process is under fault conditions respectively, are overcome and hence the monitoring charts can be interpreted appropriately. The advantage of the RADPLS over the other two methods is that it allows the confidence limits to adapt to the process prior to the introduction of the fault as shown in the first 8 hr for all monitoring charts. Additionally, it stops the adaption procedure when the samples are generated under the effect of the disturbance.

The quantitative results of the fault detection rate and false alarm rate are given in Table 7.3. It shows that RADPLS and RAMBDPLS$_T$ is a compromise between DPLS and ADPLS. The monitoring chart for the overall process and the product quality, SPE$_Y$, detect more than 92% of the faulty samples. This rate is higher than the fault detection rate attained by Yin et al. (2012) where 90% of the faulty samples were detected following the application of conventional PLS, PCA and dynamic PCA. Monitoring charts for the individual block also detect more than 89% of the faulty samples. In

addition, the application of RADPLS and RAMBDPLS$_T$ approaches decrease the false alarm rate compared to DPLS as the FAR for the monitoring charts for the overall process and the SPE$_Y$ charts were reduced by 26% and 53% respectively. This a clear indication that the monitoring charts based on RADPLS and RAMBDPLS$_T$ are appropriate for the monitoring of the TEP.

Table 7.3 – Fault detection and false alarm rates based on ADPLS and AMBDPLS$_T$ for Fault (18).

Part	Fault detection rate	False alarm rate
Overall process	92.4%	6.7%
Block 1 – Reactor	88.9%	6.7%
Block 2 - Separator	94.8%	13.3%
Block 3 – Stripper	88.1%	6.7%
Block 4 – compressor	91.1%	6.7%
Block 5 – Materials	81.2%	6.7%
SPE$_Y$	86.6%	20%
Combined index	92.4%	0%

From Figures 7.8, 7.9 and 7.10, it can be seen that the strongest response to the fault is observed in SPE$_X$ which indicates that there is a significant change in the correlation structure of the predictor variables. The separator (2) and the compressor (4) blocks are the most affected units as shown in Figure 7.9. The rest of the blocks show less of a response to the fault. This behaviour is expected since the control valve connected to the separator and the compressor reacts to the fault and hence the impact would be less in units other than the source blocks. In addition it can be seen that the fault is detected earlier in the separator (i.e. detected at 11.36 hr) than for the other blocks. The fault is detected at 13.06 hr in the compressor, stripper and the reactor. The material block is the last unit and is affected by the fault (i.e. detected at 13.42 hr). The SPE$_Y$ chart detects the fault at 13.42 hr. This was expected again as the stripper is directly related to the product quality. The delay between the stripper and the quality product occurs because the stream exiting the stripper is sent to a unit which is not included in the analysis. The detection delays for SPE$_X$ chart for the overall process and individual unit operation are summarized in Table 7.4.

The Hotelling's T^2 chart shows a much smaller response compared to SPE_X. It can be seen that the Hotelling's T^2 charts violate the limits which indicate that there is abnormal variation within the predictor variables or some of them and therefore an abnormal variation of the entire process but stabilize after sufficient time, i.e. it will reach a new steady state after a certain period of time, 12 hr to 19 hr from the onset of the fault. This is expected from engineering prospective because as the control loop reacts to the fault but stabilizes the process. During the stabilization process, the relationship between the predictor variables changes and this is reflected in Hotelling's T^2. The detection delays for the Hotelling's T^2 charts are given in Table 7.4. As shown for SPE_X charts, the fault is detected earlier, at 12.12 hr, in the Hotelling's T^2 chart for the separator block compared to other units where the fault was detected at 13.24 hr, 13.42 hr 13.42 hr for the compressor, reactor and stripper respectively. The materials block detects the fault at 14.18 hr as it the last unit to be affected by the fault.

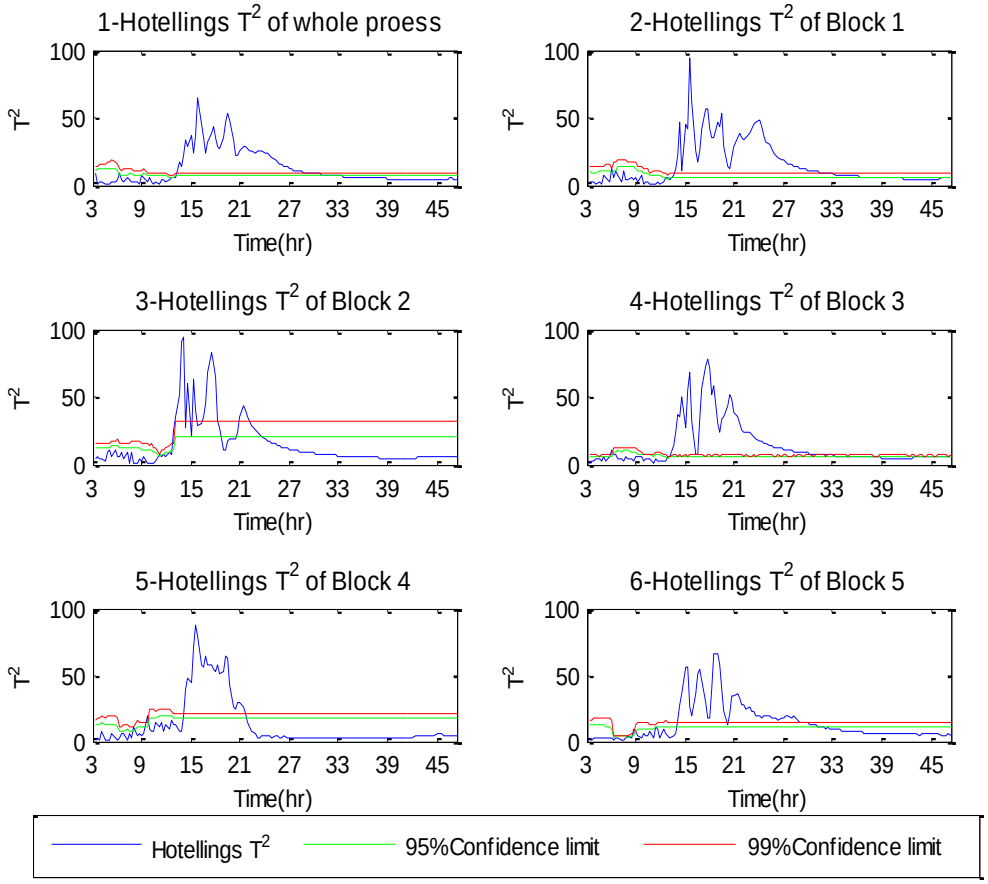

Figure 7.8 - Hotelling's T^2 for (1) overall process and (2-6) individual blocks based on RADPLS and $RAMBDPLS_T$ approach – Fault (18)

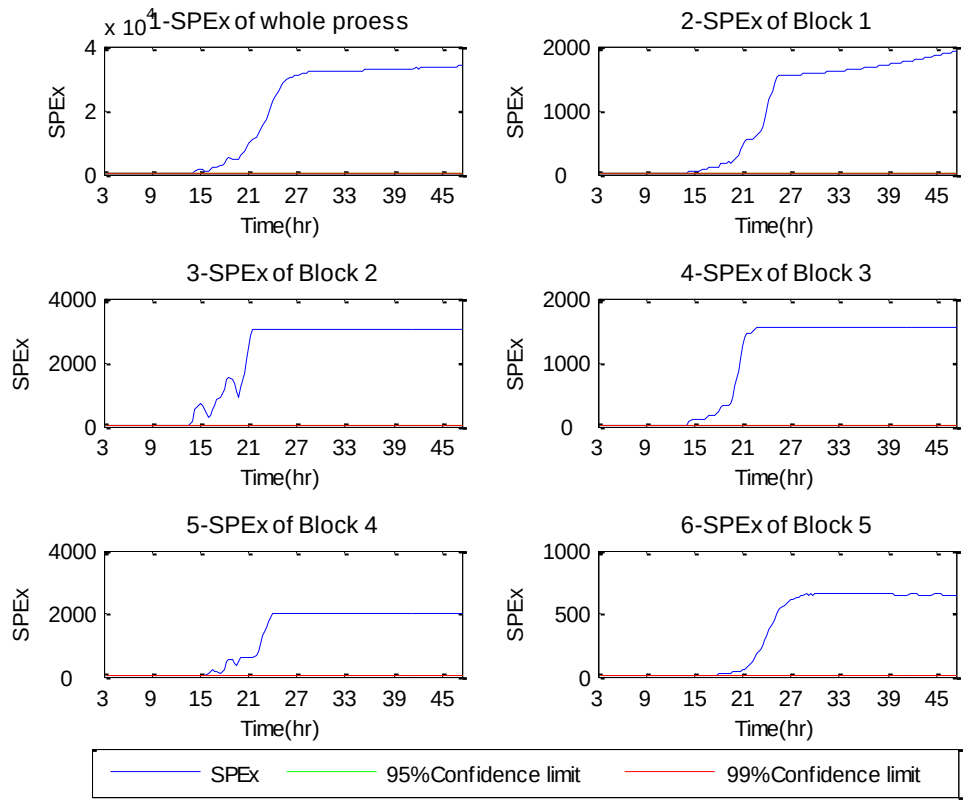

Figure 7.9 - SPE_X for (1) overall process and (2-6) individual blocks based on RADPLS and $RAMBDPLS_T$ approach –Fault (18)

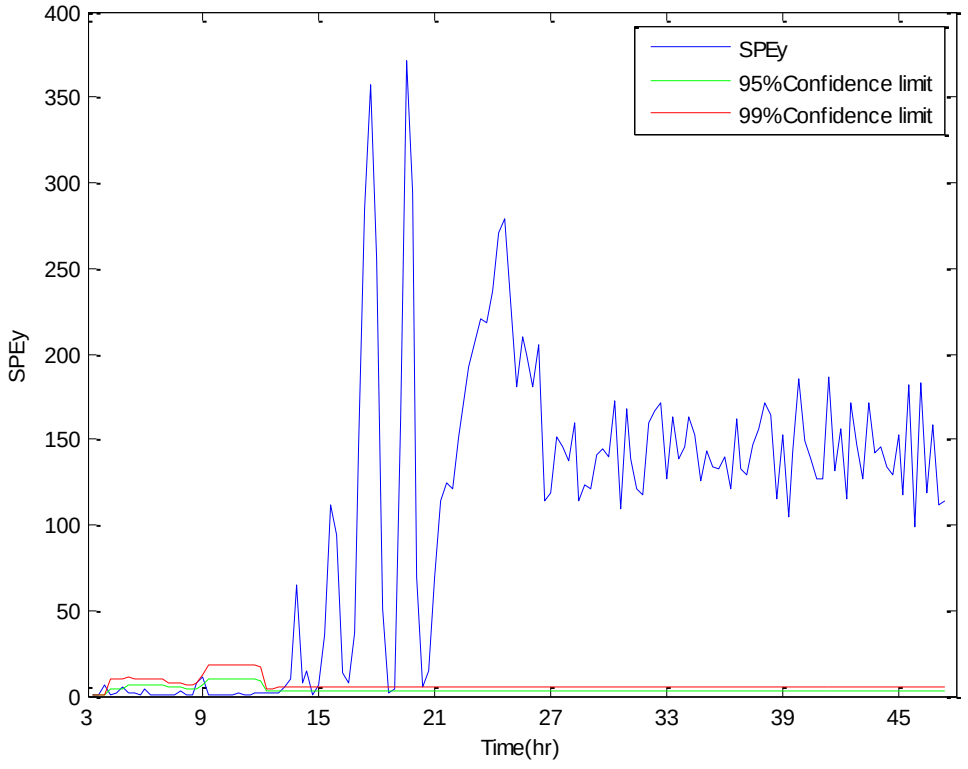

Figure 7.10- SPE_Y for the TEP based on RADPLS – Fault (18)

The detection delays recorded for Fault (18) following the application of RADPLS and $RAMBDPLS_T$ is less than the time delays provided by Chiang et al. (2001) for the same fault from the application of principal component analysis (PCA) and dynamic PCA. Chiang et al. (2001) noted that Fault (18) was detected in the Hotelling's T^2 and SPE_X monitoring charts for the overall process at 12.39 hr and 12.12 hr, which are 9 min and 18 min respectively after the time recorded in this work.

Table 7.4 – Detection delays for Fault (18)

Part	Chart	Time delay (min)	Detection time (hr)	Time delay(sample)
Overall process	Hotelling's T^2	270 min	12:30 hr	15 samples
	SPE_X	234 min	11:54 hr	13 samples
	SPE_Y	342 min	13:42 hr	19 samples
Block 1 Reactor	Hotelling's T^2	342 min	13:42 hr	19 samples
	SPE_X	306 min	13:06 hr	17 samples
Block 2 Separator	Hotelling's T^2	252 min	12:12 hr	14 samples
	SPE_X	216 min	11:36 hr	12 samples
Block 3 Stripper	Hotelling's T^2	342 min	13:42 hr	19 samples
	SPE_X	306 min	13:06 hr	17 samples
Block 4 compressor	Hotelling's T^2	324 min	13:24 hr	18 samples
	SPE_X	306 min	13:06 hr	17 samples
Block 5 Materials	Hotelling's T^2	378 min	14:18 hr	21 samples
	SPE_X	342 min	13:42 hr	19 samples

The same observations can be observed following the application of DPLS, $MBDPLS_T$, ADPLS, $AMBDPLS_T$, RADPLS and $RAMBDPLS_T$ for faults 1 and 13 as presented the following sections.

7.4.2 Case Study on Fault (1)

For Fault (1), a step change is introduced to the A/C ratio in stream 4. The process under normal operating conditions (NOC) has a 0.485, 0.005 and 0.510 mole fraction of A, B and C components in stream 4, respectively (Figure 7.1). When Fault (1) affects the process, an increase in the C feed ratio and decrease in the A feed ratio in stream 4 occurs. Under fault conditions, all the variables associated with the material balance including the pressure and level change materialising in faulty conditions (Chiang et al., 2001). Figure 7.11 show a comparison of the behaviour of variable A feed (z_1 in Table 6.3) under normal operating conditions (NOC) and under Fault (1). A significant

difference is observed between the two cases. Furthermore, half of the variables deviate from their normal operating conditions as a result of the fault (i.e. variables associated with material balance)

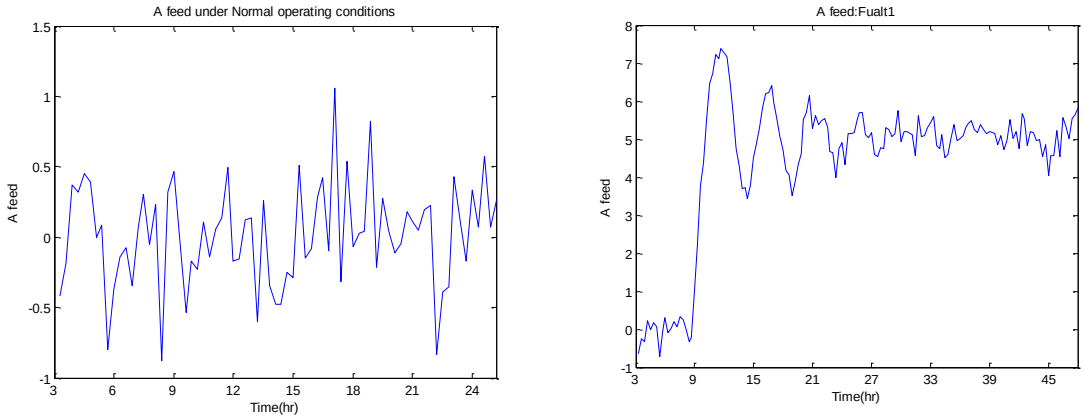

Figure 7.11 – Comparison of A feed for NOC and Fault (1)

The monitoring charts for the univariate statistics, Hotelling's, SPE_X and SPE_Y for the overall process and the individual units from the application of DPLS, $MBDPLS_T$, ADPLS and $AMBDPLS_T$ are given Appendix E. The observations following the application of these approaches for Fault (1) are similar to these for Fault (18). The quantitative results (Table 7.5) show that the monitoring charts for the overall process and the quality variable following the application of DPLS and $MBDPLS_T$ detect 97.8 % and 92.6% of the faulty samples respectively. More specifically, blocks 1, 3-5 detect 97.2 % of the faulty samples and block 2 and the SPE_Y detect 92.6 % of the faulty samples. However, the false alarm rates, for the period prior to the introduction of the fault, are very high for the overall process and the individual unit operations as shown in Table 7.5. The false alarm rate for the overall process is 33% and 60% for the reactor unit. In addition, the FAR for the SPE_Y is also high with 73.3% of the samples that represent normal operating conditions violating the confidence limits. This occurs because the confidence limits used are calculated based on the calibration data set which may not contain sufficient information to describe the current behaviour of the process.

The monitoring results from the application of ADPLS and $AMBDPLS_T$ are given in Appendix E. As observed in Fault (18), the monitoring statistics indicate the presence of the fault in the overall process and the individual unit. However, in these charts the confidence limits are allowed to adapt to the change in the process resulting in the monitoring statistics remaining within statistical control. Consequently the process is considered within statistical control state. Not only do the limits adapt to the change, but

the samples generated during the process disturbance are included in the model update. This results in decreasing the significance of the fault's effect on the monitoring charts.

The quantitative results for fault detection and the false alarm rates are presented in Table 7.5. It can be seen that the false alarm rate is significantly decreased compared to the fixed parameter DPLS approach especially for the overall process, block 1 and the monitoring chart for the output space. However, the fault detection rate decreases since the confidence limits are allowed to adapt to the changes in the monitoring statistics. From Table 7.5, it can be seen that the fault detection rate for all the individual units decreased by more than 70% compared to DPLS. Moreover, the FDR for the overall process is 84% less than the FDR based on DPLS. This indicates that the adaptive property is an advantage for a process representing nominal operation but there is a need for an indicator to stop the adaption procedure when the process is affected by a fault. For that, RADPLS and RAMBDPLS$_T$ is used.

The monitoring charts following the application of RADPLS and RAMBDPLS$_T$ are given in Figures 7.12, 7.13, 7.14 and 7.15. The combined index is presented in Figure 7.12 and it clearly indicates the process is out of statistical control. From the monitoring charts for the univariate statistics, it can be seen that the limitations observed following the application of DPLS and ADPLS, i.e. an increase in the false alarm rate when the process represents normal operation and a decrease in the fault detection rate when the process is under fault conditions respectively, are overcome and hence the monitoring charts can be interpreted appropriately. The FDR for the combined index is 97.8% (Table 7.5)

Table 7.5 - False alarm and Fault detection rates based on monitoring approaches for Fault (1).

Part	DPLS MBDPLS$_T$		ADPLS AMBDPLS$_T$		RADPLS RAMBDPLS$_T$	
	FAR	FDR	FAR	FDR	FAR	FDR
Overall process	33.3 %	97.8 %	6.7 %	12.8 %	6.7 %	97.8%
Block 1 – Reactor	60 %	97.0 %	6.7 %	16.5 %	6.7 %	97.0%
Block 2 Separator	6.7 %	92.6 %	6.7 %	18.8 %	6.7 %	97.0%
Block 3 – Stripper	6.7 %	97.0 %	6.7 %	20.3 %	6.7 %	97.8%
Block 4 – compressor	13.3 %	97.0 %	13.3 %	22.6 %	13.3 %	97.0%
Block 5 Materials	13.3 %	97.0 %	6.7 %	15.8 %	6.7 %	97.0%
Quality variables	73.3 %	92.6 %	6.7 %	10.5 %	6.7 %	97.8%
Combined index	-	-	-	-	0%	97.8%

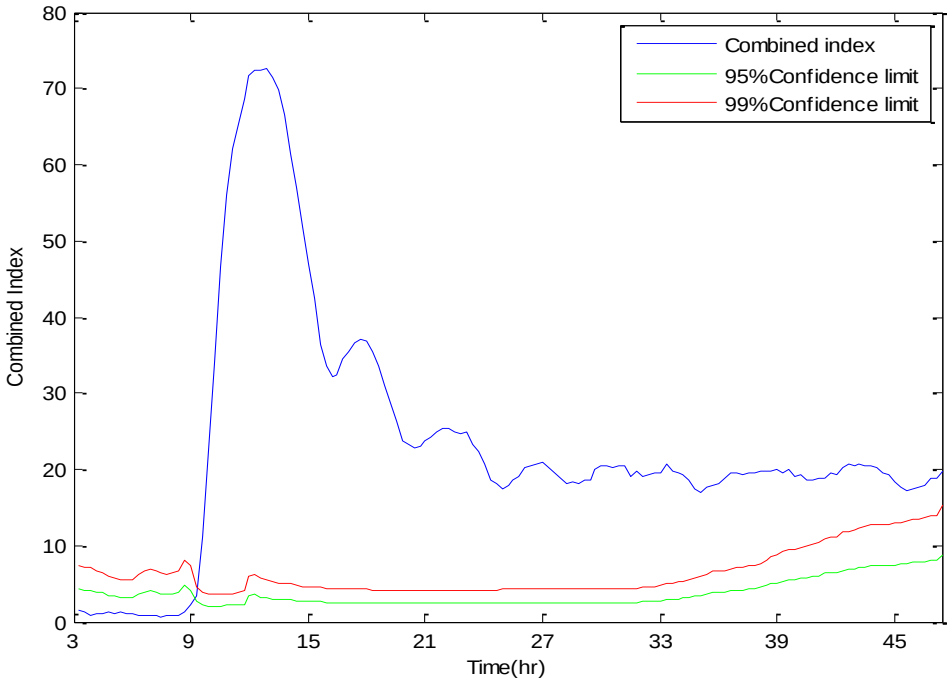

Figure 7.12 – Combined index for the TEP based on RADPLS and RAMBDPLS$_T$ approaches – Fault (1)

From Figure 7.13, it can be seen that the most significant response in term of breaching the limits is observed in the SPE$_X$ charts (Figure 7.13- subfigure 1). This indicates that the fault causes a significant change in the correlation structure of the predictor variables. This is correct since the fault occurs in the A/C ratio (total feed) and most of the predictor variables associated with the material balance including level, pressure and compositions in the process are affected. From the SPE$_X$ plots for the individual blocks, it can be seen that the fault is detected in all the blocks but with different level of significance. Block 5 (materials) and block 3 (stripper), show the strongest response which is expected since the fault occurs in the materials block and thus affects the stream going to the stripper prior to its propagation to the remaining blocks. Since the operation in the stripper is directly related to the quality product, the monitoring statistics of the output space indicates that the product quality variable is also affected by the fault (Figure 7.14). The other blocks are also affected by the fault but the impact is less than for the materials and stripper blocks. This is expected since the control loops start to react to the fault and hence, the effect of the fault reduces.

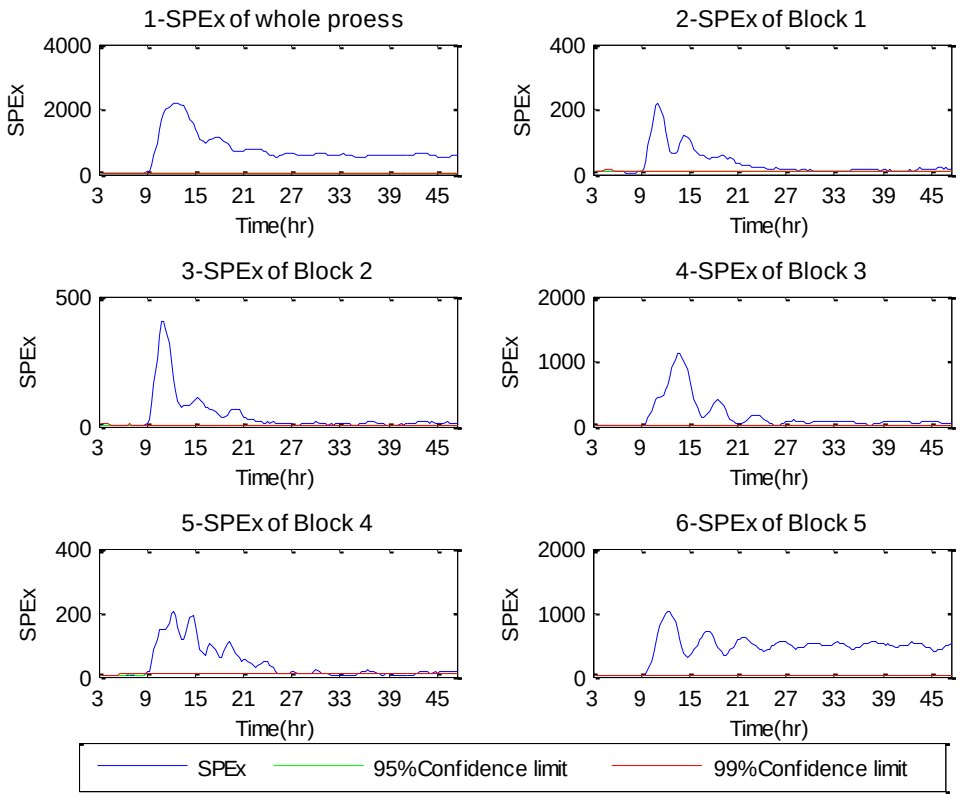

Figure 7.13 - SPE_X for (1) overall process and (2-6) individual blocks based on RADPLS and $RAMBDPLS_T$ approaches – Fault (1)

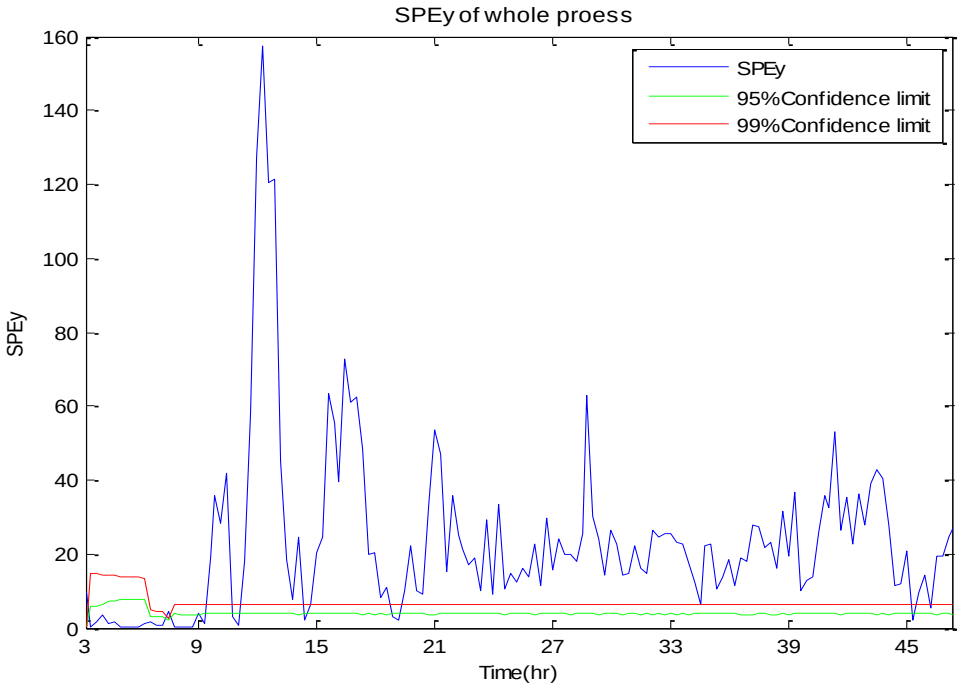

Figure 7.14 - SPE_Y for the TEP based on RADPLS approach – Fault (1).

Figure 7.15 shows the Hotelling's T^2 monitoring charts for the whole process (sub-figure 1) and the individual blocks (sub-figures 2-6). Hotelling's T^2 for the whole process indicates that there is abnormal variation within the predictor variables and the process stabilised after sufficient time. This is expected from an engineering prospective because as the control loop reacts to the fault and stabilizes the process, it will reach to a new steady state after a certain period of time, i.e. 7 hr post the onset of the fault. During the stabilization process, the variation within the predictor variables changes and this is reflected in Hotelling's T^2. The same observation can be seen in the monitoring charts for the individual unit operations. The variation in the process variables has changed significantly as a result of the fault. However, the control system reacts to the fault and stabilizes the process.

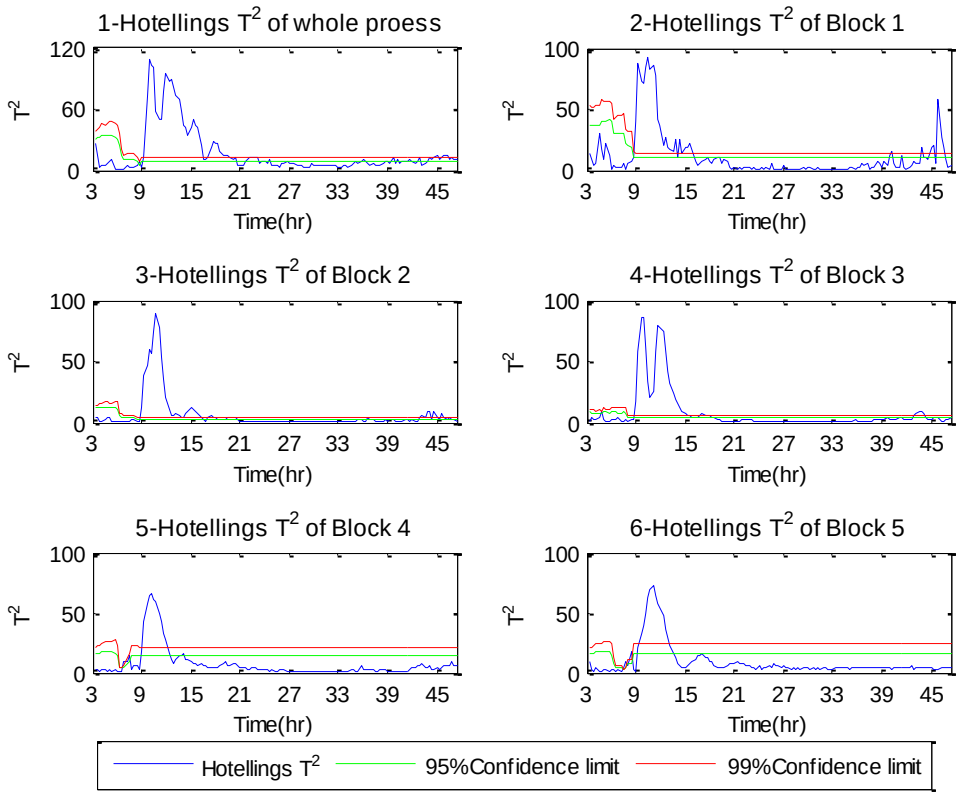

Figure 7.15 - Hotelling's T^2 for (1) overall process and (2-6) individual blocks based on RADPLS and RAMBDPLS$_T$ approach – Fault (1)

Table 7.5 summarise the fault detection rate and false alarm rate following the application of RADPLS and the RAMBDPLS$_T$. This approach results in a reduction in the number of false alarms when the process represents nominal operation compared with DPLS. The most significant improvement is in the FAR with the level for the overall process decreasing by 26.3% and for SPE$_Y$ it falls by 66.6%. The fault detection rate improves compared to ADPLS as the overall process and all the individual part detect more than 95% of the faulty samples.

The detection delays for Fault (1) are small, one to three samples corresponding to 18 min to 54 min for most of the individual blocks, compared to the detection delay for Fault (18). This conclusion was also noted by Chiang et al. (2001) who stated that the detection delay for Fault (1) was 21 min for the overall process following the application of PCA and DPCA. The detection delays for the overall and individual unit monitoring charts are given in Table 7.6. It can be seen that fault is detected earlier in materials block and it then propagates to other blocks and detected after one sample in the reactor, stripper and then in the separator and compressor, i.e. 18 min difference.

The presence of the detection delay for the TEP for all the faults is acceptable based on the time constant, approximately 2 hr, which indicates that the process requires time to respond to a change in the manipulated variables. Therefore, the fault is expected to be indicated in the monitoring charts after a period of time. In addition, this is a continuous system where the fault and the reaction of the control valves to the fault propagates between process units. Other important factors for fault propagation are the magnitude of the fault, the sampling interval and the blocking structure of the system. For example, Libo and Xiangdong (2009) show that the impact of Fault (1) for the TEP following the application of multiblock PCA was observed in different blocks at the same time.

Chen and McAvoy (1998) showed that there is a time delay in fault propagation through the different units. In their case study, they applied a larger fault magnitude, i.e. 4 times larger step change compared to the original Fault (1), hence the impact and the transfer speed differs significantly. Chen and McAvoy (1998) pointed out that for larger faults and a 5 min sampling interval, the fault was detected in the stripper at sample number 61 and it was detected in the separator at sample number 71, i.e. 10 samples difference. This corresponds to 50 min of operation, approximately 3 samples based on 18 sampling interval.

Table 7.6 – Detection delays for Fault (1)

Part	Chart	Time delay (min)	Detection Time (hr)	Time delay(sample)
Overall process	Hotelling's T^2	36 min	8:36	2 samples
	SPE_X	18 min	8:18	1 samples
	SPE_Y	54 min	8:54	3 samples
Block 1 Reactor	Hotelling's T^2	54 min	8:54	3 samples
	SPE_X	36 min	8:36	2 samples
Block 2 Separator	Hotelling's T^2	54 min	8:54	3 samples
	SPE_X	54 min	8:54	3 samples
Block 3 Stripper	Hotelling's T^2	54 min	8:54	3 samples
	SPE_X	36 min	8:36	2 samples
Block 4 compressor	Hotelling's T^2	3 min	8:54	3 samples
	SPE_X	3 min	8:54	3 samples
Block 5 Materials	Hotelling's T^2	54 min	8:54	3 samples
	SPE_X	18 min	8:18	1 samples

7.4.3 Case study on Fault (13)

Fault 13 represents a slow drift in the reaction kinetics. Figure 7.16 shows a comparison between the separator temperature under normal operating conditions and during the fault period. However, a few variables behave in a similar manner to the separator temperature and the rest of the variables remain within the steady state. Although, few variables were affected by the fault, it can be seen that the magnitude of the variable response to the fault is large compared to the normal operating condition behaviour.

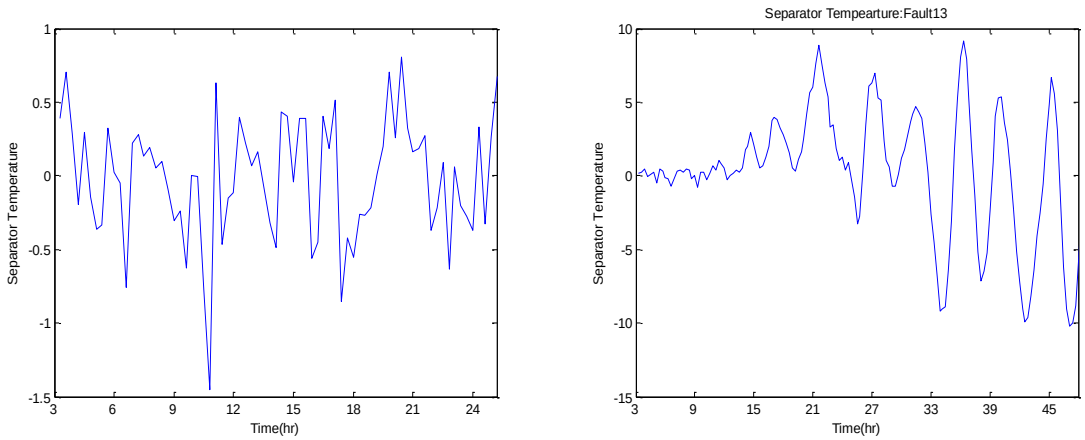

Figure 7.16 – Comparison of separator temperature for NOC and Fault (13)

Fault (13) was introduced after 8 hr of nominal operation and hence, it is expected that the monitoring metrics will be statistical control. The DPLS monitoring charts are given in Appendix E. As for in Faults (18) and (1), the statistical indices, SPE_X for the overall process and individual unit operation and SPE_Y violate the limits prior to the onset of the fault. Consequently, the number of false alarms for this period increased whilst the process was operating under normal conditions. The fault detection and false alarm rates are summarised in Table 7.7. It can be seen that the overall process, as well as the individual blocks, have the ability to detect more than 90% of the faulty sample. On the other hand, they generated a high false alarm as the FAR for the overall process and the individual charts is more than 33% of the samples. For the output space, the FAR is 46.7%. Hence, the DPLS model gives raise the false alarms and is inappropriate for monitoring the process even though it successfully detects the fault.

The monitoring results from the application of ADPLS and $AMBDPLS_T$ are given in Appendix E where the same conclusion as from Faults (1) and (18) can be derived, i.e. they reduce the false alarm rate following the application of DPLS and $MBDPLS_T$ for the overall and individual unit operation monitoring charts. However, since the confidence limits are updated, the fault is included and hence the process remains within a state of statistical control and the fault detection rate decreases. The fault detection rate and the false alarm rate following the application of ADPLS are presented in Table 7.7. The false alarm rate has decreased significantly compared with that attained for DPLS. However, the fault detection rate as shown in Table 7.7 decreases indicating a limitation of the monitoring approach and the need for a threshold to stop the adaption procedure when the incoming samples are generated from a process disturbance. Therefore, RADPLS and $RAMBDPLS_T$ are considered.

The monitoring results from the application of RADPLS and $RAMBDPLS_T$ are given in Figures 7.17, 7.18, 7.19 and 7.20 for the combined index, the whole process and the individual blocks. Table 7.7 summarise the fault detection and false alarm rates which indicate that the monitoring charts for the overall process detect more than 95.5% of the faulty samples. This rate is comparable to the FDR provided by Yin et al. (2012), 95.25% which indicated that for Fault (13), the change in the sampling interval does not result in miss detection of the fault. The FDR for the individual unit operation indicate that 92% to 95% of the faulty samples were detected. This rate is higher compared to the FDR following the application of ADPLS and $AMBDPLS_T$. On the other hand, the FAR for the overall process and the individual unit operations decreased compared to

DPLS as shown in Table 7.7. Hence, the monitoring charts can monitor process performance appropriately.

Table 7.7 - False alarm and Fault detection rates based on all monitoring approaches for Fault (13)

Part	DPLS MBDPLS$_T$		ADPLS AMBDPLS$_T$		RADPLS RAMBDPLS$_T$	
	FAR	FDR	FAR	FDR	FAR	FDR
Overall process	33.3%	93.3%	6.7%	27.8%	6.7%	95.5%
Block 1 – Reactor	33.3%	92.4%	6.7%	25.6%	6.7%	92.4%
Block 2 Separator	33.3%	93.3%	6.7%	25.6%	6.7%	95.5%
Block 3 – Stripper	33.3%	93.3%	6.7%	33.3%	6.7%	95.5%
Block 4 - compressor	20%	91.1%	13.3%	29.3%	13.3%	94%
Block 5 Materials	13.3%	92.4%	6.7%	27.1%	6.7%	92.4%
Quality variables	46.7%	89.6%	20%	12.0%	20%	75%
Combined index	-	-	-	-	0%	95.5%

Figure 7.17 shows the time series plot of the combined index. The monitoring chart for the combined index gives an enhanced fault detection index as it is calculated as a weighted combination of Hotelling's T^2 and SPE_X for the whole process. The combined index provides an indication as when to stop updating the model and the confidence limits because the process is affected by a fault thereby ensuring the robustness of the model, i.e. the model represent the process behaviour and it is resistance to outlying samples.

Figure 7.18 shows the monitoring statistics of the quality variable, SPE_Y, where it clearly indicates that the product quality variable is affected by the fault. It is shown that 75% of the faulty samples related to the product quality were successfully detected. Figures 7.19 and 7.20 show the monitoring charts for Hotelling's T^2 and SPE_X of the whole process (sub-figure 1). It can be seen from the process monitoring charts that the process remains within statistical control prior to the introduction of the fault, the false alarm rate for the overall process decreased compared to monitoring charts following the application of DPLS. Additionally, they indicate that the process is affected by the fault as 95% of the faulty samples were successfully detected.

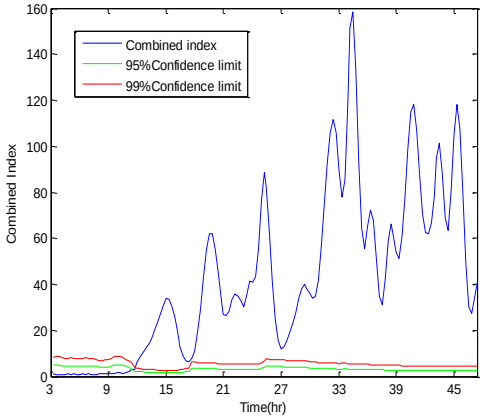

Figure 7.17 – Combined index for the TEP based on RADPLS and RAMBDPLS$_T$ approach – Fault (13)

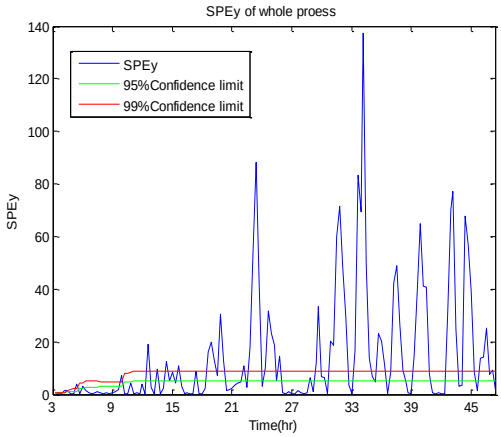

Figure 7.18- SPE$_Y$ for the TEP based on RADPLS and RAMBDPLS$_T$ approaches – Fault (13)

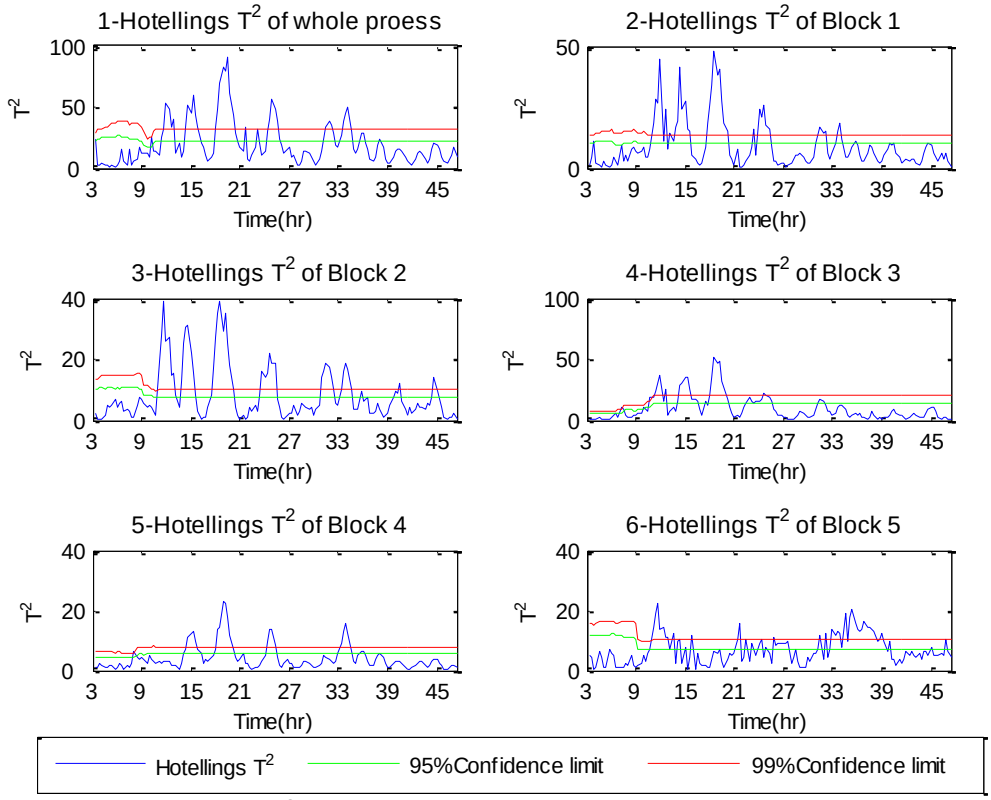

Figure 7.19 - Hotelling's T^2 for (1) overall process and (2-6) individual blocks based on RADPLS and RAMBDPLS$_T$ approaches – Fault (13)

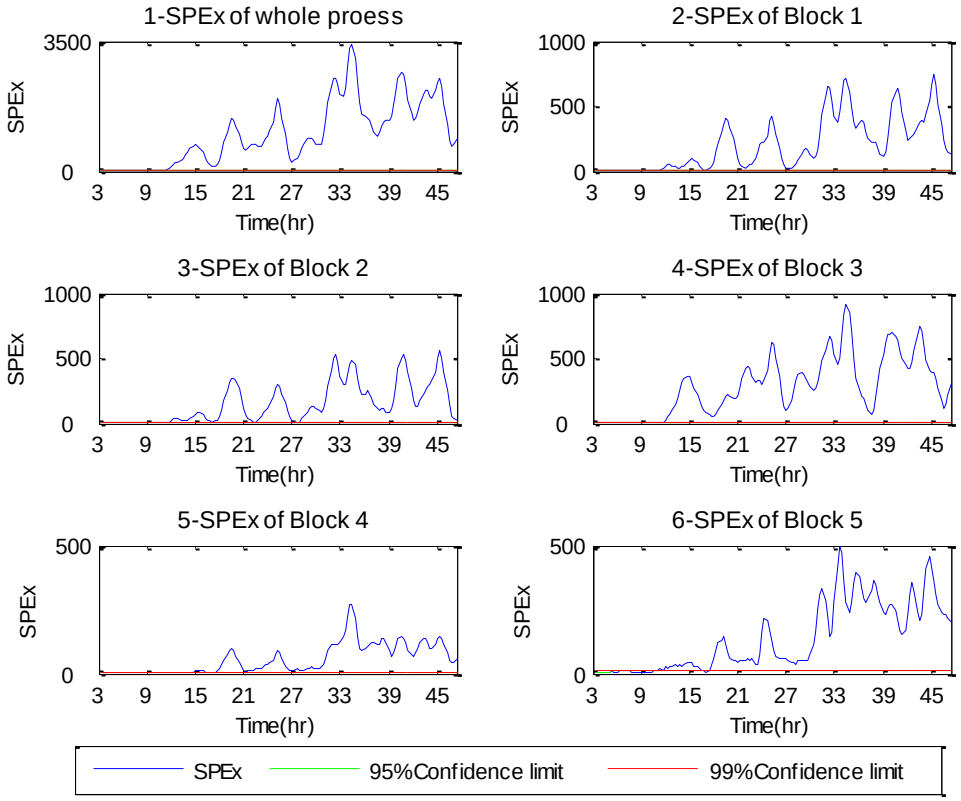

Figure 7.20 - SPE_X for (1) overall process and (2-6) individual blocks based on RADPLS and $RAMBDPLS_T$ approach – Fault13

The strongest response to the fault was observed in the SPE_X metric. More specifically, the reactor block (1), separator block (2) and stripper block (3) show the most significant effect resulting from the fault with the other blocks being less affected. In addition, the first three blocks indicate the fault earlier than the compressor and materials blocks. This is expected from a chemical engineering prospective as the fault is in the reaction kinetics which has a direct relationship with the reaction rate. In addition, most of the predictor variables associated with the reaction rate such as level, pressure and temperature are affected by this fault and since these variables are contained in different blocks, the fault affects all the process units but with different levels of impact. Table 7.8 summarizes the detection delays for the overall process and the individual unit operations. The overall SPE_X chart detects the fault at 9.48 hr, i.e. 108 min after the introduction of the fault. The recorded detection delay is 3 min earlier than the detection delay provided by Chiang et al. (2001) following the application of PCA and DPCA. Additionally, it can be seen that the fault was indicated at 9.12 hr, 9.48 hr and 9.48 hr for the separator, reactor and stripper respectively. The fault is then detected at 10.06 hr and 11.18 hr for the compressor and materials units respectively.

A much smaller effect is observed in Hotelling's T^2 and SPE_Y but they are still significant. From Figure 7.19, it can be seen that the monitoring charts for the overall process and individual unit operations violate the confidence limits with different levels of significance. The SPE_Y monitoring chart also violate the limits due to the fact that the operations in the stripper (block 3), which is related to the production of the quality variables, are affected by the fault and hence the product quality will be affected. Consequently the reaction in the stripper is affected by the slow drift and the production of product G is affected.

The detection delays for the Hotelling's T^2 and SPE_Y charts are summarised in Table 7.8. The Hotelling's T^2 chart for the overall process detects the fault at 10.24 hr, i.e. 144 min after the introduction of the fault. This delay is also comparable to the detection delay reported by Chiang et al. (2001) following the application of PCA and DPCA. The individual unit monitoring charts is detected earlier for the stripper and the reactor at 10.06 hr and 11.00 hr respectively. Other units detect the fault 18 min later than the reactor block as shown in Table 7.8.

Table 7.8 – Detection delays for Fault (13)

Part	**Chart**	**Time delay (min)**	**Detection Time (hr)**	**Time delay(sample)**
Overall process	Hotelling's T^2	144 min	10:24 hr	8 samples
	SPE_X	108 min	9:48 hr	6 samples
	SPE_Y	126min	10:06 hr	7 samples
Block 1 Reactor	Hotelling's T^2	198 min	11:18 hr	10 samples
	SPE_X	108 min	9:48 hr	6 samples
Block 2 Separator	Hotelling's T^2	198 min	11:18 hr	11 samples
	SPE_X	72 min	9:12 hr	4 samples
Block 3 Stripper	Hotelling's T^2	126 min	10:06 hr	7 samples
	SPE_X	108 min	9:48 hr	6 samples
Block 4 compressor	Hotelling's T^2	198 min	11:18 hr	11 samples
	SPE_X	126 min	10:06 hr	7 samples
Block 5 Materials	Hotelling's T^2	198 min	11:18 hr	11 samples
	SPE_X	198 min	11:18 hr	11 samples

7.4.4 Case study on Fault (10)

Fault (10) represents a random variation in the C feed temperature in stream 4. Figure 7.21 shows a comparison between a nominal stripper temperature and the behaviour pertaining to Fault 10. The investigation shows that most of the variables behave in a similar manner to the stripper temperature, i.e. large and fast oscillation resulting from the random variations.

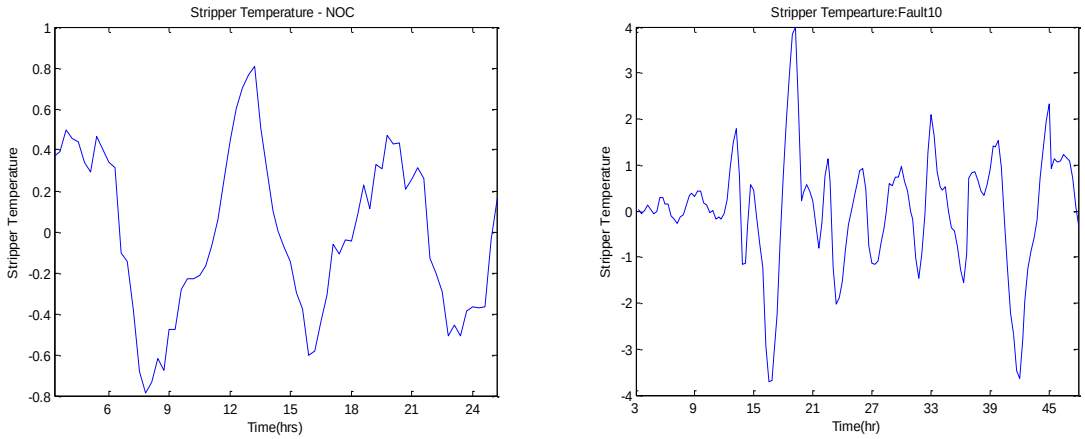

Figure 7.21 – Comparison of Stripper temperature for NOC and Fault (10)

The DPLS algorithm described in §6.4.2.2 was applied to the data generated incorporating Fault (10). The DPLS monitoring charts are given in Appendix E. The results following the application of DPLS and MBDPLS$_T$ are similar to these for Faults (1), (13) and (18). They show an increase in the false alarm rate prior to the introduction of the fault (Table 7.9). For example, the false alarm rate for SPE$_Y$ is 40%. The violation was observed for the monitoring charts for the overall process and for the individual unit operation indicating that the monitoring charts are inefficient. In addition, the fault detection ability for the whole process is low, i.e. 86.5%, compared with the other faults. However, it is higher than the FDR provided by Yin et al. (2012), 60.5%, 72% and 82.63% following the application of PCA, DPCA and conventional PLS respectively. Additionally, the fault detection ability of the individual unit operations was also less compared to the other faults with the FDR by 29.6 % and 53.3 % for the separator and reactor blocks respectively. It can then be concluded that the DPLS and MBDPLS$_T$ are inappropriate for constructing monitoring charts to monitor process performance.

The results from the application of ADPLS and AMBDPLS$_T$ to the TEP for Fault (10) are given in Appendix E. From the figures and the quantitative results (Table 7.9) it can

be concluded that ADPLS overcomes the limitations of DPLS. This is clearly seen in the reduction of the false alarm rate when the process represents nominal operation. However, the process remains within statistical control because the ADPLS allows the confidence limits to adapt to the change in the process and hence is statistically in control. The fault detection rate for the overall process is less compared to DPLS as the overall monitoring charts and the quality variable chart detect 25.6% and 8.3% of the faulty samples respectively. Furthermore, the monitoring charts for the individual units detect 14.3% to 25.6% of the faulty samples as shown in the Table 7.9. This significant reduction in the FDR indicates that the ADPLS and AMBDPLS$_T$ approaches are inappropriate for monitoring the TEP behaviour, hence RADPLS and RAMBDPLS$_T$ is considered.

The results following the application of RADPLS and RAMBDPLS$_T$ are given in Figures 7.22, 7.23, 7.24 and 7.25. Figure 7.22 shows the combined index for the TEP for Fault (10). Different to Faults (1), (13) and (18), the combined index fails to identify all the faulty samples as it only detects 70.7% compared to the other faults, where more than 90% of the faulty samples were detected. This may be a consequence of the following reasons:

- The process model updates incorrectly when the fault occurs due to the nature of the fault where the random variation, which represents large and fast oscillations, affects most of the variables and passes through the normal operating range. Consequently, some samples are identified as being generated from normal operation.
- The combined index is calculated as a function of the statistics (Hotelling's T^2 and SPE$_X$) and their limits. In the faulty period, some samples were identified as normal operating condition samples since they lie within the normal operating region, hence the limits are updated and used for the calculation of the combined index and its limit. This will have an impact on the functionality of the combined index as seen in Figure 7.22.

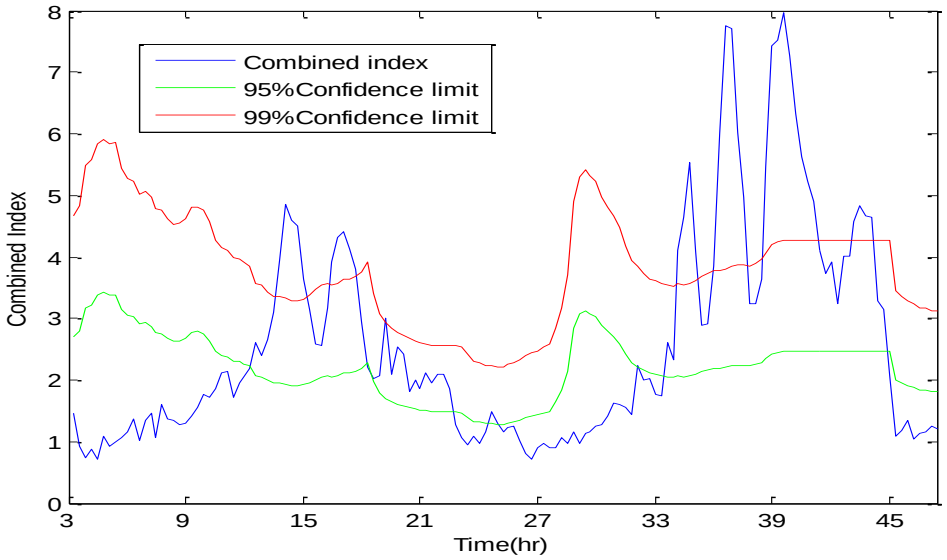

Figure 7.22 – Combined index for the TEP based on RADPLS – Fault (10)

The overall process detects 70.7% of the faulty samples which is comparable to the FDR provided by Yin et al. (2012), 60.5%, 72% and 82.63% following the application of PCA, DPCA and conventional PLS respectively. However, it is considered low compared to the detection ability for the other faults following the application of RADPLS and RAMBDPLS$_T$. The monitoring charts for the individual unit operations detect 37.6% to 69.1% of the faulty samples as shown in Table 7.9. This rate is decreased compared to the FDR for the other faults indicating that the functionality of the RADPLS and RAMBDPLS$_T$ is affected by the nature of the fault.

Table 7.9 - False alarm and fault detection rates based on all monitoring approaches for Fault (10).

Part	DPLS MBDPLS$_T$		ADPLS AMBDPLS$_T$		RADPLS RAMBDPLS$_T$	
	FAR	FDR	FAR	FDR	FAR	FDR
Overall process	13.3%	86.7%	6.7%	25.6%	6.7%	70.7%
Block 1 - Reactor	20%	53.3%	6.7%	16.5%	6.7%	38.3%
Block 2 Separator	6.7%	29.6%	6.7%	14.3%	6.7%	37.6%
Block 3 - Stripper	20%	86.7%	6.7%	23.3%	6.7%	69.1%
Block 4 - compressor	13.3%	70.4%	6.7%	21.8%	6.7%	47.4%
Block 5 Materials	6.7%	60%	6.7%	25.6%	6.7%	45.8%
Quality variables	40%	72.6%	26.7%	8.3%	26.7%	17.3%
Combined index	-	-	-	-	0%	70.7%

The monitoring charts for the overall process and the individual unit operation are given in Figures 7.23, 7.24 and 7.25. It can be seen that the fault is partially detected by the overall process and the individual unit operations. This observation is evaluated by the calculation of the FDR (Table 7.9). The detection delays for the overall and the individual unit monitoring charts are summarised in Table 7.10. It can be seen that the Hotelling's T^2, SPE_X and SPE_Y charts for the overall process detect the fault at 12.48 hr, 10.06 hr and 12.24 corresponding to 288 min, 126 min and 144 min respectively. These delays are comparable to the time delay attained by Chiang et al. (2001) following the application of PCA and DPCA. Additionally, the detection delay for the individual unit operation indicates that the fault is detected earlier in the stripper compared to the other blocks as the SPE_X and Hotelling's T^2 monitoring charts detect the fault at 10.24 hr and 10.42 hr respectively. The fault is then detected by the separator, reactor, compressor and finally the materials blocks. It is noticed that the monitoring indices fall back into a state of statistical control in some blocks which is expected as the nature of the fault is that of random variations. These variations force the process to deviate from the normal operating conditions, however, it may lead the process lying within the normal operating region hence the statistical indices remain within a state of statistical control.

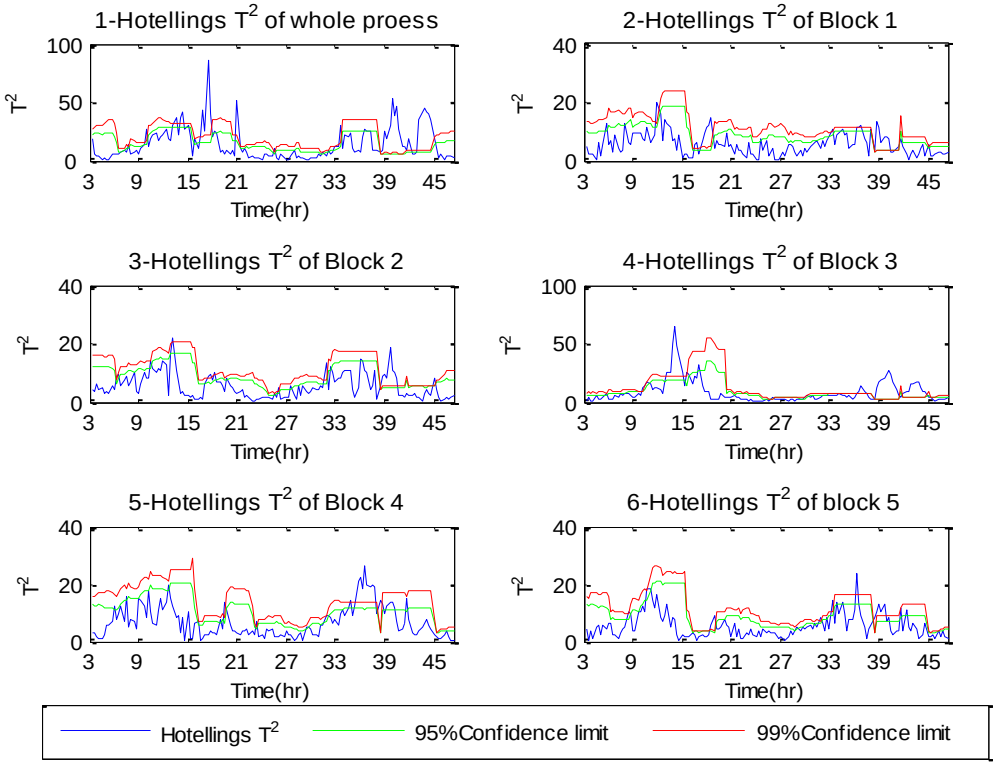

Figure 7.23 - Hotelling's T^2 for (1) overall process and (2-6) individual blocks based on RADPLS and $RAMBDPLS_T$ approaches – Fault (10)

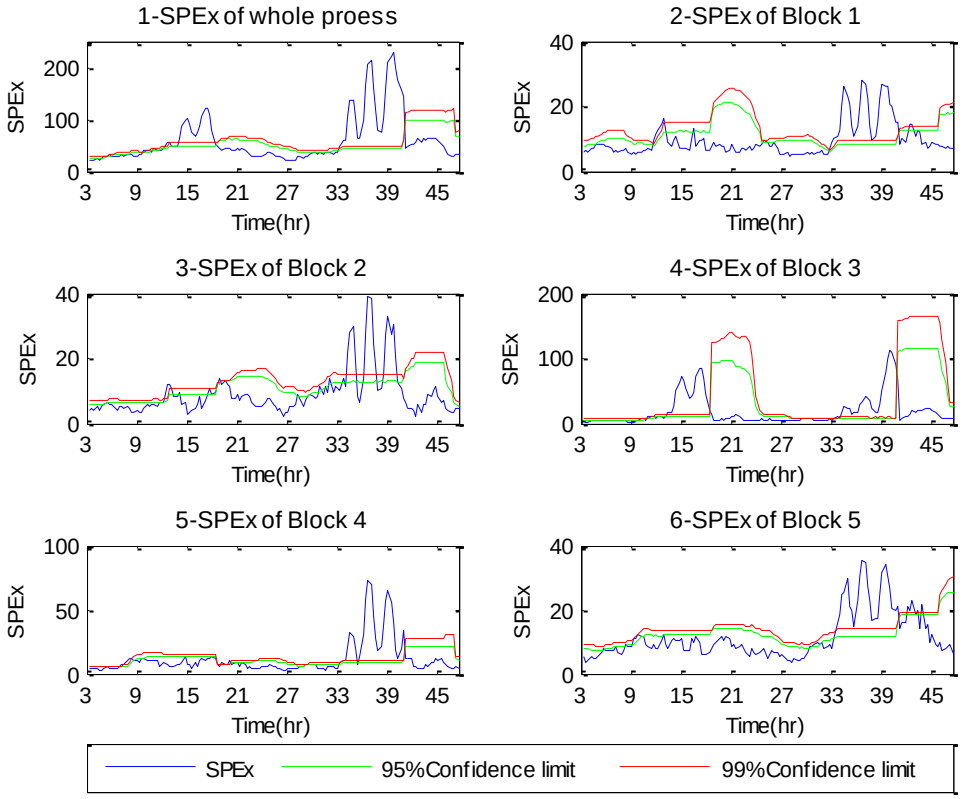

Figure 7.24 - SPE_X for (1) overall process and (2-6) individual blocks based on RADPLS and $RAMBDPLS_T$ approaches – Fault (10)

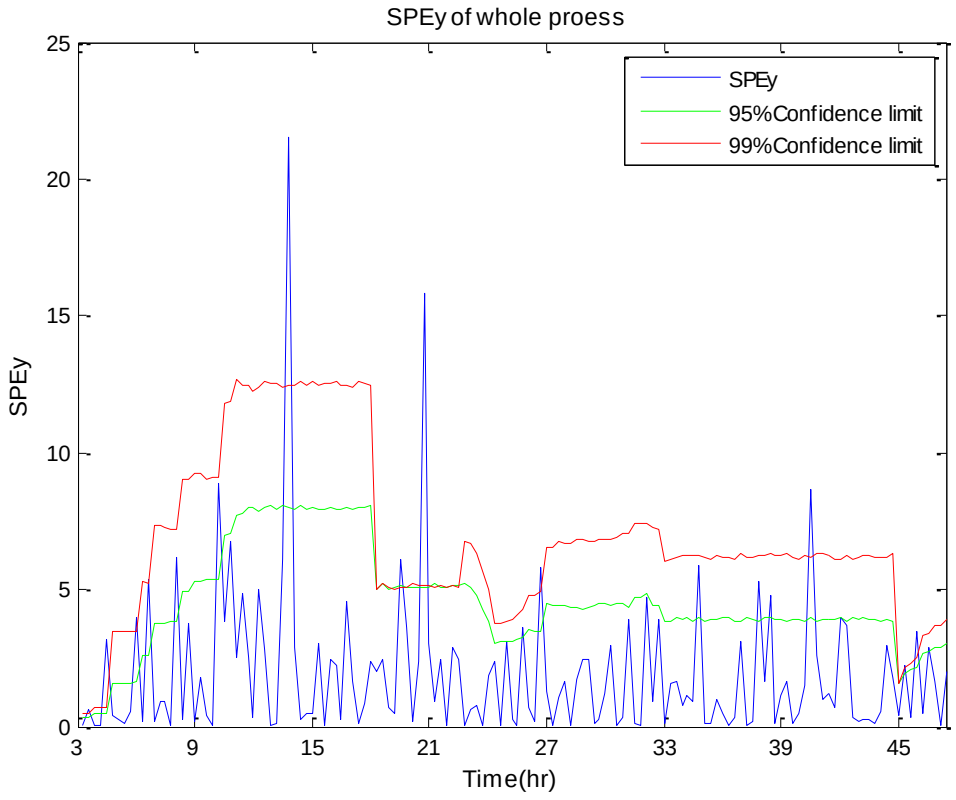

Figure 7.25- SPE_Y for the TEP based on RADPLS – Fault (10)

Table 7.10 – Detection delays for Fault (10)

Part	Chart	Time delay (min)	Detection Time (hr)	Time delay(sample)
Overall process	Hotelling's T^2	288 min	12:48 hr	16 samples
	SPE_X	126 min	10:06 hr	7 samples
	SPE_Y	144 min	10:24 hr	8 samples
Block 1 Reactor	Hotelling's T^2	234 min	11:54 hr	13 samples
	SPE_X	180 min	11:00 hr	10 samples
Block 2 Separator	Hotelling's T^2	162 min	10:42 hr	9 samples
	SPE_X	216 min	11:36 hr	12 samples
Block 3 Stripper	Hotelling's T^2	162 min	10:42 hr	9 samples
	SPE_X	144 min	10:24 hr	8 samples
Block 4 compressor	Hotelling's T^2	234 min	11:54 hr	13 samples
	SPE_X	180 min	11:00 hr	10 samples
Block 5 Materials	Hotelling's T^2	234 min	11:54 hr	13 samples
	SPE_X	198 min	11:18 hr	11 samples

7.5 Discussion and SWOT analysis

The quantitative results from the above case studies are compared in Figure 7.26 which shows the fault detection rate and false alarm rate for the three approaches for the four case studies, sub-figures a, b, c and d. It can be seen that the performance of RADPLS and the DPLS are similar. However, in the case of Fault (10) (i.e. random variations) the performance of RADPLS is affected and it fails to detect the fault. The reasons behind this observation were previously discussed in section 7.6.3. In addition, the fault detection ability for ADPLS is low compared to DPLS and RADPLS due to the adaption of the confidence limits.

On the other hand, it can be seen the false alarm rate which was calculated based on the three approaches for the different cases prior to the onset of the fault as the process was operated under normal operating conditions. In addition, the performance of the approaches is also compared for the validation data set. It can be seen that for DPLS the number of false alarms increases compared to ADPLS and RADPLS for both the faulty and validation data sets. Additionally, the performance of RADPLS is very similar to ADPLS in the case of the faulty data sets. However, when the algorithms were applied to the validation data set, RADPLS shows better performance compared to DPLS and ADPLS.

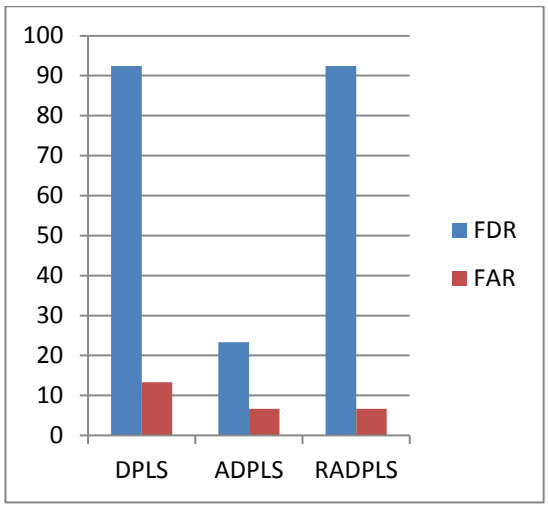

(a) Case 1 – fault (18)

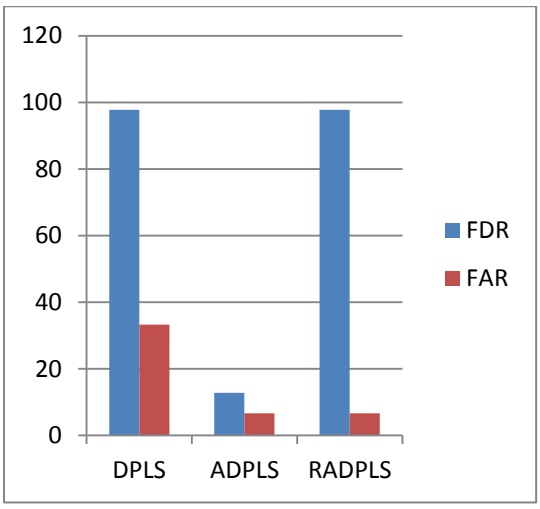

(b) Case 2 – fault (1)

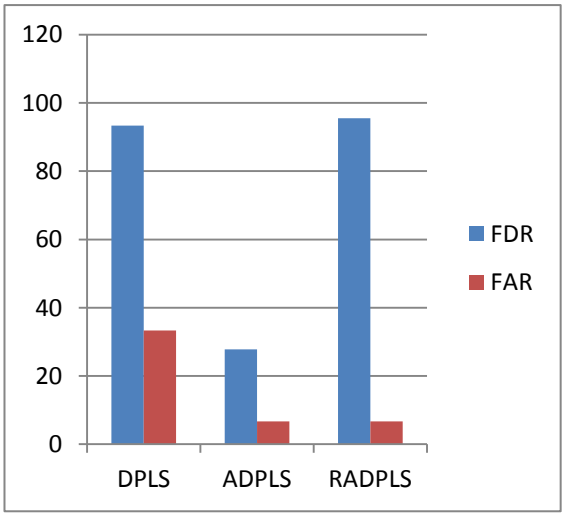

(c) Case 3 – fault (13)

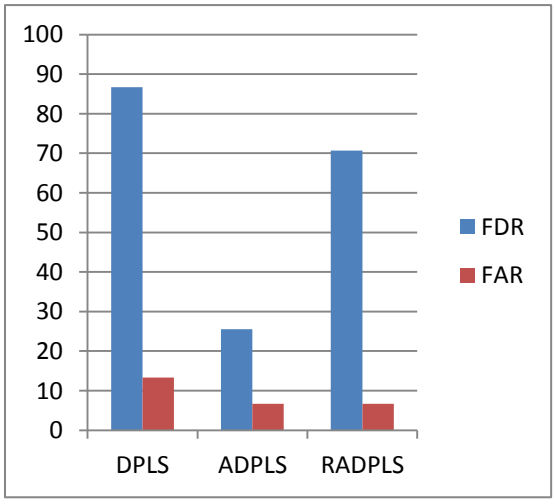

(d) Case 4 – fault (10)

Figure 7.26 - False alarm and fault detection rate for the three methods for the four different faults.

It can be concluded that RADPLS is a compromise between the other approaches as it increases the fault detection rate compared to ADPLS and decreases the false alarm rate compared to DPLS.

SWOT analysis (Strength, Weakness, Opportunities and Threat**)** is a tool used to structure qualitative or quantitative information and help organize information, present solutions, identify weaknesses and emphasize opportunities. In this work, a SWOT analysis is used to compare the performance of the proposed methods ADPLS and RADPLS (Table 7.11). The SWOT analysis is constructed based on the application of ADPLS and RADPLS to the TEP process.

Table 7.11 – SWOT analysis

Strengths	**Weaknesses**
ADPLS and AMBDPLS: - Adapts to process changes - False alarm rate is low - Easy to update the model and the confidence limits. - Ability to construct monitoring chart for the whole process and individual unit operations - Algorithm can deal with auto-correlated samples	**ADPLS and AMBDPLS:** - Updates the model when the sample represents an outlier or abnormal behaviour. - Low fault detection rate as the confidence limits are updated continuously hence, the process remain in state of statistical control.
RADPLS and RAMBDPLS: - Adapts to process changes - High false detection rate - Low false alarm rate - Resistant to statistical outliers - Resistant to non-conforming samples - Ability to construct monitoring chart for the whole process and individual unit operations - Enhanced monitoring system due to calculating an additional monitoring metric, the combined index. - Algorithm can deal with auto-correlated samples	**RADPLS and RAMBDPLS:** - Fails to identify a fault that has random variation or is of an oscillatory nature.
Opportunities	**Threats**
ADPLS and AMBDPLS: - Algorithm is useful when the data set is outliers free	**ADPLS and AMBDPLS:** - Most online data contain outliers -
RADPLS and RAMBDPLS: - The algorithm can helps the process operator by indicating abnormal behaviour. - The algorithm can be improved by incorporating other metrics	**RADPLS and RAMBDPLS:** - Time delay when sampling rate is too slow as it is required to check consecutive samples prior to model updating.

7.6 Chapter Summary and Conclusions

The approaches proposed in Chapter 6 were applied to the Tennessee Eastman process to test their efficiency in terms of fault detection and the reduction in the number of unwanted alarms (i.e. false alarms). The main conclusions are:

- From the implementation of the three methods to four different case studies, the RADPLS and RAMBDPLS$_T$ perform better than the other approaches. It can be seen as a compromise as it decreases the false alarm rate when the process represents nominal operations compared to DPLS and the MBDPLS$_T$. Furthermore, it increases the fault detection rate compared to ADPLS and AMBDPLS$_T$ (§6.7).
- However, the RADPLS and the RAMBDPLS$_T$ show a limitation when the fault represents random variation. This is due to the fact that the functionality of the combined index, which is affected by identifying samples which are faulty but would occur during normal operating conditions due to the oscillatory nature of the fault. Hence, the model and the confidence limits are updated incorrectly.
- Fault propagation was investigated for a continuous dynamic process. From the case study, it can be concluded that fault propagation in continuous dynamic system can be investigated through the calculation of the time delay between the unit operations. In addition the significance level of the monitoring charts indicates the units that are affected by the fault. More investigation needs to be conducted through contribution plots to investigate the variables most related to the fault.

Chapter 8

Conclusions and Future Work

8.1 Summary

The aim of this thesis was to contribute to the field of statistical monitoring of continuous systems exhibiting complex dynamic behaviour. The application of multivariate statistical projection approaches namely, Partial Least Squares and its extensions were investigated for the construction of monitoring schemes for both the whole process as well as for individual unit operations.

Specifically, the first part of the thesis reviewed the underpinning multivariate projection technique of partial least squares which has been shown to be efficient for the construction of monitoring schemes for high dimensional industrial processes that comprise correlated/collinear variables. Through the application of PLS to mathematical simulations that exhibited time varying and non-stationary behaviour, it was noted that conventional PLS is inappropriate and an extension, Robust Adaptive Partial Least Squares was proposed. The proposed method also has the ability to discriminate between statistical outliers and process faults. Other PLS extensions including dynamic PLS and multiblock PLS were also reviewed.

The second part of the thesis extended the proposed method and applied it to model the complex dynamic behaviour of two processes. The first one was an ammonia synthesis fixed-bed reactor, which represents a single unit operation whilst the second, was the Tennessee Eastman Process (TEP), which comprises multiple unit operations. Both processes exhibit dynamic and nonlinear behaviour. Finally the limitations of the developed methods and further work were identified.

8.5 Key Contributions and Results

- Most recursive PLS algorithms aim to update the PLS model whenever new data becomes available. In particular, for the recursive PLS with adaptive confidence limits (APLS) algorithm proposed by Wang (2003), the PLS model is updated in a sample wise manner. An issue that arises when the model is updated using statistical outliers or abnormal data results in a non-representative model of nominal process behaviour. To address this limitation, a novel technique, robust adaptive PLS (RAPLS) was proposed. In this algorithm the combined index as

well as Western electrical rule were utilised to enable the algorithm to distinguish between nominal samples, outliers and abnormal events. The application of conventional PLS, APLS and RAPLS to mathematical simulations that represented time varying and non-stationary processes showed that the RAPLS algorithm performs better compared to the conventional PLS and APLS algorithms in terms of model prediction, average run length, false alarm rate and fault detection rate. Following the application of RAPLS to test data sets, the prediction ability was observed to be slightly lower than for APLS which is expected as the algorithm prevents nonconforming data from contributing to the model. The APLS algorithm performs better compared to conventional PLS in terms of tracking the change in the process behaviour and reducing the number of false alarms. However, it fails to discriminate between a process fault and the change in the process behaviour.

- PLS assumes a linear and static relationship between variables and therefore it is not suitable in cases where a process exhibits dynamic behaviour. In addition, dynamic process typically demonstrates a degree of nonlinearity and therefore a process model that accounts for process dynamics and nonlinearity is required. To address this issue, a time series representation is incorporated within the proposed method of RAPLS. Hence a robust adaptive dynamic PLS (RADPLS) is developed. Following the application of the RADPLS algorithm to two dynamic and non-linear processes, it was observed that processes behaviour is well predicted demonstrate that the recursive variants of DPLS can be used for nonlinear processes.

- Identifying the dynamic structure of the process is application dependent so identifying the dynamic structure has been carried out separately for each industrial process simulation in this work. A number of dynamic structures have been considered and investigated to enable the selection of the most appropriate dynamic PLS model. The accurate prediction of process behaviour suggested that a dynamic structure was used, i.e. ARX (1,1,20) for the ammonia synthesis fixed-bed reactor and FIR with 6 lags based on 18 min sampling interval for the data generated from the Tennessee Eastman Process. In addition when this structure was applied along within the recursive technique, it showed significant improvement compared to the conventional PLS model in terms of fault detection, reducing the number of false alarms and model predictions.

- To the knowledge of the author, no studies have been conducted on the modelling and monitoring of the dynamic and nonlinear behaviour of the ammonia synthesis fixed-bed rector using PLS and its extension. Following the application of DPLS and the recursive variants, it was shown that the robust adaptive dynamic PLS algorithm based on an autoregressive with exogenous input time series model is more appropriate for constructing the monitoring scheme. It has the ability to detect statistical outliers, improve the predictions and reduce the number of false alarms when the process is operated under normal operating conditions. One limitation observed was when a disturbance affects the process and the threshold was unable to detect the full period of the faulty samples as the disturbance affect the process for a significantly long period. However, when the fault affects the process for shorter period, the RADPLS performs well with the fault detection rate being high compared to the adaptive dynamic PLS technique.

- The ammonia reactor fault considered which can be caused by a drop in the overall pressure or feed temperature, results in a rapid oscillation in the temperatures and ammonia concentrations. These oscillations can damage the catalyst and hence damage the reactor. A monitoring system, which provides early detection of the fault and which reduces the number of false alarms, can impact on the many factors including the ability of the operator to restore normal operation conditions. Additionally, energy saving will be achieved in terms of controlling the temperatures, preserving the quality of the product in terms of controlling the concentration and finally financial savings in terms of not damaging processes equipment.

- Several scaling techniques were considered. For the case studies considered, normalization was the most appropriate scaling approach for the data generated from the simulation of ammonia synthesis fixed-bed reactor. This conclusion was drawn following the application of DPLS to the normalised data and considering the root mean squared error (RMSE) and the coefficient of determination R^2.

- To construct a monitoring scheme for large scale processes that comprise several unit operations, multiblock PLS was used along with robust adaptive dynamic

PLS. Consequently a robust adaptive multiblock dynamic PLS (RAMBDPLS) algorithm was proposed. The methodology was applied to data from the Tennessee Eastman Process which comprised 5 unit operations. The monitoring charts derived from the application of RAMBDPLS were reliable compared to multiblock dynamic PLS and adaptive multiblock dynamic PLS, since the false alarm rate was reduced and the fault detection rate increased. In addition, fault propagation in a dynamic and nonlinear system was investigated through the calculation of the time delay before the fault being detected in the various unit operations. More specifically the fault propagates through the system and from the monitoring charts; the impact of the fault on different unit operation is investigated and hence it is evident as to which part of the process is affected by the fault.

8.6 Future work

Based on the reported research, a number of issues need further investigation providing opportunities for future research. These issues include:

- All the results presented in the thesis are based on simulated data which stimulate the behaviour of real industrial processes. Application of the proposed methods on data generated from real industrial process would give further verification of the results presented in the thesis.

- Fault isolation is the next step after fault detection. This step helps identify the variable responsible for the onset of the detected fault. Hence a more detailed analysis of the root causes required to be conducted. One of the most popular methods for fault isolation is contribution analysis. Considering the application of contribution analysis for large scale process that exhibit dynamic and nonlinear behaviour is complicated due to the complex relationships between process variable. This is a major area of research.

- In chapter 4, the threshold used was based on the combined index which showed some limitations especially in the context of oscillatory behaviour. Further research needs to be conducted into the use of different outlier detectors such as the Mahalnbios distance.

- In this work, the recursive algorithm was based on sample wise recursive PLS by Qin (1993). The application of a kernel based recursive algorithm as opposed to NIPALS based recursive algorithm is a further area of research

- In Chapter 6, the division of the whole process into individual unit operations was based on engineering knowledge. Further research into how to split the process to multiple units in the absence of the engineering knowledge would be of interest. For example, correlation analysis could help in the blocking of a system for multiblock PLS.

- The robust adaptive dynamic PLS (RADPLS) and robust adaptive multiblock dynamic PLS (RAMBDPLS) algorithm considered in this thesis are based on multiple inputs single output (MISO) data. Multiple inputs multiple outputs (MIMO) needs to be further investigated.

- The issue of selecting the window size for the calculation of the adaptive confidence limits, which in this thesis has been selected empirically for the ammonia synthesis fixed-bed reactor and Tennessee Eastman processes needs to be investigated further.

- The extension of the approach proposed by Galicia et al (2012), principal component analysis based on Bayesian supervisory approach to detect outliers for real time monitoring, to partial least squares when constructing a process model is research area of interest.

8.7 Publication from the Thesis

Conference

Altaf, B., Montague, G., Martin, E.B. (2012) Monitoring of an industrial process using robust adaptive partial least squares. *proceeding Royal Statistical Society Conference, Telford, United Kingdom,* September 3-5.

Altaf, B., Montague, G., Martin, E.B. (2012) Monitoring of an industrial process using robust adaptive multiblock partial least squares. *proceeding Saudi Scientific International Conference, London, United Kingdom,* October 11-14.

Altaf, B., Montague, G., Martin, E.B. (2013) Dynamic monitoring of the Tennessee Eastman process using PLS. *proceeding Northern Postgraduate Chemical Engineering Conference, Newcastle upon Tyne, United Kingdom,* August 8-9.

Altaf, B., Montague, G., Martin, E.B. (2013) Dynamic monitoring of the Tennessee Eastman process using Partial Least Squares and Extensions. *proceeding Royal Statistical Society Conference, Newcastle upon Tyne, United Kingdom,* September 3-5.

Journal

Altaf, B., Montague, G., Martin, E.B. (2013) Dynamic Process Monitoring of an Ammonia Synthesis Fixed-bed Reactor. *Submitted to Journal of Chemical Engineering & Technology*.

Bibliography

Abdi, H. (2010) 'Partial least squares regression and projection on latent structure regression (PLS Regression)', *Wiley Interdisciplinary Reviews: Computational Statistics*, 2(1), pp. 97-106.

Akaike, H. (1974) 'A new look at the statistical model identification', *IEEE Transactions on Automatic Control*, 19(6), pp. 716-723.

Alghazzawi, A. and Lennox, B. (2008) 'Monitoring a complex refining process using multivariate statistics', *Control Engineering Practice*, 16(3), pp. 294-307.

Alwan, L.C. and Roberts, H.V. (1988) 'Time series modeling for statistical process control', *Journal of Business & Economic Statistics*, 6(1), pp. 87-95.

Appl, M. (1999) 'Chemical Reactions and Uses of Ammonia', in *Ammonia*. Wiley-VCH Verlag GmbH, pp. 231-234.

Baffi, G., Martin, E.B. and Morris, A.J. (2000) 'Non-linear dynamic projection to latent structures modelling', *Chemometrics and Intelligent Laboratory Systems*, 52(1), pp. 5-22.

Barnett, V. and Lewis, T. (1994) *Outliers in statistical data*. 3rd edn. Chichester: Wiley & Sons.

Bersimis, S., Psarakis, S. and Panaretos, J. (2007) 'Multivariate statistical process control charts: an overview', *Quality and Reliability Engineering International*, 23(5), pp. 517-543.

Box, G.E.P. (1954) 'Some theorem on quadratic forms applied in the study of analysis of variance problems', *The Annals of Mathematical Statistics*, 25(2), pp. 290-302.

Box, G.E.P., Jenkins, G.M. and Reinsel, G.C. (2008) *Time series analysis : forecasting and control*. 4th edn. Hoboken, N.J.: John Wiley.

Box, G.E.P. and Tiao, G.C. (1965) 'A change in level of a non-stationary time series', *Biometrika*, 52(1-2), pp. 181-192.

Brauner, N. and Shacham, M. (2000) 'Considering precision of data in reduction of dimensionality and PCA', *Computers & Chemical Engineering*, 24(12), pp. 2603-2611.

Breiman, L. and Friedman, J.H. (1997) 'Predicting multivariate responses in multiple linear regression', *Journal of the Royal Statistical Society: Series B (Methodological)*, 59(1), pp. 3-54.

Brian, P.L.T., Baddour, R.F. and Eymery, J.P. (1965) 'Transient behaviour of an ammonia synthesis reactor', *Chemical Engineering Science*, 20(4), pp. 297-310.

Bro, R. and Smilde, A.K. (2003) 'Centering and scaling in component analysis', *Journal of Chemometrics*, 17(1), pp. 16-33.

Brook, D. and Evans, D.A. (1972) 'An approach to the probability distribution of CUSUM run length', *Biometrika*, 59(3), pp. 539-549.

Cateni, S., Colla, V. and Vannucci, M. (2008) 'Outlier detection methods for industrial applications', *Advances in robotics, automation and control*, pp. 265-282.

Cefic: the European Chemical Industry Council (2012) *CHIMICAL INDUSTRY PROFILE: World exports and imports of chemicals by regional share*. Available at: http://www.cefic.org/Documents/FactsAndFigures/2012/Chemicals-Industry-Profile/Facts-and-Figures-2012-Chapter-Chemicals-Industry-Profile.pdf (Accessed: 8 Jan 2013).

Chen, G. and McAvoy, T.J. (1998) 'Predictive on-line monitoring of continuous processes', *Journal of Process Control*, 8(5-6), pp. 409-420.

Chen, J. and Liu, K.C. (2002) 'On-line batch process monitoring using dynamic PCA and dynamic PLS models', *Chemical Engineering Science*, 57(1), pp. 63-75.

Chen, T. (2010) 'On reducing false alarms in multivariate statistical process control', *Chemical Engineering Research and Design*, 88(4), pp. 430-436.

Chiang, L.H., Braatz, R.D. and Russell, E. (2001) *Fault detection and diagnosis in industrial systems*. London: Springer.

Cho, J.-H., Lee, J.-M., Wook Choi, S., Lee, D. and Lee, I.-B. (2005) 'Fault identification for process monitoring using kernel principal component analysis', *Chemical Engineering Science*, 60(1), pp. 279-288.

Choi, S.W., Martin, E.B., Morris, A.J. and Lee, I.-B. (2006) 'Adaptive multivariate statistical process control for monitoring time-varying processes', *Industrial & Engineering Chemistry Research*, 45(9), pp. 3108-3118.

Christina, M.M. and Douglas, C.M. (1995) 'SPC with correlated observations for the chemical and process industries', *Quality and Reliability Engineering International*, 11(2), pp. 79-89.

Cinar, A., Palazoglu, A. and Kayihan, F. (2007) *Chemical process performance evaluation*. Boca Raton, FL: CRC/Taylor & Francis.

Cummins, D.J. and Andrew, C.W. (1995) 'Iteratively reweighted partial least squares: A performance analysis by Montecarlo simulation', *Journal of Chemometrics*, 9(6), pp. 489-507.

Dayal, B.S. and MacGregor, J.F. (1996) 'Identification of finite impulse response models: methods and robustness issues', *Industrial & Engineering Chemistry Research*, 35(11), pp. 4078-4090.

Dayal, B.S. and MacGregor, J.F. (1997a) 'Improved PLS algorithms', *Journal of Chemometrics*, 11(1), pp. 73-85.

Dayal, B.S. and MacGregor, J.F. (1997b) 'Recursive exponentially weighted PLS and its applications to adaptive control and prediction', *Journal of Process Control*, 7(3), pp. 169-179.

De Jong, S. (1993) 'SIMPLS: An alternative approach to partial least squares regression', *Chemometrics and Intelligent Laboratory Systems*, 18(3), pp. 251-263.

De Jong, S. and Ter Braak, C.J.F. (1994) 'Comments on the PLS kernel algorithm', *Journal of Chemometrics*, 8(2), pp. 169-174.

Denn, M.M. and Lavie, R. (1982) 'Dynamics of plants with recycle', *The Chemical Engineering Journal*, 24(1), pp. 55-59.

Diana, G. and Tommasi, C. (2002) 'Cross-validation methods in principal component analysis: A comparison', *Statistical Methods and Applications*, 11(1), pp. 71-82.

Dong, D. and McAvoy, T.J. (1996) 'Nonlinear principal component analysis Based on principal curves and neural networks', *Computers & Chemical Engineering*, 20(1), pp. 65-78.

Downs, J.J. and Vogel, E.F. (1993) 'A plant-wide industrial process control problem',

Computers & Chemical Engineering, 17(3), pp. 245-255.

Fornell, C. and Bookstein, F.L. (1982) 'Two structural equation models: LISREL and PLS applied to consumer Exit-voice theory', *Journal of Marketing Research*, 19(4), pp. 440-452.

Frank, I.E. and Kowalski, B.R. (1985) 'A multivariate method for relating groups of measurements connected by a causal pathway', *Analytica Chimica Acta*, 167, pp. 51-63.

Frank, P.M. (1990) 'Fault diagnosis in dynamic systems using analytical and knowledge-based redundancy: A survey and some new results', *Automatica*, 26(3), pp. 459-474.

Fyfe, C. (2005) 'Multicollinearity and Partial Least Squares', in *Hebbian Learning and Negative Feedback Networks*. Springer London, pp. 275-289.

Galicia, H., Wang, J. and He, Q. (2012) 'Adaptive outlier detection and classification for online soft sensor update', *8th International Symposium on Advanced Control of Chemical Processes*. Furama Riverfront, Singapore. pp. 402-407.

Gallagher, N.B. and Wise, B.M. (1996) 'The process chemometrics approach to process monitoring and fault detection', *Journal of Process Control*, 6(6), pp. 329-348.

Gallagher, N.B., Wise, B.M., Butler, S.W., White, D.D. and Barna, G.G. (1997) *International Symposium on Advanced Control of Chemical Processes*. Banff, Canada, 9–11 June.

Garthwaite, P.H. (1994) 'An Interpretation of Partial Least Squares', *Journal of the American Statistical Association*, 89(425), pp. 122-127.

Ge, Z. and Song, Z. (2013) *Multivariate Statistical Process Control:Process Monitoring Methods and Applications*. Springer London.

Ge, Z., Song, Z. and Gao, F. (2013) 'Review of recent research on data-based process monitoring', *Industrial & Engineering Chemistry Research*, 52(10), pp. 3543-3562.

Geladi, P. and Kowalski, B. (1986) 'Partial least square regression: A tutorial', *Analytica Chimica Acta*, 185, pp. 1-17.

Geng, Z. and Zhu, Q. (2005) 'Multiscale nonlinear principal component analysis (NLPCA) and its application for chemical process monitoring', *Industrial & Engineering Chemistry Research*, 44(10), pp. 3585-3593.

Gerlach, R.W., Kowalski, B.R. and Wold, H.O.A. (1979) 'Partial least-squares path modelling with latent variables', *Analytica Chimica Acta*, 112(4), pp. 417-421.

Gosselin, C. and Ruel, M. (2007) 'Advantages of monitoring the performance of industrial process', *12th International Symposium on Automation in Mining, Mineral and Metal Processing*, 12, pp. 33-38.

Haenlein, M. and Kaplan, A.M. (2004) 'A beginner's guide to partial least squares analysis', *Understanding Statistics*, 3(4), pp. 283-297.

Helland, I.S. (2001) 'Some theoretical aspects of partial least squares regression', *Chemometrics and Intelligent Laboratory Systems*, 58(2), pp. 97-107.

Helland, K., Berntsen, H.E., Borgen, O.S. and Martens, H. (1992) 'Recursive algorithm for partial least squares regression', *Chemometrics and Intelligent Laboratory Systems*, 14(1-3), pp. 129-137.

Himmelblau, D.M. (1978) *Fault detection and diagnosis in chemical and petrochemical processes*. New York: Elsevier Scientific Pub. Co. ; distributors for the US and Canada Elsevier North-Holland.

Hodge, V. and Austin, J. (2004) 'A survey of outlier detection methodologies', *Artificial Intelligence Review*, 22(2), pp. 85-126.

Holter, E. (2010) *Feedforward for Stabilization of an Ammonia Synthesis Reactor*. MSc thesis. Norwegian University of Science and Technology [Online]. Available at: http://urn.kb.se/resolve?urn=urn:nbn:no:ntnu:diva-9118.

Höskuldsson, A. (1988) 'PLS regression methods', *Journal of Chemometrics*, 2(3), pp. 211–228.

Hubert, M. and Branden, K.V. (2003) 'Robust methods for partial least squares regression', *Journal of Chemometrics*, 17(10), pp. 537-549.

Iketubosin, P.P. (2011) *Studies on non-linear dynamic process monitoring*. PhD thesis. Cranfield University.

Jackson, J.E. (1991) *A user's guide to principal components*. New York: Wiley.

Jackson, J.E. and Mudholkar, G.S. (1979) 'Control procedures for residuals associated with principal component analysis', *Technometrics*, 21, pp. 341-349.

Javaheri, A. and Houshmand, A.A. (2001) 'Average run length comparison of multivariate control charts', *Journal of Statistical Computation and Simulation*, 69(2), pp. 125-140.

Jolliffe, I.T. (2002) *Principal component analysis*. 2nd edn. New York: Springer.

Juricek, B.C., Seborg, D.E. and Larimore, W.E. (2001) 'Identification of the Tennessee Eastman challenge process with subspace methods', *Control Engineering Practice*, 9(12), pp. 1337-1351.

Kano, M., Hasebe, S., Hashimoto, I. and Ohno, H. (2001) 'A new multivariate statistical process monitoring method using principal component analysis', *Computers & Chemical Engineering*, 25(7-8), pp. 1103-1113.

Kano, M., Nagao, K., Hasebe, S., Hashimoto, I., Ohno, H., Strauss, R. and Bakshi, B.R. (2002) 'Comparison of multivariate statistical process monitoring methods with applications to the Eastman challenge problem', *Computers & Chemical Engineering*, 26(2), pp. 161-174.

Kaskavelis, E. (2000) *Statistical monitoring and prediction of petrochemical processes*. PhD thesis. University of Newcastle upon Tyne.

Kaspar, M.H. and Ray, H.W. (1993) 'Dynamic PLS modelling for process control', *Chemical Engineering Science*, 48(20), pp. 3447-3461.

Kaspar, M.H. and Ray, W.H. (1992) 'Chemometric methods for process monitoring and high-performance controller design', *American Institute of Chemical Engineers Journal*, 38(10), pp. 1593-1608.

Kolmanovskii, V.B., Niculescu, S.I. and Gu, K. (1999) *Decision and Control, 1999. Proceedings of the 38th IEEE Conference on*. 1999.

Kourti, T., Lee, J. and Macgregor, J.F. (1996) 'Experiences with industrial applications of projection methods for multivariate statistical process control', *Computers & Chemical Engineering*, 20(Supplement 1), pp. S745-S750.

Kourti, T. and MacGregor, J.F. (1995) 'Process analysis, monitoring and diagnosis, using multivariate projection methods', *Chemometrics and Intelligent Laboratory Systems*, 28(1), pp. 3-21.

Kourti, T., Stephen, D.B., Rom, Tauler and Beata, W. (2009) 'Multivariate statistical process control and process control, using latent variables', in *Comprehensive Chemometrics* Oxford: Elsevier, pp. 21-54.

Kresta, J., MacGregor, J.F. and Marlin, T.E. (1991) 'Multivariate statistical monitoring of process operating performanc', *The Canadian Journal of Chemical Engineering*, 69(1), pp. 35-47.

Kresta, J.V. (1992) *The application of partial least squares to problems in chemical engineering*. PhD thesis. McMaster Univeristy.

Kruger, U. and Xie, L. (2012) *Advances in statistical monitoring of complex multivariate processes: with applications in industrial process Control*. first edn. John Wiley & Sons Ltd.

Kruger, U., Zhou, Y., Wang, X., Rooney, D. and Thompson, J. (2008a) 'Robust partial least squares regression: Part I, algorithmic developments', *Journal of Chemometrics*, 22(1), pp. 1-13.

Kruger, U., Zhou, Y., Wang, X., Rooney, D. and Thompson, J. (2008b) 'Robust partial least squares regression: Part II, new algorithm and benchmark studies', *Journal of Chemometrics*, 22(1), pp. 14-22.

Ku, W., Storer, R.H. and Georgakis, C. (1995) 'Disturbance detection and isolation by dynamic principal component analysis', *Chemometrics and Intelligent Laboratory Systems*, 30(1), pp. 179-196.

Lakshminarayan, K., Harp, S. and Samad, T. (1999) 'Imputation of Missing Data in Industrial Databases', *Applied Intelligence*, 11(3), pp. 259-275.

Lakshminarayanan, S., Shah, S.L. and Nandakumar, K. (1997a) 'Modeling and control of multivariable processes: Dynamic PLS approach', *AIChE Journal*, 43(9), pp. 2307-2322.

Lakshminarayanan, S., Shah, S.L. and Nandakumar, K. (1997b) 'Modeling and control of multivariable processes: Dynamic PLS approach', *American Institute of Chemical Engineers Journal*, 43(9), pp. 2307-2322.

Lee, D.S. and Vanrolleghem, P.A. (2002) 'Monitoring of a sequencing batch reactor using adaptive multiblock principal component analysis', *Biotechnol. Bioeng.*, 82, p. 489.

Lee, G., Han, C. and Yoon, E.S. (2004) 'Multiple-fault diagnosis of the Tennessee Eastman Process based on system decomposition and dynamic PLS', *Industrial & Engineering Chemistry Research*, 43(25), pp. 8037-8048.

Lee, H.W., Lee, M.W. and Park, J.M. (2006a) 'Robust adaptive partial least squares modeling of a full-scale industrial wastewater treatment process', *Industrial & Engineering Chemistry Research*, 46(3), pp. 955-964.

Lee, J.-M., Qin, S.J. and Lee, I.-B. (2006b) 'Fault detection and diagnosis based on modified independent component analysis', *American Institute of Chemical Engineers Journal*, 52(10), pp. 3501-3514.

Lennox, B. (2005) 'Integrating fault detection and isolation with model predictive control', *Journal of Adaptive Control and Signal Processing*, 19(4), pp. 199-212.

Li, B., Morris, J. and Martin, E.B. (2002) 'Model selection for partial least squares regression', *Chemometrics and Intelligent Laboratory Systems*, 64, p. 79.

Li, G., Qin, S.J., Ji, Y. and Zhou, D. (2010) 'Reconstruction based fault prognosis for continuous processes', *Control Engineering Practice*, 18(10), pp. 1211-1219.

Libo, B. and Xiangdong, W. (2009) 'Fault detection and diagnosis of continuous process based on multiblock principal component analysis', *International Conference on Computer Engineering and Technology*. Singapore, 22-24 Jan. 2009. pp. 200-204.

Lindgren, F., Geladi, P. and Wold, S. (1993) 'The kernel algorithm for PLS', *Journal of Chemometrics*, 7(1), pp. 45-59.

Liu, H., Shah, S. and Jiang, W. (2004) 'On-line outlier detection and data cleaning', *Computers & Chemical Engineering*, 28(9), pp. 1635-1647.

Liu, Y., Xu, C. and Shi, J. (2012) 'Tennessee Eastman Process monitoring based on support vector data description', *Second International Conference on Intelligent System Design and Engineering Application (ISDEA)*. Sanya, China, 6-7 Jan. pp. 553-555.

Ljung, L. (1999) *System identification : theory for the user*. 2nd edn. Upper Saddle River, NJ: Prentice Hall PTR.

MacGregor, J.F. (1997) 'Using On-Line Process Data to Improve Quality: Challenges for Statisticians', *International Statistical Review*, 65(3), pp. 309-323.

MacGregor, J.F., Jaeckle, C., Kiparissides, C. and Koutoudi, M. (1994) 'Process monitoring and diagnosis by multiblock PLS methods', *American Institute of Chemical Engineers Journal*, 40(5), pp. 826-838.

MacGregor, J.F. and Kourti, T. (1995) 'Statistical process control of multivariate processes', *Control Engineering Practice*, 3(3), pp. 403-414.

MacGregor, J.F., Yu, H., García Muñoz, S. and Flores-Cerrillo, J. (2005) 'Data-based latent variable methods for process analysis, monitoring and control', *Computers & Chemical Engineering*, 29(6), pp. 1217-1223.

Marjanovic, O., Lennox, B., Sandoz, D., Smith, K. and Crofts, M. (2006) 'Real-time monitoring of an industrial batch process', *Computers & Chemical Engineering*, 30(10-12), pp. 1476-1481.

Martens, H., Næs, T., Arkun, Y. and Ray, H.W. (1989) *Multivariate calibration*. Chichester England ; New York: Wiley.

Martin, E.B., Morris, A.J. and Zhang, J. (1996) 'Process performance monitoring using multivariate statistical process control', *Control Theory and Applications*, 143(2), pp. 132-144.

Miletic, I., Quinn, S., Dudzic, M., Vaculik, V. and Champagne, M. (2004) 'An industrial perspective on implementing on-line applications of multivariate statistics', *Journal of Process Control*, 14(8), pp. 821-836.

Molina, G.D., Zumoffen, D.A.R. and Basualdo, M.S. (2011) 'Plant-wide control strategy applied to the Tennessee Eastman process at two operating points', *Computers & Chemical Engineering*, 35(10), pp. 2081-2097.

Montgomery, D. and Mastrangelo, C. (1991) 'Some statistical process control methods for autocorrelated data', *Journal of Quality Technology*, 23(3), pp. 179-204

Montgomery, D.C. (2005) *Introduction to statistical quality control*. 5th edn. Hoboken, N.J.: John Wiley.

Morud, J. and Skogestad, S. (1994) 'Effects of recycle on dynamics and control of chemical processing plants', *Computers & Chemical Engineering*, 18, Supplement 1, pp. S529-S534.

Morud, J.C. and Skogestad, S. (1998) 'Analysis of instability in an industrial ammonia reactor', *American Institute of Chemical Engineers Journal*, 44(4), pp. 888-895.

Mu, S., Zeng, Y., Liu, R., Wu, P., Su, H. and Chu, J. (2006) 'Online dual updating with recursive PLS model and its application in predicting crystal size of purified terephthalic acid (PTA) process', *Journal of Process Control*, 16(6), pp. 557-566.

Mujica, L.E., Vehí, J., Ruiz, M., Verleysen, M., Staszewski, W. and Worden, K. (2008) 'Multivariate statistics process control for dimensionality reduction in structural assessment', *Mechanical Systems and Signal Processing Journal*, 22(1), pp. 155-171.

Negiz, A. and Çlinar, A. (1997a) 'Statistical monitoring of multivariable dynamic processes with state-space models', *American Institute of Chemical Engineers Journal*, 43(8), pp. 2002-2020.

Negiz, A. and Çlinar, A. (1997b) 'Statistical monitoring of multivariable dynamic processes with state-space models', *American Institute of Chemical Engineers*, 43(8), pp. 2002-2020.

Nelson, P.R.C., Taylor, P.A. and MacGregor, J.F. (1996) 'Missing data methods in PCA and PLS: Score calculations with incomplete observations', *Chemometrics and Intelligent Laboratory Systems*, 35(1), pp. 45-65.

Nikolaou, M. and Vuthandam, P. (1998) 'FIR model identification: Parsimony through kernel compression with wavelets', *American Institute of Chemical Engineers Journal*, 44(1), pp. 141-150.

Nomikos, P. and MacGregor, J. (1995) 'Multivariate SPC charts for monitoring batch processes', *Technometrics*, 37(1), p. 41.

Oakland, J.S. (2008) 'Process data collection and presentation', in *Statistical Process Control*. 6th edn. Oxford: Butterworth-Heinemann, pp. 42-60.

Pell, R.J. (2000) 'Multiple outlier detection for multivariate calibration using robust statistical techniques ', *Chemometrics and Intelligent Laboratory Systems*, 52(1), pp. 87–104.

Plumb, K. (2005) 'Continuous Processing in the Pharmaceutical Industry: Changing the Mind Set', *Chemical Engineering Research and Design*, 83(6), pp. 730-738.

Qin, J.S. (1998a) 'Recursive PLS algorithms for adaptive data modeling', *Computers & Chemical Engineering*, 22(4-5), pp. 503-514.

Qin, S.J. (1993) 'Partial least squares regression for recursive system identification', *The 32nd IEEE Conference on Decision and Control*. San Antonio, TX 15-17 Dec. pp. 2617-2622.

Qin, S.J. (1998b) 'Recursive PLS algorithms for adaptive data modeling', *Computers & Chemical Engineering*, 22(4-5), pp. 503-514.

Qin, S.J. (2003) 'Statistical process monitoring: Basics and beyond', *Journal of Chemometrics*, 17(8-9), pp. 480-502.

Qin, S.J. (2012) 'Survey on data-driven industrial process monitoring and diagnosis', *Annual Reviews in Control*, 36(2), pp. 220-234.

Qin, S.J. and McAvoy, T.J. (1993) 'A data-based process modeling approach and its applications', *International Symposium of Automatic Control*. pp. 93-93.

Qin, S.J., Valle, S. and Piovoso, M.J. (2001) 'On unifying multiblock analysis with application to decentralized process monitoring', *Journal of Chemometrics*, 15(9), pp. 715-742.

Qin, S.J. and Yue, H.H. (2001) 'Reconstruction based fault identification using a combined index', *Industrial & Engineering Chemistry Research*, 40(20), pp. 4403-4414.

Raich, A. and Çinar, A. (1996) 'Statistical process monitoring and disturbance diagnosis in multivariable continuous processes', *American Institute of Chemical Engineers Journal*, 42(4), pp. 995-1009.

Ramesh, T.S., Davis, J.F. and Schwenzer, G.M. (1992) 'Knowledge-based diagnostic systems for continuous process operations based upon the task framework', *Computers and Chemical Engineering*, 16(2), pp. 109-127.

Rato, T.J. and Reis, M.S. (2013) 'Fault detection in the Tennessee Eastman benchmark process using dynamic principal components analysis based on decorrelated residuals (DPCA-DR)', *Chemometrics and Intelligent Laboratory Systems*, 125, pp. 101-108.

Realfsen, T. (2000) *Control of unstable ammonia reactor*. Trondheim, Norway.

Reynolds, J.M.R. and Lu, C.-W. (1997) 'Control charts for monitoring processes with autocorrelated data', *Nonlinear Analysis:Theory, Methods & Applications*, 30(7), pp. 4059-4067.

Ricker, N. (1995) 'Nonlinear model predictive control of the Tennessee Eastman challenge process', *Computers & Chemical Engineering*, 19(9), pp. 961-981.

Ricker, N.L. (1988) 'The use of biased least-squares estimators for parameters in discrete-time pulse-response models', *Industrial & Engineering Chemistry Research*, 27(2), pp. 343-350.

Riegel, E.R. and Kent, J.A. (2007) *Kent and Riegel's handbook of industrial chemistry and biotechnology*. 11th edn. New York: Springer.

Rippin, D.W.T. (1983) 'Simulation of single and multiproduct batch chemical plants for optimal design and operation', *Computers & Chemical Engineering*, 7(3), pp. 137-156.

Runger, G.C. (1996) 'Multivariate statistical process control for autocorrelated processes', *International Journal of Production Research*, 34(6), pp. 1715-1724.

Schafer, J.L. and Graham, J.W. (2002) 'Missing data: Our view of the state of the art', *Psychological methods*, 7(2), pp. 147-177.

Scheffer, J. (2002) 'Dealing with missing data', *Research letters in the information and mathematical sciences*, 3(1), pp. 153-160.

Seborg, D.E., Edgar, T.F. and Mellichamp, D.A. (1989) *Process dynamics and control*. New York: Wiley.

Sharratt, P.N. (1997) *Handbook of batch process design*. London: Blackie.

Simoglou, A., Martin, E.B. and Morris, A.J. (2000) 'Multivariate statistical process control of an industrial fluidised-bed reactor', *Control Engineering Practice*, 8(8), pp. 893-909.

Smilde, A.K., Westerhuis, J.A. and De Jong, S. (2003) 'A framework for sequential multiblock component methods', *Journal of Chemometrics*, 17(6), pp. 323-337.

Summers and Donna, C.S. (2010) *Quality*. 5th edn. Boston: Prentice Hall.

Tang, J., Zhao, L., Yu, W., Chai, T. and Yue, H. (2011) 'Modified recursive partial least squares algorithm with application to modeling parameters of ball mill load', *Chinese Control Conference (CCC)*. Yantai 22-24 July. pp. 5277-5282.

Tavares, G., Zsigraiová, Z., Semiao, V. and Carvalho, M.d.G. (2011) 'Monitoring, fault detection and operation prediction of MSW incinerators using multivariate statistical methods', *Journal of Waste Management*, 31(7), pp. 1635-1644.

Tessier, J., Duchesne, C., Tarcy, G.P., Gauthier, C. and Dufour, G. (2012) 'Multivariate analysis and monitoring of the performance of aluminum reduction cells', *Industrial & Engineering Chemistry Research*, 51(3), pp. 1311-1323.

U.S. Geological Survey (2008) *Minerals Yearbook: Volume I- Metals and Minerals*. Available at: http://minerals.usgs.gov/minerals/pubs/commodity/myb/ (Accessed: 25 Jan 2013).

Venkatasubramanian, V., Rengaswamy, R. and Kavuri, S.N. (2003a) 'A review of process fault detection and diagnosis: Part II: Qualitative models and search strategies', *Computers & Chemical Engineering*, 27(3), pp. 313-326.

Venkatasubramanian, V., Rengaswamy, R., Kavuri, S.N. and Yin, K. (2003b) 'A review of process fault detection and diagnosis: Part III: Process history based methods', *Computers & Chemical Engineering*, 27(3), pp. 327-346.

Venkatasubramanian, V., Rengaswamy, R., Yin, K. and Kavuri, S.N. (2003c) 'A review of process fault detection and diagnosis: Part I: Quantitative model-based methods', *Computers & Chemical Engineering*, 27(3), pp. 293-311.

Vinzi, E.V. and Russolillo, G. (2012) 'Partial least squares algorithms and methods', *Wiley Interdisciplinary Reviews: Computational Statistics*, 5(1), pp. 1-19.

Vinzi, V.E., Chin, W.W., Henseler, J. and Wang, H. (2007) *Handbook of Partial Least Squares Concepts, Methods and Applications in Marketing and Related Fields*. Dordrecht: Springer.

Wang, D. and Srinivasan, R. (2009) 'Eliminating the effect of multivariate outliers in PLS-based models for inferring process quality', *Computer Aided Chemical Engineering*, 26, pp. 755-760.

Wang, X., Kruger, U. and Lennox, B. (2003) 'Recursive partial least squares algorithms for monitoring complex industrial processes', *Control Engineering Practice*, 11(6), pp. 613-632.

Wang, X., Kruger, U., Lennox, B. and Goulding, P. (2001) 'A novel multiblock method using latent variable partial least squares', *American Control Conference*. Arlington, VA, 25-27 Jun. pp. 3136-3141.

Wangen, L.E. and Kowalski, B.R. (1989) 'A multiblock partial least squares algorithm for investigating complex chemical systems', *Journal of Chemometrics*, 3(1), pp. 3-20.

Weighell, M., Martin, E.B. and Morris, A.J. (1997) 'Fault diagnosis in industrial process manufacturing using MSPC', *IEE Colloquium on Fault Diagnosis in Process Systems*. London, 21 Apr. pp. 41-43.

Westerhuis, J.A. and Coenegracht, P.M.J. (1997) 'Multivariate modelling of the pharmaceutical two-step process of wet granulation and tableting with multiblock partial least squares', *Journal of Chemometrics*, 11(5), pp. 379-392.

Westerhuis, J.A., Kourti, T. and MacGregor, J.F. (1998) 'Analysis of multiblock and hierarchical PCA and PLS models', *Journal of Chemometrics*, 12(5), pp. 301-321.

Westerhuis, J.A. and Smilde, A.K. (2001) 'Deflation in multiblock PLS', *Journal of Chemometrics*, 15(5), pp. 485-493.

Wold, H. (1966) 'Estimation of principal components and related models by iterative least squares', *Multivariate analysis*, 1, pp. 391-420.

Wold, S. (1978) 'Cross-validatory estimation of the number of components in factor and principal component models', *Technometrics*, 20(4), pp. 397-405.

Wold, S. (1992) 'Nonlinear partial least squares modelling II. Spline inner relation', *Chemometrics and Intelligent Laboratory Systems*, 14(1-3), pp. 71-84.

Wold, S. (1994) 'Exponentially weighted moving principal components analysis and projections to latent structures', *Chemometrics and Intelligent Laboratory Systems*, 23(1), pp. 149-161.

Wold, S., Eriksson, L., Trygg, J. and Kettaneh, N. (2004) 'The PLS method-partial least squares projections to latent structures-and its applications in industrial RDP (research, development, and production)', *Computational Statistics: 16th Symposium*. Prague,Czech Republic, 23-27 Aug. p. 349.

Wold, S., Esbensen, K. and Geladi, P. (1987) 'Principal component analysis', *Chemometrics and Intelligent Laboratory Systems*, 2(1-3), pp. 37-52.

Wold, S., Kettaneh, N. and Tjessem, K. (1996) 'Hierarchical multiblock PLS and PC models for easier model interpretation and as an alternative to variable selection', *Journal of Chemometrics*, 10(5-6), pp. 463-482.

Wold, S., Ruhe, A., Wold, H. and Dunn, I.W. (1984) 'The collinearity problem in linear regression. The partial least squares (PLS) approach to generalized inverses', *Journal on Scientific and Statistical Computing*, 5(3), pp. 735-743.

Wold, S. and Sjöström, M. (1998) 'Chemometrics, present and future success', *Chemometrics and Intelligent Laboratory Systems*, 44(1-2), pp. 3-14.

Wold, S., Sjöström, M. and Eriksson, L. (2001) 'PLS-regression: a basic tool of chemometrics', *Chemometrics and Intelligent Laboratory Systems*, 58(2), pp. 109-130.

Wood, R.K. and Berry, M.W. (1973) 'Terminal composition control of a binary distillation column', *Chemical Engineering Science*, 28(9), pp. 1707-1717.

Yacoub, F. and MacGregor, J.F. (2003) 'Analysis and optimization of a polyurethane reaction injection molding (RIM) process using multivariate projection methods', *Chemometrics and Intelligent Laboratory Systems*, 65(1), pp. 17-33.

Yin, S., Ding, S.X., Haghani, A., Hao, H. and Zhang, P. (2012) 'A comparison study of basic data-driven fault diagnosis and process monitoring methods on the benchmark Tennessee Eastman process', *Journal of Process Control*, 22(9), pp. 1567-1581.

Zhou, D., Li, G. and Qin, S.J. (2010) 'Total projection to latent structures for process monitoring', *American Institute of Chemical Engineers*, 56(1), pp. 168-178.

APPENDIX A

1. Statistically Inspired Modification of PLS (SIMPLS)

It is an alternative approach to partial least squares proposed in (De Jong, 1993) and it is summarised as follows:

For each latent variable h = 1,2 …. a and $\mathbf{S} = \mathbf{X}'\mathbf{Y}_0$, $\mathbf{Y}_0 = \mathbf{Y} - \text{mean}(\mathbf{Y})$

1. Compute $\mathbf{q}_h$ the dominant eigenvector of $\mathbf{S}_h'\mathbf{S}_h$
2. $\mathbf{w}_h = \mathbf{S}_h\mathbf{q}_h$, $\mathbf{t}_h = \mathbf{X}_h\mathbf{w}_h$, $\mathbf{t}_h$=$\mathbf{t}_h$-mean ($\mathbf{t}_h$)
3. $\mathbf{w}_h = \mathbf{w}_h/\|\mathbf{w}_h\|$ and $\mathbf{t}_h$=$\mathbf{t}_h/\|\mathbf{t}_h\|$
4. $\mathbf{p}_h$=$\mathbf{X}'\mathbf{t}_h$ and store $\mathbf{p}_h$ into $\mathbf{P}$ column
5. $\mathbf{q}_h$=$\mathbf{Y}_0'\mathbf{t}_h$ and store $\mathbf{q}_h$ into $\mathbf{Q}$ column
6. $\mathbf{u}_h$=$\mathbf{Y}_0\mathbf{q}_h$ and $\mathbf{v}_h = \mathbf{p}_h$
7. If h>1
   a. $\mathbf{v}_h = \mathbf{v}_h(\mathbf{v}_h'\mathbf{p}_h)$
   b. $\mathbf{u}_h$= $\mathbf{u}_h$-$\mathbf{t}_h'\mathbf{u}_h$)

   Otherwise

   $$\mathbf{v}_h = \mathbf{v}_h/sqrt(\mathbf{v}_h'\mathbf{v}_h)$$

   $$\mathbf{S}_h = \mathbf{S}_h - \mathbf{v}_h(\mathbf{v}_h'\,\mathbf{S}_h)$$

8. Store $\mathbf{w}_h, \mathbf{t}_h, \mathbf{q}_h, \mathbf{p}_h, \mathbf{u}_h, \mathbf{v}_h$ and go for the next dimension

2. Kernel PLS

It is an alternative approach to partial least squares proposed (Lindgren et al., 1993) and it is summarised as follows:

1. For each latent variable h = 1,2 …. a
2. Compute the kernel matrix $\mathbf{X}'\mathbf{Y}\mathbf{Y}'\mathbf{X}$
3. Calculate the PLS weight vector $\mathbf{w}_h$ as the eigenvector corresponded to the largest eigenvalue of $(\mathbf{X}'\mathbf{Y}\mathbf{Y}'\mathbf{X})_h$ using singular value decomposition (SVD)
4. Calculate $\mathbf{r}_h$ for h>1 as $\mathbf{r}_h = (\mathbf{I} - \mathbf{r}_{h-1}\,\mathbf{p}_{h-1})\,\mathbf{w}_h$
5. Calculate the first loading vector $\mathbf{p}_h$ for $\mathbf{X}$ as
$$\mathbf{p}_h' = \frac{\mathbf{r}_h'\,(\mathbf{X}'\mathbf{X})_h}{\mathbf{r}_h'\,(\mathbf{X}'\mathbf{X})_h\,\mathbf{r}_h}$$
6. Calculate the first loading vector $\mathbf{p}_h$ for $\mathbf{Y}$ as
$$\mathbf{q}_h' = \frac{\mathbf{r}_h'\,(\mathbf{X}'\mathbf{Y})_h}{\mathbf{r}_h'\,(\mathbf{X}'\mathbf{X})_h\,\mathbf{r}_h}$$
7. Update the covariance matrices as:
$$(\mathbf{X}'\mathbf{X})_{h+1} = (\mathbf{I} - \mathbf{w}_h\,\mathbf{p}_h)'(\mathbf{X}'\mathbf{X})_h\,(\mathbf{I} - \mathbf{w}_h\mathbf{p}'_h)$$
$$(\mathbf{X}'\mathbf{Y})_{h+1} = (\mathbf{I} - \mathbf{w}_h\,\mathbf{p}_h)'(\mathbf{X}'\mathbf{Y})_h$$

3. Modified kernel PLS (1)

The original kernel PLS is modified by simplifying step 7, update the covariance matrices as:

$$(\mathbf{X}'\mathbf{X})_{\mathbf{h+1}} = (\mathbf{X}'\mathbf{X})_{\mathbf{h}} - \mathbf{p}_h \mathbf{p}'_h (\mathbf{t}'_h \mathbf{t}_h) \qquad \mathbf{T} = \mathbf{XR}$$
$$(\mathbf{X}'\mathbf{Y})_{\mathbf{h+1}} = (\mathbf{X}'\mathbf{Y})_{\mathbf{h}} \mathbf{p}_h \mathbf{q}'_h (\mathbf{t}'_h \mathbf{t}_h)$$

4. Modified kernel PLS (2)

This modification was proposed by Dayal and MacGregor (1997a). They proved that only one of the data matrices needs to be deflated, i.e. the only necessary deflation in step 7 is

$$(\mathbf{X}'\mathbf{Y})_{\mathbf{h+1}} = (\mathbf{X}'\mathbf{Y})_{\mathbf{h}} \mathbf{p}_h \mathbf{q}'_h (\mathbf{t}'_h \mathbf{t}_h) \text{ where } \mathbf{T} = \mathbf{XR}$$

5. Relation between Conventional PLS and MBPLS$_T$

5.1 scores relationship

- Denote $\theta_{b,i} = \|\boldsymbol{X}_{b,i}\boldsymbol{u}_i\|$, $i = 1,2,..a$

- From the MBPLS$_T$ in chapter 3, we have

$\boldsymbol{t}_{T,i} = \boldsymbol{T}_i \boldsymbol{w}_{T,i}$

$\propto \boldsymbol{T}_i \boldsymbol{T}'_i \boldsymbol{u}_i$

$= [\boldsymbol{t}_{1,i}, \boldsymbol{t}_{2,i}, \ldots, \boldsymbol{t}_{B,i}] [\boldsymbol{t}_{1,i}, \boldsymbol{t}_{2,i}, \ldots, \boldsymbol{t}_{B,i}]' \boldsymbol{u}_i$

$= \sum_{b=1}^{B} \boldsymbol{t}_{b,i} \boldsymbol{t}'_{b,i} \boldsymbol{u}_i$ since $\boldsymbol{t}_{b,i} = \boldsymbol{X}_{b,i}\boldsymbol{w}_{b,i}$ we have

$= \sum_{b=1}^{B} \boldsymbol{X}_{b,i}\boldsymbol{w}_{b,i}\boldsymbol{w}'_{b,i} (\boldsymbol{X}'_{b,i} \boldsymbol{u}_i)$ since $\boldsymbol{w}_{b,i} = \boldsymbol{X}_{b,i}\boldsymbol{u}_i / \|\boldsymbol{X}_{b,i}\boldsymbol{u}_i\|$ we have

$= \sum_{b=1}^{B} \boldsymbol{X}_{b,i}\boldsymbol{w}_{b,i}\boldsymbol{w}'_{b,i} (\boldsymbol{w}_{b,i}\, \theta_{b,i})$ since $\boldsymbol{w}'_{b,i}\boldsymbol{w}_{b,i}=1$ we have

$= \sum_{b=1}^{B} \boldsymbol{X}_{b,i}\boldsymbol{w}_{b,i}\, \theta_{b,i}$ since $\boldsymbol{w}_{b,i} = \boldsymbol{X}_{b,i}\boldsymbol{u}_i / \theta_{b,i}$ we have

$= \sum_{b=1}^{B} \boldsymbol{X}_{b,i} \boldsymbol{X}_{b,i}\boldsymbol{u}_i$

$= [\boldsymbol{X}_{1,i}, \boldsymbol{X}_{2,i}, \ldots, \boldsymbol{X}_{B,i}] [\boldsymbol{X}_{1,i}, \boldsymbol{X}_{2,i}, \ldots, \boldsymbol{X}_{B,i}]' \boldsymbol{u}_i$ *

Since $\boldsymbol{u}_i = \boldsymbol{Y}_i \boldsymbol{q}_i / \boldsymbol{q}'_i \boldsymbol{q}_i$ and $\boldsymbol{q}'_i \boldsymbol{q}_i = 1$ and $\boldsymbol{q}_i = \boldsymbol{Y}'_i \boldsymbol{t}_{T,i}$

$$\boldsymbol{u}_i = \boldsymbol{Y}_i \boldsymbol{Y}'_i \boldsymbol{t}_{T,i} \qquad **$$

Substituting * in ** we have

$$\boldsymbol{u}_i = \boldsymbol{Y}_i \boldsymbol{Y}'_i [\boldsymbol{X}_{1,i}, \boldsymbol{X}_{2,i}, \ldots, \boldsymbol{X}_{B,i}] [\boldsymbol{X}_{1,i}, \boldsymbol{X}_{2,i}, \ldots, \boldsymbol{X}_{B,i}]' \boldsymbol{u}_i$$

Since the conventional PLS scores $\mathbf{u}_i$ and $\mathbf{t}_i$ are the eigenvalue of $\mathbf{Y}_i \mathbf{Y}'_i \mathbf{X}_i \mathbf{X}'_i$ and

$\mathbf{X}_i\,\mathbf{X'}_i\mathbf{Y}_i\,\mathbf{Y'}_i$ respectively. We need to show that $\mathbf{Y}_i = \boldsymbol{Y'}_i$ and $\mathbf{X}_i = [\boldsymbol{X}_{1,i}, \boldsymbol{X}_{2,i}, \ldots, \boldsymbol{X}_{B,i}]$ for each i and this can be proved from the identically of residuals.

5.2 Residual relationship

- Utilising the MBPLS$_T$ residual relationship for the ith latent variable we have

$\boldsymbol{X}_{b,i+1} = \boldsymbol{X}_{b,i} - \boldsymbol{t}_{T,i}\,\boldsymbol{p}'_{b,i}$ since $\boldsymbol{p}_{b,i} = \boldsymbol{X'}_{b,i}\boldsymbol{t}_{T,i}\,/\boldsymbol{t'}_{T,i}\,\boldsymbol{t}_{T,i}$

$= (\boldsymbol{I} - \boldsymbol{t}_{T,i}\,\boldsymbol{t'}_{T,i}\,/\boldsymbol{t'}_{T,i}\,\boldsymbol{t}_{T,i})\boldsymbol{X}_{b,i}$

For the conventional PLS we have

$$\mathbf{X}_{i+1} = \left(\mathbf{I} - \frac{\mathbf{t}_i\mathbf{t}'_i}{\mathbf{t}_i\mathbf{t}'_i}\right)\mathbf{X}_i$$

by partitioning the $\mathbf{X}_i = [\mathbf{X}_{1,i}, \mathbf{X}_{2,i} \ldots\ldots \mathbf{X}_{B,i}]$ we got

$$\mathbf{X}_{b,i+1} = (\mathbf{I} - \mathbf{t}_i\,\mathbf{t'}_i\,/\mathbf{t'}_i\,\mathbf{t}_i)\mathbf{X}_{b,i}$$

And the similar derivation can be obtained for the output residuals

$\mathbf{Y}_{i+1} = (\mathbf{I} - \mathbf{t}_i\,\mathbf{t'}_i\,/\mathbf{t'}_i\,\mathbf{t}_i)\mathbf{Y}_i$ since $\mathbf{Y}_{i+1} = \mathbf{Y}_i - \mathbf{t}_i\,\mathbf{q}'_i$ and $\mathbf{q}_i = \mathbf{Y'}_i\mathbf{t}_i\,/\mathbf{t'}_i\,\mathbf{t}_i$

$\boldsymbol{Y}_{i+1} = (\boldsymbol{I} - \boldsymbol{t}_{T,i}\,\boldsymbol{t'}_{T,i}\,/\boldsymbol{t'}_{T,i}\,\boldsymbol{t}_{T,i})\boldsymbol{Y}_i$

Score and residual equivalence by induction

Since $\boldsymbol{X}_{b,1} = \mathbf{X}_{b,1} = \mathbf{X}_b$ and $\boldsymbol{Y}_1 = \mathbf{Y}_1 = \mathbf{Y}$

From scores relations we have $\boldsymbol{t}_{T,1} \propto \boldsymbol{X}_1\boldsymbol{X}'_1\,\boldsymbol{Y}_1\boldsymbol{Y}'_1\boldsymbol{t}_{T,1}$ and $\mathbf{u}_1 \propto \boldsymbol{Y}_1\boldsymbol{Y}'_1\boldsymbol{X}_1\boldsymbol{X}'_1\mathbf{u}_1$

Hence both $\boldsymbol{t}_{T,1}$ and $\mathbf{t}_1$ are the first eigenvector of $\mathbf{X}_1\mathbf{X}'_1\,\mathbf{Y}_1\mathbf{Y}'_1$ and both $\boldsymbol{u}_1$ and $\mathbf{u}_1$ are the first eigenvector of $\mathbf{Y}_1\mathbf{Y}'_1\mathbf{X}_1\mathbf{X}'_1$. This proves $\boldsymbol{t}_{T,1} = \mathbf{t}_1$ and $\boldsymbol{u}_1 = \mathbf{u}_1$

Assume $\boldsymbol{t}_{T,i} = \mathbf{t}_i$, $\boldsymbol{u}_i = \mathbf{u}_i$, $\mathbf{X}_i = [\mathbf{X}_{1,i}, \mathbf{X}_{2,i} \ldots\ldots \mathbf{X}_{B,i}]$ and $\mathbf{Y}_i = \boldsymbol{Y}_i$ and from residual relationship

$\boldsymbol{X}_{b,i+1} = (\boldsymbol{I} - \boldsymbol{t}_{T,i}\,\boldsymbol{t'}_{T,i}\,/\boldsymbol{t'}_{T,i}\,\boldsymbol{t}_{T,i})\boldsymbol{X}_{b,i} = (\boldsymbol{I} - \boldsymbol{t}_{T,i}\,\boldsymbol{t'}_{T,i}\,/\boldsymbol{t'}_{T,i}\,\boldsymbol{t}_{T,i})\mathbf{X}_{b,i}$

Therefore

$$\mathbf{X}_{i+1} = [\mathbf{X}_{1,i+1}, \mathbf{X}_{2,i+1} \ldots\ldots\ldots \mathbf{X}_{B,i+1}]$$

Similarly

$$\mathbf{Y}_{i+1} = \left(\mathbf{I} - \frac{\mathbf{t}_i\mathbf{t}'_i}{\mathbf{t}_i\mathbf{t}'_i}\right)\mathbf{Y}_i = \boldsymbol{Y}_{i+1}$$

Applying these relations to scores relationship, it can be proved that

$$\boldsymbol{t}_{T,i+1} = \mathbf{t}_{T,1} \text{ and } \boldsymbol{u}_{i+1} = \mathbf{u}_{i+1}$$

5.3 Equivalence of weight and loadings MBPLS$_T$ and PLS

From conventional PLS algorithm in Chapter 3 we have

$\mathbf{w}_i = \mathbf{X}'_i u_i / \|\mathbf{X}'_i \mathbf{u}_i\|$

Partitioning $\mathbf{X}_i = [\mathbf{X}_{1,i}, \mathbf{X}_{2,i} \ldots\ldots \mathbf{X}_{B,i}]$ we got

$\mathbf{w}_{b,i} = \frac{\mathbf{X}'_{b,i}\mathbf{u}_i}{\|\mathbf{X}'_{b,i}\mathbf{u}_i\|} \propto \mathbf{X}'_{b,i}\mathbf{u}_i$ *

From the MBPLS$_T$ algorithm and by Substituting $\mathbf{X}'_{b,i}$ for $\boldsymbol{X}'_{b,i}$ we have

$$\mathbf{w}_{b,i} = \frac{\boldsymbol{X}'_{b,i}\mathbf{u}_i}{\|\boldsymbol{X}'_{b,i}\mathbf{u}_i\|} = \frac{\mathbf{X}'_{b,i}\mathbf{u}_i}{\|\mathbf{X}'_{b,i}\mathbf{u}_i\|} = \frac{\boldsymbol{w}_{b,i}}{\|\boldsymbol{w}_{b,i}\|}$$

From MBPLS$_T$ algorithm

$$\boldsymbol{w}_{b,i} = \frac{\boldsymbol{X}'_{b,i}\mathbf{u}_i}{\|\boldsymbol{X}'_{b,i}\mathbf{u}_i\|}$$

By multiplying the previous step by $\mathbf{u}'_i \boldsymbol{X}_{b,i}$

$$\|\boldsymbol{X}'_{b,i}\mathbf{u}_i\| = \frac{\boldsymbol{X}'_{b,i}\mathbf{u}_i}{\boldsymbol{w}_{b,i}} = \boldsymbol{X}'_{b,i}\mathbf{u}_i \Big/ \frac{\boldsymbol{X}'_{b,i}\mathbf{u}_i}{\|\boldsymbol{X}'_{b,i}\mathbf{u}_i\|} = \|\boldsymbol{X}'_{b,i}\mathbf{u}_i\| \quad \frac{\boldsymbol{X}'_{b,i}\mathbf{u}_i}{\boldsymbol{X}'_{b,i}\mathbf{u}_i} = \|\boldsymbol{X}'_{b,i}\mathbf{u}_i\| = \|\mathbf{X}'_{b,i}\mathbf{u}_i\| \quad **$$

By multiplying the previous step by $\mathbf{u}'_i \boldsymbol{X}_{b,i}$

$(\mathbf{u}'_i \boldsymbol{X}_{b,i})\boldsymbol{w}_{b,i} = \mathbf{u}_i \boldsymbol{t}_{b,i}$ ***

From MBPLS$_T$ algorithm we have

$$\boldsymbol{w}'_{T,i} = \frac{\boldsymbol{T}'_i \boldsymbol{u}_i}{\|\boldsymbol{T}'_i \boldsymbol{u}_i\|} \propto \boldsymbol{u}'_i \boldsymbol{T}_i$$

Since $\boldsymbol{T}_i = [\boldsymbol{t}_{1,i}, \boldsymbol{t}_{2,i}, \ldots\ldots \boldsymbol{t}_{B,i}]$ we got

$\boldsymbol{w}'_{T,i} = \boldsymbol{u}'_i [\boldsymbol{t}_{1,i}, \boldsymbol{t}_{2,i}, \ldots\ldots \boldsymbol{t}_{B,i}]$

$= [\boldsymbol{u}'_i \boldsymbol{t}_{1,i}, \boldsymbol{u}'_i \boldsymbol{t}_{2,i}, \ldots\ldots \boldsymbol{u}'_i \boldsymbol{t}_{B,i}]$

From ***

$\boldsymbol{w}'_{T,i} = [(\mathbf{u}'_i \boldsymbol{X}_{1,i})\boldsymbol{w}_{1,i}, (\mathbf{u}'_i \boldsymbol{X}_{2,i})\boldsymbol{w}_{2,i}, \ldots\ldots (\mathbf{u}'_i \boldsymbol{X}_{B,i})\boldsymbol{w}_{B,i}]$

From **

$$\boldsymbol{w'}_{T,i} = [\|\mathbf{X'}_{1,i}\mathbf{u}_i\|, \|\mathbf{X'}_{2,i}\mathbf{u}_i\|, \ldots., \|\mathbf{X'}_{B,i}\mathbf{u}_i\|] \quad \text{Since } \mathbf{w}_{b,i} = \frac{\boldsymbol{X'}_{b,i}\mathbf{u}_i}{\|\boldsymbol{X'}_{b,i}\mathbf{u}_i\|}$$

$$\propto [\|\mathbf{w}_{1,i}\| \, \|\mathbf{w}_{2,i}\|, \ldots. \|\mathbf{w}_{b,i}\|]$$

5.4 Equivalence of loadings

From $MBPLS_T$

$$\boldsymbol{p}_{b,i} = \boldsymbol{X'}_{b,i}\boldsymbol{t}_{T,i} / \boldsymbol{t'}_{T,i}\boldsymbol{t}_{T,i}$$

Since $\boldsymbol{t}_{T,i}$ and $\mathbf{t}_i$ are equivalence from 5.1 and 5.2

$$\boldsymbol{p}_{b,i} = \boldsymbol{X'}_{b,i}\mathbf{t}_i / \mathbf{t'}_i\mathbf{t}_i \qquad **$$

From conventional PLS algorithm

$$\boldsymbol{p}_i = \boldsymbol{X'}_i\mathbf{t}_i / \mathbf{t'}_i\mathbf{t}_i$$

By partitioning $\mathbf{X}_i = [\mathbf{X}_{1,i}, \mathbf{X}_{2,i} \ldots. \mathbf{X}_{B,i}]$ we got

$$\mathbf{p}_{b,i} = \boldsymbol{X'}_{b,i}\mathbf{t}_i / \mathbf{t'}_i\mathbf{t}_i \quad ***$$

By comparing ** and *** we got

$$\boldsymbol{p}_{b,i} = \mathbf{p}_{b,i}$$

6. Residuals plots for time varying process – calibration data set

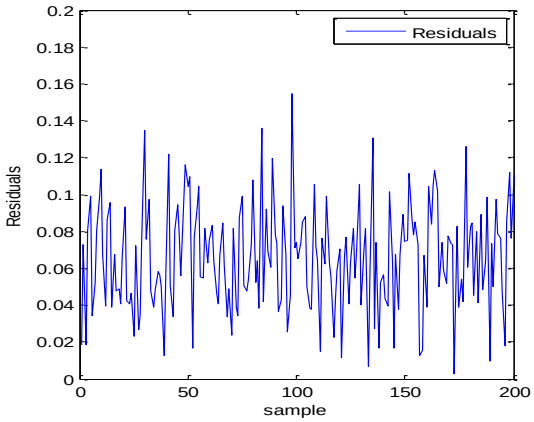

Figure 1- Time series plot of the residuals for the first quality variable

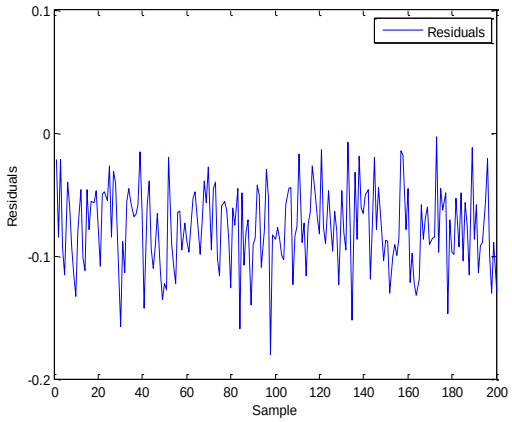

Figure 2 - Time series plot of the residuals for the second quality variable

7. Residuals plots for time varying process – validation data set

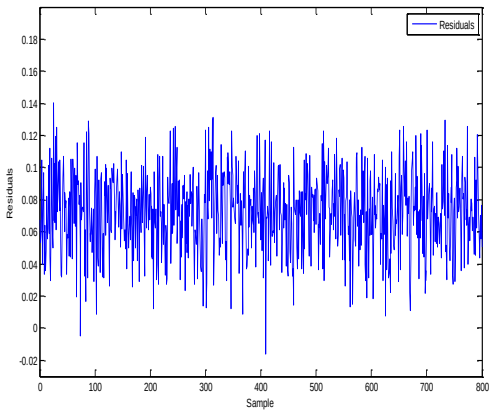

Figure 3 -Time series plot of the residuals for the first quality variable

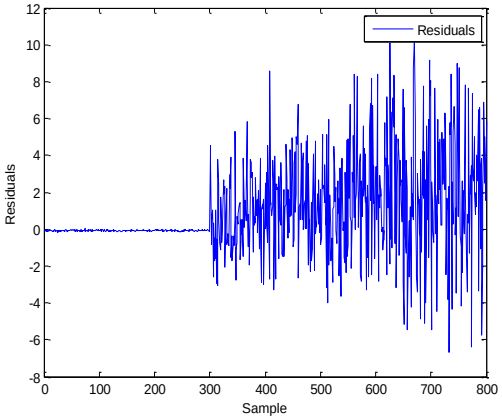

Figure 4 - Time series plot of the residuals for the second quality variable

8. Residuals plots for time varying process – test data set

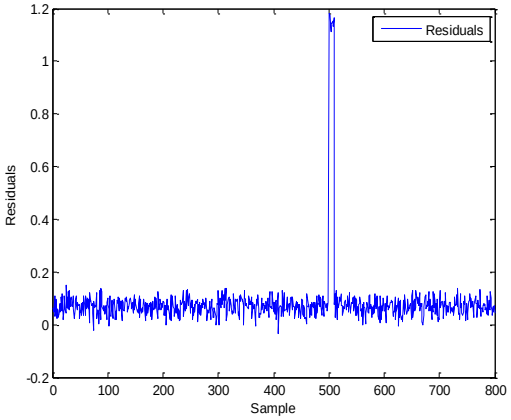

Figure 5 - Time series plot of the residuals for the first quality variable

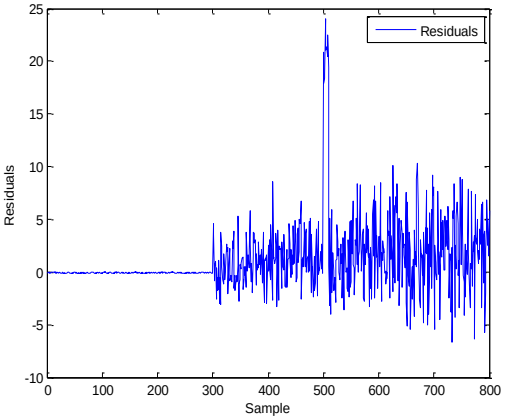

Figure 6 - Time series plot of the residuals for the second quality variable

9. Residuals plots for non-stationary process – calibration data set

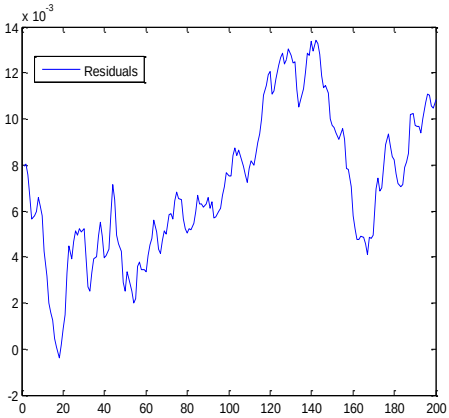

Figure 7 - Time series plot of the residuals for the first quality variable

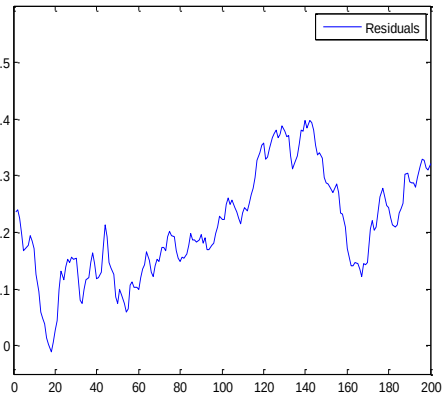

Figure 8 - Time series plot of the residuals for the second quality variable

10. Residuals plots for non-stationary process – validation data set

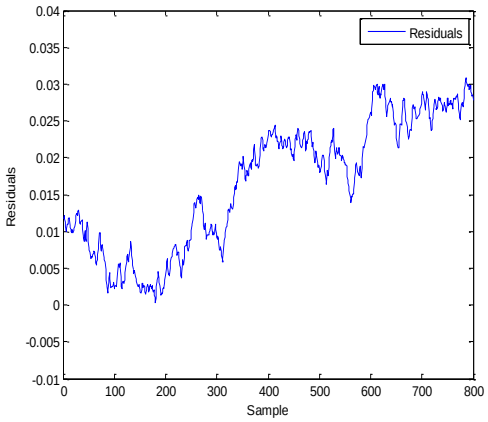

Figure 9 - Time series plot of the residuals for the first quality variable

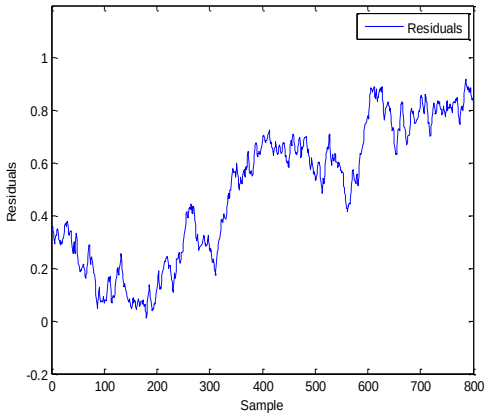

Figure 10 - Time series plot of the residuals for the second quality variable

11. residuals plots for non-stationary process – test data set

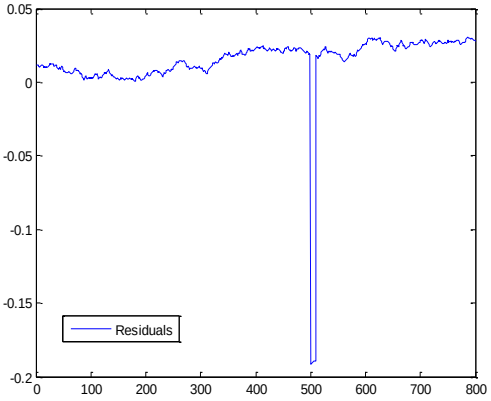

Figure 11-Time series plot of the residuals for the first quality variable

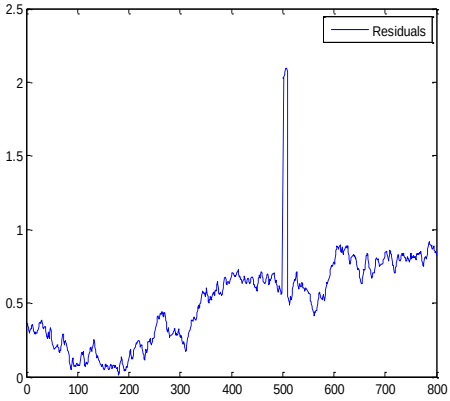

Figure 12-Time series plot of the residuals for the second quality variable

Appendix B

1. Recursive Kernel Algorithm

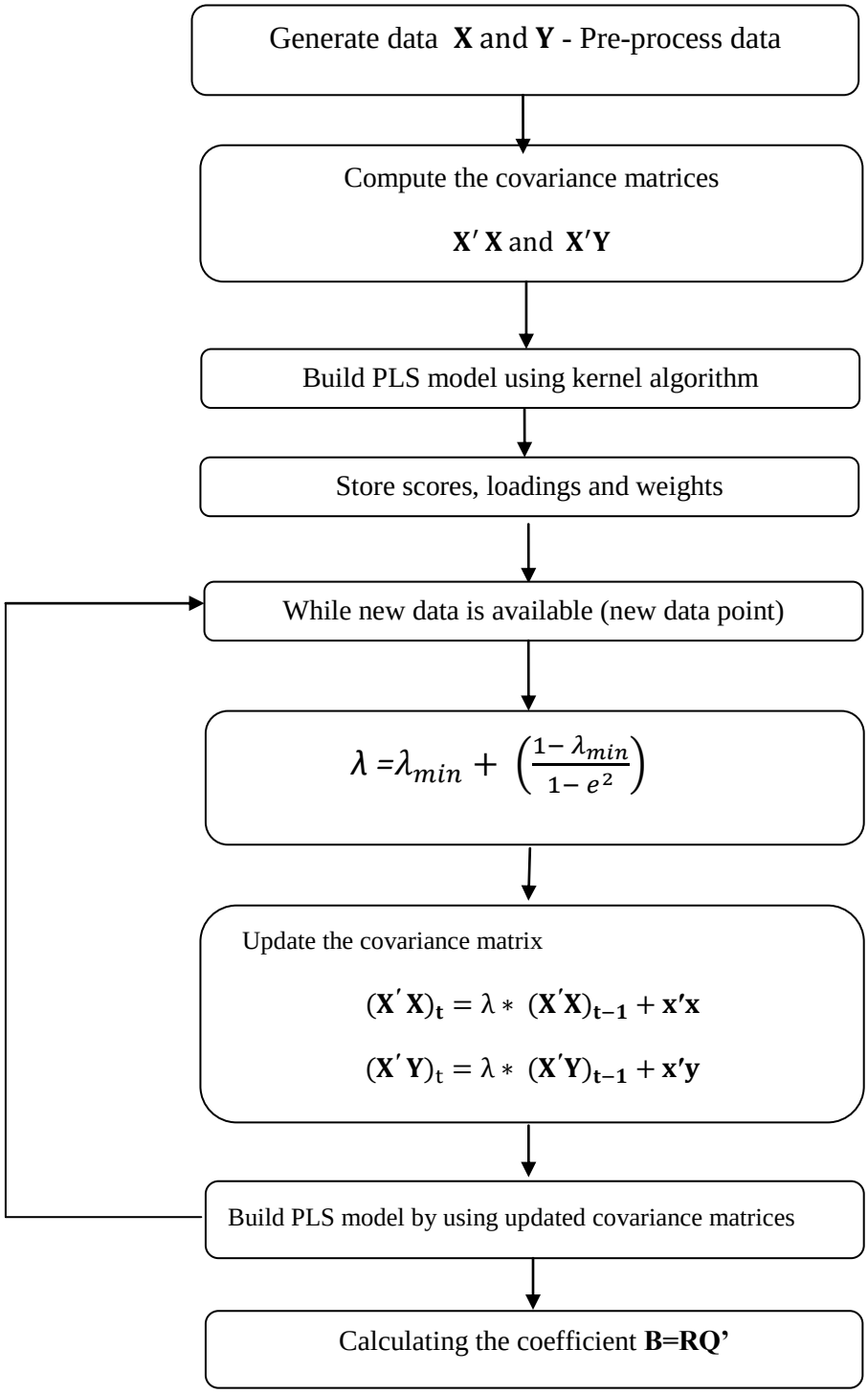

Where $(\mathbf{X}'\mathbf{X})_{t-1}$, $(\mathbf{X}'\mathbf{Y})_{t-1}$ are the covariance matrices at time t-1

$(\mathbf{X}'\mathbf{X})_t$, $(\mathbf{X}'\mathbf{Y})_t$ are the updated covariance matrices at time t

x (1×m) new predictor vector, **y** (1× k) new response vector

λ is a variable forgetting factor, λ_{min} the minimum value of the forgetting

2. Time varying process –Adaptive PLS – Validation data set

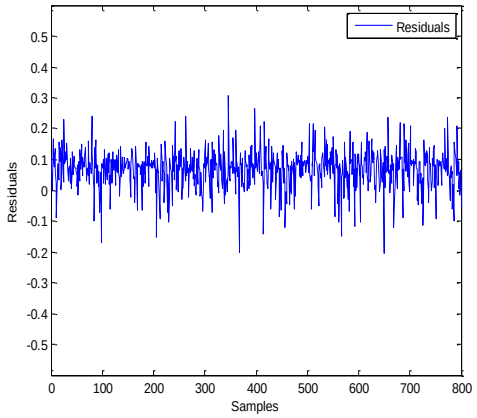

Figure 13- Residual of first quality variable – APLS for validation data set

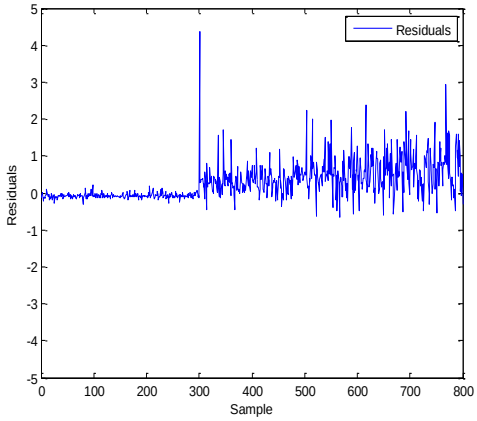

Figure 14- Residual of second quality variable – APLS for validation data set

3. Time varying process –Adaptive PLS – Test data set

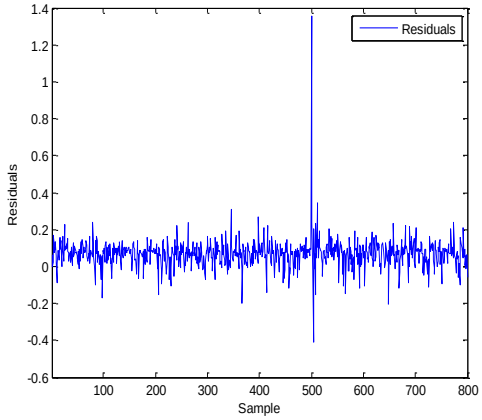

Figure 15 - Residual of first quality variable –APLS for test data set

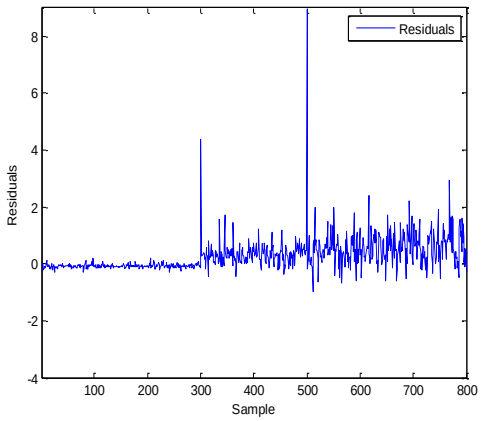

Figure 16 - Residual of second quality variable –APLS for test data set

4. Time varying process –RAPLS – Test data set

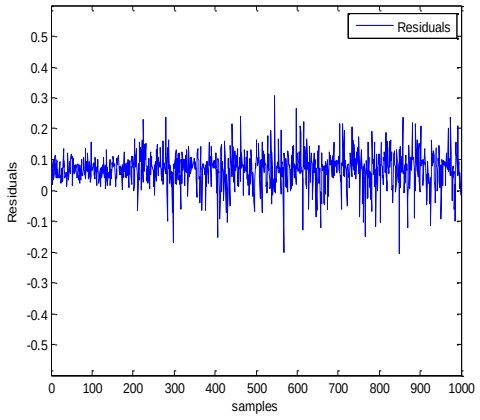

Figure 17 - Residual of first quality variable –RAPLS for test data set

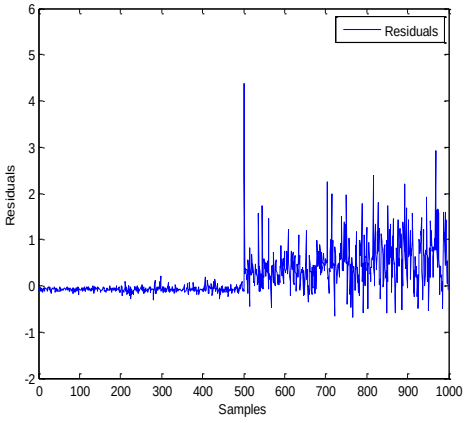

Figure 18 - Residual of Second quality variable –RAPLS for test data set

5. Residual of first quality variable –RAPLS for validation data set

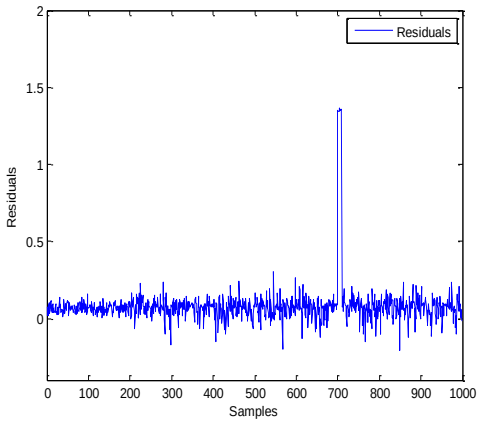

Figure 19 - Residual of first quality variable –RAPLS for validation data set

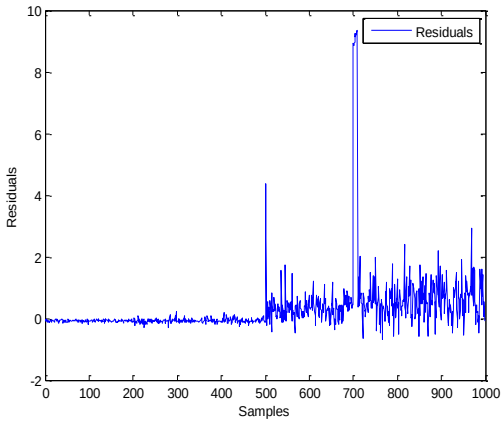

Figure 20 - Residual of Second quality variable –RAPLS for validation data set

6. Time series plot of outliers weight –RAPLS for validation data set

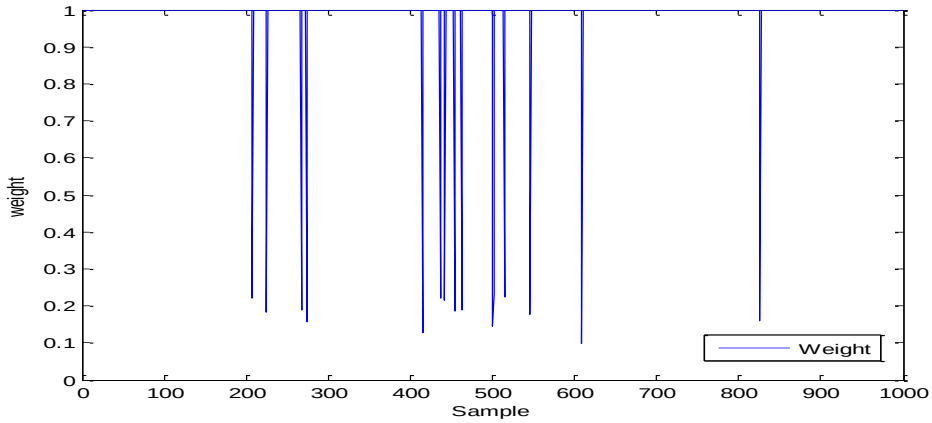

Figure 21 - Outliers weight –RAPLS for validation data set

7. Time series plot of outliers weight –RAPLS for test data set

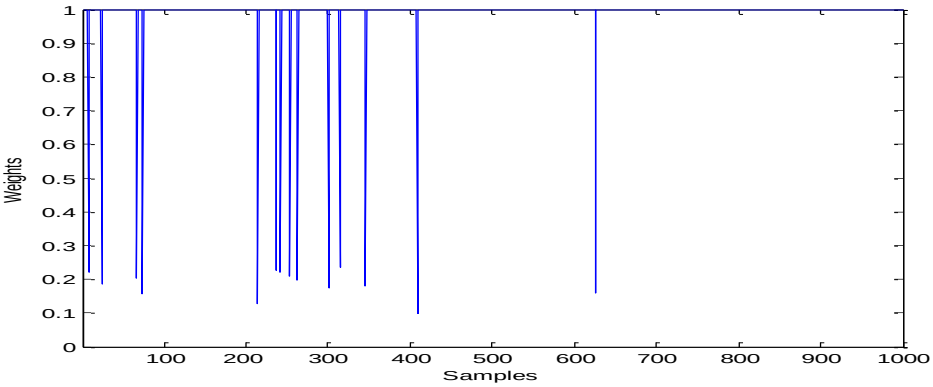

Figure 22- Outliers weight –RAPLS for test data set

8. Non-stationary process –Adaptive PLS –Validation data

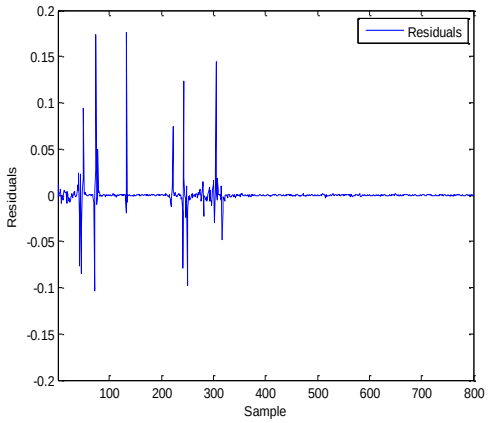

Figure 23 - Residual of first quality variable –APLS for validation data set

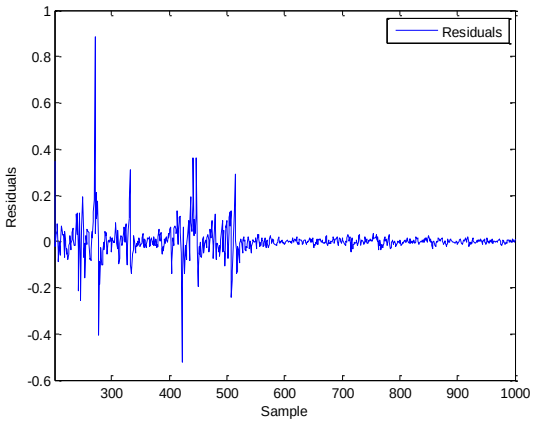

Figure 24 - Residual of Second quality variable –APLS for validation data set

9. Non-stationary process –Adaptive PLS –test data

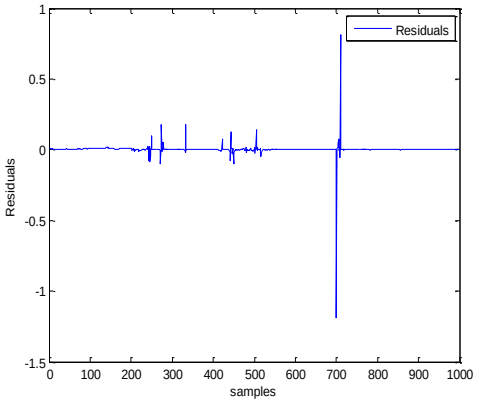

Figure 25 - Residual of first quality variable –APLS for test data set

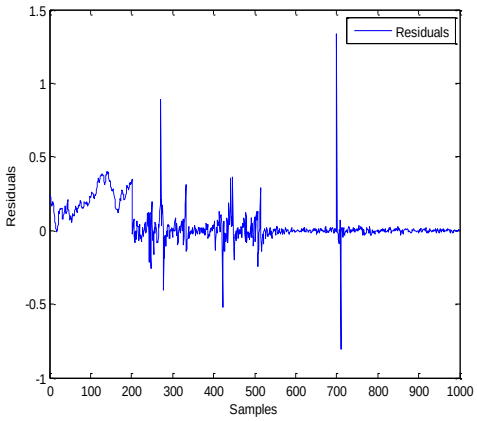

Figure 26 -Residual of Second quality variable –APLS for test data set

10. Non-stationary process –Robust Adaptive PLS – Validation data

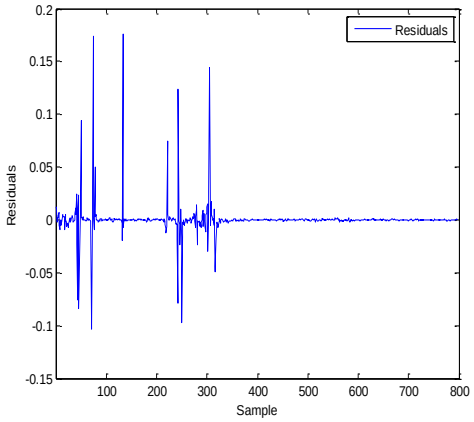

Figure 27 - Residual of first quality variable – RAPLS for validation data set

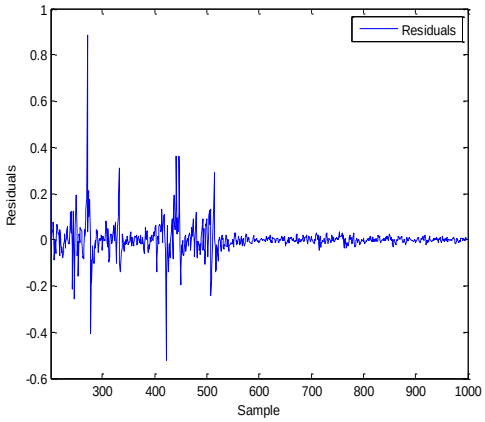

Figure 28 - Residual of Second quality variable –RAPLS for validation data set

11. Non-stationary process –Robust Adaptive PLS –test data

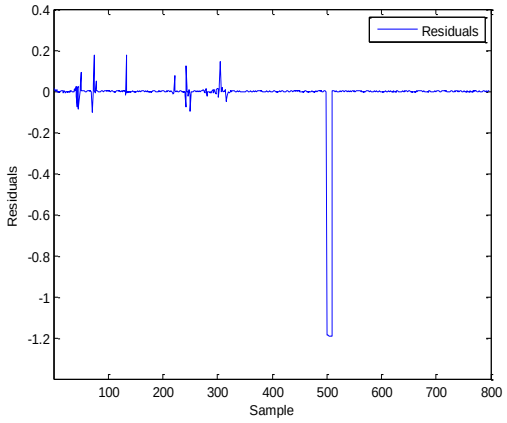

Figure 29 - Residual of first quality variable –APLS for test data set

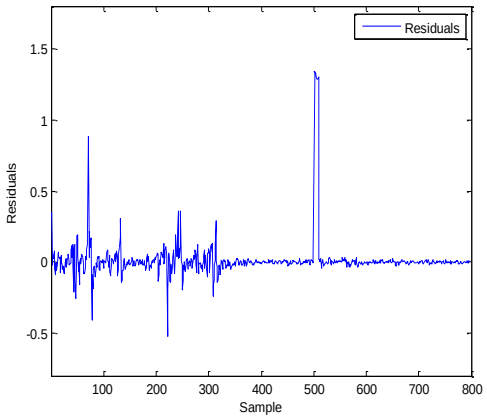

Figure 30 - Residual of Second quality variable –APLS for test data set

12. Time series plot of outliers weight –RAPLS for validation data set

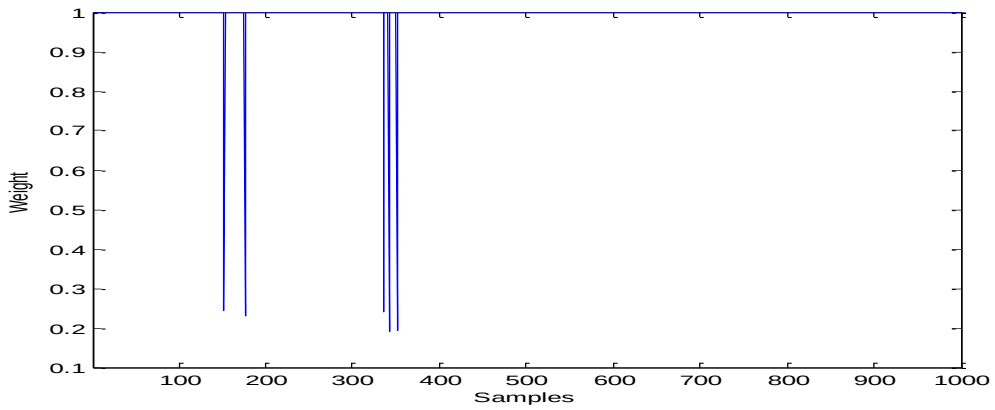

Figure 31 - Outliers weight –RAPLS for validation data set

13. Time series plot of outliers weight –RAPLS for test data set

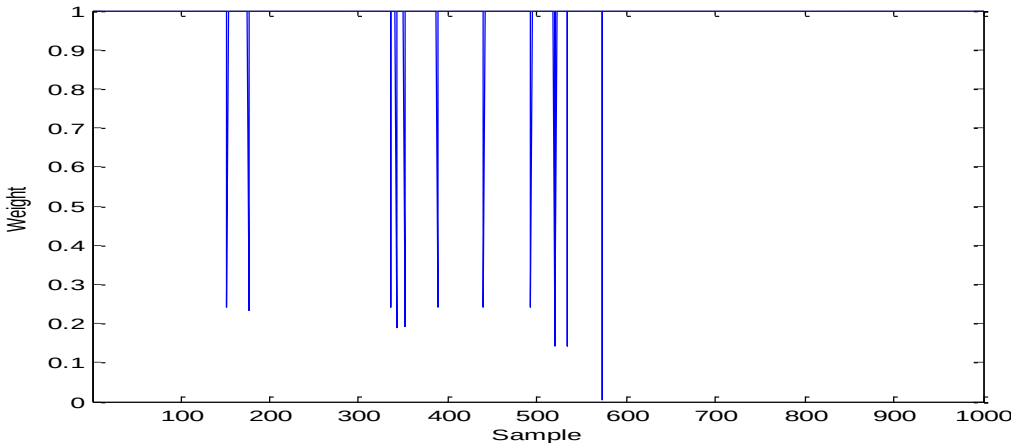

Figure 32- Outliers weight –RAPLS for test data set

14. Confidence limits for Hotelling T^2

- As mentioned latent variables are linear combinations of the original variables. Therefore they approximately normally distributed.
- T^2 related to F distribution, considering that mean and covariance are estimated from the data

  $\frac{N\,(N-a)}{a\,(N^2-1)}\,T^2 \sim F_{a,N-a}$
- For given α, the process is in state of statistical control if

  $T^2 < \frac{a\,(N^2-1)}{N\,(N-a)}\,F_{a,N-a}$
- If the mean is accurately known and only the covariance are estimated, the control limit is given by:
- If N is large, the estimations of the mean and the covariance are accurate hence the T^2 monitoring index will be approximated with χ^2 with a degree of freedom

15. Confidence limits for Squared prediction error

- Jackson, J. E. and Mudholkar, G. S. (1979) developed the following limits for the squared prediction error monitoring statistics.

  $SPE_{\alpha} = \theta_1\left(\frac{C_\alpha\sqrt{2\theta_2 h_0^2}}{\theta_1} + 1 + \frac{\theta_2 h_0(h_0-1)}{\theta_1^2}\right)$

  Where $\theta_i = \sum_{j=a+1}^{m} \lambda_j^i$ and $h_0 = 1 - \frac{2\theta_1\theta_3}{3\theta_2^2}$

16. Weight value for time variant and nonstationary processes

Weight value used to weight the outlying samples – Time variant processes

Weight type	Value 1	Value 2	Value 3	Final used weight
Caushy	Weight = 1.7 RMSEC=0.06 RMSEV=0.59	Weight = 0.99 RMSEC=0.037 RMSEV=0.57	Weight = 0.3 RMSEC=0.12 RMSEV=0.97	Fair function Weight value =0.99
Fair	Weight = 1.7 RMSEC=0.06 RMSEV=0.61	Weight = 0.99 RMSEC=0.03 RMSEV=0.56	Weight = 0.3 RMSEC=0.1 RMSEV=0.95	

Weight value used to weight the outlying samples – Nonstationary processes

Weight type	Value 1	Value 2	Value 3	Final used weight
Caushy	Weight = 1.7 RMSEC=0.08 RMSEV=0.085	Weight = 0.99 RMSEC=0.02 RMSEV=0.07	Weight = 0.3 RMSEC=0.07 RMSEV=0.085	Fair function Weight value =0.99
Fair	Weight = 1.7 RMSEC=0.09 RMSEV=0.085	Weight = 0.99 RMSEC=0.01 RMSEV=0.06	Weight = 0.3 RMSEC=0.07 RMSEV=0.09	

Appendix C

1. Input matrix response to a step change in overall pressure at t=1000 sec

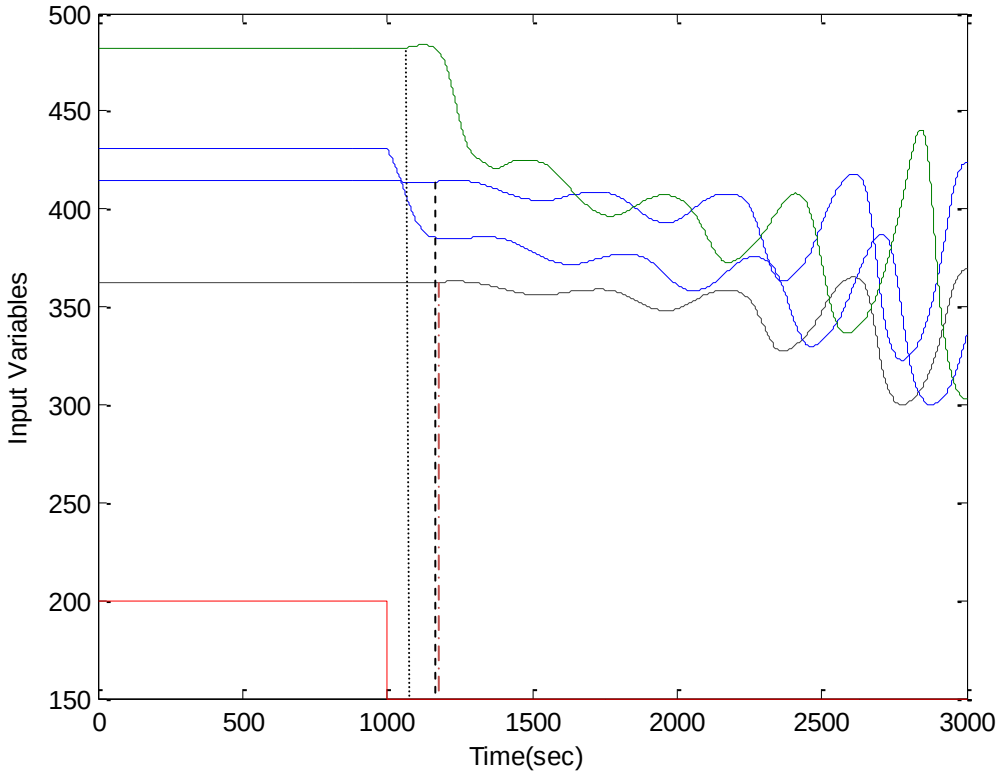

Figure 33 – input variables

2. Modelling results of different sampling periods and different dynamic structures

Sampling frequency	Dynamic structure	RMSEC	RMSEV	% Variance captured
25 sec	No	0.000266	0.0014	95%
25 sec	ARX(1,1,3)	0.000265	0.0012	96.01%
25 sec	ARX(1,1,10)	0.00024	0.0011	94.18%
25 sec	ARX(3,3,1)	0.0004	0.0013	89.97%
15 sec	No	0.00049	0.0011	94.87%
15 sec	ARX(1,1,3)	0.00045	0.0010	95.51%
15 sec	ARX(1,1,10)	0.00044	0.00045	95.55%
15 sec	ARX(3,3,1)	0.00056	0.0011	85.17%
10 sec	No	0.0004	0.00098	95.00%
10 sec	ARX(1,1,3)	0.00034	0.00093	95.24%
10 sec	ARX(1,1,10)	0.00032	0.0009	97.29%
10 sec	ARX(3,3,1)	0.0004	0.00094	95.80%
5 sec	No	0.00048	0.0016	92.00%
5 sec	ARX(1,1,3)	0.00041	0.00089	93.89%
5 sec	ARX(1,1,10)	0.00041	0.00088	95.46
5 sec	ARX(3,3,1)	0.00039	0.00097	92.77%

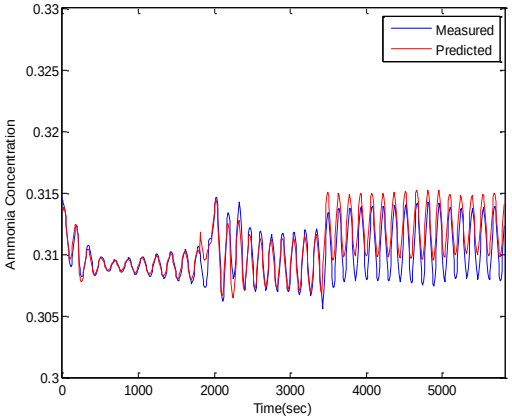

Figure 34 - 25sec sampling interval-Static PLS

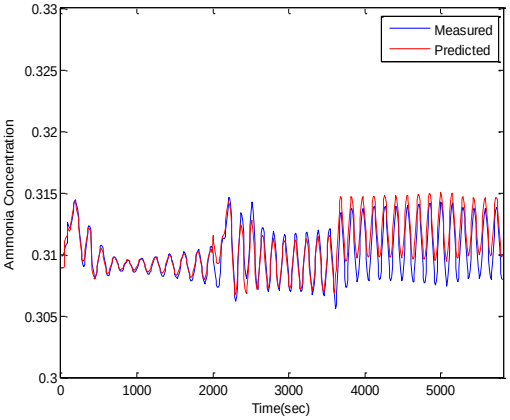

Figure 35 - 25sec sampling interval - ARX(1,1,3)

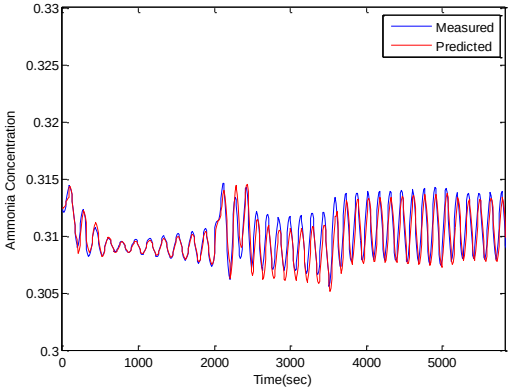

Figure 36 - sampling interval 25sec-ARX(1,1,10)

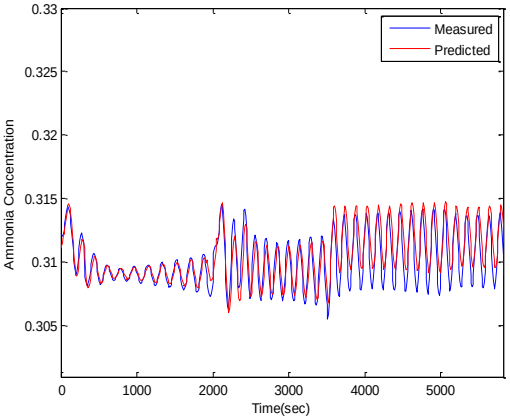

Figure 37 - sampling interval 25sec - ARX(3,3,1)

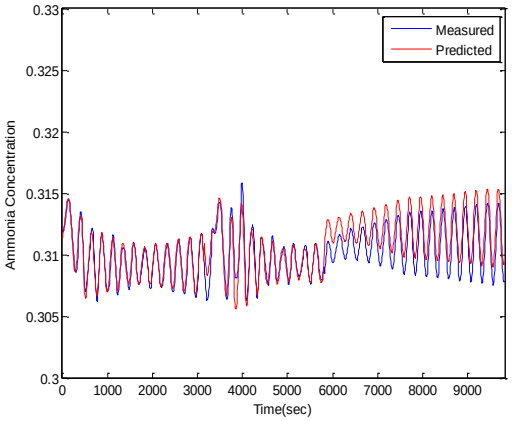

Figure 38 - sampling interval 15 sec - Static PLS

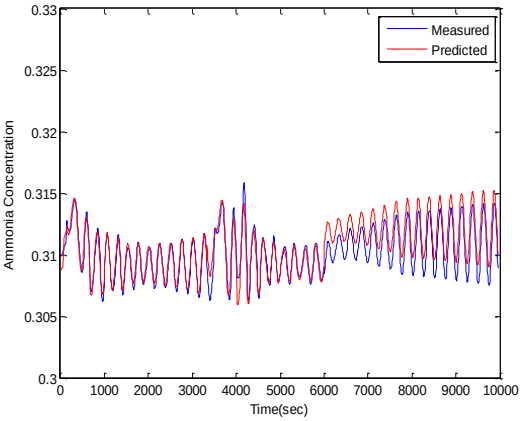

Figure 39 – Sampling interval 15sec ARX(1,1,3)

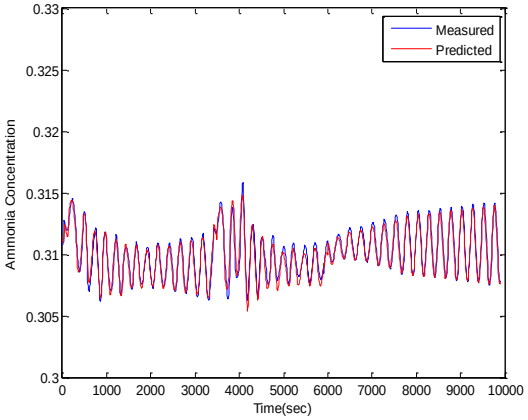

Figure 40 - Sampling interval 15sec ARX(1,1,10)

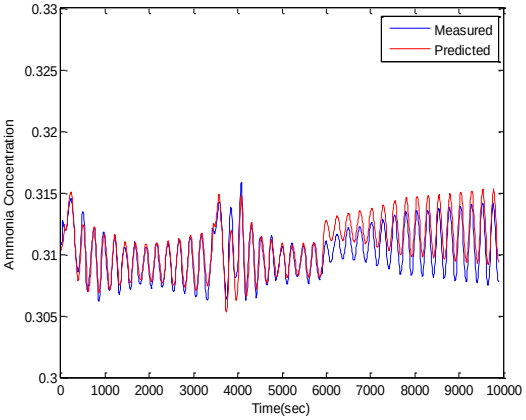

Figure 41 - Sampling interval 15sec ARX(3,3,1)

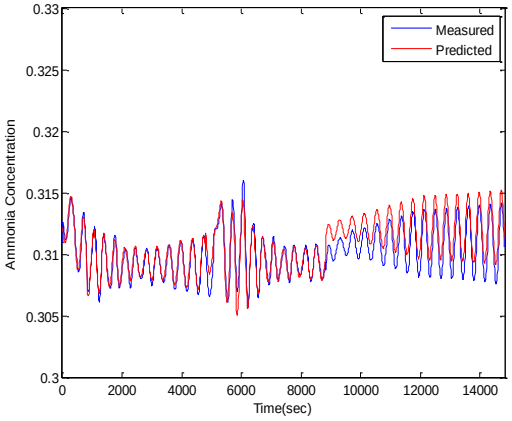

Figure 42 - Sampling interval 10 sec - Static PLS

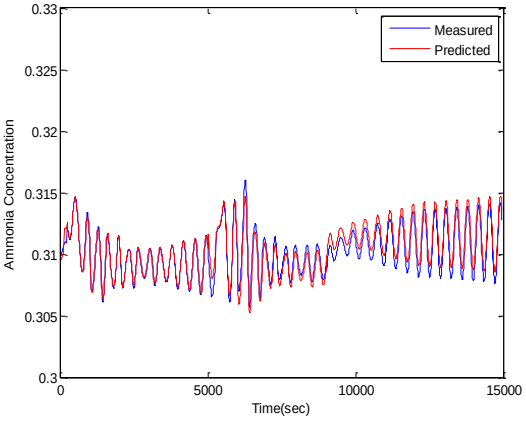

Figure 43 - Sampling interval 10sec ARX(1,1,3)

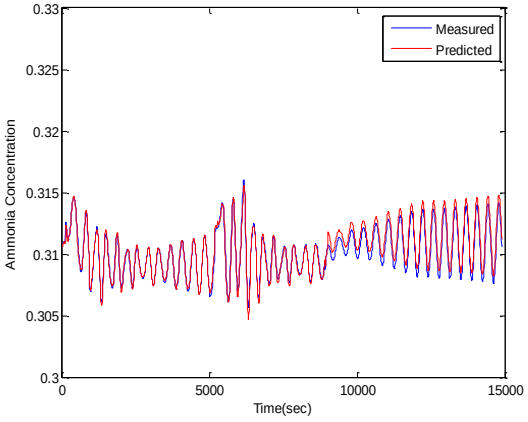

Figure 44 - Sampling interval 10 sec ARX(1,1,10)

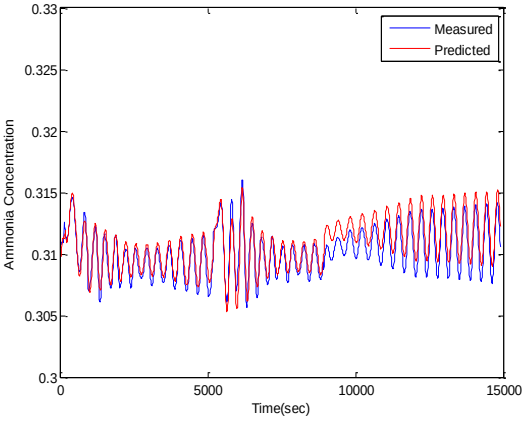

Figure 45 - Sampling interval 10sec ARX(3,3,1)

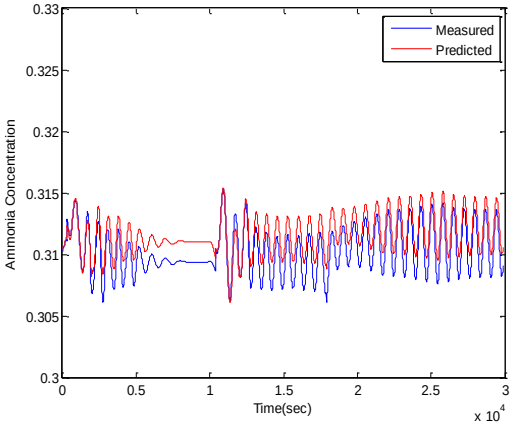

Figure 46 - Sampling interval 5sec Static PLS

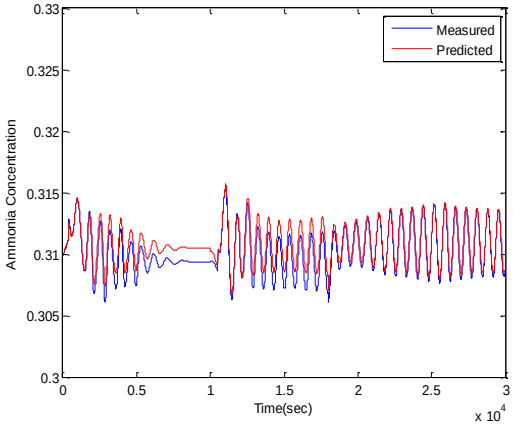

Figure 47 - Sampling interval 5sec ARX(1,1,3)

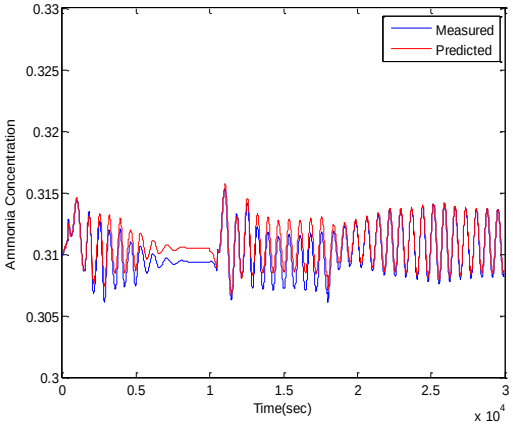

Figure 48 - Sampling interval 5sec ARX(1,1,10)

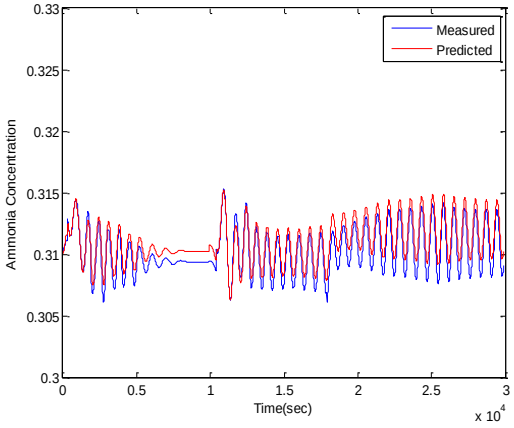

Figure 49 - Sampling interval 5sec ARX(3,3,1)

3. Modelling of ammonia Synthesis reactor based on 10 sampling period and ARX(1,1,3)

Dynamic PLS (DPLS) was applied to the normalized data and the dynamic structure identified in Chapter 6(§ 6.7.1). The first step was to determine the number of latent variables LVs by the use of cross validation approach. Figure 1 shows the RMSE of the calibration and RMSE of cross validation. Both indices indicate that three latent variables are appropriate to model the process. Table 1 shows that four latent variables correspond to 96.43 % of the total amount of variance explained in the X-block and 95.24 % of the variance explained in the output.

Table 1- Percentage variance captured from DPLS model

LV	X-block		Y-block	
	%Variance	% Cumulative	%Variance	% Cumulative
1	49.91	49.91	66.76	66.76
2	22.27	72.18	25.28	92.04
3	20.02	92.20	2.07	94.12
→ 4	4.23	96.43	1.13	95.24
5	2.05	98.48	0.99	96.23
6	1.22	99.70	0.57	96.80
7	0.30	100.00	0.07	96.87
8	0.00	100.00	0.03	96.90
9	0.00	100.00	0.00	96.90
10	0.00	100.00	0.00	96.90
11	0.00	100.00	0.00	96.90

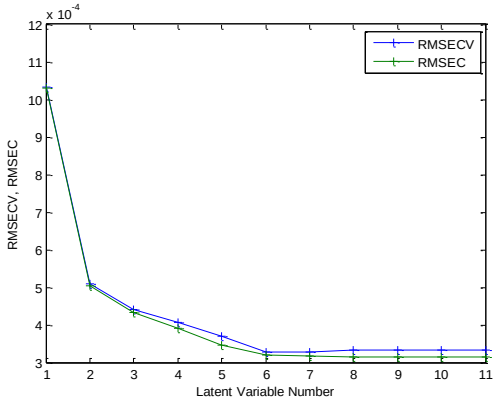

Figure 50 - Cross validation results for determining the number of *LVs*

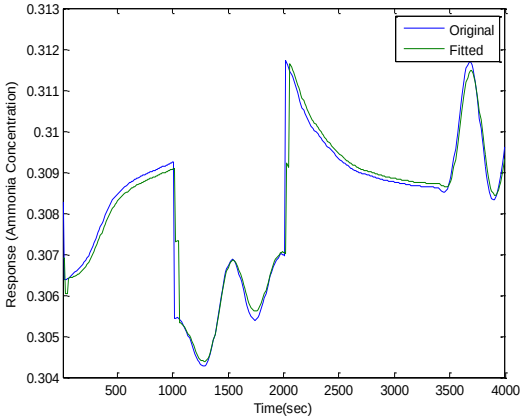

Figure 51 - Time series plot of the original and fitted response

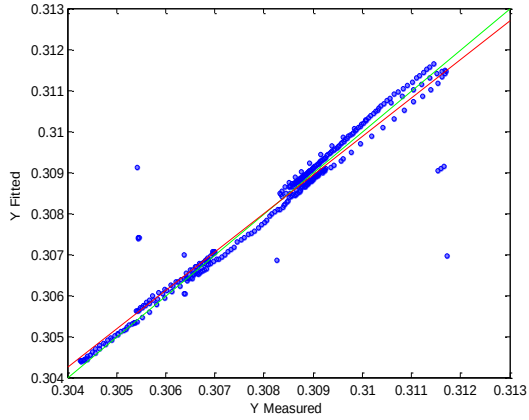

Figure 52 - Original vs. fitted response

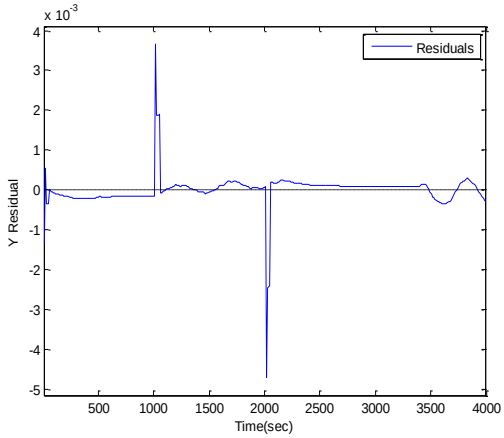

Figure 53 - Time series plot of the residuals for reference model

The results from applying the DPLS model to the validation data sets are presented in Figure 5 to Figure 6. It can be seen that the model dose not well fit the data.

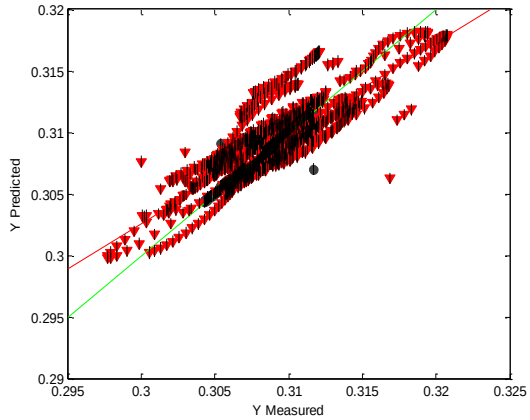

Figure 54 - Measured vs. predicted response of validation data set

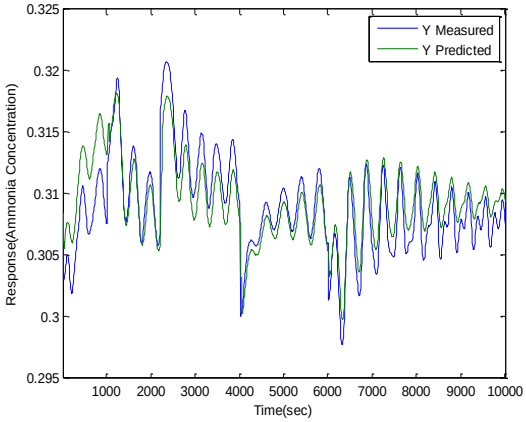

Figure 55 - Time series of measured and predicted response of validation data set

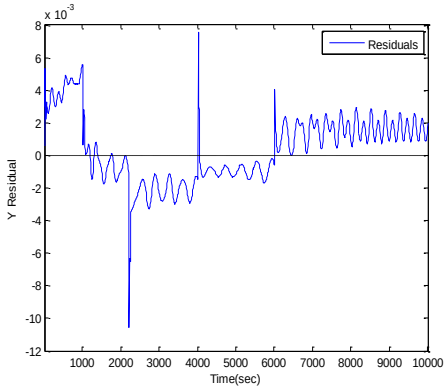

Figure 56 - Time series plot of the residuals for validation data set

The results from applying the DPLS model to the two testing data sets corresponding case1 and case 2

Case1- Testing data sets

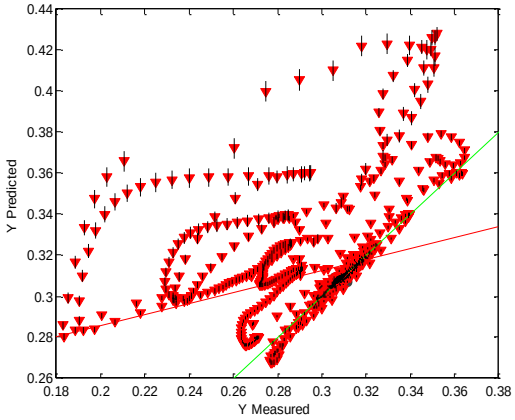

Figure 57 - Measured vs. predicted response of test data set – Case1

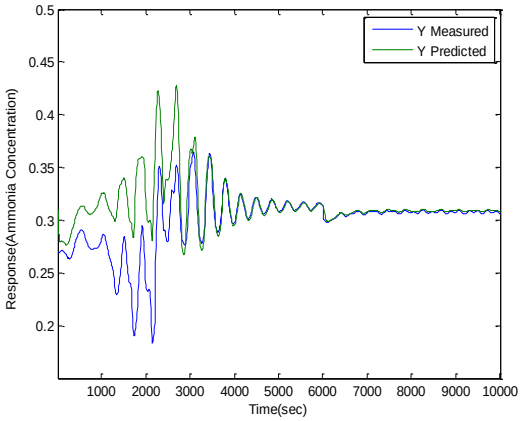

Figure 58 - Time series of measured and predicted response of test data set – Case 1

Case2- Testing data set

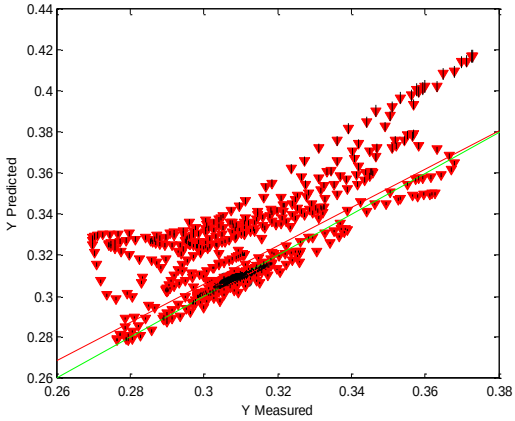

Figure 59 - Measured vs. predicted response of test data set – Case2

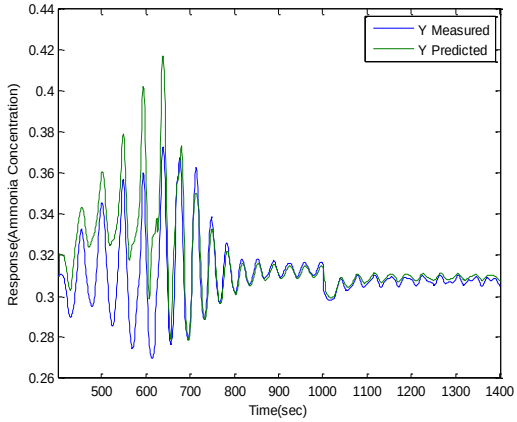

Figure 60 - Time series of measured and predicted response of test data set-Case2

4. Modelling of ammonia Synthesis reactor based on 10 sampling period and ARX(3,3,1)

Dynamic PLS (DPLS) was applied to the normalized data and the dynamic structure identified in Chapter 6(§ 6.7.1). The first step was to determine the number of latent variables LVs by the use of cross validation approach. Figure 1 shows the variance captured by the model. It can be seen that 4 latent variables are appropriate to model the process. Table 2 shows that four latent variables correspond to 95.84% of the total amount of variance explained in the X-block and 95.80% of the variance explained in the output.

Table 2- Percentage variance captured from DPLS model

LV	X-block		Y-block	
	%Variance	% Cumulative	%Variance	% Cumulative
1	51.05	51.05	68.17	68.17
2	21.10	72.15	25.41	93.58
3	19.54	91.69	1.62	95.20
→ 4	4.15	95.84	0.60	95.80
5	1.96	97.81	0.55	96.35
6	1.43	99.24	0.25	96.60
7	0.22	99.46	0.23	96.83
8	0.19	99.64	0.05	96.89
9	0.17	99.81	0.04	96.93
10	0.13	99.94	0.04	96.96
11	0.03	99.97	0.05	97.01
12	0.01	99.98	0.10	97.11
13	0.01	99.99	0.06	97.17
14	0.01	100.00	0.01	97.18
15	0.00	100.00	0.01	97.19
16	0.00	100.00	0.03	97.22
17	0.00	100.00	0.01	97.23
18	0.00	100.00	0.00	97.23
18	0.00	100.00	0.00	97.23
20	0.00	100.00	0.00	97.23

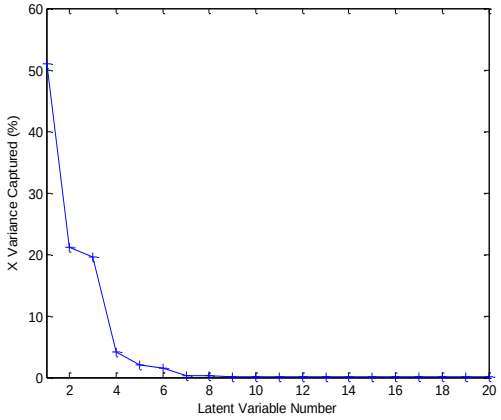

Figure 61 - Variance captured by individual latent variables

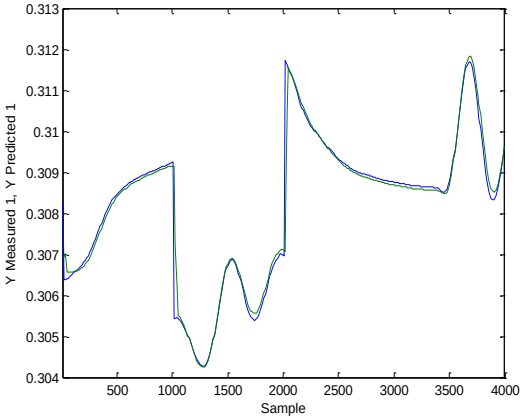

Figure 62 -Time series plot of the original and fitted response

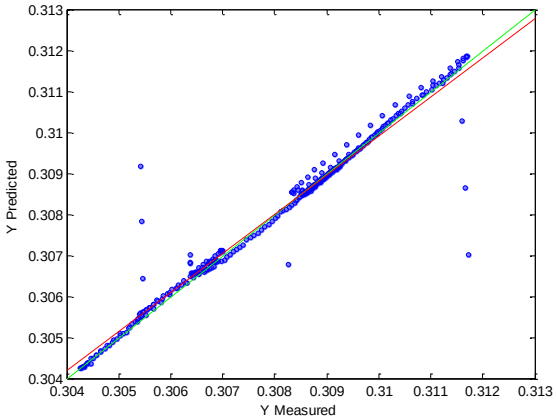

Figure 63 - Original vs. fitted response

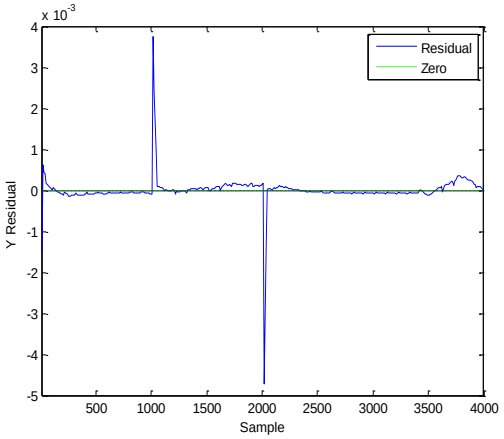

Figure 64 - Time series plot of the residuals for reference model

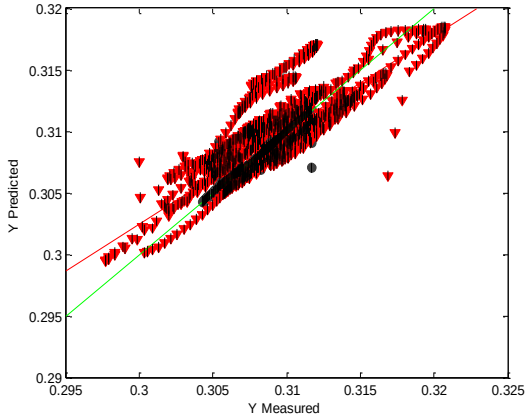

Figure 65 -Measured vs. predicted response of validation data set

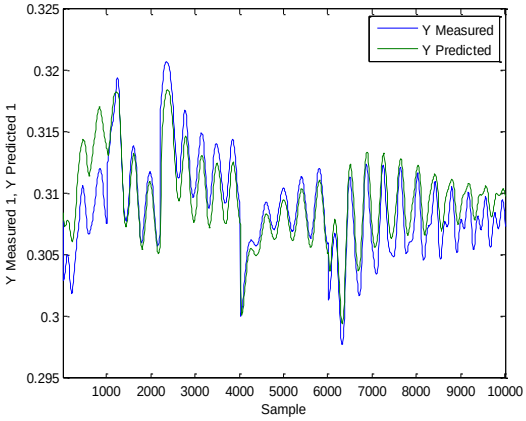

Figure 66 - Time series of measured and predicted response of validation data set

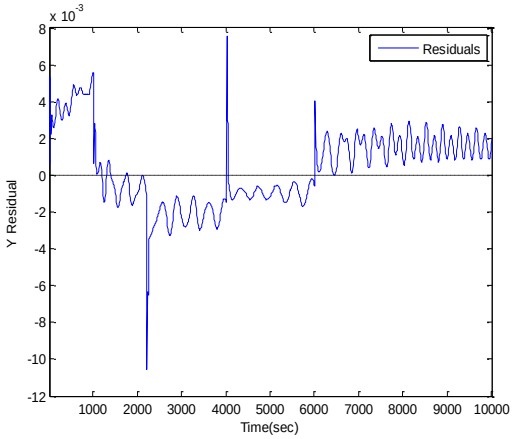

Figure 67 -Time series plot of the residuals for validation data set

Case1- Testing data sets

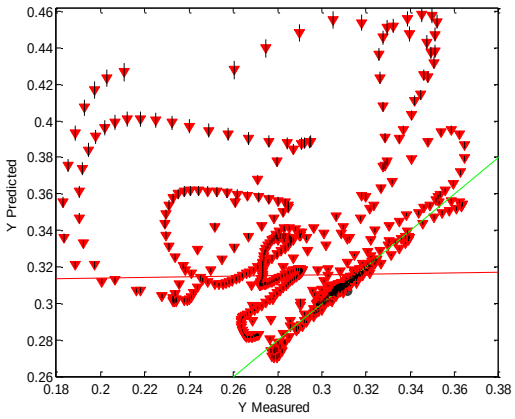

Figure 68 - The measured vs. predicted response (case 1-DPLS)

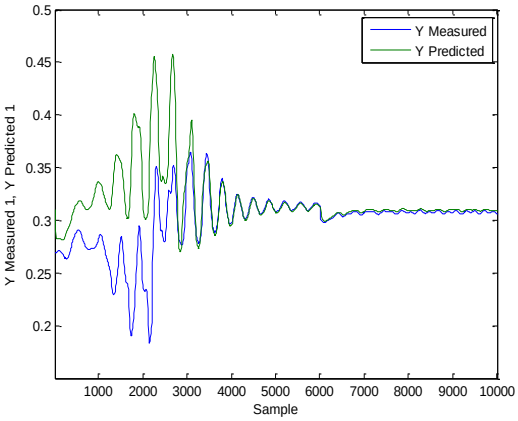

Figure 69 - Time series plot of the measured and predicted response (case 1-DPLS)

Case2- Testing data set

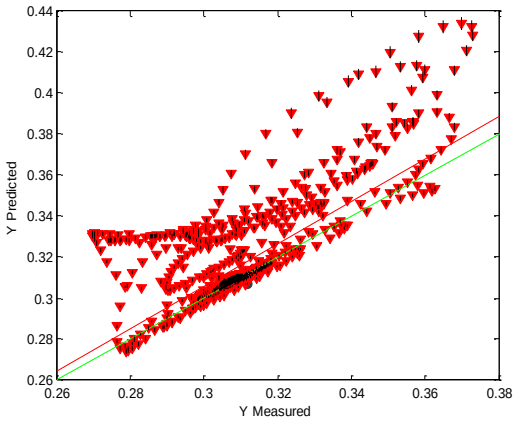

Figure 70 - The measured vs. predicted response (case 2-DPLS)

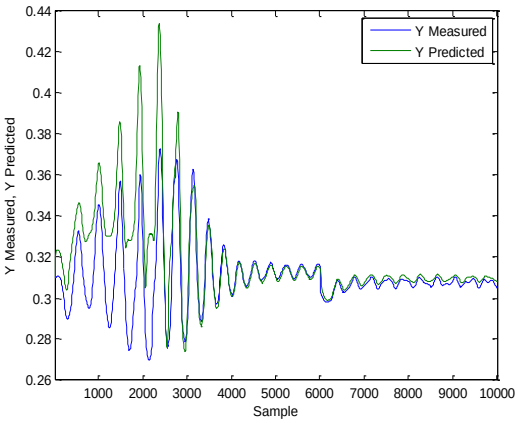

Figure 71 - Time series plot of the measured and predicted response (case 2-DPLS)

5. Residuals for the application of ADPLS to validation data set

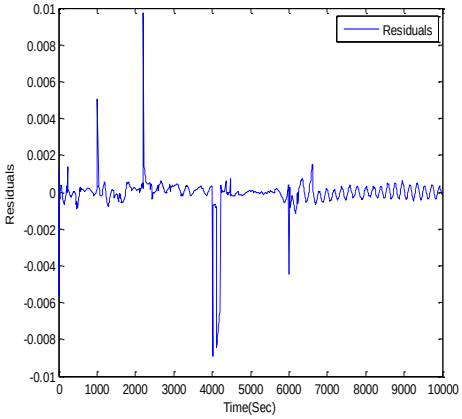

Figure 72 -Residuals for the application of ADPLS to validation data set –Fixed LVs

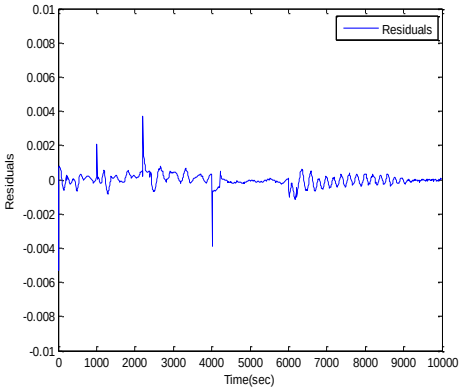

Figure 73 - Residuals for the application of ADPLS to validation data set-variable LVs.

6. Residuals for the application of ADPLS to the test data set (case 1)

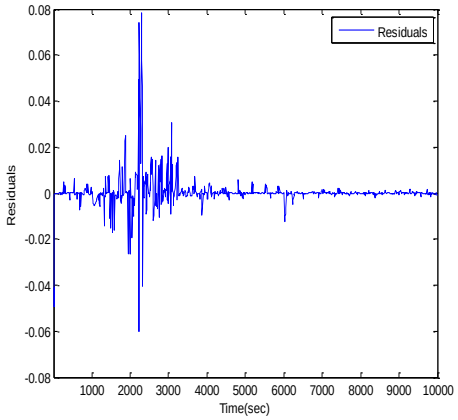

Figure 74 - Residuals for the application of ADPLS to test data set – Fixed LVs

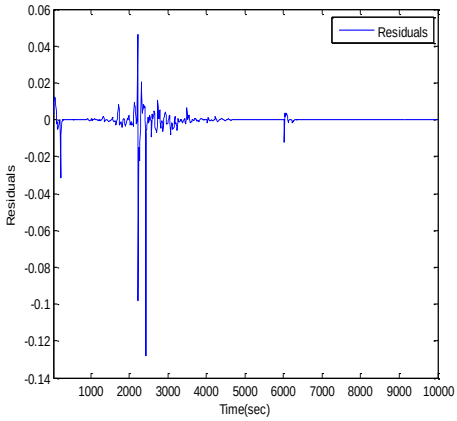

Figure 75 - Residuals for the application of ADPLS to test data set- variable LVs.

7. Residuals for the application of ADPLS to the test data set (case 2)

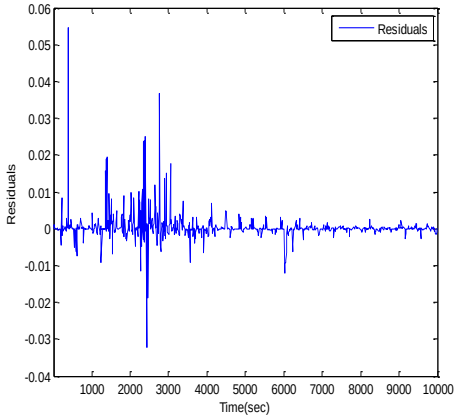

Figure 76 - Residuals for the application of ADPLS to test data set – Fixed LVs

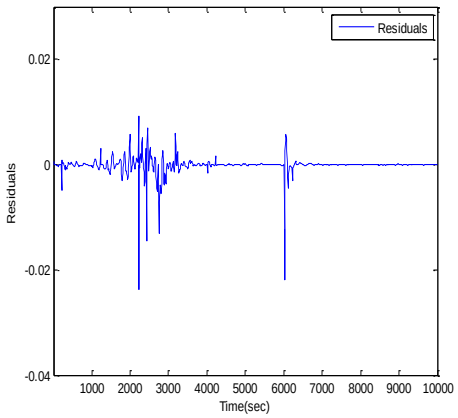

Figure 77 - Residuals for the application of ADPLS to test data set- variable LVs.

8. Residuals for the application of RADPLS to the validation data set

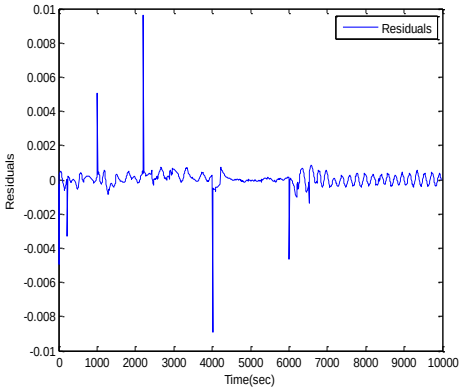

Figure 78 - Residuals for the application of ADPLS to test data set – Fixed LVs

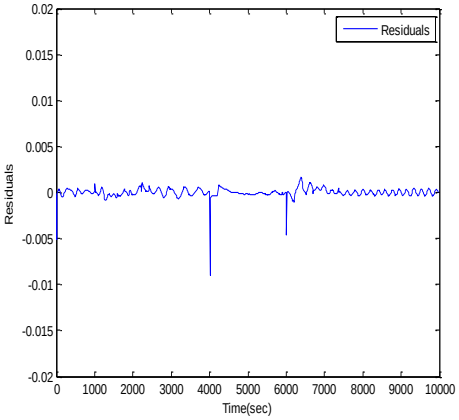

Figure 79 - Residuals for the application of ADPLS to test data set- variable LVs.

9. Residuals for the application of RADPLS to the test data set (case 1)

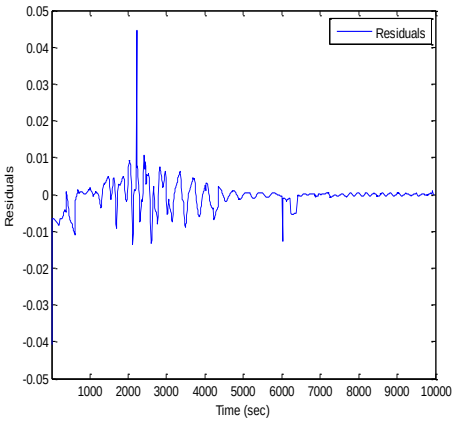

Figure 80 - Residuals for the application of RADPLS to test data set – Fixed LVs

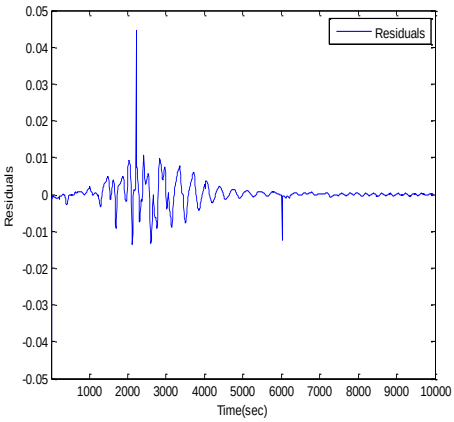

Figure 81 - Residuals for the application of RADPLS to test data set- variable LVs.

10. Residuals for the application of RADPLS to the test data set (case 2)

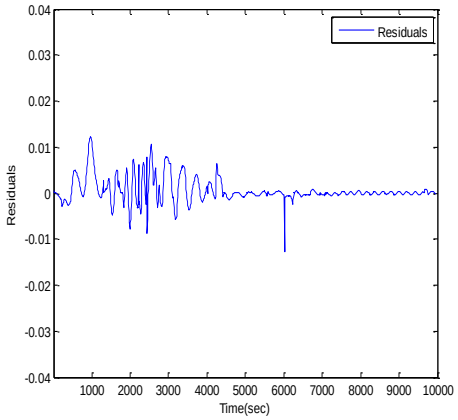

Figure 82 - Residuals for the application of RADPLS to test data set –Fixed LVs

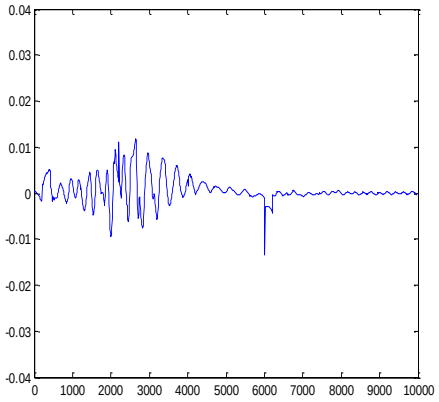

Figure 83 - Residuals for the application of RADPLS to test data set- variable LVs.

11. Weight value used to weight the outlying samples – Ammonia Reactor

Weight type	Value 1	Value 2	Value 3	Final used weight
Caushy	Weight = .90 RMSEV=0.00059	Weight = 1.5 RMSEV=0.0009	Weight = 0.2 RMSEV=0.0006	Fair function Weight value =0.90
Fair	Weight = 0.90 RMSEV=0.00057	Weight = 1.5 RMSEV=0.00087	Weight = 0.2 RMSEV=0.00062	

Appendix D

1- Monitoring statistics of static PLS model (6 LV) based on auto-scaled data.

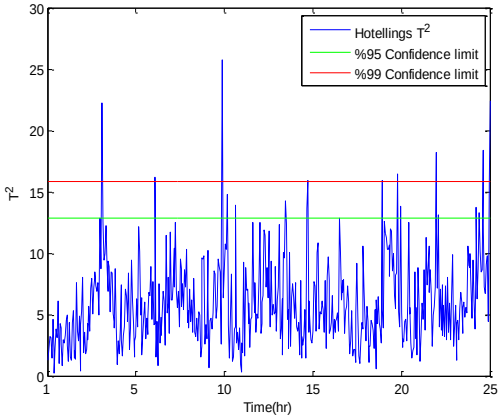

Figure 84 – Hotelling's T² for static PLS model (6 LV)- Auto-scaled calibration data set

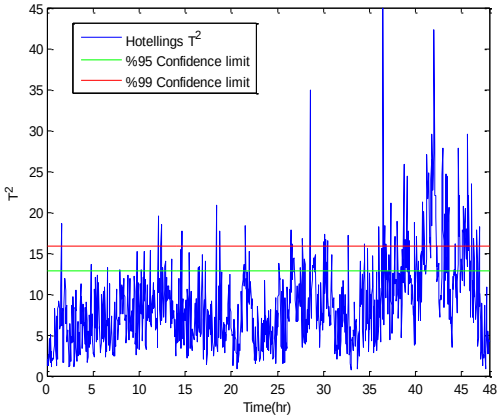

Figure 85 – Hotelling's T² for static PLS model (6 LV)- Auto-scaled validation data set

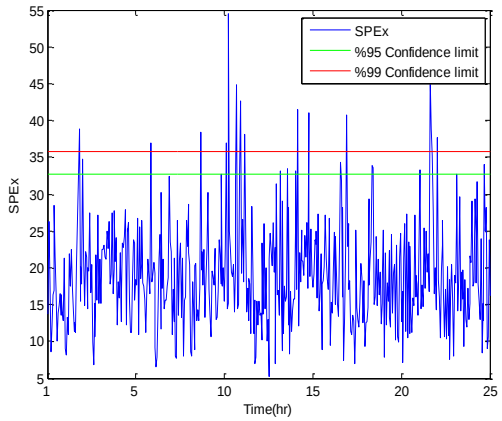

Figure 86 – SPE_X for static PLS model (6 LV)- Auto-scaled calibration data set

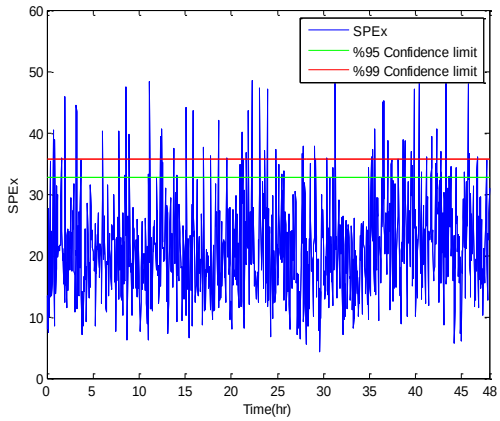

Figure 87 – SPE_X for static PLS model (6 LV)- Auto-scaled validation data set

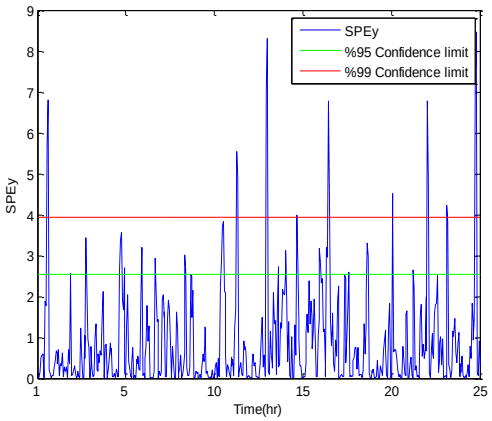

Figure 88 – SPE_Y for static PLS model (6 LV)- Auto-scaled calibration data set

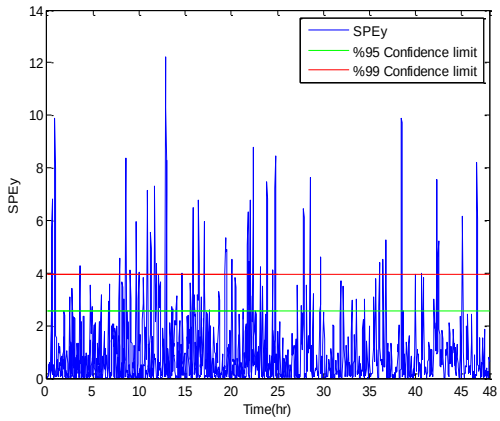

Figure 89 – SPE_Y for static PLS model (6 LV)- Auto-scaled validation data set

Calibration

Part	Chart	FAR 95%
whole process	Hotelling's T^2	7.2
	SPE_X	9.2
	SPE_Y	8.6

Validation

Part	Chart	FAR 95%
whole process	Hotelling's T^2	30%
	SPE_X	42%
	SPE_Y	37%

2- Monitoring statistics of the static PLS model (6 *LV*) based on block-scaled data

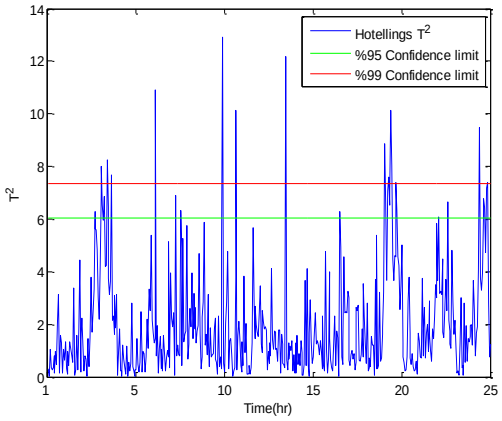

Figure 90 – Hotelling's T^2 for static PLS model (3 *LV*)- Block-scaled calibration data set

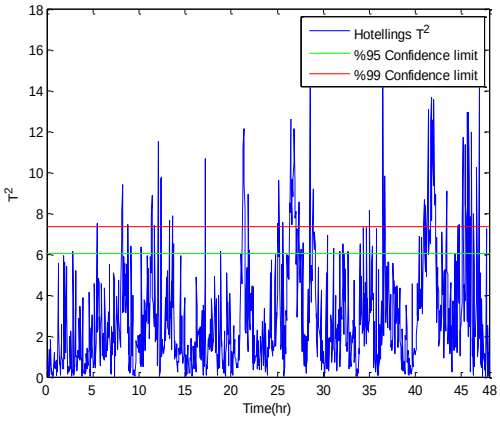

Figure 91 – Hotelling's T^2 for static PLS model (3 *LV*)- Block -scaled validation data set

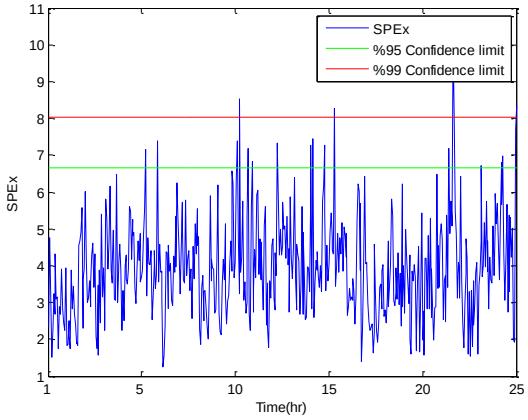

Figure 92 – SPE_X for static PLS model (3 *LV*)- block-scaled calibration data set

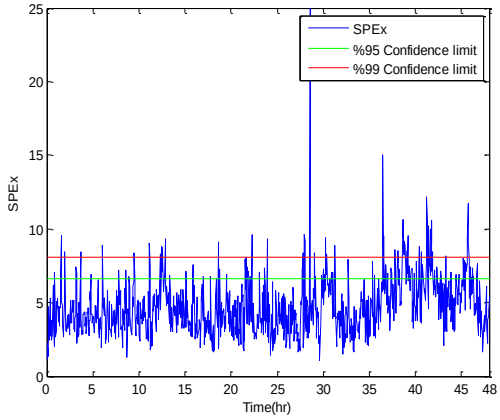

Figure 93 – SPE_X for static PLS model (3 *LV*)- Block -scaled validation data set

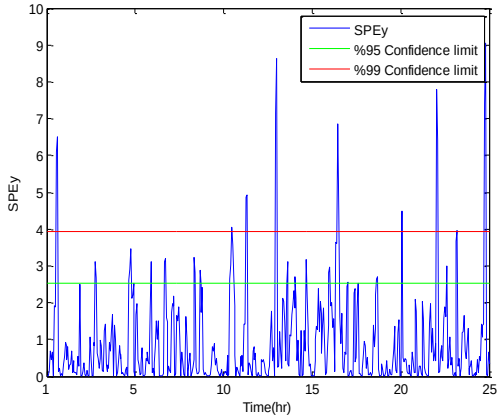

Figure 94 – SPE_Y for static PLS model (3 LV)- Block -scaled calibration data set

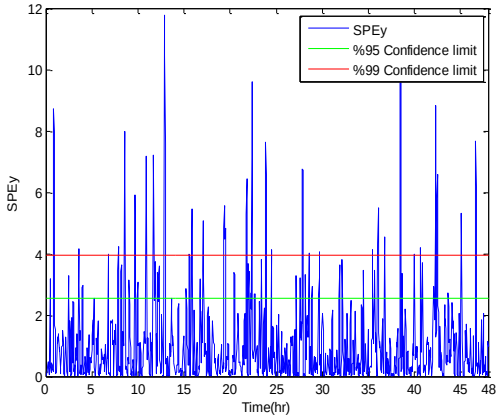

Figure 95 – SPE_Y for static PLS model (3 LV)- Block -scaled validation data set

Calibration

Part	Chart	FAR 95%
whole process	Hotelling's T^2	6.6
	SPE_X	8.7
	SPE_Y	8.3

Validation

Part	Chart	FAR 95%
whole process	Hotelling's T^2	29%
	SPE_X	38%
	SPE_Y	35%

Appendix E

1. Monitoring charts using DPLS and MBDPLS$_T$ for Fault (1)

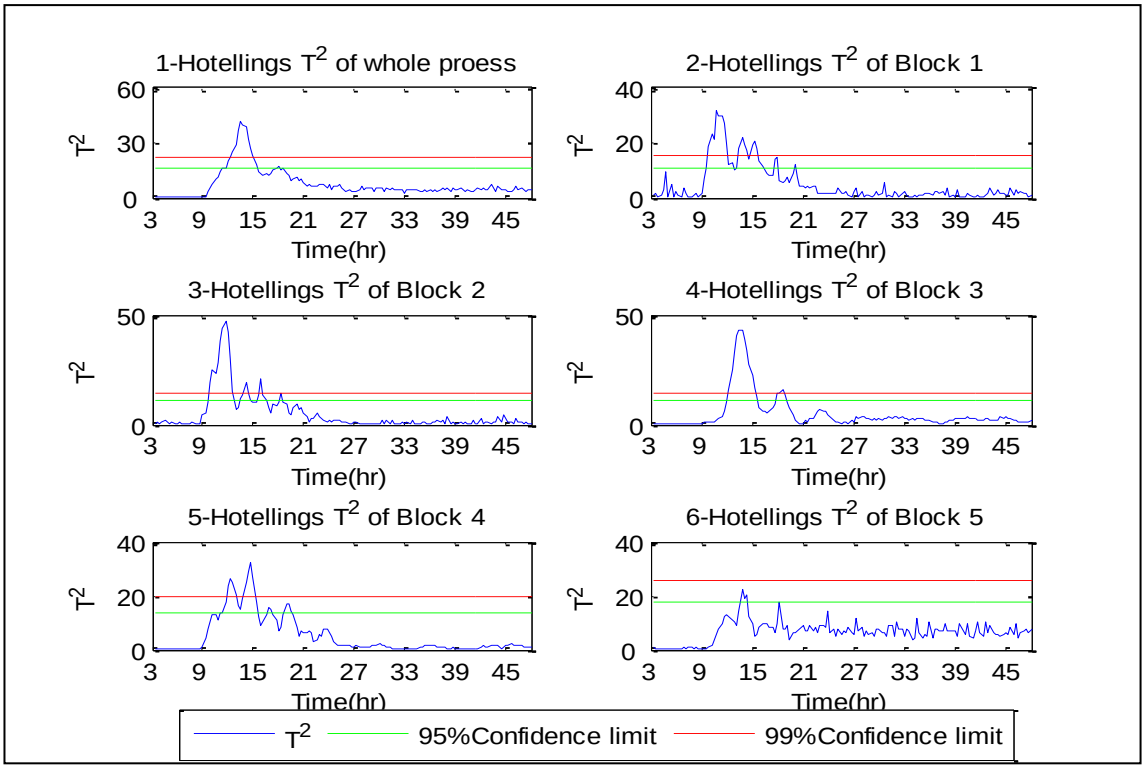

Figure 96 - Hotelling's T^2 for (1) overall process and (2-6) individual blocks based on DPLS and MBDPLS$_T$ approaches – Fault (1)

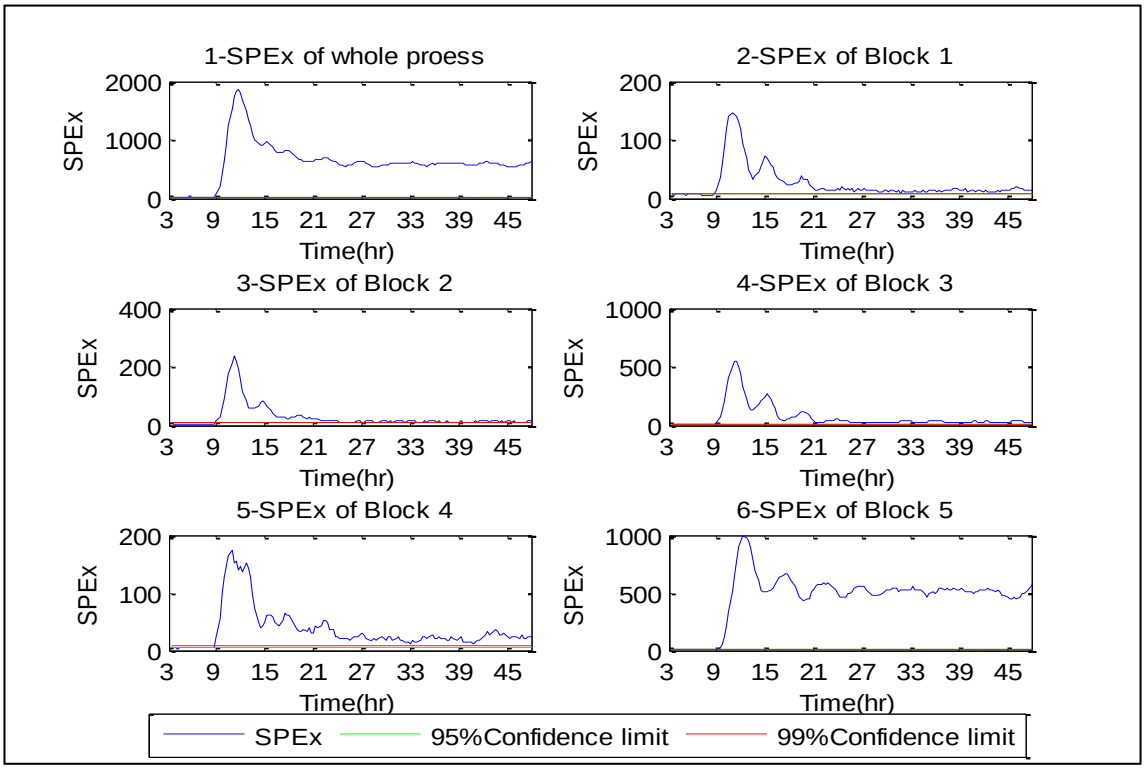

Figure 97 - SPE$_X$ for (1) overall process and (2-6) individual blocks based on DPLS and

MBDPLS$_T$ approaches – Fault (1)

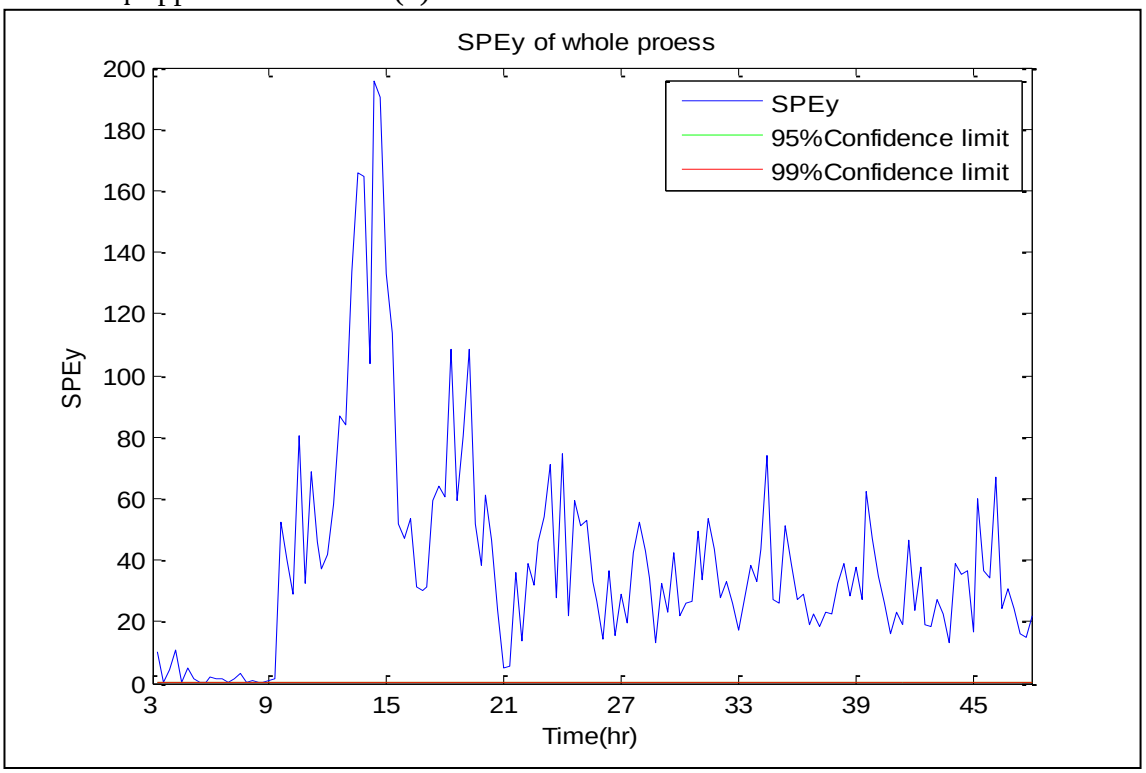

Figure 98- SPE$_Y$ for the TEP based on DPLS and MBDPLS$_T$ approaches – Fault (1)

2. Monitoring charts using ADPLS and AMBDPLS$_T$ for Fault (1)

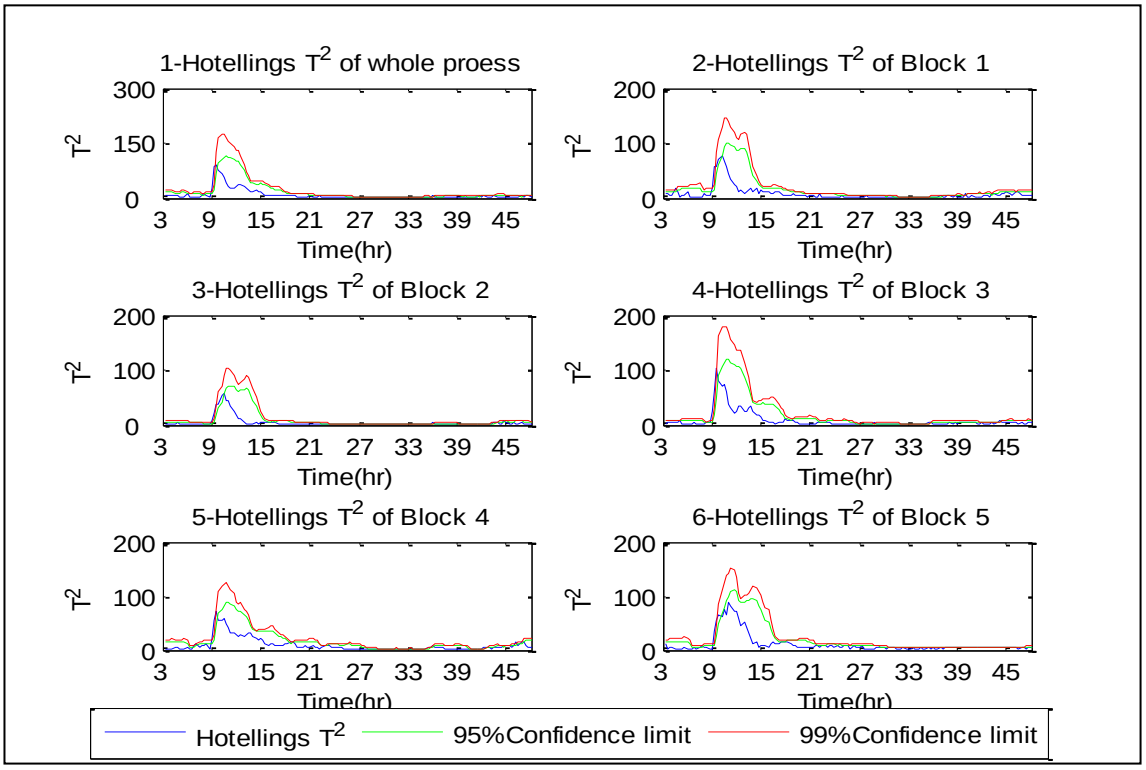

Figure 99 - Hotelling's T^2 for (1) overall process and (2-6) individual blocks based on ADPLS and AMBDPLS$_T$ approaches – Fault (1)

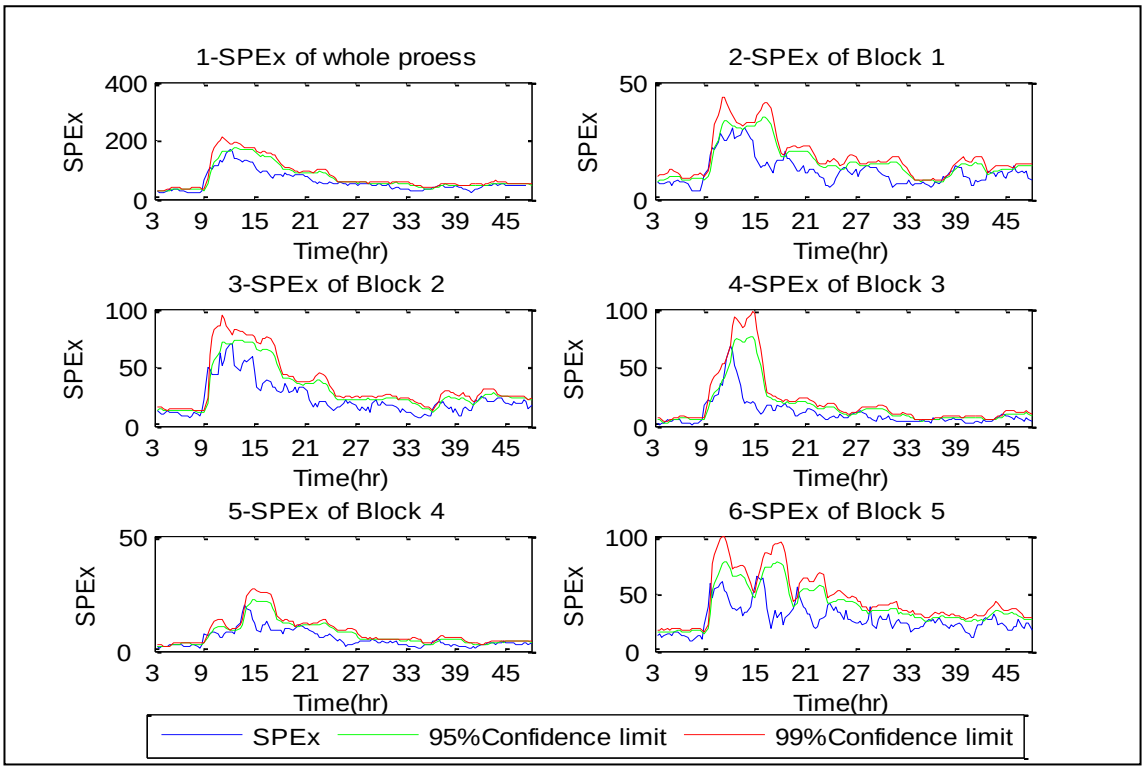

Figure 100 - SPE_X for (1) overall process and (2-6) individual blocks based on ADPLS and $AMBDPLS_T$ approaches – Fault (1)

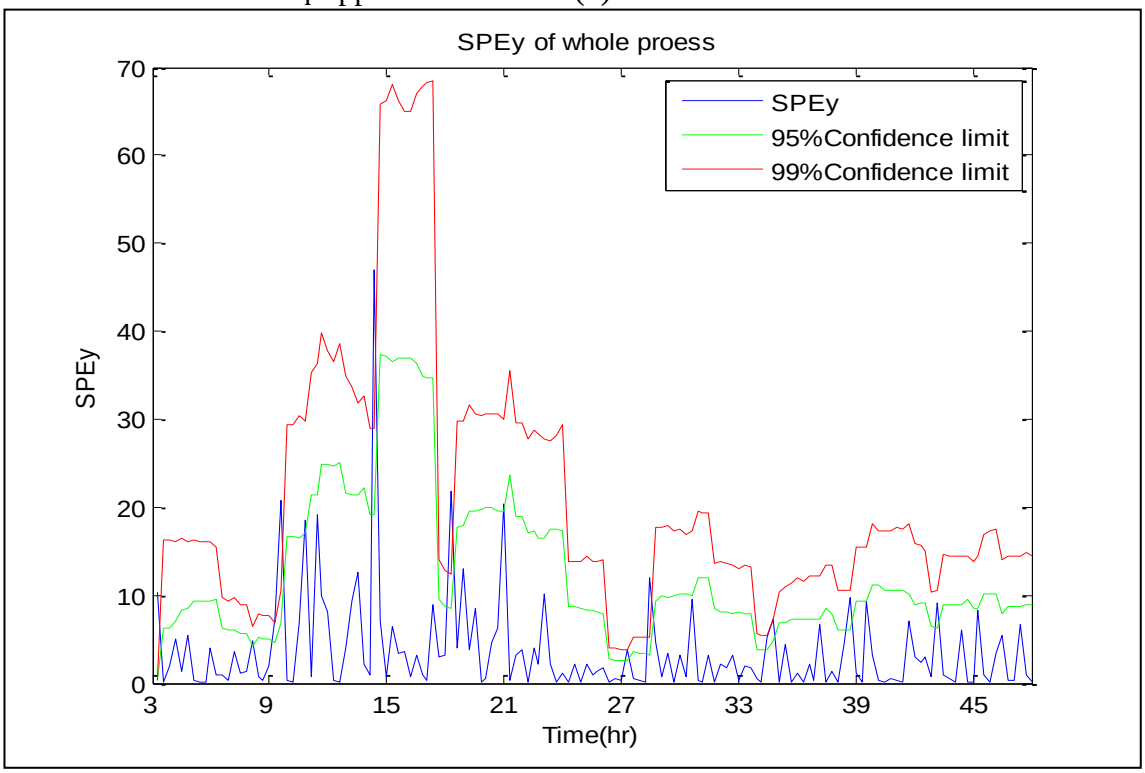

Figure 101 - SPE_Y for the TEP based on ADPLS and $AMBDPLS_T$ approaches – Fault (1)

3. Monitoring charts using DPLS and MBDPLS$_T$ for Fault (13)

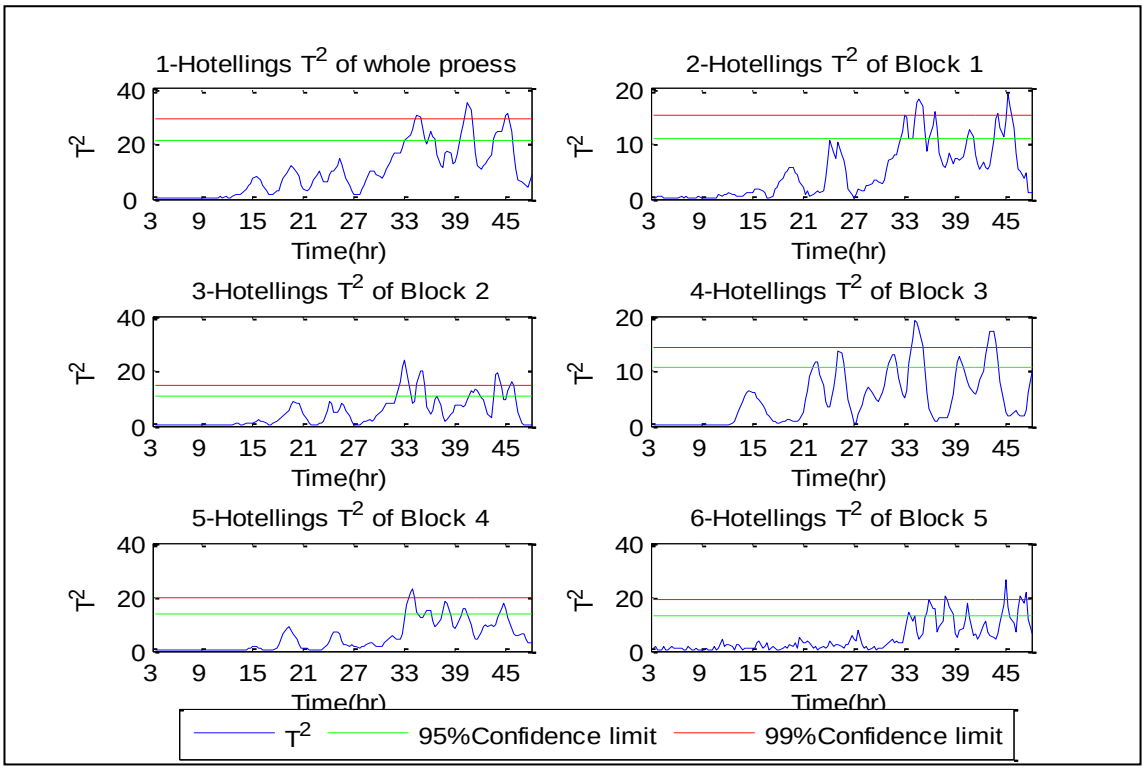

Figure 102 - Hotelling's T^2 for (1) overall process and (2-6) individual blocks based on DPLS and MBDPLS$_T$ approaches – Fault (13)

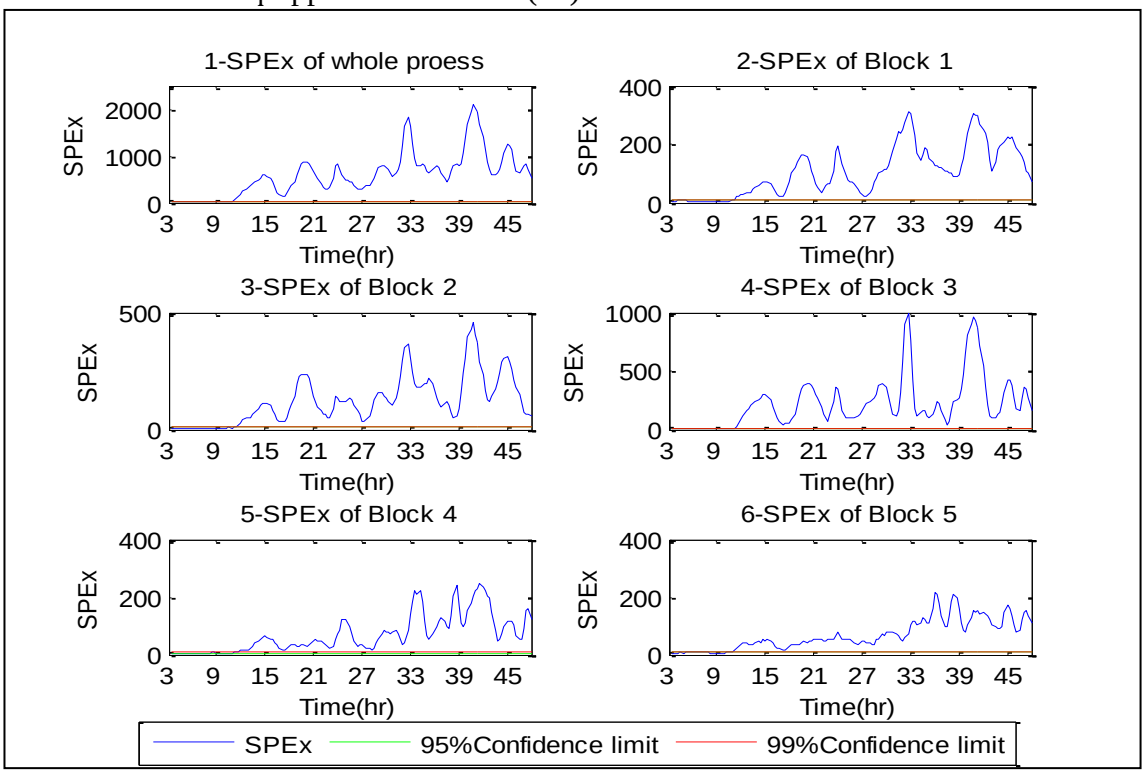

Figure 103 - SPE$_X$ for (1) overall process and (2-6) individual blocks based on DPLS and MBDPLS$_T$ approach –Fault13

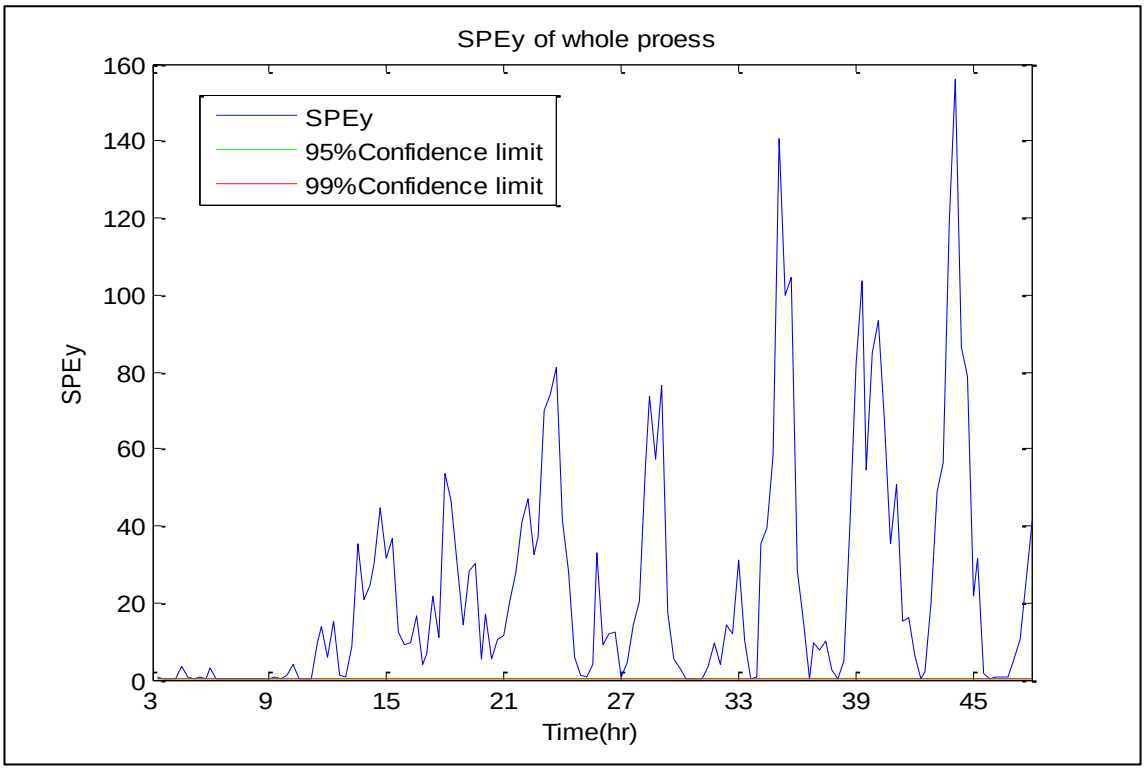

Figure 104 - SPE_Y for the TEP based on DPLS and $MBDPLS_T$ approaches – Fault (13)

4. Monitoring charts using ADPLS and $AMBDPLS_T$ for Fault (13)

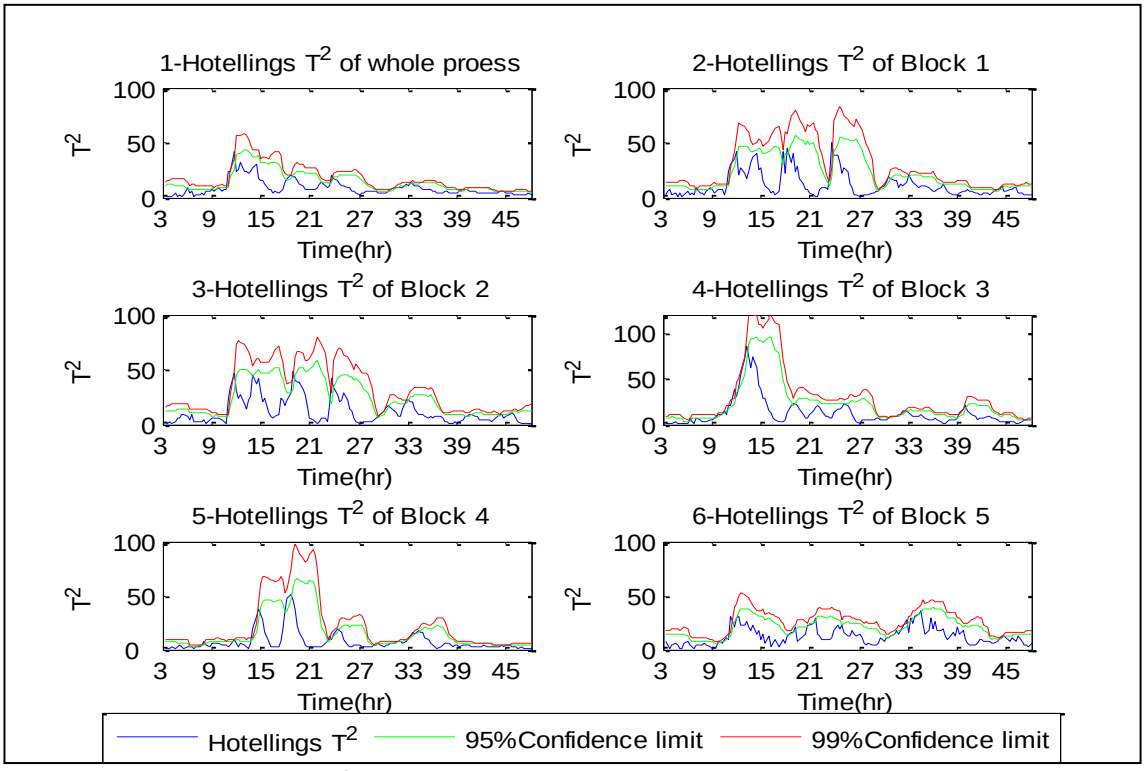

Figure 105 - Hotelling's T^2 for (1) overall process and (2-6) individual blocks based on ADPLS and $AMBDPLS_T$ approaches – Fault (13)

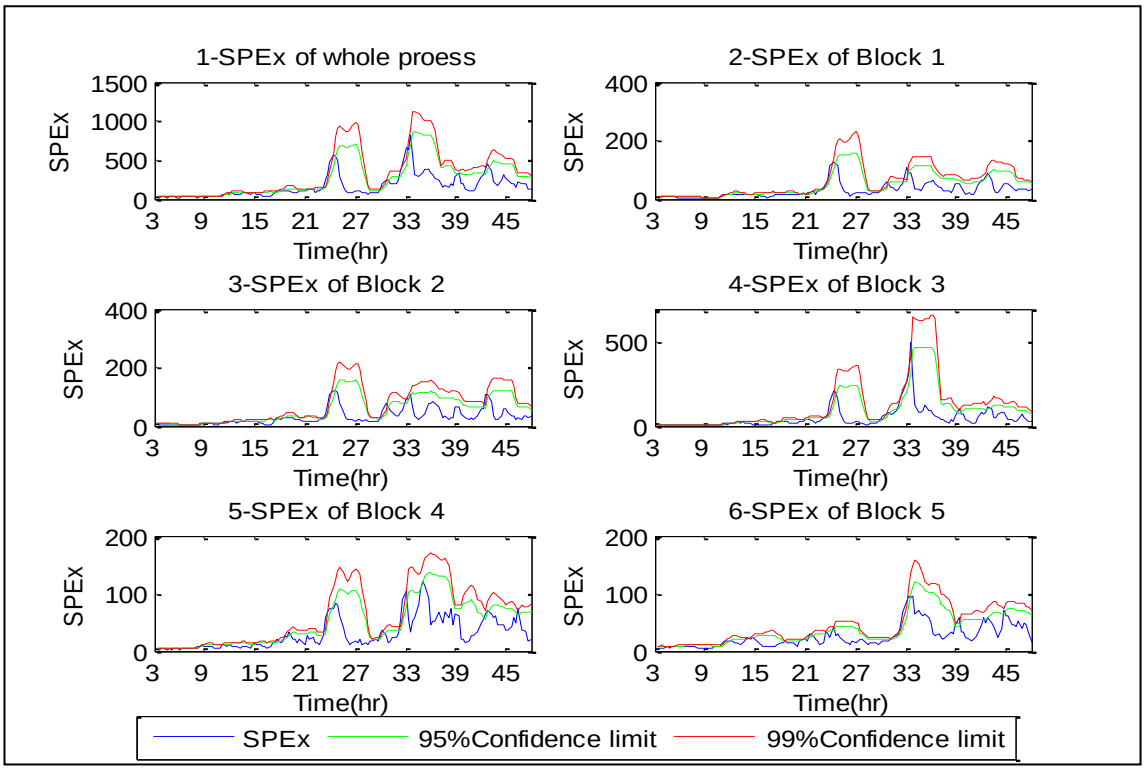

Figure 106 - SPE_X for (1) overall process and (2-6) individual blocks based on ADPLS and $AMBDPLS_T$ approaches – Fault (13)

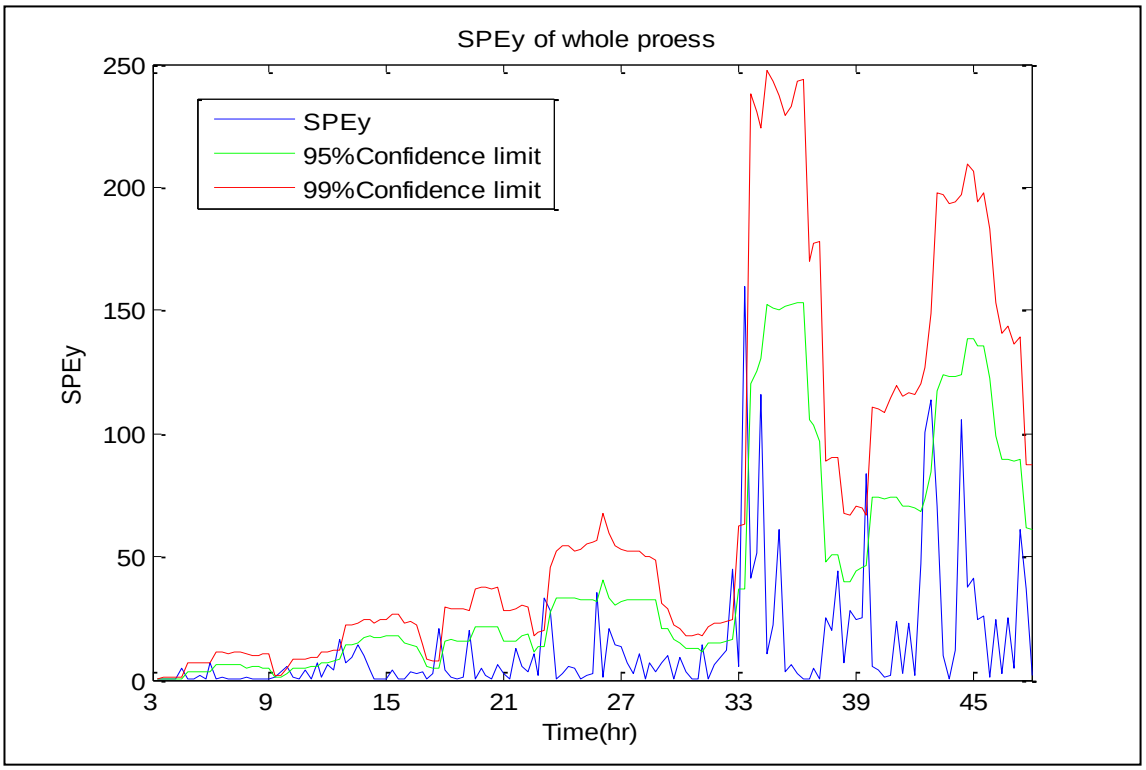

Figure 107 - SPE_Y for the TEP based on ADPLS and $AMBDPLS_T$ approaches – Fault (13)

5. Monitoring charts using DPLS and MBDPLS$_T$ for Fault (10)

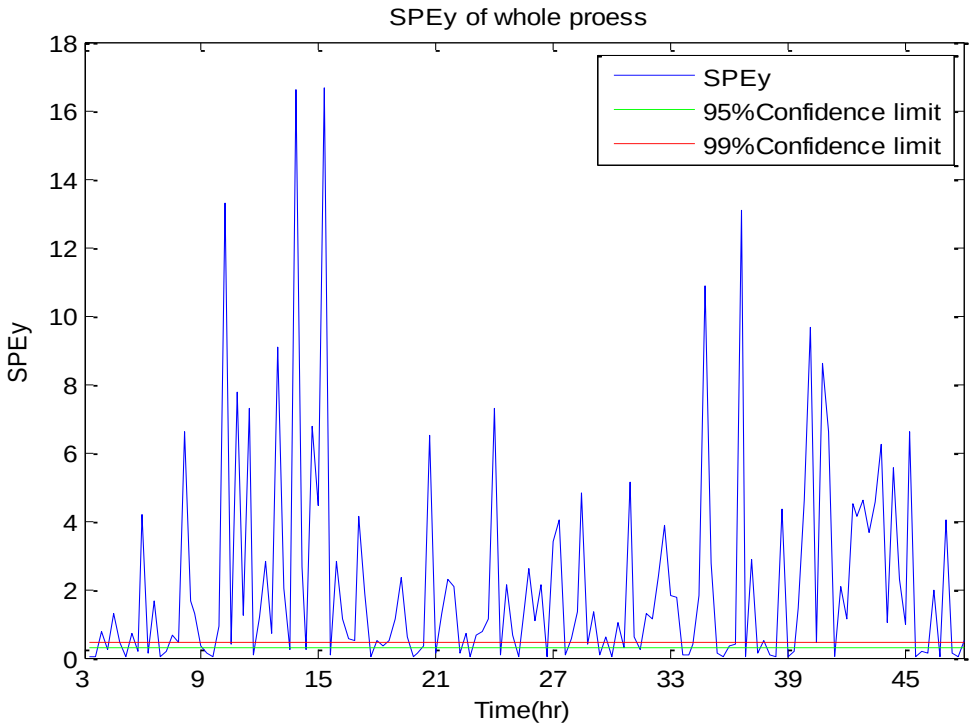

Figure 108 - SPE$_Y$ for the TEP based on DPLS and MBDPLS$_T$ – Fault (10)

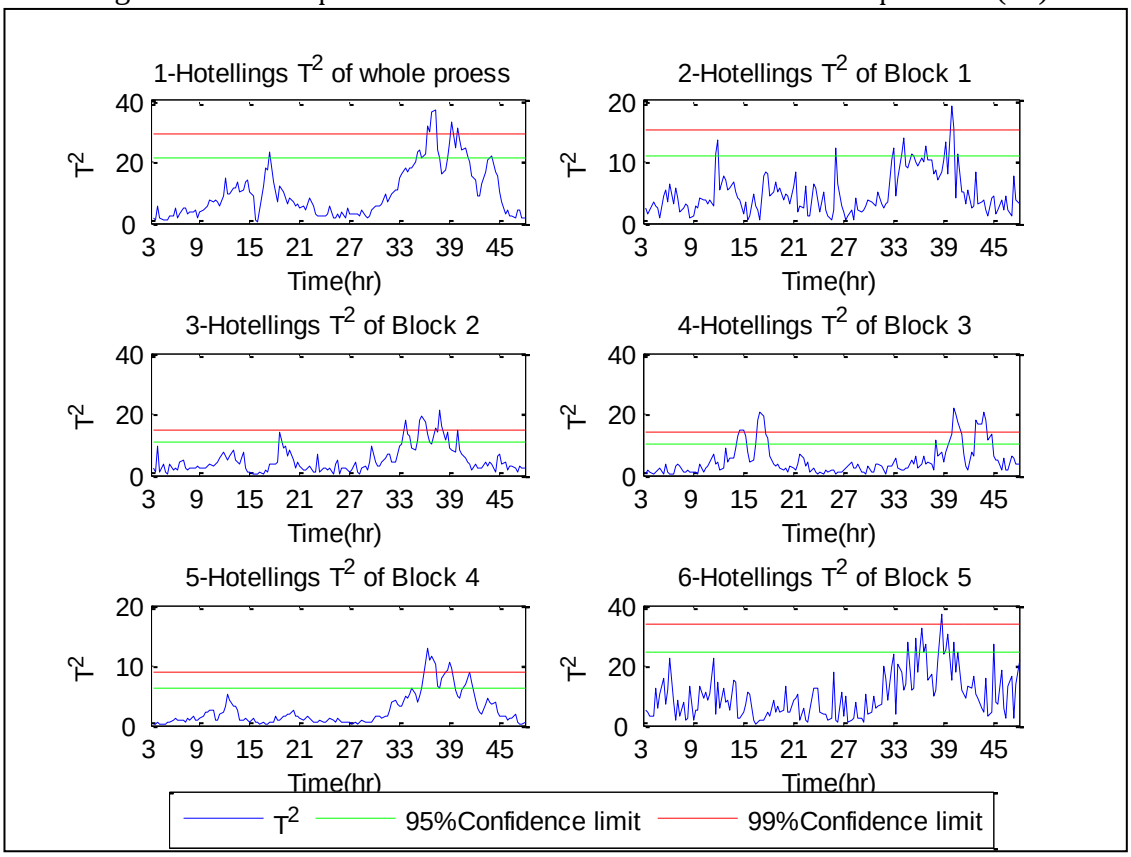

Figure 109 - Hotelling's T^2 for (1) overall process and (2-6) individual blocks based on DPLS and MBDPLS$_T$ approach – Fault (10)

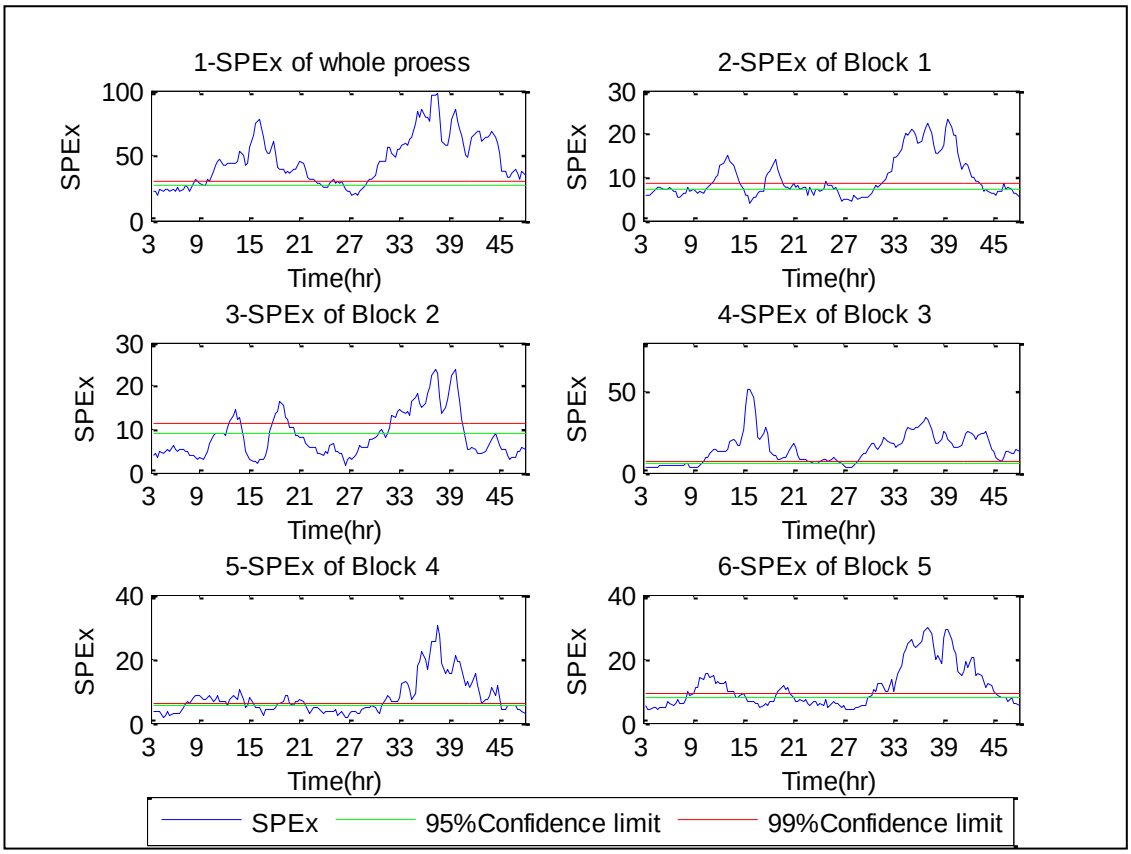

Figure 110 - SPE_X for (1) overall process and (2-6) individual blocks based on DPLS and $MBDPLS_T$ approaches – Fault (10)

6. Monitoring charts using ADPLS and $AMBDPLS_T$ for Fault (10)

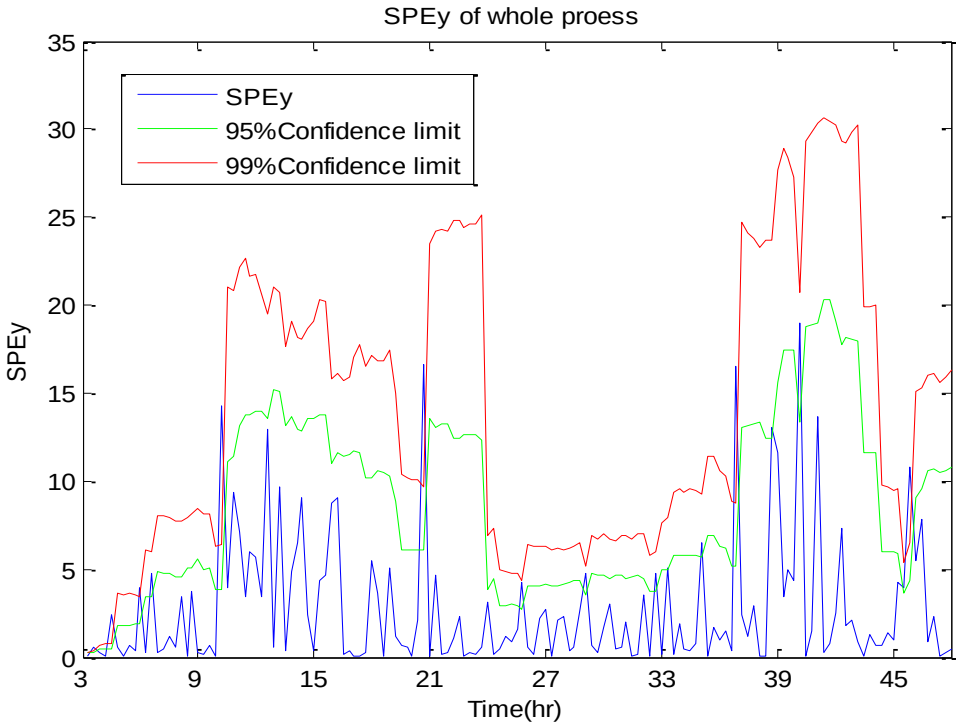

Figure 111 - SPE_Y for the TEP based on ADPLS – Fault (10)

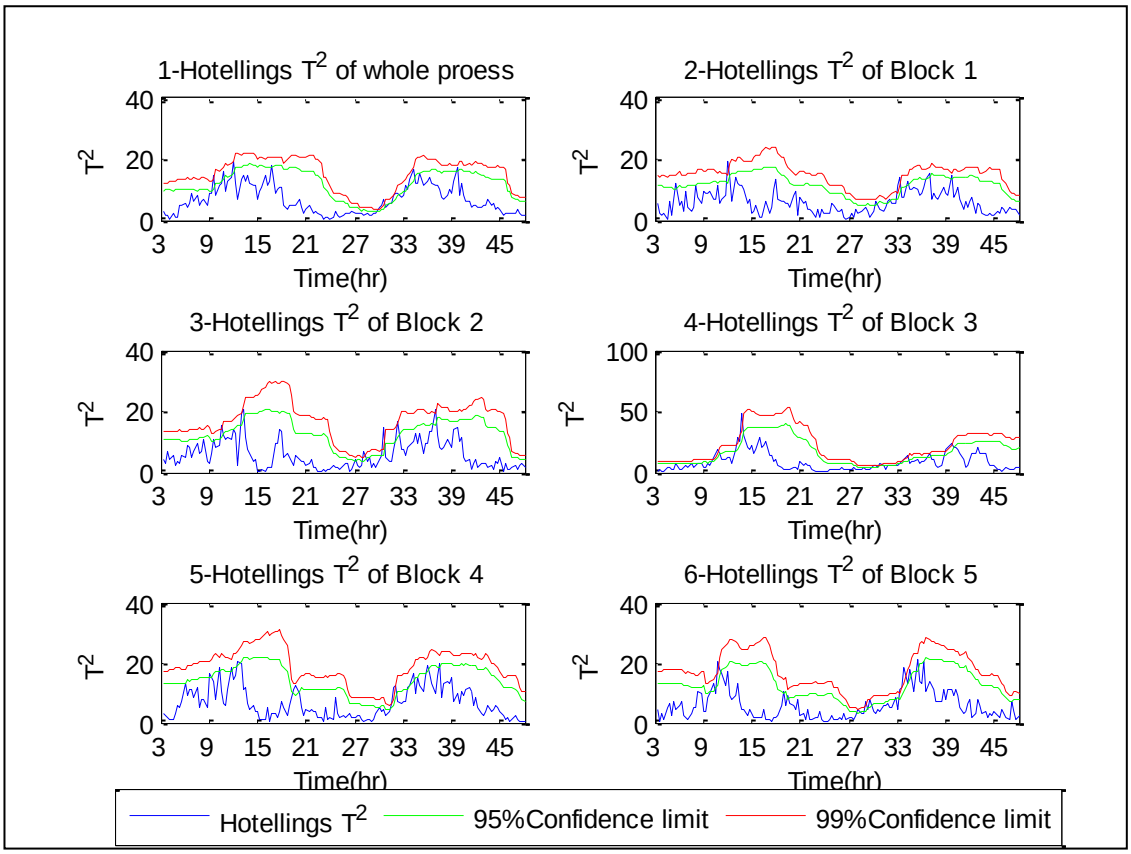

Figure 112 - Hotelling's T^2 for (1) overall process and (2-6) individual blocks based on ADPLS and AMBDPLS$_T$ approaches – Fault (10)

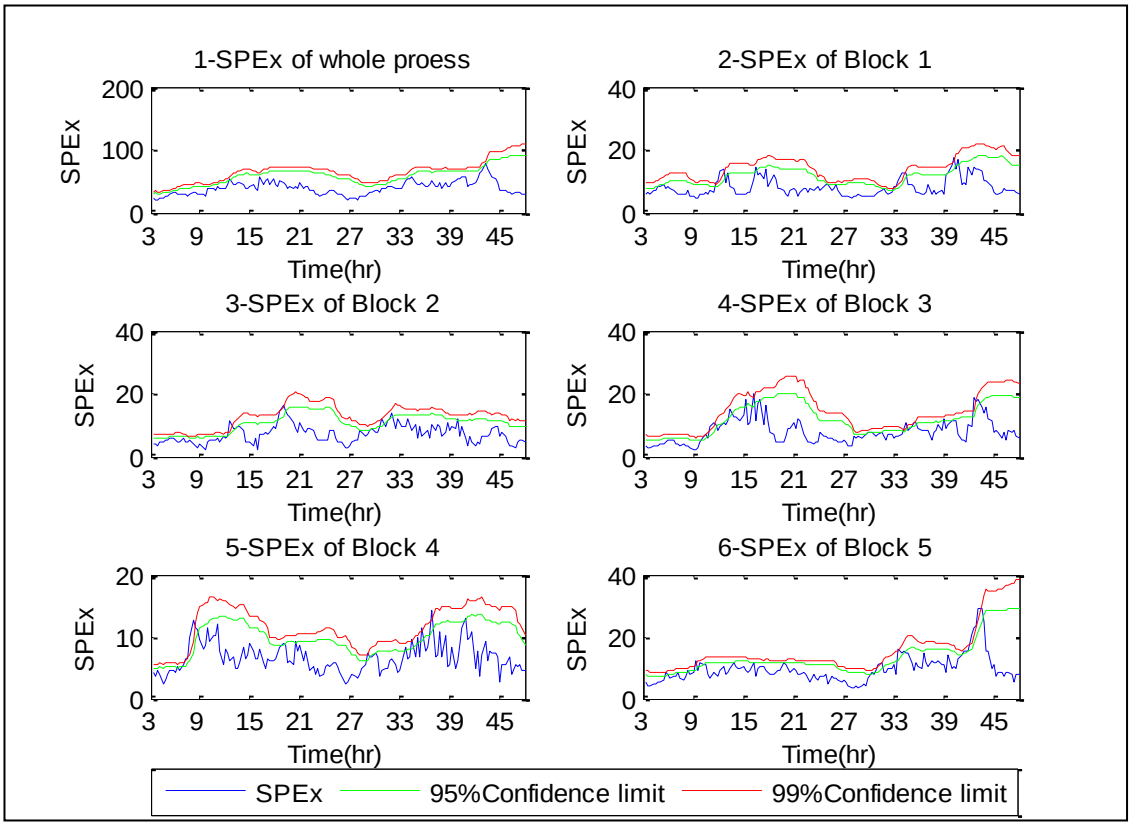

Figure 113 - SPE_X for (1) overall process and (2-6) individual blocks based on ADPLS and AMBDPLS$_T$ approach – Fault (10)